IAEA TECDOC SERIES

IAEA-TECDOC-1927

Environmental Transfer of Radionuclides in Japan following the Accident at the Fukushima Daiichi Nuclear Power Plant

Report of Working Group 4
Transfer Processes and Data for Radiological Impact Assessment
Subgroup 2 on Fukushima Data

IAEA Programme on Modelling and Data for Radiological Impact Assessments (MODARIA II)

IAEA
International Atomic Energy Agency

ENVIRONMENTAL TRANSFER OF RADIONUCLIDES IN JAPAN FOLLOWING THE ACCIDENT AT THE FUKUSHIMA DAIICHI NUCLEAR POWER PLANT

The following States are Members of the International Atomic Energy Agency:

AFGHANISTAN
ALBANIA
ALGERIA
ANGOLA
ANTIGUA AND BARBUDA
ARGENTINA
ARMENIA
AUSTRALIA
AUSTRIA
AZERBAIJAN
BAHAMAS
BAHRAIN
BANGLADESH
BARBADOS
BELARUS
BELGIUM
BELIZE
BENIN
BOLIVIA, PLURINATIONAL STATE OF
BOSNIA AND HERZEGOVINA
BOTSWANA
BRAZIL
BRUNEI DARUSSALAM
BULGARIA
BURKINA FASO
BURUNDI
CAMBODIA
CAMEROON
CANADA
CENTRAL AFRICAN REPUBLIC
CHAD
CHILE
CHINA
COLOMBIA
COMOROS
CONGO
COSTA RICA
CÔTE D'IVOIRE
CROATIA
CUBA
CYPRUS
CZECH REPUBLIC
DEMOCRATIC REPUBLIC OF THE CONGO
DENMARK
DJIBOUTI
DOMINICA
DOMINICAN REPUBLIC
ECUADOR
EGYPT
EL SALVADOR
ERITREA
ESTONIA
ESWATINI
ETHIOPIA
FIJI
FINLAND
FRANCE
GABON
GEORGIA
GERMANY
GHANA
GREECE
GRENADA
GUATEMALA
GUYANA
HAITI
HOLY SEE
HONDURAS
HUNGARY
ICELAND
INDIA
INDONESIA
IRAN, ISLAMIC REPUBLIC OF
IRAQ
IRELAND
ISRAEL
ITALY
JAMAICA
JAPAN
JORDAN
KAZAKHSTAN
KENYA
KOREA, REPUBLIC OF
KUWAIT
KYRGYZSTAN
LAO PEOPLE'S DEMOCRATIC REPUBLIC
LATVIA
LEBANON
LESOTHO
LIBERIA
LIBYA
LIECHTENSTEIN
LITHUANIA
LUXEMBOURG
MADAGASCAR
MALAWI
MALAYSIA
MALI
MALTA
MARSHALL ISLANDS
MAURITANIA
MAURITIUS
MEXICO
MONACO
MONGOLIA
MONTENEGRO
MOROCCO
MOZAMBIQUE
MYANMAR
NAMIBIA
NEPAL
NETHERLANDS
NEW ZEALAND
NICARAGUA
NIGER
NIGERIA
NORTH MACEDONIA
NORWAY
OMAN
PAKISTAN
PALAU
PANAMA
PAPUA NEW GUINEA
PARAGUAY
PERU
PHILIPPINES
POLAND
PORTUGAL
QATAR
REPUBLIC OF MOLDOVA
ROMANIA
RUSSIAN FEDERATION
RWANDA
SAINT LUCIA
SAINT VINCENT AND THE GRENADINES
SAN MARINO
SAUDI ARABIA
SENEGAL
SERBIA
SEYCHELLES
SIERRA LEONE
SINGAPORE
SLOVAKIA
SLOVENIA
SOUTH AFRICA
SPAIN
SRI LANKA
SUDAN
SWEDEN
SWITZERLAND
SYRIAN ARAB REPUBLIC
TAJIKISTAN
THAILAND
TOGO
TRINIDAD AND TOBAGO
TUNISIA
TURKEY
TURKMENISTAN
UGANDA
UKRAINE
UNITED ARAB EMIRATES
UNITED KINGDOM OF GREAT BRITAIN AND NORTHERN IRELAND
UNITED REPUBLIC OF TANZANIA
UNITED STATES OF AMERICA
URUGUAY
UZBEKISTAN
VANUATU
VENEZUELA, BOLIVARIAN REPUBLIC OF
VIET NAM
YEMEN
ZAMBIA
ZIMBABWE

The Agency's Statute was approved on 23 October 1956 by the Conference on the Statute of the IAEA held at United Nations Headquarters, New York; it entered into force on 29 July 1957. The Headquarters of the Agency are situated in Vienna. Its principal objective is "to accelerate and enlarge the contribution of atomic energy to peace, health and prosperity throughout the world''.

IAEA-TECDOC-1927

ENVIRONMENTAL TRANSFER OF RADIONUCLIDES IN JAPAN FOLLOWING THE ACCIDENT AT THE FUKUSHIMA DAIICHI NUCLEAR POWER PLANT

REPORT OF WORKING GROUP 4
TRANSFER PROCESSES AND DATA
FOR RADIOLOGICAL IMPACT ASSESSMENT
SUBGROUP 2 ON FUKUSHIMA DATA

IAEA PROGRAMME ON MODELLING AND DATA
FOR RADIOLOGICAL IMPACT ASSESSMENTS (MODARIA II)

INTERNATIONAL ATOMIC ENERGY AGENCY
VIENNA, 2020

COPYRIGHT NOTICE

For further information on this publication, please contact:

Terrestrial Environment Laboratory
International Atomic Energy Agency
Vienna International Centre
PO Box 100
1400 Vienna, Austria
Email: Official.Mail@iaea.org

Printed by the IAEA in Austria
October 2020

IAEA Library Cataloguing in Publication Data

Names: International Atomic Energy Agency.
Title: Environmental transfer of radionuclides in Japan following the Accident at the Fukushima Daiichi Nuclear Power Plant / International Atomic Energy Agency.
Description: Vienna : International Atomic Energy Agency, 2020. | Series: IAEA TECDOC series, ISSN 1011–4289 ; no. 1927 | Includes bibliographical references.
Identifiers: IAEAL 20-01352 | ISBN 978–92–0–117920–3 (paperback : alk. paper) |
ISBN 978–92–0–118020–9 (pdf)
Subjects: LCSH: Radioecology. | Radioisotopes. | Nuclear chemistry. | Fukushima Nuclear Disaster, Japan, 2011.

FOREWORD

Protection of the public and the environment from harmful effects of ionizing radiation originating from anthropogenic or natural radionuclides in the environment requires quantitative assessment of exposure levels. For this purpose, radioecological models are commonly used to describe environmental transfer of radionuclides and their accumulation in various compartments or biological entities, including humans. The predictive and explanatory powers of a radioecological model depend on the plausibility of the underlying assumptions and model parameters. Observations and experimental data provide a basis for sensible parameterizations of the radioecological models, thus making them fit for specific exposure situations and improving their plausibility and predictive power.

Since the 1980s, the IAEA has been organizing programmes of international model comparison and testing. These programmes have helped to improve modelling approaches through both exchange of data and the enhancement of modelling capabilities in Member States. IAEA publications on this subject over the past three decades demonstrate the comprehensive nature of the programmes and provide a record of the associated advances.

From 2016 to 2019, the IAEA organized a programme entitled Modelling and Data for Radiological Impact Assessments (MODARIA II), a follow-up of the preceding MODARIA programme (2012–2015), mainly aimed at testing the performance of radioecological and dose assessment models, developing new and improving existing models, analysing radioecological data, and providing an international forum for exchange and collaboration. The seven working groups of the MODARIA II programme addressed various complementary thematic areas, such as remediation and decision making, exposures in urban and rural environments following accidents, modelling radionuclide releases to the environment, analysis and evaluation of radioecological data, radiation exposures and effects on wildlife, biosphere modelling for long term safety assessments of waste disposal facilities, and marine modelling.

This publication presents the outcomes of Working Group 4 — Transfer Processes and Data for Radiological Impact Assessment — relating to radioecological transfer parameters in the environment in Japan following the accident at the Fukushima Daiichi nuclear power plant in 2011. The publication presents experiences gained in Japan after the accident, compares post-accident data with pre-accident data collected in Japan and existing data originated from other parts of the world, and focuses on integration of the Japan specific outcomes into the global framework of radioecological knowledge.

The IAEA is grateful to all the participants of Working Group 4 and in particular the main drafting group members: S. Fesenko (Russian Federation), S. Hashimoto (Japan), B. Howard (United Kingdom, working group leader), G. Pröhl (Germany), K. Tagami (Japan, subgroup leader). The IAEA acknowledges the efforts of M. Thorne (United Kingdom) and H. Yasuda (Japan), who reviewed the final draft document and provided valuable comments and suggested edits. The IAEA officers responsible for this publication were A. Iurian and A. Ulanowski of the IAEA Environment Laboratories.

EDITORIAL NOTE

This publication has been prepared from the original material as submitted by the contributors and has not been edited by the editorial staff of the IAEA. The views expressed remain the responsibility of the contributors and do not necessarily represent the views of the IAEA or its Member States.

Neither the IAEA nor its Member States assume any responsibility for consequences which may arise from the use of this publication. This publication does not address questions of responsibility, legal or otherwise, for acts or omissions on the part of any person.

The use of particular designations of countries or territories does not imply any judgement by the publisher, the IAEA, as to the legal status of such countries or territories, of their authorities and institutions or of the delimitation of their boundaries.

The mention of names of specific companies or products (whether or not indicated as registered) does not imply any intention to infringe proprietary rights, nor should it be construed as an endorsement or recommendation on the part of the IAEA.

The authors are responsible for having obtained the necessary permission for the IAEA to reproduce, translate or use material from sources already protected by copyrights.

The IAEA has no responsibility for the persistence or accuracy of URLs for external or third party Internet web sites referred to in this publication and does not guarantee that any content on such web sites is, or will remain, accurate or appropriate.

CONTENTS

1. INTRODUCTION 1

1.1. BACKGROUND 2
1.2. OBJECTIVE 3
1.3. SCOPE 3
1.4. STRUCTURE 4

2. ECOSYSTEMS AND PROCESSES 7

2.1. THE NATURAL ENVIRONMENT AROUND THE FDNPP 7
2.2. TRANSFER PROCESSES IN THE ENVIRONMENT 8
2.3. BASIC TERMS AND DEFINITIONS 11

3. THE FUKUSHIMA DAIICHI NUCLEAR POWER PLANT ACCIDENT 23

3.1. INITIAL RELEASES OF RADIONUCLIDES IN THE ATMOSPHERE AND COUNTERMEASURES 23
3.1.1. Radioactive releases in the atmosphere and deposition in the terrestrial environment 23
3.1.2. Initial countermeasures and remediation in the terrestrial environment 26
3.2. RADIONUCLIDES IN FRESHWATERS 26
3.3. RADIONUCLIDES IN THE MARINE ENVIRONMENT 27
3.3.1. Deposition and releases into the Pacific Ocean 27
3.3.2. Dispersion of radionuclides in the marine environment 28
3.4. SUMMARY OF CHAPTER 3 29

4. AGRICULTURAL SYSTEMS 31

4.1. INTERCEPTION AND WEATHERING 32
4.1.1. Mass interception of Fukushima fallout radionuclides by edible parts of herbaceous plants 32
4.1.2. Approach used to estimate interception 33
4.1.3. Weathering half-lives for calculation of mass interception 33
4.1.4. Calculation of mass interception for edible part of crops 39
4.1.5. Summary and limitations 41
4.2. BEHAVIOUR OF RADIOCAESIUM IN AGRICULTURAL SOIL 41
4.2.1. Introduction 42
4.2.2. Soil characteristics governing radiocaesium sorption and mobility in soil 42
4.2.3. The relationship between *RIP* and soil properties 42
4.2.4. The impact of flood irrigation on radiocaesium behaviour in rice paddy fields 45
4.2.5. Relationship between $\boldsymbol{K}$d and *CR* in Japanese agricultural soils 48
4.2.6. Summary and limitations 48
4.3. TRANSFER OF RADIOCAESIUM TO CROPS 49
4.3.1. Transfer to rice 50
4.3.2. Transfer to green tea 64
4.3.3. Transfer to fruit 68
4.3.4. Transfer to other agricultural crops 90
4.4. TRANSFER TO FARM ANIMALS 103

4.4.1. Introduction 103
4.4.2. ***Fm***, ***Ff*** and *CR* values 106
4.4.3. Radiocaesium distribution in animal tissues 110
4.4.4. Biological half-life 110
4.4.5. Summary and limitations 111
4.5. CONCLUSIONS 112

5. FOREST ECOSYSTEMS 129

5.1. INTRODUCTION 129
5.2. RADIOCAESIUM TRANSFER TO TREE COMPARTMENTS 134
5.2.1. Introduction 134
5.2.2. Interception and weathering 135
5.2.3. Soil to tree transfer 140
5.2.4. K fertilization effect 144
5.2.5. Heartwood/Sapwood ^{137}Cs concentration ratio 146
5.2.6. Radiocaesium activity concentrations in pollen 149
5.2.7. Radiocaesium transfer in forest soil 150
5.2.8. Half-life values in needles, branches and bark 154
5.3. TRANSFER TO MUSHROOMS 156
5.4. TRANSFERS TO EDIBLE WILD PLANTS 159
5.5. TRANSFER TO GAME 161
5.5.1. ***T***ag values for game 161
5.5.2. $CR_{meat\text{-}soil}$ and $CR_{meat\text{-}water}$ data for game species 164
5.5.3. Effective half-lives for game animals 165
5.5.4. Radiocaesium distribution in wild boar and Asian black bear tissues 166
5.5.5. Transfer to game summary and data limitations 167
5.6. SUMMARY AND CONCLUSIONS 168

6. CATCHMENTS AND RIVERS 179

6.1. INTRODUCTION 179
6.2. RADIOCAESIUM RUN-OFF IN CATCHMENTS 180
6.2.1. Radiocaesium run-off before the FDNPP accident 180
6.2.2. Run-off of radiocaesium after the FDNPP accident 182
6.2.3. Time dependence of ^{137}Cs of river water 192
6.2.4. Summary and limitations. 196
6.3. ESTIMATION OF THE FRESHWATER DISTRIBUTION COEFFICIENT *K*D 197
6.3.1. Introduction 197
6.3.2. The distribution coefficient ***K***d(a)-SS parameter 198
6.3.3. $K_{d(a)\text{-}SS}$ before the FDNPP accident 199
6.3.4. $K_{d(a)\text{-}SS}$ after the FDNPP accident 200
6.3.5. Summary and limitations 205
6.4. UPTAKE OF RADIOCAESIUM BY FRESHWATER FISH 206
6.4.1. Introduction 206
6.4.2. Data collection 206
6.4.3. Concentration Ratios for freshwater biota before the FDNNP accident 207
6.4.4. Concentrations ratios for different fish species after the FDNPP accident 207

6.4.5. Fish size effect on concentration ratios....209
6.4.6. Concentration ratios for other aquatic organisms....212
6.4.7. Detailed analysis for radiocaesium transfer to lake fish....212
6.4.8. Comparison of ^{137}Cs concentration ratios before and after the FDNPP accident....214
6.4.9. Summary and limitations....216
6.5. EFFECTIVE HALF-LIVES OF RADIOCAESIUM IN LAKE BIOTA....217
6.5.1. Summary and limitations....218

7. MARINE SYSTEMS....229

7.1. INTRODUCTION....229
7.2. CONCENTRATION RATIOS FOR EDIBLE MARINE SPECIES....230
7.2.1. Definitions of concentration ratios (*CR*) for edible marine species....230
7.2.2. Datasets....230
7.2.3. CR_{GF} values derived from global fallout (1984–2010)....231
7.2.4. CR_a values after the FDNPP accident....234
7.2.5. Effective half-lives (T_a) of CR_a for returning to pre-accident CR values after the FDNPP accident....238
7.3. SEDIMENT DISTRIBUTION COEFFICIENT....241
7.3.1. Outline of monitoring programme....241
7.3.2. Data sources....241
7.3.3. Temporal changes of ^{137}Cs in seawater and sediment, and K_d before the FDNPP accident....242
7.3.4. Variation of $\boldsymbol{K}$d before the FDNPP accident....245
7.3.5. Temporal changes of ^{137}Cs in seawater and sediment, and $K_{d(a)}$ after the FDNPP accident....248
7.4. SUMMARY....254
7.4.1. Pre-FDNPP accident (1984–2010)....254
7.4.2. After the FDNPP accident....255
7.5. LESSONS LEARNED FROM THE ACCIDENT....256
7.5.1. Importance of systematic monitoring on a long-term basis:....256
7.5.2. CR_{GF} and CR_a values as indicators of ^{137}Cs transfer to species in host vs post-accident conditions:....256
7.5.3. Temporal changes of $\boldsymbol{K}$d values:....256
7.5.4. *CR* vs $\boldsymbol{K}$d(a) values:....256
7.6. LIMITATIONS....257
7.7. REFERENCES....257

8. FOOD AND CULINARY PROCESSING....263

8.1. INTRODUCTION....263
8.2. DEFINITIONS AND CONCEPTS....264
8.3. PROCESSING OF CEREALS....265
8.4. PROCESSING OF SOYBEAN....267
8.5. VEGETABLES AND FRUITS....268
8.6. BEVERAGES....270
8.6.1. Tea brewing....270
8.6.2. Alcoholic drinks....273
8.7. FOOD PROCESSING OF ANIMAL PRODUCTS AND FISH....273

8.7.1. Meat 273
8.7.2. Fish 274
8.7.3. Insects 275
8.8. WILD EDIBLE PLANTS AND MUSHROOMS 276
8.8.1. Wild edible plants (Sansai) 276
8.8.2. Mushrooms 276
8.9. SUMMARY AND LIMITATIONS 278

9. CONCLUSIONS 283
9.1. INTRODUCTION 283
9.2. LESSONS LEARNED FROM POST-ACCIDENT STUDIES 284
9.3. SPECIFIC FINDINGS 285
9.4. KEY RADIOECOLOGICAL LESSONS 291

APPENDIX I. 293

APPENDIX II. 299

APPENDIX III. 301

APPENDIX IV. 321

APPENDIX V. 329

ABBREVIATIONS 337

CONTRIBUTORS TO DRAFTING AND REVIEW 339

LIST OF WORKING GROUP 4, SUBGROUP 2 PARTICIPANTS 343

1. INTRODUCTION

GERHARD PRÖHL
Consultant, GERMANY

JOANNE BROWN, ALEXANDER ULANOWSKI
International Atomic Energy Agency

Radiological assessment is required to evaluate the radiological hazards associated with routine and accidental releases of radionuclides to the environment, both for supporting decision making during normal operation of nuclear facilities and for emergency management and remediation of areas affected by enhanced levels of radioactivity. Following the release of radionuclides to the environment, radiation exposure of members of the public are assessed using radiological models describing transfer of radionuclides through different ecosystems and compartments of the environment [1.1]. Such models serve as a key element of the regulatory control of nuclear facilities and activities in planned, existing and emergency exposure situations. The reliability of such models depends on a well-informed description of the environmental conditions and on high quality data that can be applied to represent radionuclide transfer through the environment.

For many years, the IAEA has supported the development of models for radiological assessments for members of the public and has provided guidance on appropriate application of these models [1.1, 1.2]. The IAEA has coordinated the collation of appropriate data sets to quantify the transfer of radionuclides in the terrestrial and aquatic environment [1.3–1.6]. This has been carried out in the framework of the international model test and comparison programmes comprising: Biosphere Modelling and Assessment (BIOMASS) in 1996–2002, Environmental Models for Radiation Safety (EMRAS) in 2003–2007 and 2009–2011) and Modelling and Data for Radiological Impact Assessment (MODARIA I and II) in 2012–2015 and 2016–2019. As one of the many results of these programmes, the "Handbook of Parameter Values for the Prediction of Radionuclide Transfer in Terrestrial and Freshwater Environments" [1.4] was published which serves as a key document for many IAEA Members States when performing radiological impact assessments for facilities and activities to ensure compliance with the IAEA Safety Standards [1.7, 1.8].

The programme MODARIA II, implemented in the period 2016–2019, addressed the following topics: (a) assessment and decision making of existing exposure situations for NORM and nuclear legacy sites (work group 1); (b) assessment of exposures and countermeasures in urban environments (work group 2); (c) assessments and control of exposures to the public and biota for planned releases to the environment (work group 3); (d) transfer processes and data for radiological impact assessment (work group 4); (e) exposure and effects to biota (work group 5); (f) biosphere modelling for long term safety assessments of high level waste disposal facilities (work group 6); (g) assessment of fate and transport of radionuclides released in the marine environment (work group 7).

The activities of the work group 4 were focused on environmental transfer of radionuclides and, specifically, its subgroup 2 dealt with radioecological observations and outcomes following the nuclear accident on the Fukushima Daiichi NPP (FDNPP) on 11 March 2011. Correspondingly, this document summarises the work of the subgroup and presents outcomes of radioecological observations and studies done in Japan before and after the accident.

1.1. BACKGROUND

As a consequence of the FDNPP accident in Japan, radionuclides were released to both terrestrial and aquatic environments. Due to the prevailing wind directions during the accident, radionuclides deposited on both the Pacific Ocean and on land. The highest depositions on land were observed in a north-westerly direction from the FDNPP [1.9].

Immediately after the accident, intensive monitoring programmes were initiated to determine gamma-dose rates and their time-dependence, and to identify radionuclide activity concentrations in environmental media such as soil, plants, foodstuffs, surface waters, sediments and aquatic species. In the early phase of the FDNPP accident, major contributors to the environmental contamination were mainly ^{133}Xe, ^{131}I, and ^{132}Te/^{132}I, which have physical half-lives of a few days as well as by the longer-lived ^{134}Cs and ^{137}Cs, with physical half-lives of 2.06 years and 30.2 years, respectively. Traces of ^{90}Sr and long-lived plutonium isotopes were also released, but the resulting activity concentrations in the environment were difficult to distinguish from that deposited following the testing of nuclear weapons in the atmosphere in the 1950s and 1960s. Over longer timescales, only the radiocaesium isotopes (^{134}Cs and ^{137}Cs) that has remained in the environment were relevant for assessment of potential radiation exposure to humans and other organisms.

Many measurements were performed at different locations in close proximity to, and at further distances from, the FDNPP. Based on the results of such measurements, radiation doses to people were estimated for evaluating the radiological significance of the radionuclide releases and to decide on the necessity of protective and remedial actions to ensure that radiation doses to people remain as low as reasonably achievable. The measurements were also used to ensure compliance with reference levels for radiation doses to people and limits of activity concentrations in foodstuffs. Restrictions to prevent the consumption of these products were established by the Japanese authorities in response to the accident.

In parallel to the extensive monitoring of radiocaesium in the environment in Japan, scientific studies were initiated to investigate the behaviour of radionuclides in the environment. The research focused on radionuclide interception by forest trees and a few agricultural plants, the uptake of radionuclides by rice and other agricultural crops, the transfer of radiocaesium from feed to animal food products such as meat, milk and eggs, the uptake of radionuclides by freshwater fish and marine seafood and the transport of radiocaesium in catchments areas, rivers and lakes and its transport to the Pacific Ocean. The behaviour of radionuclides deposited onto the Pacific Ocean, or subsequently released afterwards, has also been addressed with large scale monitoring of water, sediment and seafood. The major part of Fukushima Prefecture is covered by forest, so research projects were established in forests to quantify the rate of reduction of the external gamma dose rate from radiocaesium and to better understand soil chemistry. The studies are also evaluating the distribution of radiocaesium within different components of trees (wood, bark and leaves) to gain knowledge about the amount of radiocaesium in timber and firewood, wild plants, fungi and wild animals, and to analyse the time trends of activity concentrations in such products.

Until 2010, most of the experience related to the transfer of radionuclides in the environment has been gained in Europe and North America starting in the mid-1950s. The data derived from Fukushima related research allowed extension and validation of the available data, primarily for radiocaesium, and can contribute to the improvement of radiological models.

The data compiled in this report are mainly based on peer reviewed publications. These data were largely elaborated by those Japanese institutes leading the work in their respective fields.

The studies analysed in this report do not necessarily include all the work performed in Japan to study the transfer of radionuclides in the environment.

1.2. OBJECTIVE

The goal of this report is to compile and analyse the radioecological information gained in Japan following the FDNPP accident in 2011 to improve the worldwide capability to quantify the transfer of radionuclides in the environment. The report includes information acquired during programmes implemented for monitoring radiocaesium activity concentrations as well as research projects set up to investigate specific topics on the environmental transport of radiocaesium and, to a much lesser extent, radioiodine.

The objectives of the report are:

- To analyse the environmental transfer parameters for radionuclides released from the FDNPP accident in the context of the assessment of exposures to people;

- To compare the environmental transfer data observed in Japan with that collated by other countries. The latter includes globally collated data related to weapons' fallout, and data from Europe after the Chernobyl accident;

- To explore whether, and to which extent, the environmental transfer parameters determined in Japan are specific to the environmental conditions of the areas affected by the deposition of radionuclides, or whether they can also be applied to other areas for the assessment of radiological impacts to people and the environment. Specific consideration is given to the transfer of radionuclides to rice. For each environmental system considered, suitable parameter values for use in Japan and other countries with similar environmental and agricultural conditions are collated where possible. Parameters are identified where data are scarce and further information is needed;

- To identify the environmental factors in the areas affected by the deposition of radionuclides that have had a notable impact on the transfer of radionuclides such as climate, soil types, agricultural practice, forest management, customs and living habits;

- To identify topics addressed in IAEA documents on the assessment of radiological impacts to people and the environment that require updating to appropriately address the experience gained following the FDNPP accident.

1.3. SCOPE

This report covers radionuclide transfer in terrestrial and aquatic environments with a focus on radiocaesium isotopes. The data collected and analysed are relevant for estimating the transfer of radionuclides through food chains to humans and for assessing radiation doses due to intake of food. This publication is primarily intended to provide information to IAEA Member States on environmental transfer data from Japan after the release of radionuclides to the environment from the FDNPP. The report covers the following topics:

- Interception of radionuclides on, and loss from, plant surfaces;
- Translocation of radionuclides in plants;
- Behaviour of radiocaesium in soil;
- Uptake of radionuclides from soil by rice and other agricultural crops and vegetables;

- Uptake and distribution of radiocaesium in forest trees;
- Uptake of radiocaesium by wild edible plants;
- Transfer of radiocaesium to wild animals;
- Transfer of radionuclides from feedstuffs to edible animal products, including milk and meat;
- Behaviour of radiocaesium in aquatic ecosystems, including freshwaters, coastal areas and the ocean and transfer to edible aquatic organisms;
- Transport of radiocaesium from catchments through rivers and lakes to the ocean;
- Modification of radionuclide activity concentrations in food products during food processing and culinary preparation.

Additionally, the report compares the parameter values derived after the FDNPP accident in Japan with international values. Data or pathways that are specific for the environmental conditions in Japan are identified as are transfer parameters values that are applicable to environmental conditions in other countries.

1.4. STRUCTURE

This report consists of nine chapters and five appendices. An overview on the relevant ecosystem and processes are given in Chapter 2. Chapter 3 provides a short overview on the accident. Chapters 4 and 5 address the radionuclide transfer in agricultural and forest systems respectively. Chapter 6 is devoted to the behaviour of radiocaesium in catchments areas and the uptake by freshwater fish. The transfer of radiocaesium in marine system is discussed in Chapter 7. The modification of radionuclide activity concentrations in foods during processing and culinary preparation is addressed in Chapter 8. Chapter 9 summarizes the conclusions and lessons learned from the FDNPP accident with regard to the environmental transport of radionuclides and the implications for the assessment of ingestion doses following large-scale depositions of radionuclides, with particular emphasis on radiocaesium.

REFERENCES

[1.1] INTERNATIONAL ATOMIC ENERGY AGENCY, Generic Models for Use in Assessing the Impact of Discharges of Radioactive Substances to the Environment, Safety Reports Series 19, IAEA, Vienna (2001).

[1.2] INTERNATIONAL ATOMIC ENERGY AGENCY, Generic Models and Parameters for Assessing the Environmental Transfer of Radionuclides from Routine Releases, Safety Series 57, IAEA, Vienna (1982).

[1.3] INTERNATIONAL ATOMIC ENERGY AGENCY, Handbook of Parameter Values for the Prediction of Radionuclide Transfer in Temperate Environments, Technical reports series TRS-364, IAEA, Vienna (1994).

[1.4] INTERNATIONAL ATOMIC ENERGY AGENCY, Handbook of Parameter Values for the Prediction of Radionuclide Transfer in Terrestrial and Freshwater Environments, Technical Reports Series 472, IAEA, Vienna (2010).

[1.5] INTERNATIONAL ATOMIC ENERGY AGENCY, Sediment Distribution Coefficients and Concentration Factors for Biota in the Marine Environment, Technical Reports Series 422, IAEA, Vienna (2004).

[1.6] INTERNATIONAL ATOMIC ENERGY AGENCY, Quantification of Radionuclide Transfer in Terrestrial and Freshwater Environments for Radiological Assessments, TECDOC Series 1616, IAEA, Vienna (2009).

[1.7] INTERNATIONAL ATOMIC ENERGY AGENCY, Prospective Radiological Environmental Impact Assessment for Facilities and Activities, General Safety Guides GSG-10, IAEA, Vienna (2018).

[1.8] INTERNATIONAL ATOMIC ENERGY AGENCY, Regulatory Control of Radioactive Discharges to the Environment, General Safety Guides GSG-9, IAEA, Vienna (2018).

[1.9] INTERNATIONAL ATOMIC ENERGY AGENCY, The Fukushima Daiichi Accident, Non-serial Publications, IAEA, Vienna (2015).

2. ECOSYSTEMS AND PROCESSES

SERGEY FESENKO
Russian Institute of Agricultural Radiology and AgroEcology, RUSSIAN FEDERATION

GERHARD PRÖHL
Consultant, GERMANY

BRENDA J. HOWARD
University of Nottingham, Nottingham, UNITED KINGDOM
UK Centre for Ecology and Hydrology, UNITED KINGDOM

KEIKO TAGAMI
National Institutes for Quantum and Radiological Science and Technology, Chiba, JAPAN

MASASHI KUSAKABE
Marine Ecology Research Institute, Tokyo, JAPAN

YICHI ONDA
University of Tsukuba, Tsukuba, JAPAN

SHOJI HASHIMOTO
Forestry & Forest Products Research Institute, Tsukuba, JAPAN

ANDRA-RADA IURIAN
ALEXANDER ULANOWSKI
International Atomic Energy Agency

2.1.THE NATURAL ENVIRONMENT AROUND THE FDNPP

The Fukushima Daiichi Nuclear Power Plant (FDNPP) is located about 230 km north-east of Tokyo on the Pacific Ocean coast of Honshu, the main island of Japan. Offshore of the FDNPP, the ocean depth increases steadily, reaching some 200 m at 50 km from the coast. The area is located at the junction of two currents of the North Pacific: the Oyashio[1] transporting cold, less saline water southward and the Kuroshio[2] transporting warm, saline waters northwards along the south coast of Japan and then to the East (see Fig. 2.1). Additionally, the Tsugaru Warm Current flows from the Sea of Japan through the Tsugaru Strait between north of Honshu and Hokkaido and then southward along the east coast of Honshu [2.1–2.3].

Fukushima Prefecture is located in the southern part of the Tohoku region, the northern part of the Honshu. The Tohoku region is characterized by mountain ranges running from North to South. Some peaks have an altitude of more than 1500 m. The mountain ranges divide the region into two areas with different climates being influenced by the Sea of Japan and the Pacific Ocean, respectively.

The Abukuma Mountains, located in the Eastern part of the Fukushima Prefecture are gentle hills with an average altitude of about 600 m; the highest peak has an altitude of nearly 1200 m. This mountain range is characterized by small valleys, forests and agricultural fields that are

[1] The Oyashio current that is also known as the Kurile current is a cold subarctic ocean current. It circulates counterclockwise in the western North Pacific Ocean
[2] The Kuroshio is also known as the Japan current is a north-flowing current on the west side of the North Pacific

located in the east, between the Abukuma Mountains and the Pacific Ocean. In the Abukuma River plain, many river tributaries join with the Abukuma River, which runs into the Pacific Ocean. West of the Abukuma Mountains many small lakes are present with Lake Inawashiro being the largest with an area of approximately 100 km^2 (Fig. 2.1).

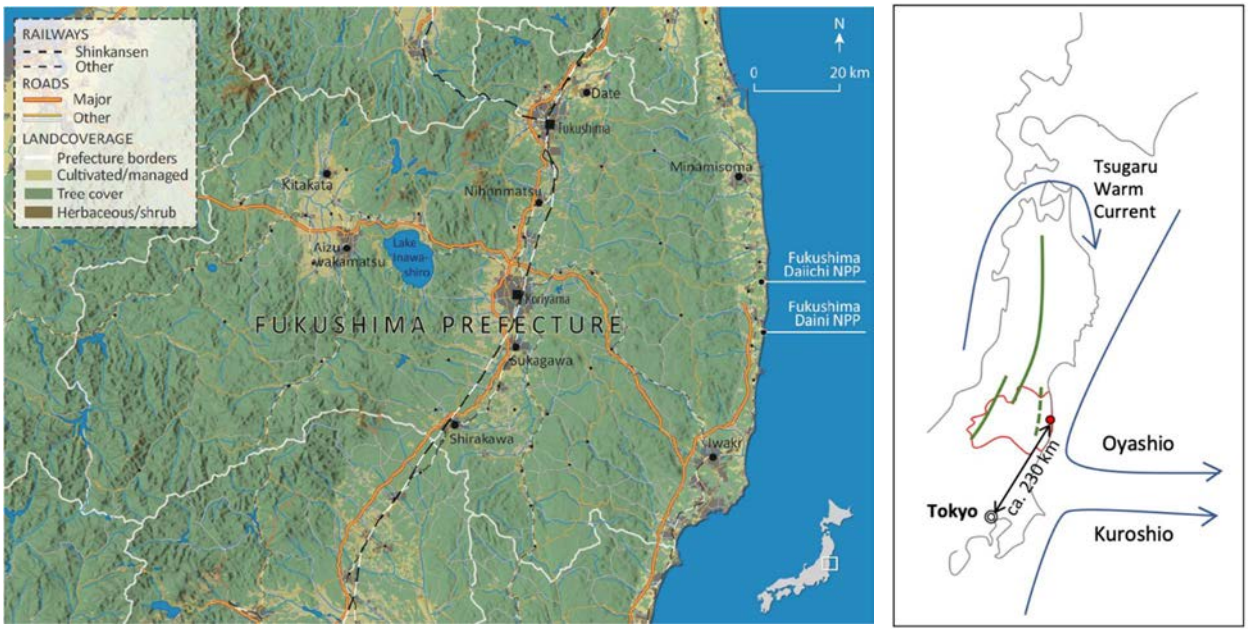

FIG. 2.1. Geographical features of Fukushima Prefecture [2.1].

The western part of Fukushima Prefecture is characterized by warm summers and relatively cold winters with heavy snowfall. In the eastern part, the climate has both inland and Pacific coastal characteristics. Although temperatures occasionally rise to very high values, summers are cooler, and winters are milder than in the western part.

The Tohoku region is characterized by a mixture of paddy fields, farmlands, deciduous forest and evergreen coniferous trees. About 80% of Fukushima Prefecture is covered by mountains, and 70% is covered by forests. Within Fukushima Prefecture, from North to South, the natural vegetation changes from evergreen broadleaf forests to deciduous broadleaf forests.

The forests in the areas affected by the FDNPP accident are mainly located on mountainous catchments with agricultural land confined to the lower slopes and valley floors where there are many paddy fields [2.2].

Fukushima Prefecture is famous for organic farming, producing high quality rice, fruits, soybeans, and buckwheat. The prefecture also produces vegetables (sweet potato, spinach, cucumbers, tomato etc.) and wheat. Processed fruits including the local speciality, Anpogaki (dried persimmon) also generate additional income to the prefecture.

2.2.TRANSFER PROCESSES IN THE ENVIRONMENT

Radionuclides released to the environment are dispersed in different media (air, water, soil and sediment) through various physical and chemical processes. Following accidental releases

affecting large areas, knowledge about the behaviour of radionuclides in the environment is essential to estimate radiological impacts to the population, to assess the further development of radiation levels and activity concentrations in the environment and to explore options for actions that mitigate the consequences. From radionuclides in the environment, exposures to people are potentially caused by the following pathways:

- Inhalation of radionuclides during the passage of the radioactive plume;
- Inhalation of particle-bound radionuclides resuspended from soil;
- External exposure during the passage of the plume;
- External exposure from radionuclides deposited on the ground and surfaces;
- Ingestion of radionuclides with food and drinks following their transfer through food chains.

Radionuclides in environmental media are taken up at different rates by the organisms which live in the respective environments and by people who use the environment or consume foods produced in such areas. Additionally, humans and other organisms are exposed to external gamma and beta radiation from radionuclides in environmental media.

The main transfer processes for radionuclides in the environments and the exposure pathways for humans are shown in Figure 2.2. In this document, the terrestrial environment is defined as a media encompassing the following components: the atmosphere (particularly, the troposphere), soils, sediments and both surface- and ground-waters and the living organisms with which they are associated. The marine environment includes marine waters, aquatic organisms and sediments.

The main components of the environment addressed in this report are:

- The near-surface atmosphere, which comprises the regions above the ocean surface in the marine environment or above the ground or freshwater surfaces in the terrestrial environment, including both the layers above and below the plant canopy;
- The soil that comprises minerals and organic material, water and air. The characteristics of these various components are influenced by the biotic and abiotic conditions in soil;
- Terrestrial plants;
- Freshwater and marine bodies;
- Aquatic organisms;
- Wild and domesticated animals in the terrestrial environment.

The main processes and phenomena associated with the transfer of radionuclides in the environment and resulting exposures to radiation are:

- Interception of deposited radionuclides by vegetation;
- Loss of radionuclides from vegetation due to weathering;
- Transport of radionuclides within plants (translocation);
- Uptake of radionuclides by plants from soil;
- Vertical migration of radionuclides in soil;

- Sorption of radionuclides to soil constituents and the resulting decline of bioavailability;
- Surface run-off of radionuclides in catchment areas;
- Transfer of radionuclides from feed to animal products;
- Sedimentation of radionuclides in terrestrial and marine waters;
- Uptake of radionuclides by aquatic organisms (freshwater and marine);
- Modification of radionuclide activity concentrations in foodstuffs during culinary processing and food preparation.

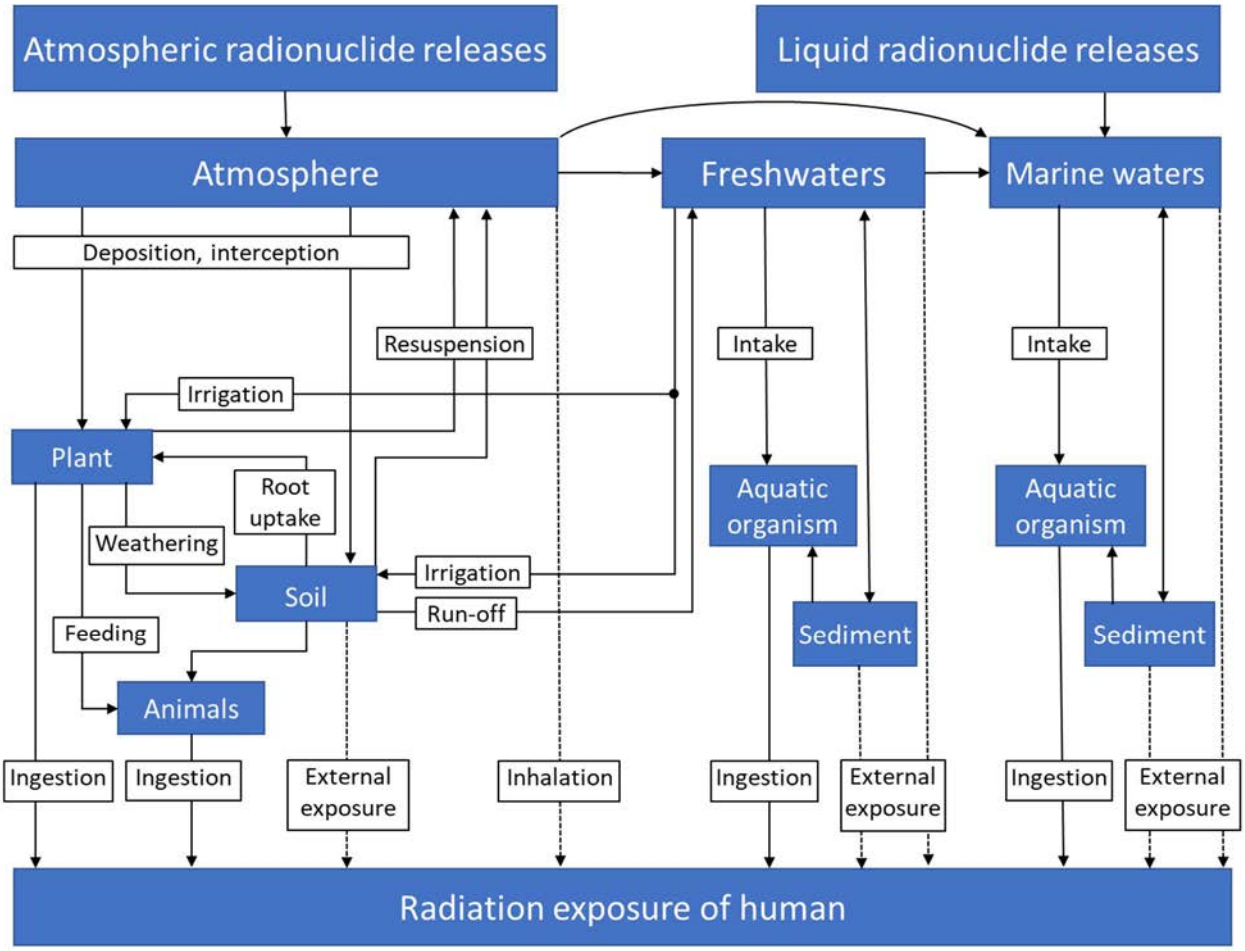

FIG. 2.2. Example of major exposure pathways to humans. The dashed lines show pathways that are not considered in this document.

In the long-term, soil and bottom sediments in the aquatic environment are the most important media for the terrestrial and freshwater environments from which radionuclides can be taken up by agricultural crops and animals as well as wild species.

Terrestrial and freshwater environments are closely connected. Some terrestrial organisms obtain food or drinking water from the aquatic environment and through surface run-off water. Conversely, the terrestrial environment can serve as a source of radionuclides for freshwater

environments. Water from rivers and lakes may be used as irrigation water for agricultural crops.

The freshwater environment includes catchments, streams, rivers, lakes and sediments, whilst the marine environment includes tidal zones, coastal waters and marine sediments. Radionuclides can be taken up from these environmental media by a wide range of organisms such as phytoplankton, zooplankton, invertebrates, sessile aquatic plants, fish, water-based amphibians, crustaceans, mammals and birds that obtain dietary components from the aquatic (freshwater/marine) environment.

People may incorporate radionuclides mainly via inhalation, consumption of drinking water and ingestion of plant and animal food. The intake of foodstuffs depends on individual habits and diets. For example, some people may consume mainly food from the food distribution system, whilst others may prefer locally produced foods.

The uptake of radionuclides by plants and animals in terrestrial, freshwater, estuarine and marine environments is an essential transport process that needs to be quantified for the assessment of radiological impacts. Mathematical models are generally used in assessment studies to simulate the transport of radionuclides to humans.

The transfer of radionuclides from soil to plants depends strongly on soil properties. For the purpose of radiological assessments, a simple soil classification system based on texture and organic matter content was used in the most recent IAEA Handbook of Parameter Values for the Prediction of Radionuclide Transfer in Terrestrial and Freshwater Environments [2.4–2.5]. Four soil groups: “sand”, “loam”, “clay” and “organic soil” were defined for radiological assessments. These classes are mostly based on grain-size distributions with clays typically being ≤ 0.004 mm, sands ≥ 0.06 to 2 mm (gravels are above this) and loams being intermediate. For this scheme, the soils were grouped according to the percentages of sand and clay minerals and the organic matter (OM) content in the soil based on the FAO soil classification [2.6]. For the analysis of the uptake of radionuclides by agricultural crops, the IAEA also introduced a plant classification system based on fourteen plant groups: cereals, maize, rice, leafy vegetables, non-leafy vegetables, leguminous vegetables, root crops, tubers, fruits, grasses (cultivated species), fodder leguminous (cultivated species), pasture (species mixture–natural or cultivated), herbs and other crops [2.4].

In this report, a more detailed species-oriented approach has been adopted, but which also specifies groups of plants according the above classification, where possible. Classification of Japanese soils based on the original Japanese names in respect to the FAO/UNESCO soil classification [2.6] is given in Table I.1, whilst the main soil properties of the basic Japanese soil groups are presented in Table 2.1.

2.3.BASIC TERMS AND DEFINITIONS

The definitions used in this document are mainly adopted from the ICRU Report 65 [2.9] and the IAEA TECDOC-1616 [2.4]. Generic parameters and units used across the whole document are presented in Table 2.2. More specific definitions and adaptations of the general terms to describe actual situations and environmental compartments can be found in the related chapters.

TABLE 2.1. SOIL PROPERTIES OF JAPANESE SOIL GROUPS [2.7–2.8]

Soil types	Bulk density (kg DM/dm^3)		Texture(major)	pH (H_20)	Total carbon (%)
	Standard	Range			
Andosols and Wet andosols	0.65	0.5–0.8	Light clay, Clay Loam, Heavy Clay	5.2–6.8	2.2–9.0
Gleyed andosols	0.6	0.5–0.7	Clay Loam	5.4–6.2	2.6–7.3
Brown forest soils and Gley upland soils	0.8	0.8–0.9	Clay Loam, Light Clay	5.0–7.0	1.0–4.7
Brown lowland soils	0.8	0.7–0.9	Sandy Loam, Clay Loam	5.6–7.0	0.6–3.1
Grey lowland soils	0.9	0.7–1.1	Light Clay, Clay Loam	5.3–6.5	1.2–3.4

TABLE 2.2. QUANTITIES AND UNITS USED IN THE DOCUMENT

Name	Symbol used in:			Definition
	ICRU Report 65	IAEA publications	Current document	
Foliar uptake				
Interception fraction (unitless)	—	α, f	f	The interception fraction is the ratio of the activity initially retained on the plant per unit area (A_i in Bq/m^2) and the total activity deposited on the terrestrial surface (soil plus vegetation) (A_t in Bq/m^2).
Mass interception fraction (m^2/kg)	—	f_B	f_B	The mass interception fraction (f_B) is the interception fraction (f) divided by the standing biomass in kg/m^2, dry mass.
Translocation factor (unitless)	f_{tr}	f_{tr}	f_{tr}	The translocation factor is the ratio of the radionuclide activity concentration (A_m in Bq/kg) in one tissue, typically an edible tissue, divided by the radionuclide activity concentration (A_m in Bq/kg) in another tissue of the same plant or crop
Weathering half-life	T_w	T_w	T_w	The time taken for the quantity of radionuclides on and in plants to be reduced by half due to impact of rain, irrigation, surface abrasion, tissue ageing, leaf fall and other processes.
Resuspension ratio (m^{-1})	K	K_s	K_s	The resuspension ratio is the ratio of the radionuclide activity concentration (A_v in Bq/m^3), measured in air or water to the deposition density (A_α in Bq/m^2) measured on the soil or sediment surface).
Transfer parameters				
Distribution coefficient (L/kg)	K_d	K_d	K_d	K_d is the ratio of the radionuclide activity concentration (Bq/kg) in the solid phase (usually on a dry mass basis) to the radionuclide activity concentration (A_v in Bq/L) in the liquid phase.

TABLE 2.2. QUANTITIES AND UNITS USED IN THE DOCUMENT (cont.)

Name	Symbol used in:			Definition
	ICRU Report 65	IAEA publications	Current document	
Aggregated transfer factor (m^2/kg)	C_{ag}	T_{ag}	T_{ag}	T_{ag} is the radionuclide activity concentration (Bq/kg) in a specified component per unit area activity density, (A_a in Bq/m^2) in the soil.
Normalized activity concentration	—	—	NC	*Nc* is the ratio of radionuclide activity concentration in environmental compartment (Bq/kg) to the total activity intercepted by plants + activity deposited on soil) initial deposition density (Bq/m^2)
Concentration ratio [unitless]	C_r	B_v, F_v, TF	CR	*CR* is the ratio of the activity concentration of radionuclide in the receptor compartment to that in the donor compartment.
Feed transfer coefficient (d/L, d/ kg]	C_{fr}	F_m, F_f	F_m, F_f	Feed transfer coefficient is the radionuclide activity concentration in the receptor tissue or animal product (milk, meat, eggs) (Bq/kg wet mass or Bq/L) divided by the daily radionuclide intake of the animal (Bq/d)
		Food processing		
Food processing factor (unitless)	—	P_f	P_f	The food processing factor is the ratio of the activity concentration of the radionuclide in a given food item when ready for consumption (Bq/kg) to the concentration of the radionuclide in the food before processing and preparation (Bq/kg FM).
Food processing retention factor (unitless)	f_{fp}	F_r	F_r	The food processing retention factor is the fraction of the total activity of a radionuclide in the raw product retained in the food after processing (Bq in processed food per Bq in raw material).
Half-life (s)	$T_{1/2}$	$T, T_{1/2}$	$T, T_{1/2}$	The time taken for the quantity of a specified material (e.g. a radionuclide) in a specified place to decrease by half as a result of any specified *process* or *processes* that follow exponential patterns like *radioactive* decay.

Most of parameters used in this document are originally defined for equilibrium conditions, e.g., the concentration of radionuclides in environmental compartments is assumed to be at steady state with respect to the intake rate. However, this is rarely the case both in laboratory and field conditions. Concentrations of radionuclides in biological or physical compartments, such as biota species or solids in freshwater ecosystems, are continuously subject to slow or fast changes due to changes of radionuclide concentration in the surrounding environment or intake conditions. If such changes are much slower than parameters of the kinetics of radionuclide accumulation in the environmental compartments the status of this process can be regarded as corresponding to a quasi-steady state condition.

Parameters determined from measurements of radionuclide concentrations in compartments that are not in equilibrium are normally called "apparent" [2.5] or "effective" parameters [2.11]. This is especially the case following short-term radionuclide releases to the environment.

Therefore, many of the processes analysed in this report are quantified based on such "apparent" parameters.

The *interception fraction f* (or interception coefficient) is measured immediately after the deposition of radionuclides before processes such as weathering, leaching and loss of biomass cause activity losses from the plant. The interception coefficient depends on the plant surface characteristics, the deposition mode (wet and/or dry deposition), meteorological conditions, the chemical form of the radionuclide, the standing biomass density, leaf area index, species, plant part, and on the stage of development of the plant or tree canopy [2.10]. To take account of some of these factors, the interception fraction can be normalized to the standing biomass B of vegetation (kg/m^2, DM). This quantity is termed the mass interception fraction f_B (m^2 /kg):

$$f_B = \frac{f}{B}. \tag{2.1}$$

Application of this parameter for interception in assessments facilitates estimation of the internal dose from the ingestion of foods [2.5] because the measurement of the standing biomass of the crop is not required.

Radiocaesium intercepted by plants is removed from the plant surfaces by *weathering* processes such as rain wash-off, abrasion and defoliation. Therefore, the amount of radiocaesium in the canopy decreases with time. The loss of radiocaesium from plants surfaces by wash-off can be expressed by single or the double exponential functions. The weathering rate depends on radionuclide solubility, its adsorption by the plant surface and the radionuclide penetration into the inner tissues. The structure of the plant epidermis, senescence and defoliation, and shedding of old epicuticular wax also may affect the weathering rate. Interactions of these factors may explain the differences in weathering half-lives among radionuclides, plant species and their growth stages.

Effective, ecological, biological and physical half-lives describe the reduction of radionuclides in environmental or biological compartments where that reduction can be approximated by a single component loss model:

$$C(t) = C_0 e^{-\frac{\ln 2}{T}t}, \tag{2.2}$$

or a two-component loss model:

$$C(t) = C_0 \left(\alpha\, e^{-\frac{\ln 2}{T_1}t} + (1-\alpha)\, e^{-\frac{\ln 2}{T_2}t} \right), \tag{2.3}$$

where T is the half-life, and T_1 and T_2 are the half-lives corresponding to the fast and slow loss components. Thus, the assumption behind this approach is that the observed reductions follow exponential patterns, similar to radioactive decay.

The application of the half-lives depends on the purpose. In this report, the effective half-life, the ecological half-life or the biological half-life are used to quantify radionuclide reductions in environmental compartments or organism tissues, and to express T, days (d) or years (y) are used instead of seconds. Half-live depends on radionuclide properties, media and compartments considered.

The *physical* half-life $T_{1/2}$ is radionuclide specific, it is used to describe radioactive decay. $T_{1/2}$ is the time required for the activity to decrease, by a radioactive decay process, by a half.

The *effective* half-life T_{eff} is specific to each radionuclide, medium and compartment of interest and is defined as the time required for the radionuclide concentration in the specific compartment to be reduced to half of the initial value as a result of all environmental factors, including radioactive decay:

$$\frac{1}{T_{\text{eff}}} = \sum \frac{1}{T_i}\,, \tag{2.4}$$

where T_i is the half-life for process i.

The *ecological* half-life T_{eco} is the time taken for the activity concentration of a radionuclide in a specified place to halve as a result of all relevant processes, except for radioactive decay:

$$\frac{1}{T_{\text{eco}}} = \frac{1}{T_{\text{eff}}} - \frac{1}{T_{1/2}}\,. \tag{2.5}$$

Some simple illustrations of the relationship among effective half-life, ecological half-life and physical half-life are given in Fig. 2.3.

The *biological* half-life T_b is the time taken for the quantity of a material in a specified tissue, organ or region of the body (for any specified type of biota) to halve as a result of biological removal processes.

The *resuspension ratio* K_s is used to quantify the transfer of radionuclides from the soil surface to the near-surface air. Transfers from sediment to water, from water to air, and from other surfaces (e.g. urban surfaces) to air can all be quantified using this parameter. The processes are highly time-dependent due to episodic events such as strong winds and floods. Radionuclide migration from the surface to deeper soil layers reduces the radionuclide activity that is available for resuspension. It is important to specify the assumed thickness of the compartment, since contamination deeper than a few mm is usually not available for resuspension. In addition to weather and disturbance events, K_s is sensitive to the nature of the surface and to the characteristics of the material being resuspended [2.10]. Temporal fluctuations can be dampened by time-averaging.

The *translocation factor* f_{tr} (or translocation ratio or translocation coefficient) is often used to estimate the radionuclide activity concentration in an unmeasured tissue from another tissue in the same plant which has been measured, often onto which deposition has occurred. The parameter may be used to estimate radionuclide activity concentrations in fruits, seeds, specific edible vegetables or different tree compartments. It depends on the element, and factors such as chemical form, time since deposition, species, growth stage, and nutrition status.

The translocation factor can be calculated in several ways. For instance, as the radionuclide activity concentration in the edible tissue (Bq/kg DM or FM) divided by the activity concentration in another tissue of the same plant or crop. Alternatively, it can be calculated as the radionuclide activity concentration in the edible tissue (Bq/kg, DM or FM) divided by the activity (Bq) contained on the mass of foliage covering a square metre of land surface (Bq/m^2).

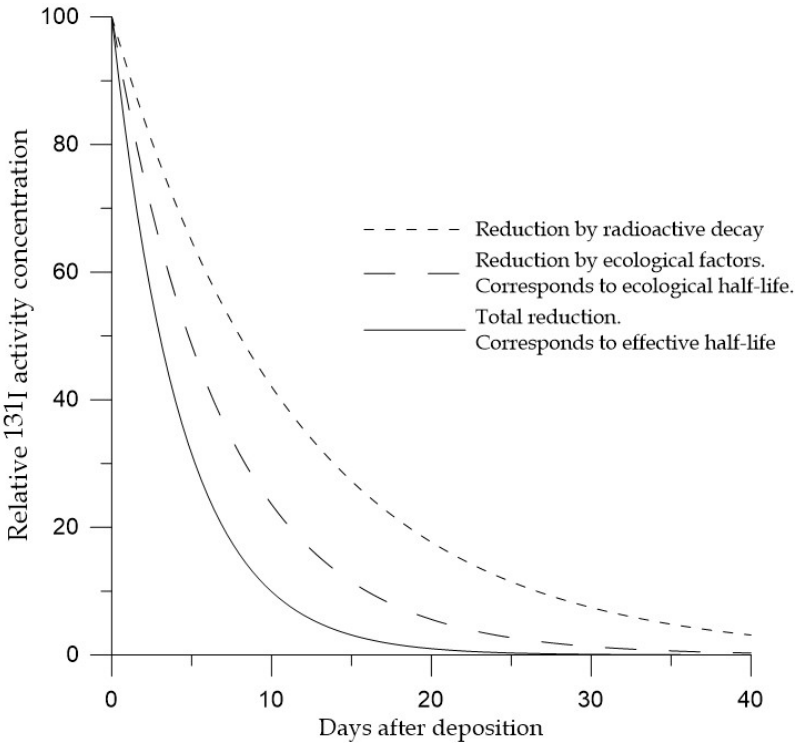

FIG. 2.3. Conceptual example of typical changes in ^{131}I activity conentrations in environmental compartments after single deposition event. The following half-lives are assumed: $T_{1/2}$ = 8.03 d, T_{eco} = 4.8 d, T_{eff} = 3 d.

For needles of coniferous trees that consist of needles mixture with ages from 1 years of 4–5 years old, the translocation factor was defined as follows:

$$f_{tr} = \frac{\text{activity concentration in newly emerged needles}}{\text{activity concentration in old needles}} \left[\frac{\frac{\text{Bq}}{\text{kg DM}}}{\frac{\text{Bq}}{\text{kg DM}}} \right] \qquad (2.6)$$

The *distribution coefficient* K_{d} (L/kg) depends on the radionuclide properties; the properties of solid and liquid media, laboratory or field conditions, attainment of equilibrium; ratio of solid to liquid mass, chemical form of radionuclide etc. The definition of K_{d} theoretically assumes (i) *equilibrium*, i.e. steady-state equilibrium based on totally reversible processes, (ii) sorption is independent of the radionuclide activity concentration in the aqueous phase, and (iii) the concentration of free or unoccupied surface sorption sites is much greater than the concentration of bound radionuclide. In some contamination situations, and especially in aquatic systems, some of these assumptions (or maybe all of them) are not fully achievable. To indicate such situations, the apparent distribution coefficient $K_{d(a)}$ has been used in this document to identify assessments of the distribution coefficients that may not fulfil the above assumptions.

In this document, several options for $K_{d(a)}$ quantification have been used in different chapters depending on the media of interest and the contamination scenario:

- In Chapter 4 (Agricultural systems), K_d is used to describe the radionuclide mobility in soil; it is defined as the ratio of the activity concentration (Bq/kg) in the solid phase (usually on a DM basis) to the activity concentration in (Bq/L) of the liquid phase;

- In Chapter 6 (Catchments and rivers), the K_d is considered as the ratio of the activity concentration of a radionuclide in the solid phase (for either suspended solid or bottom sediment) and the liquid phase (dissolved constituent). Both sediment type definitions are in compliance with that previously used in TRS 472 [2.5], making the data presented here directly comparable with those reported in that document;
- In Chapter 7 (Marine systems), the K_d is defined as the ratio of the ^{137}Cs activity concentrations in bottom sediments (average concentration of the upper 0–3 cm bottom sediment layer) and in water.

The *aggregated transfer factor* T_{ag} (m^2/kg) was originally developed to quantify transfers from soil to plants and animals in natural and semi-natural ecosystems. The T_{ag} does not necessary imply that the soil is the only source of radionuclide transfer to plant or animal tissues. T_{ag} may encompass many transfer processes including root uptake, translocation, soil adhesion, direct soil ingestion, etc. It may have lower variations in the case of transfers from soil because it factors out the effects of the differences in soil bulk density between organic and mineral soils. The aggregated transfer factor depends on the radionuclide, and on the receptor and source compartments, and on the use a wet or dry mass basis for the receptor compartment [2.7]. For some ecosystems, such as forests or fruit plantations, the estimation of the amount of radionuclide in soil is difficult due to the radionuclide interception in the tree canopies, and the subsequent radionuclide transfer from the crowns to the soil. This should also be taken into account for grassland. These processes may continuously modify the radionuclide activity concentrations in the forest soil-litter system; this is especially the case in the short-term after the deposition.

The radionuclide activity in soil is quantified based on the total radionuclide deposition per unit area (Bq/m^2) in soil [2.5]. Two major sources of the information on deposition per unit area that were used in this report for estimating T_{ag} values:

- Direct measurements of radionuclide activity concentrations in soil samples and further assessment of the total radionuclide inventory per unit area;
- Airborne surveys that allows measurements of the deposition of gamma-emitters with some spatial resolution with the aid of gamma-spectrometry.

Ideally, these methods should provide similar data, although they can be different in the short-term after deposition.

Some information derived from the monitoring of radiocaesium in the products was available only at the level of individual municipalities, without indication of sampling points. In such cases, the T_{ag} values were calculated as a ratio of radiocaesium activity concentrations in the product calculated for each municipality, and an average deposition density taken for the same municipality.

The T_{ag} does not necessary imply that the soil is the only source of radionuclide transfer to plant or animal tissues.

Normalized concentrations NC are defined as radionuclide concentrations in specific environmental media (Bq/kg) divided by the *initial* total deposition density (Bq/m^2). In the forest chapter, the *NC* approach is used to quantify time-dependent concentration in litterfall, stemflow and through fall, tree compartments and forest products. The NC values are based on airborne survey data that were performed in the affected areas annually. The concept of NC is

similar to T_{ag}, but NC is normalized to the estimated initial total inventory of radionuclide deposited on the forest ecosystem and not to the inventory in the soil.

The *concentration ratio* CR (dimensionless, kg/kg or L/kg) is used to describe a radionuclide transfer to a variety of different environmental compartments, different species and tissues in different contamination scenarios. For example, the CR values in marine and freshwater species are inherently different from the steady-state pre-accident data and the separate notation CR_a (apparent concentration ratio) has been used to emphasize that after radionuclide release equilibrium will not be achieved instantaneously. It underlines the dynamic nature of the parameter after the accident.

The CR concept has been widely used in this document to quantify *root uptake* of radionuclides from the soil; CR is defined as ratio of radiocaesium activity concentration in plants (Bq/kg, DM) to activity concentration in soil (Bq/kg, DM).

For *radionuclide transfer to animals*, CR is defined as the ratio of the radionuclide activity concentration in animal product (Bq/kg, FM) divided by the mean radionuclide concentration in the animal diet (Bq/kg, DM) under equilibrium conditions. The advantage of the application CR is that daily dietary intake (that is often the main source of uncertainty) is excluded from the assessment; therefore, the variability of the CR values is lower than that of the feed transfer coefficients estimated based on the same data. The application of CR is useful in field studies where the feed intake in most cases cannot be directly measured and is often assumed. However, in many circumstances when the diet is comprised of a number of foodstuffs, the relative proportions of all dietary components will be required to apply CR values in assessments.

For radionuclide transfer to freshwater or marine organisms in the aquatic environment, CR is defined as the ratio of radionuclide activity concentration in organisms (Bq/kg, FM) to that in host water (Bq/kg or L).Organisms living in water intake radionuclides directly from diet and their host water whilst retaining a balance of osmotic pressure between the host water and the body of the organism. Transfer of radionuclides in the aquatic environment occurs to all organisms either directly or indirectly from their host water, so the host water concentration was used to calculate CR rather than their diet.

The CR was also applied to describe the radionuclide distribution between hardwood and sapwood of the woody plants.

The CR depends on the radionuclide, the type of organism, the receptor and source compartments and whether data are reported relative to wet or dry mass of each compartment. Soil-to-plant CR (also commonly termed transfer factor) values are given in this document mainly on a DM basis, for both plants and soil. If the CR values have been expressed relative to FM, the FM/DM conversion factors are given in Tables I.2 and I.3 and can be also found in the IAEA TECDOC-1616 [2.7]. Thus, radionuclide transfers to fresh vegetables and fruits are quantified in this report using both FM and DM bases.

The *feed transfer coefficient* is widely adopted for quantifying transfer to milk F_m, (d/L), meat F_f (d/kg) and other animal products. It depends on the radionuclide, animal species, and animal product (meat, milk, eggs). It also depends on feed type and source of contamination. The tissues or product activity concentration are assumed to be in equilibrium with respect to the daily dietary radionuclide intake [2.5, 2.8].

The *food processing factor* P_f (Bq/kg in processed food per Bq/kg in raw product) considers the reduction of radionuclide activity concentrations in food after preparation, whilst the *food processing retention factor* F_r addressed to the reduction of the total radionuclide activity following a culinary procedure. Examples of food processing and preparation include milling, washing, peeling, pickling, boiling, baking and frying. The methods used to determine the sample masses before and after processing and preparation need to be specified. Both quantities vary according to the radionuclide, the type of food, and the varying conditions of preparation (e.g. temperature, time, etc.). Since the mass of the processed food can differ from that of the raw product, an additional parameter, namely, the *processing efficiency* P_e, which represents the ratio of the wet mass of processed food M_{pf} divided by the mass of original raw material M_{rf} is required to convert the food processing factor to the food processing retention factor:

$$P_e = \frac{M_{\text{pf}}}{M_{\text{rf}}}. \tag{2.7}$$

Thus, F_r can be calculated based on P_f and P_e:

$$F_r = P_f P_e. \tag{2.8}$$

Most of the transfer parameters presented in this document are given on a dry mass basis, for both plants and soil, to reduce uncertainty. In those cases where concentration ratios or radionuclide activity concentrations in environmental samples were reported relative to wet mass, the wet mass/dry mass conversion factors given in Tables I.2 and I.3 were applied.

REFERENCES

[2.1] INTERNATIONAL ATOMIC ENERGY AGENCY, The FDNPP accident, Technical Volume 4, Radiological Consequences, IAEA, Vienna (2015).

[2.2] INTERNATIONAL ATOMIC ENERGY AGENCY, The FDNPP accident, Technical Volume 5, Post-accident Recovery, IAEA, Vienna (2015).

[2.3] UNITED NATIONS, Sources, Effects and Risks of Ionizing Radiation (Report to the General Assembly), UNSCEAR 2013 Report, Vol. I, Scientific Annex A: Levels and Effects of Radiation Exposure Due to the Nuclear Accident after the 2011 Great East-Japan Earthquake and Tsunami, Scientific Committee on the Effects of Atomic Radiation (UNSCEAR), UN, New York (2014).

[2.4] INTERNATIONAL ATOMIC ENERGY AGENCY, Quantification of Radionuclide Transfers in Terrestrial and Freshwater Environments for Radiological Assessments, IAEA-TECDOC-1616, IAEA, Vienna (2009).

[2.5] INTERNATIONAL ATOMIC ENERGY AGENCY, Handbook of Parameter Values for the Prediction of Radionuclide Transfer in Terrestrial and Freshwater Environments, Technical Reports Series No. 472, IAEA, Vienna (2010).

[2.6] FOOD AND AGRICULTURE ORGANISATION, UNITED NATIONS EDUCATIONAL, SCIENTIFIC AND CULTURAL ORGANIZATION, Soil map of the world 1: 5 000 000. UNESCO, Paris (1994).

[2.7] MINISTRY OF AGRICULTURE FORESTRY AND FISHERIES, Basic Data for Soil. http://www.maff.go.jp/j/seisan/kankyo/hozen_type/h_sehi_kizyun/pdf/ntuti4.pdf (in Japanese)

[2.8] NATIONAL AGRICULTURE AND FOOD RESEARCH ORGANIZATION (NARO); Japanese Soil Inventory, https://soil-inventory.dc.affrc.go.jp/explain.html

[2.9] INTERNATIONAL COMMISSION ON RADIATION UNITS AND MEASUREMENTS, ICRU Report 65. Quantities, Units and Terms in Radioecology, Journal of the ICRU (2001).

[2.10] INTERNATIONAL ATOMIC ENERGY AGENCY, Modelling of resuspension, seasonality and losses during food processing, Report of the Terrestrial Working group. IAEA-TECDOC-647, ISSN 1011-4289, IAEA, Vienna (1992).

[2.11] MINISTRY OF EDUCATION, CULTURE, SPORTS, SCIENCE AND TECHNOLOGY, JAPAN, Standard Tables of Food Composition in Japan – 2015 – (Seventh Revised Edition), http://www.mext.go.jp/en/policy/science_technology/policy/title01/detail01/1374030.htm

[2.12] ISAKARI, K., Calcium contents in certain foods (Part 9), Journal of Home Economics of Japan **21** (1970) 301 (in Japanese).

[2.13] ITABASHI, M. TAKAMURA, N., Nutritional compositions of the leaves of Fuki (*Petasites japonicus* Miq.), Tsuwabuki (*Ligulariatussilaginea* Makino), Gobo (*Arctiumlappa* L.) and Gishigishi (*Rumex japonicus* Houttuyn), Nippon Shokuhin Kogyo Gakkaishi **32** (1985) 120 (in Japanese).

[2.14] IZUMI, M. SAITO, Y., Vitamin C content in the edible portion of wild plant,Journal of Home Economics of Japan **33** (1982) 158 (in Japanese).

[2.15] KIYONO, Y., AKAMA, A., IWAYA, M., YOSHIDA, Y. The transfer of radiocesium released in the 2011 Fukushima Daiichi Nuclear Power Station Accident to petioles of wild butterbur (*Petasites Japonicus*), Bulletin of the Forestry and Forest Products Research Institute **17** (2018) 249.

[2.16] KIYONO, Y., KOMATSU, M., AKAMA, A., MATSUURA, T., ET AL., The transfer of radiocesium released in the 2011 Fukushima Daiichi Nuclear Power Station Accident to leaves of wild *Osmunda japonica*, an edible fern, Bulletin of the Forestry and Forest Products Research Institute **17** (2018) 217 (in Japanese with English abstract).

[2.17] ONO, M., HAYASHI, M., ABE, M., The Composition of Some Wild Plants, Journal of Home Economics of Japan **28** (1977) 76 (In Japanese).

[2.18] SAITO, Y., IZUMI, M., Amount of mineral elements in edible wild plants, Journal of Home Economics of Japan **36** (1985) 351 (In Japanese).

[2.19] SAITO, Y., IZUMI, M., OHSAWA, A. Amounts of dietary fiber and the other general components in edible portion of wild plants, Journal of Japanese Society of Food and Nutrition **34** (1981) 468 (in Japanese).

[2.20] SHISHIDO, I., KODAMA, E. Nutritional ingredients of wild vegetables of the Akita district (1), Report of the Akita Prefecture Institute of Public Health **10** (1966) 55 (in Japanese).

[2.21] SHISHIDO, I., KODAMA, E., Nutritional ingredients of wild vegetables of the Akita district (3), Report of the Akita Prefecture Institute of Public Health **12** (1968) 202 (in Japanese).

[2.22] SHISHIDO, I., KODAMA, E., Nutritional ingredients of wild vegetables of the Akita district (4), Report of the Akita Prefecture Institute of Public Health **13** (1969) 239 (in Japanese).

[2.23] SHISHIDO, I., KODAMA, E., Nutritional ingredients of wild vegetables of the Akita district (5), Report of the Akita Prefecture Institute of Public Health **14** (1970) 173 (in Japanese).

[2.24] SHISHIDO, I., KODAMA, E., Nutritional ingredients of wild vegetables of the Akita district (6), Report of the Akita Prefecture Institute of Public Health **15** (1971) 297 (in Japanese).

[2.25] TAGAMI, K., UCHIDA S., Distribution and food processing effect of radiocaesium in fertile shoots of field horsetail (*Equisetum arvense*): comparison of direct deposition and root uptake results after the Fukushima Daiichi Nuclear Power Plant Accident. Radioisotopes **61** (2012) 511 (in Japanese).

[2.26] TAGAMI, K., UCHIDA, S., Comparison of food processing retention factors of ^{137}Cs and ^{40}K in vegetables. Journal of Radioanalytical Nuclear Chemistry **295** 3 (2013) 1627.

3. THE FUKUSHIMA DAIICHI NUCLEAR POWER PLANT ACCIDENT

GERHARD PRÖHL
Consultant, GERMANY

SERGEY FESENKO
Russian Institute of Agricultural Radiology and AgroEcology, RUSSIAN FEDERATION

This chapter provides a short summary of the dispersion of radionuclides in the environment following the accident in the Fukushima Daiichi Nuclear Power Plant (FDNPP). A detailed description and analysis of the accident is given in [3.1] and [3.2].

3.1. INITIAL RELEASES OF RADIONUCLIDES IN THE ATMOSPHERE AND COUNTERMEASURES

3.1.1. Radioactive releases in the atmosphere and deposition in the terrestrial environment

The tsunami following the Great Eastern Earthquake on 11 March 2011 caused an accident at the Fukushima Daiichi Nuclear Power Plant (FDNPP). Consequently, radionuclides were released into the terrestrial and aquatic environment.

Releases into the atmosphere continued over several weeks. A wide spectrum of radionuclides was released, most of them with half-lives of hours to days; examples are ^{133}Xe (5.2 d), ^{136}Cs (13.6 d), ^{132}Te (3.26 d), ^{132}I (2.3 h) and ^{133}I (20.8h). Strontium and plutonium isotopes were also released, however, in most of the evacuated areas, the amounts deposited could hardly be distinguished from the strontium and plutonium that had previously been deposited following the testing of nuclear weapons in the atmosphere in the 1950s and 1960s [3.2]. Due to the prevailing westerly winds that occurred after the accident, most of the radionuclides were dispersed over the Pacific Ocean. However, the releases on 12, 14 and 15 March and around 20–23 March caused depositions of ^{131}I, ^{134}Cs and ^{137}Cs and other radionuclides on inhabited areas, agricultural land, forests, rivers and lakes. The deposition patterns in these areas varied considerably due to the varying release rates of the different radionuclides with time, combined with changes in wind direction, heterogeneous precipitation, the physical and chemical form of the radionuclide and the topography of the affected area [3.2, 3.3].

The deposition of radionuclides on the ground and water bodies is influenced by many factors including the land use (largely forest, agricultural land, and inhabited areas), the stage of development of trees and other vegetation and the amount of precipitation that occurred during the passage of the radioactive plumes. Most deposition occurred in Fukushima Prefecture, but the Iwate, Miyagi, Ibaraki, Tochigi, Gunma and Chiba prefectures were also affected. Initially, the most important radionuclides regarding the resulting exposure to people [3.2], were ^{134}Cs (2.1 a), ^{137}Cs (30.1 a), ^{131}I (8.05 d), and ^{129m}Te (33.6 d); in the long-term only ^{134}Cs and ^{137}Cs are relevant in determining doses to people.

Immediately after the onset of the accident, emergency protective actions for the public were implemented including evacuation, sheltering, application of stable iodine for blocking the further uptake of radioiodine by the thyroid, restrictions on the consumption of food and drinking water, and relocation. The evacuation of the 20 km-zone around the FDNPP started on 11 March 2011 and was completed a day later. In the area within a 20-30 km radius, the population was ordered to stay indoors, then voluntary evacuation was recommended. Because

in some locations, the criteria for relocation were exceeded beyond 30 km from the reactor, voluntary evacuation was also recommended in those areas.

Subsequently, a comprehensive monitoring programme was initiated including measurements of ambient dose rates and of radionuclide activity concentrations in soil, crops, food and feed for animals. Where necessary, protective actions were implemented in the agricultural areas and restrictions were placed on the consumption and distribution of food and on the consumption of drinking water.

The highest ^{137}Cs and ^{134}Cs depositions occurred north-west of the FDNPP. Figure 3.1 shows a map of ^{137}Cs deposition density (decay corrected to 14 June 2011), which is based on measurements of soil samples. The highest value of 15.5 MBq/m^2 ^{137}Cs was recorded just north of the FDNPP. The ^{134}Cs/^{137}Cs ratio of the deposit — determined for March 2011 — was approximately 1 [3.3]. The activity per unit area decreases with time due to physical decay; since ^{134}Cs decays much faster than ^{137}Cs, the ^{134}Cs/^{137}Cs ratio will drop to 0.04 by March 2021.

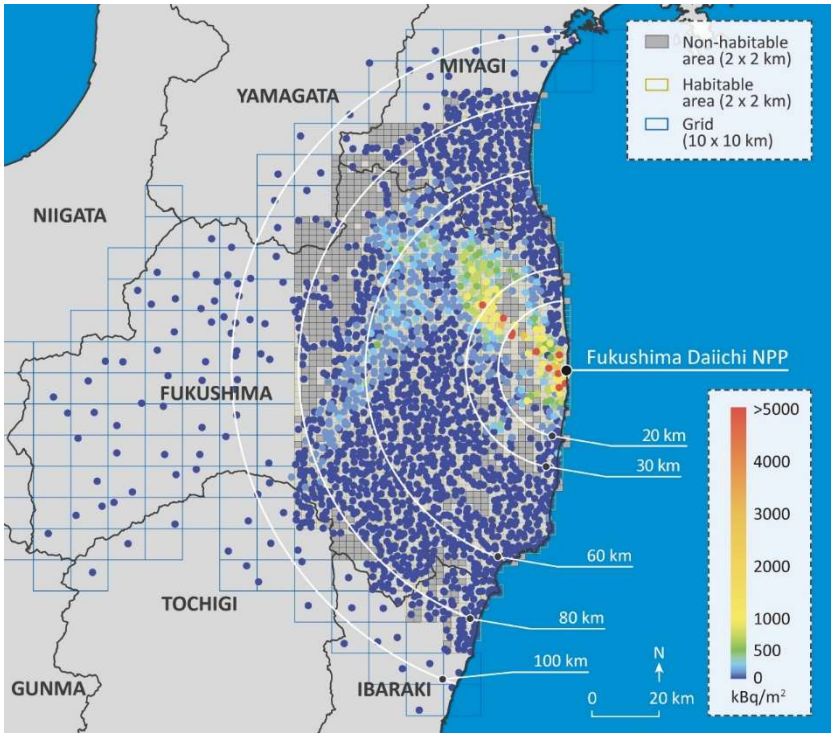

FIG. 3.1. Deposition density of ^{137}Cs based on soil sampling, decay corrected to 14 June 2011 [3.2].

Radiocaesium activity concentrations in soil exceeded 1000 Bq/kg DM in the eastern part and in a narrow area in the central part of Fukushima Prefecture, and in some of the northern part of Tochigi Prefecture. Rice cultivation was restricted for areas with radiocaesium activity concentrations higher than 5000 Bq/kg DM. Such relatively high activity concentrations were not detected outside the evacuated areas ([3.2]).

Direct deposition of ^{131}I, ^{134}Cs and ^{137}Cs onto the crops was measured for a few types of leafy vegetables and evergreen fruits and relatively high activity concentrations of radioiodine and radiocaesium were found in vegetables. However, the releases occurred before the beginning of the growing periods of most crops in Fukushima Prefecture. Agricultural animals, including

dairy cows, were housed and being fed with stored feed. Therefore, rice and many other crops and animal products were not affected by direct contamination of leaves, and the long-term uptake of radiocaesium from soil was the dominant contamination route. In southern prefectures, vegetation was further developed, but the deposition in these regions was relatively low and close to, or below, the detection limit in many areas.

About 70% of the Fukushima Prefecture is covered by forest, which was also affected by direct deposition of radionuclides. The initial retention of radionuclide deposits by trees was relatively high for evergreen coniferous forests. In March 2011, the leaves of deciduous trees were not emerged; therefore, compared to coniferous forest, a higher fraction of radionuclides was deposited directly onto the forest soil. Some wild animals, plants, and mushrooms in forests were relatively highly contaminated with ^{134}Cs and ^{137}Cs compared with agricultural crops. Further details can be found in [3.2].

Based on the additional annual effective dose estimated in autumn of 2011, the contaminated areas were arranged into two zones, as shown in Fig 3.2. “The Special Decontamination Area (SDA)” includes the areas where evacuation was ordered or recommended. The Intensive Contamination Survey Area (ICSA) includes those municipalities where the additional annual effective dose in the first year was estimated to be between 1 and 20 mSv for individuals in some parts of the municipality. According to the model used at that time, a γ-dose rate of 0.23 μSv/h corresponded to an effective dose of 1 mSv in one year [3.4]. In these municipalities monitoring surveys were conducted to identify areas requiring decontamination and remediation measures [3.5].

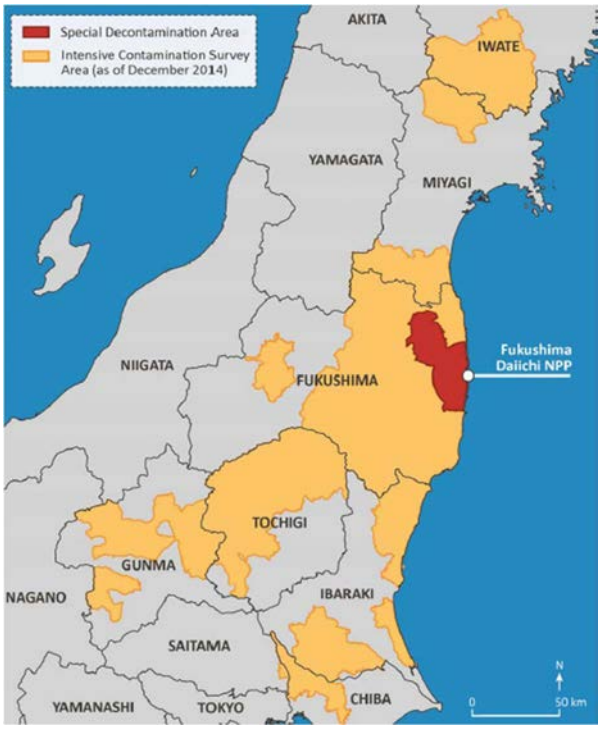

FIG. 3.2. Zones in the vicinity of the FDNPP: The Special Decontamination Area (shaded red) and the Intensive Contamination Survey Area (shaded orange) [3.2].

3.1.2. Initial countermeasures and remediation in the terrestrial environment

After the accident, limits for radionuclide activity concentrations in food were applied and a food surveillance programme was implemented. Therefore, long-term exposures of the population were dominated by external exposure from radionuclides deposited on the ground, while the exposures due to ingestion of radioactively contaminated food was of minor importance.

In 2011, remedial activities were initiated and took several years in the ICSA. The programme focused on the reduction of external exposure to people but measures to reduce activity concentrations in crops and animals were also implemented. The remediation work included (see [3.6, 3.7]):

- **Houses:** removal of deposits from the roof, gutters and any decking, wiping roofs and walls, vacuum sanding, high pressure washing;
- **Gardens, parks, school yards:** removal of topsoil and grass;
- **Roads:** high pressure washing and cleaning of ditches
- **Gardens and trees:** removal of topsoil and fallen leaves, mowing, high pressure washing, removal thin layers of surfaces in inhabited areas;
- **Farmland:** removal of weed grass and topsoil, enhanced application of potassium fertilizer, ploughing/deep ploughing;
- **Animal husbandry:** monitoring of animal feed and live animals;
- **Forests:** removal of fallen leaves and lower twigs and pruning on forest boundaries.

Decontamination of surfaces was carried out following a standard procedure which included several different remediation measures. Soil removal was mainly applied in private gardens to reduce external exposures which also caused a reduction of radionuclide activity concentrations in garden vegetables. Remediation activities for farmland were implemented on a case by case basis, depending on the radiocaesium activity concentrations in soil and the farmer's preference. Decontamination of forests was, in general, limited to the outer borders of woodland in the vicinity of residential and frequently visited agricultural areas to reduce external exposure in adjacent houses.

3.2. RADIONUCLIDES IN FRESHWATERS

The accidental releases and deposition of radionuclides also affected the freshwater systems in the north-west of the Fukushima Prefecture, which is a mountainous area covered by forests, with many rivers and lakes. Intensive monitoring of radionuclides in rivers and lakes was conducted to determine activity concentrations in water and sediments. Figure 3.3 shows a map of this area indicating the catchments of the river systems. For selected monitoring points, ^{137}Cs activity concentration in water is given as measured in August 2012; at that time ^{137}Cs-activity concentrations were (with one exception) below 1 Bq/L. At some locations, activity concentrations of strontium (^{89}Sr and ^{90}Sr) and plutonium (^{238}Pu and ^{239,240}Pu) were also measured and found well below 0.1 Bq/L, which is similar to previous background values measured before the FDNPP accident [3.2].

Radionuclides deposited on catchment areas are subject to surface run-off processes, which transport radiocaesium with the river water largely to the Pacific Ocean. The run-off is influenced by a complex interaction of physical-chemical properties of the deposited radionuclides, the area's topography, the land-use, and the vegetation cover. The run-off of radionuclides is a slow, long-term process which is still ongoing. During the passage of typhoons, the loss of radiocaesium from the catchment may temporarily be enhanced.

In freshwater systems, the highest radiocaesium activity concentrations occurred in bottom sediments due to the strong sorption of caesium to fine particles. However, their contribution to the γ-dose rate in the surrounding environment is negligible due to the shielding effect of water. Therefore, sediments were only removed in selected cases, when the riverbanks or the lake shore were used for leisure activities. Contaminated sediments were also removed from ponds used for the irrigation of rice. High radiocaesium activity concentrations in some freshwater fish from rivers and lakes were observed; restrictions on fishing were put into force, where radiocaesium activity concentrations were above the permissible limit.

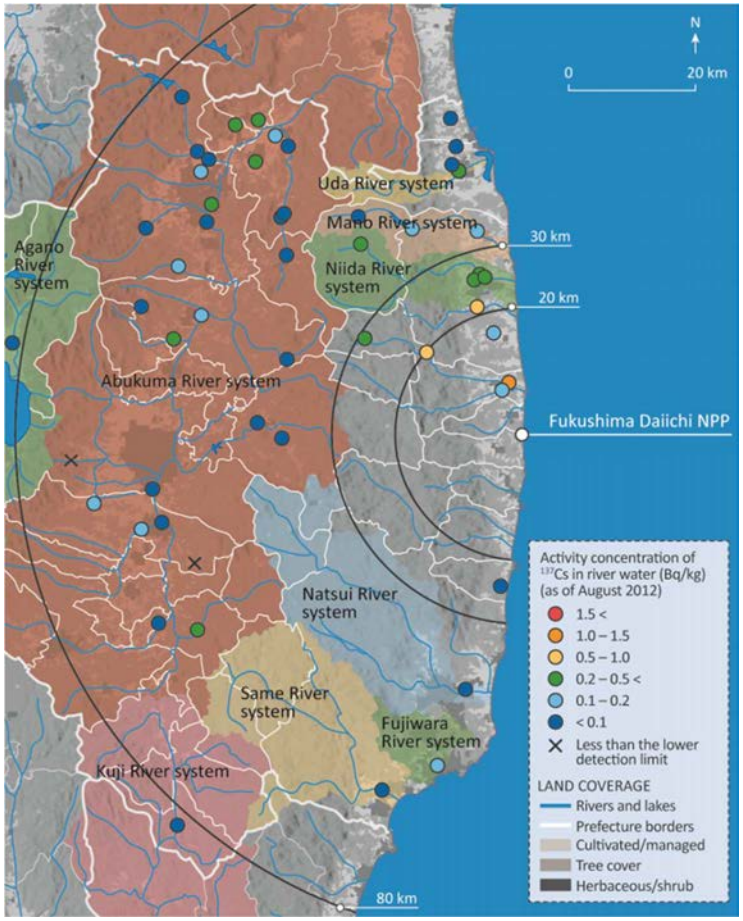

FIG. 3.3. Map of the river catchments affected by deposition of radionuclides in the north-west of the FDNPP (after [3.2]). The different colours represent different catchments, bold white lines represent prefecture borders, other white lines represent borders of municipalities.

3.3. RADIONUCLIDES IN THE MARINE ENVIRONMENT

3.3.1. Deposition and releases into the Pacific Ocean

Radionuclides have been introduced to the Pacific Ocean via two pathways: (a) initial releases of radionuclides to the atmosphere followed by their subsequent deposition from the atmosphere to the ground and the seawater surface, and (b) the direct liquid releases from the FDNPP. The following contamination routes played a significant role [3.2]:

- Deposition of radionuclides released to the atmosphere onto the ocean surface (March 2011);
- Unintended release of water containing high levels of radionuclides (early April 2011);
- Planned discharge of water from storage tanks containing low levels of radionuclides (early April 2011);
- Unintended release of water with moderate levels of radionuclides (May 2011);
- Inflow of groundwater to the Ocean that was contaminated due to contact with reactor the reactor or the reactor components (May 2011–present);
- Run-off of radionuclides deposited onto catchments due to processes such as precipitation, erosion, floods and tides (ongoing).

Atmospheric deposition on the ocean and the direct release of highly radioactive water from a pit adjacent to Unit 2 of the reactor were the most important sources [3.2]. Large amounts of seawater injected to cool the reactors and the structural damage of some of the pressurized containment vessels led to the main direct releases of radionuclides to the ocean. More details on the radionuclide discharges to the Pacific Ocean are provided in [3.2].

3.3.2. Dispersion of radionuclides in the marine environment

The FDNPP is located in a region of confluence of two wind-driven western boundary currents of the North Pacific: the Kuroshio, which transports warm, saline seawater northwards along the south coast of Japan and then eastward, and the Oyashio, which transports cold, less saline seawater southwards [3.8].

The dispersion of radionuclides in the ocean depends on the movement of the ocean currents, the mixing of surface waters with deep seawaters, the sedimentation of radionuclides to the sea bottom and the topography of the ocean floor. Dispersion in the shallow shelf seawaters is primarily driven by winds, tides and freshwater inputs.

Marine monitoring began on 21 March 2011. Figure 3.4 presents results of the seawater monitoring for ^{137}Cs for several monitoring points close to the Fukushima Daiichi and Daini NPPs and at distance 30 km of the shore. The results cover the period from 21 March to 31 July 2011. The highest values in the marine environment were observed from the end of March to the beginning of April 2011.

The highest activity concentrations shown in Fig. 3.4 were located in a small area at the release point to the seawater and rapidly declined in the first few weeks. The ^{137}Cs activity concentrations in surface waters continued to decrease in the following years.

Sea monitoring programmes were established following the accident and comprising collection and measurement of seawater, sediment and marine biota, and fish [3.9]. Measurements were made of seawater close to the FDNPP and intensive monitoring of fish was performed. In many cases, radiocaesium activity concentrations in fish and seafood greatly exceeded the permissible limit of 100 Bq/kg FM. The highest reported value for radiocaesium in fish outside the 20 km radius exclusion zone in the period March 2011 to March 2012 was 14 400 Bq/kg FM. In the subsequent year, the highest radiocaesium value in fish was 3300 Bq/kg FM. Since the FDNPP accident all fishing has been suspended in the area adjacent to the shore of Fukushima Prefecture. Meanwhile, beyond 30 km from the FDNPP, ^{137}Cs activity concentrations in seawater have returned to pre-accident levels.

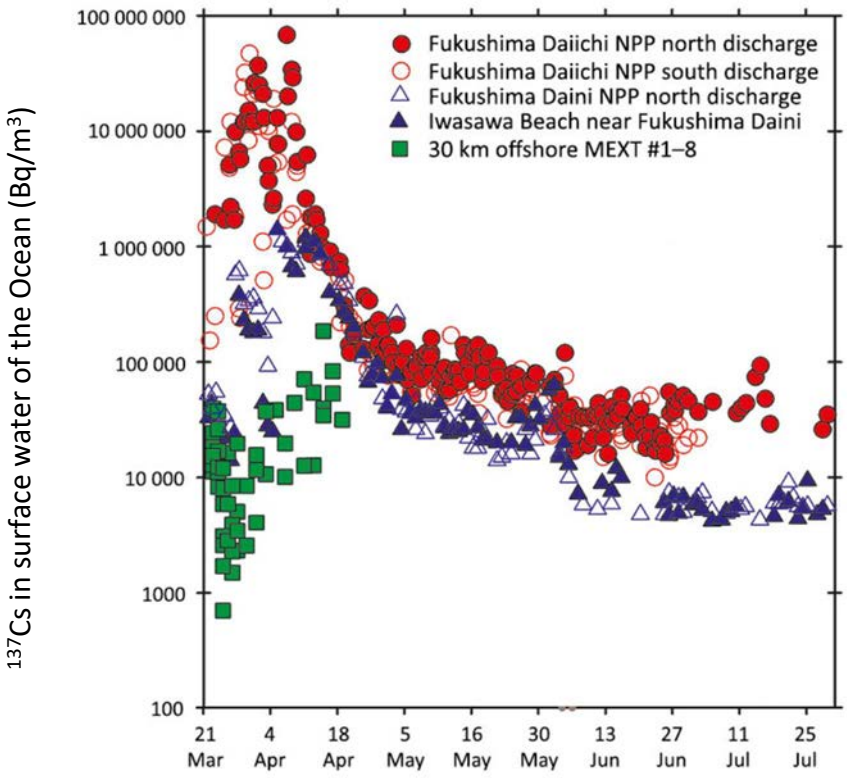

FIG. 3.4. Activity concentration of ^{137}Cs in surface ocean seawater (Bq/m^3) from 21 March to 31 July 2011 for two sites near the Fukushima Daiichi NPP, Fukushima Daini NPP, Iwasawa Beach near the Fukushima Daini NPP and 30 km offshore. Pre-accident ^{137}Cs activity concentrations in seawater are a few Bq/m³ and not shown (adapted from [3.2]).

3.4. SUMMARY OF CHAPTER 3

- The releases of radionuclides during the accident at the Fukushima Daiichi Nuclear Power Plant affected the terrestrial, freshwater and marine environments;
- A wide range of radionuclides were released, most of them with half-lives of hours, days and weeks. Among them, only radiocaesium was significant, as a long-term potential source of exposure to humans in the environment;
- Following deposition, a rapid decline of radionuclide activity concentrations in the environment and ambient equivalent dose rates was observed due to physical decay and natural attenuation processes;
- Low permissible limits for radiocaesium in food, food restrictions and strict food monitoring were very effective in limiting exposures to people due to intakes of food;
- External exposure from radionuclides deposited on the ground is the most important exposure pathway for people;
- Comprehensive countermeasures were implemented in 2011 and remediation during the following years focused on the reduction of radiocaesium activity concentrations and related ambient equivalent dose rates in residential areas and in areas used for leisure purposes (e.g. riverbanks) or irrigation (lakes);
- The behaviour of radiocaesium in the environment and the resulting exposures to people is the result of a complex interaction of a wide range of factors such as deposition

density, time of the year, soil type, topography, land use, agricultural practice, and living habits;

- Detailed investigations were initiated in Japan to study the behaviour of radiocaesium under the specific environmental conditions in the affected areas. These efforts were also intended to explore whether the observations made were consistent with the global experience available regarding the behaviour of radiocaesium or were specific for Fukushima Prefecture;

REFERENCES

[3.1] UNITED NATIONS SCIENTIFIC COMMITTEE ON THE EFFECTS OF ATOMIC RADIATION (UNSCEAR), Sources, Effects and Risks of Ionizing Radiation, UNSCEAR 2013 Report to the General Assembly with Scientific Annexes; VOLUME I Scientific Annex A: Levels and Effects of Radiation Exposure Due to the Nuclear Accident after the 2011 Great East-Japan Earthquake and Tsunami, New York (2014).

[3.2] INTERNATIONAL ATOMIC ENERGY AGENCY, The Fukushima Daiichi Accident Technical Volume 4/5 Radiological Consequences, IAEA, Vienna (2015).

[3.3] INTERNATIONAL ATOMIC ENERGY AGENCY, The Fukushima Daiichi Accident Technical Volume 1/5 Description and Context of the Accident, IAEA, Vienna (2015).

[3.4] INTERNATIONAL ATOMIC ENERGY AGENCY, The Fukushima Daiichi Accident Technical Volume 4/5 Radiological Consequences, IAEA, Vienna (2015).

[3.5] SAITO, K. et al., Summary of temporal changes in air dose rates and radionuclide deposition densities in the 80 km zone over five years after the Fukushima Nuclear Power Plant accident, Spec. Issue Five Years Fukushima **210** (2019) 105878.

[3.6] INTERNATIONAL ATOMIC ENERGY AGENCY, The Fukushima Daiichi Accident Technical Volume 3/5 Emergency Preparedness and Response, IAEA, Vienna (2015).

[3.7] INTERNATIONAL ATOMIC ENERGY AGENCY, The Fukushima Daiichi Accident Technical Volume 5/5 Post-Accident Recovery, IAEA, Vienna (2015).

[3.8] YASUDA, I., Hydrographic Structure and Variability in the Kuroshio-Oyashio Transition Area, J. Oceanogr. **59** 4 (2003) 389.

[3.9] NUCLEAR REGULATION AUTHORITY (NRA), Implementation Guides on Sea Area Monitoring in FY2013, (2013).

4. AGRICULTURAL SYSTEMS

KEIKO TAGAMI
National Institute of Radiological Sciences, National Institutes for Quantum and Radiological Science and Technology, JAPAN

MAMORU SATO
Faculty of Agriculture, Fukushima University, JAPAN

TAKURO SHINANO
Laboratory of Plant Nutrition, Research Faculty of Agriculture, Hokkaido University, JAPAN

HIROFUMI TSUKADA
Institute of Environmental Radioactivity (IER), Fukushima University, JAPAN

SHINICHIRO UEMATSU
University of Tsukuba, JAPAN

SADAO EGUCHI
Institute for Agro-Environmental Sciences, National Agriculture and Food Research Organization, JAPAN

SHIGEO UCHIDA
National Institute of Radiological Sciences, National Institutes for Quantum and Radiological Science and Technology, JAPAN

NORIKO YAMAGUCHI
Institute for Agro-Environmental Sciences, National Agriculture and Food Research Organization, JAPAN

FRANCA CARINI
Università Cattolica del Sacro Cuore, ITALY

MIQUEL VIDAL
Universitat de Barcelona, SPAIN

DAISUKE TAKATA
Faculty of Agriculture, Fukushima University, JAPAN

SHIGETO FUJIMURA
Agricultural Radiation Research Centre, Tohoku Agricultural Research Centre, National Agriculture and Food Research Organization, JAPAN

TAKASHI SAITO
Hama Agricultural Regeneration Research Centre, Fukushima Agricultural Technology Centre, JAPAN

NOBUYOSHI ISHII
National Institute of Radiological Sciences, National Institutes for Quantum and Radiological Science and Technology, JAPAN

HISAYA MATSUNAMI
Agricultural Radiation Research Centre, Tohoku Agricultural Research Centre, National Agriculture and Food Research Organization, JAPAN

YUICHI ONDA
University of Tsukuba, JAPAN

YONG-HO CHOI
Korea Atomic Energy Research Institute (KAERI), KOREA

NICK BERESFORD
UK Centre for Ecology and Hydrology, UNITED KINGDOM

SERGEY FESENKO
Russian Institute of Agricultural Radiology and AgroEcology, RUSSIAN FEDERATION

GERHARD PRÖHL
Consultant, GERMANY

BRENDA J. HOWARD
University of Nottingham, UNITED KINGDOM
UK Centre for Ecology and Hydrology, UNITED KINGDOM

JOANNE BROWN
International Atomic Energy Agency

This chapter provides a synthesis of data on the transfer of radiocaesium to agricultural crops and farm animals in Japan after the FDNPP accident. The main processes for radiocaesium transfer to crops are discussed and the available data for Japan are presented and compared with data from before the FDNPP accident, where possible. The processes considered include interception, weathering, translocation, uptake from soil to crops, and transfers from crops to farm animals.

Some general concepts and methodologies that are relevant for the transfer of all radionuclides to food crops are described in Sections 4.1 (mass interception and weathering) and 4.2 (soil).

For three important crops in Japan, rice, fruit and tea, separate sections are provided that present and discuss transfer parameter data collected after the FDNPP accident. Data for other crops are compiled in an additional section. Effective half-lives for the different types of crops are also included in each section. Key processes that affect the extent of transfer of radiocaesium are described.

4.1. INTERCEPTION AND WEATHERING

4.1.1. Mass interception of Fukushima fallout radionuclides by edible parts of herbaceous plants

Radionuclides released from the FDNPP accident were deposited onto many agricultural areas of Eastern Japan resulting in contamination of crops with radiocaesium and radioiodine. Fresh green vegetables need to be harvested when they are still tender to ensure that they are suitable for consumption in salads or for preservation by processes such as pickling. Following the deposition of radionuclides onto green vegetables, the initial radionuclide activity concentration of the vegetables is described by the interception factor, which quantifies the amounts of deposited radionuclides retained by the edible parts of the plant. Therefore, the interception factor is a key quantity needed for estimating the exposure arising from ingestion of recently contaminated fresh vegetables. Estimation of the time-dependence of radionuclide activity concentrations in green vegetables in the emergency response phase and the transition phase greatly assists the management of such crops. In combination with data from radionuclide monitoring of agricultural plants, it facilitates an optimized implementation of countermeasures and further implementation of remedial options. Retention goes beyond the discussion in this section and it is partially discussed for fruit in sub-section 4.3.3.

Interception of radionuclides by vegetation depends on the vegetation density, the contributions of dry and wet deposition to the total deposition, the chemical properties of the radionuclide and the amount of rainfall (if wet deposition contributes to the total deposition) [4.1]. In this section, mass interception data determined after the FDNPP accident are summarized and compared with those previously reported in international literature.

4.1.2. Approach used to estimate interception

To calculate the interception fraction following a deposition event, data are needed on the standing biomass (kg/m^2 DM) for converting the radionuclide activity per unit mass (Bq/kg DM) into the radionuclide activity per unit area (Bq/m^2). For wild plants, the radionuclide activity per unit area is difficult to measure because several wild species often grow together in the same area. For vegetables, monoculture is generally used making it potentially simpler to measure the standing biomass per unit area. However, during the initial few days after an accident it is unlikely that time can be devoted to the collection of such data.

Therefore, instead of the theoretically preferable interception based on area, the mass interception fraction (f_B) is more often determined which is defined as the ratio between the radionuclide activity concentration in vegetation (Bq/kg DM) and the total radionuclide activity deposited per unit area (Bq/m^2) as defined in IAEA TRS 472 [4.2]. The approach avoids the need to determine the standing biomass per unit area of a plant. The normalization of the initial radionuclide activity in plants to the total deposition is especially useful if f_B is determined specifically for edible parts of fresh vegetables, since it facilitates the estimation of the internal dose from the ingestion of foods.

The interception parameter is important as a starting point for estimating the time–dependence of radionuclide concentrations in plants. Whereas in TRS 472, the mass interception factor was applied to the total above-ground part of the crop, in this section the interception parameter has been applied specifically to the edible part of fresh vegetables such as broccoli and spinach. For these plants, such a simplification is appropriate because the edible parts are a major fraction of the standing biomass. Since the monitoring of fresh vegetables did not start immediately after the deposition occurred, the initial radionuclide activity concentration of green vegetables was back calculated from monitoring data.

4.1.3. Weathering half-lives for calculation of mass interception

Radionuclide activity concentration in plants that arise from interception subsequently decline due to what is commonly termed a weathering effect which encompasses all processes that lead to a loss of radionuclide contamination from the surface of plants. Biomass dilution due to plant growth can also contribute to the time dependence of radionuclide activity concentrations in crops. The decrease, due to weathering and growth dilution, is normally characterized by a single exponential function, which is quantified by determining the effective half-lives, T_{eff}, of radionuclides in plants, especially in the edible part of crops.

4.1.3.1. Weathering half-lives (T_{eff} and T_{eco}) of ^{131}I and radiocaesium in edible part of crops

The T_{eff} can be used to back–calculate the radionuclide activity concentration in vegetables at the time of deposition as shown in Fig. 4.1.

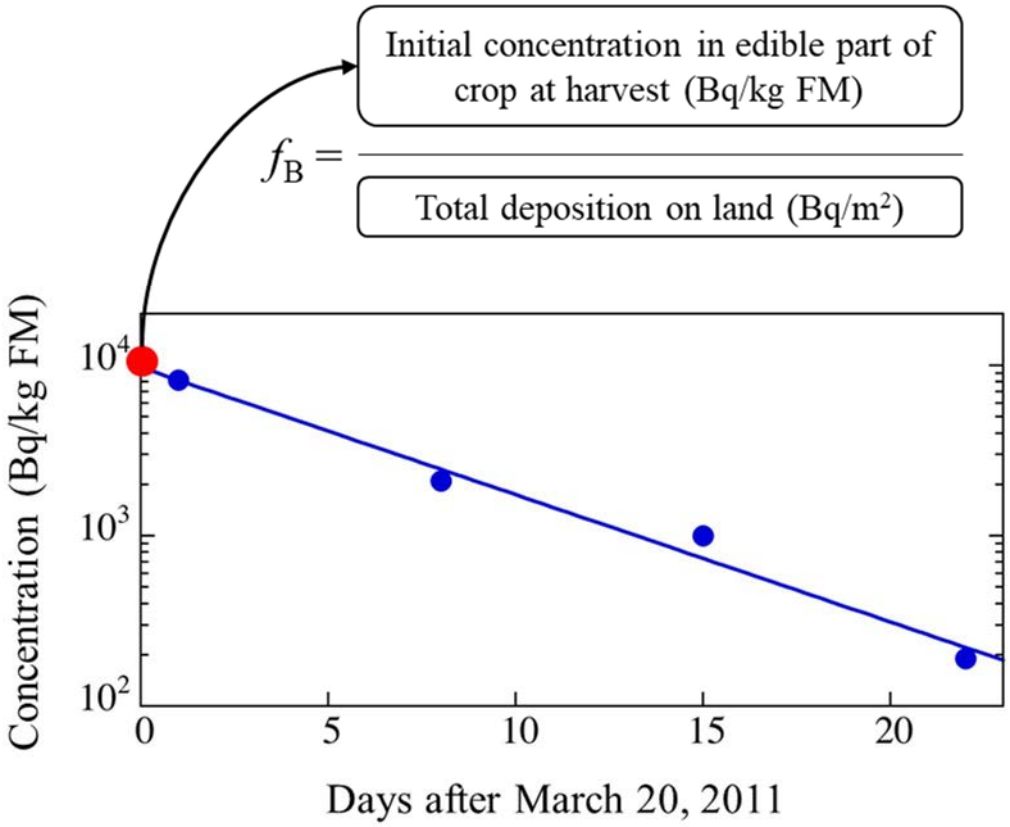

FIG. 4.1. An example of back-calculating the initial ^{137}Cs activity concentration (red) from measured monitoring data (blue).

Farmers want to have a long harvesting period to maintain a continuous income. Therefore, planting can occur over an extended period so there are crops present with different biomasses at any one time, which is particularly important for cropping of fresh vegetables. The sampling scheme, given in Fig. 4.2, shows how the stage of development of various plants differs over the growing period. Plants are harvested when they have reached a suitable size which occurs at different times for each crop. Plants removed during the first harvest were most affected after the FDNPP accident. By the time of subsequent harvests, there had been more time since deposition, during which a greater proportion of radionuclides were lost from plant surfaces due to weathering. Additionally, the radionuclide activity concentration in the plant decreased due to the greater increase of biomass during growth after the time of deposition, which had a diluting effect.

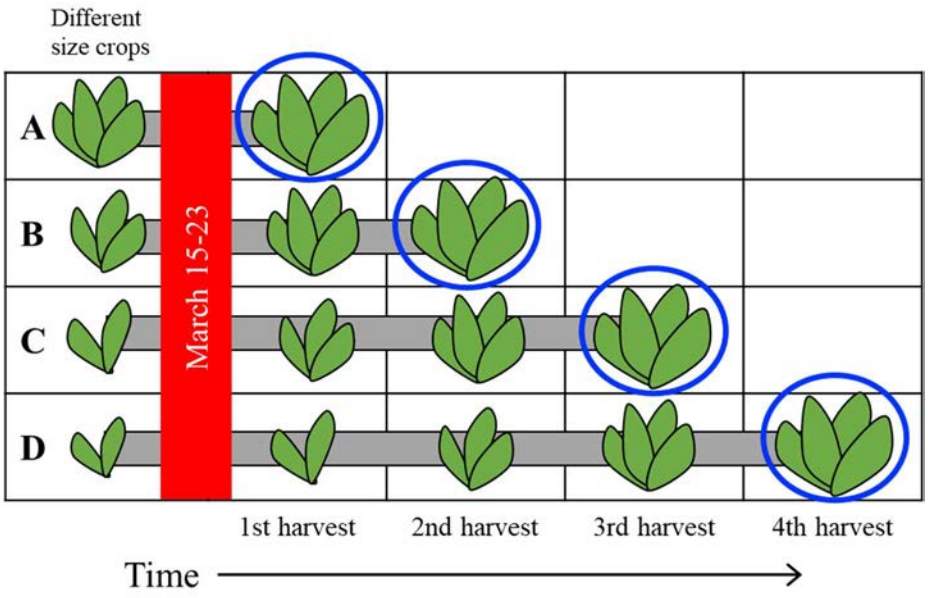

FIG. 4.2. Schematic of growth dilution of radionuclide activity concentrations in leafy vegetables with time, after deposition occurred. Horizontal axis is time, and the vertical axis shows the size of the plants at the time of the accident, A>B>C>D (The largest plant on the vertical axis was harvested at the 1st harvest, and the smallest plant on the vertical axis was harvested at the 4th harvest).

The FDNPP accident occurred on 11 March 2011. Relatively heavy depositions of radionuclides on land occurred primarily in two periods from 15 to 16 March and from 20 to 23 March 2011. For most areas in the Kanto plain, where many data sets were collected, deposition was heaviest on 21 March. Because the number of deposition data collection sites in earlier period were limited, 20 March, at the beginning of the later period, was selected as the target date for the initial activity concentration.

In Japan, from winter to early spring, fresh vegetables are harvested over a period of several weeks. Until early June 2011, continuous monitoring of fresh vegetables (edible part, not washed) was carried out where radionuclide activity concentrations in a vegetable crop once exceeded, or were close to, the provisional limits applied in 2011 of 2000 Bq/kg FM for ^{131}I and 500 Bq/kg FM for total radiocaesium (^{134}Cs+^{137}Cs). The measurements were performed every one or two weeks. Data sets from municipalities with continuous monitoring data (3 to 5 times in a month) for specified vegetables, such as cabbage and spinach, were used to derive the T_{eff} of the radionuclide activity concentration in crops.

Relevant data were obtained from food monitoring datasets of the Ministry of Health, Labour and Welfare [4.3] and from observations for wild butterbur measured by Tagami and Uchida [4.4]. The selected data complied with the following criteria:

- Crops were grown outside (not in a greenhouse);
- At least three continuous sampling data records existed for a specified crop (e.g., spinach) in a municipality;
- Sampling started in March 2011 (Because the loss of deposited radionuclides is rapid immediately after the deposition onto plants later initiation of continuous sampling

would not appropriately represent the weathering and growth dilution in the initial phase);
- Pearson's correlation p-value was lower than 0.05 from statistical fitting of data for each crop observation.

Derived T_{eff} data for leafy vegetables and flowering head crops are summarized in Table 4.1 (see also the detailed data Table II.1). The reported values were limited to those where the correlation coefficients of the statistical fits exceeded 0.88. Clearly, if sampling start dates were from 12 to 15 March 2011, then the fitting results would differ from those for datasets for which sampling started from 20 to 25 March 2011.

TABLE 4.1. SUMMARY OF EFFECTIVE T_{EFF} AND ECOLOGICAL T_{ECO} (IN PARENTHESIS) HALF-LIVES (D) OF RADIOCAESIUM (^{137}CS OR ^{134,137}CS) AND ^{131}I IN FRESH VEGETABLES AFTER THE FDNPP ACCIDENT

Crop type	Radionuclide	N[a]	Effective (ecological) half–life (d)					
			AM[b]	SD[c]	GM[d]	GSD[e]	Minimum	Maximum
Leafy vegetables: Japanese butterbur, kakina, and kukitachina, spinach	^{137}Cs or ^{134,137}Cs	8	7.8 (7.9)	2.3 (2.3)	7.4 (7.5)	1.5 (1.5)	3.2 (3.2)	10.5 (10.6)
Leafy vegetables: Japanese butterbur, kakina, komatsuna, kukitachina, spinach	^{131}I	23	4.1 (9.8)	1.0 (5.3)	4.0 (8.6)	1.3 (1.7)	2.2 (3.0)	6.0 (23.3)
Flowering head: broccoli, turnip rape, purple–stem mustard	^{131}I	6	4.2 (10.6)	1.0 (8.1)	4.1 (9.1)	1.2 (1.7)	3.5 (6.7)	6.2 (27.1)

[a] the number of data points used in analysis
[b] arithmetic mean
[c] standard deviation
[d] geometric mean
[e] geometric standard deviation (unitless)

The T_{eff} data showed that radioactivity concentrations in fresh vegetables declined quickly. Radiocaesium data are combined as the differing physical half-lives had a minor effect on T_{eff} half-lives over the time period considered. Nevertheless, to remove the physical decay effect, T_{eco} values were also calculated. The GM of T_{eco} values for radiocaesium and radioiodine in leafy vegetables were 7.4 and 8.6 days, respectively, which were not significantly different (ANOVA test). The T_{eco} data for flowering heads were not significantly different between leafy vegetables and flowering heads for ^{131}I. Similarly, the data compilation of T_{eco} in TRS 472 [4.2] suggested that there was little difference in weathering half-lives for ^{137}Cs and ^{131}I in grass.

4.1.3.2. Weathering half-lives (T_{eff} and T_{eco}) of ^{131}I and radiocaesium in weeds

Further assessments of weathering half-life were carried out utilising data for weeds collected for the Fukushima plant-monitoring programme of the Ecological Radioactivity Monitoring centre of Fukushima [4.5]. Sampling started only 3–4 days after initial deposition occurred on 18 March 2011 initially at six sites in Iitate village (sampling site code: 2-1), Kawamata town (2-2), Tamura city (2-3), Minamisoma city (2-4), Ono town (2-5) and Iwaki city (2-6) in

Fukushima Prefecture. As for the crop data, the radionuclide activity concentrations in the weeds were affected by various weathering processes.

Data on the early time trends of ^{131}I and ^{137}Cs activity concentrations in weeds for these first eight weeks after 11 March 2011 are presented in Fig. 4.3. Associated calculation of the weathering half-life was based on these data with T_{eco} and T_{eff} for ^{131}I and T_{eff} for ^{137}Cs given in Table 4.2. GM values of T_{eff} for ^{131}I and ^{137}Cs activity concentrations in the weeds agreed well with that for edible part of crops (Table 4.2). Similar trends for perennial grasses in Japan were reported by Fesenko et al. [4.6].

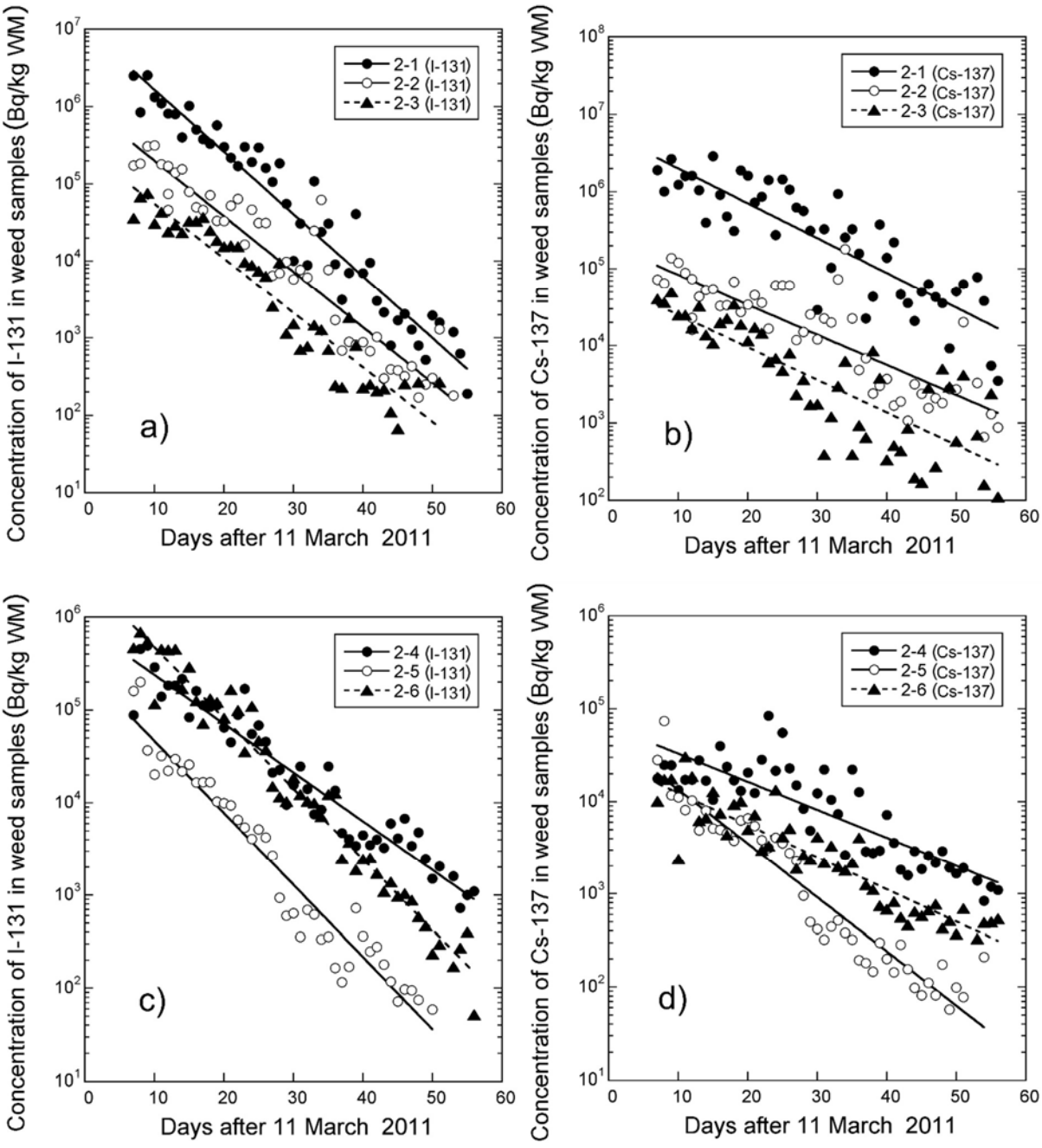

FIG. 4.3. Time trends of ^{131}I (a, c) and ^{137}Cs (b, d) activity concentrations in weeds at six emergency monitoring sites near the FDNPP; the figure legends show the sampling site codes (see text).

TABLE 4. 2. EFFECTIVE (T_{eff}) AND ECOLOGICAL (T_{eco}) WEATHERING HALF–LIVES OF ^{131}I AND ^{137}CS IN WEED SAMPLES COLLECTED AT SIX EMERGENCY MONITORING SITES (SEE FIG. 4.3) IN FUKUSHIMA PREFECTURE FROM 18 MARCH TO 6 MAY 2011

Sampling site [a]	^{131}I				^{137}Cs			
	N [b]	T_{eff} (d)	T_{eco} (d)	R^2 [c]	N	T_{eff} (d)	T_{eco} (d)	R^2
2-1	48	3.7	7.0	0.93	49	6.7	6.7	0.74
2-2	48	4.2	8.7	0.90	51	7.7	7.7	0.70
2-3	42	4.3	9.1	0.91	49	7.1	7.1	0.65
2-4	49	5.7	19.9	0.92	49	9.9	9.9	0.71
2-5	43	3.9	7.5	0.94	46	5.2	5.2	0.91
2-6	49	3.9	7.8	0.96	49	8.7	8.7	0.84
GM	n.a.[d]	4.2	9.3	n.a.	n.a.	7.4	7.4	n.a.

[a] sampling site code, see Fig. 4.3
[b] the number of data points used for analysis
[c] the squared correlation coefficient
[d] not applicable

Analysis of data collected over a longer period of 300 days [4.5] suggested that root uptake became the major pathway about 100 days after the FDNPP accident occurred (Fig. 4.4).

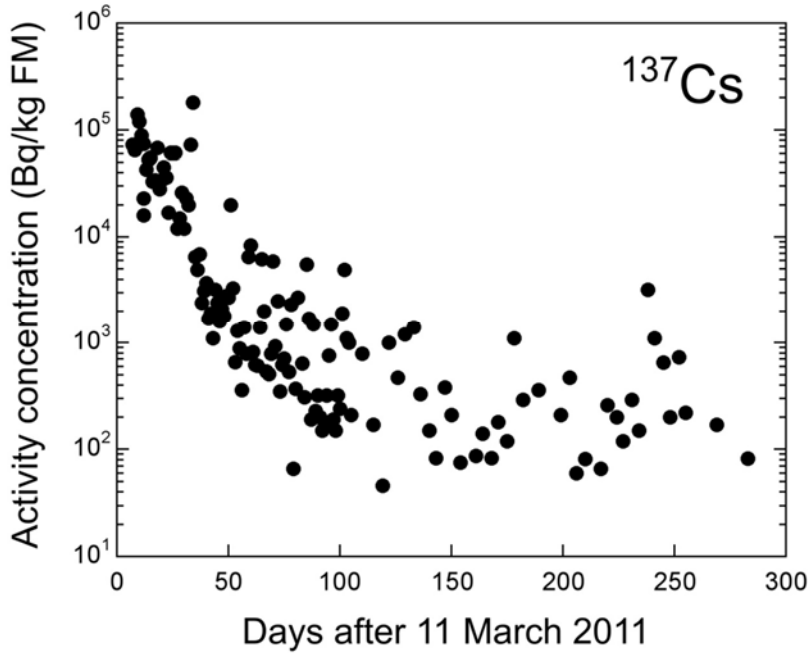

FIG. 4.4. Long-term monitoring of ^{137}Cs activity concentrations in weeds collected at emergency monitoring site 2-1 near the FDNPP (see also TABLE 4.2 and FIG. 4.3).

The T_{eco} estimated for both ^{131}I and ^{137}Cs are reasonably consistent with values derived after the Chernobyl accident. The mean T_{eco} value for ^{131}I in plants after the Chernobyl accident was 8.8 days, whilst that for ^{137}Cs was 17.0 days with a range of 9.0 to 34 days [4.1]. The narrow ranges for T_{eco} after the FDNPP accident compared with those after the Chernobyl accident may be explained by the smaller size of the affected area and the lower diversity of environmental conditions [4.7].

4.1.4. Calculation of mass interception for edible part of crops

The f_B is usually based on dry mass (DM), however, a fresh mass (FM) basis was used for edible crops as it was easier to use in the prevailing conditions soon after the FDNPP accident. The concepts underpinning the calculation are shown in Fig. 4.1.

The T_{eco} values derived above were used for estimation of the initial radionuclide activity concentrations in crop samples at the time of deposition. Online deposition data for the relevant municipalities for the crops considered were used [4.8]. For some municipalities, deposition data were not available, so daily deposition data from neighbouring municipalities were applied. All daily deposition data were decay corrected to 20 March 2011 and the total deposition was estimated. The mass interception fractions summarized in Table 4.3 were estimated for ^{131}I and $^{134,137}Cs$ on leafy vegetables [4.4] (see also detailed data in Table II.2).

TABLE 4.3. MASS INTERCEPTION FRACTION f_B (M²/KG FM) FOR RADIOCAESIUM (^{137}CS OR ^{134,137}CS) AND ^{131}I ESTIMATED FOR LEAFY VEGETABLES AFTER THE FDNPP ACCIDENT

Plant species	Radionuclide	N [a]	Mass interception fraction f_B (m²/kg FM)					
			AM [b]	SD [c]	GM [d]	GSD [e]	Minimum	Maximum
Leafy vegetables (Japanese butterbur, kakina, kukitachina, spinach)	^{137}Cs or $^{134,137}Cs$	8	0.167	0.153	0.099	3.4	0.014	0.43
Leafy vegetables (Japanese butterbur, kakina, komatsuna, kukitachina, spinach)	^{131}I	17	0.094	0.073	0.072	2.2	0.016	0.30

[a] the number of data points used for analysis
[b] arithmetic mean
[c] standard deviation
[d] geometric mean
[e] geometric standard deviation (unitless)

These data were converted to a DM basis using dry matter content information collated in the Standard Tables of Food Composition in Japan [4.9] allowing comparison with the data collated in IAEA TRS 472 (Table 4.4). The applied dry/wet ratio for spinach was 0.076, and for *Brassica rapa* crops (kakina, kukitachina) it was 0.117. For Japanese butterbur, a dry/wet ratio of 0.15 was applied based on field data.

The estimations for the mass interception fractions based on monitoring data obtained after the FDNPP accident are consistent with findings reported after the Chernobyl accident.

Measured $^{134,137}Cs$ activity concentrations in rye and Italian ryegrass collected on 31 March 2011 in Tochigi Prefecture, 112 km south-southwest of the FDNPP were supplemented later

with radiocaesium deposition to soil (Bq/m^2) allowing f_B estimation [4.10]. The estimated interception fraction and mass interception fraction values are shown in Table 4.5. The values for f_B are within the range of those reported by [4.11] measured in Chiba Prefecture, and also similar to the Chernobyl fallout values [4.2].

TABLE 4.4. MASS INTERCEPTION FRACTION f_B (M²/KG DM) OF ^{137}CS AND ^{131}I ESTIMATED FOR LEAFY VEGETABLES AFTER THE FDNPP ACCIDENT AND COMPARISON WITH DATA IN TRS-472 [4.2]

Plant species	Source	Radio-nuclide	N [a]	Mass interception fraction f_B (m^2/kg DM)					
				AM [b]	SD [c]	GM [d]	GSD [e]	Min	Max
Leafy vegetables (Japanese butterbur, kakina, kukitachina, spinach)	Fukushima	^{137}Cs	8	1.7	1.6	1.0	3.4	0.12	4.6
Grass (TRS 472)	Chernobyl	Cs	—[f]	—	—	1.1	—	—	—
Leafy vegetables (Japanese butterbur, kakina, komatsuna, kukitachina, spinach)	Fukushima	^{131}I	17	1.0	0.7	0.81	2.1	0.14	2.6
Grass (TRS 472)	Chernobyl	^{131}I	—	—	—	0.7	—	—	—
Grass and clover (TRS 472)	Experiment with simulated rain	^{131}I	6	—	—	3.0	2.1	1.1	8.7
Mean of 5 species (TRS 472) (Fescue, bush clover, spruce, maple & goldenrod)	Experiment with simulated rain	^{131}I	5	—	—	0.27	—	—	—

[a] the number of data points used for analysis
[b] arithmetic mean
[c] standard deviation
[d] geometric mean
[e] geometric standard deviation (unitless)
[f] no data

TABLE 4.5. AVERAGE INTERCEPTION FRACTION (F) AND MASS INTERCEPTION FRACTION (F_B) OF RADIOCAESIUM (^{134,137}CS) ON 31 MARCH 2011 IN TOCHIGI AND CHIBA PREFECTURES

Plant species	N	f	f_B (m²/kg)	Reference
Rye (*Secale cereale* L.)	3	0.24	0.48	[4.10]
Italian ryegrass (*Lolium multiflorum Lam.*)	3	0.53	0.99	[4.10]
Mugwort, giant butterbur, dandelion, Japanese dock, field horsetail, wild onion)	6	—[a]	0.9 (Range: 0.5–1.3)	[4.11]

[a] no data

4.1.5. Summary and limitations

4.1.5.1.Summary

Observations and analysis after both the FDNPP accident and the Chernobyl accident give similar values for f_B for ^{131}I and ^{137}Cs. The data are also in general agreement with those from controlled experiments reported in TRS 472 [4.2]. The similarity indicates that the mass interception factor is a robust concept for estimating initial activity concentrations is crops after deposition of radionuclides.

The initial T_{eco} over the first few weeks following deposition onto perennial weeds are consistent with those calculated for edible leafy vegetables.

4.1.5.2.Limitations

Interception quantifies the initial retention of radionuclides by vegetation during a specific deposition event. Following interception, radionuclides are subject to weathering which reduces the radionuclide activity on vegetation. Under field conditions in accidental situations, the simultaneous measurement of radionuclides deposited on the ground and retained by vegetation is difficult to achieve. However, availability of food monitoring and deposition data made it possible to derive the interception fraction.

Estimation of the mass interception fraction from monitoring measurements carried out under emergency conditions introduces several sources of uncertainties. Data collection after the FDNPP accident was not carried out immediately after the heavy deposition occurred, but a few days later. Simplification was necessary to enable the assumption of a single deposition event. The initial radionuclide activity concentrations were not directly measured but were estimated by back-calculation using T_{eco} for ^{137}Cs and ^{131}I, determined from monitoring data.

The mass interception fraction, according to the definition in IAEA TRS 472 [4.2], is estimated for the total above-ground plant parts. In the assessment after the FDNPP accident, the mass interception factor was also applied to the edible parts of plants, such as broccoli and spinach, which gave similar values to the total above-ground value. The approach is consistent with the definition of the mass interception factor, which normalizes the interception to the mass, so the consideration of a specific plant part should not be significantly different from the consideration of the total plant.

The mass interception fraction depends on the deposition mode. Plants were contaminated with both dry and wet deposition, so it was difficult to identify which deposition form contributed most to the contamination of the vegetables.

The data in TRS 472 were given on a DM basis; however, FM data would be more appropriate when considering radionuclide retention by vegetables under emergency and other situations. Provision of conversion factors from dry-to-wet and wet-to-dry would be helpful when quantifying interception data sets in future.

4.2.BEHAVIOUR OF RADIOCAESIUM IN AGRICULTURAL SOIL

In this section, radiocaesium behaviour in agricultural soil in Japan is described after the FDNPP accident. Data are provided on the radiocaesium interception potential (*RIP*), distribution coefficient (K_d) and the relationship with the soil-plant concentration ratio (*CR*).

4.2.1. Introduction

Agricultural soils are ploughed to a depth that depends on the crop requirements and the management techniques used by farmers. The ploughing depth in Japan normally varies between 10–25 cm. Ploughing and mixing soil disperses deposited radioactive materials resulting in similar activity concentrations in the ploughed soil layers. In rice paddy fields, surface water paddling, and submerged soil conditions are typical during the growing period. A compacted subsurface layer with low permeability is formed under the plough layer, at a depth of typically 12–18 cm. Thus, the management of paddy fields and the consequences for radiocaesium distribution are uniquely different from those of dry fields (i.e. not irrigated) used for other crops.

4.2.2. Soil characteristics governing radiocaesium sorption and mobility in soil

Radiocaesium sorption in soils is controlled by ionic exchange at two types of sites: the high-affinity frayed edge sites (FES), which are inter-lattice sites that are found at the end of expanded clay layers, and the low-affinity regular exchange sites (RES) that are found in organic matter phases and at external positions in clay minerals [4.12, 4.13]. Except for soils with high organic matter content or a negligible 2:1 phyllosilicate content, the FES dominate radiocaesium sorption. A fraction of radiocaesium adsorbed to FES may migrate into the interlayer sites; due to the interlayer collapse of micaceous minerals, Cs is bound irreversibly [4.12, 4.14–4.16].

Because the FES capacity is difficult to measure, the Radiocaesium Interception Potential (*RIP*) of soil is used to estimate the capacity of a given soil to specifically sorb Cs [4.17, 4.18]. The *RIP* relates to the content and selectivity of expandable clays, especially illite and other 2:1 phyllosilicate, in which FES are present. The *RIP* becomes a key parameter to predict radiocaesium interactions and subsequent mobility in soils in the short-term after a radioactive release.

Radiocaesium sorption is also affected by the NH_4^+ and K status in the solid and solution phases of soil. The sorption pattern of radiocaesium and the amount of K and NH_4^+ accessible for plants (K is an essential element for plant growth) eventually play a major role in radiocaesium root uptake. Potassium is added to agricultural soil as a fertilizer so dissolved K concentrations are generally high in agricultural soils. The NH_4^+ concentration and availability in agricultural soils may be affected by the application of nitrogen fertilizer, the redox potential and other factors such as decomposition of organic nitrogen, nitrogen uptake by crops, nitrification and the types of expandable clay minerals present to which NH_4^+ can be sorbed or fixed [4.19].

4.2.3. The relationship between *RIP* and soil properties

4.2.3.1. Understanding the RIP concept

As described in the previous section, *RIP* is a parameter that reflects the sorption capacity and selectivity of soil to sorb radiocaesium. In a soil homo-ionically saturated with K or NH_4^+, the sorption of radiocaesium at the FES depends on the total capacity of these sites, the sorption selectivity of Cs compared with that of K or NH_4^+ ($K_c^{\mathrm{FES}}(Cs/X)$) and the concentration of K or NH_4^+ in the contact aqueous phase (m_x), as shown in the following equation:

$$K_d^{\mathrm{FES}}(Cs) = \frac{[FES]}{m_x}\ K_c^{\mathrm{FES}}\left(\frac{Cs}{X}\right), \tag{4.1}$$

in which *RIP* is defined from the $K_d^{\mathrm{FES}}(Cs) \times m_x$ product.

The *RIP* can be determined for both K and NH_4^+ scenarios (RIP_K and RIP_N), although it is more commonly determined for a K scenario, after pre-equilibrating the soil sample with a solution containing a controlled amount of K (often 0.5 mmol L^{-1}). *RIP* is experimentally determined under laboratory conditions that ensure that sorption of ^{137}Cs only occurs on FES. Before spiking carrier-free radiocaesium to soil, the regular exchange sites (*RES*, negative charge sites with low Cs selectivity) are masked using a silver thiourea complex (AgTU) [4.17] or Ca^{2+} [4.18].

In field conditions, soil solution is composed of various cations and the *RES* is not completely masked by the cations present so part of radiocaesium can be adsorbed onto *RES* in addition to the *FES*. The radiocaesium that is weakly adsorbed on *RES* is gradually redistributed to *FES* with time due to the higher selectivity of *FES* for radiocaesium than *RES*.

According to its definition, the *RIP* value, modulated by the K and NH_4^+ concentrations in the soil solution, is a good predictor of the radiocaesium distribution coefficient in FES [4.20].

4.2.3.2. RIP in Japanese soils grouped according to soil classification

Based on the *RIP* values, 88 worldwide soils were subdivided into 12 soil groups. Reported *RIP* values for Histosols, Podzols, Ferrasols, Anthrosols and Andosols were lower than for other soil groups (Table 4.6) [4.21].

The soil groups with lower *RIP* values were characterized by a lower content of 2:1 aluminosilicate mineral. In contrast, *RIP* values of Calcisols, Chernozems, Cambisols and Vertisols tended to be higher than the other soil groups. However, the number of observations for the different soil types varies widely making systematic comparisons of all soil types difficult. Micaceous minerals widely occur within igneous, metamorphic and sedimentary rocks, but they are not the key factor for determining soil classification. The prevalence of these minerals is one of the reasons why the *RIP* values vary widely even within a category. The relationship between *RIP* and soil properties, regardless of soil classification, is examined in the following section.

There are only a few studies evaluating the *RIP* for different soil types in Japan before the FDNPP accident [4.22, 4.23], but several studies have measured *RIP* afterwards. *RIP* data for different soils are presented in Table 4.6 (data from [4.21, 4.24–4.33]). The *RIP* values of farmland soil in Fukushima prefecture and surrounding regions [4.27, 4.30–4.32], are mostly within the range for similar soils reported for other countries [4.21, 4.24–4.26, 4.28, 4.29, 4.33–4.37]. However, the *RIP* values of Andosols (volcanic ash soil), which covers about 18% of agricultural land in Fukushima, are lower than those of other soil types in Japan. The dominant clay minerals of Andosols are low-crystalline minerals such as allophane and imogolite, and the *RIP* values of these low-crystalline minerals are low because of the lack of FES.

RIP values for farmland soils in the areas severely affected by the Chernobyl accident have not been widely reported. However, *RIP* values of some pasture soils (Podzols, Histosols) collected from Russia and Belarus [4.24] were 24–455 (mmol/kg) (GM 163 mmol/kg), which were lower than most *RIP* values reported for soils in Fukushima prefecture and surrounding areas. Therefore, soil *RIP* in most contaminated areas of Fukushima prefecture are likely to be higher than those of most soils affected by the Chernobyl NPP accident.

TABLE 4.6. *RIP* (MMOL/KG) FOR SOILS GROUPED ACCORDING TO SOIL CLASSIFICATION

Location	Soil Classification	N [a]	*RIP* (mmol/kg)			
			GM [b]	GSD [c]	Minimum	Maximum
Japan (Fukushima, Tochigi, Iwate and Miyagi prefectures)	All soil types	1131	1290	2.2	73	12 700
	Andosols	248	690	2.3	73	6170
	Fluvisols	706	1460	1.9	170	12 700
	Cambisols	168	1950	2.0	190	8720
Other Countries	All soil types	338	940	5.4	1.8	13 300
	Andosols	11	390	2.5	94	1320
	Anthrosols	4	330	2.1	140	800
	Calcisols	6	7510	1.6	4220	12 100
	Cambisols	18	3020	2.5	540	12 900
	Chernozems	6	5960	1.3	4510	8590
	Ferrasols	9	240	3.3	26	1410
	Gleysols	13	1000	4.4	91	10 100
	Histosols	16	55	5.9	5	1190
	Inceptisols	5	1170	1.9	450	1840
	Luvisols	39	800	6.1	23	13 300
	Nitisols	7	1900	3.1	320	4920
	Podzols	20	86	6.6	1.8	2120
	Regosols	8	2060	3.6	230	9650
	Vertisols	7	3310	1.8	1820	8210

[a] the number of data points used in analysis
[b] geometric mean
[c] geometric standard deviation (unitless)

4.2.3.3.RIP grouped according to the clay and organic matter contents

The content of micaceous minerals in soil is a determining factor for *RIP* values of soils [4.38, 4.39]. However, the contribution of micaceous minerals to basic soil properties such as CEC and clay contents is low, therefore, *RIP* values are not simply related to basic soil properties. The *RIP* values of soils with a low silt and clay content, or high organic matter content are typically lower than that of the other soil types. For soils collected near Fukushima prefecture, the *RIP* is significantly negatively correlated with organic matter content [4.27, 4.30–4.32], because the higher the OM content, the lower the silt and clay contents. The *RIP* values were significantly correlated with the clay content in soils from northern Belgium and with the pH, clay content and fine silt content in soils from southern Belgium [4.37]. Absalom et al. [4.40] estimated *RIP* based on clay contents of European soils, whereas Gil-Garcia et al. [4.20] showed that silt and clay contents explained more than 60% of *RIP* variance, regardless of soil type and organic matter content.

Taking into account the correlations of soil properties with *RIP* and available data obtained in Japan, *RIP* values have been grouped according to the contents of clay and total carbon

(representing organic matter) in Table 4.7 (data from [4.21, 4.25, 4.27, 4.29, 4.32, 4.34, 4.37]). There is a clear trend showing that the higher the clay content in the soils considered the higher the *RIP* value.

TABLE 4.7. *RIP* (MMOL/KG DM) FOR JAPANESE SOILS GROUPED ACCORDING TO CARBON AND CLAY CONTENTS

Carbon content (g/kg DM)	Clay content (g/kg DM)	N [a]	*RIP* (mmol/kg DM)				
			GM [b]	GSD [c]	Minimum	Maximum	95% CI [d]
>35	>300	58	1240	2.8	87	11 200	180–8090
	200–300	87	750	2.7	150	6100	190–4690
	100–200	69	720	2.3	150	4600	180–3850
	<100	27	630	4.1	12	4502	27–4240
25–35	>300	36	1780	2.2	320	9650	420–9280
	200–300	53	1510	1.8	430	6790	520–4490
	100–200	72	980	2.1	97	5400	290–3590
	<100	25	260	3.7	26	3500	32–3200
15–25	>300	70	1950	2.0	420	13 300	670–6760
	200–300	128	1720	1.8	500	9620	650–4740
	100–200	90	1250	2.0	240	6130	320–3400
	<100	45	980	2.5	190	6310	200–4420
<15	>300	30	2310	2.7	330	12 900	390–12 500
	200–300	38	2330	1.7	670	5720	680–5330
	100–200	68	1670	2.10	190	7410	530–6610
	<100	30	750	6.2	1.8	10 500	5.3–9020

[a] the number of data points used in analysis
[b] geometric mean
[c] geometric standard deviation
[d] confidence interval

The range in the organic matter content of the soils considered is rather small which limits the comparison of the data. There is a tendency for *RIP* values to be higher in soils with low organic matter contents, but the data are not consistent when the OM content of the Clay<100 g/kg DM range is considered.

4.2.4. The impact of flood irrigation on radiocaesium behaviour in rice paddy fields

Flood irrigation is carried out in paddy fields to provide an appropriate environment for the growth of rice plants, such as maintaining a moderate root temperature and retaining soil particles. The periodic gentle flooding of paddy fields during the planting period leads to variation in the redox conditions (precipitation or dissolution of iron oxide-hydroxide and other minerals) (Fig. 4.5) and may vary the composition of the soil solution (e.g., K and NH_4) and *RIP* [4.41]. Such changes may also affect radiocaesium sorption and mobility in soil through changes in soil–soil solution K_d between under flooded and unsaturated conditions.

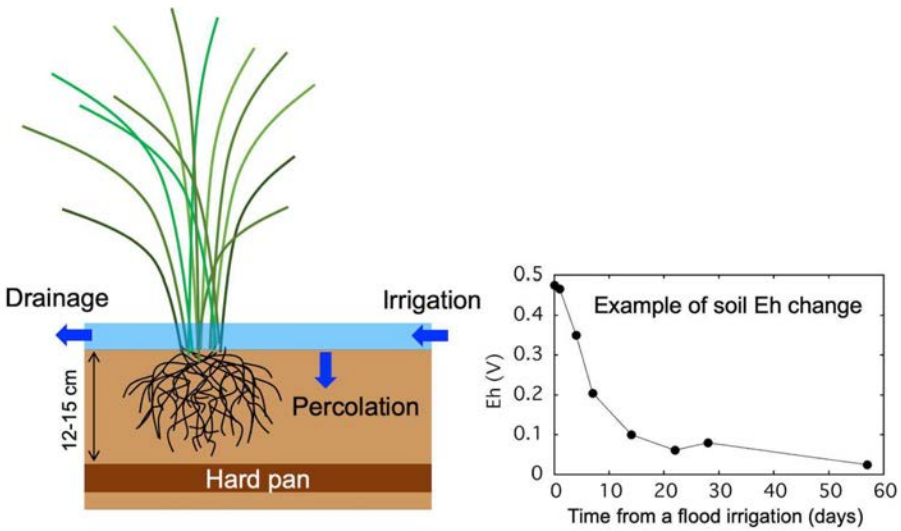

FIG. 4.5. Schematics of rice cultivation methodology in Japan

Closed system radiotracer experiments in laboratories have been carried out to study the influence of flood irrigation on radiocaesium mobility in soil. Lower K_d values for radiocaesium have been measured under flooded conditions compared with unsaturated conditions [4.42, 4.43]. These findings were thought to be related to higher concentrations of NH_4^+ in soil water under flooded conditions than under unsaturated conditions. Conversely, Uematsu et al. [4.44] reported that the dissolved fraction of radiocaesium (spiked with ^{134}Cs) in soil was significantly lower under flooded conditions than under unsaturated conditions, suggesting that the effect of competition with K^+ and NH_4^+ on radiocaesium exchange was not significantly different between flooded and unsaturated conditions. This finding is supported by Tagami and Uchida [4.45] who carried out a radiotracer experiment using Andosol and Grey lowland soil. After application of ^{137}Cs, these soils were kept under saturated or flooded conditions and ^{137}Cs was extracted from soil with 0.05M $CaCl_2$ to identify water soluble and Ca exchangeable fractions. There was no difference in the relative amount of extracted ^{137}Cs with time between flooded and unsaturated conditions for Andosol and Grey lowland soils (Fig. 4.6).

During normal flood irrigation of paddy fields, water moves gently over the soil surface to minimize soil erosion. Suspended solids with different physicochemical characteristics in the irrigation water from e.g. rivers, lakes, ponds, and groundwater wells can be released to paddy fields. The suspended soil particles can be removed from the paddy fields via surface and subsurface drainage water. After unplanned situations (e.g. typhoons) when enormous amounts of water enter the paddy field, *RIP* can either decrease thereafter due to runoff of soil particles leading to either a decrease in the clay content or increase due to an input of fine particles to the flooded area [4.41]. Water management in rice paddies can significantly affect the mass balances of soil components and may modify physicochemical characteristics including clay content, organic matter content, *RIP*, CEC, exchangeable K and nitrogen concentration.

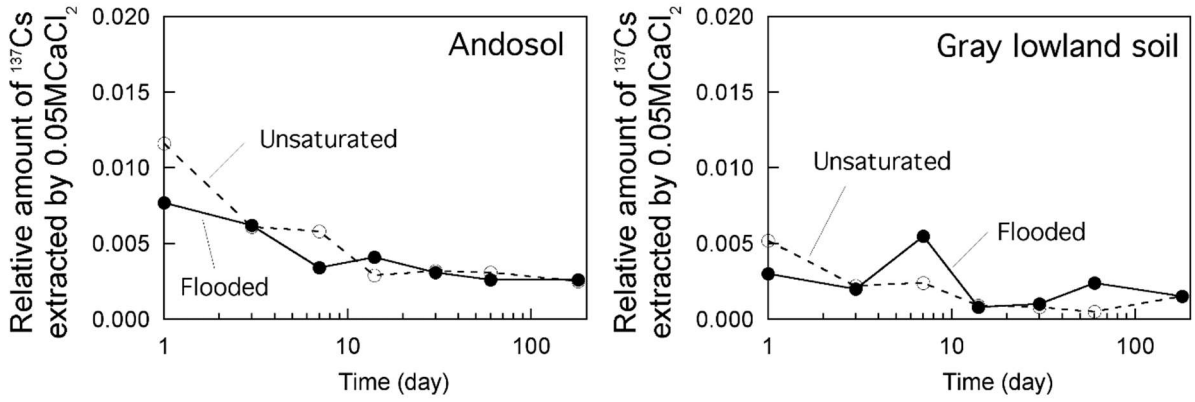

FIG. 4.6. Time dependence on the amount of 0.05M $CaCl_2$ extractable ^{137}Cs (water soluble + exchangeable fractions) in Andosol and Grey lowland soil under flooded and unsaturated conditions.

These various studies suggest that the impact of flooding on the concentrations of K^+, NH_4^+ and of radiocaesium in the soil solution, and on the *RIP* need to be carefully considered in contaminated paddies. Uematsu et al. [4.44] determined soil solution sampling-based K_d from pot-culture experiments in different soils under either unsaturated conditions or flooded conditions. The soils were collected in Fukushima prefecture after the FDNPP accident and spiked with ^{134}Cs followed by incubation for 28 days. The $K_d$values (see Table 4.8) under flooded conditions were higher than those under unsaturated conditions by 1.5 times on average ($p<0.05$, paired *t*-test). K in soil solution (K_{ss}) was approximately a factor of 2 lower, whereas NH_4 in soil solution (NH_{4ss}) did not change. The changes of K_{ss} due to flooding would affect K_d and *RIP* values.

TABLE 4.8 CHANGES IN K AND NH_4 STATUS AND K_D DUE TO FLOODING FOR 28 DAYS

Soil type	Under unsaturated conditions				Under flooded conditions			Ratios		
	K_{ss} (mM)	$NH_{4,ss}$ (mM)	*RIP* (mM/kg DM)	K_d (L/kg DM)	$K_{,ss}$ (mM)	$NH_{4,ss}$ (mM)	K_d (L/kg DM)	$K_{ss,\ flood}$ / $K_{ss,unsat}$	$NH_{4ss,\ flood}$ / $NH_{4ss,unsat}$	$K_{d,flood}$ / $K_{d,unsat}$
Glaysol	0.45	0.39	1586	1320	0.29	0.31	1790	0.64	0.79	1.4
Andosol	0.68	0.72	685	320	0.37	0.44	600	0.54	0.61	1.9
Glaysol	0.96	0.68	399	130	0.51	0.92	290	0.53	1.35	2.2
Glaysol	0.47	0.59	831	1350	0.39	1.22	810	0.83	2.07	0.6
Glaysol	0.96	0.67	833	340	0.38	1.16	520	0.40	1.73	1.5
Glaysol	0.10	0.32	1757	3320	0.05	0.19	6730	0.50	0.59	2.0
Glaysol	0.14	0.43	650	360	0.12	0.61	390	0.86	1.42	1.1
Glaysol	0.38	0.48	1706	1780	0.17	0.63	4380	0.45	1.31	2.5
Glaysol	0.19	0.61	256	240	0.09	0.60	370	0.47	0.98	1.6
Geometric mean	0.37	0.53	4.2	620	0.21	0.58	940	0.56	1.11	1.5

4.2.5. Relationship between K_d and *CR* in Japanese agricultural soils

The solid-liquid distribution coefficient K_d (L/kg DM) in soil is a parameter that may be used when elucidating and/or predicting the root uptake of a radionuclide in soil-plant systems (Chapter 2). It is generally assumed that the K_d of radiocaesium will be correlated with the soil-to-plant *CR* of radiocaesium, but few studies have tested this assumption. The relationship between K_d and *CR* can be described as follows (IAEA TRS 472 [4.2])

$$CR = \frac{B_p}{K_d}, \tag{4.2}$$

where B_p is the bioaccumulation factor and refers to the radionuclide plant to soil solution ratio (L/kg DM).

Uematsu et al. [4.31, 4.44] determined soil solution sampling-based K_d values from pot experiments in different soils under either unsaturated or flooded conditions before sowing. Soil-to-plant *CR* values for paddy rice and ryegrass (see Table 4.9) are available that could be related to the respective K_d values. The logarithm of the *CR* values of all rice plant shoots and ryegrass samples and the corresponding K_d values are plotted in Fig. 4.7. There is no statistically significant correlation between *CR* and K_d values between the species ($p > 0.05$, paired *t*-test); however, the data demonstrate that *CR* values for both species similarly decrease with the increase of K_d values.

For the dataset presented in Table 4.9, Uematsu et al. [4.44] plotted the radiocaesium activity concentration in the plants against the ratio of radiocaesium to K concentrations in soil water for both flooded rice plants and ryegrass on a log-log plot (Fig. 4.8). Both quantities are correlated well with $P < 0.001$. This correlation indicates that the *CR* for rice plants grown under flooded conditions may be predicted using both the K_d and the K concentration in soil solution. The ryegrass data are consistent with those of Smolders et al. [4.29], who reported a significant correlation between radiocaesium in ryegrass and *CR* of radiocaesium to K in soil water for Belgian soils (Fig. 4.8).

4.2.6. Summary and limitations

4.2.6.1. Summary

The K_d value might increase in paddy field soil during gentle flooding under typical water management for rice. The probable increase is due to the competitive sorption of radiocaesium and K^+ in flooded soils and it might cause a decrease of CR. However, some differences were observed in the changes of K_d values obtained for flooded and unsaturated conditions. Other factors, such as an increase in NH_4^+ concentration during flooding can affect the binding of radiocaesium to soil components and, a general increase of K_d values during flooding has not yet been verified.

Soil *RIPs* in most contaminated areas of Fukushima prefecture are higher than those of the radioecologically sensitive regions, with Histosols and Podzols, around the Chernobyl NPP.

TABLE 4.9. K_d (L/KG) VALUES FOR SPIKED ^{134}CS AND THE SOIL-TO-PLANT CONCENTRATION RATIO *CR* (KG SOIL DM / KG PLANT DM) FOR RYEGRASS AND RICE SHOOTS (DATA ADAPTED FROM UEMATSU ET AL. [4.31, 4.44])

Soil type	Land use	Clay (%)	Under unsaturated conditions		Under flooded conditions	
			K_d (L/kg)	*CR*, ryegrass (kg soil DM/kg plant DM)	K_d (L/kg)	*CR*, rice shoots (kg soil DM/kg plant DM)
Gleysol	Paddy	12.9	1320	0.46	1790	0.033
Andosol	Paddy	23.1	320	0.77	600	0.08
Gleysol	Paddy	11.5	130	2.04	290	0.23
Gleysol	Paddy	7.5	1350	0.59	810	0.31
Gleysol	Paddy	15.5	340	0.32	520	0.17
Gleysol	Paddy	18.5	3320	0.65	6730	0.22
Gleysol	Paddy	22.3	360	8.0	390	3.0
Gleysol	Paddy	25.9	1780	0.69	4380	0.11
Gleysol	Paddy	15.8	240	4.5	370	3.7
Andosol	Upland	23.0	2430	0.019	— [a]	—
Andosol	Grassland	15.2	1640	0.10	—	—
Andosol	Grassland	14.8	8380	0.19	—	—
Cambisol	Grassland	18.1	530	0.009	—	—
Gleysol	Grassland	20.2	14 100	0.14	—	—
Cambisol	Grassland	6.8	530	0.11	—	—
Andosol	Grassland	8.4	100	1.6	—	—
Andosol	Grassland	23.4	670	0.066	—	—
Andosol	Grassland	30.7	1680	0.010	—	—
Cambisol	Grassland	15.0	4730	0.013	—	—
Gleysol	Grassland	27.1	1220	0.062	—	—
Acrisol	Grassland	12.7	170	0.13	—	—
Acrisol	Forest	10.9	250	0.12	—	—

[a] no data

4.2.6.2. Data limitations

Under laboratory conditions, a negative correlation was observed between K_d and *CR*. Further data is needed to better describe the *CR* vs. K_d dependence in a range of different soils present in Japan and elsewhere.

4.3.TRANSFER OF RADIOCAESIUM TO CROPS

In the initial three sub-sections of this section, the transfer of radiocaesium is described for three of the most important crops in Japan, namely rice, green tea and fruits. Thereafter, a section is addressed to transfers of radiocaesium to other crops. Some of the transfer parameter data were derived from crops grown on soil that had been remediated by the addition of extra potassium. The role of exchangeable potassium in soil in influencing the *CR* values for radiocaesium was critical to the development of remediation approaches after the FDNPP. Therefore, for each section, the relationship between radiocaesium *CR* for the crop and the exchangeable potassium status in soil is discussed, where relevant. Effective half-lives T_{eff} are also reported where possible.

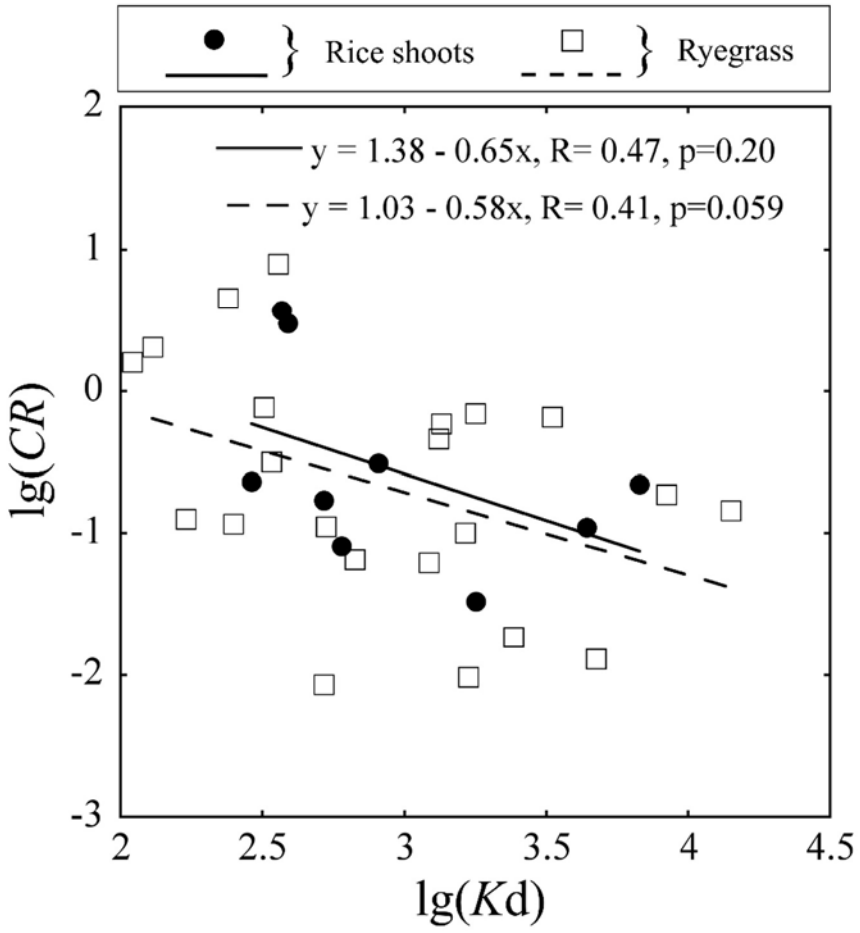

FIG. 4.7. Correlations between soil K_d and CR for rice shoots and ryegrass (adapted from [4.44])

4.3.1. Transfer to rice

4.3.1.1. Introduction

Rice is an important staple food in Japan. Typically, planting of rice seedlings starts at the end of April or early May in Fukushima Prefecture. Rice planting had not commenced at the time of the FDNPP accident in March 2011. By the time that rice growth began, radionuclide deposition from the nuclear power plant had greatly decreased and, therefore, interception was not a major transfer pathway for radiocaesium. Subsequent potential transfer to rice plants was via root uptake.

Initially, after the FDNPP accident, the provisional limit was 500 Bq/kg FM for radiocaesium in rice (which was applied in 2011 until the next rice harvesting season in 2012) [4.46]. To avoid producing rice with radiocaesium concentrations exceeding the limit, a conservative soil-to-rice *CR* of 0.1 [4.47] was assumed to derive an upper limit of radiocaesium activity concentration in soil used for rice production of 5000 Bq/kg DM [4.48]. The IAEA publication TRS 472 [4.2] provides a GM *CR* value of 0.0083 for rice but this lower value was deemed to be not appropriate to use for deriving the soil cultivation limit value because it refers to equilibrium conditions.

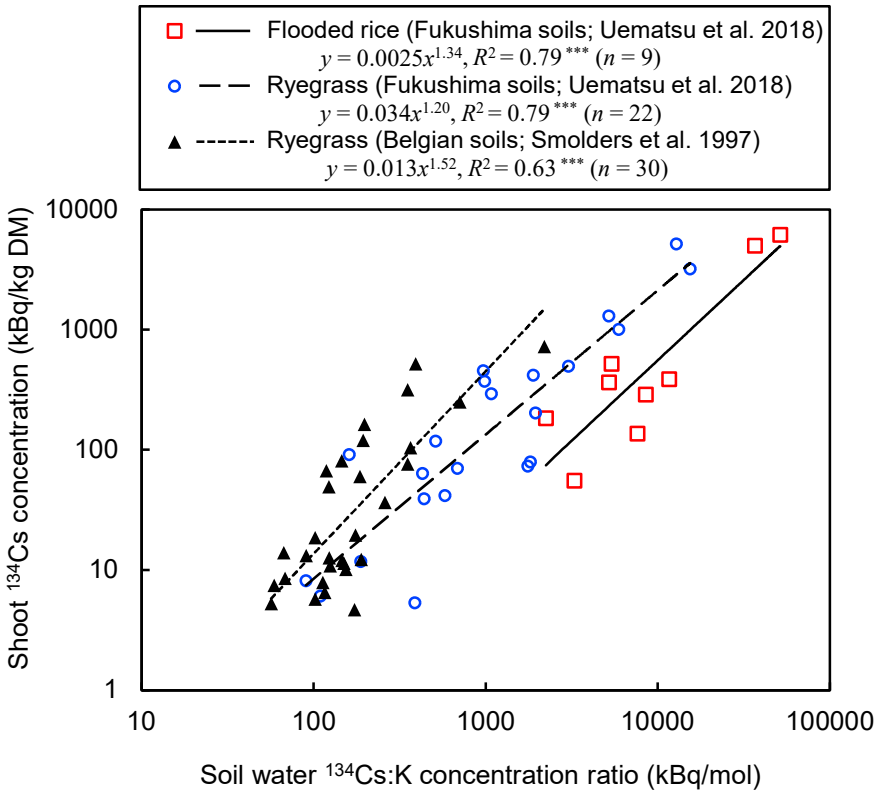

*FIG. 4.8. Positive correlations between the plant ^{134}Cs concentration and the concentration ratio of ^{134}Cs to K in soil water. The correlations are presented for flooded rice and ryegrass grown in pots with soils collected from the areas affected by the FDNPP accident and for ryegrass grown in Belgian soils. Regression equations and the squared correlation coefficient R^2 values are shown in the legend (significance ***: $P < 0.001$. Data adapted from Smolders et al. [4.29] and Uematsu et al. [4.44].*

Many measurement data for soil and brown rice samples collected both before and after the FDNPP accident are available. The rice data considered here are for unpolished brown rice with the husk removed. Polished rice (or white rice) is produced by removing the outer layer of the rice grain (the bran layer, ca. 10% of the brown rice grain by weight) and is the most commonly consumed type of rice in Japan. Analysis of the brown rice data is more appropriate than that of white rice because food monitoring has been carried out for brown rice. According to the data on food processing (see Chapter 8), on average about 40% of the total radiocaesium in brown rice is retained in white rice. Brown rice radiocaesium activity concentrations have been reported to be 2.1 ± 0.3 times higher than those of white rice [4.49, 4.50].

4.3.1.2. Uptake of radionuclides from soil

The availability of radiocaesium deposited onto soil decreases with time due to fixation of Cs to soil particles (termed as “aging effect”) [4.2]. Therefore, the soil-to-brown rice *CR* values initially derived, especially in 2011 and 2012, were obtained in non-equilibrium conditions and the radiocaesium activity concentration in plants was expected to decrease with time after the FDNPP accident.

Paddy fields are flooded during the planting period, thus the redox conditions in soil and also the soil solution composition (e.g., dilution of K and increase in NH_4) changed with time. These changes could have affected radiocaesium bioavailability in soil, thus radiocaesium transfer to paddy rice has been separately compiled before [4.51] and after the FDNPP accident. More

recent studies after the FDNPP accident have also compared radiocaesium transfer to rice for the same soil under flooded and unsaturated conditions [4.52–4.54].

Continuous soil flooding under field conditions did not significantly increase the soil-to-brown-rice *CR* of stable Cs compared with intermittent irrigation (1.2-fold increase, $P > 0.05$; [4.52]). In contrast, a field experiment in Japan revealed that continuous soil flooding enhanced the *CR* of ^{137}Cs (Fukushima-accident-derived) to brown rice by 1.7-fold compared with intermittent irrigation, where the difference was significant ($p < 0.05$; [4.54]). Conversely, another field experiment with rice in Japan showed that the *CR* of stable Cs to brown rice under flooded conditions was only a factor 1.2 higher than under unsaturated conditions ($P > 0.05$; [4.53]). The results of these studies suggest that soil flooding might affect the amounts of bioavailable radiocaesium in soil, but the effect is of minor importance.

4.3.1.3.Data set for estimation of CR values for brown rice

Radiocaesium activity concentrations in brown rice, associated soil data and derived *CR* values were collated into a dataset from journal papers and institute reports either in Japanese or English. Data for paddies treated with normal fertilization rates, fertilizer without K (hereafter, no-K), and no fertilizer application conditions were collated from sampled rice paddies and from pot experiments. A normal K fertilizer application rate was defined as the amount of fertilizer added annually by the farmers before the accident. Since soil conditions differ in each paddy field, it is difficult to specify the amount of fertilizer added for each individual paddy data source. Paddies that received additional K treatment as part of a remediation programme were not included.

There are many papers studying the effect of potassium fertilizer on soil to plant uptake of radiocaesium, but only a few *CR* values were reported for normal fertilizer applications after the FDNPP accident. In contrast, all the *CR* values reported before the accident were for normal fertilizer conditions. If fertilizer conditions were not mentioned in literature sources, it was assumed that normal fertilizer application was utilised. The cultivar grown is often not specified in the literature, so it was assumed that all data were for the most common Japonica variety of rice. Evidence for substantial variation in *CR* values for different rice cultivars was reported [4.55]; however, cultivars classified as high radiocaesium accumulators by Ohmori et al. [4.55] were not consistently in agreement with those identified by Kojima et al. [4.56]. Therefore, all cultivar data provided were combined.

Data were accepted from literature sources if they fulfilled one of the following criteria:

- *CR* values of radiocaesium were reported;
- The radiocaesium (^{137}Cs or ^{134}Cs+^{137}Cs) activity concentration in both brown rice and soil were reported, allowing a calculation of *CR* values;
- Data available in figures which provided radiocaesium (^{137}Cs or ^{134}Cs+^{137}Cs) activity concentrations in both rice and soil, from which *CR* values could be calculated.

Data where only the *CR* values were given in a figure were not included because they were often plotted against soil exchangeable potassium concentration making it difficult to identify which data values represent normal, no-K or no fertilizer application. Data from five studies [4.47, 4.50, 4.57–4.59] before and thirty-six [4.49, 4.54, 4.56, 4.60–4.91] after the FDNPP accident were used in the dataset to derive *CR* values for brown rice in Japan.

4.3.1.4.CR data for brown rice

Because radiocaesium activity concentrations in brown rice are usually higher than in white rice [4.1], the *CR* values of radiocaesium for white rice were lower than those of brown rice. Thus, to derive *CR* values for the more frequently consumed white rice, the brown rice *CR* values can be divided by 2, as discussed in sub-section 4.3.1.1. Soil groups for the *CR* data have been classified following the approach used in the IAEA publication TRS 472 [4.2], based on the FAO classification shown in Table 4.10.

In 2011, the GM of *CR* values for organic soil in Japan was about 3-fold higher than that for clay soils from TRS 472 (ANOVA test, $p = 0.023$). The numbers of data for sand and loam soil groups were small, so further analysis was not possible. From 2012 onwards, the data available for different soil groups were not sufficient to statistically compare *CR* values for rice.

CR values are also presented using the soil classification system commonly used in Japan (e.g., Fluvisol, Andosol and Cambisol and for soils that are commonly present in Japanese paddy fields) (Table 4.11). There were no significant differences between the *CR* values classified by soil types using this approach.

TABLE 4.10. CONCENTRATION RATIOS *CR* (KG SOIL DM / KG PLANT DM) OF RADIOCAESIUM FROM SOIL TO BROWN RICE IN JAPAN BEFORE (IAEA TRS 472 [4.2]) AND AFTER THE FDNPP ACCIDENT

Condition	Fertilizer application (soil type) [a]	Year	N [b]	Concentration ratio *CR* (kg soil DM / kg plant DM)			
				GM [c]	GSD [d]	Minimum	Maximum
Pre-FDNPP accident							
Field	Normal (all soil types)	1991–2000	144	4.1×10^{-3}	2.7	3.9×10^{-4}	4.1×10^{-2}
	Normal (all soil types)	2001–2007	59	3.2×10^{-3}	2.8	4.3×10^{-4}	4.1×10^{-2}
	(sand)	2001–2007	8	2.5×10^{-3}	5.2	4.3×10^{-4}	4.1×10^{-2}
	(clay)	2001–2007	5	2.4×10^{-3}	2.6	7.7×10^{-4}	9.5×10^{-3}
	(loam)	2001–2007	28	2.8×10^{-3}	2.2	8.7×10^{-4}	2.4×10^{-2}
	(organic)	2001–2007	3	4.3×10^{-3}	2.2	1.7×10^{-3}	6.9×10^{-3}
TRS 472	Not specified (all soil types)		466	8.3×10^{-3}	6.2	1.3×10^{-4}	6.1×10^{-1}
Post-FDNPP accident							
Field	Normal (all soil types)	2011	74	1.3×10^{-2}	3.5	9.7×10^{-4}	1.7×10^{-1}
	(sand)	2011	1	1.4×10^{-2}	— [e]	—	—
	(clay)	2011	12	1.5×10^{-2}	2.15	6.0×10^{-3}	5.1×10^{-2}
	(loam)	2011	3	2.0×10^{-2}	5.64	2.8×10^{-3}	7.5×10^{-2}
	(organic)	2011	11	4.0×10^{-2}	1.82	1.5×10^{-2}	1.5×10^{-1}
Field	No-K, no fertilizer	2011	11	1.4×10^{-2}	3.6	2.3×10^{-3}	9.4×10^{-2}
Pot [f]	Normal	2011	8	1.2×10^{-2}	2.3	4.7×10^{-3}	4.2×10^{-2}
Field	Normal (all soil types)	2012	82	6.2×10^{-3}	2.7	4.9×10^{-4}	8.6×10^{-2}
	(clay)	2012	1	1.1×10^{-3}	—	—	—
	(organic)	2012	8	1.1×10^{-2}	2.73	1.7×10^{-3}	3.9×10^{-2}
Field	Unknown [g]	2012	30	4.7×10^{-3}	—	5.3×10^{-4}	1.8×10^{-1}
Field	No-K, no fertilizer	2012	13	1.1×10^{-2}	4.1	1.8×10^{-3}	1.3×10^{-1}

TABLE 4.10. CONCENTRATION RATIOS *CR* (KG SOIL DM / KG PLANT DM) OF RADIOCAESIUM FROM SOIL TO BROWN RICE IN JAPAN BEFORE (IAEA TRS 472 [4.2]) AND AFTER THE FDNPP ACCIDENT (cont.)

Condition	Fertilizer application (soil type) [a]	Year	N [b]	Concentration ratio *CR* (kg soil DM / kg plant DM)			
				GM [c]	GSD [d]	Minimum	Maximum
Pot [f]	Normal	2012	12	1.8×10^{-2}	2.9	4.2×10^{-3}	9.0×10^{-2}
Field	Normal (all soil types)	2013	52	4.9×10^{-3}	3.9	3.9×10^{-4}	4.2×10^{-1}
	(sand)	2013	3	2.8×10^{-2}	10.6	6.2×10^{-3}	4.2×10^{-1}
	(organic)	2013	11	1.0×10^{-2}	2.7	3.3×10^{-3}	4.5×10^{-2}
Field	Unknown [g]	2013	62	2.3×10^{-3}	—	2.4×10^{-4}	1.4×10^{-2}
Field	Normal (all soil types)	2014	43	3.7×10^{-3}	3.8	4.5×10^{-4}	6.9×10^{-2}
	(organic)	2014	8	2.0×10^{-2}	2.02	8.0×10^{-3}	6.0×10^{-2}
Field	Unknown [g]	2014	117	1.9×10^{-3}	—	2.7×10^{-4}	1.9×10^{-1}
Field	No-K, no fertilizer	2013–2014	9	3.1×10^{-2}	5.2	2.0×10^{-3}	1.6×10^{-1}
Field	Unknown [g]	2015	97	2.3×10^{-3}	—	2.2×10^{-4}	2.6×10^{-2}

[a] data for paddies treated with normal fertilization rates, without K fertilizer (no-K), and no fertilizer application conditions; soil types in parentheses; not specified means there is no information on fertilizer status
[b] the number of measurements above detection limit
[c] geometric mean
[d] geometric standard deviation (unitless)
[e] no data
[f] using soil samples taken from contaminated soil in 2011
[g] additional data from Yamamura et al. [4.92] (see text), the level of fertilization is unknown compared to normal application of fertilizer before the accident

TABLE 4.11. RAIOCAESIUM CONCENTRATION RATIOS CR (KG SOIL DM / KG PLANT DM) FROM SOIL TO BROWN RICE FOR JAPANESE SOIL GROUPS BEFORE AND AFTER THE FDNPP ACCIDENT (DATA FROM [4.50])

Year	Soil group	N [a]	GM [b]	GSD [c]	Minimum	Maximum
1995–2007	Andosol	15	3.1×10^{-3}	1.8	9.8×10^{-4}	6.9×10^{-3}
	Fluvisol	60	3.1×10^{-3}	2.9	7.7×10^{-4}	4.1×10^{-2}
	Gleysol	48	4.5×10^{-3}	2.8	3.9×10^{-4}	2.9×10^{-2}
2011	Andosol	10	1.7×10^{-2}	1.4	1.2×10^{-2}	2.8×10^{-2}
	Fluvisol	25	4.4×10^{-3}	2.1	9.7×10^{-4}	3.7×10^{-2}
	Gleysol	9	2.5×10^{-2}	2.3	6.3×10^{-3}	7.7×10^{-2}
2012	Fluvisol	54	4.8×10^{-3}	2.2	4.9×10^{-4}	4.4×10^{-2}
2013	Fluvisol	18	2.2×10^{-3}	3.3	3.9×10^{-4}	2.9×10^{-2}
2014	Fluvisol	17	2.1×10^{-3}	2.1	5.3×10^{-4}	7.1×10^{-3}

[a] the number of data used for analysis
[b] geometric mean
[c] geometric standard deviation

For field data with normal fertilizer conditions, the geometric mean *CR* value and GSD for rice in 2011 was significantly higher by a factor of 3–4 than that before the FDNPP accident (Fig. 4.9). It was also significantly higher by a factor of about 3 than *CR* values for the later years, 2013 and 2014 ($p<0.001$). The 2012 data had a tendency to be higher than before the accident, but not significantly ($p <0.05$) [4.50].

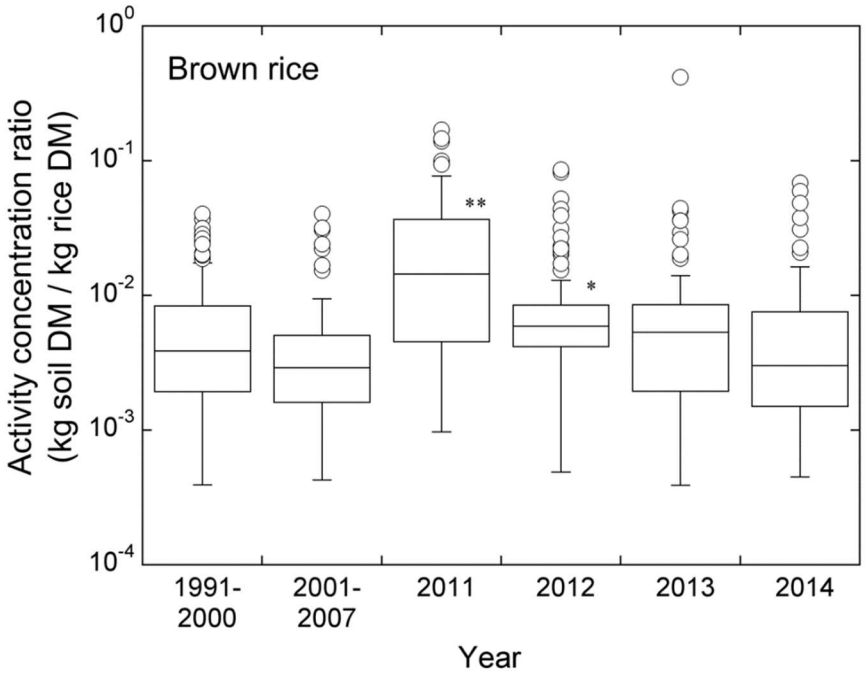

FIG. 4.9. Comparison of the soil-to-brown rice activity concentration ratio for radiocaesium before and after the FDNPP accident for field data with normal fertilizer conditions. The upper and lower quartiles are given by the box, whiskers show 10% and 90% values. Asterisks show ANOVA test results: $p<0.01$ (**) and $p<0.05$ (*)

4.3.1.5.Influence of K fertilizer on CR values

The K fertilizer status of soils has a major influence on Cs uptake by plants, and so the *CR* values from experiments, with either no K or no fertiliser are listed separately from field data with normal fertilizer conditions in Table 4.10. The "no-K/no-fertilizer" application data are compared with normally fertilized soil in Fig. 4.10. In 2011 and 2012, *CR* values for the variants "normal fertilizer application" and "no-K/no-fertilizer" were not significantly different. However, in 2013–2014, the GM of the *CR* values for these two variants were significantly—by about a factor of 7—higher than the "normal fertilizer" data ($p < 0.02$). A comparison of the *CR* data groups combined for 2011, 2012 and 2013–2014 showed no significant difference (Student's *t*-test), for the combined no-K/no-fertilizer data.

As part of the remediation strategy, additional K fertilizer was applied to selected paddy fields, which was not normal practice before the accident. Because additional potassium fertilizer was applied where necessary, in Fukushima Prefecture, the total radiocaesium activity concentrations in all brown rice has remained below the standard limit in Japan of 100 Bq/kg FM since 2015. A large dataset of CR values for brown rice collected by the Ministry of Agriculture, Forestry and Fisheries (MAFF) from Fukushima Prefecture has been summarized and evaluated by Yamamura et al. [4.92]; these data were separately reported in Table 4.10 (indicated as "unknown" in the column "Fertilizer application"):

- The conditions for the fertilizer application were not specified or compared with the normal pre-accident application. Therefore, it was not clear if the K fertiliser rate was similar to that before the accident or had been enhanced as part of the remediation programme;
- Many measurements were made in 2012–2015 in three districts, comprising 215 in Hamadori, 268 in Nakadori, and 75 in Aizu. However, only the ranges and median values of *CR* for brown rice were reported for the three districts.

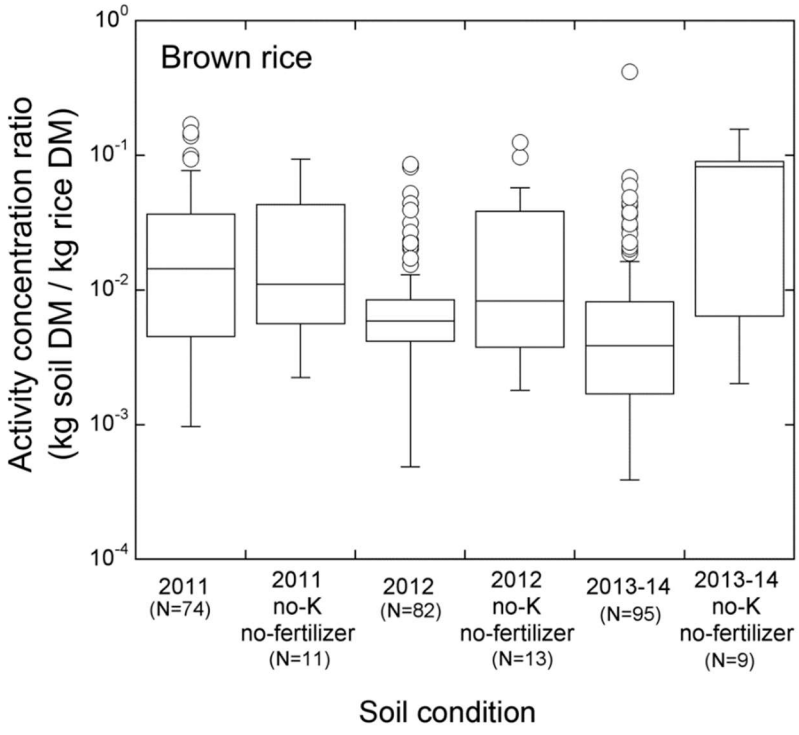

FIG. 4.10. Soil-to-brown rice activity concentration ratios of radiocaesium observed in paddies with normal fertilizer and no-K and no fertilizer applications in 2011–2014 (combined 2013–2014 data).

4.3.1.6.Effective half-life of CR values

In the 1960s, during and after the peak of nuclear weapons tests in the atmosphere, there was measurable interception of deposited fallout radionuclides by plants. By the 1980s, this contamination route was no longer relevant, so pre-accident *CR* values (1987–2007) represent uptake from the soil via the roots. The *CR* values varied in this period by more than an order of magnitude with a GM of about 5×10^{-3} in brown rice; CR showed a very slow decline with time (T_{eff} = 29 a) (Fig. 4.11) [4.47, 4.50, 4.59]. The data are consistent with the *CR* (soil-plant) values for rice in IAEA TRS 472 [4.2] because data by Komamura et al. [4.47] and Uchida and Tagami [4.59] accounted for most of the rice *CR* data for Cs in the IAEA report.

A slower reduction in the ^{137}Cs bioavailability in soil can be anticipated in the future compared with the decline observed between 2011 and 2012. Thus, in the long-term, *CR* values for rice are likely to be similar to those shown for 1987 to 2007. As an example, ^{137}Cs activity concentrations in rice taken from an environmental monitoring site near a nuclear power station in Miyagi Prefecture are shown in Fig. 4.12 (data only shown since 2011) [4.93]. The figure

shows the levelling off ^{137}Cs activity concentrations in rice after only 2–3 years following the FDNPP accident.

4.3.1.7.Balance of radiocaesium in paddy fields

The transfer of radionuclides from irrigation water to rice cultivated in paddy fields is potentially an important pathway for this crop. Water management of paddy fields varies under different climate conditions, and the scheme described here is generally used in the most affected Kanto and Tohoku areas. Paddy fields are ploughed in early-mid April and flooded with irrigation water in mid-late April. Rice plants are transplanted into the paddy fields in early-late May. The fields are flooded until July, and then the supply of irrigation water stops for ca. 1–2 weeks to change the redox status in soil (from reducing to oxidising conditions). Afterwards, the height of the water is controlled, varying from 0 to several cm repeatedly in 5–7-day cycles. During this period, the number of rice flowers and the grain mass increase. No more irrigation water is added to the fields during the period of 20–25 days before harvest.

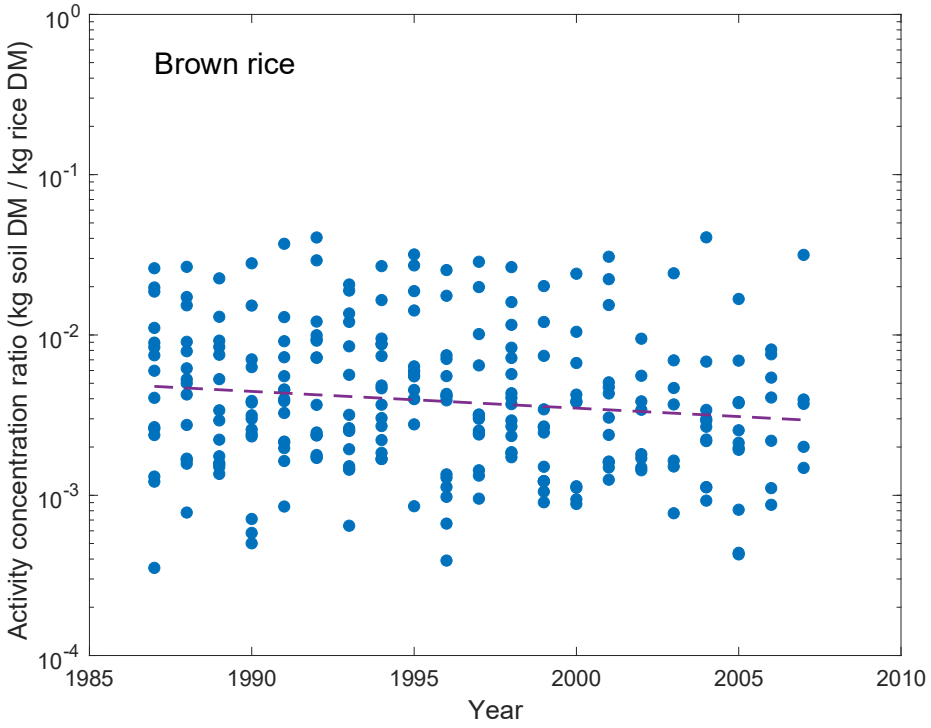

FIG. 4.11. Variation with time in pre-accident CR values of ^{137}Cs for brown rice.

The input of radiocaesium to paddy fields is due to inflow of irrigation water taken directly from contaminated catchments and/or from irrigation ponds. The radiocaesium balance in and out of the paddies can be quantified using:

$$\text{Balance of radiocaesium (\%)} = \frac{(FD + IN - BI - OUT)(\text{Bq/m}^2)}{\text{Activity concentration in soil (Bq/m}^2)} \times 100\% \qquad (4.3)$$

where *FD* is deposited radiocaesium (Bq/m^2), *IN* is inflow of radiocaesium via irrigation (Bq/m^2), *BI* is radiocaesium in biomass of above-ground parts of rice plants (Bq/m^2), and *OUT* is outflow via irrigation (Bq/m^2).

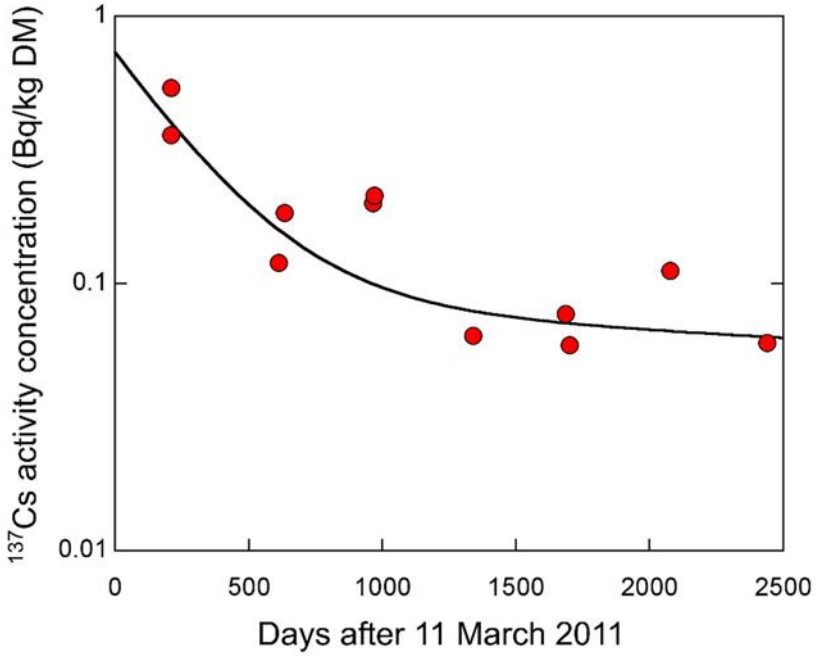

FIG. 4.12. Time-dependence of ^{137}Cs activity concentrations in brown rice from a single site in Miyagi Prefecture.

The balance of radiocaesium for a number of paddy fields after the 2011 accident (2011–2015) is given in Table 4.12. Over the years for which measurements were made, the mean balance was only −(0.49 ± 0.96)%. The low value indicates that radiocaesium in paddy fields is not being accumulated via the inflow. Radiocaesium in the paddy fields slightly decreased with time, and there was no evident seasonal pattern of inflow and outflow. The data also show that the radiocaesium content of paddy field does not greatly change before or after rice cultivation [4.16].

The potential importance of irrigation water has been considered for paddy fields in Fukushima Prefecture. When rice plants were grown in two grey lowland soils, each containing 180–250 Bq/kg DM of ^{137}Cs, and treated with irrigation water containing 0–1 Bq/L ^{137}Cs, the ^{137}Cs activity concentrations in the rice grain did not increase compared with controls [4.94]. Monitoring data for river water and irrigation water from lakes outside of the exclusion zone consistently showed radiocaesium activity concentrations below 1 Bq/L in September 2011 [4.95]. Therefore, it was clear that radiocaesium transfer from irrigation water to rice is negligible in most paddy fields in Fukushima Prefecture and the main source of radiocaesium for rice plants is radiocaesium in the soil [4.96].

TABLE 4.12. BALANCE OF RADIOCAESIUM OF INFLOW AND OUTFLOW OF IRRIGATION WATER IN PADDY FIELDS IN FUKUSHIMA PREFECTURE FROM 2011 TO 2015 (DATA FROM [4.16]).

Year	N [a]	Balance of radiocaesium (%)		
		Arithmetic mean ± SD	Minimum	Maximum
2011	1	−3.0	n.a.[b]	n.a.
2012	8	−2.2 ± 0.40	−1.0	0.13
2013	3	−1.2 ± 1.22	−2.5	–0.06
2014	2	0.20 ± 0.06	0.16	0.24
2015	2	0.04 ± 0.08	−0.02	0.09
All	16	−0.49 ± 0.96	−3.0	0.24

[a] the number of paddy fields
[b] not applicable

4.3.1.8.Loss of ^{137}Cs from paddy fields by paddling and irrigation

The loss of ^{137}Cs deposited to rice paddies during paddling and irrigation was studied in June 2011 and 2014 by comparing the outflow of ^{137}Cs and suspended sediments in a paddy field where the top 5–10 cm of soil was removed before cultivation with a control paddy [4.97]. Similar data for normal paddy fields were collected in 2014 [4.98]. The losses due to puddling and during the irrigation period are shown in Table 4.13.

TABLE 4.13. LOSS OF ^{137}CS FROM RICE PADDIES DURING CULTIVATION OF PADDY FIELDS

Site	Observation period	Initial ^{137}Cs deposition (kBq/m^2)	Loss of ^{137}Cs due to puddling (Bq/m^2)	Loss of ^{137}Cs during the irrigation period (Bq/m^2)	Loss of initial ^{137}Cs deposition (%/year)	Reference
Kawamata (normal cultivation)	2011	200	1240	102	0.67	[4.97]
Kawamata (surface scraped)	2011	5	48	317	7.3	[4.97]
Paddy A [a]	2014	231	5.8	0	0.003	[4.98]
Paddy B [a]	2014	208	3.2	3.1	0.003	[4.98]
Paddy C [b]	2014	121	26	14	0.032	[4.98]
Paddy D [b]	2014	210	40	92	0.063	[4.98]
Paddy E [b]	2014	207	42	0	0.020	[4.98]
Paddy F [b]	2014	287	79	0	0.028	[4.98]

[a] Ten-ei village, Fukushima Prefecture
[b] Minamisoma city, Fukushima Prefecture

Run-off from the paddies in 2011 has led to an input of radiocaesium into the receiving systems; however, the total amount was small and many paddy fields in the more highly contaminated

areas were not cultivated in 2011. After 2011, the losses of ^{137}Cs were consistently lower. The data are in general agreement with the data above on the balance of ^{137}Cs in rice paddies.

4.3.1.9.Effect of increased potassium application on rice cultivation

Radionuclide transfer to crops is affected by many different factors such as soil clay content, exchangeable K^+ status, pH, NH^+_4 concentration and organic matter content [4.1]. The importance of potassium in influencing ^{137}Cs transfer to crops was found many decades ago in studies on the environmental behaviour of global fallout radionuclides [4.99]. Increased administration of potassium fertilisers and other treatments were recommended to reduce radiocaesium uptake by plants and widely applied for many years in the areas affected by the Chernobyl accident in 1986 [4.100]. Phosphorus application, control of pH, ploughing and improvement in soil quality through drainage was also used to reduce *CR* of crops [4.101]. The reduction effect of phosphorus fertilizer was considered to occur via regulation of the Cs:K ratio in the solution [4.102]. Unlike affected areas after the Chernobyl accident, the effectiveness of phosphorus and pH in reducing radiocaesium *CR* was not confirmed in Japan. A major reason for the lack of effect of phosphorus and pH regulation was that conventional farming practice in Japan supports high level of soil fertility and stable levels of organic matter and soil pH.

Systematic analysis of the effects of nutrient (K^+) status on *CR* values carried out after the FDNPP accident showed that only a small fraction of contaminated agricultural soils had a relatively low fertility. The application of additional potassium was shown to ensure that adequate exchangeable K^+ was present in soil to minimise radiocaesium uptake. Additional potassium application was identified as the most effective additive for regulation of Cs uptake by crops in areas affected by the FDNPP accident. A threshold value of 25 mg K_2O /100 g soil DM was used to identify agricultural fields which needed additional K fertilisation to reduce radiocaesium *CR* values for rice [4.103]. Less readily available, non-exchangeable, potassium, (such as TPB-soluble potassium and/or hot nitrate extractable potassium) may also contribute to the regulation of Cs uptake [4.104].

An example of small-scale field study

An example of the reduction effect of the application of potassium in rice cultivation was demonstrated for paddy fields in Oguni, Date City in 2011 [4.105]. In these paddies, rice cultivation was conducted using the same soil management practices as applied before the FDNPP accident. The ^{134,137}Cs activity concentration in brown rice in several paddy fields exceeded the provisional permissible limit of 500 Bq/kg FM at that time, so planting in 2012 was prohibited by the government. Planting was resumed on the condition that additional potassium was applied in 2013 to achieve a minimum exchange potassium concentration of 25 mg K_2O 100/g DM in the soil. The remediation treatment (added-K), was compared with two experimental control paddy fields where there was no additional K applied (non-K), as in the previous soil management system.

The arithmetic mean and range of ^{137}Cs activity concentrations in the added-K and non-K treatment paddy soils were similar at 1980 (1220–2950, n = 29) and 2260 (1930–2590, n = 2) Bq/kg DM, respectively. After rice harvest, the arithmetic mean and range of exchangeable K concentration in added-K soils was 34 (16–107) and was much lower in non-K soils at 10 (6–13) mg K_2O/100 g DM soil. The arithmetic mean and range of ^{137}Cs activity concentrations in brown rice (n = 29) harvested in the added-K fields were also reduced to 6.1 and 1.1–24 Bq/kg FM, respectively, whereas the arithmetic mean and range for brown rice (n=2) in the non–K

fields was 105 and 94–115 Bq/kg FM, which exceeded the lower standard limits in 2013 of 100 Bq/kg FM (including ^{134}Cs).

A large-scale study in Fukushima prefecture by MAFF

Based on an evaluation of remedial options implemented after the FDNPP accident, a large number of *CR* values were collated for soils with measured potassium concentrations. Exchangeable potassium is routinely measured as an indicator of the availability of potassium in the soil.

The large-scale studies showed that *CR* values decreased sharply when exchangeable potassium in soil increased. (Fig. 4.13).

MAFF measured radiocaesium activity concentrations in soil and rice in a large number of paddy fields throughout Fukushima prefecture [4.92] and *CR* values were calculated (Table 4.14). There was a large percentage of rice samples (varying from 81% in 2012 to 17% in 2015) where the ^{137}Cs activity concentration was below detection limits[3] and the minimum *CR* is occasionally overestimated due to the use of the detection limit as default activity concentration in such cases. To avoid exceeding the standard limit of radiocaesium in rice, MAFF developed statistical models to describe the effect of K fertilizer on radiocaesium activity concentrations in rice.

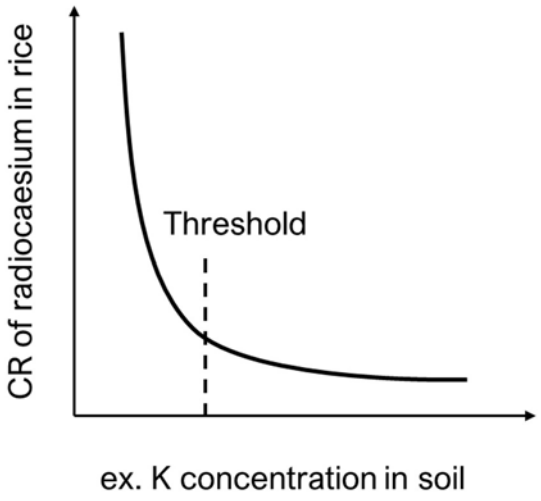

FIG. 4.13. Theoretical relationship between soil exchangeable K and CR of radiocaesium in rice grains

Values in Table 4.14 were only calculated for samples with radiocaesium activity concentrations that exceeded the detection limit, so these data do not fully reflect the time dependences of *CR* values. The major outcomes of the study were that (1) *CR* was highly dependent on soil potassium availability, and (2) *CR* decreased rapidly from 2012 to 2013 in

[3] In 2012, the minimum detection limit was higher than in subsequent years.

rice, but less rapidly from 2013–2015, and (3) a longer observation time is required to assess the ongoing trend.

TABLE 4.14. RADIOCAESIUM ACTIVITY CONCENTRATION RATIOS *CR* (KG SOIL DM / KG RICE FM) FROM SOIL TO RICE IN 2012–2017 FROM LARGE SCALE OBSERVATION BY MAFF [4.92]

Year	N [a]	M [b]	Radiocaesium *CR* (kg soil DM / kg rice FM)				Exchangeable K (mg K/kg soil DM)	
			GM [c]	GSD [d]	Minimum	Maximum	Minimum	Maximum
2012	158	128	5.7×10^{-3}	4.3	4.6×10^{-4}	1.7×10^{-1}	33	1400
2013	78	18	2.1×10^{-3}	3.2	2.2×10^{-4}	1.2×10^{-1}	33	490
2014	162	44	1.9×10^{-3}	2.7	2.4×10^{-4}	1.8×10^{-1}	26	540
2015	181	63	2.0×10^{-3}	2.7	2.1×10^{-4}	2.4×10^{-2}	51	690
2016	172	22	1.6×10^{-3}	3.1	1.3×10^{-4}	9.8×10^{-2}	20	590
2017	143	24	1.1×10^{-3}	3.2	1.8×10^{-4}	9.2×10^{-2}	39	470

[a] the number of measured samples
[b] the number of samples with radiocaesium activity concentrations above detection limit, for which statistics are shown
[c] geometric mean
[d] geometric standard deviation

It was initially difficult to develop suitable remediation procedures based on a soil concentration limit for rice paddies because there was a large variation in *CR* values within crop samples. Therefore, the focus was on studies to determine the factors controlling the variations in *CR*. Based on data obtained within the monitoring programme, as listed in Table 4.14 for rice, [4.92] suggested a simple statistical model to estimate the variability of the relationship between radiocaesium *CR* values and the exchangeable potassium concentration in the soil:

$$CR^{\text{expect}} = \exp\left(b_0 + b_1 \ln(K_{\text{ex}})\right) \quad (4.4)$$

Where CR^{expect} is the expected *CR* values and K_{ex} is the concentration of exchangeable potassium in soil at the time of harvest (mgK/kg DM). The parameter b_1 is constant, while b_0 depends on year and was derived by fitting to the concentration ratios for the years 2012–2017 (Table 4.15).

TABLE 4.15. PARAMETERS OF EQ. (4.4) DESCRIBING DEPENDENCE OF RADIOCAESIUM ACTIVITY CONCENTRATION RATIOS FOR CEREALS ON EXCHANGEABLE POTASSIUM IN THE SOIL

Species	b_0						b_1
	2012	2013	2014	2015	2016	2017	
Rice	0.61	0.23	0.47	0.51	0.39	−0.03	−1.26

Using these parameters, the relationship between soil exchangeable potassium concentration and *CR* values is presented in Fig. 4.14. The vertical axis shows a log scale of *CR* data thus the shape of the curves for all years were consistent with those in Fig. 4.13. The grey bars show the CR values calculated using the detection limit as default for the measurements with radiocaesium activity concentrations below the detection limit.

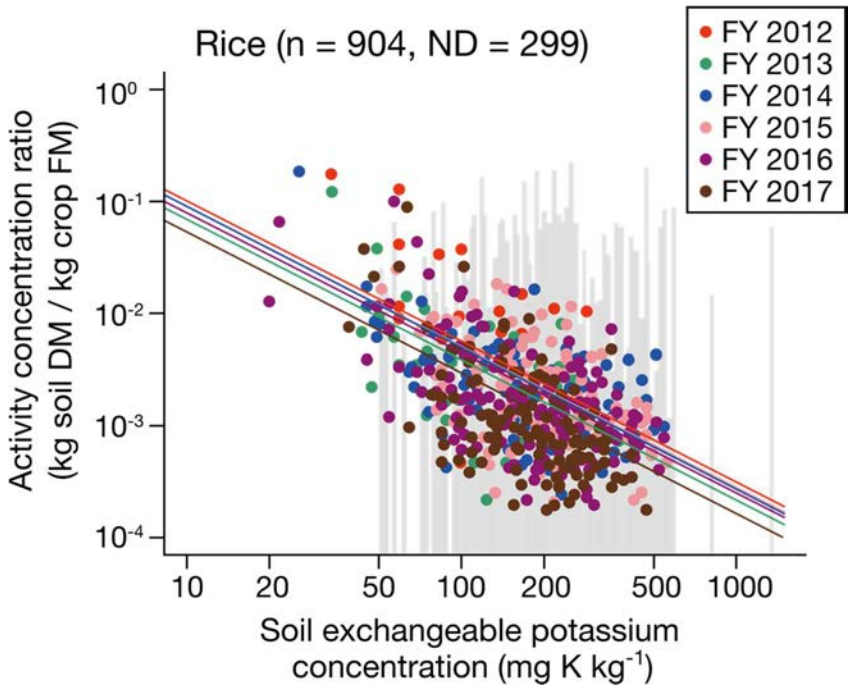

FIG. 4.14. Relationship between soil exchangeable potassium concentration K_{ex} (mg K/kg) and radiocaesium activity concentration ratio CR (kg soil DM / kg plant FM) for brown rice (n = number of analysed samples; FY = fiscal year). Tops of the grey bars in the figure are CR values calculated using the detection limit for radiocaesium for a number (ND) of samples in which radiocaesium activity concentration were below the detection limit

4.3.1.10. Summary and limitations

Summary

Rice is a staple food in Japan and the concentration ratio (*CR*) data soil to rice are important to estimate the internal doses to people from this crop. Since rice was planted after the deposition of radionuclides, the uptake of radiocaesium from the soil to rice is the dominant process; the use of irrigation water containing radiocaesium was not a major source of radiocaesium to rice.

Before the FDNPP accident, the concentration ratios reported for rice were determined for quasi equilibrium conditions. These data were not applicable in the first years after the FDNPP accident because the freshly deposited radiocaesium in soil was initially slightly more mobile than in subsequent years.

Compilation of soil-to-brown rice *CR* values showed that the transfer of radiocaesium in 2011 for normal fertilizer conditions was 3 to 4 times higher than before the accident. *CR* values in 2012 were still increased, but less enhanced than in 2011, but the CR values in the subsequent

years—when approaching equilibrium conditions in soil—returned rapidly to values similar to those before the FDNPP.

Paddy fields in Japan are generally well-fertilised with high application of potassium fertilizers and/or manure. Before the FDNPP accident, there were some small areas, especially rice paddies, that were not well fertilized because excessive K fertilizer application can negatively affect rice quality. A level of 25 mg/kg of exchangeable potassium was used to identify agricultural fields that needed additional potassium fertilizer to reduce radiocaesium in rice.

In 2011, on experimental rice paddies, normal cultivation including flooding, puddling, irrigation and drainage, led to losses from paddy fields of less than 1% of the ^{137}Cs inventory present. In the following years, when radiocaesium was less available for surface run-off because it was mixed with deeper soil layers, consequently, much lower loss rates of well below 0.05% were reported.

Limitations

Most of the data were collected for soils that were supplied with sufficient potassium for intensive rice production.

Soil characteristics affect radiocaesium fixation to the soil solid phase. Currently, only a few data are available on the effect of soil characteristics, especially after 2011 and there is little variation in *CR* as a function of soil type evident from currently available data. Data on the classification method based on soil types by IAEA in TRS 472 are included in Table 4.14. Limited evidence showed that radiocaesium transfer to rice differed between the clay and organic soil groups in 2011 but more data are needed for statistical analysis.

4.3.2. Transfer to green tea

4.3.2.1 Introduction

In Japan, tea plant (*Camellia sinensis* L.) cultivation is mainly aimed at the production of green tea. Tea plants grow from March to November, so growth had already started in some regions at the time of the FDNPP accident. In February and March, before the first new shoots of the year appear, the tea tree canopy is pruned to ensure the growth of good quality new shoots which can be easily harvested. From April to August, tea shoots are harvested two or three times. The final autumn trimming is carried out in October (The Annual Scientific Conference of Tea, [4.106]). A schematic of a tea plant field is shown in Fig. 4.15.

Due to the management method, radionuclides that were directly deposited onto tea plants, which mainly occurred in March 2011, were partially removed during the initial routine pruning event. The pruning made it difficult to determine the interception of radionuclides by tea plants. In tracer studies [4.107, 4.108], transfer to plants was below measurable levels when soil was contaminated, but when above-ground plant parts were contaminated, radiocaesium was measured in new shoots having emerged after radionuclide deposition. These data enabled estimation of the amount of radiocaesium in new shoots that had been translocated from other parts such as old leaves, stems and trunks of contaminated tea plants.

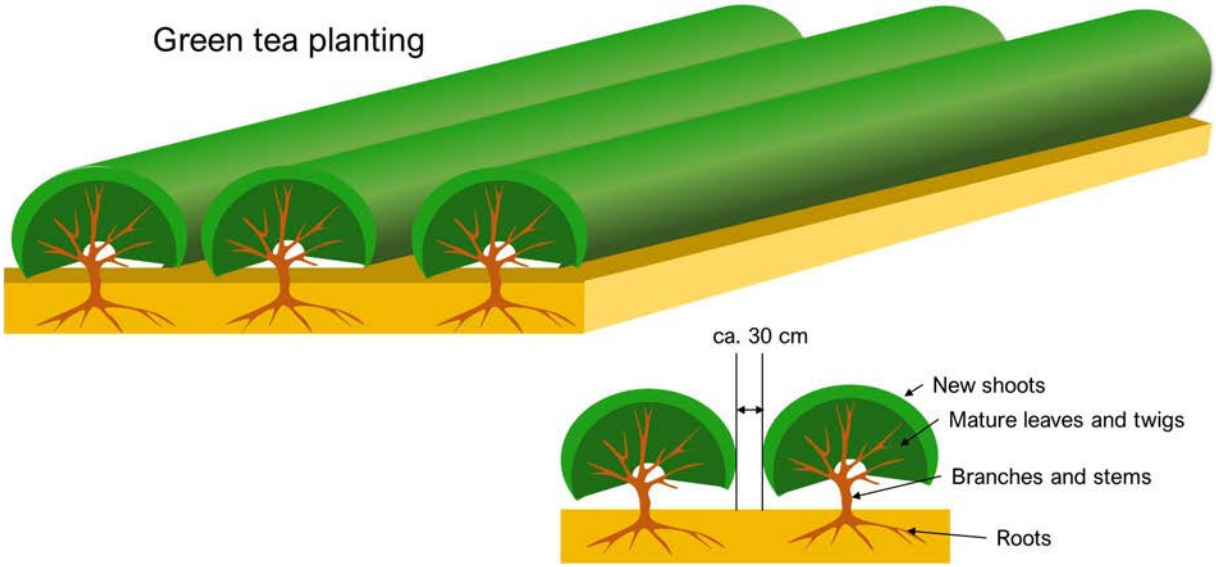

FIG. 4.15. Diagram of tea plant cultivation methodology in Japan

4.3.2.1.Relationship between radiocaesium concentrations in old leaves and new shoots

The translocation factor (f_{tr}) was calculated using the measured radiocaesium activity concentration in new shoots of green tea (Bq/kg DM) divided by the concentration in old leaves (Bq/kg DM) at harvest (Chapter 2) [4.109–4.116] In the study of Shiraki et al. [4.110], radiocaesium data for new leaves were provided in Bq/kg FM so the values were converted using a dry/wet ratio of 0.263 using data from Shiraki et al. [4.112].

The f_{tr} values are plotted after the FDNPP accident for 2011 to 2014 in Fig. 4.16. In 2011, translocation was expected to be small as radiocaesium was deposited onto old leaves (arithmetic mean f_{tr}=0.8). However, in March 2012, one year after the accident, the f_{tr} values increased sharply indicating that the new shoots had higher radiocaesium activity concentrations than the old leaves (in this case, old leaves emerged in 2011). Even in 2013 and 2014, the arithmetic mean of f_{tr} was still well above 1.0. These observations are consistent with the behaviour of potassium in perennial plants. Before the dormant period, caesium is transported from the old leaves to the stems and roots, then it is remobilized when the new leaves emerge.

An approach for quantifying translocation has been developed to utilise data from a radiotracer experiment using tea plants where a ^{137}CsCl solution was coated on existing leaves, and three weeks later radiocaesium had translocated to four subsequently developed new leaves [4.117]. Application of a ^{137}CsCl solution to the upper surface of existing leaves led to less ^{137}Cs uptake and translocation to new shoots compared with application to the lower surface. ^{137}Cs activity concentrations (Bq/kg DM) were measured in the following samples:

- Tea leaves existing at the time of deposition;
- Tea leaves at harvest that existed at deposition;
- Tea leaves at harvest that developed after radionuclide deposition.

Results are summarized in Table 4.16. Laboratory data were lower than 1.0 which is consistent with the field observation in 2011.

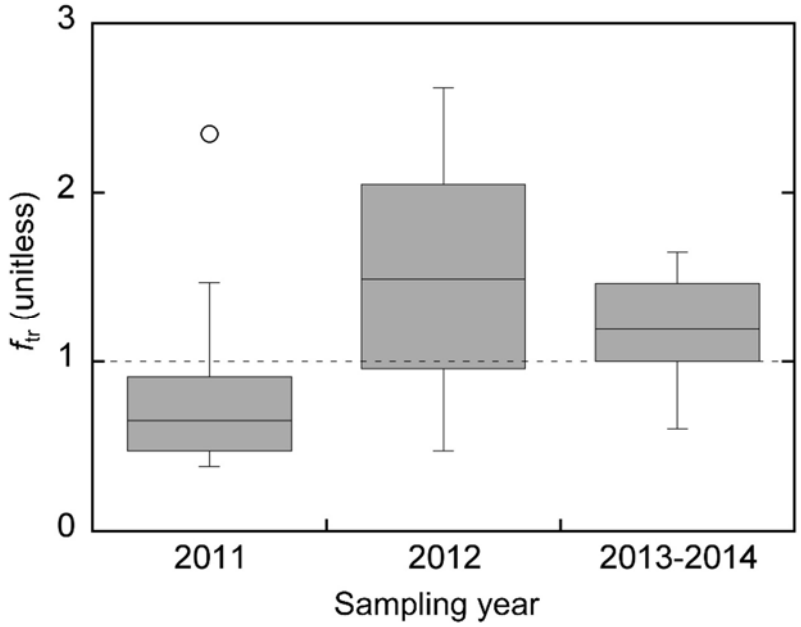

FIG. 4.16. Mass translocation ratios between new shoots and old leaves of tea plants in 2011–2014

TABLE 4.16. TRANSLOCATION FACTOR (f_{TR}) FROM OLD LEAVES FOR TEA SHOOTS (DATA FROM [4.117])

^{137}Cs application to old leaves:	Source	Time lapse after contamination	f_{tr} on activity concentrations at sampling	f_{tr} based on the initial concentration in old leaves
Upper surface	^{137}CsCl	3 weeks	0.09	0.09
Lower surface	^{137}CsCl	3 weeks	0.65	0.45

4.3.2.2. Concentration ratios for green tea

Honda and Miyazaki [4.113] removed the above-ground part of tea plants on 23 March 2011 in Saitama Prefecture, just after the period of highest deposition from the FDNPP accident. Diagrams of the cutting point and subsequent growth are shown in Fig. 4.17. The radiocaesium activity concentrations in these samples, arising only from root uptake, in 2012–2014 were less than 2.1 Bq/kg FM; ^{137}Cs activity concentrations before accident were less than 0.1 Bq/kg FM [4.93].

4.3.2.3.Ecological half-lives

Continuous measurements of ^{137}Cs in newly grown tea shoots at the same sampling sites enabled the estimation of the time-dependence of radiocaesium uptake and retention [4.118]. For data sets with only a one-year sampling period, a single exponential function provided a good fit to the data. For a longer timescale, effective half-lives were derived using a double exponential analysis. Data on half-lives for short-term measurements and over longer timescales are summarized in Table 4.17.

FIG. 4.17. Diagrams showing green tea treated on 23 March 2011 in a green tea field [4.113] and the new shoots growing image several months after the treatment.

TABLE 4.17. FAST AND SLOW EFFECTIVE HALF-LIVES T_{EFF} (D) OF ^{137}CS IN NEW SHOOTS OF TEA PLANTS AFTER THE FDNPP ACCIDENT

Fraction	N [a]	T_{eff} (d)				Reference
		GM [b]	GSD [c]	Minimum	Maximum	
Fast T_{eff}	14	50	1.6	26	105	[4.109, 4.115, 4.116, 4.119]
Slow T_{eff}	11	416	1.8	222	1538	[4.113–4.116, 4.118, 4.119]

[a] the number of T_{eff} data
[b] geometric mean
[c] geometric standard deviation (unitless)

Values of T_{eff} derived from Japanese data after the Chernobyl accident were also calculated using environmental monitoring data (Table 4.18). There was no significant difference between the short or longer T_{eff} observed after the Chernobyl and FDNPP accidents.

TABLE 4.18. FAST AND SLOW EFFECTIVE HALFLIVES T_{EFF} (D) OF ^{137}CS IN TEA LEAVES OBSERVED AFTER THE CHERNOBYL ACCIDENT

Fraction	N [a]	T_{eff} (d)				Reference
		GM [b]	GSD [c]	Minimum	Maximum	
Fast T_{eff}	9	66	1.8	25	125	[4.118, 4.120]
Slow T_{eff}	9	902	3.5	342	15900	[4.118, 4.120]

[a] the number of T_{eff} data
[b] geometric mean
c geometric standard deviation (unitless)

4.3.2.4.Summary and limitations

Summary

Data on transfer parameters for green tea plants are reported here for the first time in an international compilation.

The transfer of radiocaesium to tea leaves via root uptake from soil was similar to that reported for herbaceous plants. However, the radiocaesium activity concentrations in new shoots were greater than those that would be expected due to soil uptake due to translocation from plant parts that were contaminated during the initial deposition after the accident. The translocation ratio from old leaves to new leaves increased in the second year after the FDNPP accident compared with the first year and declined thereafter. Available data indicate that the increase in 2012 was due to significant remobilization of radiocaesium that was stored in old leaves, stems and roots of the tea tree during the winter period.

The *CR* values were low for green tea, therefore, soil to plant uptake was relatively small compared with the translocation from plant surfaces.

Effective half-lives after the FDNPP accident and the Chernobyl accidents were similar for both the fast and slow fractions in Japanese tea plants.

Limitations

Tea plant management, such as controlling the tree shape and the schedule of pruning differs between countries. Tea plants are intensively managed in Japan and trees are frequently pruned which decreased the amount of radiocaesium attached to the above-ground part of trees, especially in old leaves and twigs. However, if the trees are not frequently pruned then the rate of removal of radiocaesium may be lower than reported after the FDNPP.

4.3.3. Transfer to fruit

4.3.3.1.Introduction

Fukushima Prefecture is a major producer of deciduous fruit in Japan [4.121]. Fukushima had the 2nd highest peach production amongst all 47 prefectures in Japan both before and after the FDNPP accident, so the production rate did not greatly change. Similarly, production of Japanese pear was the third highest production in 2010 among all prefectures (producing 9% of the total harvest in Japan) and was the 4th highest producer in 2017 (8% of the total). In contrast, for persimmon, Fukushima produced 7% of the total harvest in 2010, which was the 4th largest prefecture production in Japan, but in 2017 the production rate in Fukushima prefecture decreased to only 4% of the total persimmon harvest. The changes with time in production quantities are shown in Fig. 4.18 for peach and persimmon [4.122].

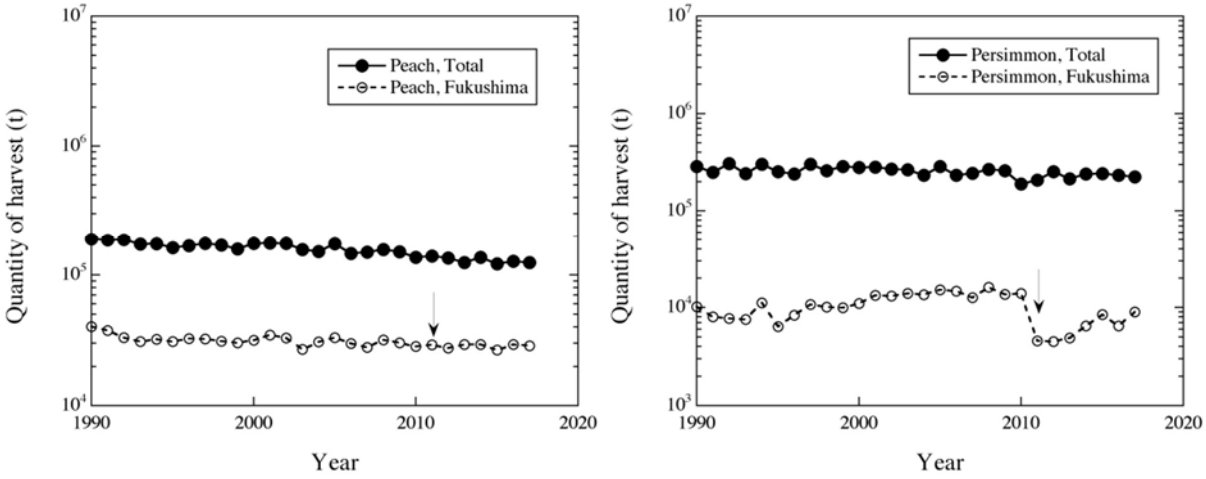

FIG. 4.18. Quantities of annual harvest for peach and persimmon in Fukushima prefectures and all Japan. The arrow shows the time of FDNPP accident.

Fruit consumption is important both locally in the prefectures nearer to the FDNPP and in Japan as a whole. The fruit produced is eaten fresh, dried or cooked depending on the type of fruit. Persimmon is often consumed as dried astringent persimmon (Hoshi-gaki) and semi-dried astringent persimmon (Ampo-gaki), both are inedible when fresh and are characterized by strong astringency [4.123]. Semi-dried persimmon fruit is a local specialty in Date city (northern Fukushima), and production is under voluntary suspension in relevant areas. Drying fruit can lead to higher radiocaesium activity concentrations and, therefore, a higher probability of exceeding activity limits.

After the FDNPP accident, radiocaesium activity concentrations in different types of fruit exceeded activity limits for foodstuffs in Japan in 2011, leading to restrictions on fruit production in Fukushima Prefecture. From May 2011, a few fruit samples had radiocaesium activity concentrations that exceeded the provisional activity limits of 500 Bq/kg FM effective until 31 March 2012. The activity limit was reduced to 100 Bq/kg FM from 1 April 2012 [4.124]. The initial activity limit was exceeded in only 28 samples of eight different fruit types, most of these samples were taken in Fukushima Prefecture. The maximum radiocaesium activity concentration measured in fruit was in the fruit of the evergreen Yuzu tree, which is related to the lemon tree. The fruit has little flesh and an acidic taste and is mainly used for its zest in traditional dishes, and in jam, liquor and as an additive in miso, which is a fermented soybean paste.

Typical flowering periods and maximum reported radiocaesium activity concentrations in fruits are summarised in Table 4.19.

Fruit is the structure of angiosperms that develops from the ovary (“true” fruit) or its appendage (“false” fruit) after fecundation as the enclosed seed or seeds mature. Fruit are produced from woody trees (e.g., apple, peach, grape, and cherry), perennial shrubs (e.g., blueberry, gooseberry, redcurrant) and herbaceous plants (e.g., banana, melon, and strawberry). This section is largely focused on woody fruit trees which intercepted and partially retained radionuclides released after the FDNPP accident in the above-ground/or aerial parts of the plant. Information for some perennial shrubs is also included. Herbaceous fruit plants, such as strawberries, musk melons and watermelons, are not considered because they are cultivated

under cover in controlled conditions in Japan and their production was not affected by the FDNPP accident.

TABLE 4.19. RADIOCAESIUM ACTIVITY CONCENTRATION IN VARIOUS FRUIT IN FUKUSHIMA PREFECTURE WHERE PERMISSIBLE LEVELS WERE EXCEEDED (ADAPTED FROM HAMADA ET AL. [4.125]).

Fruit type (English – Japanese [a] and Latin names)	Typical flowering period	^{134,137}Cs (Bq/kg FM)	Sampling date in 2011
Japanese apricot – Ume, *Prunus mume*	Late Feb–Mid March	760	9 June
Loquat – Biwa, *Eriobotrya japonica*	November–December	530	13 July
Fig – Ichijiku, *Ficus carica*	April	520	19 July
Yuzu – *Citrus junos*	Beginning of June	2400	24 August
Chestnut – Ohshu-guri, *Castanea crenata*	Late May–start of June	2040	5 September
Pomegranate – Zakuro, *Punica granatum*	Late May–June	560	13 October
Persimmon – Kaki, *Diospyros kaki*	Late May–start of June	670	4 November
Kiwi fruit – *Actinidia deliciosa*	Middle May–late May	1120	14 November
Japanese pear – *Pyrus pyrifolia* var. *culta*	Middle April–late April	48	17 August
Apple – *Malus pumila* Mill	Late April–mid May	99	2 November
Sweet cherry – *Prunus avium (L)*	April	96	2 June
Blueberry – *Vaccinium virgatum* Aiton	May–start of June	270	5 July

[a] Japanese name given where it differs from English translation.

4.3.3.2.Key processes involved in radionuclide transfer to fruit

The main processes governing the transfer of radionuclides to fruit after deposition are illustrated in Fig. 4.19. and are described below in the context of the experience in Japan following the FDNPP accident with a focus on woody fruit trees.

Interception of radionuclides by the exposed surfaces of the tree, absorption and subsequent translocation to the fruit

Woody fruit trees intercepted and partially retained radionuclides released after the FDNPP accident in the above-ground/aerial parts of the plant. The intercepted radionuclides could then be translocated to the fruit in subsequent annual harvests following deposition. The deposition of radiocaesium due to the FDNPP accident in March 2011 occurred when most deciduous fruit trees, except for Japanese apricot, were in the dormant stage prior to bud burst. Therefore, most deciduous fruit trees had not developed leaves, and only the bark was directly contaminated.

Radiocaesium in the outer bark of the tree could therefore be translocated, and partially stored in the storage organs (wood, roots), and subsequently be transferred to fruits in subsequent annual harvests [4.126]. Epiphytic lichens and bryophytes hosted by some trees in old orchards may comprise an additional external storage component for intercepted radionuclides. These species have a high interception and storage capacity of water and pollutants and can release them in the stemflow providing a secondary source of contamination [4.127, 4.128].

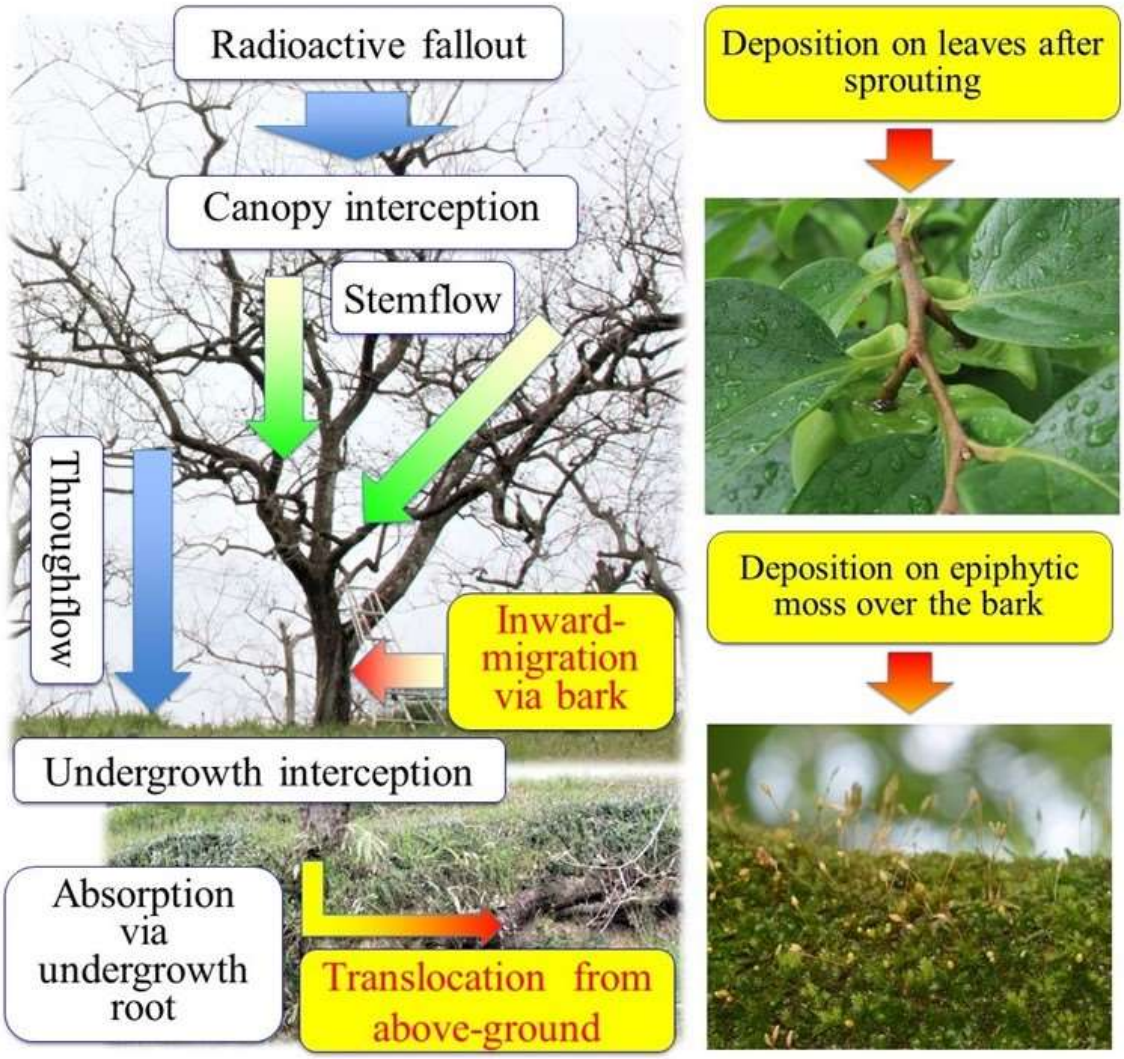

FIG. 4.19. Major transfer processes resulting in redistribution of radionuclides in deciduous orchard during dormancy: case of persimmon.

Uptake of radionuclides from the soil via roots

Radionuclides in the soil can be taken up into trees and plants via the root system and be translocated to fruit during its development. In Japan, measurements made of activity concentrations in soil showed that, at least until autumn 2011, more than 80% of the radiocaesium in the soil in orchards remained in the top 3 cm [4.129, 4.130]. The upper soil layer contains roots of undergrowth plants that grow under the fruit trees in most orchards, but not roots of fruit trees which are predominantly located lower down the soil profile [4.131]. It was therefore considered to be unlikely that root uptake of radiocaesium by fruit trees was initially important after the FDNPP accident.

The process of root uptake may have become gradually more important in subsequent years following the accident due to radiocaesium slowly migrating down the soil profile. The speed

of ^{137}Cs migration after the accident was quantified from 15 April 2011 over 6 years in five orchard soils with different textures with a migration rate of 0.4 to 1.0 cm/a [4.131].

Two other processes which may be important in specific situations, but which normally do not contribute significantly to radionuclide activity concentrations in fruit from trees, are (i) direct deposition onto developing fruit; and (ii) soil contamination of fruit due to resuspension and soil adhesion onto fruit, such as herbaceous fruit plants (e.g. strawberries), that grow close to the soil surface.

4.3.3.3.Transfer of radiocaesium to fruit

Parameter values of radiocaesium transfer to fruit are summarized and compared with those observed after the Chernobyl accident [4.132–4.136] and from experimental studies [4.137–4.141]. Knowledge on quantification of the transfer of radionuclides to fruit has been summarised in IAEA documents on the human food chain radionuclide transfer parameters [4.1, 4.2, 4.142].

Different methods that can be used to quantify the transfer of radiocaesium to fruit are outlined and the relevant data are reported. A large number of methods of quantification have historically been used to reflect the complex nature of radiocaesium transfer to fruit. A consistent notation is used here of "f-s", "f-l" or "f-b" to denote transfer from soil to fruit, leaf to fruit or bark to fruit, respectively.

Aggregated transfer factors

One method of estimating the overall transfer of radionuclides to fruit is to derive the ratio between the radionuclide activity concentration in fruit (Bq/kg, FM or DM) at harvest and the radionuclide deposition per unit area (Bq/m^2) in soil (i.e. T_{ag} as defined in Section 2.3). The calculated $T_{\mathrm{ag}}^{\mathrm{f\text{-}s}}$ uses soil as a reference compartment to normalise the data; this does not necessarily mean that the soil is the source of the contamination. T_{ag} values implicitly include contributions from all transfer processes leading to activity concentrations in fruit but do not identify which of these processes are significant, insignificant or not present at the time that the T_{ag} is measured. Commonly, the amount in soil is quantified on the basis of the amount of radionuclide deposited per unit area (Bq/m^2) at the time of deposition, to give the aggregated transfer factor, termed $T_{\mathrm{ag}}^{\mathrm{f\text{-}s}}$ (m^2/kg) and defined as:

$$T_{\mathrm{ag}}^{\mathrm{f\text{-}s}} = \frac{A_f}{A_{\mathrm{s}}} \tag{4.5}$$

where A_f is the activity concentration in mature fruit at harvest (Bq/kg FM) and A_{s} is the activity per unit area of soil at the time of deposition (Bq/m^2).

Alternatively, the aggregated transfer factor, $T_{\mathrm{ag}}^{\mathrm{f\text{-}s}}$ can be expressed using a deposition estimate based on a mass value, calculated as Bq/kg DM in soil. In this case, the aggregated transfer factor ($T_{\mathrm{ag}}^{\mathrm{f\text{-}s}*}$) is defined as follows:

$$T_{\mathrm{ag}}^{\mathrm{f\text{-}s}*} = \frac{A_f}{A_{\mathrm{s}*}} \tag{4.6}$$

where $A_{\mathrm{s}*}$ is the radionuclide activity per unit mass of soil at the time of deposition in averaged over the top 20 cm (Bq/kg DM). The units are therefore (kg soil DM / kg fruit FM).

These two expressions of overall transfer to fruit using T_{ag} values reflect the same transfer processes but are normalised to the amount of radionuclide in soil expressed in different units. To distinguish between these terms in the text, the terms $T_{ag}^{f\text{-}s}$ and $T_{ag}^{f\text{-}s*}$ are used to present the data expressed as per unit area of soil and per unit mass of soil, respectively.

The $T_{ag}^{f\text{-}s}$ factors (m^2/kg FM) using measurements of activity in soil or aerial surveys of deposition to determine the fruit T_{ag} values from fruit monitoring data derived after the FDNPP accident are given in Table 4.20.

TABLE 4.20. AGGREGATED TRANSFER FACTOR VALUES $T_{AG}^{F\text{-}S}$ FOR RADIOCAESIUM IN HARVESTED FRUIT FROM TREES CONTAMINATED IN 2011 AFTER THE FDNPP ACCIDENT

Type of fruit	Month	N	$T_{ag}^{f\text{-}s}$ (m^2/kg FM)	Reference
Japanese apricots	May–June	71	$(2.0–6.0) \times 10^{-3}$	[4.143]
Cherries	May–June	13	$(7.0–1.0) \times 10^{-3}$	[4.143]
Peaches	July–August	148	$(4.0–5.0) \times 10^{-4}$	[4.143]
Grapes	July–August	— [a]	$(2.0–3.0) \times 10^{-4}$	[4.143]
Apples	September–November	56	$(3.0–7.0) \times 10^{-4}$	[4.143]
Pears	September–November	32	$(2.0–3.0) \times 10^{-4}$	[4.143]
Persimmon	October	1	9.7×10^{-4}	[4.123]

[a] no data

Data from after the FDNPP accident (Table 4.20) show that the transfer to fruit was highest for Japanese apricots and cherries in Fukushima prefecture harvested in May – June, 2 months after the accident. Higher $T_{ag}^{f\text{-}s}$ values would also be expected for fruit growing in areas at lower-elevation, where trees and shrubs were at a more developed growth stage at the time of deposition. The $T_{ag}^{f\text{-}s}$ values were one order of magnitude lower for those fruits that were at a dormant stage, i.e. before emergence of leaves and fruit buds at the time of deposition, such as apples, pears and grapes, as shown in Table 4.20.

$T_{ag}^{f\text{-}s}$ values were also reported in the first year after the Chernobyl accident (Table 4.21). Higher values were consistently reported for fruit harvested in 1986 after the Chernobyl accident compared with those measured in 2011 after the FDNPP accident. A possible reason for the difference is that the FDNPP accident deposition occurred earlier in the year when few fruit trees had started to produce buds and leaves so radiocaesium interception by the above-ground part of the tree and any subsequent translocation was lower. The higher $T_{ag}^{f\text{-}s}$ values in Table 4.20 are for fruit species that already had well developed foliage at the time of deposition, such as Japanese apricots and cherries (harvested in May and June) and are broadly similar to those observed in orchard fruit after the Chernobyl accident in 1986. In contrast, the lowest $T_{ag}^{f\text{-}s}$ values measured in grapes in Northern Italy in 1986 after the Chernobyl accident are similar to most of the values measured after the FDNPP accident in Japan; in both cases, deposition occurred just before, or about the time of, leaf emergence.

The $T_{ag}^{f\text{-}s}$ for fruit harvested in the year following deposition for both accidents are within two orders of magnitude and vary in a range of 10^{-4}–10^{-2} m^2/kg FM.

Table 4.22 gives $T_{ag}^{f\text{-}s*}$ values, i.e. the aggregated transfer factor expressed via radiocaesium activity concentrations in soil (Bq/kg DM). These data were reported after the FDNPP accident for fruit harvested in 2011. The $T_{ag}^{f\text{-}s*}$ values cannot be directly compared to the data in Tables 4.20 and 4.21. However, if an approximate conversion is carried out between Bq/kg and Bq/m^2 for soil depth of 20 cm, the $T_{ag}^{f\text{-}s*}$ values in Table 4.22 are broadly consistent with those in Table 4.20, i.e. in the order of (1–10) × 10^{-4} m^2/kg.

TABLE 4.21. AGGREGATED TRANSFER FACTOR $T_{AG}^{F\text{-}S}$ (M^2/KG FM) VALUES FOR RADIOCAESIUM IN HARVESTED FRUIT FROM TREES CONTAMINATED IN 1986 IN SOUTHERN EUROPE AFTER THE CHERNOBYL ACCIDENT

Type of fruit	Period in 1986	N [a]	$T_{ag}^{f\text{-}s}$ (m^2/kg FM)	Reference
Hazelnut	August–September	36	3.2×10^{-2}	[4.133] [b]
Chestnut	October–November	— [d]	2.4×10^{-3}	[4.133] [b]
		—	$< 5.0 \times 10^{-3}$	[4.133] [b]
		—	2.5×10^{-3}	[4.133] [b]
Olive	October–February	3	$< 3.8 \times 10^{-3}$	[4.133] [b]
Walnut	September–November	—	5.8×10^{-3}	[4.133] [b]
Pear	June–September	5	3×10^{-3}	[4.136]
		—	3×10^{-3}	[4.144] [c]
Apricots	June–July	—	1×10^{-2}	[4.144] [c]
Sour cherry	June–August	2	3×10^{-2}	[4.145] [c]
		1	3×10^{-2}	[4.145] [c]
		5	2×10^{-2}	[4.145] [c]
Cherry	June–July	3	5×10^{-3}	[4.136] [c]
		—	3×10^{-2}	[4.144] [c]
Peach	July–August	5	3×10^{-3}	[4.136] [c]
		2	3×10^{-3}	[4.136] [c]
		—	1×10^{-2}	[4.144] [c]
Apple	July–October	6	3×10^{-3}	[4.136] [c]
		—	2.1×10^{-3}	[4.133] [b]
		—	$(2–4) \times 10^{-3}$	[4.144] [c]
Grapes	August–September	21	2×10^{-4}	[4.146] [c]
		9	4×10^{-4}	[4.146] [c]
		4	3×10^{-3}	[4.146] [c]

[a] the number of data used in analysis
[b] Note: $T_{ag}^{f\text{-}s}$ was defined as a translocation coefficient, assuming that the deposition measured in the soil was the same as that on the leaves
[c] as reported by Renaud and Gonze [4.143]
[d] no data

TABLE 4.22. AGGREGATED TRANSFER FACTORS $T_{AG}^{F\text{-}S*}$ (KG DM / KG FM) OF RADIOCAESIUM IN HARVESTED FRUIT FROM TREES CONTAMINATED BY FDNPP ACCIDENT DEPOSITION IN 2011

Type of fruit, cultivar	Year	Soil type	N	$T_{ag}^{f\text{-}s*}$ (kg soil DM/kg fruit FM)	Reference
Cherry[a]	2011	Loamy soil	4	$(3.0–5.4) \times 10^{-2}$	[4.129]
Peach[a]	2011	Loamy soil	7	$(1.4–3.3) \times 10^{-2}$	[4.129]
Grape[a]	2011	Loamy soil	3	$(8.5–16) \times 10^{-3}$	[4.129]
Pear[a]	2011	Loamy soil	3	$(5.0–20) \times 10^{-3}$	[4.129]
Apple[a]	2011	Loamy soil	3	$(1.0–2.0) \times 10^{-2}$	[4.129]
Persimmon[a]	2011	Loamy soil	4	$(1.8–3.2) \times 10^{-2}$	[4.129]
Peach, Akatsuki[b]	2011	Loamy soil+leaf mold (8:5)	4	4.3×10^{-2}	[4.148]
Peach, Akatsuki[b]	2011	Loamy soil+leaf mold (8:5)	4	0.18	[4.148]
Peach, Akatsuki[c]	2011	Loamy soil	3	8.7×10^{-3}	[4.149]
Peach, Akatsuki[c]	2011	Loamy soil	3	7.3×10^{-3}	[4.149]
Peach, Chiyohime[d]	2011	Loamy soil	3	0.15	[4.150]
Japanese apricot, Baigo[d]	2011	Andosols	3	0.51	[4.150]
Japanese chestnut[e]	2011	Brown lowland	3	0.19–0.31	[4.151]
Japanese chestnut[f]	2011	Brown lowland	3	$(8.2–27) \times 10^{-2}$	[4.151]
Japanese chestnut[g]	2011	Andosols	3	$(4.9–11) \times 10^{-2}$	[4.151]
Japanese chestnut[h]	2011	Andosols	3	$(3.9–10) \times 10^{-2}$	[4.151]

[a] In open field. The number of replicates refers to orchards. Fruits were collected from three to five trees in each orchard and combined into one sample per orchard. The soil ^{137}Cs activity concentration (Bq/kg, DM) for a 20-m soil depth was assumed to be one quarter of that measured in the 5-cm topsoil layer.

[b] Data from Tokyo Graduate School of Agricultural and Life Science, located approximately 230 km southwestern area from the FDNPP. These are calculated from data for peaches planted in containers in field conditions in the year of the FDNPP accident. The concentration in the soil was converted to a depth of 20 cm using the ^{137}Cs activity concentrations at 0-5 cm and 5-20 cm. Concentration in fresh pulp was converted using 8.81 for the ratio of fresh matter to dry matter.

[c] Data from Samegawa, Fukushima prefecture, located approximately 60 km southwest from the FDNPP. The concentration in the soil was converted to a depth of 20 cm using the ^{137}Cs concentrations at 0–5, 5–10, 10–15 and 20–25 cm in depth. Concentration in fresh pulp was converted using 8.81 for the ratio of fresh weight to dry weight, which was calculated based on Takata et al. [4.150].

[d] Data in open field obtained at the Tokyo Graduate School of Agricultural and Life Science, located approximately 230 km southwestern area from the FDNPP.

[e] Data from a farmer's orchard in Fukushima prefecture. The soil ^{137}Cs activity concentration for a 20-cm depth was assumed to be three-fourths of that measured in the 0–15 cm topsoil layer (same hereafter). More than thirty years old trees were measured.

[f] Data from a farmer's orchard in Fukushima prefecture; more than sixty years old trees were measured.

[g] Data from an orchard of Institute of Fruit Tree and Tea Science, NARO in Tsukuba. Six to twenty years old trees were measured.

[h] Data from an orchard at the Institute of Fruit Tree and Tea Science, NARO in Tsukuba. Six to twelve years old trees were measured.

Concentration Ratio $CR_{f\text{-}s}$ for uptake from soil to fruit

The concentration ratio $CR_{f\text{-}s}$ between fruit and soil from the transfer process of root uptake is a commonly used transfer parameter for many crops and is defined as:

$$CR_{f\text{-}s} = \frac{A_f}{A_{s*}} \tag{4.7}$$

where A_{s*} is the averaged radionuclide activity concentration in the upper 20 cm of soil (Bq/kg DM).

Measurements of $CR_{f\text{-}s}$ for radiocaesium in Japan have been made following the FDNPP accident by growing fruit trees in soil containing radiocaesium; the measured $CR_{f\text{-}s}$ values are given in Table 4.23 for woody trees and shrubs. Geometric mean values for both woody trees and shrubs are given along with the range of $CR_{f\text{-}s}$ values, averaging across all soil types in Table 4.24.

Table 4.25 gives compiled $CR_{f\text{-}s}$ values for radiocaesium for woody trees and shrubs measured in field studies and experiments before 2011. The data in the table are from IAEA TRS 472 [4.2] with 6 additional values for woody trees (sandy soil) giving a total of 21 values; this leads to a small change in the geometric mean from 5.8×10^{-3} to 4.1×10^{-3}. A comparison of the geometric means for both woody trees and shrubs from before 2011 and the Japanese measurements for radiocaesium show that the values and associated ranges are similar (see Table 4.23 and Table 4.25) with the exception of data for blueberry growing on peat. It is, therefore, appropriate to combine all the values of $CR_{f\text{-}s}$ for predicting transfers of radiocaesium to woody trees and shrubs. The combined geometric means and ranges are given in Table 4.26.

TABLE 4.23. CONCENTRATION RATIOS $CR_{F\text{-}S}$ OF RADIOCAESIUM IN JAPANESE FRUIT GROWN IN CONTAMINATED SOIL UNDER DIFFERENT EXPERIMENTAL CONDITIONS IN 2012–2016

Type of fruit, cultivar	Year	Soil type	N	$CR_{f\text{-}s}$ (kg soil DM / kg fruit	Reference
Peach, Hakuho[a]	2012	Loamy soil	3	4.1×10^{-4}	[4.129]
Peach, Akatsuki[b]	2012	Loamy soil	3	$(7.0 \pm 0.71) \times 10^{-4}$	[4.129]
Peach, Akatsuki[b]	2013	Loamy soil	3	$(6.5 \pm 3.2) \times 10^{-5}$	[4.152]
Peach, Akatsuki[b]	2014	Loamy soil	3	$(4.4 \pm 1.9) \times 10^{-4}$	[4.152]
Peach, Akatsuki[b]	2015	Loamy soil	3	$(1.9 \pm 0.18) \times 10^{-4}$	[4.152]
Peach, Akatsuki[b]	2016	Loamy soil	3	$(8.2 \pm 3.1) \times 10^{-4}$	[4.152]
Peach, Hikawa Hakuho[b]	2013	Loamy soil	3	$(5.2 \pm 1.9) \times 10^{-4}$	[4.152]
Peach, Hikawa Hakuho[b]	2014	Loamy soil	3	$(3.9 \pm 3.0) \times 10^{-4}$	[4.152]
Peach, Hikawa Hakuho[b]	2015	Loamy soil	3	$(1.7 \pm 0.86) \times 10^{-4}$	[4.152]
Peach, Hikawa Hakuho[b]	2016	Loamy soil	3	$(2.9 \pm 1.5) \times 10^{-4}$	[4.152]
Persimmon, Hachiya[a]	2015	Loamy soil	2	$(8.5 \pm 0.97) \times 10^{-3}$	[4.147]
Persimmon, Hachiya[b]	2015	Loamy soil	3	$(1.8 \pm 1.2) \times 10^{-3}$	[4.152]
Grape, Pione[a]	2012	Loamy soil	3	2.1×10^{-3}	[4.129]
Grape, Campbell early[c]	2012	Sandy loam[g] + soil and mulch[h]	4	1.7×10^{-3}	[4.153]
Grape, Campbell early[d]	2012	Sandy loam[g] + soil and mulch[h]	4	4.0×10^{-3}	[4.153]
Grape, Campbell early[a]	2012	Sandy loam[g] + soil and mulch[h]	4	2.7×10^{-3}	[4.153]
Grape, Muscat bailey A [c]	2012	Sandy loam[g] + soil and mulch[h]	4	2.9×10^{-3}	[4.153]

TABLE 4.23. CONCENTRATION RATIOS $CR_{\text{F-S}}$ OF RADIOCAESIUM IN JAPANESE FRUIT GROWN IN CONTAMINATED SOIL UNDER DIFFERENT EXPERIMENTAL CONDITIONS IN 2012–2016 (cont.)

Type of fruit, cultivar	Year	Soil type	N	$CR_{\text{f-s}}$ (kg soil DM / kg fruit	Reference
Grape, Muscat bailey A[d]	2012	Sandy loam[g] + soil and mulch[h]	4	5.7×10^{-3}	[4.153]
Grape, Muscat bailey A[a]	2012	Sandy loam[g] + soil and mulch[h]	4	4.4×10^{-3}	[4.153]
Fig, Houraishi[c]	2012	Sandy loam[g] + soil and mulch[h]	4	2.7×10^{-2}	[4.153]
Fig, Houraishi[d]	2012	Sandy loam[g] + soil and mulch[h]	4	7.1×10^{-3}	[4.153]
Blueberry[e]	2013	Andosols with high ^{137}Cs	3	3.0×10^{-4}	[4.154]
Blueberry[e]	2013	Andosols with mid-level ^{137}Cs	3	3.2×10^{-3}	[4.154]
Blueberry[e]	2013	Andosols with mid-level ^{137}Cs + extra K	3	8.8×10^{-4}	[4.154]
Blueberry[e]	2013	Andosols with low ^{137}Cs	2	3.5×10^{-2}	[4.154]
Blueberry[f]	2013	Peat moss	3	1.4×10^{-1}	[4.154]

[a] fruit trees were transferred from greenhouses into 7 litre pots with contaminated soil
[b] fruit trees were transferred from greenhouses into 7 litre pots with contaminated and well-mixed soil
[c] fruit trees were transferred from greenhouses into 7 litre pots with top 0–5 cm layer of contaminated soil
[d] fruit trees were transferred from greenhouses into 7 litre pots with 5–15 cm layer of contaminated soil
[e] fruit trees were transferred from greenhouses into 7 litre pots with a high, mid and low radiocaesium activity concentration
[f] fruit trees were transferred from greenhouses into 7 litre pots with peat moss; a filtrated (0.45 μm membrane) radiocaesium solution was used to irrigate the pots
[g] contaminated soil from Date and Tokyo
[h] commercial source of uncontaminated soil and mulch growing medium

TABLE 4.24. CONCENTRATION RATIOS $CR_{\text{F-S}}$ OF RADIOCAESIUM IN JAPANESE FRUIT GROWN USING CONTAMINATED SOIL UNDER DIFFERENT EXPERIMENTAL CONDITIONS IN 2012–2016

Fruit type	N[a]	Radiocaesium concentration factor $CR_{\text{f-s}}$ (kg soil DM / kg fruit FM)		
		GM[b]	GSD[c]	Range
Woody tree fruit	21	12×10^{-4}	4.6	$(0.65–270) \times 10^{-4}$
Shrub fruit	5	53×10^{-4}	12.8	$(3–1400) \times 10^{-4}$

[a] the sample size
[b] geometric mean
[c] geometric mean (unitless)

TABLE 4.25. CONCENTRATION RATIOS $CR_{F\text{-}S}$ OF RADIOCAESIUM FOR FRUIT FROM IAEA TRS 472 AND UPDATED FOR WOODY TREE FRUIT

Type of fruit, cultivar	Soil type	N [a]	$CR_{f\text{-}s}$ (kg soil DM / kg fruit FM)			
			GM [b]	GSD [c]	Minimum	Maximum
IAEA TRS 472						
Woody tree fruit (apple, pear, peach, orange, apricot, olive, grapevine)	All	15	5.8×10^{-3}	4.4	8.6×10^{-4}	8.0×10^{-2}
	Clay	2	1.1×10^{-3}	1.4	8.8×10^{-4}	1.4×10^{-3}
	Loam	5	3.5×10^{-3}	2.4	9.4×10^{-4}	9.2×10^{-3}
	Sand	4	1.5×10^{-2}	5.2	1.9×10^{-3}	8.0×10^{-2}
	Organic	1	3.7×10^{-2}	—[d]	—	—
	Others	3	6.0×10^{-3}	5.4	8.6×10^{-4}	1.9×10^{-2}
UPDATED VALUES (TRS 472 and MODARIA II [e])						
Woody tree fruit (apple, pear, peach, orange, apricot, olive, grapevine)	All	21	4.1×10^{-3}	3.7	8.6×10^{-4}	8.0×10^{-2}
	Sand	10	4.2×10^{-3}	4.3	1.0×10^{-3}	8.0×10^{-2}
IAEA TRS 472 [f]						
Shrub fruit (gooseberry, blackcurrant, raspberry, redcurrants)	All	6	2.1×10^{-3}	2.2	6.9×10^{-4}	5.7×10^{-3}
	Clay	2	1.8×10^{-3}	2.4	9.8×10^{-4}	3.3×10^{-3}
	Loam	2	3.2×10^{-3}	2.3	1.8×10^{-3}	5.7×10^{-3}
	Others	2	1.5×10^{-3}	3.0	6.9×10^{-4}	3.3×10^{-3}

[a] the number of data
[b] geometric mean
[c] geometric standard deviation (unitless)
[d] no data
[e] The IAEA programme "Modelling and Data for Radiological Impact Assessments" (MODARIA) II. https://www-ns.iaea.org/projects/modaria/modaria2.asp
[f] CR is termed F_v in TRS 472

TABLE 4.26. REVISED CONCENTRATION RATIOS $CR_{F\text{-}S}$ OF RADIOCAESIUM FOR FRUIT PLANTS

Type of fruit, cultivar	Soil type	N [a]	$CR_{f\text{-}s}$ (kg soil DM / kg fruit FM)			
			GM [b]	GSD [c]	Minimum	Maximum
Woody fruit tree	All	42	2.3×10^{-3}	4.7	6.5×10^{-5}	8.0×10^{-2}
Shrub fruit	All	11	3.2×10^{-3}	5.9	3.0×10^{-4}	1.4×10^{-1}

[a] the number of data
[b] geometric mean
[c] geometric standard deviation (unitless)

4.3.3.4.Transfer of radiocaesium to fruit by interception and translocation

Measurements have been made of translocation from tree or plant parts to fruit following deposition after the FDNPP accident. These have been expressed in several ways depending on the types of experiments being undertaken or the field measurements made. The quantities that have been measured are:

Concentration ratios for deciduous fruits to leaf $CR_{\text{f-l}}$ in 2011 for the year of FDNPP accident expressed as:

$$CR_{\text{f-l}} = \frac{A_f}{A_l} \tag{4.8}$$

where A_l is the radiocaesium activity concentration in leaf at harvest (Bq/kg FM). Note that a few values are expressed on a DM basis and this ratio is unitless.

The transfer rate $TR_{\text{f-l}}$ of radiocaesium to fruit via leaves expressed as:

$$TR_{\text{f-l}}(\%) = \frac{B_f}{B_l} \times 100\% \tag{4.9}$$

where B_f is the activity of radiocaesium in fruit (Bq), not necessarily at harvest condition, and B_l is the activity of radiocaesium in leaves (Bq) at fruit sampling. The intercepted activity of radiocaesium is the residual activity in leaves after treatment (spray or paste).

Concentration ratio for deciduous fruits to bark $CR_{\text{f-b}}$ in 2011 for the year of the FDNPP accident expressed as:

$$CR_{\text{f-b}} = \frac{A_f}{A_b} \tag{4.10}$$

where A_b is the radiocaesium activity concentration in bark (Bq/kg, FM or DM) of the main trunk and scaffold limbs. The bark activity should reflect the initial interception and be measured soon after deposition.

These quantities are discussed below and compared, where possible, with data collected from other experimental work and field measurements made after the Chernobyl accident.

Quantity 1: Concentration ratios $CR_{\text{f-l}}$ for deciduous fruits to leaf in Japan after the FDNPP accident

The measured $CR_{\text{f-l}}$ values in fruit from experimental studies in Japan after the FDNPP accident are given in Tables 4.27 and 4.28, expressed both as the ratio of activity concentration in mature fruit to leaves at 2011 harvest on a FM basis and a DM basis, respectively.

$CR_{\text{f-l}}$ values measured in experimental studies after the Chernobyl accident are given in Table 4.29. The data given on a DM basis can be compared with the data from Japan following the FDNPP accident in Tables 4.27 and 4.28. The $CR_{\text{f-l}}$ values cover a similar range for orchard fruit, being within a range of 0.1 to 1.7. The Chernobyl data expressed on a FM basis in Table 4.29 cannot be compared directly with the Japanese data in Tables 4.27 and 4.28.

TABLE 4.27. CONCENTRATION RATIOS FOR DECIDUOUS FRUITS TO LEAF $CR_{\text{F-L}}$ (KG LEAF FM / KG FRUIT FM) VALUES FOR RADIOCAESIUM AND FRUIT AFTER THE FDNPP ACCIDENT AT 2011 HARVEST

Type of fruit, cultivar	Year	N [a]	Concentration ratio $CR_{\text{f-l}}$ at harvest (kg leaf FM / kg fruit FM)	Reference
Apple	2011	3	0.21 ± 0.07	[4.155]
Japanese apricot, Baigo	2011	—[b]	0.30	[4.150]
Blueberry	2011	11	0.19–1.48	[4.156]
Cherry	2011	7	0.29 ± 0.08	[4.155]
Chestnuts	2011	1	0.06	[4.157]
Chestnuts	2012	1	0.56	[4.157]
Chestnuts	2013	2	0.87– 1.7	[4.158]
Grape	2011	3	0.23 ± 0.07	[4.155]
Peach	2011	7	0.17 ± 0.08	[4.155]
Peach, Akatsuki	2011	—	0.23–0.36	[4.150]
Pear	2011	2	0.12 ± 0.09	[4.155]
Persimmon	2011	3	0.29 ± 0.09	[4.155]

[a] the number of data
[b] no data

TABLE 4.28. CONCENTRATION RATIOS FOR DECIDUOUS FRUITS TO LEAF $CR_{\text{F-L}}$ (KG LEAF DM / KG FRUIT DM) VALUES FOR RADIOCAESIUM AND FRUIT AFTER THE FDNPP ACCIDENT

Type of fruit, cultivar	Year	N [a]	Concentration ratio $CR_{\text{f-l}}$ at harvest (kg leaf DM / kg fruit DM)	Reference
Japanese apricot	2012	1	0.38	[4.80]
Blueberry	2012	5	0.38–1.1	[4.154, 4.159]
Chestnuts	2013	8	0.51–1.7	This work, [4.158, 4.160]
Chestnuts	2014	3	0.3–0.44	[4.160]
Kiwi fruit	2012	1	0.52	[4.80]
Pear	2012	2	0.55 ± 0.14	[4.80]
Persimmon	2011	2	0.11 ± 0.01	[4.161]
Persimmon	2011	2	0.10–0.11	This work
Persimmon	2012–2017	7	0.36–0.89	This work

[a] the number of data analysed

TABLE 4.29. CONCENTRATION RATIOS FOR DECIDUOUS FRUITS TO LEAF $CR_{\text{F-L}}$ VALUES FOR RADIOCAESIUM AND FRUIT AFTER THE CHERNOBYL ACCIDENT

Type of fruit	Year	N [a]	$CR_{\text{f-l}}$ at harvest	Reference
			(kg leaf DM / kg fruit DM)	
Apple	1986	1 [b]	0.43	[4.132]
Pear	1986	1 [b]	0.11	[4.132]
Peach	1986	1 [b]	1.3	[4.132]
Grapevine	1986	1 [b]	1.9	[4.132]
			(kg leaf DM / kg fruit FM) [c]	
Cherry	1986	3	0.029	[4.136]
Peach	1986	7	0.13	[4.136]
Apple	1986	6	0.094	[4.136]
Pear	1986	5	0.031	[4.136]

[a] the number of data analysed
[b] combined sample from fruits taken from several trees
[c] CR_{f-l} values are GM values from the data in Anguissola Scotti and Silva [4.136]

Quantity 2: The transfer factor $TR_{\text{f-l}}$ of radiocaesium to fruit via leaves

The transport of radiocaesium to fruits via leaves can be influenced by the stage of contamination (seasonality), precipitation intensity, age of branch and tree, cultivar and tree species, distance between fruit and the contaminated leaf, dilution effect from growth and yield. The measurements made from experimental field studies in Japan in 2011 are given in Table 4.30 for the woody tree fruit persimmon, cherry and grape. Transfer factor $TR_{\text{f-l}}$(%) of ^{137}Cs applied to leaves after the fruit growing stage were similar for persimmon, cherry and grape at 8.4%–16.4%, 14.3% and 19.1%–22.5% respectively. In the persimmon, the $TR_{\text{f-l}}$ (%) was also found to be dependent on the distance between fruit and the spiked leaves [4.147] as was previously shown experimentally for apples by [4.137] and [4.138].

An additional experiment was reported by [4.147] in which 160 Bq/L of ^{137}Cs solution was sprayed on four occasions over young peach trees planted in pots before leaf bud burst. The measured activity concentration in peaches was 3.5 Bq/kg fruit FM.

$TR_{\text{f-l}}$(%) has been previously examined in experimental research on woody trees carried out before the FDNPP accident and have been compiled elsewhere [4.162]. These data are summarised in Table 4.31 and are for the first harvest after radionuclides were applied to leaves under various experimental conditions. Values of 1.8%–9.6% for grapes [4.139, 4.140, 4.163, 4.164], 1%–47% for apples [4.137, 4.138, 4.140, 4.141], 13% for Satsuma orange [4.165] and 12.8% for pears [4.140] have been measured. The range of measured values for woody trees is consistent with the values measured in Japan in the experimental studies after the FDNPP accident.

TABLE 4.30. THE TRANSFER FACTOR $TR_{F\text{-}L}$ (%) OF RADIOCAESIUM TO FRUIT VIA CONTAMINATED LEAVES FROM EXPERIMENTAL STUDIES IN JAPAN AFTER THE FDNPP ACCIDENT

Type of fruit, cultivar	Soil type	N [a]	$TR_{f\text{-}l}$ (%)	Reference
Persimmon, Hachiya [b]	Loamy soil	2	10.2 ± 3.2	[4.147]
Persimmon, Hachiya [c]	Loamy soil	3	16.4 ± 5.0	[4.147]
Persimmon, Hiratanenashi [b]	Loamy soil	4	8.4 ± 2.6	[4.147]
Persimmon, Hiratanenashi [c]	Loamy soil	6	8.8 ± 4.3	[4.147]
Cherry, Napoleon [d]	Loamy soil	3	14.3 ± 4.9	[4.147]
Grape, Adumasizuku [d]	Loamy soil	4	12.6 ± 2.3	[4.147]
Grape, Adumasizuku [d]	Loamy soil	2	19.1 ± 13.1	[4.147]
Grape, Adumasizuku [d]	Loamy soil	2	22.5 ± 24.8	[4.147]

[a] the number of data analysed
[b] contaminated in the young fruit period
[c] contaminated in the fruit-growing period
[d] contaminated in the beginning of ripening

TABLE 4.31. THE TRANSFER FACTOR $TR_{F\text{-}L}$(%) OF RADIOCAESIUM FROM LEAF TO FRUIT OBSERVED IN EXPERIMENTS BEFORE 2011

Type of fruit, cultivar	Time of contamination	$TR_{f\text{-}l}$ (%)	Distance from fruit	Reference
Satsuma mandarin	Flowering stage	12	—[a]	[4.165]
Satsuma mandarin	Fruit growing period	13	—	[4.165]
Apple, Aroma	Fruit ripening	1	—	[4.138]
Apple, Golden Delicious	Green fruit stage	47	—	[4.140]
Apple, Gloster	Fruit growing period	39	—	[4.137]
Apple, Jonagold[b]	Fruit growing period	42	0 cm	[4.137]
	Fruit growing period	0.4	25 cm	[4.137]
	Fruit growing period	0.1	50 cm	[4.137]
Apple		4–12	—	[4.141]
Apple		1–4	—	[4.141]
Grape, Pinot Blanc	Beginning of ripening	1.8	—	[4.164]
Grape, Pinot Blanc	Beginning of ripening	3.7	—	[4.164]
Grape, Pinot Blanc	Beginning of ripening	9.6	—	[4.163]
Grape, Chardonnay	Green fruit stage	5.5	—	[4.140]
Grape, Müller–Thurgau [b]	Fully developing stage of the first leaf	7	—	[4.139]
		9	—	[4.139]
Pear, Conference	Green fruit stage	12.8	—	[4.140]
Blueberry	Green fruit stage	0.7	—	[4.166]
Gooseberry	Green fruit stage	3.4	—	[4.166]
Redcurrant	Green fruit stage	2	—	[4.166]

[a] no data
[b] samples collected 2 and 3 months following contamination

Quantity 3: Concentration ratio for woody tree fruits to bark ($CR_{\text{f-b}}$) in the year of the FDNPP accident

The measurements of the concentration ratio $CR_{\text{f-b}}$, expressed on a FM basis, made in experimental field studies in Japan in 2011 are given in Table 4.32. The times of measurement of the concentration in bark are also reported; these values are used for the purposes of calculating a *CR* value shortly after deposition.

TABLE 4.32 CONCENTRATION RATIO $CR_{\text{F-B}}$ FOR FRUITS TO BARK IN JAPAN IN 2011, FOLLOWING THE FDNPP ACCIDENT

Type of fruit, cultivar	Time of measurement of bark	Bark measured	$CR_{\text{f-b}}$ (kg bark FM / kg fruit FM	Reference
Grape	25 May 25 in 2011	Scaffold limbs	1.1×10^{-4}	[4.147]
Pear	25 May 25 in 2011	Scaffold limbs	1.0×10^{-4}	[4.147]
Peach	14 June 14 in 2011	Scaffold limbs	2.9×10^{-3}	[4.147]
Persimmon	18 October 2011	Scaffold limbs	1.5×10^{-3}	[4.147]
Persimmon	31 January 2012	Trunk	6.8×10^{-3}	[4.147]

A study carried out by Katana et al [4.137] measured the transfer from bark to fruit for apples in which the bark was contaminated with Cs at different distances from the developing fruit. The results of this study are expressed, similarly to Quantity 2, as $TR_{\text{f-b}}$(%), i.e., percentage of the activity of radiocaesium in fruit (Bq) from the applied activity of radiocaesium on bark (Bq); the values were 1.8% and 0.2% for contamination of the bark 25 cm and 50 cm from the fruit, respectively. This study confirms the transfer from bark of woody trees to fruit observed in the Japanese studies; the transfer was similar to that from leaves to fruit when the contamination was added away from the growing fruit. Takata et al [4.148] also calculated the transfer from the whole tree to peaches (Bq in fruit / Bq in plant), where contamination of the tree occurred before bud burst, so this is effectively the same as the transfer from bark to fruit and can be compared to the values in Table 4.32. The calculated $TR_{\text{f-b}}$ was 3.9–4.0.

Measurements made on the dynamics of transfer to woody tree fruit in Greece after the Chernobyl accident [4.134, 4.135] also provide evidence that some of the radiocaesium stored in the above-ground parts of trees following deposition is transferred to fruit in the following years as concentrations in fruit are higher than can be attributed to root uptake from the soil.

4.3.3.5. Effective half-life of temporal changes of the ^{137}Cs activity concentration in mature fruit

Using the measured radiocaesium concentrations in fruit after the FDNPP accident, effective half-lives in fruit have been estimated using the approach described in Chapter 2.

T_{eff} values can be useful to predict activity concentrations in fruit over time following deposition when activity concentrations in fruit have been measured in the first harvest after deposition. They implicitly include all the transfer processes and their time dependence; however, they are likely to be specific to the actual deposition event and time of year of the accident, particularly in the first few years following deposition.

T_{eff} values measured after the Chernobyl and FDNPP accidents are summarised in Table 4.33. This includes data from experiments carried out between 2011 and 2018 on effective half-lives on young and mature orchard fruit [4.167].

TABLE 4.33. MEAN (RANGE) OF EFFECTIVE HALF-LIFE(S) T_{EFF} OF ^{137}CS IN DIFFERENT FRUIT SPECIES AFTER THE CHERNOBYL AND FDNPP ACCIDENTS

Fruit	Chernobyl accident		Reference	FDNPP accident		Reference
	Year	T_{eff} (d)		Year	T_{eff} (d)	
Apple	1987–1990	314	[4.134] [a]	2011–2012	223	[4.143] [g]
	1987–1993	507	[4.168] [b]	2011–2013	330 (308–352)	[4.169] [h]
	1986–1988	188	[4.133] [c]	2011–2018	170 (fast) 2017 (slow)	[4.167] [i]
Apple (immature fruit)		—		2012–2018	876	[4.167] [i]
Apricot	1987–1990	281, 307	[4.134] [a]		—	
Japanese Apricot		—		2011–2012	172	[4.143] [g]
		—		2012–2013	277	
		—		2011–2013	226 (183–303)	[4.169] [h]
		—		2011–2017	106 (fast) 924 (slow)	[4.167] [l]
(Immature fruit)		—		2012–2017	130 (fast) 2617 (slow)	[4.169] [l]
Blueberry		—		2011–2013	179	[4.169] [h]
Cherry	1987–1995	220 (fast) 1150 (slow)	[4.135] [d]	2011–2012	190	[4.143] [g]
				2012–2013	598	
		—		2011–2018	183 (fast) 1318 (slow)	[4.167] [i]
Cherry (Immature fruit)		—		2012–2018	100 (fast) 1199 (slow)	[4.167] [i]
Chestnut		—		2011–2013	245	[4.169] [h]
				2011–2013	318	[4.169] [h]
Gooseberries	1987–1990	220	[4.168] [e]		—	
Grapes				2011–2012	210	[4.143] [g]
Hazelnut	1986–1988	145 ± 18 (AM) 144 (GM)	[4.133] [c]		—	
	1988–1992	730	[4.168] [f]		—	
Olive	1987–1990	303	[4.134] [a]		—	
	1986–1988	177	[4.133] [c]		—	

TABLE 4.33. MEAN (RANGE) OF EFFECTIVE HALF-LIFE(S) T_{EFF} OF ^{137}CS IN DIFFERENT FRUIT SPECIES AFTER THE CHERNOBYL AND FDNPP ACCIDENTS (cont.)

Fruit	Chernobyl accident		Reference	FDNPP accident		Reference
	Year	T_{eff} (d)		Year	T_{eff} (d)	
Peach	1987–1990	307	[4.134] [a]	2011–2012	186	[4.143] [g]
		—		2011–2013	237 (230–248)	[4.169] [h]
		—		2011–2016	188 (fast) 945 (slow)	[4.167] [i]
(Immature fruit)		—		2011–2017	59 (fast) 419 (slow)	[4.167] [i]
Pear	1987–1990	252, 237	[4.134] [a]		—	
	1987–1993	449	[4.168] [b]		—	
Japanese pear		—		2011–2012	264	[4.143] [g]
		—		2011–2018	175 (fast) 2522 (slow)	[4.167] [i]
Japanese pear (immature fruit)		—		2011–2018	214 (fast) 2314 (slow)	[4.167] [i]
Japanese Persimmon		—		2011–2013	371 (208–475)	[4.169] [h]
		—		2011–2018	141 (fast) 846 (slow)	[4.167] [m]
Japanese Persimmon (immature fruit)		—		2012–2018	248 (fast) 4151 (slow)	[4.167] [m]
Walnut	1986–1988	264	[4.133] [c]		—	

— no data

[a] Every year two samples of fruits were collected from each of five fruit trees in each of two farms in Northern Greece.

[b] Each year, 10–50 apple and pear samples were collected at the same sites from 4 of the 9 provinces of Austria. Apple: n=37. Pear: n=9. Mean values for the 4 provinces were calculated.

[c] Apple, olive and walnut were estimated on samples harvested in two years: 1986 and 1988 in the North of Latium (Rome). Hazelnuts: data is the average of 7 different plantations collected over three years in the North of Latium (Rome).

[d] Fruit from 3 sweet cherry trees in two farms collected from 1987 to 1990 as described in note a, supplemented with additional data collected during the years 1991–1995.

[e] Gooseberries: The investigation was carried out on a single gooseberry bush in Vienna.

[f] Hazelnuts: The annual average was used of about 50–200 import hazelnut samples taken per year. For this fruit that is imported the author supposes that the average value for 1987could incorporate a bias and he would correct the T_{eff} from 730 to 490 days.

[g] Different fruit species were gathered from selected municipalities of the Fukushima Prefecture in 2011, 2012 and 2013. They were gathered at varying dates: May–June 2011 for apricots and cherries, September–November for apples and pears. Peaches in July–August and grapes at early fall.

[h] Open source food monitoring data by the Ministry of Health Labour and Welfare were used for analysis.

[i] Research carried out for eight years 2011–2018. Each year, fruits were sampled from the same 3 trees.

[l] Each year fruits were sampled from the same 2 trees

[m] As at point i, with the difference that fruit trees were washed after the accident.

T_{eff} values for fruit were calculated by fitting the ^{137}Cs activity concentration from 2011 to 2018 to a one- or two-component exponential model. Long-term changes in ^{137}Cs activity concentrations in mature fruit could be described by two decreasing components, one of which is a rapid decrease over the first three years after the FDNPP accident, followed by a slower component.

Half-life values of the rapid component of ^{137}Cs in mature fruit were in the order of months after the FDNPP accident, as shown in Table 4.33. These values are similar to those observed after the Chernobyl accident [4.135].

4.3.3.6.Modelling

The modelling of the transfer of radionuclides to fruit was addressed as part of the IAEA Programme on BIOsphere Modelling and ASSessment (BIOMASS) [4.142]. The Fruits Working Group had the aim of improving capabilities for modelling the uptake of radionuclides by fruit. Part of this work was to gain consensus on important transfer processes and to develop a conceptual model for estimating activity concentrations in fruit following deposition. The review of models at the start of the BIOMASS programme showed that all fruit models included processes associated with air, leaf and fruit in some way and also included a soil to fruit pathway in various levels of detail. None looked at the impact of radionuclides in debris and ground cover. In considering a conceptual model, the role of wood and stems was recognised as part of the translocation of radionuclides following interception onto the plant or tree but was not ranked as an important process and it was identified that knowledge on this process was poor.

The models used for transfer to fruit at that time typically assumed interception by the plant or tree during the period from leaf bud to harvest and only uptake from the soil outside this period. Consequently, uptake outside the growing season was predicted to be low, particularly for trees for which the $CR_{f\text{-}s}$ values are relatively low. An example of this effect can be seen for the FARMLAND model for fruit [4.170] where predicted activity concentrations at the first harvest after deposition are given for deposition occurring when foliage and fruit are present and during the dormant stage for apple trees. In this case, the estimated activity concentrations were 4 Bq/kg FM and 0.03 Bq/kg FM per 1000 Bq/m^2, respectively.

The situation in Japan after the FDNPP accident has shown that for woody trees, the translocation of radiocaesium from deposition onto the bark of trees is an important contributor to the activity concentrations in fruit at harvest. In this case, there was no foliar contamination as deposition occurred before bud burst but high activity concentrations were measured in fruit as shown in Table 4.19.

For situations where foliar deposition occurs, the interception of radiocaesium by leaves and translocation to the fruit is likely to be the dominant transfer process with an additional contribution from translocation from bark to fruit. From the data presented in Tables 4.31 and 4.32, the radiocaesium in fruit due to leaf to fruit transfer can be seen to be 10 to 100 times more than that due to bark to fruit transfer. This conclusion is supported by measurements of ^{137}Cs activity concentrations in fruit of the yuzu evergreen tree in orchards near the Fukushima Agricultural Technology Centre (FARC). The measured activity concentration in yuzu fruit was 365 Bq/kg FM, which was approximately 20 times higher than the mean value of 19.0 Bq/kg FM for deciduous fruit trees in the FARC orchard [4.147], located within 2 km of the Yuzu fruit trees in 2011.

Sato [4.147] proposed a compartment model of the radiocaesium pathway in orchards contaminated during the dormancy phase, based on the conceptual model proposed by the

BIOMASS Working Group [4.142]. The model is shown in Fig. 4.20. Two additional components were added to the BIOMASS conceptual model to include the transfer of radiocaesium from Epiphytic moss which can subsequently transfer to bark and the role of undergrowth in orchards (mainly Kentucky Bluegrass and White Clover, and weeds such as *Digitaria cilialis. Capsella bursa–pastoris and Plantago asiatica*) that can influence the downward migration of radiocaesium [4.131].

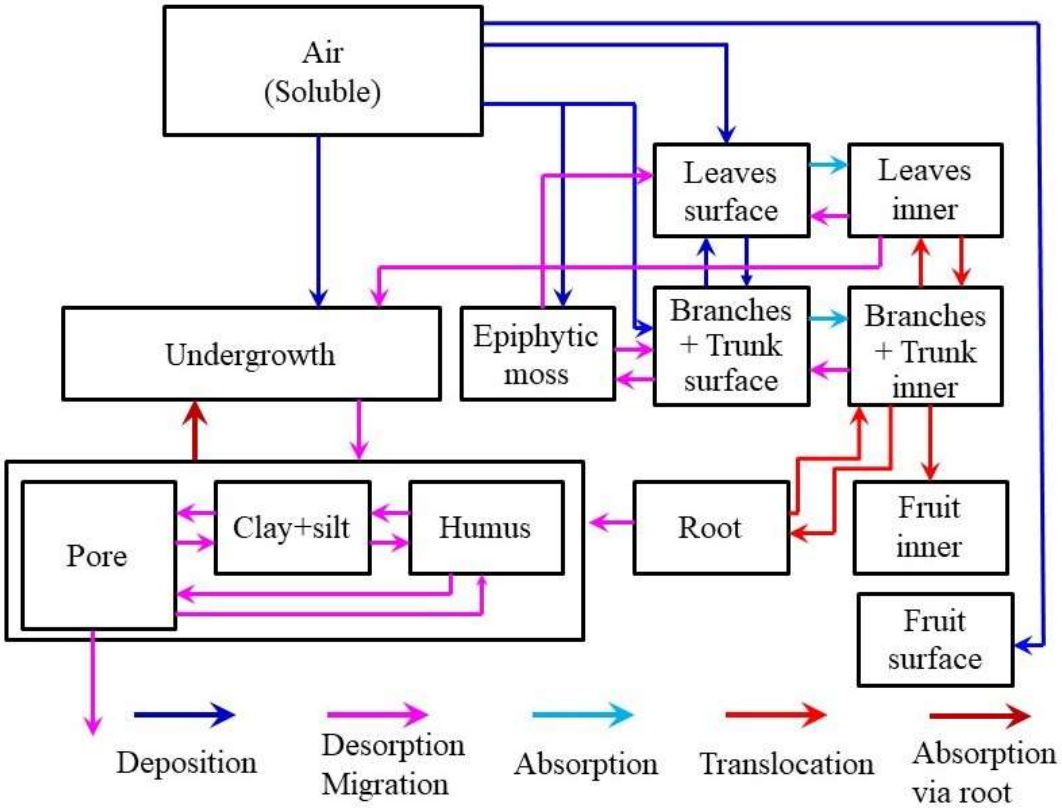

FIG. 4.20. Compartment model of the radiocaesium pathway in orchards (adapted after [4.147]).

Monte Carlo simulations were made using the compartment model in Fig. 4.20 (further detail in Fig. 4.21) to validate the additional components of the model that were added to take account of the transfer of radiocaesium from orchard undergrowth to the underlying upper soil layer. The temporal changes in ^{137}Cs activity concentration at 6 to 9 cm depth in 5 orchards were reproduced by Monte Carlo simulation as shown in Fig. 4.21 [4.147]. The figure shows an increase in the activity concentration in the upper soil layer measured and predicted over a 5-year period from the time of initial deposition. This could lead to an increase in activity concentrations from root uptake for fruit trees with fine roots in the upper layer of the soil, such as yuzu trees [4.171]. The radiocaesium in the upper soil layer could also, with time become available for uptake from the soil to other orchard trees due to migration down the soil column.

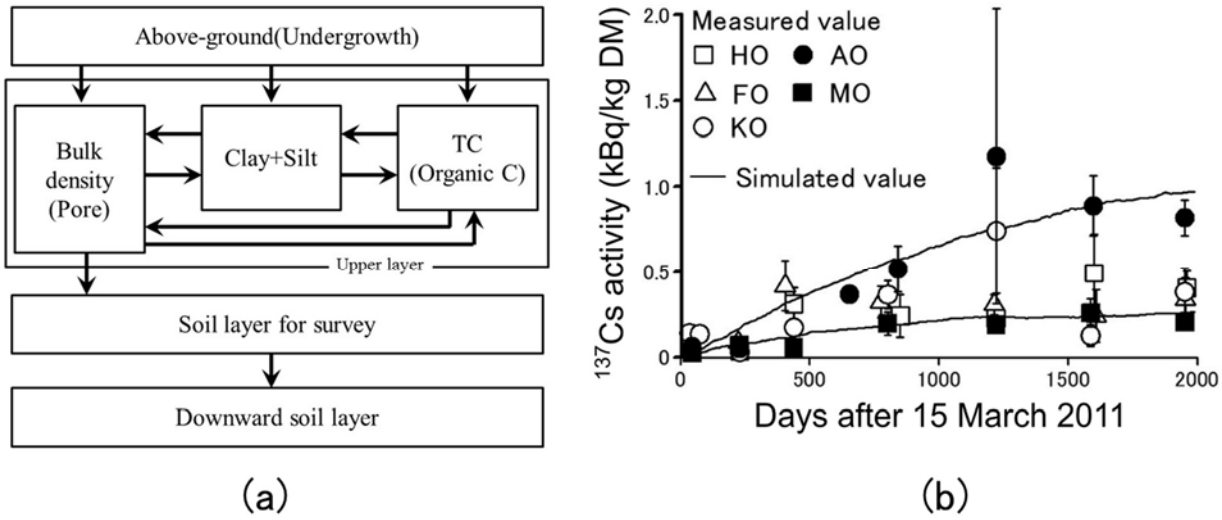

FIG. 4.21. A compartment model (a) and results of a Monte Carlo simulation (b) of the temporal changes in ^{137}Cs activity concentration in 6 to 9 cm depth in 5 orchards (adapted after [4.147]). HO, AO are peach orchards, FO, MO and KO are apple orchards.

4.3.3.7.Summary and limitations

Summary

The quality and quantity of data on the transfer of radiocaesium to fruit trees has been significantly enhanced after the FDNPP accident.

A comparison of data from the FDNPP accident and the Chernobyl accident has shown that, where the data can be compared, (i.e. for similar scenarios) the transfer parameters are broadly similar for woody fruit trees and shrubs.

The relative importance of different transfer processes for radiocaesium in contributing to activity concentrations in fruit is highly variable and depends on the time of year of deposition, the type of fruit (woody tree, shrub or other perennial plants). For example, soil was not an important source for most fruit trees soon after deposition in March after the FDNPP accident, whereas it potentially was for the yuzu tree which has fine roots in the upper soil layer. If deposition had occurred after bud burst, as was the case or the Chernobyl accident in April 1986, the role of foliar interception and translocation to fruit would have been the dominant transfer process and led to higher activity concentrations in harvested fruit. This is observed in the aggregated transfer factors ($T_{ag}^{f\text{-}s}$) in the year of deposition which are one order of magnitude lower after the FDNPP accident than after the Chernobyl accident for most orchard fruit.

The phenological stages of many fruit trees at the time of the FDNPP accident highlighted the role of bark in the process of absorption and translocation to fruit. This translocation can occur regardless of whether the tree is dormant at the time of deposition. Because fruit trees are perennial plants, their surface tissues (bark) are capable of intercepting, absorbing and translocating deposited radionuclides throughout the year and so translocation to fruit was evident in the first few years after the FDNPP accident.

The usefulness of aggregated transfer factors (T_{ag}) for fruit has been illustrated. These transfer factors include all transfer processes and are normalized to the activity deposition in soil. They

can be used to estimate the activity concentrations in fruit without requiring detailed knowledge of the actual amounts of radiocaesium intercepted by leaves, fruit and bark. For the situation where the transfer from bark is the dominant process, but there is only limited quantitative data on the interception of radiocaesium by bark that could be used in a model, this approach is particularly useful and robust.

Old orchards may host epiphytic lichens and bryophytes, which enhance the interception capacity by bark and can provide an external storage component feeding the stemflow with radionuclides in the first years after deposition.

Undergrowth plants growing under the fruit trees in most orchards constitute a component that can facilitate radiocaesium migration to the underlying upper soil layer.

The retention of radiocaesium in bark and subsequent transfer to fruit highlighted the suitability of bark-washing as an early phase countermeasure against contamination of fruit trees. More than 90% of municipalities in Fukushima Prefecture conducted bark-washing in orchards.

Limitations

Methods used to quantify transfer to fruit need to be carefully evaluated and better information is needed to inform the selection of which transfer parameter is most appropriate in different contamination situations.

Despite the potential importance of bark interception, little information is currently available on radioactive contamination mechanisms in orchards in the dormancy period and on the inward migration of radiocaesium via bark.

The importance of the transfer process from bark to fruit for other elements, such as strontium, is not known. For example, is this transfer process expected to follow the general rule of mobility for elements in terrestrial foodchains?

On-going measurements in orchard fruit in Japan will be useful to determine the timescale over which the translocation of radiocaesium from bark to fruit should be considered explicitly in model predictions and on what timescale this process is implicitly included in measured *CR* values between soil and fruit.

The sources of data compiled for this chapter include monitoring, site-specific sampling and research, and differences may arise due to the features of these different sources. Monitoring programmes provide data from sample sizes and sources not consistent among years. Experimental data are site-specific and are often derived from the same individual trees, as this is usually done to reduce the biological variability.

Half-lives calculated from monitoring data start from one year after the accident, while those from experimental data use also values from the year of the accident. Furthermore, they reflect different methodologies of sampling. These aspects need to be discussed to derive the most reliable parameters for modelling.

Only limited validation has currently been carried out of models quantifying radiocaesium pathways in orchards after the FDNPP accident.

The time of year that deposition occurred after the FDNPP highlighted the potential importance of interception and subsequent translocation of radiocaesium from bark to fruit over a number of subsequent years but particularly in the first harvest after deposition.

The application of a $CR_{\text{f-s}}$ between fruit and soil in the year of FDNPP accident in orchards would not have been appropriate to describe the transfer of radiocaesium to harvested fruit in 2011. This is the approach that would have been adopted by many of the fruit transfer models being used for dose assessment.

Transfer pathways for fruit vary considerably with growth characteristics and plant structure, emphasizing the importance of quantifying radiocaesium transfer appropriately for different types of fruit. Therefore, careful consideration needs to be given to selection of a suitable transfer parameter to adopt to adequately quantify radiocaesium transfer to fruit.

Selection of remediation options needs to take into account the ecological diversity in fruit crops and the time of year that deposition occurs.

4.3.4. Transfer to other agricultural crops

4.3.4.1.Introduction

Data on the transfer of radiocaesium to other perennial crops, including translocation for two perennial plants, *CR* values and T_{eff} values are presented here. The crops considered including soybean, buckwheat, leafy vegetables, fruit vegetables and root crops.

4.3.4.2.Translocation and concentration ratios between old leaves and new shoots in perennial crops

Perennial plants have surface structures that may be exposed to deposited radionuclides. As was shown to occur for green tea, intercepted radiocaesium on the surfaces of these plants may be translocated to other plant parts including new growth which is subsequently harvested for consumption.

New shoots need potassium and since caesium is a strong analogue of potassium, radiocaesium is also accumulated in new shoots or growing tissues [4.172]. After the FDNPP accident, newly emerged tissues of plants contained radiocaesium, even though these tissues were not directly contaminated, because radiocaesium was absorbed and translocated from old tissues in 2011 [4.173]. Such mechanisms were quantified above for green tea. They have been applied here to derive the translocation factor, f_{tr} values from data derived from sampling of giant butterbur and bamboo shoots in April and May 2011 (Table 4.34).

For bamboo shoots, at 50 days after the contamination, f_{tr} was about 0.005 (N=1), thus 0.5% of the radiocaesium activity concentration in bamboo leaves was found in new shoots, which is much lower than in giant butterbur and green tea. In the Kanto plain and in Fukushima Prefecture, bamboo shoots emerge from the ground surface in late April to early May. The growing shoots use nutrients stored in roots and the mature bamboo tree. Because above-ground parts of bamboo trees were directly contaminated, absorbed radiocaesium was translocated via the nutrient transfer mechanism and transferred to bamboo shoots. In addition, radiocaesium is taken up through roots from the soil. In field studies, more than 95% of radiocaesium was immobilized by soil in which bamboo plants were growing. It is likely that, for bamboo shoots in 2011, radiocaesium from the soil to plant pathway provided only a small portion of total radiocaesium in bamboo shoots [this work].

TABLE 4.34. ^{131}I, ^{137}CS AND ^{134}CS MASS TRANSLOCATION FACTOR f_{TR} FOR NEW SHOOTS OF GIANT BUTTERBUR AND BAMBOO FROM OLD LEAVES FOLLOWING THE FDNPP ACCIDENT

Plant type and target tissue	Nuclide	Time after contamination on 20 March 2011 (d)	f_{tr} at time of sampling (unitless)	f_{tr} using initial concentration in old leaves (unitless)
Giant butterbur	^{131}I	24	0.28	0.034
	^{131}I	29	0.49	0.029
	^{137}Cs	24	0.48	0.062
	^{137}Cs	29	0.95	0.042
Bamboo edible part	^{131}I	50	<0.005	—
	^{137}Cs	50	0.005	—
	^{134}Cs	50	0.005	—

— no data

For giant butterbur, f_{tr} was similar to that observed for green tea in 2011 (Table 4.16). Giant butterbur is a perennial plant; during winter, most of its above-ground parts senesce. In February to March, flower shoots start to grow followed by new above-ground leaves which emerge 2–3 weeks after the flower shoots growing period. At the time of the FDNPP accident, small leaves were present on the ground, and in April the new shoots of the plant grew rapidly probably because of the use of carbohydrates produced during photosynthesis from older plant tissue. Back calculation of initial ^{131}I and ^{137}Cs activity concentrations in leaves on March 20th (leaf blade plus petiole) was used to derive the translocation factor, f_{tr} for giant butterbur (Table 4.34). The results were similar to those for green tea for radiocaesium application on the upper surface leaf [4.117]. However, for giant butterbur and bamboo, data were taken from only one sampling site in each case, so it is difficult to estimate variability in the data in Table 4.41.

4.3.4.3.Activity concentration ratios for crops

Soybean and buckwheat

Soybean and buckwheat are major crops produced in the areas affected by the FDNPP accident. Most of the contaminated fields used to grow these crops were under comprehensive monitoring provided by MAFF since 2012 [4.121, 4.174–4.178]. The monitoring programme included measurements of exchangeable potassium—before planting and at the time of harvest—and radiocaesium activity concentrations in soil and crop. The GM, GSD and minimum *CR* values given in Table 4.35 were only calculated for samples with radiocaesium activity concentrations that exceeded the detection limit[4]. Thus, these data do not fully reflect the time dependences of *CR* values. As with rice, *CR* values were highly dependent on soil potassium availability, which is considered further in sub-section 4.3.4.5.

[4] In 2012, the minimum detection limit was higher than in subsequent years.

In site specific studies, such as reported by Li et al. [4.179], the CR values for soybean (grain) have been within the range of MAFF data in Table 4.35.

Other vegetables and crops

Data on radiocaesium *CR* values for leafy vegetables, non-leafy vegetables, leguminous vegetables, root crops, tubers, and fodder grasses measured in 2011 and 2012 are presented in Tables 4.36 and 4.37 [4.60, 4.121, 4.174–4.178, 4.180–4.182]. For the crops considered, there was no above-ground plant growth in March 2011, so interception and translocation did not occur. The soil to plant *CR* values for edible crops varied over 4 orders of magnitude, with geometric means ranging from 7.2×10^{-5} (Chinese cabbage) to 1.9×10^{-1} (rape seed). For crops sown in autumn and grown over winter, such as rape seed, foliar uptake might have contributed to the *CR* values, but no relevant data are available.

TABLE 4.35. ACTIVITY CONCENTRATION RATIOS *CR* FOR ^{137}CS TO SOYBEAN AND BUCKWHEAT IN 2012–2017

Crop	Year	N [a]	M [b]	Radiocaesium activity concentration ratio *CR* (kg soil DM / kg plant FM)				Exchangeable K in soil (mg/kg DM)	
				GM [c]	GSD [d]	Min [e]	Max	Min	Max
Soybean	2012	42	1	3.0×10^{-2}	2.6	3.4×10^{-3}	2.1×10^{-1}	74	640
	2013	50	1	8.7×10^{-3}	2.8	1.6×10^{-3}	1.1×10^{-1}	45	1400
	2014	59	8	4.9×10^{-3}	3.1	5.3×10^{-4}	3.5×10^{-2}	75	1300
	2015	58	12	4.3×10^{-3}	2.5	7.8×10^{-4}	2.1×10^{-2}	100	1200
	2016	43	0	3.6×10^{-3}	2.8	3.3×10^{-4}	3.3×10^{-2}	77	100
	2017	31	4	2.7×10^{-3}	3.2	2.8×10^{-4}	2.2×10^{-2}	140	1100
Buckwheat	2012	23	3	2.1×10^{-2}	1.9	8.3×10^{-3}	7.5×10^{-2}	90	1000
	2013	51	7	9.4×10^{-3}	1.8	3.4×10^{-3}	4.4×10^{-2}	92	790
	2014	39	8	6.5×10^{-3}	2.0	1.5×10^{-3}	2.1×10^{-2}	96	1100
	2015	53	9	5.8×10^{-3}	2.3	1.6×10^{-3}	4.3×10^{-2}	130	800
	2016	43	5	6.6×10^{-3}	2.2	1.5×10^{-3}	8.6×10^{-2}	92	900
	2017	25	2	4.2×10^{-3}	2.1	4.7×10^{-4}	2.4×10^{-2}	99	830

[a] the total number of measured samples
[b] the number of samples with radiocaesium activity concentrations below detection limit
[c] geometric mean (only for data above detection limit)
[d] geometric standard deviation (only for data above detection limit)
[e] minimum *CR* is occasionally overestimated due to the detection limit

There were some clear differences between the transfers of ^{137}Cs to different edible crops. The lowest transfer was for non-leafy vegetables (including cucumber, eggplant, green pepper and tomato), followed by leafy vegetables and root crops (2–3 time higher than those to non-leafy vegetables) and, finally, asparagus and beans (6–10 times higher than those for non-leafy vegetables. The transfer of radiocaesium to sunflower grain that is used for sunflower oil production was about four-fold higher than that to other edible crops. The transfer of radiocaesium to non-edible parts of non-leafy vegetables and leguminous (seeds and pods)

vegetables was general higher than that to edible parts (Table 4.43). These observations are mostly consistent with data obtained before the FDNPP accident [4.2].

TABLE 4.36. SOIL TO PLANT RADIOCAESIUM ACTIVITY CONCENTRATION RATIOS *CR* (KG SOIL DM / KG PLANT FM) OF AFTER THE FDNPP ACCIDENT IN 2011 AND 2012

Plant species	Year	N [a]	Mean [b]	GSD [c]	Minimum	Maximum
Leafy vegetables						
Komatsuna	2011	3	7.3×10^{-4}	1.6	5.3×10^{-4}	1.2×10^{-3}
Komatsuna	2012	8	2.1×10^{-3}	2.6	3.5×10^{-4}	5.0×10^{-3}
Mustard	2012	6	4.0×10^{-3}	1.3	3.0×10^{-3}	5.9×10^{-3}
Spinach	2011	1	2.3×10^{-3}	n.a.[e]	n.a.	n.a.
Chinese chives	2011	1	2.2×10^{-4}	n.a.	n.a.	n.a.
Welsh onion	2011	1	1.7×10^{-3}	n.a.	n.a.	n.a.
Cabbage	2011	1	1.8×10^{-4}	n.a.	n.a.	n.a.
Chinese cabbage	2011	1	7.2×10^{-5}	n.a.	n.a.	n.a.
Lettuce	2011	1	2.1×10^{-4}	n.a.	n.a.	n.a.
Shinobufuyuna	2011	1	4.7×10^{-2}	n.a.	n.a.	n.a.
Shinobufuyuna	2012	1	1.2×10^{-2}	n.a.	n.a.	n.a.
Oilseed rape (leaves)	2012	2	3.0×10^{-3}	n.a.	2.4×10^{-3}	3.5×10^{-3}
IAEA TRS 472 (kg DM/kg DM)		290	6.0×10^{-2}	6.0	3.0×10^{-4}	9.8×10^{-1}
Non–leafy vegetables						
Broccoli	2011	2	1.1×10^{-3}	n.a.	6.8×10^{-3}	1.5×10^{-3}
Broccoli	2012	1	1.7×10^{-4}	n.a.	n.a.	n.a.
Asparagus	2011	4	5.6×10^{-4}	4.2	1.7×10^{-4}	4.1×10^{-3}
Cucumber	2011	3	1.2×10^{-4}	1.2	1.0×10^{-4}	1.4×10^{-4}
Cucumber	2012	1	6.7×10^{-5}	n.a.	n.a.	n.a.
Tomato	2011	7	5.0×10^{-4}	2.4	1.4×10^{-4}	2.0×10^{-3}
Eggplant	2011	1	1.6×10^{-4}	n.a.	n.a.	n.a.
Green pepper	2011	1	3.3×10^{-4}	n.a.	n.a.	n.a.
Strawberry	2012	1	1.9×10^{-4}	n.a.	n.a.	n.a.
IAEA TRS 472 (kg DM/kg DM)		38	2.1×10^{-2}	4.1	7.0×10^{-4}	7.3×10^{-1}
Leguminous vegetables (seeds and pods)						
Field bean	2011	1	1.0×10^{-3}	n.a.	n.a.	n.a.
Soybean, young	2011	2	2.8×10^{-3}	n.a.	2.0×10^{-3}	3.5×10^{-3}
Soybean, young	2012	1	3.0×10^{-3}	n.a.	n.a.	n.a.
IAEA TRS 472 (kg DM/kg DM)		126	4.0×10^{-2}	3.7	1.0×10^{-3}	7.1×10^{-1}

TABLE 4.36. SOIL TO PLANT RADIOCAESIUM ACTIVITY CONCENTRATION RATIOS *CR* (KG SOIL DM / KG PLANT FM) OF AFTER THE FDNPP ACCIDENT IN 2011 AND 2012 (cont.)

Plant species	Year	N [a]	Mean [b]	GSD [c]	Minimum	Maximum
Root crops						
Japanese radish	2011	1	2.0×10^{-3}	n.a.	n.a.	n.a.
Japanese radish	2012	1	1.8×10^{-4}	n.a.	n.a.	n.a.
Turnip	2011	1	1.5×10^{-4}	n.a.	n.a.	n.a.
Turnip	2012	1	8.8×10^{-4}	n.a.	n.a.	n.a.
Carrot	2011	1	7.7×10^{-4}	n.a.	n.a.	n.a.
Carrot	2012	1	4.1×10^{-4}	n.a.	n.a.	n.a.
Burdock	2012	1	5.4×10^{-4}	n.a.	n.a.	n.a.
IAEA TRS 472 (kg DM/kg DM)		81	4.2×10^{-2}	3.0	1.0×10^{-3}	8.8×10^{-1}
Tubers						
Taro	2011	1	2.2×10^{-4}	n.a.	n.a.	n.a.
Taro	2012	1	8.7×10^{-4}	n.a.	n.a.	n.a.
Yacon	2011	1	1.2×10^{-4}	n.a.	n.a.	n.a.
Sweet potato	2011	2	4.4×10^{-3}	n.a.	3.4×10^{-3}	5.3×10^{-3}
Sweet potato	2012	2	1.4×10^{-3}	n.a.	8.7×10^{-4}	1.9×10^{-3}
Potato	2011	1	6.9×10^{-4}	n.a.	n.a.	n.a.
Yamanoimo	2012	1	2.8×10^{-3}	n.a.	n.a.	n.a.
IAEA TRS 472 (kg DM/kg DM)		138	5.6×10^{-2}	3.0	4.0×10^{-3}	6.0×10^{-1}
Seeds						
Sunflower	2011	5	7.6×10^{-3}	2.1	3.1×10^{-3}	1.8×10^{-2}
Rapeseed	2011	5	1.9×10^{-1}	2.7	5.9×10^{-2}	4.1×10^{-1}
Perilla	2012	2	3.3×10^{-3}	n.a.	2.5×10^{-3}	4.1×10^{-3}
Maize						
Grain	2011	1	4.3×10^{-4}	n.a.	n.a.	n.a.
IAEA TRS 472 (kg DM/kg DM)		67	3.3×10^{-2}	3.0	3.0×10^{-3}	2.6×10^{-1}

[a] the number of data
[b] depending on data availability, either GM (geometric mean) for N≥3 or AM (arithmetic mean) for N=2 or single value
[c] geometric standard deviation for samples with N≥3
[e] not applicable

The highest transfer measured was reported for fodder grass crops (Table 4.37). Accumulation of radiocaesium in the fodder crops was, on average, nearly three orders of magnitude higher than that of non-leafy vegetables with a particularly high transfer for Italian ryegrass (0.2 kg soil DM / kg plant FM). A high *CR* value was also measured for Orchard grass (0.5 kg soil DM / kg plant FM) that commonly grows between fruit trees. The data for grass is taken from the second cut after the accident, so the high *CR* values for perennial grasses are less likely to be

strongly influenced by retention of intercepted material than the first cut. However, it is still affected by foliar uptake, the higher CR values are probably due to the relatively high uptake from soil mat, litter on the surface of the field, and vertical grow of contaminated above-ground foliage below the cutting level into the cutting zone.

When comparing the *CR* values in Table 4.36 with those from IAEA TRS 472 [4.2], the *CR* values for non-leafy and root crops are nearly one order of magnitude lower; the values in Table 4.36 have been converted from fresh mass (FM) plant to dry mass (DM) plant (ca. 10% of the matter content for these crops from Chapter 2 attachment 2.2) for comparison with TRS 472. The geometric mean *CR* values for all fodder grass in Table 4.37 based on low sample numbers in Fukushima affected areas are similar to those provided in the TRS 472 (kg DM / kg DM). These differences may be due to higher application of potassium fertilizer in Japan associated with the high fertility of agricultural soil.

TABLE 4.37. RADIOCAESIUM ACTIVITY CONCENTRATION RATIOS *CR* (KG SOIL DM / KG PLANT FM) FROM SOIL TO FODDER GRASSES AND EDIBLE AND NON-EDIBLE PARTS OF CROPS IN 2011 AFTER THE FDNPP ACCIDENT

Crops	*CR* of edible crop parts (kg soil DM / kg plant FM)				*CR* of non-edible crop parts (kg soil DM / kg plant FM)			
	N [a]	Mean [b]	Minimum	Maximum	N	Mean [b]	Minimum	Maximum
Corn (silage)	n.a.[c]	n.a.	n.a.	n.a.	1	3.0×10^{-3}	n.a.	n.a.
Sudan grass	n.a.	n.a.	n.a.	n.a.	1	2.9×10^{-2}	n.a.	n.a.
Italian ryegrass [d]	n.a.	n.a.	n.a.	n.a.	1	2.0×10^{-1}	n.a.	n.a.
Orchard grass [d,e]	n.a.	n.a.	n.a.	n.a.	1	5.1×10^{-1}	n.a.	n.a.
Fodder grasses, all soils	n.a.	n.a.	n.a.	n.a.	4	4.8×10^{-2}	3.0×10^{-3}	5.1×10^{-1}
Grasses fodder (TRS 472), all soils (kg DM/kg DM)	n.a.	n.a.	n.a.	n.a.	64	6.3×10^{-2}	4.8×10^{-3}	9.9×10^{-1}
Leafy vegetables, all soils	10	6.9×10^{-4}	7.2×10^{-5}	4.7×10^{-2}	4	1.0×10^{-3}	2.5×10^{-4}	2.9×10^{-3}
Non-leafy vegetables, all soils	18	4.0×10^{-4}	1.2×10^{-4}	4.1×10^{-3}	6	3.1×10^{-3}	1.6×10^{-3}	6.5×10^{-3}
Leguminous vegetables, all soils	3	1.9×10^{-3}	1.0×10^{-3}	3.5×10^{-3}	2	1.0×10^{-2}	4.2×10^{-3}	1.6×10^{-2}
Root crops, all soils	3	6.1×10^{-4}	1.5×10^{-4}	2.0×10^{-3}	3	2.1×10^{-3}	5.1×10^{-4}	4.8×10^{-3}
Tubers, All soils	5	8.0×10^{-4}	1.2×10^{-4}	5.3×10^{-3}	4	2.2×10^{-3}	2.2×10^{-4}	1.0×10^{-2}

[a] the number of data
[b] depending on data availability, either GM (geometric mean) for N≥3 or AM (arithmetic mean) for N=2 or single value
[c] geometric standard deviation for samples with N≥3
[d] term used for fodder
[e] both Italian rye grass and orchard grass may also be contaminated by foliar uptake

The *CR* values for some vegetables can be directly compared with those reported for 1970–2008 in Japan (Fig. 4.22) [4.183]. In the dataset, measurements that would be affected by direct

deposition from global weapons fallout were removed. The geometric mean *CR* value of 8.0 × 10^{-3} kg soil DM / kg plant FM for leafy vegetables reported before the FDNPP accident, had a range from 2.0 × 10^{-5} to 0.5 kg soil DM / kg plant FM [4.183] which is in agreement with both the derived values in the first year after the FDNPP accident and TRS 472 values.

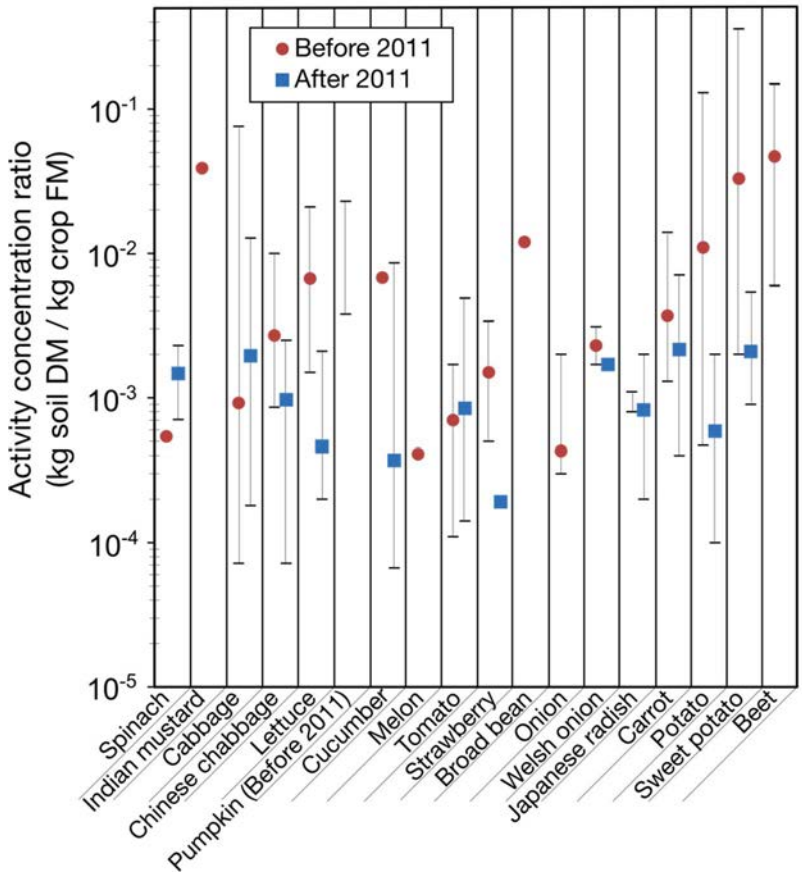

FIG. 4.22. Concentration ratios CR (kg soil DM / kg crop FM) for a range of different crops. Red circles show the data before 2011, and blue squares indicate the data after 2011. The bars represent minimum and maximum values (adapted after [4.183]]. The dataset used for CR values after 2011, although consistent with that reported in Table 4.36, also contains additional CR data for other crops.

4.3.4.4.Effect of soil properties

Studies were conducted to evaluate the effect of soil type on radiocaesium transfer [4.184, 4.185]. *CR* values were derived in pot experiments [4.184, 4.185] for various crops grown in different soil types present in the affected area, namely, grey lowland, brown forest, andosol or "Kuroboku-do" in Japanese and brown lowland (TABLE 4.38). The *CR* values for cucumber, tomatoes and peppers grown on brown forest soil tended to be higher than those of other soil types. However, further interpretation of the *CR* values was not possible because the number of observations is low and there was no information provided on soil characteristic such as exchangeable potassium and pH.

4.3.4.5.Varietal differences

Selection of plant varieties of a crop type that have low radiocaesium transfer from soil to the crop may be used as part of a remediation strategy of contaminated areas. Varietal difference

studies were implemented in the areas affected by the FDNPP accident. Data have been collated from studies carried out by the Fukushima branch of Tohoku Agricultural Research Centre of National Agriculture and Food Research Organization (NARO) which were largely focused on vegetables such as cabbage, spinach, broccoli, green onion, turnip, Japanese radish, carrot, and Amaranthus [4.186]. The dataset also includes studies on soybean [this work], and on Amaranthus (whole plants) and kenaf in 2011–2013 by Ogata et al. [4.187] and Shinano et al. [4.188]. The effect of varietal differences observed within a growing season in these different studies, which involved comparison of between 3 to 33 varieties of the above crops, is shown in FIG. 4.23.

TABLE 4.38. RADIOCAESIUM ACTIVITY CONCENTRATION RATIOS *CR* (KG SOIL DM / KG PLANT FM) FOR VARIOUS CROPS GROWN ON DIFFERENT SOIL TYPES IN 2011

Plant species	Soil type [a]	N	*CR* (kg soil DM / kg plant FM)
Cucumber	Grey lowland	3	7.0×10^{-4}
	Andosol	3	2.7×10^{-4}
	Brown forest	3	8.6×10^{-3}
Tomato	Grey lowland	3	8.0×10^{-4}
	Andosol	3	2.9×10^{-3}
	Brown forest	3	4.9×10^{-3}
Eggplant	Grey lowland	3	9.0×10^{-4}
	Andosol	3	4.5×10^{-3}
	Brown forest	3	3.4×10^{-3}
Green pepper	Grey lowland	3	3.0×10^{-4}
	Andosol	3	2.2×10^{-3}
	Brown forest	3	4.7×10^{-3}
Cabbage	Brown forest	— [b]	5.3×10^{-3}
	Andosol	—	1.6×10^{-3}
	Grey lowland	—	1.0×10^{-3}
	Brown lowland	—	3.5×10^{-3}
“Komatsuna” (mustard spinach)	Brown forest	—	2.6×10^{-3}
	Andosol	—	7.0×10^{-4}
	Grey lowland	—	1.3×10^{-3}
	Brown lowland	—	1.8×10^{-3}

[a] Brown forest: clay 5%, silt 9%, fine sand 34%, coarse sand 52%
Andosol: clay 23%, silt 31%, fine sand 24%, coarse sand 21%
Grey lowland: clay 20%, silt 24%, fine sand 36%, coarse sand 20%
Brown lowland: clay 19%, silt 24%, fine sand 46%, coarse sand 11%
[b] no data

To provide better comparisons between species and varieties, the data for soybean and Amaranthus are shown separately in Fig. 4.24 because the *CR* values for these species were higher than those for vegetables. Data for vegetables including cabbage, spinach, broccoli, leaf green onion, turnip, Japanese radish, and carrot (Fig. 4.23) are given in a FM basis (kg soil DM / kg plant FM) whereas values for soybean and Amaranthus are given on a DM basis (kg soil DM / kg plant DM) (Fig. 4.24).

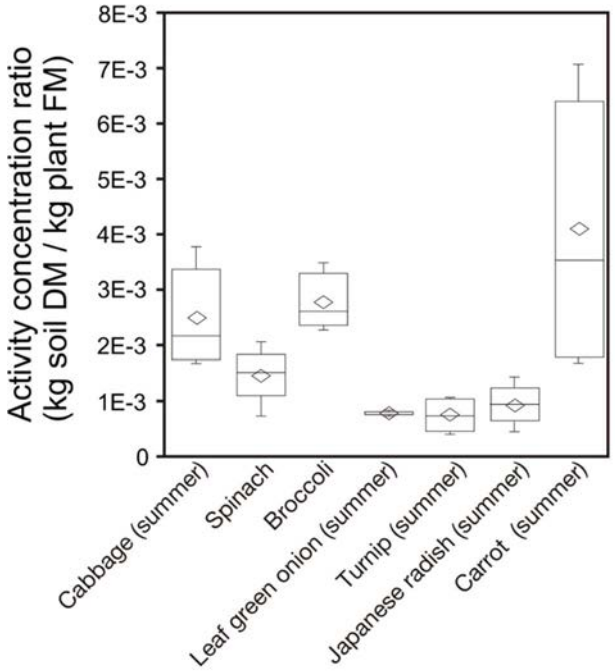

FIG. 4.23. Varietal difference in radiocaesium activity concentration ratio CR (kg soil DM / kg plant FM) within different crops.

The data provided in Figure 4.22 are the basis for the selection of suitable crop types to plant in contaminated agricultural fields, allowing optimized use of the affected land. In general, the variation in *CR* between different crops is in most cases higher than within varieties of a crop [4.2, 4.56, 4.189, 4.190]. Most likely, this is due to the limited number of plant varieties used in Japan compared with the world-wide spectrum of varieties cultivated [4.188].

The large variation in *CR* values both between and within crop species made it difficult to develop suitable remediation procedures based on a soil concentration limit for the range of edible crops.

The data for the three important crops, i.e., rice, soybean and buckwheat, have been collated to derive the relationship between the *CR* values for ^{137}Cs (Table 4.39). The ratios have been calculated separately for each year and each crop, and the geometric mean subsequently calculated. There are clear differences between the transfer of ^{137}Cs, which decreased in the order of soybean > buckwheat > brown rice.

4.3.4.6. Effect of potassium on CR values in Fukushima prefecture for soybean and buckwheat

For rice, a threshold value of 25 mg K_2O/100 g soil DM for soil was established to identify agricultural fields that needed additional K fertilisation to reduce radiocaesium *CR* values. *CR* also gradually decreased with increasing exchangeable K in soil for soybean and buckwheat. For buckwheat and soybean, threshold values were initially set for the first crop at 50 mg K_2O/ 100 g soil DM for more contaminated areas where crop radiocaesium activity concentrations in crops might exceed 100 Bq/kg FM. Subsequently, the values were reduced to 30 and 25 mg K_2O/100 g soil DM, respectively [4.191].

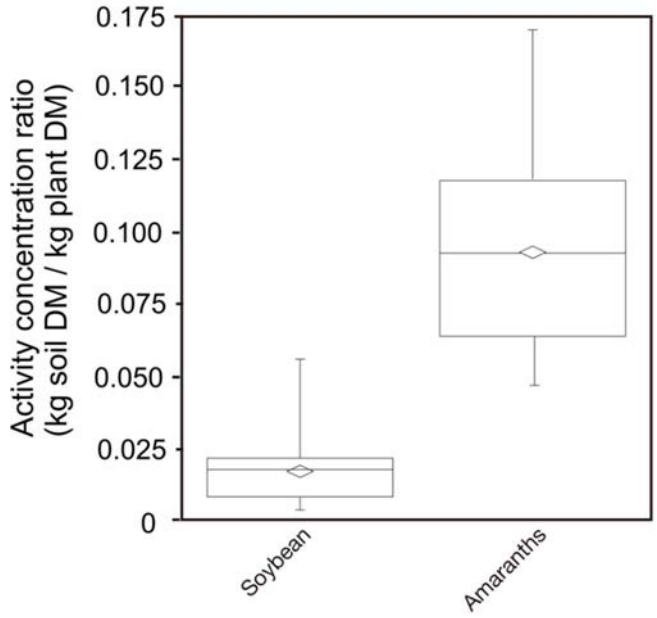

FIG. 4.24. Varietal difference in radiocaesium activity concentration ratio CR (kg soil DM / kg plant DM) within crops.

TABLE 4.39. RELATIONSHIPS BETWEEN RADIOCAESIUM ACTIVITY CONCENTRATION RATIOS *CR* FOR BUCKWHEAT, BROWN RICE AND SOYBEAN FOR 2012–2016

Parameters	Ratio of *CR* for different crops		
	Buckwheat/Rice	Buckwheat/Soybean	Soybean/Rice
Geometric mean (GM)	4.8	1.2	3.9
Arithmetic mean (AM)	4.9	1.3	4.4
Standard Deviation (SD)	1.5	0.4	2.7
Minimum	3.2	0.7	2.3
Maximum	6.2	1.7	9.1

Based on data obtained within the monitoring programme, as listed in Table 4.35 for soybean and buckwheat, Yamamura et al. [4.92] suggested a simple statistical model to estimate the relationship between radiocaesium *CR* values and the exchangeable potassium concentration in the soil using equation 4.4 in sub-section 4.3.1.9.

These empirical models developed in 2015–2017 are useful to estimate CR values from exchangeable K concentrations in soil. The b_0 and b_1 are fitted parameters which represented constants for soybean and buckwheat to be used as a function of year and which are given in Table 4.40 for 2012–2017.

TABLE 4.40. PARAMETERS OF THE STATISTICAL MODEL (EQ. 4.4) DESCRIBING DEPENDENCE OF CONCENTRATION RATIOS FOR SOYBEAN AND BUCKWHEAT ON EXCHANGEABLE POTASSIUM IN THE SOIL

Species	b_0						b_1
	2012	2013	2014	2015	2016	2017	
Soybean	−0.14	−1.22	−1.87	−2.15	−1.97	−2.38	−0.53
Buckwheat	−0.96	−1.74	−2.12	−2.21	−2.09	−2.44	−0.48

Using these parameters, the relationship between soil exchangeable potassium concentration and *CR* is presented in Fig. 4.25 for soybean and buckwheat. In 2012, for both species (see Fig. 4.25), the intercept of the curve (b_0) was the highest, thus *CR* was highest for all exchangeable K concentration range in soil. The intercepts gradually decreased in 2013 and 2014, which implies a decrease of *CR* with time. After 2014, the intercepts of the curves were almost the same, thus, relation of the radiocaesium CR and the exchangeable K concentration in soil became constant.

4.3.4.7. Effect of K fertilizer on CR values for other crops

An alternative method to describe the dependence of radiocaesium activity concentration ratio *CR* on concentration of exchangeable potassium (K_{ex}) was developed for vegetables and fodder because there were fewer data for each year. The approach [4.92], which is similar to Eq. (4.4) while using different parameterisation, was adopted:

$$CR = a\, K_{ex}^{b}\,, \tag{4.11}$$

where CR is the radiocaesium activity concentration ratio specified either on a “FM-basis”, i.e., Bq/kg plant FM per Bq/kg soil DM or on a “DM-basis”, i.e., Bq/kg plant DM per Bq/kg soil DM; K_{ex} is the concentration of exchangeable potassium in soil (mg K / kg soil DM).

The statistical model parameters for ‘komatsuna’ and cabbage are presented in Table 4.41 (based on collated data [4.186, 4.192, 4.193]).

For pasture grass (dominated by orchard grass, *Dactylis glomerata*) shown in Table 4.41, the relationship between exchangeable K and *CR* differed depending on the timing of harvesting [4.195, 4.196]. *CR* was not only affected by the exchangeable potassium concentration in soil, but also by factors such as growth status and/or sampling time.

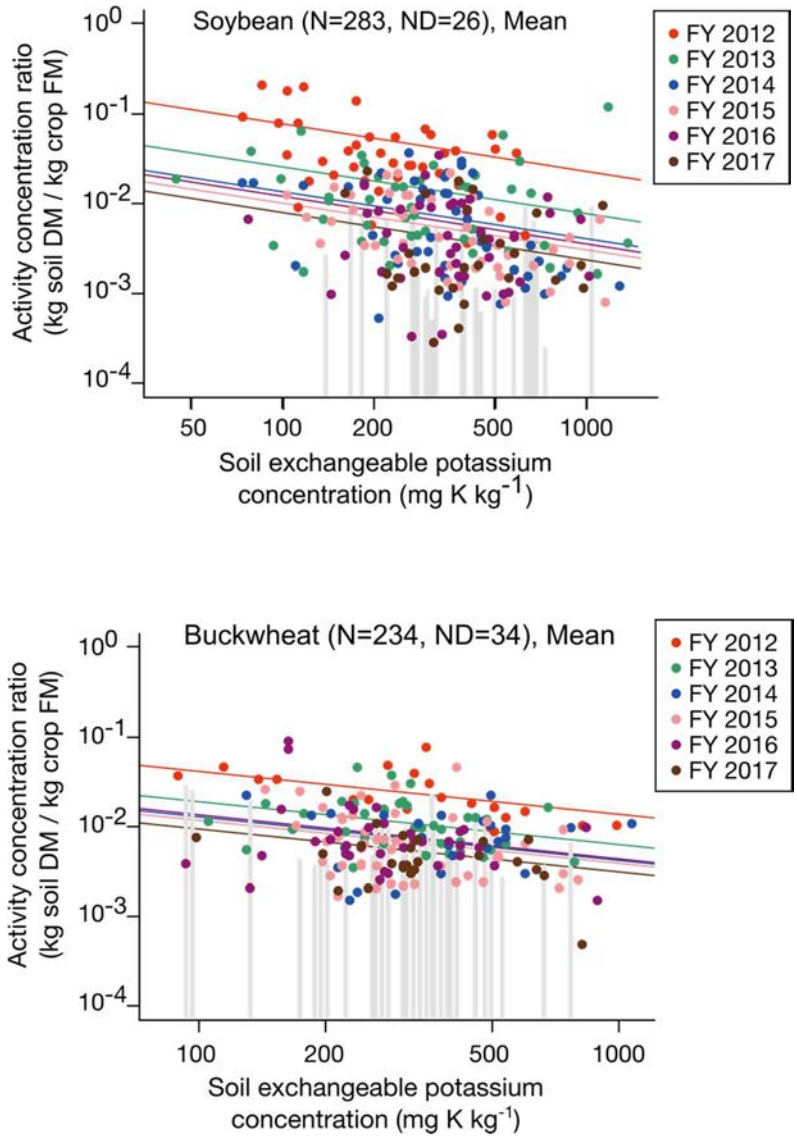

FIG. 4.25. Relationship between soil exchangeable potassium concentration and CR for soybean (top plot) and buckwheat (bottom plot); N = the number of analysed samples, FY = fiscal year. Tops of the grey bars in the figure are CR values calculated using the detection limit for radiocaesium for a number (ND) of samples in which radiocaesium activity concentration were below the detection limit.

Farmers in mountainous areas in Japan tend to use weeds grown in the levee of paddy fields as a feed for their livestock, especially for goats. The major weed species used for feed include mugwort (*Artemisia indica* var. *maximowiczii*), sweet vernal grass (*Anthoxanthum odoratum*), and tall fescue (*Festuca arundinacea*). As for crops, the *CR* values decreased as soil exchangeable potassium concentration increased [4.194] as shown in Table 4.41.

TABLE 4.41 PARAMETERS OF THE STATISTICAL MODEL (EQ. 4.11) DESCRIBING DEPENDENCE OF RADIOCAESIUM ACTIVITY CONCENTRATION RATIOS FOR VEGETABLES AND GRASSES ON CONCENTRATION OF EXCHANGEABLE POTASSIUM IN THE SOIL

Crop	Year	N [a]	*a*	*b*	R^2 [b]	Reference
Leafy vegetables (FM-basis [c])						
Komatsuna	2012	12	0.22	−0.76	0.87	[4.192]
Cabbage [d]	2011	36	0.0271	−0.85	0.35	[4.194]
Fodder (FM-basis)						
Pasture grass [e]	2012	72	33.02	−0.093	0.32	[4.195]
Weed plants used as animal feed (DM-basis [f])						
Anthoxanthum odoratum	2013	12	11.7	−0.97	0.62	This work
Festuca arundinacea	2013	22	0.46	−0.57	0.14	This work
Miscanthus sinensis	2013	11	0.022	−0.036	0.0028	This work
Artemisi indica var. Maximowiczii	2013	30	27.5	−1.1	0.62	This work

[a] the number of data
[b] the squared correlation coefficient, explains the strength of the relationship between the two variables
[c] *CR* in units (Bq/kg plant FM per Bq/kg soil DM)
[d] combined data for 4 different soils
[e] data were extracted from a figure and data for *CR*=0 were deleted from the calculation
[f] *CR* in units (Bq/kg plant DM per Bq/kg soil DM)

4.3.4.8. Radiocaesium transfer from drinking water sludge to vegetables

Both drinking water and sewage sludge were contaminated with radiocaesium (^{134}Cs and ^{137}Cs) after the FDNPP accident. Sludge from drinking water and sewage treatments is sometimes applied to agricultural fields to enhance the nutrient status of the soil. The sludge is generated during cleaning processes applied to ensure that river water and sewage effluents (from houses and industry) discharged to rivers used for drinking water meet water quality regulations.

During these cleaning processes, water soluble caesium (Cs^+), bound to organic matter or to soil particles, is partially retained in the sludge. About 10% of the Cs entering the sewage treatment plant has been reported to be transferred to the sewage sludge [4.68].

In Japan, some potting compost mix products used for growing plants contain sludge at a maximum mixing fraction of 30 vol.%. Studies were conducted to clarify whether the use of this medium would lead to enhanced radiocaesium activity concentrations in plants [4.197, 4.198]. A pot experiment using soil with contaminated drinking water sludge was carried out and the radiocaesium transfer from soil to leafy vegetables (“Komatsuna” and “Chingensai”) was measured; the results are shown in Table 4.42. The arithmetic mean *CR* values were 7.9×10^{-2} and 1.1×10^{-1} (kg soil DM / kg plant FM), for “Komatsuna”, and “Chingensai”, respectively, which were within the range of 4.1×10^{-2} to 1.7×10^{-1} (kg soil DM/kg plant FM), as previously reported for Japanese leafy vegetables [4.199]. These data suggest that radiocaesium binds strongly to drinking water sludge. The results were also consistent with studies by [4.200] which showed that the application of deionized water, ozone micro-bubble water and ozone gas bubbling in deionized water to drinking water sludge containing 4.2 kBq/kg DM of ^{137}Cs did not extract measurable amounts of ^{137}Cs.

TABLE 4.42. ACTIVITY CONCENTRATION RATIOS OF RADIOCAESIUM FOR SOIL CONTAINING DRINKING WATER SLUDGE

Plant species	N [a]	Concentration ratio CR (kg soil DM / kg plant FM)						Reference
		AM [b]	SD [c]	GM [d]	GSD [e]	Min	Max	
"Komatsuna"	6	7.9×10^{-3}	3.1×10^{-2}	7.0×10^{-2}	1.8	2.2×10^{-2}	0.1	[4.197, 4.198]
"Chingensai"	4	1.1×10^{-2}	3.3×10^{-2}	1.1×10^{-2}	1.4	7.2×10^{-2}	0.15	[4.198]

[a] the number of reported data
[b] arithmetic mean
[c] arithmetic standard deviation
[d] geometric mean
[e] geometric standard deviation (unitless)

4.3.4.9. Summary and limitations

Summary

The *CR* of soybean and buckwheat is higher than that for rice. The *CR* values for soybean and buckwheat gradually decrease with increasing soil potassium concentration as well as time, as occurred for rice.

The *CR* values for fodder grass derived from the measurements in Fukushima-affected areas are similar to those provided in TRS 472 (kg soil DM/kg plant DM). However, values for other leafy vegetables and root vegetables are much lower than the geometric mean values in TRS 472 [4.2].

The variations in CR between different crops are, in most cases, larger than within (inter-cultivar) varieties of crops, which is in agreement with pre-accident observations.

Limitations

There were few data for translocation for many crops. Therefore, the results achieved are associated with some uncertainties.

The effect of potassium fertilizer on *CR* values for other crops is clear, but the parameter values proposed here might be limited only to the areas in Fukushima. Further data comparisons among different sampling areas are needed.

4.4.TRANSFER TO FARM ANIMALS

4.4.1. Introduction

Compared with European countries, consumption of animal products is low in Asian countries, including Japan. After the FDNPP accident, ^{131}I activity concentrations in dairy cow milk were extensively monitored to ensure that milk entering the food chain did not exceed 300 Bq/L (provisional regulation value in Japan [4.46]). Monitoring data for ^{131}I and total radiocaesium (^{134}Cs+^{137}Cs) in cow milk are shown in Fig. 4.26 for the first 80 days after the accident [4.3].

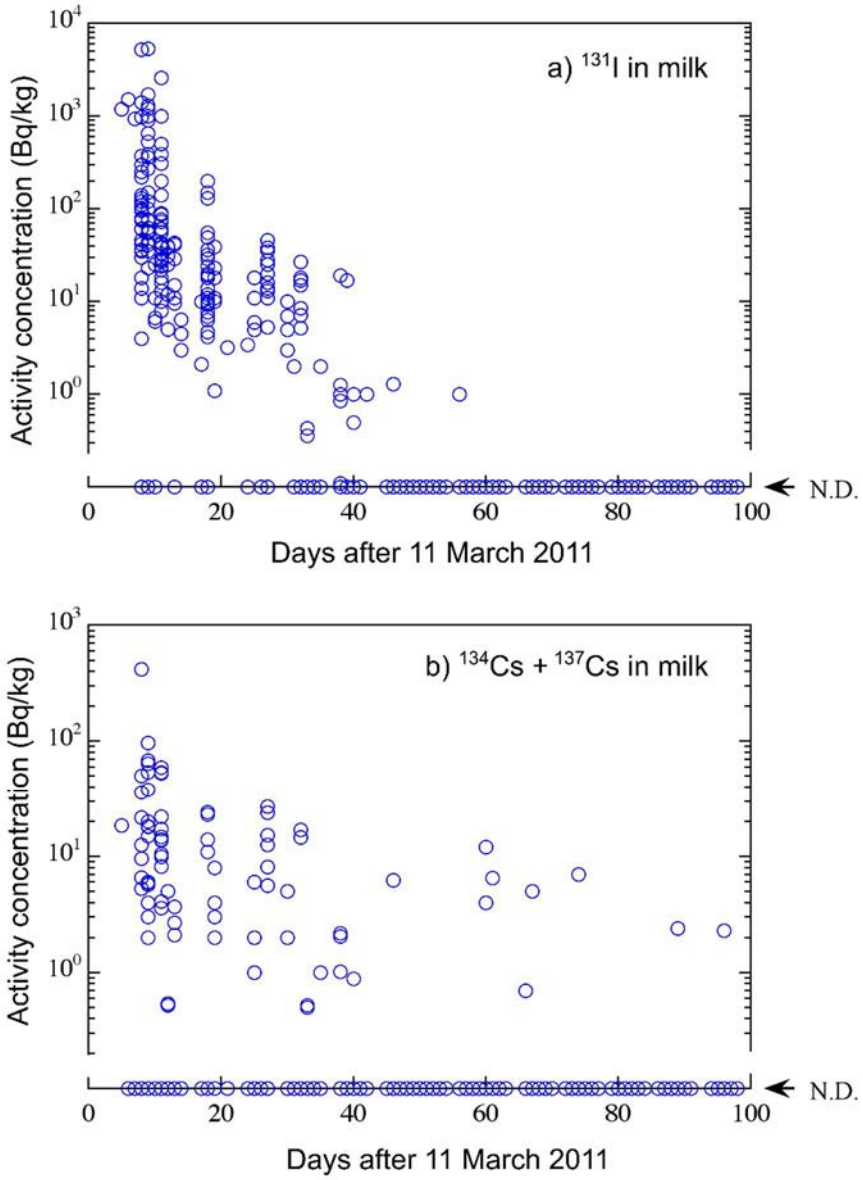

FIG. 4.26. Concentrations of ^{131}I and radiocaesium (^{134}Cs+^{137}Cs) in cow milk observed after the FDNPP accident. Not detected (N.D.) data are on the N.D. line in both figures.

The ^{131}I and total radiocaesium (^{134}Cs+^{137}Cs) activity concentrations in milk after the FDNPP accident were much lower than those occurring after the Chernobyl accident. The main reasons for the comparatively low measured values are that:

- The FDNPP accident occurred before the vegetation growing season, so dairy animals were not fed on plants that were directly contaminated by radionuclide deposition on the surface of vegetation;
- Most dairy animals in Japan are permanently housed, being fed with uncontaminated feed in stalls;
- The sale of milk was rapidly prohibited from highly contaminated areas;
- The provisional activity limits for ^{131}I and radiocaesium in foodstuffs were set at low values.

In contrast to the Chernobyl accident, milk was not consumed from cows that had been grazing outdoors on highly contaminated pasture. Since directly contaminated grass was not used in the first year, root-uptake became the major pathway leading to contamination of animal feeds.

After the FDNPP accident, there were relatively few contaminated animal data compared with the Chernobyl accident. Based on Chernobyl experience [4.201], some animals were fed with uncontaminated feed (i.e. clean feeding) to reduce radionuclide activity concentrations in tissues. In the first few months after the accident, there were no violations of the provisional regulation value of 500 Bq/kg FM of total radiocaesium concentration in animal tissues.

About 90 days after the accident, exceedance of the regulation value occurred for nine months in beef (Fig. 4.27). In Japan, after the harvesting of rice, the rice straw is spread onto fields to dry during the winter season, after which it is collected to use it as feed for beef animals and as a component of cattle beds. The FDNPP accident occurred at the end of the winter season, just before rice straw collection, so radionuclides were deposited onto the rice straw. In areas where deposition amounts of radiocaesium were low (<10 kBq/m^2), the radiocaesium activity concentrations in rice straw exceeded several hundreds of Bq/kg DM, because the dried rice straw had a low biomass. Consumption of the rice straw led to elevated radiocaesium activity concentrations in beef and thus all beef was monitored for the following five years; some prefectures continued all beef monitoring even in 2019.

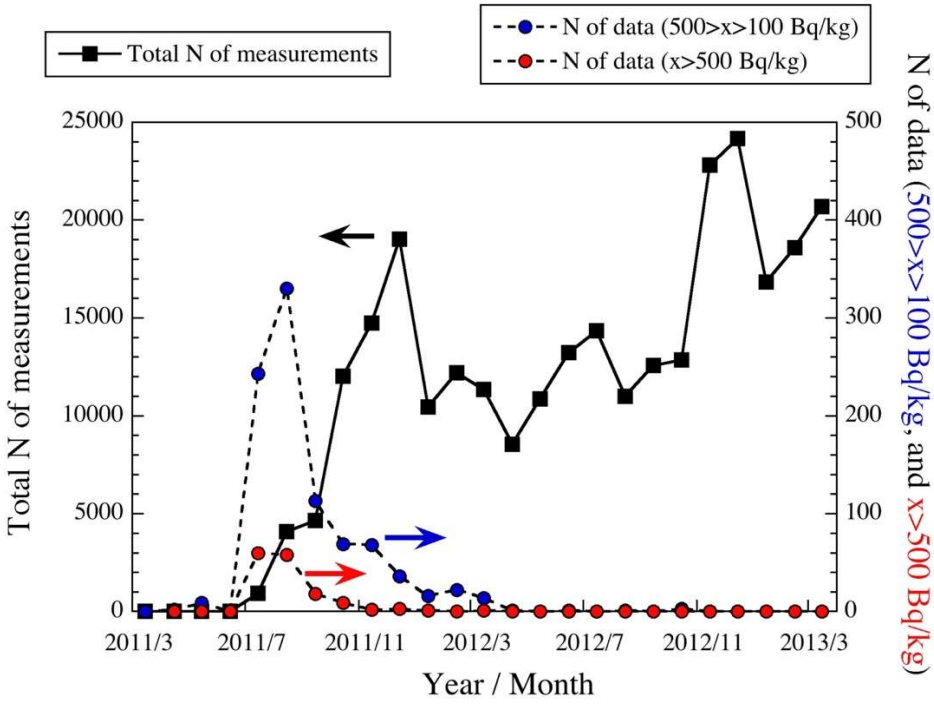

FIG. 4.27. The number N of monthly monitoring data for radiocaesium $^{134}Cs+^{137}Cs$ in beef, including the total number of samples (black squares and solid curve, left axis), the number of samples with activity concentration exceeding the provisional regulatory limit 500 Bq/kg FM effective until September 2012 (red circles, dashed curve, right axis) and the standard regulatory limit of 100 Bq/kg FM [4.124] used afterwards (blue circles, dashed line, right axis)

For pigs and chickens, feeds were usually imported from overseas which helped to prevent exceedance of the provisional regulatory value (500 Bq/kg FM). Subsequently, a strategy which encouraged the use of national products was applied (to avoid chemically treated imports). The use of locally produced rice was encouraged so the transfer of radiocaesium from rice to pigs and chickens was measured to ensure that transfer of radiocaesium would not lead to violations of the provisional regulatory value for foodstuff.

From 1 April 2012, the Japanese government applied standard limits that were 1/5th of the provisional regulatory value (except for beef, for which standard limits were applied from September 2012). To ensure that the radiocaesium activity concentrations in animal products complied with the revised Japanese regulatory values, feed to milk (F_m) and feed to meat (F_f) transfer coefficients and concentration ratios (*CR*) were determined.

A small dataset has been created of transfer parameter values for farm animals containing data from seven studies carried out after the FDNPP accident. Three pre-Fukushima studies were also added (in Japanese) that had not been included in the animal product compilation in the IAEA TRS 472 [4.2]. Information sources were mostly papers published in scientific journals; some data were collated from institutional reports.

4.4.2. F_m, F_f and *CR* values

Information on transfer parameters for animal products of radioiodine and radiocaesium reported in Japan are given in Tables 4.43–4.45. The transfer parameter values reported after the FDNPP accident were similar to those reported in international literature [4.2, 4.202].

TABLE 4.43. TRANSFER COEFFICIENT F_m (d/L) AND ACTIVITY CONCENTRATION RATIO CR (kg/L) OF RADIOIODINE FOR DAIRY FARM ANIMALS IN JAPAN

Animal	Year	N [a]	F_m (d/L) [b]	Minimum	Maximum	*CR* (kg/L)	Reference
Goat	2011	14	0.28	0.06	0.6	— [c]	[4.203]
Cow	2011	8	0.0036	0.001	0.0062	—	[4.203]
Cow	2011	1	—	n.a. [d]	n.a.	0.13	[4.204]

[a] the number of reported data
[b] inhalation may also have occurred
[c] no data
[d] not applicable

Previously recommended values are given in Table 4.46 for comparison. There are previously reported relationships whereby F_f and F_f/F_m for smaller animals are higher than those for larger animals. This phenomenon does not mean there are changes in absorption and transfer to tissues or with age or between species [4.216, 4.217]. The reason for these observations is largely due to the way how F_f is calculated. F_f is the dietary *CR* divided by the food intake rate. There is no real reason to think *CR* will change that much with age or species as this does not occur for other elemental concentrations in meat. However, the dry matter food intake increases with age and, therefore, the amount of radionuclide ingested increases and hence F_f decreases [4.217, 4.218]. The *CR* is a more robust parameter to use as it is not age dependent and expected to be relatively constant across animal types (see IAEA TRS 472 [4.2]). This can be seen to be the case for data for poultry from Japan in Fig. 4.28, where the uncertainty of *CR* is lower than that of F_f.

TABLE 4.44. TRANSFER COEFFICIENT F_f (d/kg) AND ACTIVITY CONCENTRATION RATIO *CR* (kg/kg) OF RADIOCAESIUM (^{137}CS, ^{134}CS) FOR ANIMAL TISSUE PRODUCTS IN JAPAN [a]

Animal	Tissue	Year	N [b]	F_f (d/kg)			*CR* (kg/kg)			Comment	Reference
				Mean [c]	Minimum	Maximum	Mean [c]	Minimum	Maximum		
Cattle	Muscle	2012	8	0.038	0.019	0.072	0.16	0.10	0.25	4 animals fed for 6 months	Calculated from Yonnai et al. [4.205]
Cattle	Liver	2012	4	0.010	0.0049	0.024	0.042	0.026	0.095	4 animals fed for 6 months	Calculated from Yonnai et al. [4.205]
Cattle	Heart	2012	3	0.025	0.013	0.035	0.099	0.065	0.13	3 animals fed for 6 months	Calculated from Yonnai et al. [4.205]
Cattle	Muscle	2013	4	0.016	0.014	0.019	0.11	0.10	0.13	4 animals fed for 1 month	[4.206]
Cattle	Muscle	2014	4	0.016	0.015	0.018	0.11	0.10	0.13	4 animals fed for 1 month	[4.206]
Pig	Muscle	2012	1	0.40	n.a. [d]	n.a.	0.93	n.a.	n.a.	6 castrated pigs in 3 pens, mean of n=3 fed for 3 weeks	[4.207]
Pig	Liver	2012	1	0.33	n.a.	n.a.	0.78	n.a.	n.a.	6 castrated pigs in 3 pens, mean of n=3, fed for 3 weeks	[4.207]
Pig	Digestive tract	2012	1	0.30	n.a.	n.a.	0.69	n.a.	n.a.	6 castrated pigs in 3 pens, mean of n=3, fed for 3 weeks	[4.207]
Chicken	Thigh	2011	2	1.9	1.7	2.0	0.30	0.27	0.33	1 animal fed from 0 to 12 weeks (n=1) and 5 animals fed from 0 to 17 weeks	Calculated from Miyano and Sato [4.208]
Chicken	Breast	2011	2	1.8	1.5	2.2	0.30	0.23	0.36	1 animal fed from 0 to 12 weeks (n=1) and 5 animals fed from 0 to 17 weeks	Calculated from Miyano and Sato [4.208]
Chicken	Gizzard	2011	1	0.90	n.a.	n.a.	0.14	n.a.	n.a.	1 animal fed from 0 to 12 weeks (n=1) and 5 animals fed from 0 to 17 weeks	Calculated from Miyano and Sato [4.208]
Horse	Muscle	2011	1	0.023	n.a.	n.a.	0.23	n.a.	n.a.	6 horses fed for 8 weeks	Calculated from Manabe et al. [4.209]

[a] Uptake via ingestion of contaminated silage (root uptake, Fukushima fallout)
[b] the number of data
[c] geometric mean (GM) for N > 2, arithmetic mean (AM) otherwise
[d] not applicable

TABLE 4.45. TRANSFER COEFFICIENT F_m (d/L) AND ACTIVITY CONCENTRATION RATIO *CR* (kg/L) OF RADIOCAESIUM FOR COW MILK IN JAPAN

Year	N [a]	F_m (d/L)			*CR* (kg/L)			Comment	Reference
		Mean [b]	Minimum	Maximum	Mean [b]	Minimum	Maximum		
2011	5/4[c]	0.0023	0.00037	0.017	0.010	0.0094	0.0125	Ingestion of intercepted radiocaesium and inhalation of Fukushima fallout	[4.204, 4.210, 4.211]
2012	3	0.0020	0.0015	0.0035	0.043	0.032	0.073	Ingestion of silage (root uptake of Fukushima fallout)	[4.212]
1988	10	0.0031	0.0022	0.0043	— [d]	—	—	Ingestion of grass (intercepted Chernobyl deposition)	[4.213, 4.214]
1990	2	0.0050[d]	0.0037	0.0063	0.012[d]	0.010	0.014	Ingestion of grass (root uptake of global fallout)	[4.215]

[a] the number of data
[b] geometric mean (GM) for N > 2, arithmetic mean (AM) otherwise
[c] 5 values for F_m, 4 values for *CR*
[d] no data

During outdoor grazing, some radiocaesium in soil adhered to plant surfaces and could be ingested by animals, but the transfer from soil, even when it is more highly contaminated than the plants, is usually low compared with plant material [4.219]. When chickens in Japan were fed with contaminated brown forest soil with 3900–4500 Bq/kg DM ^{137}Cs, the F_f value in chicken breast ranged from 0.04–0.05 d/kg FM, whereas the F_f for chickens fed with normal feed containing 110 Bq/kg FM ^{137}Cs was higher at 1.5 d/kg FM.

TABLE 4.46. RADIOCAESIUM TRANSFER PARAMETERS FOR ANIMAL PRODUCTS

Transfer parameter	Animal product	Geometric mean	Minimum	Maximum	Reference
F_m(d/L)	cow milk	0.0046	0.0006	0.068	[4.2]
F_m(d/L)	cow milk	0.0049	0.0006	0.057	[4.202] [a]
CR (kg/L)	cow milk	0.11	0.0036	0.69	[4.2]
CR (kg/L)	cow milk	0.084	0.0036	0.90	[4.202] [a]
F_f (d/kg)	beef	0.022	0.0047	0.096	[4.2]
F_f (d/kg)	pork	0.2	0.12	0.4	[4.2]
F_f (d/kg)	chicken	2.7	1.2	5.6	[4.2]

[a] Developed during MODARIA I; values from TRS 472 [4.2] are given for comparison, but these are now superseded by Howard et al [4.202]

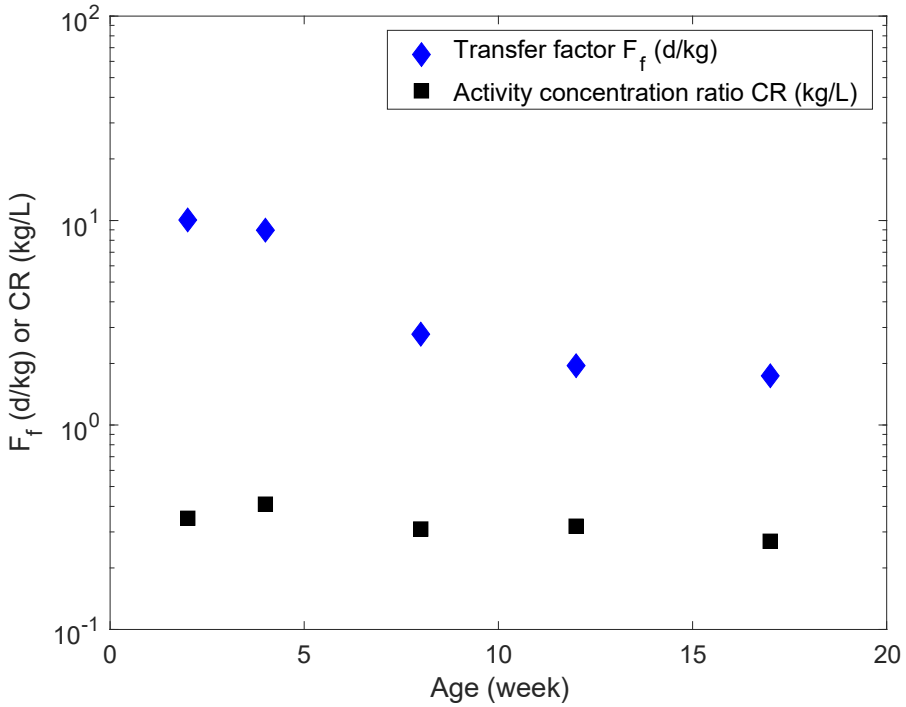

FIG. 4.28. Transfer factor F_f and activity concentration ratio CR of radiocaesium for chicken of various age (data from [4.208]).

4.4.3. Radiocaesium distribution in animal tissues

In the areas abandoned after the FDNPP accident, cattle were released from housing and subsequently grazed outdoors on highly contaminated vegetation. Some cattle were captured from August to November 2011 [4.220], September to November 2011 [4.221] and October to November 2013 [4.222] and measurements were made of the radiocaesium activity concentrations in their tissues. The ratio of the radiocaesium activity concentration in each tissue of abandoned cattle to that in *biceps femoris* muscle is shown in Fig. 4.29. The radiocaesium activity concentration was significantly higher (ANOVA test, $p<0.02$) in *biceps femoris* than in tongue, liver, kidney and heart, and that in liver was significantly lower (ANOVA test, $p<0.05$) than all the other tissues measured.

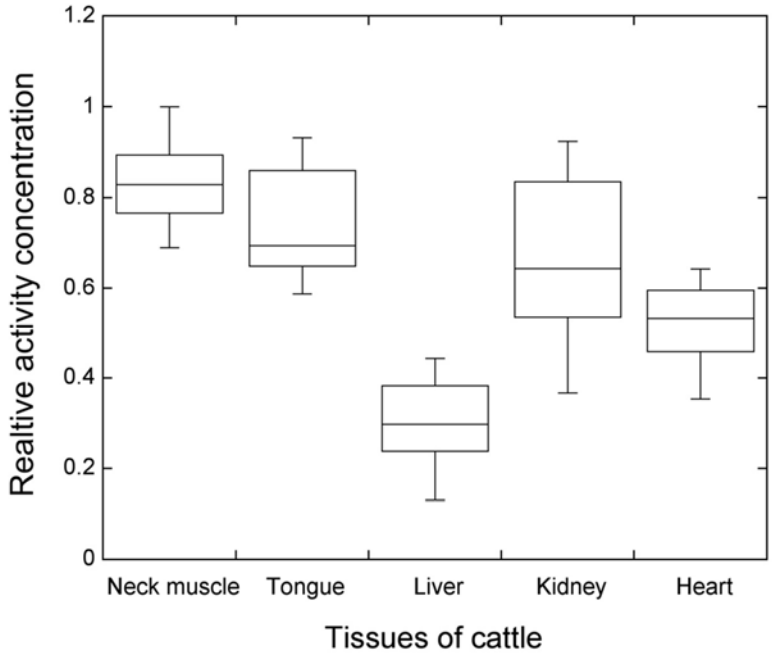

FIG. 4.29. Activity concentration of radiocaesium in different cattle tissues (neck muscle, tongue, liver, kidney, heart) normalised to activity concentration in the biceps femoris muscle (n=12).

4.4.4. Biological half-life

Clean feeding before slaughter is a commonly used remediation measure for agricultural animals contaminated due to radionuclide intake after accidents [4.201]. The loss rate of radiocaesium in animal tissues when contaminated animals are fed on uncontaminated feed is commonly quantified using the biological half-life (T_b). Data for T_b for the breeds in Japan, reported after the FDNPP accident are summarized in Table 4.47. In this table, single exponential functions were derived by fitting the time-dependence of radiocaesium in meat, because only short-term studies (up to 40 days) were carried out. Furthermore, due to high detection limits (~10–50 Bq/kg FM), many subsequent measurements were below detection limits so the slow component of loss was not measurable, and a double exponential function could not be derived.

Live monitoring was used as a management method in many countries after the Chernobyl accident to identify animals that needed clean feeding and to ensure that radiocaesium activity

concentrations were below permissible limits when slaughtered. However, due to the low radiocaesium activity concentrations in most agricultural animals in Japan, and the low standard limit of 100 Bq/kg FM for beef, live monitoring of animals was not appropriate for large-scale implementation. Furthermore, in highly contaminated areas, the surface deposits of radiocaesium contributed significantly to on-site measurements of living animals.

To ensure that animals were below standard limits prior to slaughter, live monitoring measurement methods were developed in Japan using blood sampling (e.g. Koga et al.[4.223]) which could detect the very low radiocaesium activity concentration in most animals. In dairy cows and beef cattle [4.206, 4.224, 4.225], ^{137}Cs activity concentrations in blood decreased with a T_b of 9.7 days which was similar to that observed for cow's milk. A second, longer half-life of about 50 days was derived for blood, but no equivalent data were identified for milk in Japan.

A recent review of T_b data suggest that there are two components of loss for Cs with half-lives of about 1.4 days (80% of total activity) and 15 days (20% of total activity) for milk and about 9 days (56% of total activity) and 53 days (44% of total activity) for beef [4.226].

TABLE 4.47. SINGLE EXPONENTIAL FUNCTION BIOLOGICAL HALF-LIVES OF IODINE AND CAESIUM IN JAPANESE FARM ANIMAL TISSUES.

Animal product	Element	N [a]	Biological half-life T_b (d)	Range	Reference
Cow, milk	I	1	6.5	n.a.[b]	[4.204]
Cow, milk	Cs	3	6.5	4.3−12.4	[4.204, 4.211, 4.227]
Cow, whole body	Cs	2	45	43−46	[4.206]
Cattle, meat	Cs	10	20	14−27	[4.224, 4.225]

[a] the number of data
[b] not applicable

4.4.5. Summary and limitations

4.4.5.1. Summary

Animal products were much less important as a source of internal exposure in Japan after the FDNPP accident compared with the Chernobyl accident. The prevailing animal management practices (e.g. housing dairy animals) in Japan led to low radionuclide intake by animals and, correspondingly, to relatively low contribution of farm animal products to internal exposure due to ingestion of the Japanese diet.

The importance of radioiodine in milk was low as dairy animals were housed indoors and fed on stored feed. Therefore, milk ingestion was much less significant than it had been after the Chernobyl accident.

The transfer parameter data obtained were similar to those in the international literature.

4.4.5.2. Limitations

Because livestock production and consumption are not as important in Japan as in Europe and America, few data were available on transfer to animal products.

The unexpected temporary increase in radiocaesium activity concentrations in some beef samples in the summer of 2011 due to feeding of rice straw that was exposed to radionuclide deposition in March 2011, constitutes an example of the need to consider all potential pathways after an accident.

Transfer to farm animals has often been reported as a transfer coefficient (F_m or F_f) which varies with animal liveweight. The size of cattle varies between countries, and *CR* might be more suitable to estimate concentrations in meat as it is a more generic parameter than the transfer coefficient.

4.5.CONCLUSIONS

Before the FDNPP accident, only a small number of field observations of CR for crops had been carried out in Japan [4.47, 4.58, 4.59]. After the FDNPP accident, numerous studies were carried out of radiocaesium behaviour in soil-crop systems and, to a lesser extent, agricultural animal systems, generating many new data on ^{137}Cs bioavailability.

Systematic analysis of the effects of nutrient (K^+) status on radiocaesium activity and CR values that commenced after the FDNPP accident showed that only a small proportion of contaminated agricultural soils had a relatively low fertility. Therefore, CR values were generally similar to, or lower than, international values. The occurrence of radioecologically sensitive soils with high uptake of radiocaesium over decades after the Chernobyl accident [4.100] was not observed in Japan.

REFERENCES

[4.1] INTERNATIONAL ATOMIC ENERGY AGENCY, Quantification of Radionuclide Transfer in Terrestrial and Freshwater Environments for Radiological Assessments, TECDOC Series 1616, IAEA, Vienna (2009).

[4.2] INTERNATIONAL ATOMIC ENERGY AGENCY, Handbook of Parameter Values for the Prediction of Radionuclide Transfer in Terrestrial and Freshwater Environments, Technical Reports Series 472, IAEA, Vienna (2010).

[4.3] MINISTRY OF HEALTH LABOUR AND WELFARE (MHLW), Levels of Radioactive Contaminants in Foods Tested in Respective Prefectures. The Results of Radionuclide in Foods Samples until 31 March 2012 (Provisional Regulation), MINISTRY OF HEALTH LABOUR AND WELFARE (MHLW), Japan (2012).

[4.4] TAGAMI, K., UCHIDA, S., Mass interception factor of I-131 and Cs-137 derived from the Fukushima Daiichi accident, The 68th Annual Meeting of Japan Society for Analytical Chemistry Book of Abstracts, Chiba (2019).

[4.5] MINISTRY OF EDUCATION, CULTURE, SPORTS, SCIENCE AND TECHNOLOGY (MEXT), Readings of the Environmental Monitoring Samples (Weed), MINISTRY OF EDUCATION, CULTURE, SPORTS, SCIENCE AND TECHNOLOGY (MEXT), Japan (2012).

[4.6] FESENKO, S., SHINANO, T., ONDA, Y., DERCON, G., Dynamics of radionuclide activity concentrations in annual natural plants, agricultural crops and of external dose rate after the Fukushima Daiichi Nuclear Power Plant accident, J. Environ. Radioact. (2020).

[4.7] HOWARD, B.J., FESENKO, S., BALONOV, M., PRÖHL, G., NAKAYAMA, S., A Comparison of Remediation After The Chernobyl and Fukushima Daiichi Accidents, Radiat. Prot. Dosimetry **173** 1–3 (2016) 170.

[4.8] MINISTRY OF EDUCATION, CULTURE, SPORTS, SCIENCE AND TECHNOLOGY (MEXT), THE SECRETARIAT OF THE NUCLEAR REGULATION AUTHORITY, Radioactivity Concentration Analysis of Iodine in the Distribution Survey of Radioactive Substances, MINISTRY OF EDUCATION, CULTURE, SPORTS, SCIENCE AND TECHNOLOGY (MEXT), Japan (2019).

[4.9] MINISTRY OF EDUCATION, CULTURE, SPORTS, SCIENCE AND TECHNOLOGY (MEXT), Standard Tables of Food Composition in Japan, Seventh Revised Version, MINISTRY OF EDUCATION, CULTURE, SPORTS, SCIENCE AND TECHNOLOGY (MEXT), Japan (2015).

[4.10] SUNAGA, Y., HARADA, H., KAWACHI, T., Weathering half-life of radioactive cesium for winter rye (Secale cereale L.) and Italian ryegrass (Lolium multiflorum Lam.) directly contaminated by the 2011 Fukushima Daiichi Nuclear Power Station accident, Soil Sci. Plant Nutr. **61** 2 (2015) 200.

[4.11] TAGAMI, K., UCHIDA, S., ISHII, N., Interception of Te-132, I-131 and Radiocaesium Depositions by Wild Herbaceous Plants, ICOBTE 2015 Abstract Book, Fukuoka (2015) 258.

[4.12] VIDAL, M. et al., Two approaches to the study of radiocaesium partitioning and mobility in agricultural soils from the Chernobyl area, Analyst **120** 6 (1995) 1785.

[4.13] GIL-GARCÍA, C.J., RIGOL, A., VIDAL, M., Comparison of mechanistic and PLS-based regression models to predict radiocaesium distribution coefficients in soils, J. Hazard. Mater. **197** (2011) 11.

[4.14] NAKAMARU, Y., ISHIKAWA, N., TAGAMI, K., UCHIDA, S., Role of soil organic matter in the mobility of radiocesium in agricultural soils common in Japan, INTERFACES Pollut. 2006 **306** 1 (2007) 111.

[4.15] YAMAGUCHI, N., Adsorption mechanism of radiocesium on soil, J. Jpn. Soc. Soil Phys. **126** (2014) 11.

[4.16] EGUCHI, S., Behavior of radioactive cesium in agricultural environment, J. Jpn. Soc. Soil Phys. **135** (2017) 9.

[4.17] CREMERS, A., ELSEN, A., PRETER, P.D., MAES, A., Quantitative analysis of radiocaesium retention in soils, Nature **335** 6187 (1988) 247.

[4.18] WAUTERS, J., VIDAL, M., ELSEN, A., CREMERS, A., Prediction of solid/liquid distribution coefficients of radiocaesium in soils and sediments. Part two: A new procedure for solid phase speciation of radiocaesium, Appl. Geochem. - APPL GEOCHEM **11** (1996) 595.

[4.19] YAMAGUCHI, N. et al., Behavior of radiocaesium in soil-plant systems and its controlling factor., Bull. Natl. Inst. Agro-Environ. Sci. 31 (2012) 75.

[4.20] GIL-GARCÍA, C., RIGOL, A., VIDAL, M., New best estimates for radionuclide solid–liquid distribution coefficients in soils, Part 1: radiostrontium and radiocaesium, J. Environ. Radioact. **100** 9 (2009) 690.

[4.21] VANDEBROEK, L., VAN HEES, M., DELVAUX, B., SPAARGAREN, O., THIRY, Y., Relevance of Radiocaesium Interception Potential (RIP) on a worldwide scale to assess soil vulnerability to 137Cs contamination, J. Environ. Radioact. **104** (2012) 87.

[4.22] NAKAO, A., THIRY, Y., FUNAKAWA, S., KOSAKI, T., Characterization of the frayed edge site of micaceous minerals in soil clays influenced by different pedogenetic conditions in Japan and northern Thailand, Soil Sci. Plant Nutr. **54** 4 (2008) 479.

[4.23] NAKAO, A., FUNAKAWA, S., KOSAKI, T., Hydroxy-Al polymers block the frayed edge sites of illitic minerals in acid soils: Studies in southwestern Japan at various weathering stages, Eur. J. Soil Sci. - EUR J SOIL SCI **60** (2009) 127.

[4.24] CAMPS, M., RIGOL, A., VIDAL, M., RAURET, G., Assessment of the Suitability of Soil Amendments To Reduce 137Cs and 90Sr Root Uptake in Meadows, Environ. Sci. Technol. **37** 12 (2003) 2820.

[4.25] JOUSSEIN, E., KRUYTS, N., RIGHI, D., PETIT, S., DELVAUX, B., Specific Retention of Radiocesium in Volcanic Ash Soils Devoid of Micaceous Clay Minerals, Soil Sci. Soc. Am. J. **68** 1 (2004) 313.

[4.26] KONOPLEVA, I., KLEMT, E., KONOPLEV, A., ZIBOLD, G., Migration and bioavailability of (137)Cs in forest soil of southern Germany, J. Environ. Radioact. **100** 4 (2009) 315.

[4.27] NAKAO, A. et al., Relationships between Paddy Soil Radiocesium Interception Potentials and Physicochemical Properties in Fukushima, Japan, J. Environ. Qual. **44** 3 (2015) 780.

[4.28] SANCHEZ, A.L. et al., High Plant Uptake of Radiocesium from Organic Soils Due to Cs Mobility and Low Soil K Content, Environ. Sci. Technol. **33** 16 (1999) 2752.

[4.29] SMOLDERS, E., VAN DEN BRANDE, K., MERCKX, R., Concentrations of 137Cs and K in Soil Solution Predict the Plant Availability of 137Cs in Soils, Environ. Sci. Technol. **31** 12 (1997) 3432.

[4.30] TAKEDA, A. et al., Relationship between the radiocesium interception potential and the transfer of radiocesium from soil to soybean cultivated in 2011 in Fukushima Prefecture, Japan, J. Environ. Radioact. **137** (2014) 119.

[4.31] UEMATSU, S. et al., Predicting radiocaesium sorption characteristics with soil chemical properties for Japanese soils, Sci. Total Environ. **524–525** (2015) 148.

[4.32] YAMAGUCHI, N. et al., Radiocesium interception potential of agricultural soils in northeast Japan, Soil Sci. Plant Nutr. **63** 2 (2017) 119.

[4.33] ZIBOLD, G., KLEMT, E., KONOPLEVA, I., KONOPLEV, A., Influence of fertilizing on the 137Cs soil–plant transfer in a spruce forest of Southern Germany, J. Environ. Radioact. **100** 6 (2009) 489.

[4.34] GIL-GARCÍA, C.J., RIGOL, A., RAURET, G., VIDAL, M., Radionuclide sorption–desorption pattern in soils from Spain, Appl. Radiat. Isot. **66** 2 (2008) 126.

[4.35] GOMMERS, A., GÄFVERT, T., SMOLDERS, E., MERCKX, R., VANDENHOVE, H., Radiocaesium soil-to-wood transfer in commercial willow short rotation coppice on contaminated farm land, J. Environ. Radioact. **78** 3 (2005) 267.

[4.36] SANCHEZ, A.L. et al., Predictions of in situ solid/liquid distribution of radiocaesium in soils, J. Environ. Radioact. **63** 1 (2002) 35.

[4.37] WAEGENEERS, N., SMOLDERS, E., MERCKX, R., A Statistical Approach for Estimating the Radiocesium Interception Potential of Soils, J. Environ. Qual. **28** 3 (1999) 1005.

[4.38] DELVAUX, B., KRUYTS, N., CREMERS, A., Rhizospheric Mobilization of Radiocesium in Soils, Environ. Sci. Technol. **34** 8 (2000) 1489.

[4.39] NAKAO, A., OGASAWARA, S., SANO, O., ITO, T., YANAI, J., Radiocesium sorption in relation to clay mineralogy of paddy soils in Fukushima, Japan, Sci. Total Environ. **468–469** (2014) 523.

[4.40] ABSALOM, J.P. et al., Predicting Soil to Plant Transfer of Radiocesium Using Soil Characteristics, Environ. Sci. Technol. **33** 8 (1999) 1218.

[4.41] CAMPS, M., HILLIER, S., VIDAL, M., RAURET, G., Laboratory experiments to predict changes in radiocaesium root uptake after flooding events, J. Environ. Radioact. **67** 3 (2003) 247.

[4.42] WANG, G., STAUNTON, S., Dynamics of caesium in aerated and flooded soils: experimental assessment of ongoing adsorption and fixation, Eur. J. Soil Sci. **61** 6 (2010) 1005.

[4.43] WAKABAYASHI, S., ITOH, S., TAKAHASHI, S., Influence of flooding on exchangeability and release of stable and radioactive cesium in contaminated paddy soil, Soil Sci. Plant Nutr. **63** 2 (2017) 110.

[4.44] UEMATSU, S., VANDENHOVE, H., SWEECK, L., VAN HEES, M., SMOLDERS, E., Radiocaesium bioavailability to flooded paddy rice is related to soil solution radiocaesium and potassium concentrations, Plant Soil **428** 1 (2018) 415.

[4.45] TAGAMI, K., UCHIDA, S., Aging effect on technetium behaviour in soil under aerobic and anaerobic conditions, Toxicol. Environ. Chem. **56** 1–4 (1996) 235.

[4.46] MINISTRY OF HEALTH LABOUR AND WELFARE (MHLW), Handling of food contaminated by radioactivity, MINISTRY OF HEALTH LABOUR AND WELFARE (MHLW), Japan (2011).

[4.47] KOMAMURA, M., TSUMURA, A., YAMAGUCHI, N., KIHOU, N., KODAIRA, K., Monitoring 90Sr and 137Cs in rice, wheat and soil in Japan from 1959 to 2000, Misc. Publ. Natl. Inst. Agro-Environ. Sci. Jpn. **28** (2005).

[4.48] MINISTRY OF AGRICULTURE, FORESTRY AND FISHERIES (MAFF), Index-value of radiocaesium concentration in soil considering transfer of radiocaesium to rice, MINISTRY OF AGRICULTURE, FORESTRY AND FISHERIES (MAFF), Japan (2011).

[4.49] KIHOU, N., INOUE, T., KURISHIMA, K., OHSE, K., Measurement of radioactivities in soil and grains of rice and wheat, Proceedings of Environmental Radioactivity Survey and Studies No. 54, Ministry of Education, Culture, Sports, Science and Technology, Tokyo (2013) p. 9.

[4.50] TAGAMI, K., TSUKADA, H., UCHIDA, S., HOWARD, B.J., Changes in the Soil to Brown Rice Concentration Ratio of Radiocaesium before and after the Fukushima Daiichi Nuclear Power Plant Accident in 2011, Environ. Sci. Technol. **52** 15 (2018) 8339.

[4.51] UCHIDA, S., TAGAMI, K., SHANG, Z.R., CHOI, Y.H., Uptake of radionuclides and stable elements from paddy soil to rice: a review, J. Environ. Radioact. **100** 9 (2009) 739.

[4.52] MORENO-JIMÉNEZ, E. et al., Sprinkler irrigation of rice fields reduces grain arsenic but enhances cadmium, Sci. Total Environ. **485–486** (2014) 468.

[4.53] NISHIYAMA, S., OKAZAKI, M., BABA, M., QUEVEDO, M.A., Quantification of Cs, K, and Rb in rice (Oryza sativa) cultivated under paddy and upland conditions, Microchem. J. **127** (2016) 22.

[4.54] WAKABAYASHI, S. et al., Influence of water management and fertilizer application on 137Cs and 133Cs uptake in paddy rice fields, J. Environ. Radioact. **157** (2016) 102.

[4.55] OHMORI, Y. et al., Difference in cesium accumulation among rice cultivars grown in the paddy field in Fukushima Prefecture in 2011 and 2012, J. Plant Res. **127** 1 (2014) 57.

[4.56] KOJIMA, K. et al., Characterization of 140 Japanese and world rice collections cultivated in Nihonmatsu-city in Fukushima in terms of radiocesium activity concentrations in seed grains and straws to explore rice cultivars with low radiocesium accumulation, J. Radioanal. Nucl. Chem. **314** 2 (2017) 1009.

[4.57] KAMEI-ISHIKAWA, N., TAGAMI, K., UCHIDA, S., Estimation of 137Cs Plant Root Uptake Using Naturally Existing 133Cs, J. Nucl. Sci. Technol. **45** sup6 (2008) 146.

[4.58] TSUKADA, H., HASEGAWA, H., HISAMATSU, S., YAMASAKI, S., Rice uptake and distributions of radioactive 137Cs, stable 133Cs and K from soil, Environ. Pollut. **117** 3 (2002) 403.

[4.59] UCHIDA, S., TAGAMI, K., Soil-to-plant transfer factors of fallout 137Cs and native 133Cs in various crops collected in Japan, J. Radioanal. Nucl. Chem. **273** 1 (2007) 205.

[4.60] ENDO, S., KAJIMOTO, T., SHIZUMA, K., Paddy-field contamination with 134Cs and 137Cs due to Fukushima Dai-ichi Nuclear Power Plant accident and soil-to-rice transfer coefficients, J. Environ. Radioact. **116** (2013) 59.

[4.61] FUJIMURA, S. et al., Difference in Cs-137 concentration of brown rice between the years of 2011 and 2012 in Fukushima Prefecture, J. Radioanal. Nucl. Chem. **303** 2 (2015) 1147.

[4.62] FUJIMURA, S. et al., Accumulation of (137)Cs by rice grown in four types of soil contaminated by the Fukushima Dai-ichi Nuclear Power Plant accident in 2011 and 2012, J. Environ. Radioact. **140** (2015) 59.

[4.63] FUJIMURA, S. et al., The inhibitory effects of potassium chloride versus potassium silicate application on (137)Cs uptake by rice, J. Environ. Radioact. **153** (2016) 188.

[4.64] FUJITA, T., SAKUMA, Y., FUJISAWA, Y., Radiocaesium transfer factor is low in rice variety, Fukuhibiki, for feeding cattle, (2015).

[4.65] FUJITA, T., SAKUMA, Y., FUJISAWA, Y., Time dependence of radiocesium concentration in rice for feed, (2015).

[4.66] GOTO, I., NINAKI, T., Application effects of zeolite on uptake of radioactive cesium in rice plants, Jpn. J. Soil Sci. Plant Nutr. **85** 2 (2014) 121.

[4.67] II, I. et al., Radioactive Caesium Concentration of Lowland Rice Grown in the Decontaminated Paddy Fields in Iitate-Village in Fukushima, RADIOISOTOPES **64** 5 (2015) 299.

[4.68] ISHIKAWA, S. et al., Low-cesium rice: mutation in OsSOS2 reduces radiocesium in rice grains, Sci. Rep. **7** 1 (2017) 1.

[4.69] KATO, N. et al., Potassium fertilizer and other materials as countermeasures to reduce radiocesium levels in rice: Results of urgent experiments in 2011 responding to the Fukushima Daiichi Nuclear Power Plant accident, Soil Sci. Plant Nutr. **61** 2 (2015) 179.

[4.70] KONDO, M. et al., Exchangeable Cs/K ratio in soil is an index to estimate accumulation of radioactive and stable Cs in rice plant, Soil Sci. Plant Nutr. **61** 1 (2015) 133.

[4.71] MIYAZAKI, N., Measures to reduce uptake of radiocaesium by rice plant. 1. Application of potassium fertilizer, Bull. Tochigi Agric. Exp. Stn. **78** (2018) 9.

[4.72] MIYAZAKI, N., Measures to reduce uptake of radiocaesium by rice plant. 4. Application of materials to keep exchangeable K concentration, Bull. Tochigi Agric. Exp. Stn. **78** (2018) 29.

[4.73] MIYAZAKI, N., Measures to reduce uptake of radiocaesium by rice plant. 5. Effect of water management to decrease transfer of radiocaesium, Bull. Tochigi Agric. Exp. Stn. **78** (2018) 33.

[4.74] MIYAZAKI, N., DEGUCHI, M., Measures to reduce uptake of radiocaesium by rice plant. 3. Effect of application time of potassium fertilizer, Bull. Tochigi Agric. Exp. Stn. **78** (2018) 25.

[4.75] MIYAZAKI, N., SEKIGUCHI, M., DEGUCHI, M., YOSHIZAWA, H., Measures to reduce uptake of radiocaesium by rice plant. 2. Changes of soil-to-rice transfer factor in wet andosols with continuous organic fertilizer application, Bull. Tochigi Agric. Exp. Stn. **78** (2018) 17.

[4.76] NIIZUMA, K., WAKABAYASHI, K., Radiocesium concentration change with time collected from the same paddy field: 2011 and 2013, Fukushima Prefectural Agriculture Center, (2013).

[4.77] NISHIWAKI, J., ASAGI, N., KOMATSUZAKI, M., MIZOGUCHI, M., NOBORIO, K., Progress in field experiments of continuous application of organic matter to restore rice production at radiocesium-decontaminated paddy fields in Iitate village, and present situation of Iitate village, J. Jpn. Soc. Soil Phys. **135** (2017) 33.

[4.78] ODA, K., MURAMATSU, Y., OHNO, T., FUJIMURA, S., YOSHIOKA, K., Distribution of radiocesium in rice paddy fields and its transfer into rice plants, Proceedings of the 13th Workshop on Environmental Radioactivity, Vol. KEK Proceedings 2012-6, High Energy Accelerator Research Organization, Tsukuba (2012) 177.

[4.79] OHMORI, Y. et al., The effect of fertilization on cesium concentration of rice grown in a paddy field in Fukushima Prefecture in 2011 and 2012, J. Plant Res. **127** 1 (2014) 67.

[4.80] OHSE, K. et al., Concentration of radiocesium in rice, vegetables, and fruits cultivated in the evacuation area in Okuma Town, Fukushima, J. Radioanal. Nucl. Chem. **303** 2 (2015) 1533.

[4.81] ONO, Y., SATO, K., Comparison of radiocaesium concentration in different types of paddy rice varieties, Project Report, Fukushima Agricultural Research Center (2013).

[4.82] ONO, Y. et al., Variation in rice radiocesium absorption among different cultivars, Research Report Special Issue on Radioactive Material Countermeasures, Fukushima Agricultural Research Center (2013).

[4.83] OZUTSUMI, Y., NAGAMINE, T., HATANAKA, T., DOSHU, N., The influence of applying radioactive cesium-polluted cattle manure compost on rice quality, Nihon Chikusan Gakkaiho **88** (2017) 339.

[4.84] SAITO, T., 137Cs concentration changes in brown rice with time under no potassium fertilizing condition, Department of Environment and Crop Nutrition, Fukushima Agricultural Center, Fukushima (2015).

[4.85] SAITO, T. et al., Effect of potassium application on root uptake of radiocesium in rice, Proceeding Int. Syst. Environ. Monit. Dose Estim. Resid. Accid. TEPCO's Fukushima Daiichi Nucl. Power Stn. Kyoto Univ. Res. React. Inst. Press Kyoto (2012) 165.

[4.86] SAITO, T. et al., Effect of application timing of potassium fertilizer on root uptake of 137Cs in brown rice, J. Radioanal. Nucl. Chem. **303** 2 (2015) 1585.

[4.87] SATO, S., NIIZUMA, K., What is the risk of reduced exchangeable potassium content in paddy soil? Diagnosis can be made by paddy rice cultivation without potasium, Project Report, Department of Environment and Crop Nutrition, Fukushima Agricultural Center (2016).

[4.88] SEKIMOTO, H., YAMADA, T., HOTSUKI, T., MATSUZAKI, A., MIMURA, T., Desirable levels of exchangeable K and Ca and their concentration in the soil solution to reduce uptake of radioactive Cs by rice plants., Jpn. J. Soil Sci. Plant Nutr. **85** 2 (2014) 148.

[4.89] TSUJIMOTO, M., MIYASHITA, S., NGUYEN, H.T., NAKASHIMA, S., A correlation between the transfer factor of radioactive cesium from soil into rice plants and the grain size distribution of paddy soil in Fukushima, Radiat. Saf. Manag. **15** (2016) 1.

[4.90] YAMANISHI, H. et al., Environmental Radiation Survey in Kawamata-Machi, Fukushima-Ken: Measurement of Radiocesium in Soil and Plants, The International Symposium on Environmental Monitoring and Dose Estimation of Residents after Accident of TEPCO's Fukushima Daiichi Nuclear Power Stations, Vol. 14, Kyoto University Research Reactor Institute Press, Kyoto (2012) 49.

[4.91] YANG, B. et al., Temporal changes of radiocesium in irrigated paddy fields and its accumulation in rice plants in Fukushima, Environ. Pollut. Barking Essex 1987 **208** Pt B (2016) 562.

[4.92] YAMAMURA, K. et al., A statistical model for estimating the radiocesium transfer factor from soil to brown rice using the soil exchangeable potassium content, J. Environ. Radioact. **195** (2018) 114.

[4.93] NUCLEAR REGULATION AUTHORITY (NRA), Environmental Radiation Database, NUCLEAR REGULATION AUTHORITY (NRA) (2019).

[4.94] SUZUKI, Y. et al., Effect of the concentration of radiocesium dissolved in irrigation water on the concentration of radiocesium in brown rice, Soil Sci. Plant Nutr. **61** 2 (2015) 191.

[4.95] MINISTRY OF ENVIRONMENT (MOE), Radioactive Material Monitoring in the Water Environment and around Fukushima Prefecture. Public Water Areas, MINISTRY OF ENVIRONMENT (MOE), Japan (2019).

[4.96] TSUKADA, H., NIHIRA, S., WATANABE, T., TAKEDA, S., The 137Cs activity concentration of suspended and dissolved fractions in irrigation waters collected from

the 80 km zone around TEPCO's Fukushima Daiichi Nuclear Power Station, J. Environ. Radioact. **178–179** (2017) 354.

[4.97] WAKAHARA, T., ONDA, Y., KATO, H., SAKAGUCHI, A., YOSHIMURA, K., Radiocesium discharge from paddy fields with different initial scrapings for decontamination after the Fukushima Dai-ichi Nuclear Power Plant accident, Environ. Sci. Process. Impacts **16** 11 (2014) 2580.

[4.98] MIYAZU, S. et al., Measurement and estimation of radiocesium discharge rate from paddy field during land preparation and mid-summer drainage, J. Environ. Radioact. **155–156** (2016) 23.

[4.99] EVANS, E.J., DEKKER, A.J., PLANT UPTAKE OF Cs-137 FROM NINE CANADIAN SOILS, Can. J. Soil Sci. **46** 2 (1966) 167.

[4.100] FESENKO, S.V. et al., An extended critical review of twenty years of countermeasures used in agriculture after the Chernobyl accident, Sci. Total Environ. **383** 1–3 (2007) 1.

[4.101] ALEXAKHIN, R. et al., Fluxes of Radionuclides in Agricultural Environments: Main Results and Still Unsolved Problems, Luxembourg (1996) 1192.

[4.102] BERESFORD, N.A. et al., Thirty years after the Chernobyl accident: What lessons have we learnt?, J. Environ. Radioact. **157** (2016) 77.

[4.103] MINISTRY OF AGRICULTURE, FORESTRY AND FISHERIES (MAFF), Points to Reduce Radiocaesium Concentration in Rice at Rice Production Fields, MINISTRY OF AGRICULTURE, FORESTRY AND FISHERIES (MAFF), Japan (2013).

[4.104] EGUCHI, T. et al., Influence of the nonexchangeable potassium of mica on radiocesium uptake by paddy rice, J. Environ. Radioact. **147** (2015) 33.

[4.105] TSUKADA, H., OHSE, K., Concentration of radiocaesium in rice and irrigation water, and soil management practices in Oguni, Date, Fukushima, Integr. Environ. Assess. Manag. **12** 4 (2016) 659.

[4.106] AGRONOMY SECTION OF THE ANNUAL SCIENTIFIC CONFERENCE OF TEA, Recent Trend of Plucking and Skiffing of Tea Plant in Japan, Tea Res. J. **1977** 46 (1977) 74.

[4.107] SHIRAKI, Y., TAKEDA, H., OKAMOTO, T., KITA, N., Washing of Fallout Radioactive Cesium in Tea Plants Grown in Kanagawa Prefecture, Tea Res. J. **115** (2013) 21.

[4.108] IBARAKI PREFECTURE, Report on behaviour of radiocaesium in tea plant and soil of North-inland tea plantation in Ibaraki and the effect of cutting in tea shoots to reduce radiocaesium concentration (3-y results after the Fukushima nuclear accident), (2014).

[4.109] SHIRAKI, Y., KITA, N., YAMADA, Y., Distribution and reduction of fallout radioactive caesium in tea plants grown in Kanagawa Prefecture, Radioisot. Tokyo **61** 5 (2012) 261.

[4.110] SHIRAKI, Y., TAKEDA, H., OKAMOTO, T., KITA, N., Periodic Changes in Radioactive Cesium Concentration of Tea Plants Grown in Kanagawa Prefecture after the Fukushima Daiichi Nuclear Power Plant Accident, Tea Res. J. **115** (2013) 1.

[4.111] SHIRAKI, Y., TAKEDA, H., OKAMOTO, T., KITA, N., The correlation of the radiocaesium concentration of new shoots harvested in 2012 and old leaves, and new shoots harvested in 2011 grown in Kanagawa prefecture, Radioisotopes **62** 4 (2013) 183.

[4.112] SHIRAKI, Y., TAKEDA, H., OKAMOTO, T., KITA, N., Translocation of Radioactive Cesium in Tea Nursery Stocks and its Distribution in the Branches and Trunks of the Matured Tea Bush, Tea Res. J. **115** (2013) 11.

[4.113] HONDA, Y., MIYAZAKI, Y., Reduction techniques of radioactive cesium and dynamics of radioactive cesium in tea plants and tea plantation soil in Saitama Prefecture, Saitama NouSouKen Res. Bull. **15** (2016) 25.

[4.114] SEKIYAMA, K. et al., Yearly changes in radioactive cesium concentrations and quantities in tea plants and tea garden soil and factors affecting yearly changes in Chiba Prefecture, CAFRC Res. Bull. **8** (2016) 69.

[4.115] HIRONO, Y., NONAKA, K., Time series changes in radiocaesium distribution in tea plants (Camellia sinensis (L.)) after the Fukushima Dai-ichi Nuclear Power Plant accident, J. Environ. Radioact. **152** (2016) 119.

[4.116] HIRONO, Y., NONAKA, K., Changes in radiocesium activities with new shoots growth of tea, Jpn. J. Soil Sci. Plant Nutr. **86** 4 (2015) 303.

[4.117] IKKA, T. et al., Radiocesium uptake through leaf surfaces of tea plants (Camellia sinensis L.), J. Environ. Radioact. **182** (2018) 70.

[4.118] TAGAMI, K., UCHIDA, S., SHINANO, T., PRÖHL, G., Comparisons of effective half-lives of radiocesium in Japanese tea plants after two nuclear accidents, Chernobyl and Fukushima, J. Environ. Radioact. **213** (2020) 106109.

[4.119] SHIRAKI, Y., TAKEDA, H., OKAMOTO, T., Radioactive cesium concentration in new shoots of tea plants cultivated in Kanagawa Prefecture, Tea Res. J. **117** (2014) 35.

[4.120] UNLÜ, M.Y. et al., Natural effective half-life of 137Cs in tea plants, Health Phys. **68** 1 (1995) 94.

[4.121] MINISTRY OF AGRICULTURE, FORESTRY AND FISHERIES (MAFF), Annual Report of Ministry of Agriculture, Forestry and Fisheries Affiliated Radioactivity Research: H26 Report, Agriculture, Forestry and Fisheries Research Council, Japan, MINISTRY OF AGRICULTURE, FORESTRY AND FISHERIES (MAFF), Japan, Tokyo (2017).

[4.122] PORTAL SITE OF OFFICIAL STATISTICS OF JAPAN, Japan Statistical Data, PORTAL SITE OF OFFICIAL STATISTICS OF JAPAN (2019).

[4.123] TAGAMI, K., UCHIDA, S., Concentration change of radiocaesium in persimmon leaves and fruits. Observation results in 2011 Spring-2013 Summer, Radioisotopes **63** 2 (2014) 87.

[4.124] MINISTRY OF HEALTH LABOUR AND WELFARE (MHLW), Notice No. 0315 Article 1 of the Department of Food Safety, MINISTRY OF HEALTH LABOUR AND WELFARE (MHLW), Japan (2012).

[4.125] HAMADA, N., OGINO, H., FUJIMICHI, Y., Safety regulations of food and water implemented in the first year following the Fukushima nuclear accident, J. Radiat. Res. (Tokyo) **53** 5 (2012) 641.

[4.126] TAKATA, D. et al., Remobilization of radiocaesium derived from Fukushima nuclear power plant accident in the following year in ‘Akatsuki’peach trees, Hortic. Res. **11** suppl 2 (2012) 353.

[4.127] SATO, M., TAKASE, T., YAMAGUCHI, K., Development of methods for collecting the stemflow on the trunk of trees contaminated with radioactive fallout, J. Agric. Meteorol. **73** 2 (2017) 73.

[4.128] SATO, M., TAKASE, T., YAMAGUCHI, K., Effects of bark washing and epiphytic moss on 137Cs activity concentration in bark and stemflow in Japanese persimmon (Diospyros kaki Thunb.), J. Environ. Radioact. **178–179** (2017) 360.

[4.129] SATO, M., TAKATA, D., TANOI, K., OHTSUKI, T., MURAMATSU, Y., Radiocesium transfer into the fruit of deciduous fruit trees contaminated during dormancy, Soil Sci. Plant Nutr. **61** 1 (2015) 156.

[4.130] SATO, M. et al., Use of different surface covering materials to enhance removal of radiocaesium in plants and upper soil from orchards in Fukushima prefecture, J. Environ. Radioact. **196** (2019) 204.

[4.131] SATO, M. et al., Vertical Migration of 137Cs in Japanese Orchards after the Fukushima Daiichi Nuclear Power Plant Accident, Hortic. J. **88** 2 (2019) 150.

[4.132] BALDINI, E., BETTOLI, M.G., TUBERTINI, O., Effects of the Chernobyl pollution on some fruit trees, Adv. Hortic. Sci. **1** 2 (1987) 77.

[4.133] MONTE, L., QUAGGIA, S., POMPEI, F., FRATARCANGELI, S., The behaviour of 137Cs in some edible fruits, J. Environ. Radioact. **11** 3 (1990) 207.

[4.134] ANTONOPOULOS-DOMIS, M., CLOUVAS, A., GAGIANAS, A., Radiocesium dynamics in fruit trees following the Chernobyl accident, Health Phys. **61** 6 (1991) 837.

[4.135] ANTONOPOULOS-DOMIS, M., CLOUVAS, A., GAGIANAS, A., Long term radiocesium contamination of fruit trees following the Chernobyl accident, Health Phys. **71** 6 (1996) 910.

[4.136] ANGUISSOLA SCOTTI, I., SILVA, S., Foliar absorption and leaf-fruit transfer of 137Cs in fruit trees, J. Environ. Radioact. **16** 2 (1992) 97.

[4.137] KATANA, H., BUNNENBERG, C., KÜHN, W., "Studies on the translocation of Cs-134 from leaves to fruit of apple trees", Environmental Impact of Nuclear Accidents, Cadarache International Symposium on Radioecology, Cadarache (1988).

[4.138] BENGTSSON, G.B., Mobility of superficially applied caesium-134 and strontium-85 in apple branches under precipitation-free conditions, Analyst **117** 7 (1992) 1193.

[4.139] ZEHNDER, H.J., KOPP, P., EIKENBERG, J., FELLER, U., OERTLI, J.J., Uptake and transport of radioactive cesium and strontium into grapevines after leaf contamination, Radiat. Phys. Chem. **46** 1 (1995) 61.

[4.140] CARINI, F., ANGUISSOLA SCOTTI, I., D'ALESSANDRO, P.G., 134Cs and 85Sr in fruit plants following wet aerial deposition, Health Phys. **77** 5 (1999) 520.

[4.141] PRÖHL, G., FIEDLER, I., KOCH-STEINDL, H., LESER, C., TREUTTER, D., Interzeption und Translokation von Radiocäsium bei Obst und Beeren, Bundesministerium für Umwelt, Naturschutz und Reaktorsicherheit, Bonn (2003).

[4.142] INTERNATIONAL ATOMIC ENERGY AGENCY, Modelling the Transfer of Radionuclides to Fruit. Report of the Fruits Working Group of BIOMASS Theme 3, Non-serial Publications, IAEA, Vienna (2003).

[4.143] RENAUD, Ph., GONZE, M.-A., Lessons from the Fukushima and Chernobyl accidents concerning the 137Cs contamination of orchard fresh fruits, Radioprotection **49** 3 (2014) 169.

[4.144] MAUBERT, H., ROUSSEL, S., Results and interpretations of observations from the South-eastern France after the Chernobyl radioactive deposits in May 1986, Report CEA/IPSN/SERE, (1988).

[4.145] SCPRI, Bulletins mensuels de mesures du Service Central de protection contre les Rayonnements ionisants, (1986).

[4.146] SILVA, S., ANGUISSOLA SCOTTI, I., FREGONI, M., VERCESI, A., Contamination radioactive du raisin en Italie, en 1986 à la suite de l'accident de la centrale nucléaire de Tchernobyl, Bull. OIV **62** 695–696 (1989) 74.

[4.147] SATO, M., Accumulation and migration of radiocesium in the deciduous fruit tree contaminated during dormancy, PhD Thesis, Fukushima University, Fukushima (2018).

[4.148] TAKATA, D. et al., Radioactivity distribution of the fruit trees ascribable to radioactive fall out. Transfer of radiocaesium from soil in 2011 when Fukushima Daiichi Nuclear Power Plant Accident happened, Radioisotopes **61** (2012) 517.

[4.149] TAKATA, D. et al., Radioactivity distribution of the fruit trees ascribable to radioactive fall out. A study on peach and grape cultivated in South Fukushima, Radioisotopes **61** (2012) 601.

[4.150] TAKATA, D. et al., Radioactivity distribution of the fruit trees ascribable to radioactive fall out. A study on stone fruits cultivated in low level radioactivity region, Radioisotopes **61** 6 (2012) 321.

[4.151] KUSABA, S., Accumulation of radioactive caesium in chestnut orchards in 2011, Project Report, NARO Fruit Tree Research Institute, Cultivation and Distribution Research Area (2011).

[4.152] KUWANA, A., ADACHI, Y., Secular change of 137Cs concentration in fruit of fruit tree, Project Report, Fruit Tree Research Institute, Fukushima Agricultural Center, Fukushima (2017).

[4.153] TAKATA, D., YASUNAGA, E., TANOI, K., Radioactivity distribution of the fruit trees ascribable to radioactive fall out (6) Effect of heterogeneity of caesium-137 concentration in soil on transferability to grape trees and fig trees, Radioisotopes **62** 8 (2013) 533.

[4.154] IWABUCHI, K., Inhibition of radiocesium absorption in a blueberry, Fukushima-Ken Nogyo Sogo Senta Kenkyu Hokoku (2014) 82.

[4.155] SATO, M., Fruit in Fukushima in the nuclear accident year: report of the first year examination to take measures against the radioactive contamination of nuclear power plant accident, Radiochem. News **26** (2012) 21.

[4.156] KUSABA, S., Accumulation of radiocaesium in blueberry orchards in 2011, Project Report, NARO Fruit Tree Research Institute, Cultivation and Distribution Research Area (2011).

[4.157] KUSABA, S., MATSUOKA, K., SAITO, T., KIHOU, N., HIRAOKA, K., Changes in radiocesium concentration in a Japanese chestnut (Castanea crenata Sieold & Zucc.) orchard following radioactive fallout, Soil Sci. Plant Nutr. **61** 1 (2015) 165.

[4.158] SASAKI, Y. et al., Translocation of Radiocesium Released by the Fukushima Daiichi Nuclear Power Plant Accident in Japanese Chestnut and Chestnut Weevil Larvae, Hortic. J. **86** 2 (2017) 139.

[4.159] KUSABA, S. et al., Changes in radiocesium concentration in a blueberry (Vaccinium virgatum Aiton) orchard resulting from radioactive fallout, Soil Sci. Plant Nutr. **61** 1 (2015) 169.

[4.160] MATSUOKA, K., KUSABA, S., NISHIO, S., HIRAOKA, K., Effects of Winter Pruning on the Concentration and Amount of Radiocaesium in Japanese Chestnut Trees after Radionuclide Deposition, RADIOISOTOPES **65** (2016) 367.

[4.161] TAGAMI, K., UCHIDA, S., Effective half-lives of ^{137}Cs from persimmon tree tissue parts in Japan after Fukushima Dai-ichi Nuclear Power Plant accident, J. Environ. Radioact. **141** (2015) 8.

[4.162] CARINI, F., BENGTSSON, G., Post-deposition transport of radionuclides in fruit, J. Environ. Radioact. **52** 2–3 (2001) 215.

[4.163] CARINI, F., LOMBI, E., Foliar and soil uptake of 134Cs and 85Sr by grape vines, Sci. Total Environ. **207** 2 (1997) 157.

[4.164] CARINI, F., ANGUISSOLA SCOTTI, I., MONTRUCCOLI, M., SILVA, S., 134Cs Foliar Contamination of Vine: Translocation to Grapes and Transfer to Wine, Berger, Austria (1996) 313.

[4.165] SHIRAISHI, Y., Studies on the Radioactive Contamination of Fruit Trees by Fission Products (V), Jpn. J. Health Phys. **8** 4 (1973) 209.

[4.166] KOPP, P., GÖRLICH, W., BURKART, W., ZEHNDER, H., "Foliar uptake of radionuclides and their distribution in the plant", Environmental Contamination Following a Major Nuclear Accident. V. 2, Vienna (1990) 37–46.

[4.167] SATO, M. et al., Long-term changes of 137Cs activity concentration in fruit and leaf of deciduous fruits during both period of young and mature fruit stage, Proceedings of the 20th Workshop on Environmental Radioactivity, High Energy Accelerator Research Organization, Tsukuba (2019) 143–148.

[4.168] MÜCK, K., Long-term effective decrease of cesium concentration in foodstuffs after nuclear fallout, Health Phys. **72** 5 (1997) 659.

[4.169] TAGAMI, K., "Effective Half-Lives of Radiocesium in Terrestrial Plants Observed After Nuclear Power Plant Accidents", Impact of Cesium on Plants and the Environment, Springer (2017) 125–138.

[4.170] BROWN, J., SIMMONDS, J.R., FARMLAND A Dynamic Model for the Transfer of Radionuclides through Terrestrial Foodchains, United Kingdom (1995) p. 76.

[4.171] SATO, M., WATANABE, Y., TAKASE, T., TAKATA, D., YAMAGUCHI, K., Verification of source of 137Cs migrated into fruits in yuzu orchard located in mountainous area and development of methods to diagnose contamination quantity in yuzu tree, Hortic. Res. Jpn. **18** Suppl.1 (2019) 69.

[4.172] HANDLEY, R., BABCOCK, K.L., Translocation of carrier-free 85Sr, 137Cs and 106Ru in woody plants, Radiat. Bot. **10** 6 (1970) 577.

[4.173] TAGAMI, K., UCHIDA, S., ISHII, N., KAGIYA, S., Translocation of radiocesium from stems and leaves of plants and the effect on radiocesium concentrations in newly emerged plant tissues, J. Environ. Radioact. **111** (2012) 65.

[4.174] MINISTRY OF AGRICULTURE, FORESTRY AND FISHERIES (MAFF), Annual Report of Ministry of Agriculture, Forestry and Fisheries Affiliated Radioactivity Research: H24 Report, Agriculture, Forestry and Fisheries Research Council, Japan,

MINISTRY OF AGRICULTURE, FORESTRY AND FISHERIES (MAFF), Japan, Tokyo (2014).

[4.175] MINISTRY OF AGRICULTURE, FORESTRY AND FISHERIES (MAFF), Annual Report of Ministry of Agriculture, Forestry and Fisheries Affiliated Radioactivity Research: H25 Report, Agriculture, Forestry and Fisheries Research Council, Japan, MINISTRY OF AGRICULTURE, FORESTRY AND FISHERIES (MAFF), Japan, Tokyo (2015).

[4.176] MINISTRY OF AGRICULTURE, FORESTRY AND FISHERIES (MAFF), Annual Report of Ministry of Agriculture, Forestry and Fisheries Affiliated Radioactivity Research: H27 Report, Agriculture, Forestry and Fisheries Research Council, Japan, MINISTRY OF AGRICULTURE, FORESTRY AND FISHERIES (MAFF), Japan, Tokyo (2018).

[4.177] MINISTRY OF AGRICULTURE, FORESTRY AND FISHERIES (MAFF), Annual Report of Ministry of Agriculture, Forestry and Fisheries Affiliated Radioactivity Research: H28 Report, Agriculture, Forestry and Fisheries Research Council, Japan, MINISTRY OF AGRICULTURE, FORESTRY AND FISHERIES (MAFF), Japan, Tokyo (2018).

[4.178] MINISTRY OF AGRICULTURE, FORESTRY AND FISHERIES (MAFF), Annual Report of Ministry of Agriculture, Forestry and Fisheries Affiliated Radioactivity Research: H29 Report, Agriculture, Forestry and Fisheries Research Council, Japan, MINISTRY OF AGRICULTURE, FORESTRY AND FISHERIES (MAFF), Japan, Tokyo (2019).

[4.179] LI, P., GONG, Y., KOMATSUZAKI, M., Temporal dynamics of 137Cs distribution in soil and soil-to-crop transfer factor under different tillage systems after the Fukushima Daiichi Nuclear Power Plant accident in Japan, Sci. Total Environ. **697** (2019) 134060.

[4.180] ENDO, R. et al., Analysis of Factors Involved in Absorption of Radioactive Caesium for Processing Tomatoes, RADIOISOTOPES **62** (2013) 275.

[4.181] SUGIURA, H., SAKAI, H., KAYAMA, Y., Change of the radiocesium concentrations of Shinobufuyuna (Brassica rapa) and cultured soil in Fukushima City, J. Jpn. Soc. Radiat. Saf. Manag. **13** 2 (2014) 159.

[4.182] AUNG, H.P. et al., Growth and 137Cs uptake of four Brassica species influenced by inoculation with a plant growth-promoting rhizobacterium Bacillus pumilus in three contaminated farmlands in Fukushima prefecture, Japan, Sci. Total Environ. **521–522** (2015) 261.

[4.183] SAITO, H., TAKEDA, S., KIMURA, H., Study on uncertainty of soil-to-plant transfer factor for the safety assessment (contract research), Japan Atomic Energy Agency (2011).

[4.184] KOBAYASHI, T., KATO, Y., TOKIWA, H., MURAMTATSU, Y., OONO, T., Transfer factors of radiocesium to vegetables cultivated on soils collected in Fukushima, Proceedings of the 13th Workshop on Environmental Radioactivity, Vol. KEK Proceedings 2012-6, High Energy Accelerator Research Organization, Tsukuba (2012).

[4.185] SAITO, S., Transfer factor of radiocaesium in cabbage grown in different soil types and exchangeable potassium concentrations, NARO (2012).

[4.186] NATIONAL AGRICULTURE AND FOOD RESEARCH ORGANIZATION (NARO), Transfer factor of radioactive cesium in soil among several summer

vegetables, NATIONAL AGRICULTURE AND FOOD RESEARCH ORGANIZATION (NARO), Japan (2011).

[4.187] OGATA, N., FUJITA, T., KATO, M., Phytoremediation of Radioactive Cesium Contaminated Soil by Cultivation of *Amaranthus* spp., Jpn. J. Crop Sci. **84** 1 (2015) 9.

[4.188] SHINANO, T. et al., Varietal difference in radiocesium uptake and transfer from radiocesium deposited soils in the genus Amaranthus, Soil Sci. Plant Nutr. **60** 6 (2014) 809.

[4.189] SCHIMMACK, W. et al., Intra-cultivar variability of the soil-to-grain transfer of fallout 137Cs and 90Sr for winter wheat, J. Environ. Radioact. **94** 1 (2007) 16.

[4.190] KOBAYASHI, T. et al., Transfer factors of radiocesium to vegetables, Bull. Fukushima Agric. Technol. Cent. Radioactive Substances. Special Issue (2014) 46.

[4.191] MINISTRY OF AGRICULTURE, FORESTRY AND FISHERIES (MAFF), About the Result of the Emergency Investigation Study for Radioactive Material Transfer Reduction Measures Establishment to Agricultural Products Depending on Field Environment, MINISTRY OF AGRICULTURE, FORESTRY AND FISHERIES (MAFF), Japan (2013).

[4.192] KOBAYASHI, T., MURAMATSU, Y., OONO, T., Inhibiting effect of absorption of radiocesium to vegetables by the zeolites, Bull. Fukushima Agric. Technol. Cent. Radioactive Substances. Special Issue (2014) 60.

[4.193] SAITO, S., KOBAYASHI, T., KATO, Y., Absorption restraint of radiocesium with potassium in cucumber cultivation, Fukushima-Ken Nogyo Sogo Senta Kenkyu Hokoku Radioactive Substances Special Issue (2014) 63.

[4.194] NATIONAL AGRICULTURE AND FOOD RESEARCH ORGANIZATION (NARO), Actual situation of the radioactive cesium contamination of the weed in levee after nuclear power plant accident, important point on using it, NATIONAL AGRICULTURE AND FOOD RESEARCH ORGANIZATION (NARO), Japan (2013).

[4.195] HARADA, H., Current status and challenges of developing technology for reducing radioactive cesium in forage crops, 2013 Self-feed Feed Utilization Study Group-Role of self-feed feed in aggressive agriculture, NARO Institute of Livestock and Grassland Science, Japan (2013).

[4.196] FUKUSHIMA PREFECTURE, Radioactive Cesium Concentration (Transfer Factor) of Orchard Grass under Renovated Grassland, (2012).

[4.197] ISHII, N., TAGAMI, K., KAWAGUCHI, I., UCHIDA, S., Root uptake of 137 Cs from sedimentation sludge-amended soils by Komatsuna (Brassica rapa var. perviridis), Radioisot. Tokyo **62** 7 (2013) 447.

[4.198] ISHII, N., TAGAMI, K., UCHIDA, S., Effect of Sludge Particle Size on Uptake of Cs-137 by Two Leaf Vegetables, J. Residuals Sci. Technol. **12** (2015) 61.

[4.199] UCHIDA, S., TAGAMI, K., HIRAI, I., Soil-to-Plant Transfer Factors of Stable Elements and Naturally Occurring Radionuclides (1) Upland Field Crops Collected in Japan, J. Nucl. Sci. Technol. **44** 4 (2007) 628.

[4.200] ISHII, N., KOISO, H., TAGAMI, K., UCHIDA, S., Elution of Radiocesium from Soil and Sludge, Kyoto, Japan (2013) 86–90.

[4.201] FESENKO, S.V. et al., Twenty years' application of agricultural countermeasures following the Chernobyl accident: lessons learned, J. Radiol. Prot. Off. J. Soc. Radiol. Prot. **26** 4 (2006) 351.

[4.202] HOWARD, B.J., WELLS, C., BARNETT, C.L., HOWARD, D.C., Improving the quantity, quality and transparency of data used to derive radionuclide transfer parameters for animal products. 2. Cow milk, J. Environ. Radioact. **167** (2017) 254.

[4.203] PARACHE, V. et al., Transfer of 131I from Fukushima to the Vegetation and Milk in France, Environ. Sci. Technol. **45** 23 (2011) 9998.

[4.204] KOBAYASHI, M. et al., Urgent study on the contamination of radionuclides in milk of dairy cows following the accident at the Fukushima Daiichi Nuclear Power Plant in Japan, Jpn. J. Zootech. Sci. **83** 1 (2012) 57.

[4.205] YONAI, M., HORINO, R., IMANARI, M., SHIBA, N., WATANABE, A., Residual radioactive cesium of pasture grass after the accident at the Fukushima Daiichi Nuclear Power Plant, and cesium levels in beef from grass-fed steers at the Tohoku Agricultural Research Center, Bull. Natl. Agric. Res. Cent. Tohoku Reg. **116** (2014) 83.

[4.206] ISHIKAWA, Y. et al., Application of zeolite could not accelerate removal of radiocesium from cattle body, NARO Institute of Livestock and Grassland Science (2014).

[4.207] OHMORI, H., SASAKI, Y., TAJIMA, K., KATSUMATA, M., Radioactive caesium concentrations in pigs fed brown rice contaminated by the Tokyo Electric Power Company Fukushima Daiichi nuclear power plant, Livest. Sci. **159** (2014) 156.

[4.208] MIYANO, H., SATO, S., The accumulation in body of radiocesium of the native chicken, Fukushima-Ken Nogyo Sogo Senta Kenkyu Hokoku Special Issue on Radioactive Material Countermeasures (2014) 110.

[4.209] MANABE, N. et al., "Effects of 'clean feeding' management on livestock products contaminated with radioactive Cesium due to the Fukushima Daiichi nuclear power plant accident", Agricultural Implications of the Fukushima Nuclear Accident, Springer, Tokyo (2016) 77–90.

[4.210] HASHIMOTO, K., TANOI, K., SAKURAI, K., The radioactivity measurement of milk from the cow supplied with the meadow grass grown in Ibaraki-prefecture, after the nuclear power plant accident, Radioisot. Tokyo **60** 8 (2011) 335.

[4.211] TAKAHASHI, T. et al., Changes in radionuclide levels in milk from the cow supplied with pasture grown in Ibaraki prefecture, after the accident in Fukushima Daiichi Nuclear Power Plant, Radioisotopes **61** 11 (2012) 551.

[4.212] OINUMA, H., SAITO, M., ODA, Y., ENDO, K., Effect of zeolite supplementation on the transfer of radioactive cesium from diet in dairy cows, Jpn. J. Zootech. Sci. **84** 3 (2013) 333.

[4.213] AII, T., KUME, S., TAKAHASHI, S., KURIHARA, M., MITSUHASHI, Toshihiko., The effect of the radionuclides from Chernobyl on iodine-131 and cesium-137 contents in milk and pastures in south-western Japan, Nippon Chikusan Gakkai-Ho **61** 1 (1990) 47.

[4.214] MITSUHASHI, T., A study on the transfer coefficient of cesium-137 in domestic milk, Bull. Natl. Inst. Anim. Ind. Jpn. (1996).

[4.215] ITO, N. et al., Transfer coefficients of 137 Cs via the forage-cow-milk pathway in Aomori Prefecture of Japan, Radioisot. Tokyo **43** 11 (1994) 695.

[4.216] MAYES, R., EAYRES, H.F., BERESFORD, N., LAMB, C.S., HOWARD, B., Changes with Age in the Absorption of Radiocaesium by Sheep, Radiat. Prot. Dosimetry **41** (1992) 83.

[4.217] BERESFORD, N.A., MAYES, R.W., BARNETT, C.L., HOWARD, B.J., The transfer of radiocaesium to ewes through a breeding cycle – an illustration of the pitfalls of the transfer coefficient, J. Environ. Radioact. **98** 1 (2007) 24.

[4.218] BERESFORD, N.A. et al., Making the most of what we have: application of extrapolation approaches in radioecological wildlife transfer models, J. Environ. Radioact. **151** (2016) 373.

[4.219] HOWARD, B.J., BERESFORD, N.A., BARNETT, C.L., FESENKO, S., Gastrointestinal fractional absorption of radionuclides in adult domestic ruminants, J. Environ. Radioact. **100** 12 (2009) 1069.

[4.220] FUKUDA, T. et al., Distribution of artificial radionuclides in abandoned cattle in the evacuation zone of the Fukushima Daiichi nuclear power plant, PloS One **8** 1 (2013) e54312.

[4.221] TAKASE, T. et al., Distribution of radiocaesium in cattle body, Fukushima Univ. Chiiki Sozo Rep. **24** (2013) 109.

[4.222] SATO, I. et al., Distribution of radioactive cesium and stable cesium in cattle kept on a highly contaminated area of Fukushima nuclear accident, Anim. Sci. J. **86** 7 (2015) 716.

[4.223] KOGA, F. et al., Presuming techniques of radiocesium concentration in muscle for beef cattle, Fukushima-Ken Nogyo Sogo Senta Kenkyu Hokoku Special Issue on Radioactive Material Countermeasures (2014) 94.

[4.224] ITO, N., Effect of Fukushima Daiichi Nuclear Power Plant accident to farm animal products and solution: studies using contaminated cattle within 20 km zone, Nippon Juishi Kai Zasshi **65** (2012) 645.

[4.225] NATSUHORI, M. et al., Pharmacokinetics of Radiocesium in Wagyu (Japanese Black Cattle), Proceedings of the Specialists' Meeting on Effects of the Fukushima Accident on Organisms around the Nuclear Power Plant Site, KURRI-EKR-15, Kyoto, Japan (2016) 141.

[4.226] BROWN, J.E. et al., Improving Models and Learning from Post-Fukushima Studies. Report of EJP-CONCERT H2020-662287, (2018).

[4.227] TAKENAKA, A., The Influence and Countermeasure of Radionuclides on Animal Production, Proceedings of the Japanese Pig Veterinary Society, Vol. 60, (2012) 7.

5. FOREST ECOSYSTEMS

SHOJI HASHIMOTO, MASABUMI KOMATSU,
NAOHIRO IMAMURA, SHINTA OHASHI
Forestry and Forest Products Research Institute, JAPAN
HIROAKI KATO
University of Tsukuba, JAPAN
KAZUYA NISHINA
National Institute for Environmental Studies, JAPAN
KEIKO TAGAMI, SHIGEO UCHIDA
National Institute of Radiological Sciences, National Institutes for Quantum and Radiological Science and Technology, JAPAN
GEORGE SHAW
University of Nottingham, UNITED KINGDOM
MIKE WOOD
University of Salford, UK
NICK BERESFORD, BRENDA HOWARD,
UKCEH, UK
SERGEY FESENKO
Russian Institute Radiology and Agroecology, RUSSIAN FEDERATION
YVES THIRY
ANDRA, FRANCE

5.1. INTRODUCTION

Approximately 70% of the territory affected by the Fukushima Daiichi accident is covered by forest (Fig. 5.1) [5.1]. Forests in Fukushima prefecture consist of about 0.34 million ha of forest plantations and 0.58 million ha of natural/semi natural forest [5.2].

Japanese forests are rich in tree species diversity. The types of species commonly present in these forests are described by their commonly used names in this chapter with their Latin names given on the first occasion. Commonly present coniferous trees include cedar (*Cryptomeria japonica*, Fig 5.2), pine (i.e., Japanese pine (mostly, *Pinus densiflora*), Fig. 5.3) and cypress (i.e., Japanese cypress (*Chamaecyparis obtusa*)). The deciduous broadleaf oak (Konara oak, *Quercus serrata*, Fig. 5.4) is also commonly present.

Brown forest soils (Cambisols and Andosols in the classification of the UN Food and Agriculture Organization) are widely distributed in the forested areas. Black soils (Andosols) and immature soils (Regosols, Arenosols, Fluvisols, and Leptosols) are also present [5.3] (Fig. 5.5). The major game animals present are Sika deer (*Cervus nippon*), Wild boar (*Sus scrofa*), and Asian black bear (*Ursus thibetanus*).

The characteristics of forest stands vary between forests (Figs. 5.2–5.4). A description of typical forests of major radioecological monitoring sites operated by the University of Tsukuba and the Forestry and Forest Products Research Institute is given in Table 5.1. In many Japanese forests, fast decomposition of organic matter occurs due to the warm and humid climate, so the organic layers of such Japanese forests are relatively thin compared with those in other temperate regions [5.4].

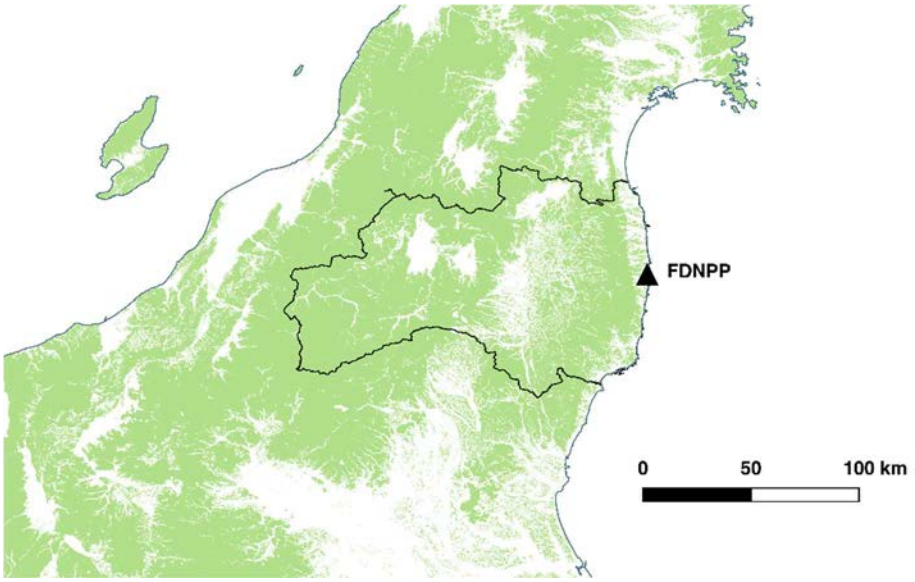

FIG. 5.1. Distributions of forests around the FDNPP [5.3]. Green shades show forested areas, the black line indicates borders of Fukushima prefecture.

FIG. 5.2. Cedar plantation forest in Ohtama village, Fukushima (Foto: Shinta Ohashi, August 2018).

Moderately moist brown forest soil is the most common soil type in Fukushima Prefecture forests. Brown forest soil often has a well-developed A_0 layer. The soils have 1.5-cm-thick organic horizon (L, F, H) with a moderately dense layer of decayed leaves. Underneath the thickly layered F-H horizon, there are often fine nutty and granular structures that are well developed for dryness [5.5].

Black soils have a thick black A-horizon below the soil surface organic layer and have relatively higher organic carbon contents than the other forest soils. The soils of the Immature category have lower organic matter contents than other soils [5.6].

In March 2011, when most radionuclides were deposited after the FDNPP accident (see Chapter 3), deciduous trees had no leaves.

TABLE 5.1. EXAMPLES OF FOREST CHARACTERISTICS IN FUKUSHIMA PREFECTURE

Site name	Tree species	Stand age (years)	Diameter at breast height (cm)	Density (trees per ha)	Soil type	Reference
Yamakiya	Cedar	33	32	800	Brown forest soil/Black soil	[5.7]
Yamakiya	Cedar	17	19	2400	Brown forest soil/Black soil	[5.7]
Yamakiya	Oak	—[a]	—	2500	Brown forest soil/Black soil	[5.8]
Kawauchi	Cedar/Oak	43	18.8/14.3	975/569	Brown forest soil	[5.9]
Kawauchi	Cypress	26	17.6	1330	Brown forest soil	[5.9]
Kawauchi	Oak	26	13.1	1750	Brown forest soil	[5.9]
Kawauchi	Cedar/Oak	57	30.9/25.8	733/255	—	[5.9]
Ohtama	Cedar	42	24.8	1117	Black soil	[5.9]
Ohtama	Pine/Oak	43	19.0/17.5	550/654	Brown forest soil	[5.9]
Ohtama	Pine/Oak	44	18.8/15.6	938/375	Brown forest soil	[5.9]
Tadami	Cedar/Oak	10	19.9/17.2	1105/133	Brown forest soil	[5.9]
Tadami	Cypress	33	20.6	2133	—	[5.9]

[a] no data

FIG. 5.3. Pine plantation forest in Kawauchi village, Fukushima in winter time (Foto: Shoji Hashimoto, November 2017).

FIG. 5.4. Oak plantation forest in Kawauchi village, Fukushima in spring time (Foto: Shinta Ohashi, April 2012).

FIG. 5.5. Soil profiles in Fukushima prefecture (left: Black soil in Otama village, taken in June 2012; middle:Brown forest soil in Kawauchi village, taken in August 2017, right: Brown forest soil in Kawauchi village, taken in August 2017) (Fotos: Shinji Kaneko and Satoru Miura).

Radiocaesium dynamics within forest ecosystems are more complex than in agricultural land (Fig. 5.6) because trees are perennial plants and forests are highly structured ecosystems. Leaves/needles, branches, bark, forest floors and soil surface organic layers were initially contaminated at the time of deposition.

The underlying mineral soil layer below the organic layer may also have been contaminated in the case of wet deposition due to radionuclide percolation from organic to mineral soil. Radiocaesium deposited on above ground vegetation was partially absorbed by the foliage, the rest gradually weathered off mainly by rain and foliar abrasion to the soil surface organic layer. Radiocaesium in the soil surface organic layer was then transferred to the mineral soil layers. The important long-term contamination pathway for trees is root uptake. Both the soil surface organic and the mineral soil layers are sources for uptake of radiocaesium by trees and understory species via roots or mycelia. The above processes lead to redistribution of radiocaesium within a forest ecosystem, eventually forming a quasi-equilibrium steady state of the radiocaesium activity concentrations in tree compartments and soil.

Two groups of transfer parameters are reported in this chapter. The first group includes parameters that describe radiocaesium dynamics in the trees and soil-tree system. The second group provides the parameters for estimating the radiocaesium activity concentrations in edible forest products and tree compartments. The data reported in this chapter are mainly based on peer reviewed papers and official reports from relevant Japanese institutions.

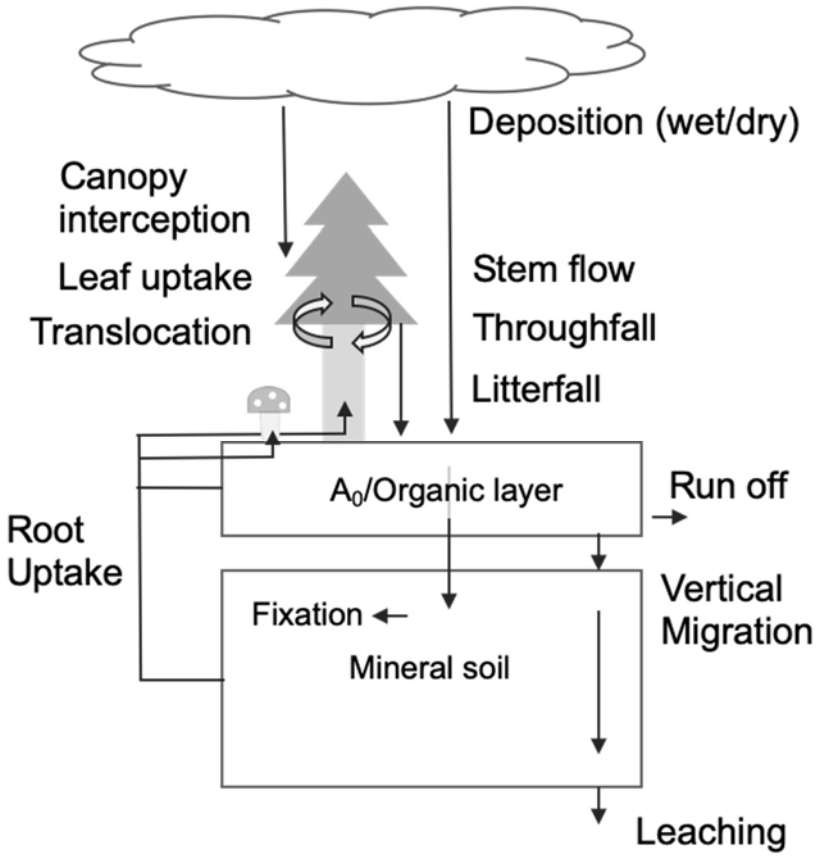

FIG. 5.6. Major dynamics of radionuclides deposited on forests after IAEA 2006 [5.10].

5.2. RADIOCAESIUM TRANSFER TO TREE COMPARTMENTS

5.2.1. Introduction

In forest ecosystems, radionuclides deposited from the atmosphere are initially mostly retained by tree canopies via a process called interception and only some of the radionuclides are directly deposited onto the soil surface. A fraction of intercepted radionuclides is subject to rapid weathering from the tree canopy to the forest floor, especially if there is rainfall subsequent to deposition [5.8–5.10]. As the migration of radionuclides from tree to soil continues, the soil becomes the largest reservoir for radionuclides. Fractions of soil associated radionuclides are taken up by trees, wild edible plants and mushrooms via roots and hyphae below ground. Radionuclides on, and within a tree, can also be translocated internally within it.

The above phenomena were well understood but were not well quantified in the emergency response phase or the transition phase after the Chernobyl accident. This is because some of these processes such as interception occurred during the first few hours or days after deposition whereas the process of radionuclide deposition occurred over a longer period of ten days. Additionally, forest monitoring systems that could have provided relevant data were not well established in forests in the Chernobyl area at the time of the accident. In the following section, parameter values are reported that quantify the transfer between, and within, tree compartments and soil that were determined using established monitoring sites in forests affected by the FDNPP accident.

5.2.2. Interception and weathering

The interception of atmospheric deposition by the tree canopies is an important process that needs to be quantified for describing the subsequent radiocaesium transfer in forests. However, in the case of accidental deposition, canopy interception fractions (*f*) are difficult to measure directly at the time of deposition as required by the definition of *f*. Radiocaesium removal from plant and tree surfaces can be assumed to be initially rapid, but then slows down with time [5.11, 5.12]. Therefore, most of the field estimates of *f* are normally based on either *(i)* measurements made soon (one or two weeks) after deposition, or (ii) back calculation using simple exponential models based on measured intercepted radionuclide activity concentrations in the tree canopies that were sampled months to years after deposition occurred. Both these options were used to estimate interception fractions in Japan. The data measured over several years after the FDNPP accident confirmed that a double exponential model was most appropriate for describing the decrease in radionuclide concentrations over time [5.8, 5.12, 5.14]. Therefore, a two-component loss model and the least squares method were applied to the data describing temporal change in radionuclide activity concentrations in the canopies of trees after the FDNPP accident to quantify parameters describing interception and weathering.

5.2.2.1. Interception fractions

Interception fraction values were reported by several research groups for forests contaminated after the FDNPP accident (Table 5.2). The definition of "Interception fraction" and more information on how it is calculated is given in Chapter 2.

The underlying measurements were made between March 2011 and February 2012. Therefore, some of the interception fraction values presented in Table 5.2 were affected to different extents by weathering processes following initial interception of atmospheric deposition and did not completely adhere to the strict definition of "Interception fraction" given in Chapter 2. Interception fraction values (f and f_B) presented in Table 5.2 were estimated using the two-component exponential model as described above [5.13]. Alternatively, the measured inventory ratio between the canopy (Bq/m^2) and the initial atmospheric input (Bq/m^2) was determined as a "Retention fraction". The fallout deposition values were based on the activity inventories reported in publications considered in Table 5.2.

The total deposition was estimated using the following methods:

- Mass balances of radiocaesium in forest canopies;
- Comparison of radiocaesium deposition to the ground on open fields and in forests based on the assumption that the total deposition inventory onto forest canopies can be represented by the measured deposition inventory on open fields near the forest;
- Sampling of mineral soil and the soil surface organic layer;
- Measurements of radiocaesium inventory in soil and organic layers;
- The radiocaesium activity concentrations in the above ground tree biomass are time dependent due to weathering and abrasion. Therefore, modelling the loss of radiocaesium from plants and back calculation gives the total radionuclide activity in plants at the time of deposition.

All the underlying data were determined by direct measurements of radiocaesium activity concentrations in soil, hydrological components (e.g., rainfall, throughfall, stemflow), and compartments of the forest system (needles, leaves, branches, litterfall and wood).

TABLE 5.2. INTERCEPTION FRACTION VALUES FOR RADIOCAESIUM BY TREES AFTER THE FDNPP ACCIDENT

Tree species	Sampling period (in 2011, unless otherwise stated)	Time since deposition (d)	^{137}Cs deposition density (Bq/m^2) [a]	Nuclides	Interception fraction f or retention fraction	Mass interception fraction f_B (m^2/kg)	Method (sample size) [b]	Reference
Interception fraction values based on measurements in the short term after the depositions								
Cedar	11–28 March	16	8×10^3	^{137}Cs, ^{134}Cs	0.93 [c]	—	Mass balance (N = 20)	[5.14]
				^{131}I	0.51[c]	—		
Cedar	11–25 March [e]	13	2.0×10^3–2.2×10^4	^{137}Cs, ^{134}Cs	0.76–0.86 [c] (0.81[f])	0.062–0.19	Mass balance (N = 3)	[5.15]
	11–29 March [e]	17			0.90 [c]	0.088		
	11–30 March [e]	18			0.33–0.75 [c] (0.55 [f])	0.016–0.050		
	11–30 March [e]	18			0.78	0.041		
	11 March–7 April [e]	26			0.40–0.50 [c] (0.45 [f])	0.016–0.023		
Cypress	11–28 March	16	8.0×10^3	^{137}Cs, ^{134}Cs	0.92 [c]	—	Mass balance (N = 20)	[5.14]
				^{131}I	0.25 [c]	—		
Cypress	11–30 March [e]	18	1.2×10^4–2.1×10^4	^{137}Cs, ^{134}Cs	0.46 [c]	0.017	Mass balance (N = 3)	[5.15]
Cypress	11 March–30 April [e]	49	1.6×10^4	^{137}Cs	0.31 [c]	—	Mass balance (N = 1)	[5.16]
Cypress	16 February 2012	341	3.3×10^4	^{137}Cs	0.56 [c]	0.019	Direct measurement (N = 12)	[5.9]
Pine	9 August	150	4.4×10^4	^{137}Cs	0.17 [c]	0.015	Direct measurement (N = 12)	[5.9]

TABLE 5.2. INTERCEPTION FRACTION VALUES FOR RADIOCAESIUM BY TREES AFTER THE FDNPP ACCIDENT (cont.)

Tree species	Sampling period (in 2011, unless otherwise stated)	Time since deposition (d)	^{137}Cs deposition density (Bq/m^2) [a]	Nuclides	Interception fraction f or retention fraction	Mass interception fraction f_B (m^2/kg)	Method (sample size) [b]	Reference
Evergreen broadleaf	11–25 March [e]	13	3.0×10^3	^{137}Cs, ^{134}Cs	0.34 [c]	0.023	Mass balance (N = 3)	[5.15]
Oak	9 August	150	4.4×10^4	^{137}Cs	0.14[c]	0.011	Direct measurement (N = 1)	[5.9]
Deciduous broadleaf	11–30 March [e]	18	2.1×10^4	^{137}Cs, ^{134}Cs	0.34 [c]	0.058	Mass balance (N = 3)	[5.15]
Interception fraction values based on back calculations								
Cedar	12 March	110	4.4×10^5	^{137}Cs	0.70 [d]	0.024–0.026	Field loss model (N = 7)	[5.13]
Cedar	9 August	150	1.0×10^4–6.3×10^5	^{137}Cs	0.68 [c] (0.15 [d])	0.0083	Direct measurement (N = 12)	[5.9]
	31 August	172			0.98 [c] (0.43 [d])	0.031		
	7 September	179			0.85 [c] (0.29 [d])	0.023		
	28 November	261			0.87 [c] (0.24 [d])	0.0092		
Oak, Pine	12 March	110	4.5×10^5	^{137}Cs	0.23 [c]	—	Field loss model (N = 6)	[5.13]

— no data
[a] arithmetic mean of interception fractions determined for multiple forest stands
[b] methodology for measurements or estimations of radiocaesium inventory in above ground tree biomass
[c] the value representing a retention fraction at the time of sample collection
[d] estimates of interception fraction at the time of initial deposition (March 11, 2011), which was derived from a back calculation by using a two-component exponential model
[e] sampling period began before the accident
[f] mean value

.

TABLE 5.3. INTERCEPTION OF RADIOCAESIUM OBSERVED AFTER THE CHERNOBYL ACCIDENT

Tree species	Sampling period	Time after deposition (d)	^{137}Cs deposition density (Bq/m^2)	Nuclides	Interception fraction *f* or retention fraction	Method (sample size) [a]	Reference
Coniferous	—	—	—	not specified	0.70–0.90 [b]	—	[5.17]
Coniferous	14 May 1986	18	1.5×10^3	^{137}Cs	0.79 [b]	Mass balance (N=3)	[5.18]
Coniferous	30 April 1986	4	2.0×10^4	^{137}Cs, ^{134}Cs	0.70 [b]	Soil and surface organic layer sampling (N=1)	[5.19]
Norway spruce	—	—	—	^{137}Cs, ^{134}Cs	0.70 [b]	—	[5.20]
Coniferous	May 1986	—	2.0×10^3	^{137}Cs	0.80–1.0 [b]	Soil sampling (N=25)	[5.21]
Coniferous	—	—	—	^{137}Cs	0.79–0.81 [b]	—	[5.22, 5.23]
Norway spruce	—	—	—	^{134}Cs	0.80 [c]	Mass balance (experiment)	[5.24]
Deciduous	May 1986	—	2.0×10^3	^{137}Cs	0.10–0.40 [b]	Soil sampling	[5.21]
Beech	—	—	—	^{137}Cs, ^{134}Cs	0.20 [b]	—	[5.20]

— no data

[a] methodology for measurements or estimations of radiocaesium inventory in above ground tree biomass

[b] the value representing a retention fraction at the time of sample collection

[c] estimates of interception fraction at the time of initial deposition derived from a mass balance calculation.

Coniferous forests (e.g., cedar, red pine) tended to have higher *f* values than deciduous broadleaf (e.g., beech, oak) forests (Table 5.2) because the deposition occurred in early spring when there were no leaves on deciduous trees. Data for interception of radiocaesium by deciduous broadleaf forests were limited. The observed *f* values for deciduous forests largely represent interception by branches and bark of the trees.

Similar data for interception were reported for forests affected by the Chernobyl accident in 1986 (Table 5.3). This suggests that the interception for both evergreen coniferous and deciduous forests is controlled by universal processes rather than by site specific conditions.

5.2.2.2. Data limitations

The smaller number of samples collected, e.g., $N \leq 3$ in cedar and cypress forests, gives less confidence in the interception fractions than those measured for other forests. Another source of the uncertainty in the interception fraction value estimates are differences in sampling times in respect to the major deposition events and the limited degree of confidence in model parameters used for back calculation of radionuclide concentrations in the tree canopy at the time of the accident.

5.2.2.3. ^{137}Cs transfer from tree canopy to the forest floor

Transport of radiocaesium intercepted by the canopy to the forest floor occurs via throughfall and stemflow and litterfall [5.8, 5.13–5.16, 5.25–5.29]. The time dependent ^{137}Cs activity concentrations, normalized to the ^{137}Cs deposition per unit area, in litterfall, throughfall and stemflow are shown in Fig. 5.7.

Throughfall and stemflow, which are both hydrological pathways, made a major contribution to the total flux of radiocaesium from the canopy to forest floor during the first days to weeks after the FDNPP accident (Kato et al., 2017 [5.13]). However, radiocaesium activity concentrations in these hydrological pathways decreased quickly. Thereafter, litterfall became the major pathway of radiocaesium transfer to the forest floor [5.8, 5.13, 5.14, 5.25, 5.26]. Parameters of the two-component exponential canopy loss model are presented in Table 5.4.

TABLE 5.4. PARAMETER VALUES FOR A TWO COMPONENT EXPONENTIAL MODEL DESCRIBING TEMPORAL EVOLUTION OF ^{137}CS ACTIVITY CONCENTRATIONS IN MAJOR RADIOCAESIUM TRANSFERS BETWEEN THE CANOPY AND FOREST FLOOR (AS SHOWN ON FIG. 5.7)

Parameter	Cedar			Deciduous broadleaf		
	Throughfall	Stemflow	Litterfall	Throughfall	Stemflow	Litterfall
C_1 (m^2/kg)	0.012	3.5×10^{-3}	0.59	9.8×10^{-3}	6.2×10^{-5}	0.24
C_2 (m^2/kg)	1.7×10^{-4}	6.8×10^{-5}	0.23	2.1×10^{-5}	2.5×10^{-5}	0.017
λ_f (year^{-1})	15	9.8	3.5	13	2.2	1.7
λ_s (year^{-1})	0.75	0.26	0.42	0.31	0.061	0.21
$T_{\text{eff},f}$ (year)	0.046	0.070	0.19	0.053	0.32	0.41
$T_{\text{eff},s}$ (year)	0.92	2.7	1.7	2.2	11	3.3
R^2	0.72**	0.89**	0.77**	0.96**	0.29*	0.87**

** $p < 0.01$, * $p < 0.05$

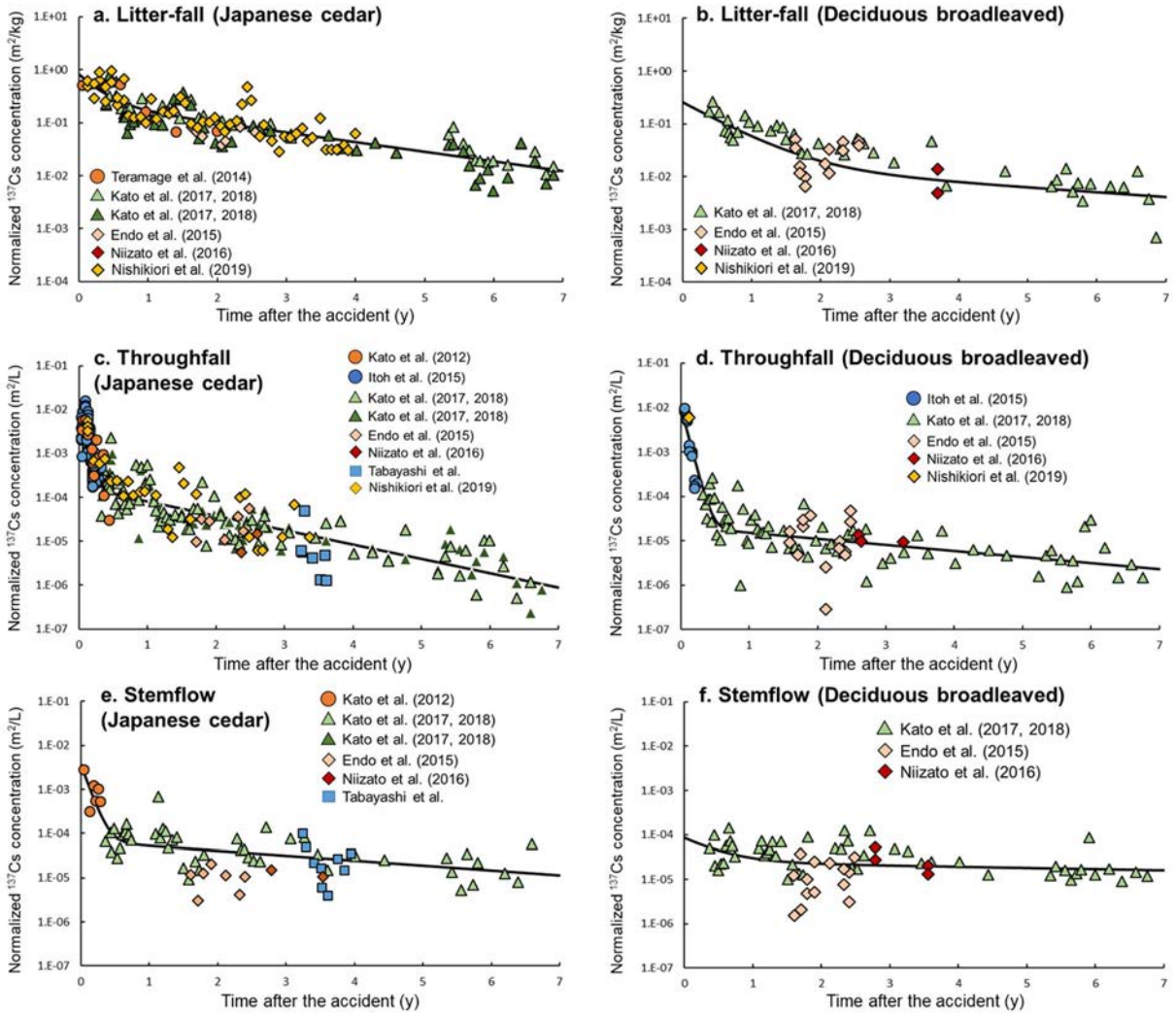

FIG. 5.7. Variations with time in ^{137}Cs activity concentrations in litterfall, throughfall, and stemflow. The normalized ^{137}Cs concentrations are plotted against time after the FDNPP accident.

The effective half-lives for the first component were less than 1 year for all the pathways transferring canopy radiocaesium to the forest floor. Conversely, the second components had longer half-lives ranging from 0.92 to 11 y. Stemflow tended to have the longest effective half-life.

5.2.3. Soil to tree transfer

5.2.3.1. Aggregated transfer factors for tree compartments

In forest ecosystems, the aggregated transfer factor, T_{ag}, is often used for quantification of radionuclide transfer to various forest compartments, including game. T_{ag} is defined as the ratio of the radionuclide activity concentration in plant or any other natural or semi-natural product (Bq/kg FM or DM) to the total deposition on the soil (Bq/m^2) [5.30] (See Chapter 2).

The total deposition to the forest floor represents the total inventory in both organic and mineral soil layers. Initially, T_{ag} was used to avoid the need for information regarding the relevant soil layers from which root uptake was taking place in semi-natural soils (such as forest soils).

Additionally, the vertical distribution of Cs is a dynamic process and varies with time [5.31]. However, application of the T_{ag} concept for forest ecosystems requires some caution because the total deposition to the forest floor can be highly variable especially soon after deposition occurs. The variation is mainly due to considerable spatial and temporal differences in interception of the deposited radionuclides by the tree canopy and in the subsequent transfer from the tree canopy to the forest floor through litterfall, throughfall or stemflow. These processes can also lead to pronounced inhomogeneity in the deposition density of forest soils.

Trees are composed of needles or leaves, branches, bark, and woody stems or trunks. T_{ag} values were derived from the literature that included both ^{137}Cs activity concentration data for tree organs and the ^{137}Cs inventory data for the soil surface organic layer and mineral soil. Samples with ^{137}Cs activity concentrations below detection limits were excluded from the assessments.

The number of data records with both ^{137}Cs activity concentration and inventory information were small, so few records were available for the derivation of T_{ag} values (Table III.1). Nevertheless, the available data clearly illustrate that the T_{ag} values and T_{ag} time dependence differed between wood and bark of different species. The decrease in T_{ag} values for needles of cedar, cypress, and pine was most rapid among all tree compartments, whilst no changes were observed in T_{ag} values for 2011–2015 for leaves of oak. The observed differences in T_{ag} values derived for evergreen coniferous and deciduous broad-leaved forests were due to direct contamination of the needles of evergreen trees during deposition of radionuclides, whereas at that time the leaves of deciduous trees such as oak had not yet appeared. The T_{ag} values for branches decreased with time. Changes in bark T_{ag} were slightly lower than those for other compartments. The T_{ag} values for wood varied for cedar, cypress and pine with no clear trend with time following deposition, whereas for oak wood T_{ag} values increased (Fig. 5.8).

5.2.3.2. Comparisons with Chernobyl studies

The T_{ag} values measured in Fukushima Prefecture varied with time. The values obtained after 4 years were compared with those measured following the Chernobyl accident in the period from 5 to 15 years after the accident [5.48]. Since both pine and oak grow in the vicinities of both the Chernobyl and Fukushima NPPs, results for these types of tree can be directly compared. Available data for other species were compiled together (Fig. 5.9).

The T_{ag} values for oak and conifer species except pine, for both wood and needles/leaves in Fukushima Prefecture were similar to those observed after the Chernobyl accident for similar time periods after initial deposition. The ranges of T_{ag} values for pine wood and needles affected by the FDNPP accident were lower than those reported for the Chernobyl accident because the Chernobyl data included relatively high T_{ag} values measured for hydromorphic soils (i.e. organic), which are not present in Fukushima Prefecture forests. Nevertheless, the geometric means of T_{ag} values for both wood and needles/leaves are similar for the Chernobyl and FDNPP affected areas.

5.2.3.3. Normalised ^{137}Cs activity concentrations in tree compartments

After the FDNPP accident, airborne survey played an important role in determining the spatial distribution of the contamination and its time dependence. The aerial gamma dose rate measurements were converted to the total radiocaesium deposition density (Bq/m^2). A series of aerial and ground truth surveys over the months and years after the FDNPP accident have provided improved estimation of the spatial and temporal variation in deposition for different

types of landscape. In the analysis presented here, data were used from the third and the fifth airborne monitoring surveys (Kato et al., 2019 [5.49]).

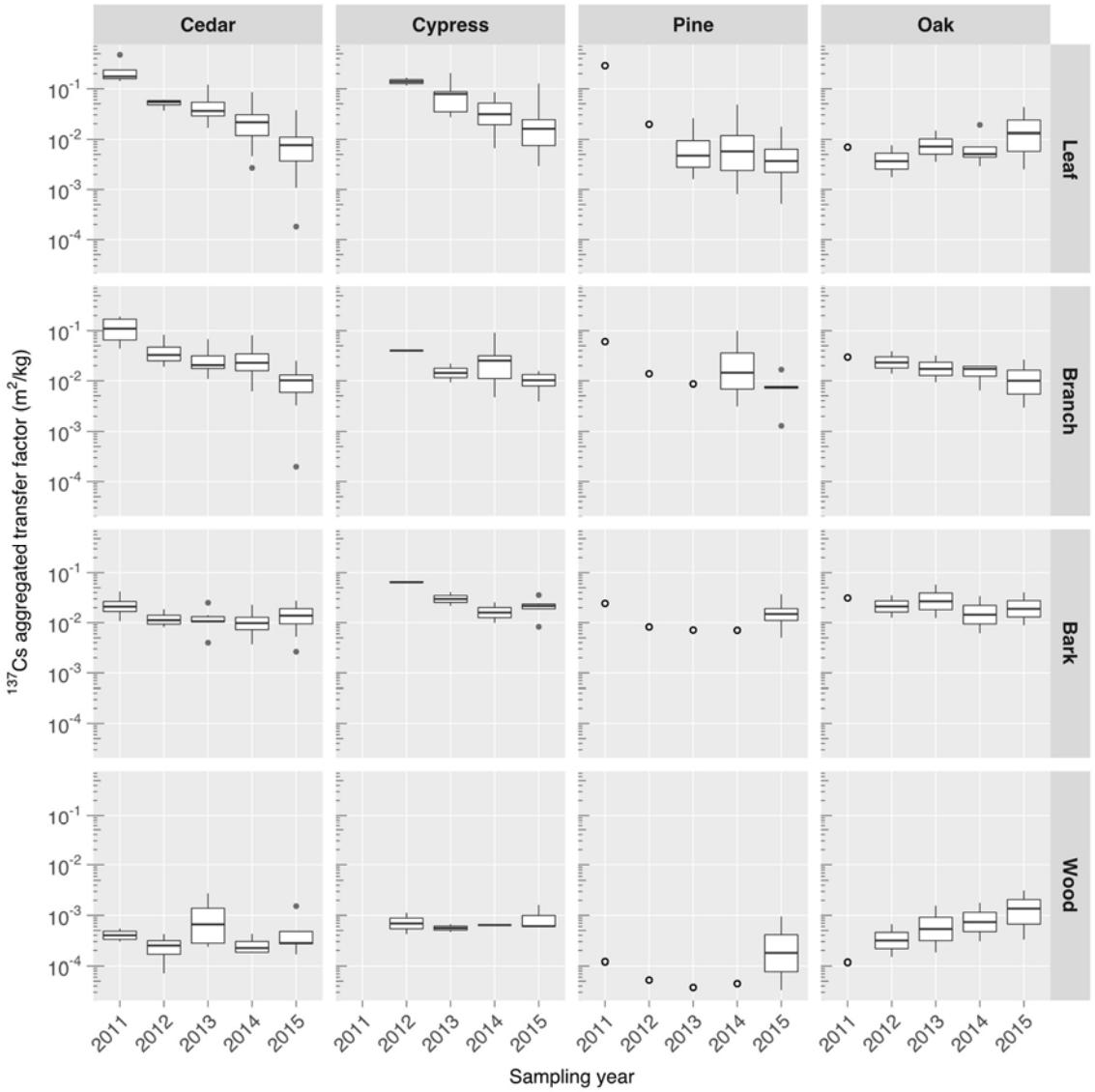

FIG. 5.8. Aggregated transfer factor, T_{ag} (m^2/kg DM) of ^{137}Cs for different tree compartments. Open circles indicate data with no replication (N=1). Based on data from [5.9, 5.21, 5.31–5.47].

The use of the normalized activity concentration (*NC),* defined as the ratio of the activity concentrations in forest compartments (leaves, needles, bark, wood) to the initial total deposition to forests (see Chapter 2; Fig. 5.10), allows the analysis of more data records for estimating the transfer of radiocaesium within forest ecosystems.

Data used for the estimation of radionuclide transfer in contaminated forests (this work) are shown in Fig. 5.11. A summary of all data entries is given in Appendix III. Most of the available data were for needles and leaves from cedar, whereas data for oak were more limited.

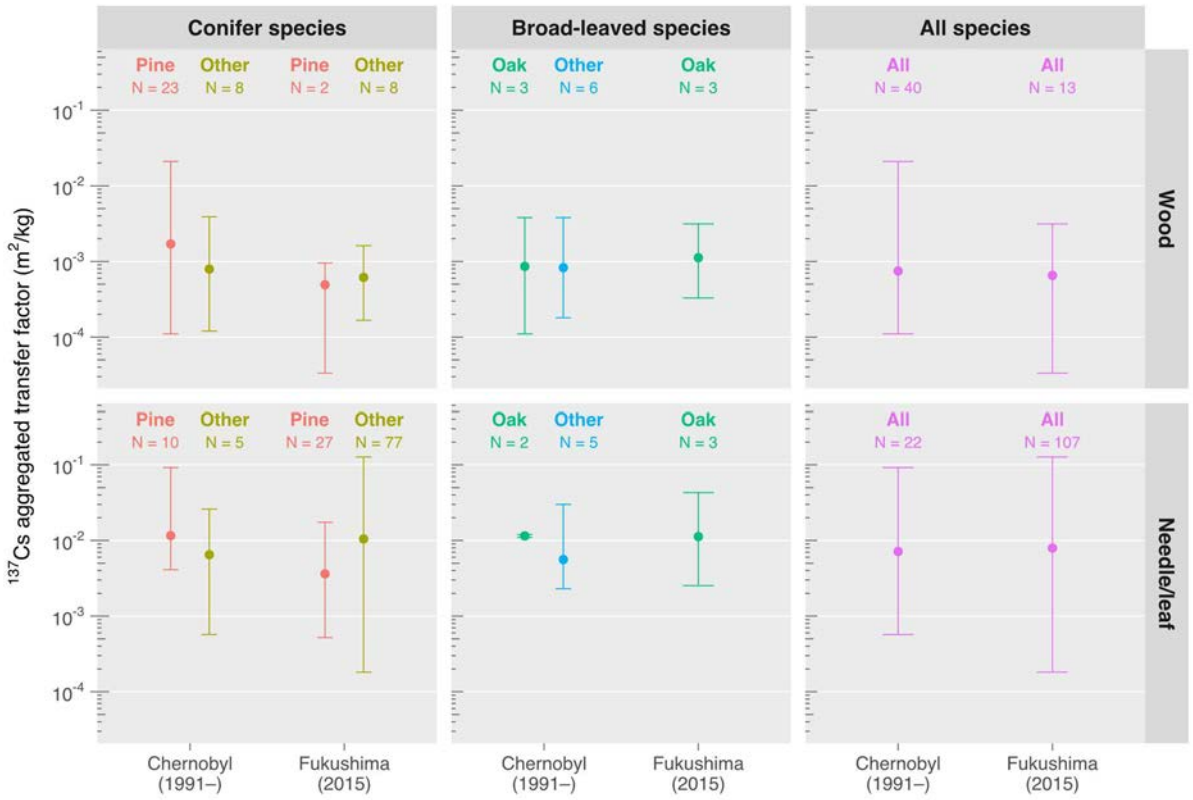

FIG. 5.9. Comparison of ^{137}Cs aggregated transfer factor (T_{ag}, m^2/kg DM) for wood and leaves of forest trees after the Chernobyl (1991–2001) and FDNPP (2015) accidents. Filled circle: arithmetic mean (N=2) or geometric mean (N>2), Error bar: range (minimum and maximum). Based on data from [5.9, 5.21, 5.31–5.47].

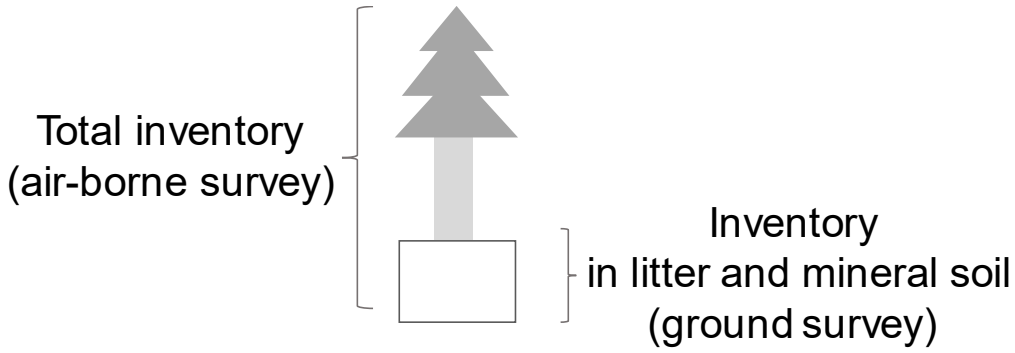

FIG. 5.10. Diagram illustrating the difference between total inventory and soil inventory.

The *NC* values for ^{137}Cs in needles of cedar, cypress and pine decreased with time. An increase with time was observed for oak leaves, probably because the FDNPP accident occurred before mid-March when the oak trees did not have leaves, whereas needles of evergreen trees were directly contaminated by the deposition. Although the data records differed in the number of different years and tree compartments, these data provide useful information to understand the

dynamics of radiocaesium in the early phase after deposition, and to validate radionuclide transfer models for forest ecosystems.

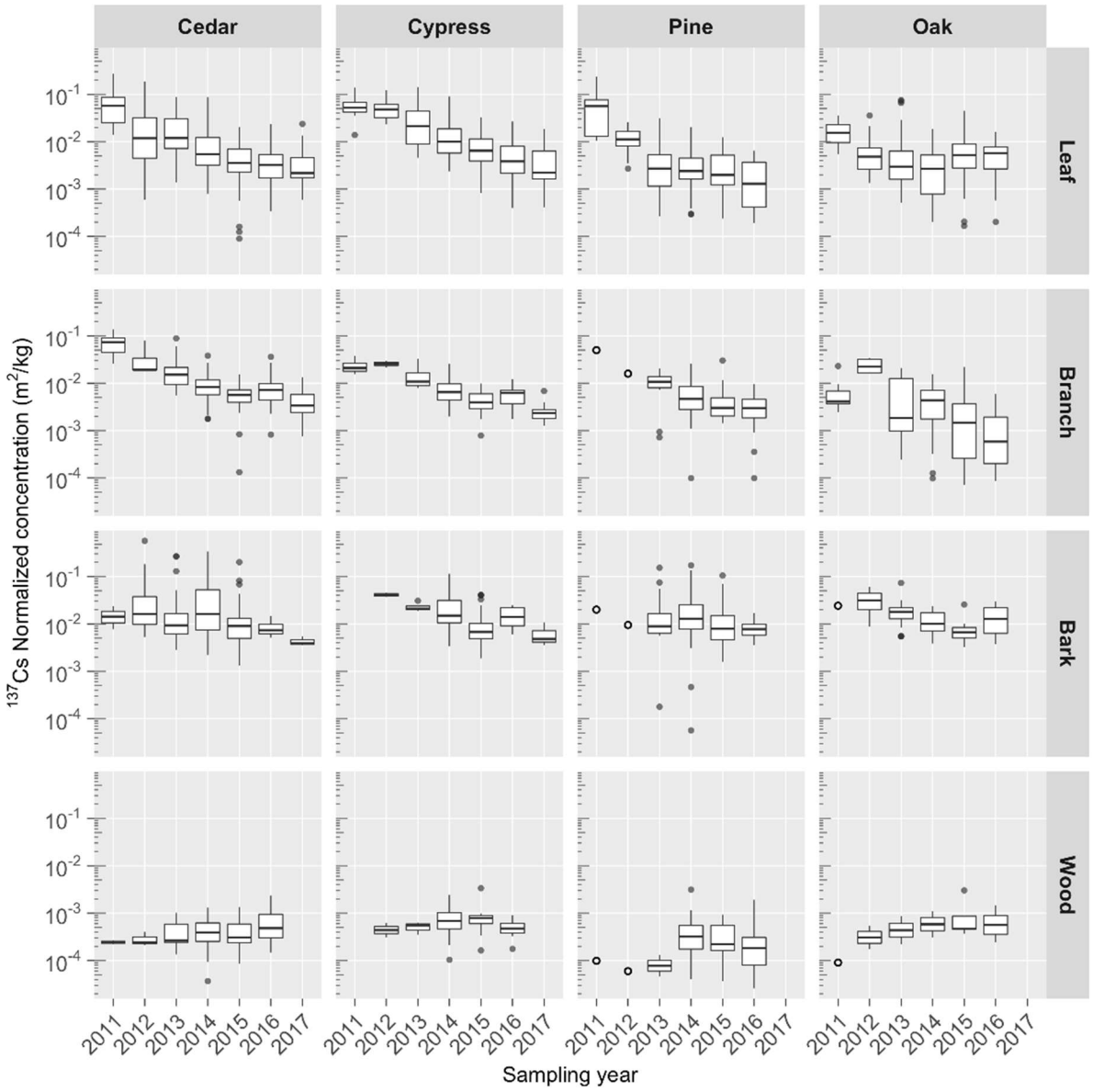

FIG. 5.11. Time-dependence of normalized activity concentrations (m^2/kg DM) of ^{137}Cs for tree compartments. Open circles indicate data with no replication (N=1).

5.2.4. K fertilization effect

The radiocaesium activity concentration in wood was lower than in directly contaminated tree parts such as needles or leaves, branches and bark. However, bark had relatively high contamination and bark ash occasionally exceeds the standard limit for general waste (8000 Bq/kg FM), which may require specific arrangements for the management of contaminated ash. In Japan, no standard limit was set for radiocaesium activity concentrations in wood used as a building material. The amount of external exposure by residence in a house made by timber obtained in Fukushima Prefecture is estimated to be small (less than 0.064 mSv/year) [5.50].

However, since radiocaesium is concentrated in ash, the standard limits for charcoal and firewood have been set to 280 and 40 Bq/kg DM, respectively, so that the resulting combustion ash does not exceed the limit for general waste. Additionally, a standard limit of 50 Bq/kg DM was also applied to logs intended for shiitake mushroom cultivation. The application of these standard limits had economic impacts and the use of logs for shiitake mushrooms is still restricted in Fukushima and surrounding prefectures. Farmers in eastern Japan pay more for less contaminated logs, although the additional costs are currently (as of July 2019) covered by TEPCO compensation. For sustainable long-term production, remediation methods are needed to produce wood that conforms to the standard limits.

A reduction of ^{137}Cs activity concentrations in cypress seedlings planted after the FDNPP accident was observed following potassium application [5.51]. Potassium applied for two years to give a total K of 83 kg/ha, resulted in a reduction of ^{137}Cs activity concentrations in needles of 88% and in stems and roots of 75% (Fig. 5.12). Based on the relationship between exchangeable potassium in soil and T_{ag} to needles, it was suggested that caesium transfer to seedlings in the control group was decreased by higher exchangeable potassium concentrations measured at the site (Fig. 5.13). The exchangeable potassium concentration in soil measured at the end of the experiment was similar between the fertilized and control groups indicating that the observed effect was short term due to the high mobility of potassium in soil. The application of potassium has also been reported to suppress stable caesium uptake by Konara oak seedlings [5.52].

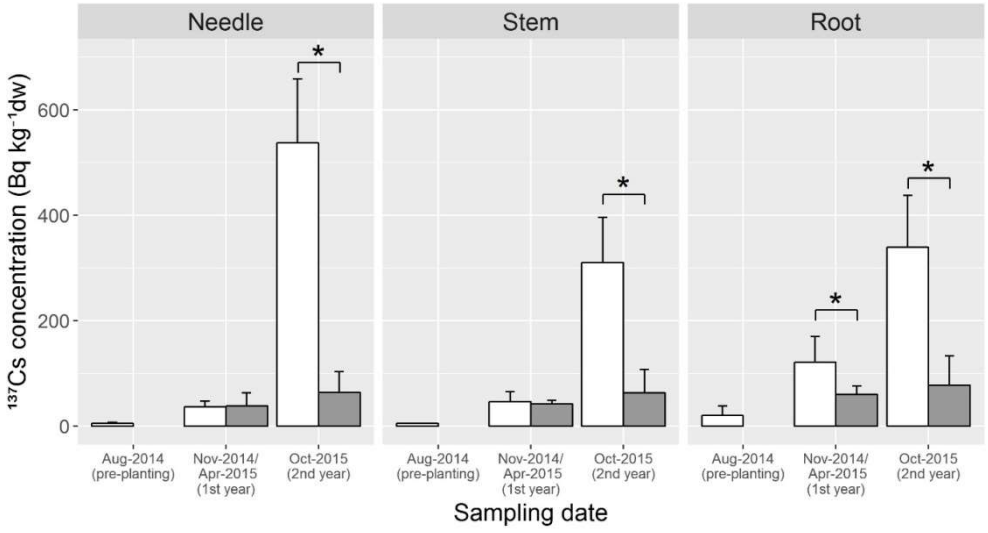

FIG. 5.12. ^{137}Cs activity concentrations in cypress seedlings sampled at control plots (open bar) and K-fertilised plots (grey bar) Komatsu et al. 2017 [5.51]). Samples collected at the same time differ significantly between treatments (nested ANOVA, $p < 0.05$, indicated by asterisk). Pre-planting samples are shown for control plots. All stem samples at pre-planting had lower values than the detection limit despite long (24 h) measurements. Subsequently, values shown for stem samples at pre-planting are the mean of detection limits.

Several studies on forest soil fertilisation were carried out after the Chernobyl accident ([5.36] [5.37], [5.53]). These examined the effect of K-fertilisation on ^{137}Cs activity concentrations in tree compartments and understory species (wild plants and berries). A reduction by a factor of 1.5–2 was reported of the ^{137}Cs activity concentration in wood of young trees following a potassium application at a rate of about 100 kg/ha [5.36]. A twofold reduction of radiocaesium

activity concentrations in new needles for single and repeated K application with rates of 5–79 kg/ha was also reported [5.37].

A summary of these data has suggested a mechanistic model for optimizing the application of fertilizers and other ameliorants for remediation of contaminated forest [5.37]. The ^{137}Cs activity concentration in berries gradually decreased with time after the application of potassium on automorphic dry forest. The activity concentration decreased to 85%, 30%, 12% and 6% for the 2nd, 3rd, 4th and 5th year respectively after potassium application. Overall, the data referenced here for the Chernobyl accident agree with research data from the Fukushima Prefecture when similar K application rates are used [5.51].

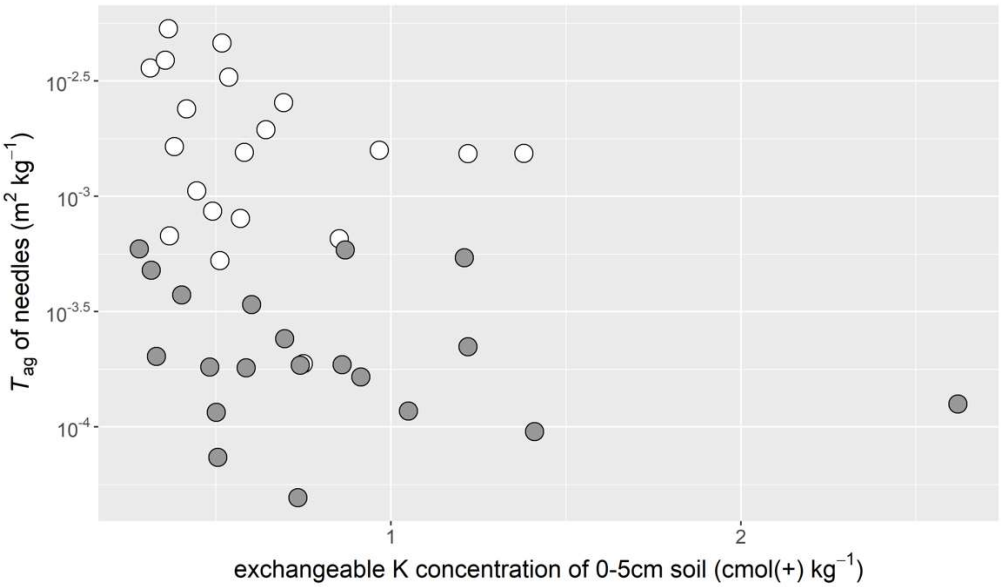

FIG. 5.13. Relationship between exchangeable K concentrations in surface soil (0–5 cm) and aggregated transfer factor values (T_{ag}) of cypress needles in control (open symbols) and K-fertilised sites (grey symbols) Komatsu et al. 2017 [5.51]. The seedlings were sampled in October 2015 at the end of the second growing season.

5.2.5. Heartwood/Sapwood ^{137}Cs concentration ratio

5.2.5.1. Fukushima data

Stem wood of mature trees consists of sapwood and heartwood, which have different physiological functions (Fig 5.14). The sapwood (outer part of the stem wood) has living parenchyma cells with radial and axial transport functions for nutrients and water; the moisture content in sapwood is generally higher than in heartwood. The heartwood (inner part of the stem wood) does not have living cells and does not transport water, but it has various species-specific heartwood constituents that support the tree. Heartwood is widely used as building material because it usually has a larger volume and higher durability than the sapwood; this is the case especially for cedar, which has a relatively large heartwood fraction. Thus, the ratio of ^{137}Cs activity concentrations in heartwood and sapwood is important for understanding the ^{137}Cs dynamics within a tree and for modelling ^{137}Cs contamination in wood.

The concentration ratios of ^{137}Cs in heartwood to sapwood (CR_{hs}) at around breast height (on a DM basis) were calculated based on data for each sampling year, study site and species (cedar, cypress, pine and oak) based on: [5.7, 5.43–5.45, 5.54–5.74]. When a study site had more than one individual measurement, the mean (arithmetic mean when N=2 and geometric mean when N>2) values of ^{137}Cs activity concentrations in the heartwood and sapwood were used for the ratio calculation.

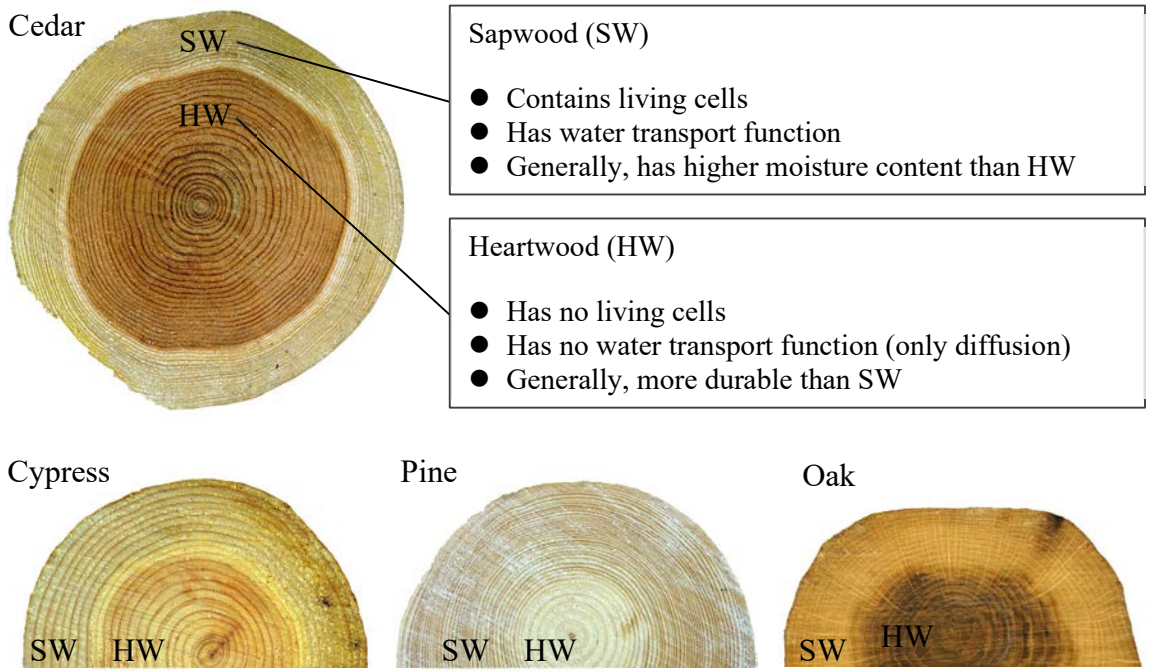

FIG. 5.14. Diagram of sapwood and heartwood

The data shows strong species specificity. CR_{hs} values in cedar, cypress and pine increased from 2011 to 2016, and the mean values reached 2.0 in cedar, but remain (as of 2016) <1.0 in cypress and pine (Fig. 5.15). Because the ^{137}Cs activity concentration in the sapwood of these 3 species remained at similar levels over time (Fig. 5.16), the increment in the CR_{hs} was caused by the gradual accumulation of ^{137}Cs in the heartwood. Conversely, the CR_{hs} values in oak remained almost constant (at about 0.3). However, because both normalized concentrations, *NC,* in sapwood and heartwood of oak showed increasing trends, it is not clear whether the ^{137}Cs distribution in the oak wood was in equilibrium. In general, the CR_{hs} values do not seem to be in equilibrium as of 2016.

5.2.5.2. Comparison with data in previous studies

Some ^{137}Cs data is available on European tree species CR_{hs} values after the Chernobyl accident. Scots pine (*Pinus sylvestris*), which is one of the major commercial tree species in Europe, had lower ^{137}Cs activity concentrations in heartwood than in sapwood (i.e. $CR_{hs} < 1$) as seen in Japanese cypress, pine and oak (Thiry et al. 2002, Yoshida et al. 2011) [5.75, 5.76]. Post-Chernobyl models for ^{137}Cs contamination of wood either assumed low ^{137}Cs activity concentrations in heartwood or did not differentiate heartwood and sapwood for species such

as Scots pine. The high CR_{hs} in Japanese cedar differs from that observed in Scots pine after the Chernobyl accident.

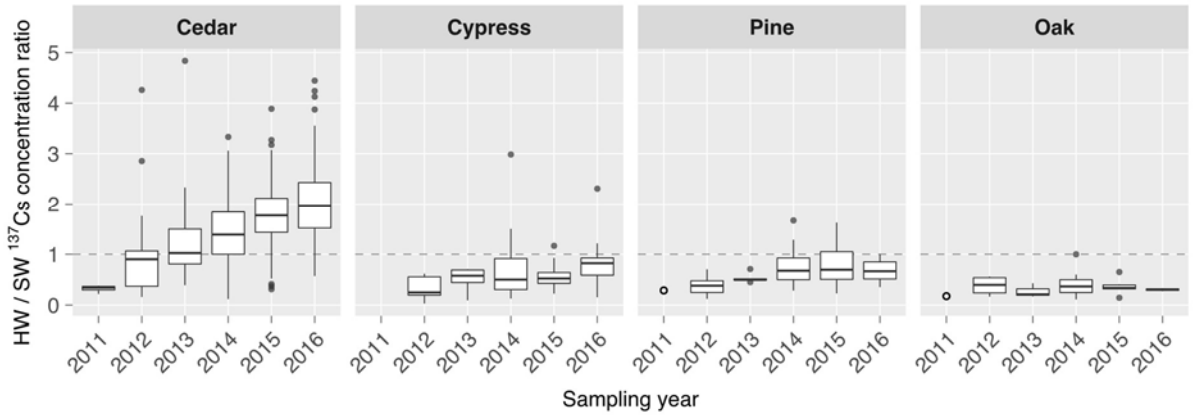

FIG. 5.15. Time series of heartwood (HW) / sapwood (SW) ^{137}Cs activity concentration ratio (dry weight basis). Open circles indicate the data with no replication (N=1). Based on: [5.7, 5.43–5.45, 5.54–5.74].

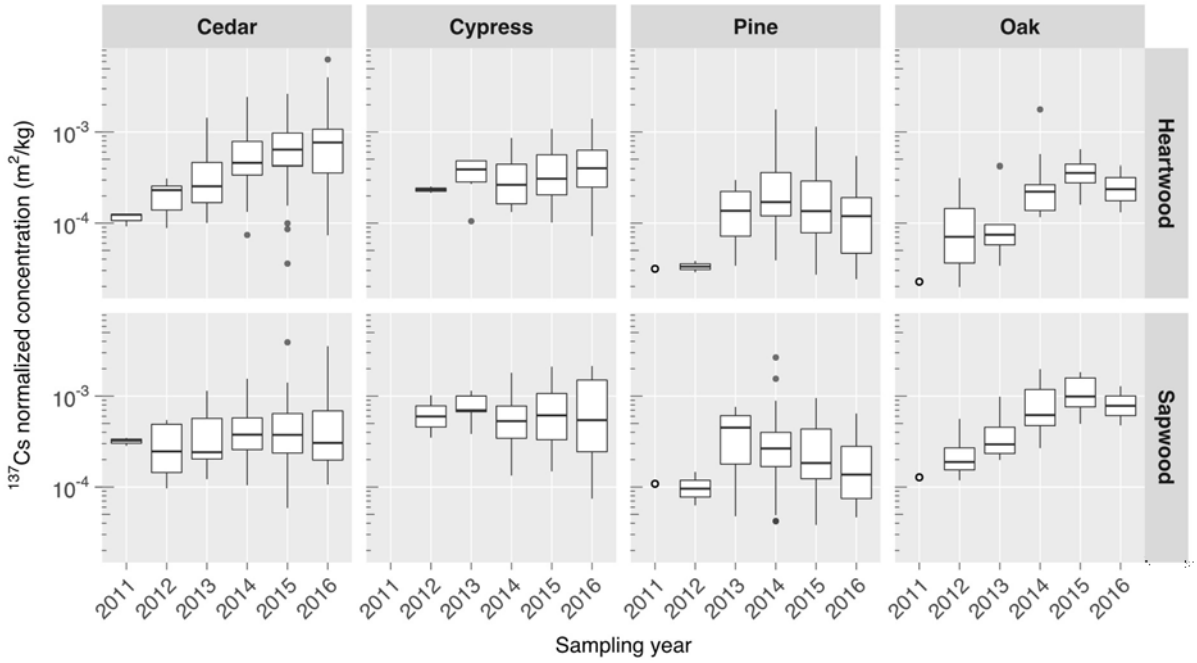

FIG. 5.16. Time series of ^{137}Cs normalized activity concentration (NC; m^2/kg DM) for heartwood and sapwood. Open circles indicate data with no replication (N=1). Based on: [5.7, 5.43–5.45, 5.54–5.74].

5.2.5.3. Data application

Many studies conducted in Japan distinguished heartwood and sapwood and measured individual activity concentrations in these tissues. Unfortunately, the mass of both heartwood

and sapwood are often not reported and therefore much of the data is not convertible to activity concentrations for whole wood.

The data suggest that, as expected from the different physiological characteristics, ^{137}Cs activity concentrations in heartwood and sapwood differ between tree species. It may be appropriate to distinguish heartwood and sapwood in modelling to simulate the dynamics of radiocaesium in forests for predicting the contamination level of wood used for commercial purposes.

5.2.6. Radiocaesium activity concentrations in pollen

The allergic reaction of some people following exposure to cedar pollen is a public health issue. This reaction, commonly known as 'hay fever' is a widespread health problem in Japan. The Forestry Agency has continuously monitored radiocaesium activity concentrations in male flowers of cedar since 2011 at 10 sites in the Fukushima Prefecture. The ^{137}Cs activity concentration dropped markedly from 2011 to 2014, thereafter declining more slowly until 2018 (see Table III.2 and Fig. 5.17). ^{137}Cs activity concentrations were also reported in cedar pollen sampled at 115 sites in 2012 in Fukushima and adjacent prefectures [5.77] (see Table III.2). The *NC* values for ^{137}Cs in 2012 were similar in the two surveys.

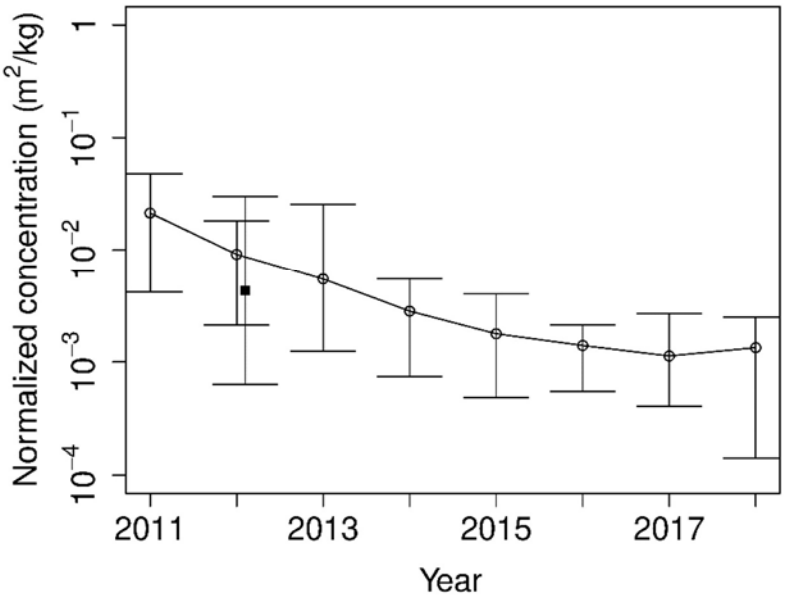

FIG. 5.17. Time series of ^{137}Cs normalized activity concentration (NC; m^2/kg DM) for cedar pollen. The data for 10 sites adopted from Forestry Agency (open circle), and for an intensive spatial sampling study [5.77] (solid rectangle). The bar indicates the minimum-mean-maximum, and the point indicates the arithmetic mean.

A strong correlation has been reported between radiocaesium activity concentrations in male flowers and needles (R^2=0.90–0.96) [5.78], suggesting that the radiocaesium concentration in pollen can be predicted from that in needles.

5.2.7. Radiocaesium transfer in forest soil

5.2.7.1. Distribution of radiocaesium between the organic layer and mineral soil

Radiocaesium intercepted by the tree canopy is gradually transferred over time to the soil surface (see sub-section 5.2.2). Therefore, the soil surface organic material (L, F, H layers) and, later, the mineral soil layer (A and B layers) becomes the major radiocaesium reservoir on a timescale of weeks to years following deposition (Table III.3). The total deposition density of radiocaesium of the upper soil layers is normally applied for calculating T_{ag} values.

To illustrate the tendency for radiocaesium migration in soil, the ratios of soil surface organic layer/mineral soil to total inventory were calculated using the airborne measurements of total deposition inventory. Since deciduous forests had no leaves at the time of the FDNPP accident, the canopy intercepted a smaller fraction of radiocaesium than occurred in evergreen forests, and most of the radiocaesium was deposited directly on the forest floor. Therefore, the geometric mean of the inventory ratio in soil surface organic layer and mineral soil was slightly higher in deciduous forests (ca. 0.8) than that in evergreen forests (ca. 0.7) where the canopy intercepted radiocaesium reducing the early transfer to the surface organic layer (Table III.3; Figs. 5.18, 5.19). Consequently, the ^{137}Cs inventory in the combined soil surface organic layer and mineral soil in deciduous forests was similar to the total deposition inventory in 2011.

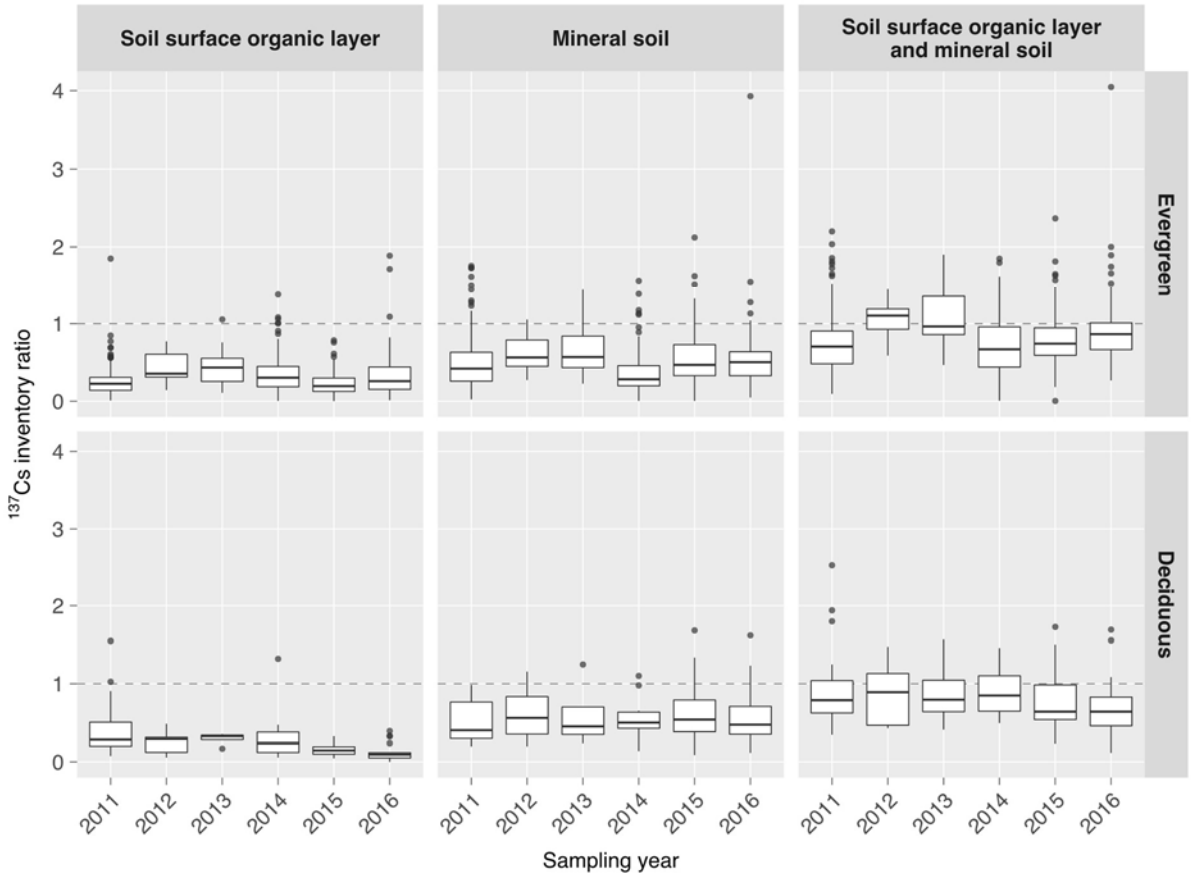

FIG. 5.18. ^{137}Cs inventory ratios of soil surface organic layer and/or mineral soil to airborne based total deposition. A value of 1 shows that the airborne and soil data give the same value. Based on: [5.7, 5.9, 5.44, 5.47, 5.55, 5.58, 5.59, 5.61–5.65, 5.79–5.90].

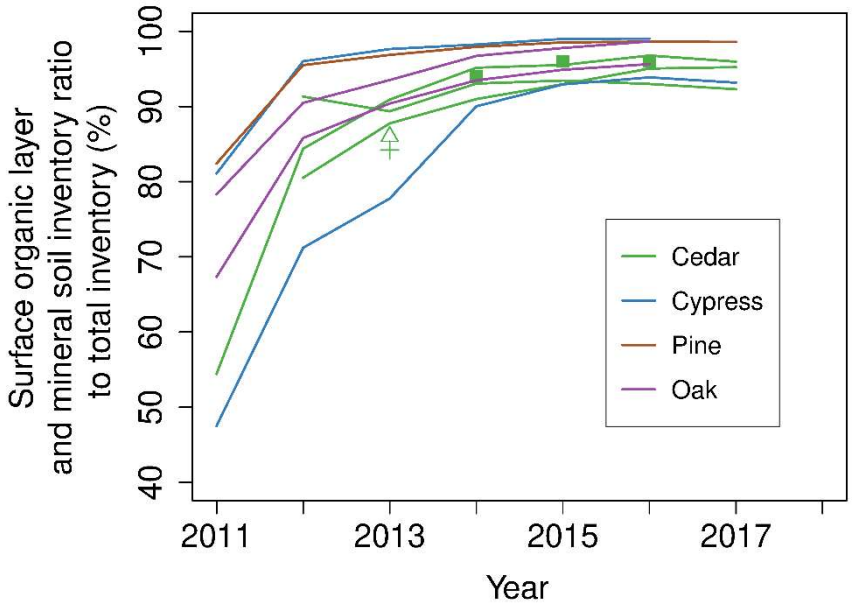

FIG. 5.19. ^{137}Cs inventory ratios of soil surface organic layer and mineral soil to total deposition observed in intensively monitored sites. Lines are from observations from the Forestry and Forest Products Research Institute [5.9]; open triangles and crosses are data from Ref. [5.7]; solid rectangles are data from Refs. [5.73, 5.74]. In these studies, total inventories were estimated by summing up each inventory measured in field surveys.

The inventory ratio in deciduous forests declined between 2011–2016 in the soil organic layer but increased in 2012 and 2013 (when the ratio of geometric means was 1) before declining in 2015 and 2016. In evergreen forests, the inventory ratios of both soil surface organic layer and mineral soil did not show clear trends. The geometric mean of the inventory ratio in the combined data for both the evergreen surface organic layer and mineral soil fluctuated between 0.7 and 0.9. The data also suggest that the proportion of the deposited radiocaesium retained in the evergreen canopy 5 years after deposition occurred decreased from 30% in 2011 to about 20% in 2016.

The transfer of radiocaesium from the above ground parts of trees to the soil, including the soil surface organic layer, has been more clearly demonstrated based on research performed in intensively monitored sites (Fig. 5.19). The data show that the combined soil layers account for varying proportions of the total inventory depending on the tree species. The combined soil layers contained more than 80% of radiocaesium in oak and pine forests in 2011. The fractions of radiocaesium in soil of the cedar and cypress forests were lower than in oak and pine forests and varied among sites from 50–80%. However, the differences were lower after 2014 and approximately 95% of the total inventory was in the combined soil layers. The high ratio for oak is probably because oak trees did not have emerged leaves in March 2011, and therefore intercepted less radiocaesium than cedar and cypress. Pine is an evergreen conifer, but the amount of foliage (needles) is lower than those observed for cedar and cypress forests.

5.2.7.2. Activity concentrations of radiocaesium in the soil surface organic layer

The *NC* for the soil surface organic layer is determined by the balance between inflow from trees and outflow to the mineral soil layer. The normalised activity concentration values, *NC,* for the soil surface organic layer decreased with time (Table III.3). Therefore, migration of ^{137}Cs to the mineral soil layer from the soil surface organic layer was greater than the migration from above ground parts of the tree to the forest floor.

5.2.7.3. Vertical distributions of radiocaesium within forest soil

Radiocaesium in the soil surface organic layer is transferred to mineral soil layers by leaching, a process that depends on the decomposition rate of organic matter. In general, in forests, radiocaesium is mainly located in the upper soil layers. The radiocaesium activity concentration decreases with increasing depth. The vertical distribution changes with time in the soil organic layer because of decomposition of the litter layer, and varies from site to site, but in the long term, radiocaesium in the upper mineral soil generally migrates to deeper soil layers in forest soils. Therefore, quantification is needed of the vertical distribution of radiocaesium to understand the radiocaesium dynamics in forest soils and to allow predictions of radiocaesium migration.

Migration of radiocaesium in soil leads to a reduction of both external dose and radionuclide transfer to trees and understorey species with time [5.31, 5.91]. Different models have been used to predict radionuclide distribution in soil [5.92, 5.93].

5.2.7.4. *Parameters for vertical distributions*

As input for such predictions, two simple parameters were derived for ^{137}Cs, (1) the fraction contained in the soil surface organic layer, and (2) position of the migration centre. As shown in Fig. 5.19, a substantial amount of radiocaesium migrates from the tree canopy to the forest soil.

The radionuclide fraction in the soil surface organic layer ($F_{l/t}$) is the ratio of the inventory in the soil surface organic layer to that in the soil surface organic and mineral layers:

$$F_{l/t} = \frac{\text{Inventory in soil organic layer}}{\text{Inventory in soil organic and mineral layers}} \quad (5.1)$$

The migration centre (X_c) was defined as ^{137}Cs activity-weighted soil depth by the following expression [5.94–5.98]:

$$X_c = \frac{\Sigma_i x_i I_i}{\Sigma_i I_i} \quad (5.2)$$

where $I_i = q_i \Delta x_i$ is the ^{137}Cs inventory (Bq/m^2) in the mineral soil layer i centred at the depth x_i (cm), having thickness Δx_i (cm) and average activity concentration q_i (Bq/m^3).

To characterize the radionuclide distribution in soil, values for the parameters above were estimated based on the analysis of 99 vertical soil profiles presented in six publications (see Table III.4); some examples of the data evaluations are given in Figs. 5.20 and 5.21.

As expected, $F_{l/t}$ drastically decreased from about 50% in 2011 to about 5% in 2017 (linear regression analysis, $p < 0.001$; see Fig. 5.20). This indicates a fast migration of radiocaesium

from the soil surface organic layers to mineral soil layers; and it also indicates that the loss of radiocaesium from the soil surface organic due to migration to the mineral soil layers is larger than the input from the tree canopy to the forest floor.

The rapid decrease in $F_{l/t}$ was also observed in several monitoring studies [5.9, 5.99]. Values for the fraction $F_{l/t}$ are also reported in studies carried out in the Russian Federation and Ukraine [5.17, 5.31, 5.40] after the Chernobyl accident. However, these studies do not include values obtained immediately after the accident.

The migration centre, X_c is closely connected to $F_{l/t}$, both parameters characterise the depth to which radiocaesium has migrated within a given time period. X_c did not show significant change with time (Fig. 5.21; linear regression analyses, p = 0.15), and was 3–4 cm on average. This implies that, once ^{137}Cs has reached the mineral soil layer, its migration significantly slows down, demonstrating a slow ^{137}Cs migration from the upper mineral soil layers to deeper mineral layers. However, ^{137}Cs migrated from soil surface organic layer into the mineral soil, in particular, in the early stage. Therefore, the values are influenced by migration from the layers above the mineral soil layer. Slow migration in mineral soil layers was also reported in post-Chernobyl studies [5.17, 5.100] and slow migration in mineral soil layers appears to be a common behaviour in forest soils.

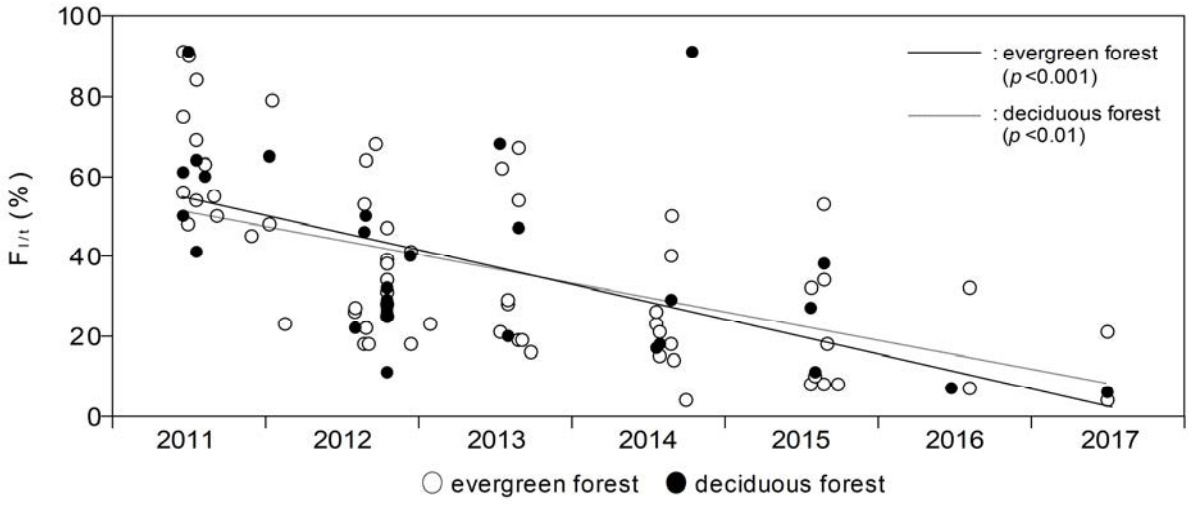

FIG. 5.20. Fraction $F_{l/t}$ (%) of the total activity in forest soil retained in the soil surface organic layer in evergreen forest and deciduous forests om 2011–2017

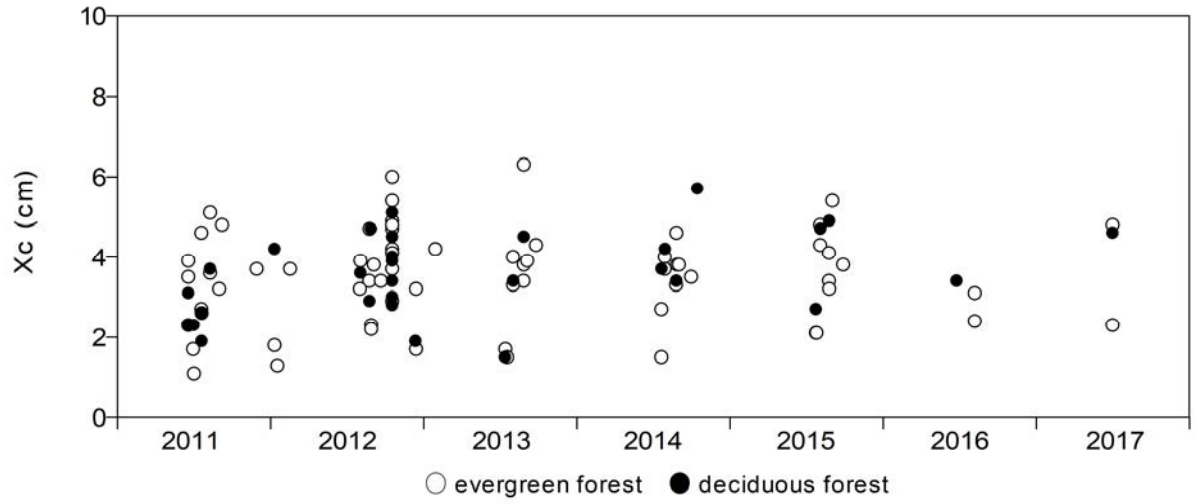

FIG. 5.21. ^{137}Cs activity migration centre X_c (cm) in mineral soil in evergreen forest and deciduous forests in 2011–2017.

5.2.8. Half-life values in needles, branches and bark

Needles/leaves (in evergreen species), branches and bark were directly contaminated by releases from the FDNPP accident. The radiocaesium activity concentrations in these tree compartments decreased because of weathering, growth, generation of new tissues and radioactive decay. The reduction of radiocaesium concentrations in these tree compartments has been quantified by analysing time series of activity concentrations. Twenty six datasets were analysed to derive half-lives, T_{eff}, for ^{137}Cs activity concentrations in different tree species as shown in Table 5.5 [5.8, 5.9, 5.101] which gives a compilation of statistically significant T_{eff} values. All reported values were based on the bulk ^{137}Cs activity concentrations so there was no subdivision of samples by factors such as the age of tissue (i.e., current or older needles for the conifer) or whether the bark was living or dead.

Table 5.6 gives statistics relevant to the T_{eff} values for different tree compartments. The T_{eff} values for cedar needles ranged from 0.76 to 2.7 years, with a mean value of 1.9 years (N=9). The T_{eff} for cypress and pine needles were within this range. The T_{eff} values for branches varied from 1.0 year (in pine) to 3.8 years. Except for red pine, T_{eff} values for branches were generally longer than those for needles. The T_{eff} values for bark were longer than those for needles and branches, except for oak bark, for which the value was 1.3 years [5.8] (Table 5.5).

Three studies included in Table 5.6 also reported non-significant regressions to the time series of ^{137}Cs activity concentrations in leaves (fitted as a first-order exponential decrease), so T_{eff} was not calculated in some cases. Thus, the data provided should be applied with caution.

The decrease of radiocaesium in tree compartments can normally be described by exponential functions after the FDNPP accident. However, there are substantial variations and, in some cases, no significant decrease in tree tissue contamination was reported. The numbers of time series where an exponential decline was not statistically significant (mainly for oak) are shown in Table 5.6. For instance, three cases were reported as non-significant for exponential loss from oak leaves [5.9].

TABLE 5.5. COMPILED T_{EFF} VALUES FOR TREE COMPONENTS

Tree type	Species	Parts	Period	T_{eff} (year)	Reference
Coniferous	Cedar	Leaves	2011–2014	0.76	[5.101]
	Cedar	Leaves	2011–2016	1.6, 2.3, 1.8, 2.1	[5.9]
	Cedar	Leaves	2011–2016	1.7, 2.7, 1.3, 1.3	[5.8]
	Cypress	Leaves	2011–2016	3.6, 2.2	[5.9]
	Pine	Leaves	2011–2016	1.0	[5.9]
	Cedar	Branch	2011–2016	2.5, 2.8, 3.3, 3.8	[5.9]
	Cypress	Branch	2011–2016	3.5, 3.5	[5.9]
	Pine	Branch	2011–2016	1.0	[5.9]
	Cedar	Bark	2011–2016	8.5	[5.9]
	Cypress	Bark	2011–2016	3.9	[5.9]
	Pine	Bark	2011–2016	6.4	[5.9]
Deciduous	Oak	Branch	2011–2016	3.6, 2.2	[5.9]
	Oak	Bark	2011–2016	6.7	[5.9]
	Oak	Bark	2012–2016	1.3	[5.8]

TABLE 5.6. SUMMARY OF T_{EFF} (YEAR) AGGREGATED FOR EACH TREE COMPARTMENT (ALL TREE DATA INCLUDED)

Tree part	Effective half-life T_{eff} (year)			The number of reports with simple exponential fit as	
	Mean	Min–Max	SD	significant	not significant
Leaf	1.7	0.76–3.6	0.78	12	3
Branch	2.9	1.0–3.8	0.89	9	0
Bark	5.3	1.3–8.5	2.8	5	7

None of the datasets analysed indicated an increase of radiocaesium activity concentration in tree tissues with time. Similar studies were made after the Chernobyl accident in the Zhitomir region (Ukraine), where an increase of radiocaesium in pine needles was reported ([5.102]). After the FDNPP accident, no decrease in ^{137}Cs activity concentrations of oak leaves has been reported as of 2015 [5.9]. However, it can be anticipated that radiocaesium activity concentrations of leaves will increase in the near future due to root uptake of ^{137}Cs from soil (see sub-section 5.2.8). Therefore, continuing field surveys are needed to elucidate the long-term dynamics in these components.

Many of the T_{eff} values presented here are based on research performed in the early stage (based on a 3- to 5-year observation period) after the FDNPP accident. Processes causing the immediate loss of intercepted radiocaesium probably have a strong influence on the observed T_{eff} values. For example, wash-off processes, as discussed in sub-section 5.2.2, strongly controlled the decrease of ^{137}Cs activity concentrations in coniferous needles and bark.

Most post-Chernobyl studies reporting half-lives started several years after the accident in 1986 [5.74]. Therefore, it is difficult to compare the T_{eff} values for trees from Chernobyl studies with those derived from the compiled Fukushima dataset.

5.3. TRANSFER TO MUSHROOMS

Mushrooms are an important foodstuff in Japan. The total annual production of edible mushrooms is 457 000 ton/year [5.103] and the mean mushroom consumption for adults is 17.0 g/d [5.104].The collection of wild mushrooms is less important than the production of cultivated mushrooms (e.g. the annual collection of *Tricholoma matsutake*, the most familiar wild mushroom species in Japan, was 69 ton in 2016 [5.105]). However, wild mushrooms are more important in mountainous areas of Japan, where collecting mushrooms is an important recreational activity for local residents [5.106, 5.107].

After the FDNPP accident, radiocaesium was measured in wild mushrooms in many areas across eastern Japan. The Japanese government restricted commercial shipping of foods with radiocaesium activity concentrations exceeding 100 Bq/kg (usually FM basis). As a result of food monitoring surveys, shipment of wild mushrooms was restricted in 110 municipalities of 10 prefectures (26 June 2019) [5.108]. The restriction is now partially lifted in 12 municipalities for specific mushroom species. As part of these restrictions, mushroom shipments were restricted on a regional basis without distinguishing between species.

Radionuclide transfer from soil to mushrooms is quantified using aggregated transfer factor (T_{ag}) values according to genus and species. T_{ag} values derived before the FDNPP accident are compiled in the IAEA TRS 472 [5.30] and a summary of this data is published elsewhere [5.109]. After the FDNPP accident, the T_{ag} values for wild mushrooms in Japan have been reported in a subsequent study [5.110] (Table 5.7).

Another approach for T_{ag} calculations was based on environmental monitoring data organised by prefectural governments. Even though site specific data on contamination of the soil at the sampling sites are not available, normalized concentrations (*NC*) for mushrooms could be calculated using estimates of the contamination obtained from airborne surveys (Table 5.8 and Appendix III). For the *NC* calculation, the geometric mean of radiocaesium deposition was calculated for each municipality and decay corrected to the date of the FDNPP accident (11 March 2011).

TABLE 5.7. Aggregated transfer factor T_{AG} (M^2/KG DM) FOR ^{137}CS IN WILD MUSHROOMS AT KAWAUCHI VILLAGE, 20–30KM FROM THE FDNPP, IN 2012 [5.110].

Mushrooms group	GM	Mean	GSD [a]	SD	Min	Max
Mycorrhizal fungal species	0.24	0.65	1.7	0.77	0.01	3.0
Saprotrophic fungal species	0.10	0.24	1.1	0.49	0.03	1.8

[a] unitless

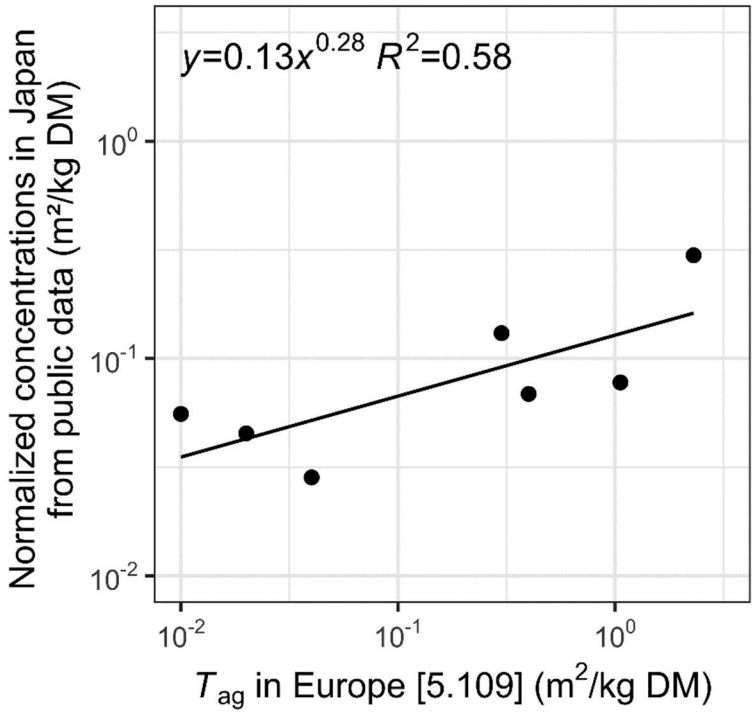

FIG. 5.22. Comparison of reported T_{ag} values in Europe after the Chernobyl accident [5.109] and NC values in Japan after the Fukushima accident derived from public data monitored by the local governments. Results for common species in the two studies were plotted.

Since the *NC* values were originally calculated on a fresh mass basis (m^2/kg FM), the data given in Table 5.8 were converted to dry mass basis (m^2/kg DM) using dry/wet ratios of mushroom species from published articles [5.111–5.120]. The *NC* values varied by about 100-fold between species. Most of the mycorrhizal species had higher *NC* values than other types of mushrooms, with the exception of some saprotrophic fungal species, which also had high *NC* values (e.g. *Pholiota lubrica*, Table III.4). The *NC* values obtained in Fukushima studies were compared with the T_{ag} values reported in Europe for seven common species [5.109] (Table 5.9 and Fig. 5.22). Although the number of species was small and the slope of the regression line is 0.28, the comparison indicated that the T_{ag} values of radiocaesium in the same species measured in Europe and Japan are within the same order of magnitude.

In Japan, sawdust mushroom cultivation is more popular for mushroom production than bed-log cultivation (Fig. 5.23). The *CR* value for shiitake mushrooms (*Lentinula edodes*) of 0.18 calculated using 64 samples with sawdust cultivation is relatively low (GSD 1.6 and range 0.062–0.63; Bq/kg FM mushroom to Bq/kg DM substrate). The radiocaesium content of such cultivated mushrooms can be further minimized by diluting the growing medium with uncontaminated sawdust.

TABLE 5.8. NORMALISED CONCENTRATION NC (m^2/kg DM) FOR ^{137}CS IN WILD MUSHROOMS

Type of mushroom	Year	N	GM (m^2/kg DM)	GSD	Min (m^2/kg DM)	Max (m^2/kg DM)
Type L, soil litter decomposing fungi	2011	12	1.6×10^{-2}	7.0	1.2×10^{-3}	0.56
	2012	8	2.5×10^{-2}	4.0	4.1×10^{-3}	0.24
	2013	14	0.16	4.6	2.1×10^{-2}	2.0
	2014	9	6.9×10^{-2}	7.8	4.1×10^{-3}	0.82
	2015	6	4.8×10^{-2}	8.5	5.2×10^{-3}	0.61
	2016	2	1.4×10^{-2}	7.1	3.5×10^{-3}	5.6×10^{-2}
	2017	3	0.22	1.2	0.19	0.27
Type M, mycorrhizal fungi	2011	84	2.4×10^{-2}	5.6	6.2×10^{-4}	2.2
	2012	66	9.6×10^{-2}	5.6	3.7×10^{-3}	1.1
	2013	36	3.9×10^{-2}	4.1	3.9×10^{-3}	2.4
	2014	34	3.1×10^{-2}	3.6	3.5×10^{-3}	0.65
	2015	29	1.8×10^{-2}	2.9	2.7×10^{-3}	0.24
	2016	28	3.4×10^{-2}	2.9	6.2×10^{-3}	0.23
	2017	34	2.2×10^{-2}	2.3	5.1×10^{-3}	0.14
Type W, wood decomposing fungi	2011	12	1.2×10^{-2}	4.2	1.2×10^{-3}	0.17
	2012	20	3.6×10^{-2}	3.8	3.1×10^{-3}	0.77
	2013	18	4.0×10^{-2}	3.2	1.6×10^{-3}	0.18
	2014	30	3.6×10^{-2}	2.0	2.3×10^{-3}	0.34
	2015	22	2.3×10^{-2}	3.0	4.0×10^{-3}	7.2×10^{-2}
	2016	21	2.9×10^{-2}	2.0	4.4×10^{-3}	0.20
	2017	25	2.9×10^{-2}	2.4	6.6×10^{-3}	0.11

TABLE 5.9. COMPARISON OF REPORTED T_{AG} VALUES IN EUROPE [5.36], [5.109]) AND *NC* VALUES DERIVED FROM THE FUKUSHIMA STUDIES

Species	D/F ratio [a]	N	GM (dry) (m^2/kg DM)	GSD	T_{ag} in Europe (m^2/kg DM)
Armillaria mellea	0.11	75	3.0×10^{-2}	2.85	4.0×10^{-2}
Cortinarius caperata	0.10	2	0.31	— [b]	2.3
Cortinarius praestans	0.10	5	4.7×10^{-2}	2.08	2.0×10^{-2}
Kuehneromyces mutabilis	0.11	1	0.14	—	0.30
Lepista nuda	0.09	10	5.8×10^{-2}	4.30	1.0×10^{-2}
Suillus grevillei	0.09	9	7.2×10^{-2}	2.09	0.40
Suillus luteus	0.09	1	8.1×10^{-2}	—	1.1

[a] D/F ratio: dry to fresh mass ratio (kg/kg) summarized from published articles. Mean values by genus were used. Since a ratio for *Kuehneromyces mutabilis* was not obtained, the mean ratio of all data excluding polypore species (with high D/F ratio) was used
[b] no data

FIG. 5.23. Cultivated shiitake mushrooms (Lentinula edodes). Left: sawdust cultivation (Photo: Hiromi Mukai), Right: bed-log cultivation (Photo: Japan Non-Wood Forest Products Promotion Association).

The annual production in Japan of shiitake mushrooms using bed-logs (usually oak trees) is 25 000 ton/year [5.105]. Bed-log cultivation is normally performed outdoors on the forest floor using wood logs taken from nearby forests. The geometric mean of the *CR* values for bed-log mushrooms of 0.43 is higher than that for sawdust cultivation (n = 48, GSD = 2.49, min = 0.037, max = 2.8, [5.121]). Consequently, bed-log shiitake mushrooms with radiocaesium activity concentrations exceeding regulatory limit values were reported in many municipalities during the first few years after the FDNPP accident. As part of the remediation strategy, the Japanese government provided guidelines for safe production such as restricting the use of contaminated logs and outdoor cultivation. The number of municipalities with shipping restrictions for bed-log shiitake mushrooms has decreased with time [5.122].

Overall, the ratios between ^{137}Cs uptake of different mushroom species observed in the areas affected by the FDNPP accident are similar to those observed for the same mushroom species obtained after the Chernobyl accident. Some differences may be explained by the different time periods for which the *CR* values were derived. Monitoring for the Chernobyl data began after a longer time period following the release of radionuclides to the environment compared to data obtained for Fukushima.

5.4. TRANSFERS TO EDIBLE WILD PLANTS

As already mentioned in Chapter 4, wild edible plants, including edible ferns and bamboos, commonly called "*Sansai*", are widely consumed by residents of the Fukushima Prefecture (Fig. 5.24). Wild plant species are also cultivated in forests and the annual production of bamboo shoots and other wild plants are about 36,000 and 14,000 tons/year, respectively [5.105]. After the FDNPP accident, shipping of edible wild plants was restricted in many prefectures [5.108]. Due to the high consumption of wild plants in mountain areas [5.106, 5.107], the contamination of wild plants was of great concern to the population of the Fukushima and some surrounding prefectures.

The aggregated transfer factors (T_{ag}) of six edible wild plants obtained from peer reviewed publications are shown in Table 5.10. *NC* values based on deposition data measured in airborne surveys are given in Table III.3. The T_{ag} and *NC* values obtained on a FM basis were converted to a DM basis using dry to fresh mass ratios obtained from published articles, as was also carried out for wild mushrooms in Section 5.3.

TABLE 5.10 AGGREGATED TRANSFER FACTOR VALUES T_{ag} (M^2/KG DM) FOR ^{137}CS IN EDIBLE WILD PLANTS [5.123–5.126]

Name	Species	Parts	N	GM (D/F ratio)	GSD [a]	Min	Max	Reference
Butterbur leafstalk	*Petasites japonicus*	Leafstalk	20	3.8×10^{-3}	3.3	4.3×10^{-4}	4.9×10^{-2}	[5.124]
Koshiabura (ja)	*Eleutherococcus sciadophylloides*	Shoot	11	3.2×10^{-2}	3.7	3.5×10^{-3}	2.7×10^{-1}	[5.123]
Zenmai (ja)	*Osmunda japonica*	Shoot	20	2.5×10^{-3}	3.0	2.8×10^{-4}	4.2×10^{-2}	[5.125]
Butterbur scape	*Petasites japonicus*	Scape	17	1.2×10^{-3} (0.13) [b]	— [c]			[5.126]
Japanese knotweed	*Fallopia japonica*	Shoot	5	8.3×10^{-4} (0.06)				[5.126]
Mugwort	*Artemisia indica var. maximowiczii*	Shoot	7	6.2×10^{-4} (0.15)				[5.126]

[a] unitless
[b] T_{ag} values from [5.126] were provided on a fresh mass basis and were converted to a DM basis using the dry to fresh mass ratio (D/F ratio, kg/kg)
[c] no data

The T_{ag} values for edible wild plants were about 10 times less than those calculated for wild mushrooms. Among the species examined, *Eleutherococcus sciadophylloides* (Japanese name: Koshiabura) had the highest T_{ag} and *NC* values and the shipment of Koshiabura has been the most widely restricted of any wild plant. Potassium availability did not explain differences in radiocaesium transfer to both *E. sciadophylloides* and other plant species, and between individuals of the *E. sciadophylloides* family [5.88, 5.127]. High radiocaesium uptake by *E. sciadophylloides* may be due to the distribution of fine roots within the soil humus layers with high radiocaesium concentrations [5.128] and the activity of symbiotic soil microorganisms [5.129].

Temporal trends of *NC* values were wild plant specific. Although some decrease after radiocaesium deposition was observed for most species, such as in the leafstalk of *Petasites japonicus* and bamboo shoots. For *E. sciadophylloides* and *Aralia elata*, increases were reported in *NC*. Ref. [5.126] reported time dependent T_{ag} values for three wild herbaceous plants and concluded that the radiocaesium reduction in wild plants was best described by a double-exponential model (Table 5.11).

TABLE 5.11 EFFECTIVE HALF-LIVES (d) FOR ^{137}CS ACTIVITY CONCENTRATIONS IN THREE WILD PLANTS. [5.126]

Name	Species	Double-exponential model			Single-exponential model	
		R^2	$T_{eff,\ fast}$ (d)	$T_{eff,\ slow}$ (d)	R^2	T_{eff} (d)
Giant butterbur	*Petasites japonicus*	0.794	230	970	0.784	530
Knotweed	*Fallopia japonica*	0.997	140	1700	0.835	420
Mugwort	*Artemisia indica* var. *maximowiczii*	0.543	100	3800	0.809	530

FIG. 5.24. Photographs of edible wild plants. Left: a scape (flowering scape) of Petasites japonicas ("Fukinotou" in Japanese). Centre: a shoot of Aralia elata ("Taranome" in Japanese). Right: a shoot of Eleutherococcus sciadophylloides ("Koshiabura" in Japanese). (All photos: Yoshiyuki Kiyono)

5.5. TRANSFER TO GAME

The transfer of radiocaesium to meat from game after the FDNPP accident was relatively high compared with that to domestic animals. This observation is consistent with the reported data after the Chernobyl accident [5.130]. The consumption and sale of game animals was banned in a number of countries after the Chernobyl accident, and also partially implemented in Japan after the FDNPP accident, because some game meat exceeded the relevant limit for total radiocaesium.

Before the FDNPP accident, food with ^{137}Cs activity concentrations that exceeded 370 Bq/kg FM could not be imported into Japan. The provisional limit for radiocaesium in meat of farm animals was initially set to 500 Bq/kg FM. This limit took into account the timing of the next harvest and the availability of food for farm animals in the months after the FDNPP accident. From October 1, 2012, a lower standard limit of 100 Bq/kg FM was also applied to meat of farm animals.

5.5.1. T_{ag} values for game

The T_{ag} approach was commonly used to describe the transfer of radiocaesium to wild game in Japan. T_{ag} values measured after the FDNPP accident have been reported in Ref. [5.131] and

further data were collated by the MODARIA I Working Group 4[5]. The Ministry of Environment (MOE), Japan, which monitored radiocaesium activity concentrations in terrestrial wildlife, has also reported data for wild animals [5.132]. The MOE data include the radiocaesium activity concentration in soil (Bq/kg DM, 0–5 cm) collected near the site where the animal was captured, enabling the calculation of concentration ratios ($CR_{\text{meat-soil}}$) for some wild animal tissues. The reported T_{ag} and $CR_{\text{meat-soil}}$ values derived in Japan after the FDNPP accident are summarized below.

T_{ag} values were collated for three mammal species (Asian black bear, wild boar and sika deer) and three bird species (green pheasant, copper pheasant and duck). All are omnivorous species, for which plants are an important part of their diet, except for sika deer, which is an herbivorous species.

The T_{ag} data in Table 5.12 are based on values from a transfer factor study [5.131] and supplemented by more recently reported data [5.133] and [5.134]. In these three studies, T_{ag} values were derived using slightly different approaches as outlined below:

(1) Game meat data from food monitoring from May 8, 2011 to December 31, 2015 (websites of MHLW [5.135]; Fukushima Prefecture [5.136]; Tochigi Prefecture [5.137]) covering 5 prefectures were matched with the geometric means of the deposition density (Bq/m^2) for the corresponding places of capture [5.131]. Radiocaesium deposition values were derived from data collected by the Ministry of Education, Culture, Sports, Science and Technology (MEXT) on seven occasions between 2011–2014 with a sampling grid 5.5 × 4.7 km² in the Fukushima Prefecture and at municipality level in other prefectures. The number of soil sampling points in each area ranged from 2 sites in areas with low to 14 sites in areas with high radiocaesium deposition (MEXT website [5.138]).
(2) Radiocaesium activity concentrations in the meat of wild boar and Asian black bear were matched with the corresponding soil data (Bq/m^2) determined during the 5th Airborne Monitoring Survey (as of 31 October 2016) conducted in Eastern Japan by the Japan Atomic Energy Agency [5.139], [5.133]. Some of these data overlapped with those used by Ref. [5.131]. Using data from May 2011 to March 2016, Ref. [5.133] applied a generalized additive mixed model which showed consistently 6-fold higher mean ^{137}Cs activity concentrations in wild boar in winter (February and March) than in summer (July and August).
(3) Wild boar measurements were compared with the mean of three soil samples collected at the site of capture [5.134]. The ^{137}Cs deposition density data and ^{137}Cs concentrations in wild boar correlated well so the uncertainties of the T_{ag} value are lower than for the other two approaches above which used more aggregated deposition data from soil monitoring or airborne surveys.

Results from analyses of these three large datasets were reported as summarized values (collated in Table 5.12) so a dataset of individual values could not be compiled. The geometric means of T_{ag} (in m^2/kg throughout) ranged from 4.7×10^{-3}–8.1×10^{-3} for sika deer, 2.6×10^{-3}–6.8×10^{-3} for wild boar, and 3.0×10^{-3}–5.5×10^{-3} for Asian black bear. Geometric mean T_{ag} values observed for game birds after the FDNPP accident (Table 5.13) did not change from

[5] MODARIA I was the IAEA programme on Modelling and Data for Radiological Impact Assessment that ran from 2012–2015. Working Group 4 undertook tasks on the analysis of radioecological data in the IAEA Technical Report Series publications to identify key radionuclides and associated parameter values for human and wildlife exposure assessment.

those reported by Ref. [5.131] because radiocaesium concentration data in birds did not exceed the detection limits. The values range from 1.0×10^{-4}–8.9×10^{-4} for green pheasant (N = 86), 1.6×10^{-3}–4.8×10^{-3} for copper pheasant (N = 50), and 2.2×10^{-4}–8.7×10^{-4} for wild duck (N = 104).

TABLE 5.12 AGGREGATED TRANSFER FACTOR T_{AG} (M^2/KG FM) OF ^{137}CS IN THREE GAME ANIMALS

Year	N	T_{ag} (m^2/kg FM)					Reference
		AM	GM	GSD	Min	Max	
Sika deer (Cervus nippon)							
2011	47	1.5×10^{-2}	8.1×10^{-3}	2.6	1.3×10^{-3}	2.3×10^{-1}	MODARIA I WG4
2012	134	1.0×10^{-2}	5.9×10^{-3}	2.6	3.6×10^{-4}	1.4×10^{-1}	MODARIA I WG4
2013	150	9.2×10^{-3}	5.8×10^{-3}	2.5	9.5×10^{-4}	7.5×10^{-2}	MODARIA I WG4
2014	133	1.1×10^{-2}	5.9×10^{-3}	3.0	4.6×10^{-4}	1.2×10^{-1}	MODARIA I WG4
2015	111	8.1×10^{-3}	4.7×10^{-3}	2.9	5.2×10^{-4}	3.7×10^{-2}	MODARIA I WG4
Wild boar (*Sus scrofa*)							
2011	167	1.4×10^{-2}	6.8×10^{-3}	2.7	4.7×10^{4}	5.4×10^{-1}	MODARIA I WG4
2012	458	9.7×10^{-3}	4.4×10^{-3}	2.6	2.1×10^{-4}	1.2	MODARIA I WG4
2013	501	9.8×10^{-3}	4.3×10^{-3}	3.3	2.9×10^{-4}	1.5×10^{-1}	MODARIA I WG4
2014	546	4.3×10^{-3}	2.6×10^{-3}	2.6	4.7×10^{-5}	8.3×10^{-2}	MODARIA I WG4
2015	612	6.1×10^{-3}	3.1×10^{-3}	2.8	8.9×10^{-5}	2.9×10^{-1}	MODARIA I WG4
2011–2016	1031	—	3.2×10^{-3}	3.4	9.2×10^{-5}	9.1×10^{-1}	Nemoto et al. (2018) [5.133]
2015	72	1×10^{-3}	9×10^{-4}	3	8×10^{-5}	6×10^{-3}	Anderson et al. (2019) [5.134]
Asian black bear (*Ursus thibetanus*)							
2011	26	8.2×10^{-3}	5.5×10^{-3}	2.3	1.6×10^{-3}	4.7×10^{-2}	MODARIA I WG4
2012	174	6.0×10^{-3}	3.9×10^{-3}	2.4	3.2×10^{-4}	6.7×10^{-2}	MODARIA I WG4
2013	83	7.0×10^{-3}	4.8×10^{-3}	2.4	9.1×10^{-4}	4.2×10^{-2}	MODARIA I WG4
2014	205	5.0×10^{-3}	3.0×10^{-3}	2.6	3.4×10^{-4}	8.0×10^{-2}	MODARIA I WG4
2015	66	5.7×10^{-3}	4.4×10^{-3}	2.2	6.0×10^{-4}	1.9×10^{-2}	MODARIA I WG4
2011–2016	271	—	2.2×10^{-3}	2.3	2.2×10^{-4}	5.3×10^{-2}	Nemoto et al. (2018) [5.133]

The range and GM of T_{ag} values for the first five years after both the Chernobyl (IAEA TECDOC-1616) [5.48] and the FDNPP accidents are summarized in Table 5.14 for the same time period. The T_{ag} values were similar after both accidents for the game animal species (deer, wild boar and pheasant). The T_{ag} data for brown bear (*Ursus arctos*) in IAEA TECDOC-1616 [5.34] is one order of magnitude higher than that for the Asian black bear. Relatively high variation might be expected in bears as they are omnivores with a very variable diet. The Asian black bear is mostly herbivorous whereas brown bears eat more meat.

TABLE 5.13. AGGREGATED TRANSFER FACTOR T_{AG} (M^2/KG FM) OF ^{137}CS IN GAME BIRDS DERIVED USING DATA COLLATED BY MODARIA I WG4

Year	N	T_{ag} (m^2/kg FM)				
		AM	GM	GSD [a]	Min	Max
Green pheasant (*Phasianus versicolor*)						
2011	27	1.4×10^{-3}	9.1×10^{-4}	2.3	2.7×10^{-4}	7.7×10^{-3}
2012	37	1.2×10^{-3}	8.0×10^{-4}	2.6	5.9×10^{-5}	3.8×10^{-3}
2013	12	4.3×10^{-4}	2.7×10^{-4}	3.2	3.3×10^{-5}	1.2×10^{-3}
2014	6	4.4×10^{-4}	3.3×10^{-4}	2.4	1.2×10^{-4}	8.6×10^{-4}
2015	4	1.6×10^{-4}	1.0×10^{-4}	2.6	5.4×10^{-5}	4.2×10^{-4}
Copper pheasant (*Syrmaticus soemmerringii*)						
2011	10	3.3×10^{-3}	2.5×10^{-3}	2.2	7.3×10^{-4}	9.0×10^{-3}
2012	21	2.6×10^{-3}	1.6×10^{-3}	2.8	2.5×10^{-4}	1.3×10^{-2}
2013	8	8.3×10^{-3}	4.8×10^{-3}	3.0	8.3×10^{-4}	3.4×10^{-2}
2014	6	3.3×10^{-3}	1.7×10^{-3}	3.4	6.1×10^{-4}	1.1×10^{-2}
2015	5	2.2×10^{-3}	1.9×10^{-3}	1.7	1.3×10^{-3}	4.6×10^{-3}
Duck (*Anas zonorhyncha, and Anas platyrhynchos*)						
2011	16	1.1×10^{-3}	8.7×10^{-4}	2.0	1.9×10^{-4}	2.9×10^{-3}
2012	46	1.3×10^{-3}	6.1×10^{-4}	2.9	9.6×10^{-5}	2.3×10^{-2}
2013	18	8.2×10^{-4}	5.5×10^{-4}	2.7	6.2×10^{-5}	2.3×10^{-3}
2014	14	5.0×10^{-4}	2.8×10^{-4}	2.9	7.4×10^{-5}	1.8×10^{-3}
2015	10	3.3×10^{-4}	2.4×10^{-4}	2.6	3.3×10^{-5}	7.7×10^{-4}

[a] unitless

T_{ag} values for wild duck calculated for areas affected by the Chernobyl and FDNPP accidents also differed, however, due to the small number of data, the uncertainty around mean data measured for the FDNPP accident was large. Further data collection would be needed to clarify whether T_{ag} values for wild duck estimated for the FDNPP and the Chernobyl accident were significantly different.

5.5.2. $CR_{meat\text{-}soil}$ and $CR_{meat\text{-}water}$ data for game species

$CR_{meat\text{-}soil}$ values were determined as the ratio of the activity concentration in meat (Bq/kg FM) and the activity concentration in soil (Bq/kg DM). The small number of available $CR_{meat\text{-}soil}$ data for green pheasant (*Phasianus versicolor*) are shown in Table 5.15 using data from MOE [5.103]. The activity in soil represents the mean concentration in the layer 0–5 cm.

$CR_{meat\text{-}water}$ values were also determined as the ratio of the activity concentration in meat (Bq/kg FM) and the activity concentration in water (Bq/L). A $CR_{meat\text{-}water}$ for the edible part of the American bullfrog (*Lithobates catesbeianus*) was calculated using data available from Refs. [5.103, 5.139].

TABLE 5.14 COMPARISON OF T_{AG} VALUES FOR ^{137}CS OBTAINED FOR FIRST 5 YEARS AFTER BOTH THE FUKUSHIMA AND CHERNOBYL ACCIDENTS

Species or group	Fukushima accident (2011–2015)		Chernobyl accident (data extracted from Ref. [5.48])	
	N	Range of GM T_{ag} values (m^2/kg FM)	N	Range of GM T_{ag} values (m^2/kg FM)
Deer	575	4.7×10^{-3} – 8.1×10^{-3} (Sika)	>807	7.6×10^{-3} – 9.4×10^{-2} (Roe)
			— [a]	2.8×10^{-2} – 5.0×10^{-2} (Red)
Wild boar	2284	9×10^{-4}– 6.8×10^{-3}	>37	4.0×10^{-3} – 6.7×10^{-2}
Bear	554	3.0×10^{-3} – 5.5×10^{-3} (Asian black)	84	4.3×10^{-2} –7.1×10^{-2} (Brown)
Pheasant	86	1.0×10^{-4} – 9.1×10^{-4} (Green)	3	3.2×10^{-4}
	50	1.6×10^{-3} – 4.8×10^{-3} (Copper)		
Wild duck	104	2.4×10^{-4} – 8.7×10^{-4}	51	2.4×10^{-3} – 1.3×10^{-2}

[a] no data

5.5.3. Effective half-lives for game animals

To analyse the time dependence of ^{137}Cs concentrations in game, effective half-lives, T_{eff}, were calculated for ^{137}Cs in game animals by plotting the T_{ag} values against the sampling date (days after 11 March 2011). The resulting T_{eff} values are summarized in Table 5.16. Since no correlations were found between time and log-transformed T_{ag} for sika deer and copper pheasant ($p>0.05$), T_{eff} values are not given for these animal species. The ^{137}Cs activity concentrations in Asian black bear, wild boar and sika deer sampled in Japan have not markedly declined over the first few years after the FDNPP accident. In Germany (Bavaria), a T_{eco} of 10.5 a for wild boar (1986–1999) and no decrease in T_{eco} for wild boar was reported in most other countries. High variation in T_{eco} values of 5.8–128 years for roe deer (1986–2002) after the Chernobyl accident had also been reported [5.140]. A longer observation period after the FDNPP accident is needed to provide a more detailed comparison with the data observed in European countries.

The reasons for the observed differences between species have not been identified yet. The diet of wild boar given in the IAEA TECDOC 1616 [5.48] is also valid for wild boar in Japan, however, the effect of intake of wild mushrooms is not evident. Seasonal changes of the intake of components of the diet of wild animals would affect T_{eff}.

TABLE 5.15 CR VALUES FOR ^{137}CS FOR OTHER GAME SPECIES RELATIVE TO SOIL OR WATER

Species	Tissue	Year	N	CR				
				Median	GM	GSD [a]	Minimum	Maximum
				$CR_{meat\text{-}soil}$ (kg DM/kg FM)				
Green pheasant	Breast muscle	2014–2015	4	1.1×10^{-2}	1.0×10^{-2}	1.3	8.3×10^{-3}	1.4×10^{-2}
	Thigh muscle	2014–2015	2	1.0×10^{-2}	— [b]	—	8.9×10^{-3}	1.2×10^{-2}
	Gizzard	2014–2015	2	7.2×10^{-3}	—	—	6.7×10^{-3}	7.7×10^{-3}
	Liver	2014–2015	2	4.5×10^{-3}	—	—	3.5×10^{-3}	5.4×10^{-3}
				$CR_{meat\text{-}water}$ (L/kg FM)				
American bullfrog	Thigh muscle	2014–2017	2	3.0×10^{3}	—	—	1.7×10^{3}	4.3×10^{3}
	Whole body	—	4	8.6×10^{2}	7.9×10^{2}	1.6	5.6×10^{2}	1.6×10^{3}

[a] unitless
[b] no data

Table 5.16 EFFECTIVE HALF-LIFE T_{EFF} (year) of ^{137}CS FOR GAME ANIMALS

Animal name	Japan 2011–2015	European countries 1986–1999 [5.48] [5.141]
Sika deer	— [a]	Roe deer: 5.8–128 Red deer: 6.1–18
Wild boar	3.2	10.5
Asian black bear	5.6	—
Green pheasant	1.2	—
Wild duck	1.8	—

[a] no data

5.5.4. Radiocaesium distribution in wild boar and Asian black bear tissues

Radiocaesium activity concentrations in wild boar muscle were higher than those in 24 other tissues measured in four adults and three juvenile animals in November 2012 and December 2013 [5.142]. Radiocaesium activity concentrations in different muscles of wild boar decreased with increasing fat content [5.143], presumably due to the relatively low radiocaesium content of fat. A similar relationship was reported for beef [5.144].

Radiocaesium activity concentrations in each tissue relative to those in muscle have been collated for five tissues of wild boar and Asian black bear [5.109, 5.138]. The mean concentration ratio for each tissue of each animal was less than 1, and, except for liver, the concentration ratio for the different tissues was not significantly different between the two animal species (Fig. 5.25).

5.5.5. Transfer to game summary and data limitations

5.5.5.1. Summary

Seasonal variations were observed in wild boar from the Fukushima area [5.133]. The highest values were found in late winter rather than in autumn as observed after the Chernobyl accident.

Where activity concentrations in tissues were differentiated, radiocaesium activity concentrations were the highest in muscle.

5.5.5.2. Data limitations

There are relatively few studies in Japan which explore the relationship of radiocaesium activity concentrations and the differences in diet between various game species. Using soil concentrations averaged over a large area for estimating T_{ag} for game may introduce a source of uncertainty, especially if the range of the individual animal or local population is small. Furthermore, the soil contamination in the animals' habitats are often highly heterogenous. Further information on the seasonality of wild boar diet would help to understand the reason for seasonal change. Differences in diet between Asian black bears and European brown bears may explain the higher T_{ag} values found in Europe.

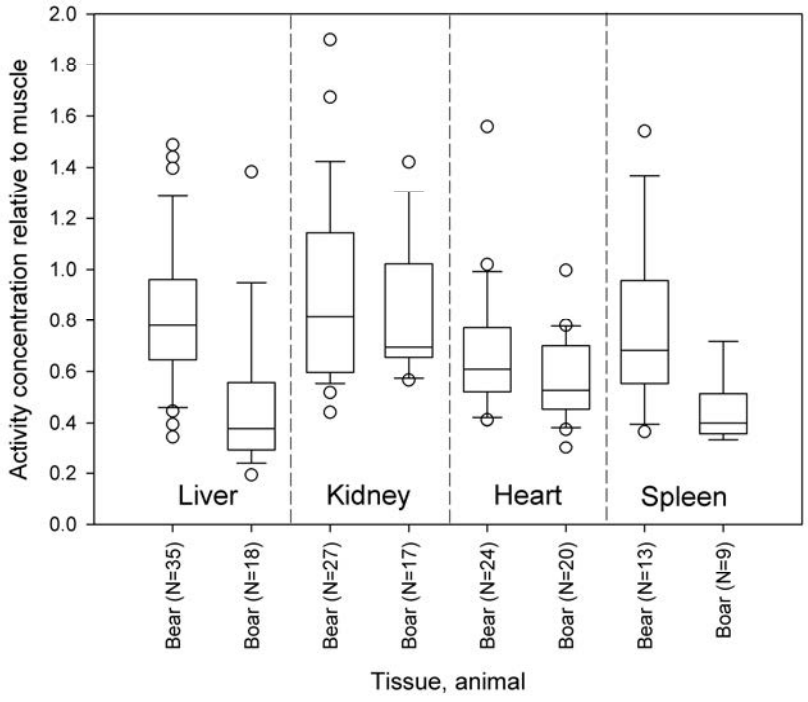

FIG. 5.25. Radiocaesium activity concentrations in liver, kidney, heart or spleen in comparison to that in muscle.

5.6. SUMMARY AND CONCLUSIONS

General features of forests in Fukushima

- Forests cover the largest part of the areas affected by the Fukushima Daiichi accident. The mountainous catchments covered by forest (about 70 % of the areas affected by the FDNPP accident) are much larger than the area covered by agricultural land (10 %);
- There is a diverse range of forest types in the affected area, including natural and planted forests of different ages;
- Forests in Japan are highly important in terms of various ecosystem services such as economic and recreational activities;
- The use of forest products in Japan is generally similar to that in other parts of the world. However, the widespread consumption of a wide range of wild edible plants differs from previous situations considered;
- Forests in Japan dominate the upstream catchments of rivers and play an important role in the conservation of water resources. In affected mountainous areas, forests are adjacent to agricultural areas with paddy fields that are often irrigated using stream waters discharged from forested catchments.

Key features of forest transfer processes observed after the Fukushima accident

- Total deposition data based on airborne surveys provided by the Japanese government were essential for the radioecological characterization of the different forest sites.
- The interception of radionuclides by deciduous trees, which had no leaves at the time of deposition in March 2011, was much less than that of coniferous trees (approximately < 30 % of the total inventory);
- Novel data were collected to study the dynamics of radiocaesium in forest ecosystems in the early and medium stages after the single deposition event. The measured decrease of radiocaesium in tree canopies during the early phase after the accident was well described by a two-component loss model;
- Throughfall and stemflow were major contributors to the radiocaesium flux from the canopy to forest floor during the first 200 days after deposition; thereafter, litterfall became the major process of radiocaesium loss from tree canopies;
- T_{ag} values for needles, bark, and branches were consistently highest in needles, followed by branches and bark whereas the lowest T_{ag} values were measured for wood. Similar patterns of radiocaesium transfer to forest trees were observed after the Chernobyl accident;
- T_{ag} values tended to decrease with time, however, the reduction of T_{ag} varied between different tree compartments. The decrease of T_{ag} values was more rapid for needles than for all other tree organs. However, the activity concentration in oak leaves remained almost unchanged over a period of 5 years;
- The T_{ag} values for oak (wood and leaves) were similar to those observed after the Chernobyl accident for similar times after the initial deposition. Conversely, T_{ag} values for wood of coniferous trees affected by the FDNPP accident were low compared with those reported after the Chernobyl accident. Continued monitoring is necessary to identify any systematic differences;
- Radiocaesium was distributed unevenly in wood (sapwood versus heartwood). The pattern and time dependency in contamination differed for the two types of wood and the tree species considered;

- The soil organic layer (including litter) and mineral soil layer became the largest radiocaesium reservoir within two years after deposition;
- The vertical distributions of radiocaesium in soils established in the first year changed slowly thereafter;
- The T_{eff} values for radiocaesium in cedar needles ranged from 0.76 to 2.7 year, with a mean value of 1.7 year. The T_{eff} values for cypress and pine needles were within this range. The T_{eff} values for branches varied from 1.0 year (in pine) to 3.8 year;
- The T_{eff} values in Fukushima Prefecture were generally shorter than those observed in affected areas around the Chernobyl NPP. However, the observation time differed; continued monitoring in Japan is needed to allow better comparisons;
- Radiocaesium activity concentrations in cedar pollen quickly reduced over a few years, in a similar time frame as that for leaves;
- The application of potassium fertilizer to forest soils substantially reduced (by 80–90%) radiocaesium transfer to trees, which is consistent with the data reported after the Chernobyl accident. Future research and cost-benefit assessment are essential before implementation of K treatment as a remediation option;
- Transfer of radiocaesium to a wide range of mushrooms and edible wild plants were extensively measured by governmental monitoring programmes. For seven common mushroom species, the *NC* values obtained after the FDNPP accident were comparable with the T_{ag} values reported after the Chernobyl accident;
- T_{ag} values for sika deer and wild boar in Japan were similar to those reported for other terrestrial game mammals in post-Chernobyl studies in TRS 472. T_{ag} values for Asian black bear were similar to those reported for sika deer and wild boar in Japan;
- The effective half-lives for radiocaesium in animals were generally shorter than those determined after the Chernobyl accident. However, T_{ag} values for Sika deer in Japan did not decline during the period 2011–2015.

Limitations, applicability to other forest biomes/situations, and future works

- In some studies, the number of sampling sites was limited which introduced uncertainties in the analysis of some data, such as the time dependency of ^{137}Cs in litterfall, throughfall, and stem flow;
- Supplementary environmental data (such as diet of game, distribution of roots in the forest soil, soil properties etc.) required for understanding accumulation of radiocaesium in forests were available only in a few studies. The lack of knowledge on the impact of such ecological data on radioecological processes constrains the evaluation of the data and long-term predictions of radiocaesium behaviour. For instance, sampled soil horizons have not been characterised for different properties that are known to affect radiocaesium mobility and distribution in soil profiles. The lack of such data limits the ability to predict the long-term dynamics of radiocaesium transfer to forest plants, mushrooms and game;
- The sampling of radiocaesium in the trunks of forest trees was mostly performed for sapwood and hardwood, which limits evaluation of whole wood contamination;
- Effective half-lives of radiocaesium in forest products (such as mushrooms, game and berries) measured after the Chernobyl accident were much longer than those for agricultural products. It is not clear whether such a difference also exists for Fukushima forests;
- The reasons of different time dependencies of radiocaesium activity concentrations in wood (e.g. slow increase for cedar vs rapid increase for oak), which is commercially the most important forest product, have not been well studied yet.

REFERENCES

[5.1] HASHIMOTO, S., UGAWA, S., NANKO, K., SHICHI, K., The total amounts of radioactively contaminated materials in forests in Fukushima, Japan., Sci. Rep. **2** (2012) 416.

[5.2] FUKUSHIMA PREFECTURE, AGRICULTURE, Forestry. and Fisheries Department, Statistics of Forest and Forestry in Fukushima Prefecture, (2017) 202 pp.

[5.3] NATIONAL LAND INFORMATION DIVISION, NATIONAL SPATIAL PLANNING AND REGIONAL POLICY BEREAU, M. of J., National Land Numerical Information Download Service, http://nlftp.mlit.go.jp/ksj-e/index.html.

[5.4] TAKAHASHI, M. et al., Carbon stock in litter, deadwood and soil in Japan's forest sector and its comparison with carbon stock in agricultural soils, Soil Sci. Plant Nutr. **56** 1 (2010) 19.

[5.5] FORESTRY AND FOREST PRODUCTS RESEARCH INSTITUTE, Atlas of Forest Soil Profiles in Japan. Vol. 2, (1981) 83 pp.

[5.6] MORISADA, K., ONO, K., KANOMATA, H., Organic carbon stock in forest soils in Japan, Geoderma **119** 1–2 (2004) 21.

[5.7] COPPIN, F. et al., Radiocaesium partitioning in Japanese cedar forests following the "early" phase of Fukushima fallout redistribution, Sci. Rep. **6** November (2016) 1.

[5.8] KATO, H. et al., Six-year monitoring study of radiocesium transfer in forest environments following the Fukushima nuclear power plant accident, J. Environ. Radioact. July (2018).

[5.9] IMAMURA, N. et al., Temporal changes in the radiocesium distribution in forests over the five years after the Fukushima Daiichi Nuclear Power Plant accident, Sci. Rep. **7** 1 (2017) 1.

[5.10] INTERNATIONAL ATOMIC ENERGY AGENCY, Environmental Consequences of the Chernobyl Accident and Their Remediation: Twenty Years of Experience, IAEA, Vienna (2006) 166 pp.

[5.11] ERTEL, J., VOIGT, G., PARETZKE, H.G., Weathering of $^{134/137}$Cs following leaf contamination of grass cultures in an outdoor experiment, Radiat. Environ. Biophys. **28** 4 (1989) 319.

[5.12] MADOZ-ESCANDE, C., GARCIA-SANCHEZ, L., BONHOMME, T., MORELLO, M., Influence of rainfall characteristics on elimination of aerosols of cesium, strontium, barium and tellurium deposited on grassland, J. Environ. Radioact. **84** 1 (2005) 1.

[5.13] KATO, H., ONDA, Y., HISADOME, K., LOFFREDO, N., KAWAMORI, A., Temporal changes in radiocesium deposition in various forest stands following the Fukushima Dai-ichi Nuclear Power Plant accident, J. Environ. Radioact. **166** (2017) 449.

[5.14] KATO, H., ONDA, Y., GOMI, T., Interception of the Fukushima reactor accident-derived ^{137}Cs, ^{134}Cs and ^{131}I by coniferous forest canopies, Geophys. Res. Lett. **39** 20 (2012) 1.

[5.15] ITOH, Y., IMAYA, A., KOBAYASHI, M., Initial radiocesium deposition on forest ecosystems surrounding the Tokyo metropolitan area due to the Fukushima Daiichi Nuclear Power Plant accident, Hydrol. Res. Lett. **9** 1 (2015) 1.

[5.16] NISHIKIORI, T. et al., Uptake and translocation of radiocesium in cedar leaves following the Fukushima nuclear accident, Sci. Total Environ. **502** (2015) 611.

[5.17] TIKHOMIROV, F.A., SHCHEGLOV, A.I., SIDOROV, V.P., Forests and forestry: radiation protection measures with special reference to the Chernobyl accident zone, Sci. Total Environ. **137** 1–3 (1993) 289.
[5.18] RONNEAU, C., CARA, J., APERS, D., The deposition of radionuclides from Chernobyl to a forest in Belgium, Atmos. Environ. **21** 6 (1987) 1467.
[5.19] BUNZL, K., SCHIMMACK, W., KREUTZER, K., SCHIERL, R., Interception and retention of Chernobyl-derived ^{134}Cs, ^{137}Cs and ^{106}Ru in a spruce stand, **78** (1989) 77.
[5.20] SCHIMMACK W, BUNZL K, KREUTZER K, RONDENKIRCHEN E, S.R., Influence of spruce (*Picea abies* L. karst) and beech (*Fagus sylvatica* L.) on the migration of radiocaesium in the soil (in German), Forstw Forschungen **39** (1991) 242.
[5.21] MELIN, J., WALLBERG, L., SUOMELA, J., Distribution and retention of cesium and strontium in Swedish boreal forest ecosystems, Sci. Total Environ. **157** (1994) 93.
[5.22] SOMBRÉ, L. et al., Long-term radiocesium behaviour in spruce and oak forests, Sci. Total Environ. **157** C (1994) 59.
[5.23] SOMBRE L, VANHOUCHE M, THIRY Y, RONNEAU C, LAMBOTTE JM, M.C., "Transfer of radiocesium in forest ecosystems resulting from a nuclear accident", Transfer of Radionuclides in Natural and Semi-Natural Environments (DESMET, G.G. et, Ed), Elsevier Applied Science (1990) 74–83.
[5.24] THIRY, Y., GARCIA-SANCHEZ, L., HURTEVENT, P., Experimental quantification of radiocesium recycling in a coniferous tree after aerial contamination: Field loss dynamics, translocation and final partitioning, J. Environ. Radioact. **161** (2016) 42.
[5.25] HISADOME, K., ONDA, Y., KAWAMORI, A., KATO, H., Migration of radiocesium with litterfall in hardwood-Japanese red pine mied forest and sugi plantation, J. Japanese For. Soc. **95** (2013) 267.
[5.26] TERAMAGE, M.T., ONDA, Y., KATO, H., GOMI, T., The role of litterfall in transferring Fukushima-derived radiocesium to a coniferous forest floor, Sci. Total Environ. **490** (2014) 435.
[5.27] LOFFREDO, N., ONDA, Y., KAWAMORI, A., KATO, H., Modeling of leachable ^{137}Cs in throughfall and stemflow for Japanese forest canopies after Fukushima Daiichi Nuclear Power Plant accident, Sci. Total Environ. **493** (2014) 701.
[5.28] ENDO, I. et al., Estimation of radioactive 137-cesium transportation by litterfall, stemflow and throughfall in the forests of Fukushima, J. Environ. Radioact. **149** (2015) 176.
[5.29] NIIZATO, T. et al., Input and output budgets of radiocesium concerning the forest floor in the mountain forest of Fukushima released from the TEPCO's Fukushima Dai-ichi nuclear power plant accident, J. Environ. Radioact. **161** (2015) 11.
[5.30] INTERNATIONAL ATOMIC ENERGY AGENCY, Technical Reports Series No. 472 Handbook of Parameter Values for the Prediction of Radionuclide Transfer in Terrestrial and Freshwater Environments, IAEA, Vienna (2010) 194 pp.
[5.31] FESENKO, S. V et al., Identification of processes governing long-term accumulation of ^{137}Cs by forest trees following the Chernobyl accident, Radiat. Environ. Biophys. **40** 2 (2001) 105.
[5.32] BELLI, M., SEMINAT Long Term Dynamics of Radionuclides in Semi-Natural Environments: Derivation of Parameters and Modelling, (2000) 105 pp.
[5.33] FOGH, C.L., ANDERSSON, K.G., Dynamic behaviour of ^{137}Cs contamination in trees of the Briansk region, Russia, Sci. Total Environ. **269** 1–3 (2001) 105.
[5.34] GOOR, F., THIRY, Y., Processes, dynamics and modelling of radiocaesium cycling in a chronosequence of Chernobyl-contaminated Scots pine (*Pinus sylvestri*s L.) plantations, Sci. Total Environ. **325** 1–3 (2004) 163.
[5.35] HUS, M., KOŠUTIĆ, K., LULIĆ, S., Radioactive contamination of wood and its products, J. Environ. Radioact. **55** 2 (2001) 179.

[5.36] IPATYEV, V., BULAVIK, I., BAGINSKY, V., GONCHARENKO, G., DVORNIK, A., Forest and Chernobyl: Forest ecosystems after the Chernobyl nuclear power plant accident: 1986-1994, J. Environ. Radioact. **42** 1 (1999) 9.
[5.37] KAUNISTO, S., ARO, L., RANTAVAARA, A., Effect of fertilisation on the potassium and radiocaesium distribution in tree stands (*Pinus sylvestris* L.) and peat on a pine mire, Environ. Pollut. **117** 1 (2002) 111.
[5.38] MCGEE, E.J. et al., Chernobyl fallout in a Swedish spruce forest ecosystem, J. Environ. Radioact. **48** 1 (2000) 59.
[5.39] PLAMBOECK, A.H., NYLÉN, T., GRIP, H., Uptake of cations under two different water regimes in a boreal Scots pine forest, Sci. Total Environ. **256** 2–3 (2000) 175.
[5.40] SHCHEGLOV, A., Biogeochemistry of Anthropogenic Radionuclides in Forest Ecosystems of Central Part of South-European Plain (in Russia), Moscow State University (1997).
[5.41] STRANDBERG, M., Radiocesium in a Danish pine forest ecosystem, Sci. Total Environ. **157** C (1994) 125.
[5.42] STREBL, F., GERZABEK, M.H., BOSSEW, P., KIENZL, K., Distribution of radiocaesium in an Austrian forest stand., Sci. Total Environ. **226** 1 (1999) 75.
[5.43] FORESTRY AGENCY, Demonstration Experiments for Revival of Forestry in Zones in Preparation for the Lifting of the Evacuation Order (Iitate Village) FY2016, 100 (2017).
[5.44] FORESTRY AGENCY, Demonstration Experiments for Revival of Forestry in Zones in Preparation for the Lifting of the Evacuation Order (Kuzuo Village) FY2015, Tokyo (2016).
[5.45] FORESTRY AGENCY, Demonstration Experiments for Revival of Forestry in Zones in Preparation for the Lifting of the Evacuation Order (Kawauchi Village) FY2015, Tokyo (2016) 105 pp.
[5.46] FORESTRY AGENCY, Monitoring of Environmental Radioactivity in National Forests in Zones in Preparation for the Lifting of the Evacuation Order FY 2015, (2016).
[5.47] FORESTRY AGENCY, Demonstration Experiments for Revival of Forestry in Zones in Preparation for the Lifting of the Evacuation Order (Kawauchi Village) FY2016, Tokyo (2017).
[5.48] INTERNATIONAL ATOMIC ENERGY AGENCY, Quantification of Radionuclide Transfer in Terrestrial and Freshwater Environments for Radiological Assessments; IAEA-TECDOC-1616, IAEA, Vienna (2009).
[5.49] KATO, H., ONDA, Y., GAO, X., SANADA, Y., SAITO, K., Reconstruction of a Fukushima accident-derived radiocesium fallout map for environmental transfer studies, J. Environ. Radioact. **210** (2019) 105996.
[5.50] TAKAHASHI, M., "To revive the forestry after the Fukushima nuclear accident", Forest Environment 2016, Forest culture association (2016).
[5.51] KOMATSU, M., HIRAI, K., NAGAKURA, J., NOGUCHI, K., Potassium fertilisation reduces radiocesium uptake by Japanese cypress seedlings grown in a stand contaminated by the Fukushima Daiichi nuclear accident, Sci. Rep. **7** 1 (2017) 1.
[5.52] KOBAYASHI, R., KOBAYASHI, N.I., TANOI, K., MASUMORI, M., TANGE, T., Potassium supply reduces cesium uptake in Konara oak not by an alteration of uptake mechanism, but by the uptake competition between the ions, J. Environ. Radioact. **208**–**209** March (2019) 106032.
[5.53] SPIRIDONOV, S.I., FESENKO, S. V., SANZHAROVA, N.I., Modelling of ^{137}Cs behaviour in the soil-plant system following the application of ameliorants, Radioprotection **40** (2005) S119.

[5.54] FORESTRY AGENCY, Validation and Development of Technology for Forest Operations FY2012, Tokyo (2013).
[5.55] FORESTRY AGENCY, Demonstration Experiments for Decontamination in Forest FY2012, 100 (2013).
[5.56] FORESTRY AGENCY, Demonstration Experiments for Decontamination in Forest FY2013, (2014).
[5.57] FORESTRY AGENCY, Validation and Development of Technology for Preventing Spread of Radionuclides in Forests FY2013, (2014).
[5.58] FORESTRY AGENCY, Demonstration Experiments for Decontamination in Forest in Preparation for the Lifting of the Evacuation Order (Minamisouma City) FY2014, (2015).
[5.59] FORESTRY AGENCY, Demonstration Experiments for Decontamination in Forest in Preparation for the Lifting of the Evacuation Order (Tamura Village Broadleaf) FY2014, 100 (2015).
[5.60] FORESTRY AGENCY, Demonstration Experiments for Decontamination in Forest in Preparation for the Lifting of the Evacuation Order (Minamisouma City) FY2015, (2016).
[5.61] FORESTRY AGENCY, Demonstration Experiments for Revival of Forestry in Zones in Preparation for the Lifting of the Evacuation Order (Tamura City) FY2015, Tokyo (2016).
[5.62] FORESTRY AGENCY, Monitoring of Environmental Radioactivity in National Forests in Zones in Preparation for the Lifting of the Evacuation Order FY 2016, (2017).
[5.63] FORESTRY AGENCY, Monitoring of Environmental Radioactivity in National Forests in Zones in Preparation for the Lifting of the Evacuation Order FY 2017, (2018).
[5.64] FORESTRY AGENCY, Demonstration Experiments for Revival of Forestry in Zones in Preparation for the Lifting of the Evacuation Order (Tamura Village Needleleaf) FY2016, 100 (2017).
[5.65] FUKUSHIMA PREFECTURE, Monitoring Survey Results of Environmental Radionuclides in Forests in Fukushima Prefecture, (2016).
[5.66] KURODA, K., KAGAWA, A., TONOSAKI, M., Radiocesium concentrations in the bark, sapwood and heartwood of three tree species collected at Fukushima forests half a year after the Fukushima Dai-ichi nuclear accident, J. Environ. Radioact. **122** (2013) 37.
[5.67] MASUMORI, M., NOGAWA, N., SUGIURA, S., TANGE, T., Radiocesium in Stem, Branch and Leaf of Cryptomeria japonica and Pinus densiflora Trees: Cases of Forests in Minamisoma in 2012 and 2013 (in Japanese with English abstract), Japanese J. For. Res. **97** (2013) 51.
[5.68] OGAWA, H. et al., Changes in the distribution of radiocesium in the wood of Japanese cedar trees from 2011 to 2013, J. Environ. Radioact. **161** (2016) 51.
[5.69] OHASHI, S., OKADA, N., TANAKA, A., NAKAI, W., TAKANO, S., Radial and vertical distributions of radiocesium in tree stems of *Pinus densiflora* and *Quercus serrata* 1.5 y after the Fukushima nuclear disaster, J. Environ. Radioact. **134** (2014) 54.
[5.70] OHASHI, S. et al., Temporal trends in ^{137}Cs concentrations in the bark, sapwood, heartwood, and whole wood of four tree species in Japanese forests from 2011 to 2016, J. Environ. Radioact. **178**–**179** (2017) 335.
[5.71] OHTE, N. et al., Monitaring of radiocesium dynamics in forests located at the north of Fukushima prefecture following the Fukushima accident (in Japanese), Gakujyutunodoukou **10** (2015) 16.

[5.72] PUMPANEN, J. et al., ^{137}Cs distributions in soil and trees in forest ecosystems after the radioactive fallout – Comparison study between southern Finland and Fukushima, Japan, J. Environ. Radioact. **161** (2016) 1.
[5.73] YOSCHENKO, V. et al., Radiocesium distribution and fluxes in the typical Cryptomeria japonica forest at the late stage after the accident at Fukushima Dai-Ichi Nuclear Power Plant, J. Environ. Radioact. **166** (2017) 45.
[5.74] YOSCHENKO, V. et al., Radioactive and stable cesium isotope distributions and dynamics in Japanese cedar forests, J. Environ. Radioact. **186** April 2017 (2018) 34.
[5.75] THIRY, Y., GOOR, F., RIESEN, T., The true distribution and accumulation of radiocaesium in stem of Scots pine (*Pinus sylvestris* L.), J. Environ. Radioact. **58** 2–3 (2002) 243.
[5.76] YOSHIDA, S., WATANABE, M., SUZUKI, A., Distribution of radiocesium and stable elements within a pine tree, Radiat. Prot. Dosimetry **146** 1–3 (2011) 326.
[5.77] KANASASHI, T., SUGIURA, Y., TAKENAKA, C., HIJII, N., UMEMURA, M., Radiocesium distribution in sugi (*Cryptomeria japonica*) in Eastern Japan: Translocation from needles to pollen, J. Environ. Radioact. **139** (2015) 398.
[5.78] AKAMA, A., KIYONO, Y., KANAZASHI, T., SHICHI, K., Survey of radioactive contamination of sugi (*Cryptomeria japonica* D. Don) shoots and male flowers in Fukushima prefecture, Japanese J. For. Environ. **55** 2 (2013) 105.
[5.79] FORESTRY AGENCY, Results of Measurements of Radiocesium Concentration in Forest Soils in Fukushima Prefecture, 100 (2012).
[5.80] FORESTRY AGENCY, Demonstration Experiments for Decontamination in Forest in Preparation for the Lifting of the Evacuation Order (Iitate Village) FY2014, Tokyo (2015).
[5.81] FORESTRY AGENCY, Demonstration Experiments for Revival of Forestry in Zones in Preparation for the Lifting of the Evacuation Order (Iitate Village) FY2015, 100 (2016).
[5.82] FORESTRY AGENCY, Demonstration Experiments for Revival of Forestry in Zones in Preparation for the Lifting of the Evacuation Order (Kuzuo Village) FY2016, Tokyo (2017).
[5.83] IMAMURA, N., LEVIA, D.F., TORIYAMA, J., KOBAYASHI, M., NANKO, K., Stemflow-induced spatial heterogeneity of radiocesium concentrations and stocks in the soil of a broadleaved deciduous forest, Sci. Total Environ. **599**–**600** (2017) 1013.
[5.84] SHOKO, I., HIDEKI, T., TATSUHIRO, N., SEIJI, H., Effect of mass of organic layers on variation in ^{137}Cs distribution in soil in different forest types after the Fukushima nuclear accident, J. For. Res. **23** 1 (2018) 28.
[5.85] KOARASHI, J. et al., Factors affecting vertical distribution of Fukushima accident-derived radiocesium in soil under different land-use conditions, Sci. Total Environ. **431** (2012) 392.
[5.86] KOARASHI, J., ATARASHI-ANDOH, M., MATSUNAGA, T., SANADA, Y., Forest type effects on the retention of radiocesium in organic layers of forest ecosystems affected by the Fukushima nuclear accident, Sci. Rep. **6** November (2016) 1.
[5.87] NAKANISHI, T., MATSUNAGA, T., KOARASHI, J., ATARASHI-ANDOH, M., ^{137}Cs vertical migration in a deciduous forest soil following the Fukushima Dai-ichi Nuclear Power Plant accident, J. Environ. Radioact. **128** (2014) 9.
[5.88] SUGIURA, Y., KANASASHI, T., OGATA, Y., OZAWA, H., TAKENAKA, C., Radiocesium accumulation properties of *Chengiopanax sciadophylloides*, J. Environ. Radioact. **151** (2016) 250.

[5.89] TAKADA, M., YAMADA, T., TAKAHARA, T., OKUDA, T., Spatial variation in the ^{137}Cs inventory in soils in a mixed deciduous forest in Fukushima, Japan, J. Environ. Radioact. **161** (2016) 35.
[5.90] TAKAHASHI, J., TAMURA, K., SUDA, T., MATSUMURA, R., ONDA, Y., Vertical distribution and temporal changes of ^{137} Cs in soil profiles under various land uses after the Fukushima Dai-ichi Nuclear Power Plant accident, J. Environ. Radioact. **139** (2015) 351.
[5.91] FESENKO, S. V et al., ^{137}Cs availability for soil to understory transfer in different types of forest ecosystems., Sci. Total Environ. **269** 1–3 (2001) 87.
[5.92] OTA, M., NAGAI, H., KOARASHI, J., Modeling dynamics of ^{137}Cs in forest surface environments: Application to a contaminated forest site near Fukushima and assessment of potential impacts of soil organic matter interactions, Sci. Total Environ. **551**–**552** (2016) 590.
[5.93] MUTO, K., ATARASHI-ANDOH, M., MATSUNAGA, T., KOARASHI, J., Characterizing vertical migration of ^{137}Cs in organic layer and mineral soil in Japanese forests: Four-year observation and model analysis, J. Environ. Radioact. **208**–**209** February (2019) 106040.
[5.94] RAMZAEV, V., BARKOVSKY, A., Vertical distribution of ^{137}Cs in grassland soils disturbed by moles (*Talpa europaea L.*), J. Environ. Radioact. **184**–**185** September 2017 (2018) 101.
[5.95] ARAPIS, G. et al., Effective migration velocity of ^{137}Cs and ^{90}Sr as a function of the type of soils in Belarus, J. Environ. Radioact. **34** 2 (1997) 171.
[5.96] KANG, S. et al., Interpreting the deposition and vertical migration characteristics of ^{137}Cs in forest soil after the Fukushima Dai-ichi Nuclear Power Plant accident, Environ. Monit. Assess. **189** 8 (2017).
[5.97] FORSBERG, S., ROSÉN, K., FERNANDEZ, V., JUHAN, H., Migration of ^{137}Cs and ^{90}Sr in undisturbed soil profiles under controlled and close-to-real conditions, J. Environ. Radioact. **50** 3 (2000) 235.
[5.98] FUJII, K. et al., Effects of radiocesium fixation potentials on ^{137}Cs retention in volcanic soil profiles of Fukushima forests, J. Environ. Radioact. **198** October 2018 (2019) 126.
[5.99] TAKAHASHI, J., ONDA, Y., HIHARA, D., TAMURA, K., Six-year monitoring of the vertical distribution of radiocesium in three forest soils after the Fukushima Dai-ichi Nuclear Power Plant accident, J. Environ. Radioact. **192** May (2018) 172.
[5.100] TIKHOMIROV, F.A., SHCHEGLOV, A.I., Main investigation results on the forest radioecology in the Kyshtym and Chernobyl accident zones, Sci. Total Environ. **157** (1994) 45.
[5.101] YOSHIHARA, T., MATSUMURA, H., HASHIDA, S. nosuke, NAKAYA, K., Radiocesium contamination in living and dead foliar parts of Japanese cedar during 2011–2015, J. Environ. Radioact. **164** (2016) 291.
[5.102] INTERNATIONAL ATOMIC ENERGY AGENCY, Modelling the Migration and Accumulation of Radionuclides in Forest Ecosystems, Report of the Forest Working Group of the Biosphere Modelling and Assessment (BIOMASS) Programme, Theme 3, IAEA, Vienna (2002) 127 pp.
[5.103] MINISTRY OF AGRICULTURE, F. and F., Trends in Supply and Demand of Mushrooms and Timber, http://www.maff.go.jp/j/tokei/sihyo/data/25.html.
[5.104] NATIONAL INSTITUTE OF HEALTH AND NUTRITION, Nutritional Intake Status Survey, http://www.nibiohn.go.jp/eiken/kenkounippon21/eiyouchousa/koumoku_syokuhin_chousa.html.
[5.105] MINISTRY OF AGRICULTURE, F. and F., Production Survey of Special Forestry Products, http://www.maff.go.jp/j/tokei/kouhyou/tokuyo_rinsan/.

[5.106] KAWARASAKI, S.H., SUGIMURA, K., Estimation of Frequency and Locality of Collection of Wild Mushroom and Wild Vegetables by Internet Search, J. Japanese For. Soc. **94** 2 (2012) 95.
[5.107] MATSUURA, T., HAYASHI, M., SUGIMURA, K., TANAKA, N., MIYAMOTO, A., Ecosystem services valuation of harvesting edible wild plants/mushrooms -A case study in Tadami Town, Fukushima prefecture-, Japanese J. For. Plan. **47** 2 (2013) 55.
[5.108] FORESTRY AGENCY, Shipping Restriction of Mushrooms and Wild Edible Plants.
[5.109] CALMON, P., THIRY, Y., ZIBOLD, G., RANTAVAARA, A., FESENKO, S., Transfer parameter values in temperate forest ecosystems: A review, J. Environ. Radioact. **100** 9 (2009) 757.
[5.110] NAKAI, W., OKADA, N., OHASHI, S., TANAKA, A., Evaluation of ^{137}Cs accumulation by mushrooms and trees based on the aggregated transfer factor, J. Radioanal. Nucl. Chem. **303** 3 (2015) 2379.
[5.111] IRISAWA, A., Research of Uptake Mechanisms of Radioactive Cesium by Mushroom and Its Behavior in Envoronment (in Japanese), Tohoku University (2016) 131 pp.
[5.112] YOSHIDA, S., MURAMATSU, Y., Concentrations of radiocesium and potassium in Japanese mushrooms, Environ. Sci. **7** 1 (1994) 63.
[5.113] YOSHIDA, S., MURAMATSU, Y., Accumulation of radiocesium in basidiomycetes collected from Japanese forests, Sci. Total Environ. **157** 1–3 (1994) 197.
[5.114] YAMADA, T. et al., Radiocaesium accumulation in wild mushrooms from low-level contaminated area due to the Fukushima Daiichi Nuclear Power Plant accident -a case study in the University of Tokyo Forests-, Radioisotopes **62** 3 (2013) 141.
[5.115] KUWAHARA, C. et al., Accumulation of radiocesium in wild mushrooms collected from a Japanese forest and cesium uptake by microorganisms isolated from the mushroom-growing soils, Sci. Total Environ. **345** 1–3 (2005) 165.
[5.116] NAKASHIMA, K. et al., Radiocesium concentrations in wild mushrooms collected in Kawauchi Village after the accident at the Fukushima Daiichi Nuclear Power Plant, PeerJ **3** (2015) e1427.
[5.117] KAWAI, H. et al., Mineral contents in edible mushrooms., Nippon Shokuhin Kogyo Gakkaishi **33** 4 (1986) 250.
[5.118] SAWADA, M., Studies on chemical components of wild mushrooms and toadstools in Japan., Bull. Univ. Tokyo For. **59** (1965) 33.
[5.119] YOSHIDA, H., Hanabiratake mushroom [*Sparassis crispa* (Wulf.: Fr.)] chemical composition cultivated on sawdust substrate beds, Mushroom Sci. Biotechnol. **12** 4 (2004) 157.
[5.120] MURAMATSU, Y., YOSHIDA, S., SUMIYA, M., Concentrations of radiocesium and potassium in basidiomycetes collected in Japan, Sci. Total Environ. **105** C (1991) 29.
[5.121] FORESTRY AND FOREST PRODUCTS RESEARCH INSTITUTE, Report of Stable Supply Projects of Safe “Mushroom Logs”, (2012) 36 pp.
[5.122] TAGAMI, K., UCHIDA, S., ISHII, N., Effects of indoor and outdoor cultivation conditions on ^{137}Cs concentrations in cultivated mushrooms produced after the Fukushima Daiichi Nuclear Power Plant accident, J. Sci. Food Agric. **97** 2 (2017) 600.
[5.123] AKAMA, A., KIYONO, Y., Radioactive Cesium Contamination of *Eleutherococcus Sciadophylloides* - Comparisons between the Regions of Different Contamination Level and the Seasons - (In Japanese with English abstract), Kanto J. For. Res. **66** 2 (2015) 255.
[5.124] KIYONO, Y., AKAMA, A., IWAYA, M., YOSHIDA, Y., The Transfer of Radiocesium Released in the 2011 Fukushima Daiichi Nuclear Power Station Accident to Petioles of Wild Butterbur (*Petasites Japonicus*) (in Japanese with English abstract), Bull. For. For. Prod. Res. Inst. **17** 3 (2018) 249.

[5.125] KIYONO, Y. et al., The Transfer of Radiocesium Released in the 2011 Fukushima Daiichi Nuclear Power Station Accident to Leaves of Wild Osmunda Japonica, an Edible Fern (in Japanese with English abstract), Bull. For. For. Prod. Res. Inst. **17** 3 (2018) 217.
[5.126] TAGAMI, K., UCHIDA, S., Changes of effective half-lives of ^{137}Cs in three herbaceous plants and bioavailable ^{137}Cs fraction in soil after the Fukushima nuclear accident, Appl. Geochemistry **85** (2017) 162.
[5.127] KENZO, T. et al., Relationship between leaf radiocesium and potassium concentrations in various tree species after the accident of Fukushima Dai-ichi Nuclear Power Plant, Kanto J. For. Res. **69** 1 (2018) 39.
[5.128] MURAMATSU, Y. et al., Transfer of radiocaesium into forest product, J. Sci. soil manure **85** 2 (2014) 117.
[5.129] YAMAJI, K. et al., Root endophytic bacteria of a ^{137}Cs and Mn accumulator plant, *Eleutherococcus sciadophylloides*, increase ^{137}Cs and Mn desorption in the soil, J. Environ. Radioact. **153** (2016) 112.
[5.130] ALEXAKHIN, R.M., SANZHAROVA, N.I., FESENKO, S. V., SPIRIDONOV, S.I., PANOV, A. V., Chernobyl radionuclide distribution, migration, and environmental and agricultural impacts, Health Phys. **93** 5 (2007) 418.
[5.131] TAGAMI, K., HOWARD, B.J., UCHIDA, S., The Time-Dependent Transfer Factor of Radiocesium from Soil to Game Animals in Japan after the Fukushima Dai-ichi Nuclear Accident, Environ. Sci. Technol. **50** 17 (2016) 9424.
[5.132] MINISTRY OF ENVIRONMENT, Monitoring Results for Wildlife, http://www.env.go.jp/jishin/monitoring/results_r-wl.html (in Japanese).
[5.133] NEMOTO, Y., SAITO, R., OOMACHI, H., Seasonal variation of Cesium-137 concentration in Asian black bear (*Ursus thibetanus*) and wild boar (*Sus scrofa*) in Fukushima Prefecture, Japan, PLoS One **13** 7 (2018) e0200797.
[5.134] ANDERSON, D. et al., A comparison of methods to derive aggregated transfer factors using wild boar data from the Fukushima Prefecture, J. Environ. Radioact. **197** (2019) 101.
[5.135] MINISTRY OF HEALTH LABOR AND WELFARE, Levels of Radioactive Contaminants in Foods Tested in Respective Prefectures, http://www.mhlw.go.jp/english/topics/2011eq/index_food_press.html.
[5.136] FUKUSHIMA PREFECTURE, Monitoring of Wild Animals (in Japanese), http://www.pref.fukushima.lg.jp/site/portal/wildlife-radiationmonitoring1.html.
[5.137] TOCHIGI PREFECTURE, Wild Boar Monitoring (in Japanese), http://www.pref.tochigi.lg.jp/g02/houdou/h23nakagawainoshishi.html.
[5.138] MINISTRY OF EDUCATION, CULTURE, SPORTS, S. and T., Extension Site of Distribution Map of Radiation Dose, https://ramap.jmc.or.jp/map/eng/.
[5.139] JAPAN ATOMIC ENERGY AGENCY, Results of Deposition of Radioactive Cesium of the Fifth Airborne Monitoring Survey and Airborne Monitoring Survey Outside 80 km from the Fukushima Dai-Ichi NPP, http://emdb.jaea.go.jp/emdb/en/portals/b1020201/.
[5.140] MOKUDAI, T. et al., Radiocesium contamination of wild animals in Gunma Prefecture based on samples from October, 2010 to August, 2014, Bull. Gunma Museum Nat. Hist. **20** (2016) 169.
[5.141] PRÖHL, G. et al., Ecological half-lives of ^{90}Sr and ^{137}Cs in terrestrial and aquatic ecosystems, J. Environ. Radioact. **91** 1–2 (2006) 41.
[5.142] TANOI, K. et al., Investigation of radiocesium distribution in organs of wild boar grown in Iitate, Fukushima after the Fukushima Daiichi nuclear power plant accident, J. Radioanal. Nucl. Chem. **307** 1 (2016) 741.

[5.143] HAYASHI, C. et al., Surveillance of Radioactive Cesium in Meats of Wild Animals Caught in Chiba Prefecture, Food Hyg. Saf. Sci. (Shokuhin Eiseigaku Zasshi) **57** 2 (2016) 32.
[5.144] NABESHI, H., KIKUCHI, H., TSUTSUMI, T., HACHISUKA, A., MATSUDA, R., Concentrations of Radioactive Cesium in Different Cuts of Beef, Food Hyg. Saf. Sci. (Shokuhin Eiseigaku Zasshi) **54** 6 (2013) 415.
[5.145] KOMATSU, M. et al., Characteristics of initial deposition and behavior of radiocesium in forest ecosystems of different locations and species affected by the Fukushima Daiichi Nuclear Power Plant accident, J. Environ. Radioact. **161** (2016) 2.
[5.146] FUKUSHIMA PREFECTURE, Monitoring Restlts of Radionuclides in Forests, https://www.pref.fukushima.lg.jp/sec/36055a/shinrinhousyasei2.html.
[5.147] MATSUNAGA, T. et al., Comparison of the vertical distributions of Fukushima nuclear accident radiocesium in soil before and after the first rainy season, with physicochemical and mineralogical interpretations, Sci. Total Environ. **447** (2013) 301.
[5.148] TSUKADA, H., SHIBATA, H., SUGIYAMA, H., Transfer of radiocaesium and stable caesium from substrata to mushrooms in a pine forest in Rokkasho-mura, Aomori, Japan, J. Environ. Radioact. **39** 2 (1998) 149.
[5.149] YOSHIDA, S., MURAMATSU, Y., OGAWA, M., Radiocesium concentrations in mushrooms collected in Japan, J. Environ. Radioact. **22** 2 (1994) 141.
[5.150] KURASAWA, S., SUGAWARA, T., HAYASHII, J., Proximate and dietary fibre analysis of mushrooms, Nippon Shokuhin Kogyo Gakkaishi **29** 7 (1982) 400.
[5.151] ITABASHI, M., TAKAMURA, N., Nutritional compositions of the leaves of Fuki (Petasites japonicus Miq.), Tsuwabuki (Ligularia tussilaginea Makino), Gobo (Arctium lappa L.) and Gishigishi (Rumex japonicus Houttuyn), Nippon Shokuhin Kogyo Gakkaishi **32** 2 (1985) 120.
[5.152] SAITO, Y., IZUMI, M., Amount of mineral elements in edible wild plants, J. Home Econ. Japan **36** 5 (1985) 351.
[5.153] SAITO, Y., IZUMI, M., OHSAWA, A., Amounts of Dietary Fiber and the Other General Components in Edible Portion of Wild Plants, Eiyo To Shokuryo **34** 5 (1981) 468.
[5.154] ISAKARI, K., Calcium Contents in Certain Foods (Part 9), J. Home Econ. Japan **21** 5 (1970) 301.
[5.155] ONO, M., HAYASHI, M., ABE, M., The Composition of Some Wild Plants, J. Home Econ. Japan **28** 1 (1977) 76.
[5.156] SHISHIDO, I., KODAMA, E., Nutritional Ingredients of Wild Vegetables of the Akita District (1), *Report of the Akita Prefecture Institute of Public Health*, Vol. 10 (1966) pp. 55–60.
[5.157] SHISHIDO, I., KODAMA, E., Nutritional Ingredients of Wild Vegetables of the Akita District (3), *Report of the Akita Prefecture Institute of Public Health*, Vol. 12 (1968) pp. 202–206.
[5.158] SHISHIDO, I., KODAMA, E., Nutritional Ingredients of Wild Vegetables of the Akita District (4), *Report of the Akita Prefecture Institute of Public Health*, Vol. 13 (1969) pp. 239–243.
[5.159] SHISHIDO, I., KODAMA, E., Nutritional Ingredients of Wild Vegetables of the Akita District (5), *Report of the Akita Prefecture Institute of Public Health*, Vol. 14 (1970) pp. 173–177.
[5.160] SHISHIDO, I., KODAMA, E., Nutritional Ingredients of Wild Vegetables of the Akita District (6), *Report of the Akita Prefecture Institute of Public Health*, Vol. 15 (1971) pp. 297–302.

6. CATCHMENTS AND RIVERS

YUICHI ONDA
University of Tsukuba, Tsukuba, JAPAN

SEIJI HAYASHI
National Institute for Environmental Studies, Tsukuba, JAPAN

SEIYA NAGAO
Kanazawa University, Kakumamachi, JAPAN

ISHII YUMIKO, HIDEKI TSUJI
National Institute for Environmental Studies, Tsukuba, JAPAN

KEISUKE TANIGUCHI
Fukushima Prefectural Centre for Environmental Creation, JAPAN

KAZUYA NISINA
National Institute for Environmental Studies, Tsukuba, JAPAN

KYUMA SUZUKI, SHUN WATANABE
Gunma Prefectural Fisheries Experiment Station, Maebashi, JAPAN

GERHARD PRÖHL
Consultant, GERMANY

PATRIC BOYER, GARCIA-SANCHEZ LAURENT
IRSN, FRANCE

6.1.INTRODUCTION

Radionuclides released to the atmosphere can be deposited onto catchments and water bodies. After the FDNPP accident, subsequent redistribution of radionuclides, mostly radiocaesium, occurred via (i) water run-off in streams and rivers (commonly termed washoff) and (ii) erosion of material from catchments, into water bodies. These processes can affect the extent to which radiocaesium is transferred into edible aquatic organisms from water and aquatic food.

After the FDNPP accident, the combination of high rainfall and intensive agricultural land-use contributed to a highly dynamic transfer of radiocaesium from catchments to rivers, lakes and irrigation ponds in Fukushima Prefecture and other neighbouring Prefectures. Various factors affecting the transfer of radiocaesium from catchments to rivers and from freshwater to aquatic organisms are discussed below.

Studies on the loss of radiocaesium from catchment areas and the impact on radiocaesium activity concentrations in surface waters have been studied in Japan over a long period of time prior to the FDNPP accident (e.g. [6.1]). An assessment of the extent of radiocaesium run-off allows an estimate of the radiocaesium flux from the catchment through rivers to the ocean, which provides essential information on the long-term fate of deposited radiocaesium after the FDNPP accident. The identification of time trends in freshwaters and freshwater organisms

following deposition on catchments and surface waters allows an assessment of the persistence of environmental contamination.

Many studies have reported on the dependence of radiocaesium run-off on land use before and after the FDNPS accident. The parameters obtained for different land uses constitute a key input that is essential to modelling the run-off of radiocaesium from catchments and the transport of radiocaesium in freshwater systems.

The text below addresses the following topics:

- Radiocaesium run-off in catchments;
- Estimation of the freshwater distribution coefficient, K_d;
- Uptake of radiocaesium by freshwater fish in rivers and streams;
- Time dependency of radiocaesium uptake and retention in freshwater lake fish.

The transfer of radiocaesium from irrigation ponds to rice paddies and the transport of radiocaesium from rice paddies is discussed in chapter 4.3.

6.2. RADIOCAESIUM RUN-OFF IN CATCHMENTS

6.2.1. Radiocaesium run-off before the FDNPP accident

6.2.1.1. Measurement of ^{137}Cs run-off on erosion plots

In Japan, there were few data reported on erosion of radionuclides from catchments with forest hill slopes and agricultural land before the FDNPP accident. Some studies were carried out to investigate soil erosion and run-off of ^{137}Cs in forests in mountainous areas of Mie and Kochi Prefectures. These studies were carried out on slopes ranging from 32 to 43 degrees [6.2, 6.3]. The aim of these pre-accident studies was to investigate the interaction of land use and soil erosion and to quantify ^{137}Cs activity concentrations originating from nuclear weapons' testing in eroded soil.

During these studies, surveys were mainly conducted using small plots with a horizontal projection length of 1.5–2 m. The characteristics of the experimental plots in Kochi and Mie Prefectures, with ^{137}Cs inventories of 2500 and 3070 Bq m^{-2} respectively, are shown in Table 6.1. Such values are typical for heavy rainfall areas in the northern hemisphere which received relatively higher amounts of global fallout in the atomic weapons testing era than areas with low precipitation.

The ^{137}Cs activity concentration in eroded soil depends on the deposition density on the original site where deposition occurred. The erosion of radionuclides is quantified by the entrainment coefficient, S_c, defined as the ratio of the radionuclide activity concentration in soil and the radionuclide deposition according to:

$$S_c = \frac{C}{A} \tag{6.1}$$

where S_c is the entrainment coefficient (m²/kg DM) at the sampling time, C is activity concentration of ^{137}Cs (Bq/kg DM) in the eroded soil and A is the initial deposition density measured at the reference site (Bq/m^2).

TABLE 6.1. CHARACTERISTICS AND RESULTS FROM RUN-OFF STUDIES FOR GLOBAL FALLOUT ^{137}CS DURING AUGUST 2004–AUGUST 2006

Vegetation cover, Sampling point	Observation period (year)	^{137}Cs-deposition density (Bq/m^2)	Slope steepness (degrees)	Slope length (m)	^{137}Cs-activity in eroded soil (Bq/kg DM)	Entrainment coefficient S_c (m^2/kg)	Mass of eroded soil per year [a)] (kg m^{-2} year^{-1})	Annual fraction of ^{137}Cs released [a] (%/year)	References
Broad-leaved forest	2.0	3070	37–39	1.8–2.0	38	0.012	0.27–0.70	0.33–0.86	[6.3, 6.4]
Japanese cypress	2.0	3070	38	1.7	32	0.010	0.94	0.97	[6.3]
Japanese cedar	2.0	3070	38	1.8	33	0.011	0.097	0.10	[6.4]
Broad-leaved forest	2.1	2500	43	1.5	48	0.019	0.004	0.008	[6.2, 6.5–6.7]
Japanese cypress (low management intensity)	1.3	2500	32	1.7	35	0.014	1.63	2.28	[6.2, 6.5–6.7]
Thinned Japanese cypress	3.4	2500	37	1.6	45	0.018	0.003	0.005	[6.2, 6.5–6.7]

[a] Average during the period from August 2014 to August 2016

6.2.1.2. Radiocaesium run-off rate from erosion plots

The entrainment coefficient S_c was calculated for each plot (Table 6.1); it varied in the range of 0.01 to 0.02 m²/kg DM. The annual loss of ^{137}Cs due to run-off differed depending on the characteristics of the understory vegetation and litter cover. It was substantially higher in small cypress forests (0.4–1.1% per year), which have little vegetation on the forest floor, than in well-managed cypress forests where ^{137}Cs losses of 0.01–0.02% per year were reported. These data were obtained on small plots with a plot length of 2 m. However, in most forests, large fractions of water and eroded material will infiltrate into the soil of the catchment area reducing the potential for erosion of radiocaesium. Thus, data for more realistic longer slopes estimated that losses of ^{137}Cs due to surface run-off was almost an order of magnitude lower [6.5] than that from the short slopes. Consequently, the run-off to streams would be expected to be an order of magnitude lower for longer slopes.

Surface run-off of rainwater and erosion of solid material was potentially high due to the high annual precipitation and the predominantly steep slopes in the studied areas. However, the data in Table 6.1 indicate that the annual run-off of ^{137}Cs was relatively low, even in the poorly managed Japanese Cypress forest. Run-off rates of ^{137}Cs in other natural or well-managed forests in both the Kochi and Mie site, were typically below 0.1% per year [6.3, 6.6]. Although downward migration of caesium in soil was slow, 40 years after the peak of nuclear weapons' testing ^{137}Cs had migrated into deeper soil layers, which are not usually subject to erosion [6.6]

An example of the headwater-scale (hillslope and stream) ^{137}Cs balance before the FDNPP accident in a cypress forest with little understorey vegetation is shown in Fig. 6.1. In this case, headwater catchment outlet quantification is only 0.013% of the ^{137}Cs-inventory lost per year due to run-off of sediments. This means that, for aged deposits, the decline of the ^{137}Cs-inventory due to run-off was negligible and the reduction in ^{137}Cs-inventory was determined by radioactive decay (2.3%/year for ^{137}Cs).

6.2.2. Run-off of radiocaesium after the FDNPP accident

6.2.2.1. Radiocaesium run-off from erosion plots

Radiocaesium run-off in field experiments on standard soil erosion plots (22.1 m × 5 m) was investigated in Kawamata, Fukushima Prefecture [6.8]. The plots, shown in Fig. 6.2., were set up on two farmland areas (farmland A1 and B1) that had not been cultivated since the end of November 2010, two grasslands areas (grassland A and B) and a forest floor in a young Japanese cedar forest. Soil tillage was performed in September 2012 on farmland (A2 and B2). All plots were located within 6 km of each other.

Experiments were also carried out on a hillslope plot in a forested area to study the run-off and mass balance of a forest soil [6.9, 6.10]. The slopes of the plots for farmland and grassland range from 4 to 10 degrees, whereas the forest plots were much steeper with slopes from 13 to 39 degrees. The data for all plots are summarized in Table 6.2.

For forests, the values for S_c ranged from 0.045 to 0.14 m²/kg DM which are higher than those determined before the FDNPP accident [6.3]. The data reflect the different depth distributions of ^{137}Cs from weapons' tests and the FDNPP accident in soil. The deposits from the FDNPP accident have not yet migrated as deep as those from weapons' fallout. Therefore, it is expected that the depth distribution of ^{137}Cs from the FDNPP accident [6.11] will gradually become more similar to that of ^{137}Cs from weapons' fallout [6.12].

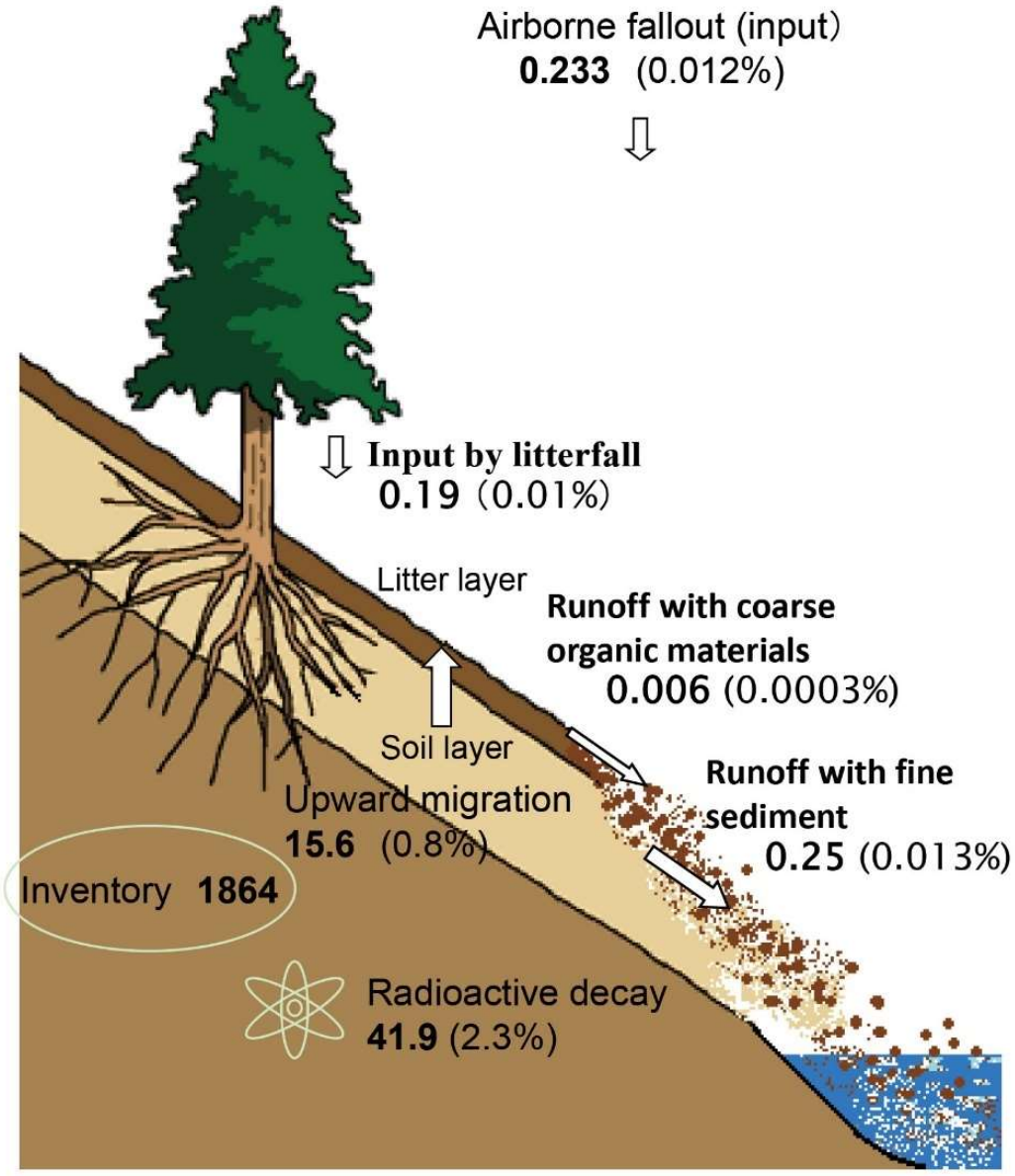

FIG. 6.1. ^{137}Cs cycling in Japanese cypress plantation catchment (Bq m^{-2} year^{-1}) and the contributions of individual components to the current mean ^{137}Cs inventory (%) (adapted from [6.2] with permission, courtesy of Elsevier)

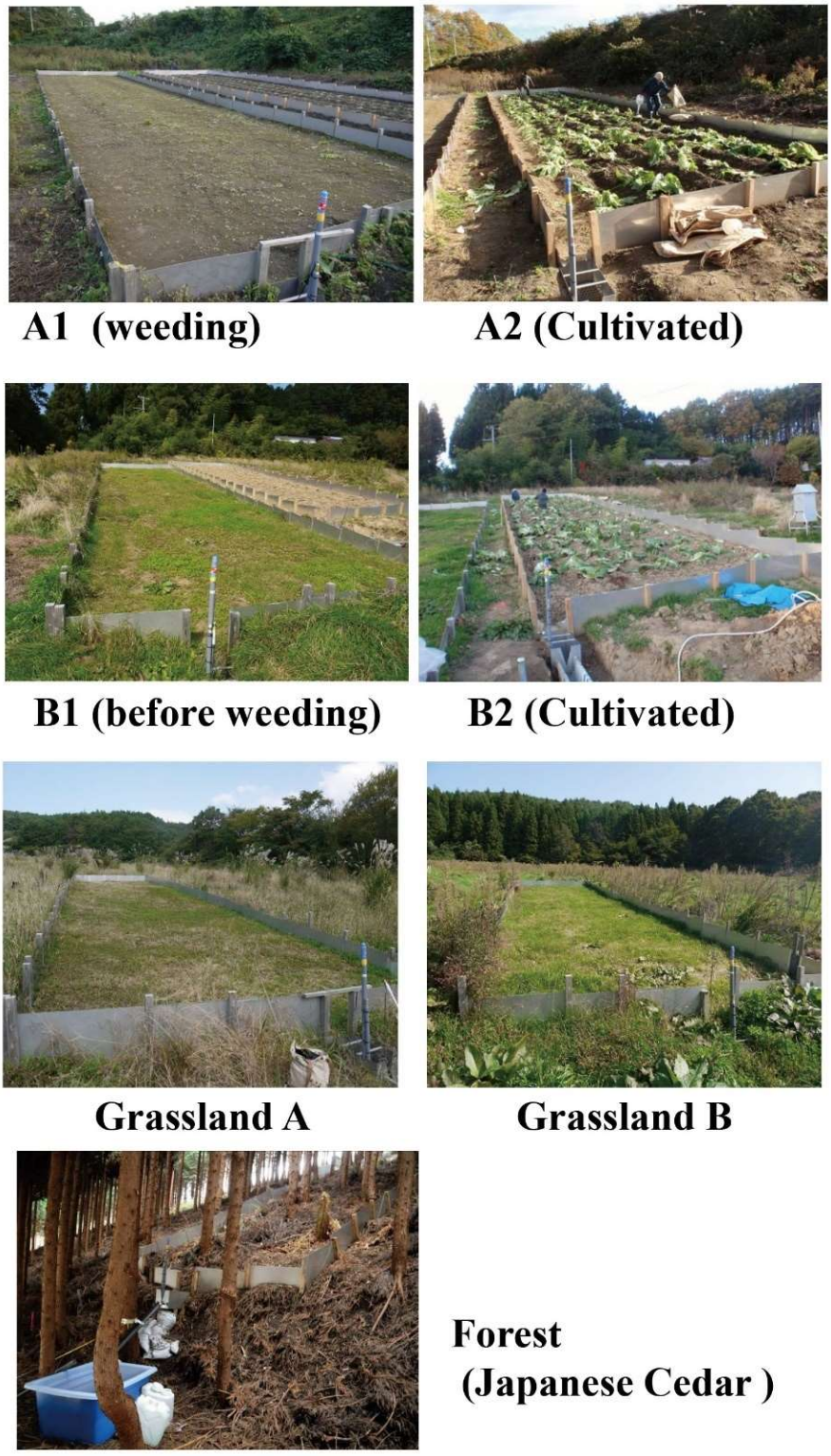

FIG. 6.2. Experimental plots for the water erosion study (Photos were taken in 2012, courtesy of Kazuya Yoshimura).

TABLE 6.2. CHARACTERISTICS OF THE SITES USED TO STUDY RADIOCAESIUM RUN-OFF AFTER THE FDNPP ACCIDENT

Type of canopy or land use	Observation period	Initial deposition density of ^{137}Cs (kBq/m^2)	Slope steepness (degrees)	Slope length (m)	^{137}Cs activity in soil (kBq/kg DM)	Entrainment coefficient S_c (m^2/kg)	Mass of eroded soil per year (kg m^{-2} year^{-1})	Annual ^{137}Cs run-off (part of initial ^{137}Cs deposition) (%/year)	Reference
Uncultivated farmland A (Before weeding)	17.07.2011–13.06.2012	372	4.4	22.1	17	0.046	0.50	2.2	[6.8, 6.13]
Uncultivated farmland A (After weeding)	13.06.2012–27.08.2014	372	4.4	22.1	11	0.030	4.1	12	[6.13]
Uncultivated farmland B (Before weeding)	17.07.2011–14.07.2013	413	9.3	22.1	21	0.051	0.028	0.14	[6.13]
Uncultivated farmland B (After weeding)	14.07.2013–30.07.2014	413	9.3	22.1	19	0.046	1.9	8.7	[6.13]
Cultivated farmland A	30.09.2012–27.08.2014	372	4.2	22.1	0.41	0.0011	7.2	7.9	[6.13]
Cultivated farmland B	30.09.2012–30.07.2014	413	10	22.1	0.42	0.001	0.90	0.91	[6.13]
Grassland A	17.07.2011–21.12.2013	557	9.7	22.1	1.3	0.0023	0.028	0.067	[6.13]
Grassland B	17.07.2011–7.08.2013	1010	9.5	22.1	10	0.099	0.019	0.019	[6.13]
Grassland C	31.07.2013–3.12.2014	260	9.5	22.1	1.9	0.0073	0.0041	0.0029	[6.13]
Cedar Forest	17.07.2011–3.12.2014	442	28	22.1	37	0.084	0.0052	0.044	[6.8, 6.13]

TABLE 6.2. CHARACTERISTICS OF THE SITES USED TO STUDY RADIOCAESIUM RUN-OFF AFTER THE FDNPP ACCIDENT (cont.)

Type of canopy or land use	Observation period	Initial deposition density of ^{137}Cs (kBq/m^2)	Slope steepness (degrees)	Slope length (m)	^{137}Cs activity in soil (kBq/kg DM)	Entrainment coefficient S_c (m^2/kg)	Mass of eroded soil per year ($kg\ m^{-2}\ year^{-1}$)	Annual ^{137}Cs run-off (part of initial ^{137}Cs deposition) (%/year)	Reference
Red Pine forest	05.2013–10.2014	170	39	2	10	0.060	0.056	0.34	[6.9] [a]
Cedar Forest	05.2013–10.2014	200	39	2	28	0.14	0.012	0.17	[6.9] [a]
Japanese Cypress Forest	05.2013–10.2014	160	39	2	19	0.12	0.18	2.1	[6.9] [a]
Deciduous broad leaved	05.2013–10.2014	110	37	2	7.7	0.070	0.26	1.8	[6.9] [a]
Deciduous broad-leaved	03.11.2013–04.10.2014	497	13	11	41	0.082	0.011	0.11	[6.10]
Deciduous broad-leaved	06.11.2013–04.10.2014	497	28.5	10	37	0.074	0.034	0.22	[6.10]
Japanese Cedar	06.11.2013–04.10.2014	487	29.5	11	22	0.045	0.061	0.15	[6.10]

[a] Estimating annual water run-off by using the ratio of rainfall during the observation period divided by mean annual rainfall

The values for S_c tended to be lower in forests than for other land uses. Soil erosion on grassland was lower than on bare soil that was treated with herbicides because the flux of soil material was inhibited by the grass canopy [6.8, 6.13]. These data indicate that radiocaesium run-off depends on both the vegetation cover and the land use. The upper soil layers with the higher ^{137}Cs activity concentrations are the main source of eroded radiocaesium in grassland whereas in cultivated land, the radiocaesium is mixed with deeper soil layers, so the values for S_c are lower.

The annual ^{137}Cs loss rates due to solid wash-off rates varied with land use and were highest on unvegetated bare soil. On cultivated soil, the loss of ^{137}Cs due to wash-off was much lower. In 2015, an increase of run-off due to a major typhoon was observed. On grassland, run-off is generally lower, with a reported range of 0.001–0.068% per year [6.8]. In forest, there was no significant change in the wash-off compared with that before the FDNPP accident [6.10]. The radiocaesium inventory on a steep hill increased due to an input of radiocaesium from litter-fall and through-fall, which compensated for the loss due to run-off from the experimental plot.

The loss of soil due to water erosion under different environmental conditions is commonly estimated by the Universal Soil Erosion Equation (USLE) [6.14], according to:

$$A = R \times K \times L \times S \times C \times P \tag{6.2}$$

where A is soil loss per unit area (ton/ha), R is the rainfall erosivity factor (MJ · ha^{-1} · mm · h^{-1}), which is calculated for a given period with n rainstorms according to:

$$R = \sum_{i=1}^{n} E_i \, I_{30i} \tag{6.3}$$

where E_i is the energy in rainfall (MJ/ha) and I_{30} is the maximum half-hour rainfall intensity (mm/h) for i^{th} storm. K is the soil erodibility factor (dimensionless), L is the slope length factor (dimensionless), S is the slope steepness factor (dimensionless), C is the cover management factor (dimensionless) and P is the support practice factor (dimensionless).

To compare the erosion of plots with different rainfall characteristics, Wakiyama et al [6.13] normalized the erosion rate to the erosivity factor, R, the slope steepness factor S and the factor K, applying R, S, and K as given in [6.8]. The factor R was estimated for each plot based on the rainfall events during the experimental period (2800–3700 MJ ·ha^{-1} mm h^{-1} for farmland and pasture plots, 4100 MJ ha^{-1} mm h^{-1} for the forest plots). The factor K is determined by soil texture; for the plots in this experiment K was obtained from the database of the National Institute for the Agro-Environmental Sciences (0.039 for farmland and pasture plots, 0.02 for the forest plots).

The data are summarized for each plot during the monitoring period in Fig. 6.3, which shows an exponential relationship between vegetation cover and the amount of ^{137}Cs lost with by eroded soil.

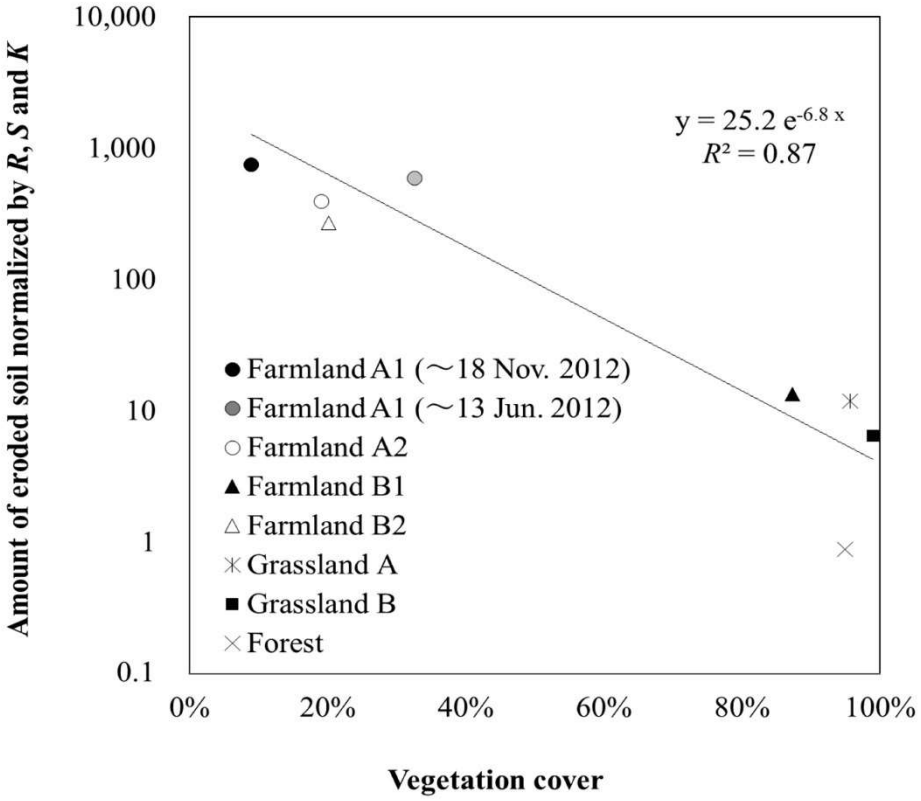

FIG 6.3. Relationship between vegetation cover and soil loss during the monitoring period (kg/ha) normalised by the rainfall erosivity factor (R), soil erodibility factor (K) and slope steepness factor (S). Vegetation cover was averaged over the monitoring period (after [6.8])

A few studies have been carried out to explore the time-dependence of the run-off rate and S_c [6.13]. Based on long-term observations, the time dependence of S_c (m^2/kg) was analyzed according to the following exponential equation:

$$S_c(t) = S_{c0}e^{-k\,t} \tag{6.4}$$

where $S_c(t)$ is the value of S_c at time t (year), S_{c0} is the intercept of S_c at $t = 0$, and k is the decrease rate constant (year^{-1}). The parameters k and S_c were determined as an average over 3-month time intervals during the experiments; the results are shown in Table 6.3 [6.13]. The variations in S_c for a given land use were lower than for S_c between land uses. No significant time trend was identified for any of the land uses. S_c appeared to decrease with time only on uncultivated land with sparse vegetation and higher erosion rates.

6.2.2.2. Time dependence of ^{137}Cs in in run-off water of forested catchments.

After deposition of ^{137}Cs onto a catchment, its subsequent transport to surface waters is highly influenced by the fraction and type of forest coverage [6.15] because deciduous and evergreen forests have different interception and retention characteristics. Data on run-off from forested catchments, obtained after the FDNPP accident since June 2011 [6.15] indicated that run-off of ^{137}Cs in dissolved form was strongly associated with the removal of ^{137}Cs from the litter layer [6.16, 6.17]. Related laboratory experiments [6.18] also indicated that elution from the litter was an important process for mobilizing ^{137}Cs. The activity concentrations of dissolved ^{137}Cs in run-off water during rainfall events were higher than during dry periods [6.19].

TABLE 6.3. PARAMETERS FOR TEMPORAL CHANGES OF S_c, THREE-MONTH WEIGHTED MEAN S_{c0} (JULY 2011 TO DECEMBER 2014)

Site	n	S_{c0} (m^2/kg)	S_c (m^2/kg)		k ($year^{-1}$)	R^2
			Min	Max		
Uncultivated farmland A (before weeding)	18	0.034	0.015	0.062	−0.075	0.0030
Uncultivated farmland A (after weeding)	37	0.060	0.018	0.070	0.23	0.19 [a]
Uncultivated farmland B (before weeding)	28	0.027	0.0079	0.14	−0.51	0.14 [a]
Uncultivated farmland B (after weeding)	19	0.047	0.010	0.077	0.036	0.00072
Cultivated farmland A	26	0.015	0.0078	0.046	0.049	0.0042
Cultivated farmland B	27	0.0043	0.0046	0.023	−0.39	0.26 [a]
Grassland A	29	0.026	0.0018	0.15	0.32	0.038
Grassland B	20	0.0080	0.0010	0.041	0.38	0.082
Grassland C	10	0.0018	0.0048	0.056	−0.61	0.13
Forest	34	0.12	0.032	3.2	0.20	0.038

[a] All coefficients of regression are statistically significant ($p < 0.05$).

The time-dependence of the entrainment coefficient of dissolved water, L_c determined for ^{137}Cs in forests were fitted to an exponential function with two components:

$$L_c(t) = \alpha e^{-k_1 t} + \beta e^{-k_2 t} \quad (6.5)$$

where $L_c(t)$ is the entrainment coefficient at time t (year), α and β (m^2/kg) are the initial contributions to the entrainment coefficient for rapid and slow components of the decline and k_1 and k_2 ($year^{-1}$) are the rate constants describing the decline of the two components of the function.

The exponential functions describing the time-dependence of the activity concentration of dissolved ^{137}Cs in run-off water up to the first 200 days after deposition and the long-term decrease are summarized in Table 6.4.

The time-dependence of the entrainment coefficient for four different catchments is shown in Fig. 6.4. The entrainment coefficient is presented for: (a) dissolved ^{137}Cs, (b) ^{137}Cs bound to coarse organic matter and (c) ^{137}Cs bound to suspended sediments respectively.

For dissolved ^{137}Cs, the fastest decline during the first phase, k_1 (measurements started in June 2011) was observed in the catchment with 100% forest. The decline in the first rapid phase was equivalent to an effective half-life T_{eff} ranging from 44 to 77 d (see Table 6.4 and Fig. 6.4). The fraction of dissolved ^{137}Cs in the run-off water was small. The rapid phase was influenced by multiple processes including the ^{137}Cs flux from tree crowns to soil due to throughfall as indicated by measurements of ^{137}Cs in throughfall, which followed the same time-dependence as dissolved ^{137}Cs in run-off water [6.20]. This observation supports the hypothesis that Cs in throughfall was an important process contributing to the early loss of radiocaesium from catchments. Thereafter, the decline was much slower [6.17], since the processes potentially releasing dissolved ^{137}Cs such as the decomposition of litter were considerably slower [6.12].

TABLE 6.4. PARAMETERS OF THE MODEL (EQ. 6.5) DESCRIBING TIME DEPENDENCE OF ^{137}CS ACTIVITY CONCENTRATION IN RUN-OFF WATER FOR SMALL CATCHMENTS IN DISSOLVED FRACTION (BOTH COMPONENTS) AND ORGANIC AND SUSPENDED SOIL FRACTIOONS (LONG-TERM COMPONENT).

Phase	Catchment [a]	Form of ^{137}Cs	Parameters (stastical significance [b])		
First			α (m²/kg)	k_1 (year^{-1})	$T_{\text{eff},1}$ (year)
	KOU	Dissolved	$(9.4 \pm 5.6) \times 10^{-7}$	4.3 ± 1.2 (**)	0.21
	IBO	Dissolved	$(7.0 \pm 9.2) \times 10^{-6}$	8.5 ± 2.8 (*)	0.12
	ISH	Dissolved	$(3.1 \pm 11) \times 10^{-5}$	14 ± 9.9	0.12
Second			β (m²/kg)	k_2 (year^{-1})	$T_{\text{eff},2}$ (year)
	KOU	Dissolved	$(3.9 \pm 0.72) \times 10^{-8}$ (**)	0.25 ± 0.11 (*)	2.2
		Org	$(1.8 \pm 0.87) \times 10^{-3}$	−0.66 ± 0.25 (*)	n.a. [c]
		SS	$(3.9 \pm 1.3) \times 10^{-2}$ (*)	0.031 ± 0.18	22
	SET	Dissolved	$(4.7 \pm 2.8) \times 10^{-8}$	0.13 ± 0.13	5.3
		Org	$(2.4 \pm 1.4) \times 10^{-2}$	0.33 ± 0.12 (*)	2.1
		SS	$(9.7 \pm 3.4) \times 10^{-2}$ (**)	0.28 ± 0.072 (**)	2.5
	IBO	Dissolved	$(2.6 \pm 1.0) \times 10^{-7}$ (*)	0.71 ± 0.12 (**)	0.98
		Org	$(6.5 \pm 1.7) \times 10^{-2}$ (**)	0.85 ± 0.074 (**)	0.82
		SS	$(4.8 \pm 2.6) \times 10^{-2}$	0.15 ± 0.25	4.6
		SS' (after decontamination)	$(1.3 \pm 1.1) \times 10^{-3}$	−0.015 ± 0.19	n.a.
	ISH	Dissolved	$(1.1 \pm 0.23) \times 10^{-6}$ (**)	0.78 ± 0.056 (**)	0.89
		Org	$(3.3 \pm 0.91) \times 10^{-2}$ (**)	0.68 ± 0.079 (**)	1.0
		SS	$(9.8 \pm 1.9) \times 10^{-2}$ (**)	0.44 ± 0.054 (**)	1.6

[a] Catchments are coded as follows:
KOU: Koutaishi catchment (cedar forest 99%, grassland 1%; average deposition density 916 kB/m^2)
SET: Setohachi catchment (cedar forest 100%; average deposition density 759 kBq m^2)
IBO: Iboishi catchment (cedar and deciduous forest 76%, grassland 23%; average deposition density 544 kBq/m^2)
ISH: Ishidaira catchment (cedar forest 81%, grassland 19%; average deposition density 298 kBq/m^2)
[b] Statistical significance of parameters shown as: (**) for p-value < 0.01 and (*) for p-value < 0.05
[c] not applicable

Radionuclide ^{137}Cs bound to organic matter declined in the second phase according to an T_{eff} of 0.82–2.1 years. The largest fraction of ^{137}Cs in run-off water of forested catchments was bound to suspended sediments. The decline in the ^{137}Cs activity concentration in run-off water bound to organic matter varied widely with reported T_{eff} values ranging from 1.6–22 years [6.17].

In the second phase (k_2), the decline of ^{137}Cs in run-off water was faster in catchments with a higher fraction of pasture than that occurring in forested catchments. This observation is in agreement with data showing a faster decline of ^{137}Cs activity concentration in grass compared with litter [6.21]. It is also consistent with the time-dependence of ^{137}Cs activity concentrations

observed in rivers linked to larger catchments ([6.22]; this work), where L_c for dissolved ^{137}Cs in run-off water was higher in forest-dominated catchments in 2018.

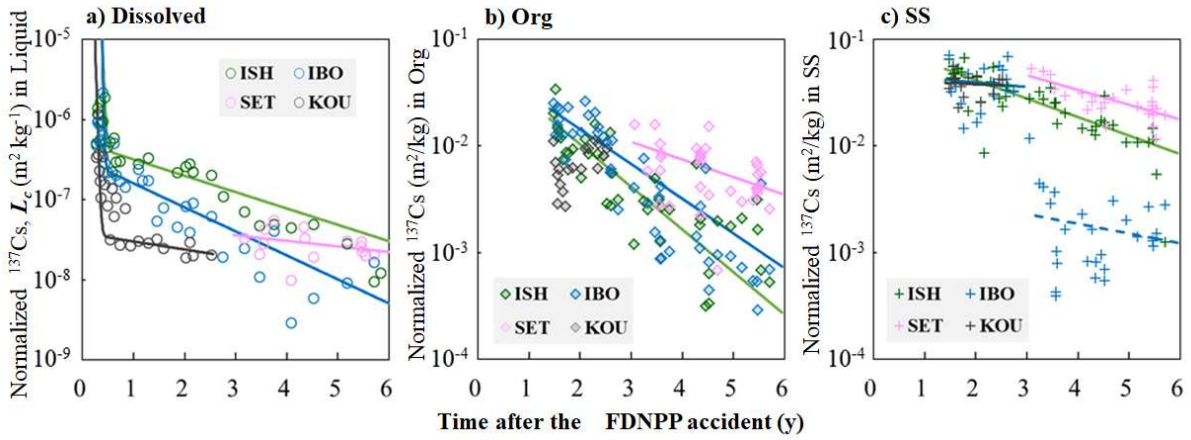

FIG 6.4. Time series of normalized ^{137}Cs in dissolved form (a), coarse organic matter (b) and suspended sediment (c) in the four catchments (Ishidairayama (ISH), Iboishiyama (IBO), Setohachiyama (SET), and Koutaishiyama (KOU)), and their fitted exponential relationships [17]

6.2.2.3. Time dependency radiocaesium run-off in urban areas

In urban environments, radiocaesium activity concentrations in suspended sediments of run-off water were higher where run-off events occurred in small catchments [6.23]. Yamashita et al. [6.24] and Murakami et al. [6.25] studied a 31 km^2 urbanised catchment in Kashiwa, Chiba Prefecture. The land use was 53% housing and 1.5% roads and the mean initial ^{137}Cs deposition density in the area was 61 kBq/m². From May 2012 to March 2013, the initial decline in the entrainment coefficient tended to be faster than from March 2013 to February 2015 (Fig. 6.2.6), but the difference was not statistically significant. Overall, the data was described as a single decline as:

$$S_c(t) = 0.18\, e^{-0.40t}\ (\mathrm{m^2/kg}), (r^2 = 0.41, p < 0.01). \quad (6.6)$$

S_c values in urban areas were significantly higher than in forested catchments throughout the period from May 2012 to February 2015. Furthermore, the rate of decline was faster in urban areas than in the forested catchments (Fig. 6.5).

A comparison of different surfaces showed that the average radiocaesium deposition density (Bq/m^2) of paved areas was about a factor of 5.5 lower than that of pasture, lawn or farmland measured 3.8 years after the fallout and based on a large dataset (n = 1119) [6.26]. The average radiocaesium deposition density on urban areas was more than a factor of 10 lower, indicating rapid removal of radiocaesium from urban areas even without decontamination. The data suggest that human activity and the type of surface materials greatly affects the rate of reduction of radiocaesium in urban areas.

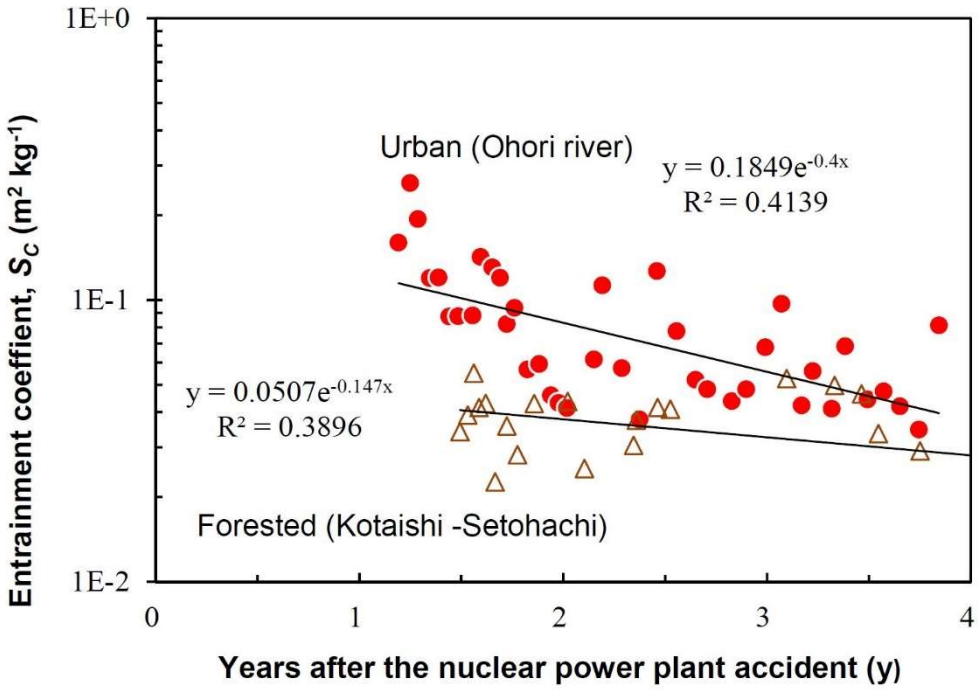

FIG. 6.5. Comparison of the time-dependence of suspended sediments in run-off water in urban [6.25] and forested catchments [6.17]

6.2.3. Time dependence of ^{137}Cs of river water

Fukushima prefecture has several large catchments with several types of land use. The rivers in these catchments transport radiocaesium to the ocean. The time-dependence of the ^{137}Cs activity concentrations in suspended sediments of river water was described by a double exponential function for the period from June 2011 to December 2015 [6.27]. At the outlet of the Abukuma River basin (Site 6 in Fig. 6.6), which is the largest river system in the affected Prefectures, the ^{137}Cs activity concentration in suspended sediment normalized to the initial average ^{137}Cs deposition in the catchment $C'(t)$, can be expressed as an exponential function with two components:

$$C'(t) = 0.868\, e^{-2.86\, t} + 0.0636\, e^{-0.309\, t}, (\mathrm{Bq/kg}). \qquad (6.7)$$

The rate constants λ_1 and λ_2 as well as the related half-lives $T_{\mathrm{eff},1}$ and $T_{\mathrm{eff},2}$ for the early and intermediate phases (June 2011–March 2012 and April 2012–March 2016) for the other rivers of Fukushima Prefecture are given in Table 6.6. Trends in the rate of decline differ between monitoring sites. A higher decrease rate λ_1 of the ^{137}Cs activity concentration in suspended sediments was reported for the early phase for monitoring sites in the main channel of the Abukuma river, compared with the concentrations in the lower order tributaries. The decline in the intermediate phase (λ_2 in range of 0.04–0.66 year^{-1}, corresponding to $T_{\mathrm{eff},2}$ in range of 1.05–16 year) was—with a few exceptions—similar to those reported for radiocaesium in suspended sediments observed in Chernobyl-affected areas in Ukraine [6.28].

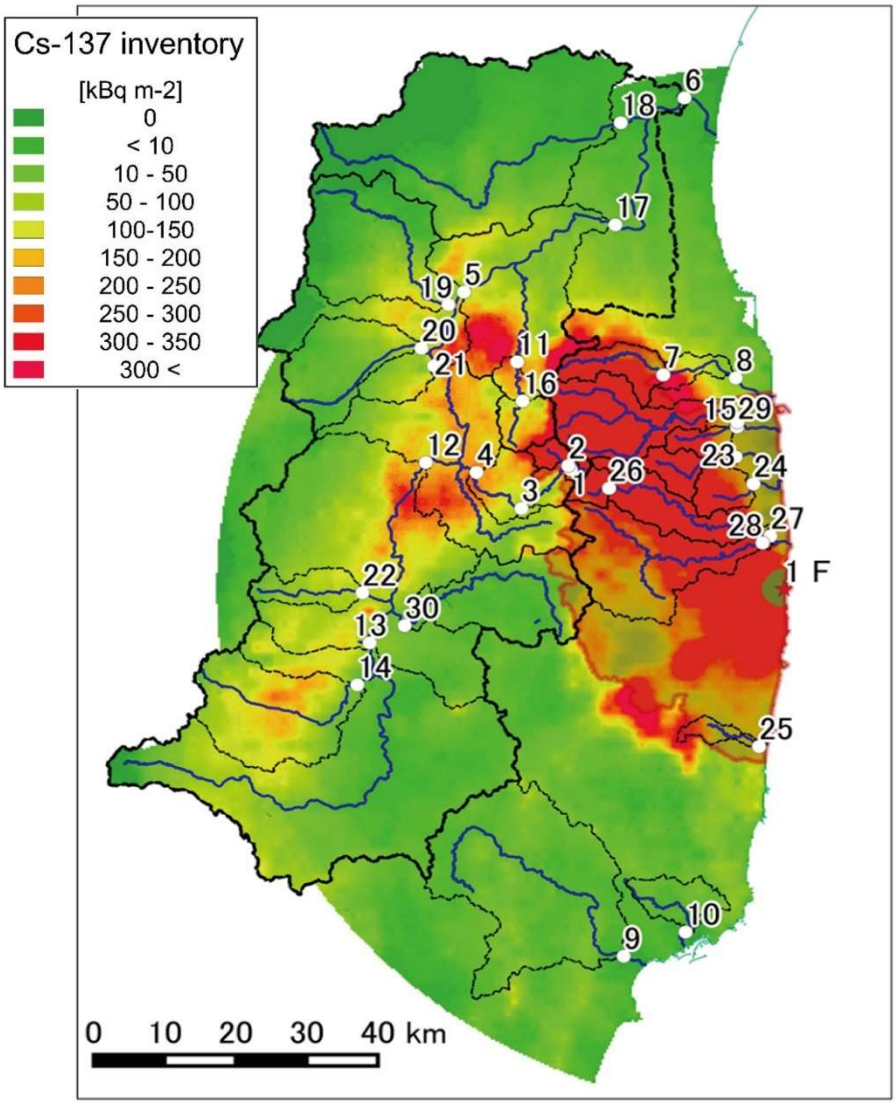

FIG. 6.6. ^{137}Cs deposition density in Fukushima Prefecture and location of the sites for monitoring ^{137}Cs activity concentrations in suspended sediments in river water. The site numbers refer to the data in Table 6.6.

TABLE 6.6. PARAMETERS ON TIME DEPENDENCE OF ^{137}CS ACTIVITY CONCENTRATIONS IN SUSPENDED SEDIMENTS IN RIVERS AFFECTED BY THE FDNPP ACCIDENT

Site name (abbreviation)	River name	River system	Catchment area (km^2)	Mean ^{137}Cs deposition in the catchment (kBq/m^2)	June 2011–March 2012 [a]		April 2012–March 2016	
					λ_1 (year^{-1})	$T_{eff,1}$ (year)	λ_2 (year^{-1})	$T_{eff,2}$ (year)
80km-area and Abukuma watershed			9862	200				
The initial evacuation area			1591	847				
Mizusakai (Miz)	Kuchibuto	Abukuma	7.5	745	0.44	1.6	0.26	2.7
Kuchibuto_Upper (KU)	Kuchibuto	Abukuma	21.4	477	1.89	0.37	0.35	2.0
Kuchibuto_Middle (KM)	Kuchibuto	Abukuma	62.8	357	2.11	0.33	0.44	1.6
Kuchibuto_Down (KD)	Kuchibuto	Abukuma	135.2	269	0.92	0.75	0.51	1.4
Fushiguro (Fus)	Abukuma	Abukuma	3644.5	95.9	3.79	0.18	0.38	1.8
Iwanuma (Iwa)	Abukuma	Abukuma	5313.2	88.4	3.10	0.22	0.47	1.5
Mano (Man)	Mano	Mano	75.6	499	— [b]	—	0.08	8.2
Ojimadazeki (Oji)	Mano	Mano	110.8	406	—	—	0.15	4.6
Matsubara (Mat)	Same	Same	570.9	40	—	—	0.19	3.7
Onahama (Ona)	Fujiwara	Fujiwara	70.1	38.8	—	—	0.33	2.1
Tsukidate (Tsuk)	Hirose	Abukuma	83.6	223	—	—	0.66	1.1
Nihonmatsu (Nih)	Abukuma	Abukuma	2380.3	81.8	—	—	0.42	1.6
Miyota (Miy)	Abukuma	Abukuma	1286.6	74.1	—	—	0.24	2.9
Nishikawa (Nis)	Shakado	Abukuma	289.4	132	—	—	0.28	2.9
Kitamachi (Kit)	Mizunashi	Niida	35.8	565	—	—	0.48	1.5
Kawamata (Kaw)	Hirose	Abukuma	56.6	229	—	—	0.63	1.1
Marumori (Mar)	Abukuma	Abukuma	4123.9	105	—	—	0.38	1.8

TABLE 6.6. PARAMETERS ON TIME DEPENDENCE OF ^{137}CS ACTIVITY CONCENTRATIONS IN SUSPENDED SEDIMENTS IN RIVERS AFFECTED BY THE FDNPP ACCIDENT (cont.)

Site name (abbreviation)	River name	River system	Catchment area (km^2)	Mean ^{137}Cs deposition in the catchment (kBq/m^2)	June 2011–March 2012 [a]		April 2012–March 2016	
					λ_1 (year^{-1})	$T_{eff,1}$ (year)	λ_2 (year^{-1})	$T_{eff,2}$ (year)
Funaoka-ohashi (Fun) [c]	Shiroishi	Abukuma	775.2	20.2	—	—	—	—
Senoue (Sen)	Surigami	Abukuma	313.3	41.9	—	—	0.29	2.4
Yagita (Yag)	Ara	Abukuma	184.6	52.7	—	—	0.04	16
Kuroiwa (Kur)	Abukuma	Abukuma	2921.4	103	—	—	0.53	1.3
Tomita (Tom)	Ouse	Abukuma	72.6	98.5	—	—	0.46	1.5
Ota (Ota)	Ota	Ota	49.9	1770	—	—	0.18	3.8
Odaka (Oda)	Odaka	Odaka	50.3	724	—	—	0.06	11
Asami (Asa)	Asami	Asami	25.8	194	—	—	0.34	2.1
Tsushima (Tsus)	Ukedo	Ukedo	25.4	954	—	—	0.40	1.7
Ukedo (Uke)	Ukedo	Ukedo	152.6	2570	—	—	0.25	2.8
Takase (Tak)	Takase	Ukedo	263.7	726	—	—	0.41	1.7
Haramachi (Har)	Niida	Niida	200.3	964	—	—	0.23	3.0
Akanuma (Aka)	Otakine	Abukuma	242.6	52.6	—	—	0.35	2.0
				Average	2.04	0.57	0.34	3.2
				SD	1.16	0.48	0.15	3.3

[a] monitoring for most sites started later than that for the first six sites, so the fast component could not be identified
[b] no data
[c] dissolved radiocaesium activity concentration only

6.2.4. Summary and limitations.

Radionuclides deposited in the terrestrial and freshwater environment are re-distributed due to run-off and erosion processes. After the FDNPP accident these processes were studied in field experiments and by analysis of data from environmental monitoring programmes.

Emphasis was given to erosion from farmland, pasture and forest, the transport of radiocaesium from rice paddies to rivers, the transport in catchments and the time-dependence of ^{137}Cs activity concentrations in suspended sediments of rivers in Fukushima Prefecture.

Loss of radiocaesium due to erosion

- The loss of radiocaesium due to water erosion depended on the land use. It increased in the order: grassland and forest < vegetated farmland < bare farmland;
- On a farmland plot, that was unvegetated during the whole year due to continuous weeding, the loss of radiocaesium due to water erosion reached about 10% per year, whereas for vegetated farmland plots erosion losses were much lower. On grassland, erosion rates were generally well below 0.01%/year;
- Erosion losses varied considerably for forested areas. In a study carried out before 2011, the loss of ^{137}Cs in experimental forest plots due to water erosion was in the range of 0.005–2.3%/year. After the FDNPP accident, in forests with steep slopes, erosion losses ranged from 0.001–0.2%/year;
- Except for bare farmland, the erosion of ^{137}Cs from affected areas was, in general, a process of minor importance.

Urban catchments

- In a catchment with more than 50% residential areas run-off, as quantified by the entrainment coefficient, was initially a factor of 3 higher than in forested areas due to the retarding effect of vegetation cover;
- The data indicated a decline in two phases, but the tendency was not statistically significant, as the observation period started only in 2012 so the first phase was not covered by the observation period. Assuming a single exponential model, run-off in the urban catchment declined from May 2012 to February 2015 with an effective half-life of 1.5 to 2 years.

Forested catchments

- In four catchments, predominantly covered by forest, the fraction of dissolved ^{137}Cs in the run-off water was small. Most ^{137}Cs in run-off water of forested catchments was bound to suspended sediments;
- Initially, activity concentrations of dissolved ^{137}Cs declined according to an effective half-life of 25–220 days; the long-term decline was equivalent to effective half-lives ranging from 0.9–4 years;
- In the medium-term, ^{137}Cs bound to organic matter declined according to an effective half-life of 0.75–1.8 years;

- The fraction of ^{137}Cs bound to suspended sediments in run-off water varied widely. Activity concentrations of ^{137}Cs bound to organic matter declined with long-term effective half-lives of 1.7–13 years.

^{137}Cs in suspended sediments of river water

Activity concentrations of ^{137}Cs bound to suspended sediment in water was monitored in rivers of Fukushima Prefecture and related tributaries.

- The dynamic changes with time could be described by an exponential function with two components;
- In general, the decline observed in the mainstream of the Abukuma river was faster than in the tributaries;
- At different monitoring sites of the Abukuma River, the initial decline was described by effective half-lives of 0.2–1.6 year, with the long-term decline T_{eff} varying in a narrower range of 1.4–2.7 years;
- In the tributaries, only the long-term component was observed. Averaged over 16 monitoring sites, the decline was equivalent to a mean effective half-life of about 3 years, with a range of 1–16 years. Similar values were reported in rivers of the Chernobyl-affected areas.

6.3. ESTIMATION OF THE FRESHWATER DISTRIBUTION COEFFICIENT K_{d}

6.3.1. Introduction

Soon after the FDNPP accident there were concerns expressed about the potential transfer of radiocaesium from freshwater systems via irrigation ponds into agricultural products such as paddy rice [6.29]. In response, several studies commenced to improve understanding of the behaviour of radiocaesium in freshwater systems and to enable predictions of the fate of dissolved (with high bioavailability) and suspended-sediments-bound radiocaesium in river systems.

The K_{d} approach is a model used to quantify the activity concentration of both particulate and dissolved radiocaesium in aquatic systems. This model is based on the K_{d} coefficient which corresponds to the solid/liquid concentrations ratio of radionuclides assuming instantaneous equilibrium, reversibility, and linearity. It is used in many models developed to simulate the dynamics of radiocaesium in rivers or lakes after releases of radionuclides to aquatic systems (e.g. [6.30, 6.31]). K_{d} values may vary over a wide range, dependent on the often dynamic and heterogenous characteristics of freshwater systems. K_{d} values depend on several co-factors such as pH, dissolved organic carbon (DOC), particulate organic carbon (POC), cation exchangeable capacity (CEC), concentrations of major elements and the concentration of suspended solids [6.32] which normally increases during rain run-off events. Therefore, in many aquatic studies, apparent $K_{\text{d(a)}}$ (see Chapter 2) was a key parameter used to model the dynamics of radiocaesium in rivers after the FDNPP accident [6.33–6.37].

Field studies have been carried out to explore the environmental factors influencing the $K_{\text{d(a)}}$ of radiocaesium after the FDNPP accident [6.27, 6.38–6.42]. The data illustrate the spatial and temporal variations of radiocaesium $K_{\text{d(a)}}$ values using comprehensive water quality data for the river systems in Fukushima Prefecture Miyagi Prefecture, Tochigi Prefecture, Gunma

Prefecture, and Chiba Prefecture. Such an analysis enables the identification of environmental factors influencing the radiocaesium $K_{d(a)}$ values.

6.3.2. The distribution coefficient $K_{d(a)\text{-}SS}$ parameter

The distribution of radiocaesium between suspended sediments and water in rivers is quantified as $K_{d(a)\text{-}SS}$ (ratio of the activity concentrations of suspended sediments and river water). This coefficient should not be mistaken for $K_{d(a)\text{-}BS}$ which is used to quantify the distribution between bottom sediments and the water column by the ratio of the activity concentrations in bottom sediment and river water.

6.3.2.1.Data collection and organization of $K_{d(a)\text{-}SS}$

Mountainous forest areas dominate the upper regions of the contaminated river catchments in Fukushima Prefecture. Highly contaminated forest litter is a significant source of dissolved radiocaesium in river catchments [6.19, 6.37, 6.43]. Therefore, dissolved radiocaesium probably originates from the leachate of the litter in the streams or rivers.

Activity concentrations of dissolved and suspended-sediment-bound ^{137}Cs, reported for 150 sites in various river systems in Fukushima Prefecture after the FDNPP accident, were analysed to derive $K_{d(a)\text{-}SS}$ distributions [6.16, 6.27, 6.39, 6.41, 6.43–6.59]. The collated published values covered the period from July 2011 to August 2014 in the Abukuma River system (197 observations) and from July 2011 to March 2018 in other rivers in the coastal region of Fukushima Prefecture (316 observations).

$K_{d(a)\text{-}SS}$ values determined before the FDNPP accident from both within and outside of Japan were also collated from international literature sources [6.1, 6.28, 6.60–6.71]. International compilations of $K_{d(a)\text{-}SS}$ values were also considered [6.72–6.74].

6.3.2.2. Data collection and organization for environmental factor analysis

To determine a relationship between river water quality and the $K_{d(a)\text{-}SS}$ value, a dataset was developed from a field campaign designed to measure environmental factors and radiocaesium activity concentrations in water and suspended matter. The data set also contained water quality data for 67 sites in 65 rivers for normal flow condition determined in East Japan (including Fukushima Prefecture) in August 2017. Tsuji et al. [6.22] describes the details of the sampling points as well as the sampling and analytical methods. The water quality parameters included pH, electrical conductivity (EC), dissolved organic carbon (DOC), inorganic cations (Na^+, Ca^{2+}, K^+, NH_4^+, Mg^{2+}) and inorganic anions (Cl^-, SO_4^{2-}, NO_2^-, NO_3^-, PO_4^{3-}). Additionally, literature data relevant for analysis of the relationship between river water quality parameters and $K_{d(a)\text{-}SS}$ values were collected from field surveys in Japan for before and after the FDNPP accident [6.38, 6.41, 6.42, 6.49, 6.60, 6.63, 6.75].

Sorption and desorption reactions of radiocaesium between river water and suspended particles or bottom sediments do not always play a dominant role in controlling the radiocaesium behaviour in a catchment area. This is because of (i) the short contact time between flowing water and radiocaesium associated with soil surfaces in affected areas and (ii) the properties of the environmental sources of dissolved radiocaesium. In contrast, vertical migration in soil occurs gradually at a relatively slow speed enabling radiocaesium sorption and desorption to soil components. Therefore, at the scale of a catchment, the dominant process is the solid/liquid fractionation in soils rather than in rivers

6.3.3. $K_{d(a)\text{-}SS}$ before the FDNPP accident

Table 6.7 presents statistical data for $K_{\mathrm{d(a)\text{-}SS}}$ measured before the FDNPP accident. The data measured during the period of global fallout and after the Chernobyl accident are shown separately. The global dataset for suspended sediment were extracted from the data collected within the IAEA MODARIA I Programme[6] and did not include Japanese data. Data are also included that were measured for various nuclear and radiological sources such as the discharge of radioactive effluents from The Chalk River Nuclear Laboratories and the contamination associated with the Goiania radiological accident.

In IAEA TRS 472 [6.72] and the MODARIA dataset, the data corresponded to field conditions. Data were exclusively for suspended matter in the MODARIA dataset, whereas data for bottom sediments and suspended matter were compiled together in TRS 472. Due to this, these two IAEA datasets are not directly comparable.

TABLE 6.7. COMPILATION OF $K_{\mathrm{D(A)\text{-}SS}}$ MEASUREMENTS IN JAPAN AND OTHER AREAS BEFORE THE FDNPP ACCIDENT

Region	N	Mean	SD	Median	GM	GSD	Min	Max	IQR [a]
Combined Measurements before the FDNPP accident									
Global data	434	9.9×10^4	1.8×10^5	3.9×10^4	4.3×10^4	3.6	2.3×10^3	2.7×10^6	1.0×10^5
Japanese data	20	7.5×10^4	7.9×10^4	4.0×10^4	4.7×10^4	2.7	1.0×10^4	3.2×10^5	7.2×10^4
Global measurements on weapons' fallout (before Chernobyl)									
Global data	27	4.5×10^4	3.0×10^4	3.2×10^4	3.6×10^4	1.9	8.5×10^3	1.4×10^5	3.3×10^4
Japanese data	5	1.1×10^5	1.3×10^5	6.1×10^4	5.4×10^4	4.2	1.0×10^4	3.2×10^5	1.2×10^5
Global measurements on Chernobyl fallout									
Global data	407	1.0×10^5	1.9×10^5	4.0×10^4	4.3×10^4	3.8	2.3×10^3	2.7×10^6	1.9×10^5
Japanese data	15	6.3×10^4	5.7×10^4	3.5×10^4	4.5×10^4	2.3	1.3×10^4	1.9×10^5	4.9×10^4
International IAEA values									
TRS472 [b]	219	— [c]	—	—	2.9×10^4	5.9	1.6×10^3	5.2×10^5	—
MODARIA I	211	—	—	—	1.4×10^5	2.7	2.3×10^3	2.7×10^6	—

[a] Inter-quartile range
[b] Data for bottom sediments and suspended matter are compiled together
[c] no data

The $K_{\mathrm{d(a)\text{-}SS}}$ values for Japan fit within the distribution of all other global data. There are no statistically significant differences between the Japanese data and any of the other datasets (Wilcoxon ranked sum: Japan vs Combined; p-value = 0.66; Japan vs weapons' fallout; p-value = 0.43; Japan vs After Chernobyl; p-value = 0.68). Comparison of the global and Japanese data extracted from the MODARIA dataset is not strictly appropriate as the TRS 472 values included not only suspended sediment, but also bottom sediment. It is therefore expected

[6] http://www-ns.iaea.org/projects/modaria/

to have a difference of around one order of magnitude between these K_d distributions and those focused only on suspended matter [6.73].

6.3.4. $K_{d(a)\text{-}SS}$ after the FDNPP accident

6.3.4.1.Time-dependence of $K_{d(a)\text{-}SS}$

Figure 6.7 presents the time-dependent values of $K_{d(a)\text{-}SS}$ derived from measured ^{137}Cs activity concentrations of dissolved and particulate forms. The underlying measurements were carried in the mainstream and tributaries of the Abukuma River and in the rivers of the coastal region of Fukushima Prefecture starting three months after the FDNPP accident. The values fluctuate considerably so a significant time trend could not be identified in either area (Mainstream of Abukuma: $R^2 = 0.00029$, $p = 0.88$; tributaries of Abukuma: $R^2 = 0.030$, $p = 0.060$; rivers in the coastal region: $R^2 = 0.0001$, $p = 0.85$). Differences in methods used in sampling suspended sediment from the rivers may contribute to the fluctuations observed. Some studies obtained samples by filtrating river water instantaneously collected at various flow conditions using a membrane filter ($Ø_{cut\text{-}off} = 0.45$ µm), grass filter ($Ø_{cut\text{-}off} = 0.7$–1.0 µm), or cartridge filter ($Ø_{cut\text{-}off} = 1.0$ µm; [6.49]). In contrast, other studies used a time-integrated SS sampler [6.76] to collect suspended sediment [6.27, 6.39]. The effect of the difference on $K_{d(a)\text{-}SS}$ has not been investigated in detail and needs further examination.

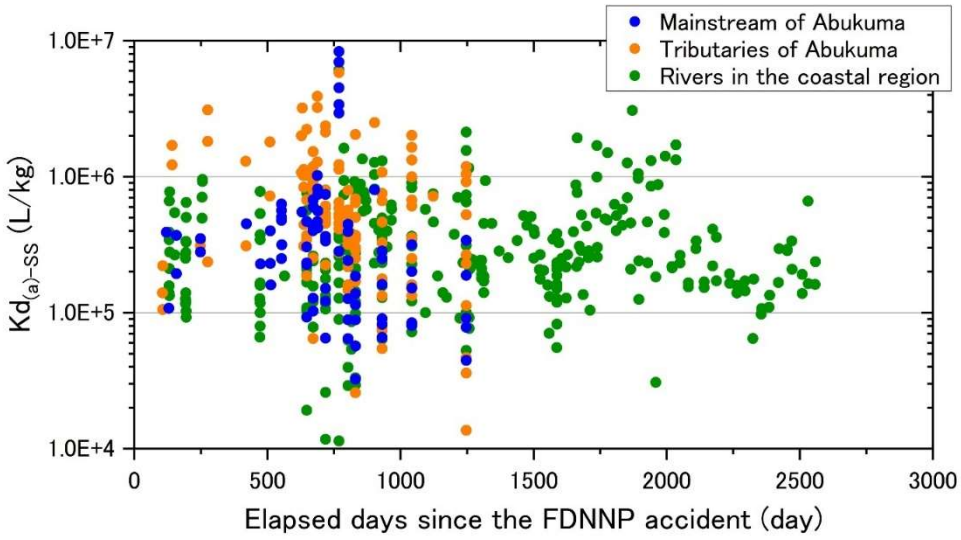

FIG 6.7. Time-dependence of the values of $K_{d(a)\text{-}SS}$ in the mainstream and the tributaries of the Abukuma River and the rivers in the coastal region of Fukushima Prefecture after the FDNPP accident.

6.3.4.2.Interaction of $K_{d(a)\text{-}SS}$ *with suspended sediment load*

The flow rate of the river may also influence $K_{d(a)\text{-}SS}$. In general, the concentration of suspended sediments increases with increasing flow rates. Due to the difficulty in safely sampling river water during storm events, there are few data that allow the derivation of $K_{d(a)\text{-}SS}$ for high flow rates in rivers. Figure 6.8 presents the dependence of $K_{d(a)\text{-}SS}$ on the concentrations of suspended sediments derived from river water sampling during rainfall events in the Mano, Hiso and Ohta

Rivers, which run through the coastal region of Fukushima prefecture [6.43, 6.57]. For all rivers, $K_{d(a)\text{-}SS}$ values tend to decrease with an increase of the river flow rate and the related increase in the *SS* concentration.

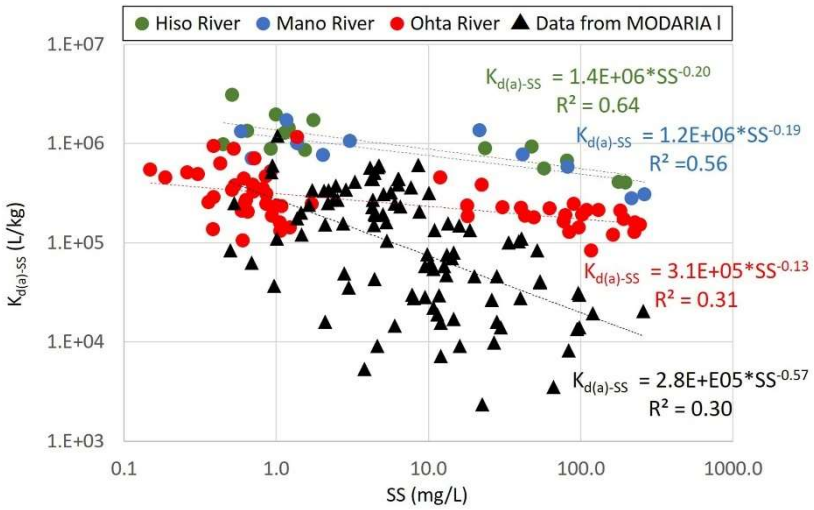

FIG. 6.8. Change in the values of $K_{d(a)\text{-}SS}$ *with the concentration of suspendent sediment (SS) in the Hiso, Mano [6.57], Ohta Rivers [6.43], and the MODARIA database [6.72–6.74].*

6.3.4.3.Site-dependence of $K_{d(a)\text{-}SS}$

Table 6.8 show the statistics of $K_{d(a)\text{-}SS}$ values derived for the mainstream and tributaries of the Abukuma River as well as for the rivers in the coastal region of Fukushima Prefecture to explore the spatial aspects of $K_{d(a)\text{-}SS}$. The values of $K_{d(a)\text{-}SS}$ show a large variation in both areas. The values for the mainstream of the Abukuma river and the rivers in the coastal region are similar, whereas the values of the tributaries of Abukuma are significantly higher (Kruskal-Wallis rank-sum test, $p < 0.001$).

TABLE 6.8. STATISTICAL VALUES OF $K_{D(A)\text{-}SS}$ IN THE MAINSTREAM AND TRIBUTARIES OF THE ABUKUMA RIVER AND OTHER RIVERS IN THE COASTAL REGION OF FUKUSHIMA PREFECTURE.

Region	N	$K_{d(a)\text{-}SS}$ (L/kg)							
		Mean	SD	Median	GM	GSD	Min.	Max.	IQR
Mainstream of Abukuma River	78	6.1×10^5	1.3×10^6	2.6×10^5	2.6×10^5	3.2	5.7×10^3	8.3×10^6	3.4×10^5
Tributaries of Abukuma River	119	8.0×10^5	8.8×10^5	5.2×10^5	4.8×10^5	3.0	1.4×10^4	5.8×10^6	7.9×10^5
Rivers in the coastal region	316	4.0×10^5	5.0×10^5	2.5×10^5	2.6×10^5	2.6	3.4×10^3	6.1×10^6	3.3×10^5
Overall	513	5.3×10^5	7.9×10^5	2.9×10^5	3.0×10^5	2.9	3.4×10^3	8.3×10^6	4.2×10^5

Comparison of $K_{d(a)\text{-}SS}$ before and after the FDNPP accident

The mean $K_{d(a)\text{-}SS}$ values measured mainly in Fukushima Prefecture after the FDNPP accident (Table 6.8) are a factor of 2–5 higher than observations made both in Japan and beyond reported after global weapons' fallout or the Chernobyl accident (Table 6.7). The post FDNPP accident means fall within the range of the pre-accident global data but exceed the maximum pre-accident observations for Japan (confounded by a small data sample). The GM of the MODARIA freshwater $K_{d(a)\text{-}SS}$ database, which constitutes the most up-to-date international collation of *in-situ* $K_{d(a)\text{-}SS}$ values at 1.35×10^5 (L/kg) with a GSD of 2.67 (L/kg) and a range of 2.3×10^3–2.7×10^6, is closer to the reported Japanese values.

The datasets of MODARIA I and of the Japanese data after the FDNPP accident are solely composed of K_d data for suspended sediments, whereas the other datasets are comprised of K_d data for suspended sediments, bottom sediments and eroded soils. It is therefore expected that there will be a difference of one order of magnitude between these compiled K_d distributions and those of suspended sediments alone [6.73]. Consequently, artefacts due to sample composition differences make it inadvisable to comment on the relative values.

The post FDNPP accident K_d values are heterogeneous covering a range of more than three orders of magnitude. The twofold difference between the GM values for Japanese data after the FDNPP accident and the MODARIA I data should not be interpreted as an indicator of real differences, when taking into account the impact of various environmental factors discussed above. Additionally, the presence of water-insoluble micro-particles with high radiocaesium activity concentrations in the fallout from the FDNPP accident may also contribute to the difference although this hypothesis needs to be verified [6.40].

In Fig. 6.9, the relationship between $K_{d(a)\text{-}SS}$ and *EC* based on measurements in some Japanese rivers before the FDNPP accident [6.60, 6.63] is compared against data after the accident. The relationship for measurements carried out before and after the FDNPP accident is similar which indicates that the rivers studied before the FDNPP accident had higher EC than those in Fukushima Prefecture. The limited number of non-Japanese studies that report both data of $K_{d(a)\text{-}SS}$ and EC indicate a similar relationship as observed in Japan (Fig. 6.9).

TABLE 6.9. STATISTICAL VALUES FOR THE RELATIONSHIP BETWEEN WATER QUALITY PARAMETERS AND $K_{D(A)}$-SS AT NORMAL FLOW CONDITIONS OF SAMPLED RIVERS IN THE EAST OF JAPAN.

Water quality parameter (X)	$\lg K_{d(a)\text{-}SS} = a \lg X + \lg b$			
	a	b	R	N
EC (mS/cm)	−1.0	4.7	−0.54	66
NH_4^+ (mg/L)	−0.48	4.9	−0.49	43
SS (mg/L)	−0.47	6.0	−0.46	66
K^+ (mg/L)	−0.74	5.8	−0.39	65
DOC (mg/L)	−0.56	5.8	−0.28	66
H^+ (mol/L)	5.5	5.3	−0.17	66

6.3.4.4.Relationship between water quality and $K_{d(a)\text{-}SS}$

To understand the relationship between major water quality parameters and $K_{d(a)\text{-}SS}$ in rivers, Fig. 6.10 shows the relationship of $K_{d(a)\text{-}SS}$ to water quality parameters such as pH, EC, SS, DOC, K^+, and NH_4^+ sampled in August 2017 [6.22]. Additionally, Table 6.9 presents the result of regression analyses. The best correlation was found with EC, followed by NH_4^+ and SS. However, the relationship to EC should not be overstated since there are also correlations amongst these parameters. In most cases, EC increases with increasing concentrations of suspended sediments, which has also an influence on the potassium concentrations. There are also correlations between ammonium concentrations, pH and DOC. A multiple regression analysis using the water quality dataset indicates that EC has the greatest influence on $K_{d(a)\text{-}SS}$ (t-value = –2.8, p-value = 0.01, n = 43; Table 6.10).

To examine the validity of the relationship between $K_{d(a)\text{-}SS}$ and EC, a double logarithmic plot was developed merging the data measured after the FDNPP accident [6.38, 6.41, 6.42, 6.49] with the data described above (Fig. 6.11). The correlation is lower for the merged data, however, $K_{d(a)\text{-}SS}$ still shows a significant negative correlation with EC (R = −0.42, $p < 0.001$, n = 106). Therefore, EC appears to be an important factor controlling the sorption-desorption processes of radiocaesium on suspended solid particles.

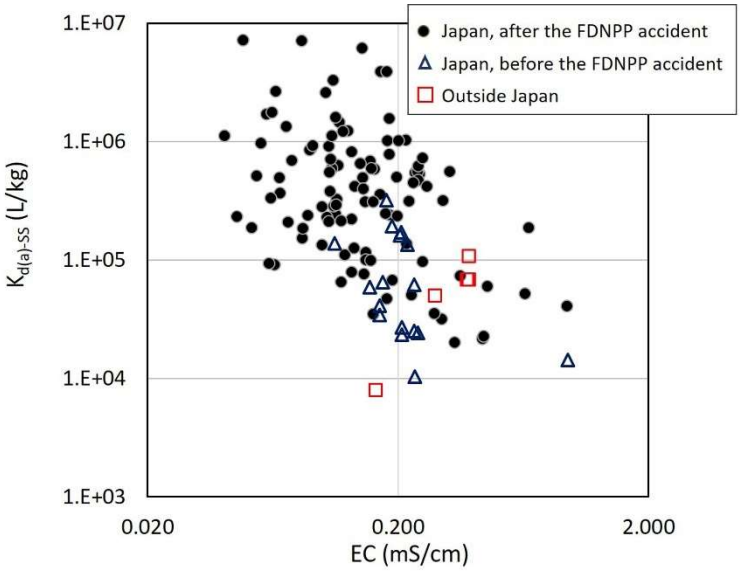

FIG. 6.9. Relationship between $K_{d(a)\text{-}SS}$ and EC in the rivers as observed in Japan before (empty blue triangles, [6.60, 6.63, 6.75]) and after (solid circles, [6.22, 6.38, 6.41, 6.42, 6.49]) the FDNPP accident and elsewhere outside Japan [6.28, 6.70].

In addition, the relationship between $K_{d(a)\text{-}SS}$ and EC in reservoirs in the evacuation order zone also has a significant negative correlation (*Fig. 6.3.5*) [6.41] (R = −0.63, p<0.001, n = 45). The values of $K_{d(a)\text{-}SS}$ in the reservoirs are generally lower than in the rivers, but the negative correlation between $K_{d(a)\text{-}SS}$ and EC in reservoirs is more pronounced than in rivers as shown by the slope of regression line in Fig.6.3.5 (reservoirs: −1.5, merged data in rivers: −0.92). In

addition to the difference in residence time of particles affecting the extent to which equilibrium is achieved between rivers and reservoirs, the difference in characteristics of suspended solids in rivers and reservoirs such as particle size distribution and organic content might affect the relationship between $K_{d(a)\text{-}SS}$ and EC.

TABLE 6.10. STATISTICAL VALUES OF A MULTIPLE REGRESSION ANALYSIS USING WATER QUALITY PARAMETERS TO EXPLAIN THE VALUES OF $K_{D(A)\text{-}SS}$ AT NORMAL FLOW RATES OF THE RIVERS IN EAST JAPAN

Water quality parameter [a]	Result of statistical test on correlation of $K_{d(a)\text{-}SS}$	
	t-value	*p*-value
EC (mS/cm)	−2.8	0.010
NH_4^+(mg/L)	−1.4	0.18
SS (mg/L)	−1.2	0.24
K^+ (mg/L)	0.50	0.62
DOC (mg/L)	−0.31	0.76
H^+(mol/L)	−0.06	0.95

[a] The analysis was conducted using data collected in 43 monitoring sites, except for the points where no NH_4^+ was detected

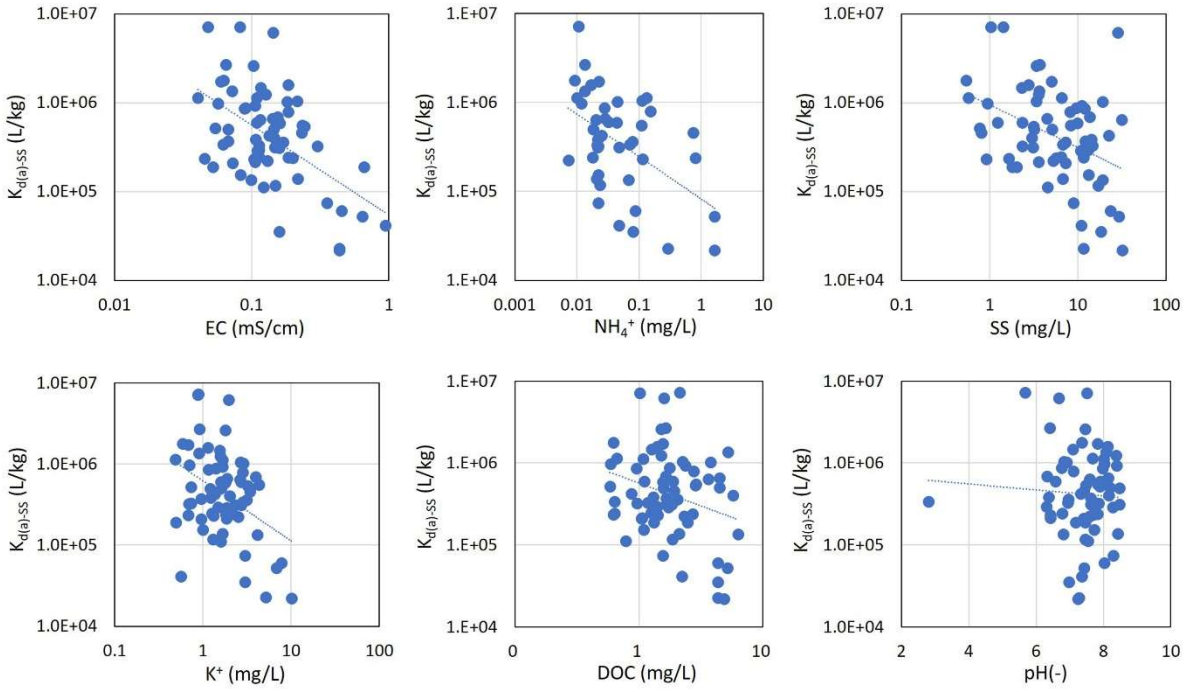

FIG. 6.10. Relationship between water quality parameters and $K_{d(a)\text{-}SS}$ during normal flow conditions for rivers in the East of Japan.

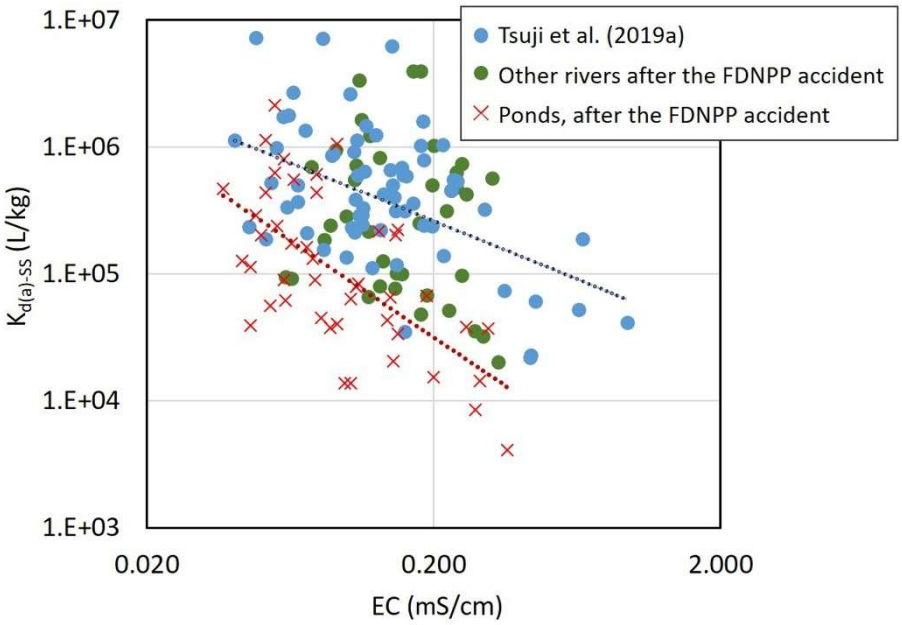

FIG. 6.11. Relationship between $K_{d(a)-SS}$ and EC in the rivers in the area affected by the FDNPP accident: Comparison with other data measured in rivers and ponds. The dashed blue and red lines show the regression between $K_{d(a)-SS}$ and EC for all data in rivers and ponds estimated by Tsukada et al [6.41] after the FDNPP accident, respectively.

6.3.5. Summary and limitations

$K_{d(a)-SS}$ values have been determined from concentrations of dissolved and suspended-sediment-bound ^{137}Cs in freshwaters of Fukushima Prefecture.

- The $K_{d(a)-SS}$ values determined for monitoring sites of the Abukuma River and tributaries and for rivers of the coastal regions span more than two orders of magnitude with most values within a range of 10^5 to 10^6 L/kg. A significant time trend could not be identified;

- The relationship of $K_{d(a)-SS}$ values with water quality parameters such as pH, electrical conductivity (EC), dissolved organic carbon (DOC), inorganic cations and anions was explored. The strongest correlation was found with EC, followed by NH_4^+ and SS;

- $K_{d(a)-SS}$ values tended to decrease with an increase of the river flow rate and the related increase of the suspended sediment concentration. The electrical conductivity increases with increasing concentrations of suspended sediments;

- The $K_{d(a)-SS}$ values for the mainstream of the Abukuma River and the rivers in the coastal region are similar (geometric mean ≈ 2.5×10^5 L/kg), whereas the mean of the values of the tributaries of the Abukuma River was a factor of 2 higher;

- For radiocaesium data reported before 2011, the Japanese $K_{d(a)-SS}$ values for suspended sediments had a geometric mean of 5×10^4 L/kg which was not significantly different from the combined global data. The GM values of $K_{d(a)-SS}$ (n = 513) for three sampling

situations reported in Japan after the FDNPP accident in Fukushima Prefecture were 5–10 fold higher than the small number of $K_{d(a)\text{-}SS}$ values (n = 20) measured before the FDNPP accident. However, it doesn't imply a clear change in $K_{d(a)\text{-}SS}$ before and after the FDNPP accident because the range of post-accident values was 2–3 orders of magnitude with minima in the order of 10^3 indicating that the pre-accident values were within the log normal distributions for Japanese data. Overall, it is clear that the $K_{d(a)\text{-}SS}$ values within the MODARIA dataset for radiocaesium with GM = 1.35×10^5 (L/kg) and GSD = 2.67 are similar and consistent with those reported in Japan both before and after the FDNPP accident.

6.4. UPTAKE OF RADIOCAESIUM BY FRESHWATER FISH

6.4.1. Introduction

The radioisotope ^{137}Cs is the most important radionuclide in the aquatic environment. With its long half-life of 30.2 y, it is persistent in the environment and is effectively taken up by aquatic organisms. The contamination of freshwater fish is a concern to the public in Fukushima Prefecture and neighbouring prefectures in Japan. Radiocaesium activity concentrations in some species in the contaminated areas still exceeded 100 Bq/kg FM (the Japanese limit of radiocaesium in most food) seven years after the Fukushima Daiichi FDNPP accident.

Radiocaesium uptake by freshwater fish and its time-dependence is quantified by the concentration ratio, *CR* (ratio of the activity concentration in biota and the total activity concentration in water, see chapter 2). *CR* is an empirical parameter that combines all possible uptake routes from water to biota including uptake of water, sediments and feed (plant or animal feed). It is widely used to quantify radionuclide transfer in aquatic ecosystems and to estimate the potential risks due to consumption of fish harvested in contaminated ecosystems [6.72, 6.77]. *CR* is used in many radioecological models to estimate uptake of radionuclides by aquatic organisms (see e.g. [6.78]).

This section summarizes *CR* values for ^{137}Cs for freshwater organisms calculated from observations in rivers and lakes in the surroundings of the FDNPP [6.79–6.82]. For fish species, the values are compiled by their functional feeding groups. Values are given for rivers and lakes separately because the *CR* values have been reported to differ between these two types of aquatic systems [6.83]. Differences in *CR* values for ^{137}Cs are discussed and compared with data obtained before the FDNPP accident [6.84] to optimize monitoring activities of aquatic organisms after radionuclide releases to freshwater bodies.

6.4.2. Data collection

The data to derive *CR* values for ^{137}Cs were mainly taken from a dataset provided by the Ministry of the Environment (MOE). Measurements of ^{137}Cs have been carried out in Fukushima Prefecture since 2011 within a monitoring program "Radioactive Material Monitoring Surveys of the Water Environment" [6.85]. Additional, reported *CR* fish data ([6.24, 6.86–6.88]) were also included in the analysis.

All *CR* values were calculated using ^{137}Cs activity concentration in fish measured as whole-body samples. The *CR* values were calculated using the total ^{137}Cs in water, including both dissolved and particulate forms, so the estimates are lower than *CR* values that have been derived using only the dissolved ^{137}Cs activity concentrations in water.

6.4.3. Concentration Ratios for freshwater biota before the FDNNP accident

Table 6.11 presents compiled *CR* values for ^{137}Cs for various freshwater organisms reported in IAEA-TECDOC-1616 [6.84] to summarize the data available before the FDNPP accident. An increase in CR values was found according to the increase of trophic level from the difference in the value between forage and piscivorous fish. From the comparison of CR values between adult frogs and tadpoles, there might be a significant difference in radiocaesium transfer for these two life-stages as pointed by Tagami et al. [6.89]. Tadpoles are generally thought to be herbivorous or detritivorous, whereas adult frogs are carnivorous.

TABLE 6.11. SUMMARY OF CR VALUES FOR ^{137}CS FOR FRESHWATER BIOTA BEFORE THE FDNNP ACCIDENT (IAEA, 2009)

Type of aquatic organisms	Tissue	N	Concentration ratio *CR* (L/kg FM)			
			GM/AM[a]	GSD/SD	Min	Max
Freshwater Fish						
Benthic Fish	Muscle	17	1400	2.2	160	3100
	Whole	11	2000	1.9	480	4400
Forage Fish	Muscle	12	1400	2.2	140	2200
	Whole	43	980	2.6	75	5200
Piscivorous Fish	Muscle	78	3100	2.5	260	15000
	Whole	91	5300	2.2	240	24000
Primary Producers		26	87	16	1.8	3300
Algae and Plants						
Macrophytes (generic)		3	390	4	170	2000
Floating-leafed Macrophytes		2	360	300	150	570
Emergent Macrophytes		16	27	8.8	1.8	1400
Freshwater Invertebrate		29	23	75	0.0054	6100
Invertebrate (edible)		20	15	120	0.0054	6100
Molluscs	Soft tissue	1	300			
Herpetofauna						
Tadpole	Whole	3	3000	1.3	2500	4000
Frog	Muscle	2	260	1.2	170	340
Frog (carcass)		2	210	64	160	250
Reptile (carcass)		9	280	1.3	130	500

[a] The arithmetical mean, AM, and the standard deviation (SD) are given if the number of observations (N) is 2

6.4.4. Concentrations ratios for different fish species after the FDNPP accident

The time trends of *CR* values for freshwater fish are given separately for lakes and rivers in Fig. 6.12 and Table IV.1. Additionally, Table IV.2 presents the time trends of ^{137}Cs activity concentrations in fish. Fish species were classified into four feeding functional groups (herbivore, planktivore, omnivore, piscivore) based on their predominant food source.

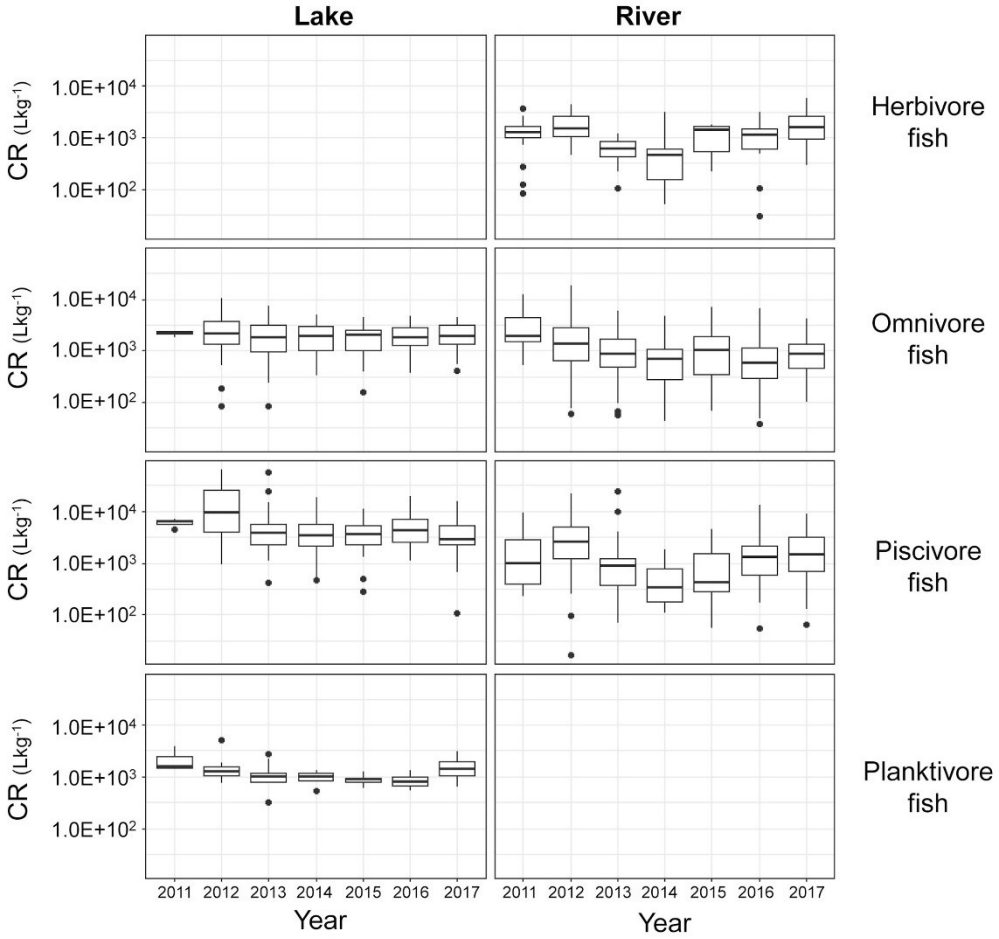

FIG. 6.12. CR values of ^{137}Cs for freshwater fish in different functional feeding groups sampled from 2011 to 2017. Dark horizontal lines represent median. Boxes represent 25th and 75th percentiles. Whiskers represent 5th and 95th percentiles. Dots indicate outliers.

Piscivorous species consume other fish and include masu salmon (*Oncorhynchus masou*), smallmouth bass (*Micropterus dolomieu*), largemouth bass (*Micropterus salmoides*), whitespotted char (*Salvelinus leucomaenis*), Japanese catfish (Silurus asotus), channel catfish (*Ictalurus punctatus*) and Japanese eel (*Anguilla japonica*).

Omnivorous species consume a diverse range of feed. Many species are within this category including crucian carp (*Carassius auratus langsdorfii*), Japanese dace (*Tribolodon hakonensis*), Japanese barbel (*Hemibarbus barbus*) and *Rhinogobius* spp.

Herbivorous species graze on macroalgea and macrophytes: only the ayu, *Plecoglossus altivelis*, was assigned to this category.

Planktivorous species consume plankton; only pond smelt, or wakasagi in Japanese, (*Hypomesus nipponensis*) was assigned to this category.

For both rivers and lakes, clear time trends in the *CR* values could not be identified for the functional groups. In lakes, an increase in *CR* values was found according to the increase of trophic level from planktivore to piscivore. There was a tendency for *CR* to decline after

reaching the highest level in 2011 or 2012 for every functional feeding group in both lakes and rivers.

Figure 6.13 and Table 6.12 show *CR* values for ^{137}Cs for various fish species which are important for fishery concerns. *CR* values were relatively stable over the five years since the FDNPP accident. Therefore, *CR* values for each fish species were calculated from measurements from 2016. Table 6.13 summarizes ^{137}Cs activity concentrations for species from 2016 to 2017.

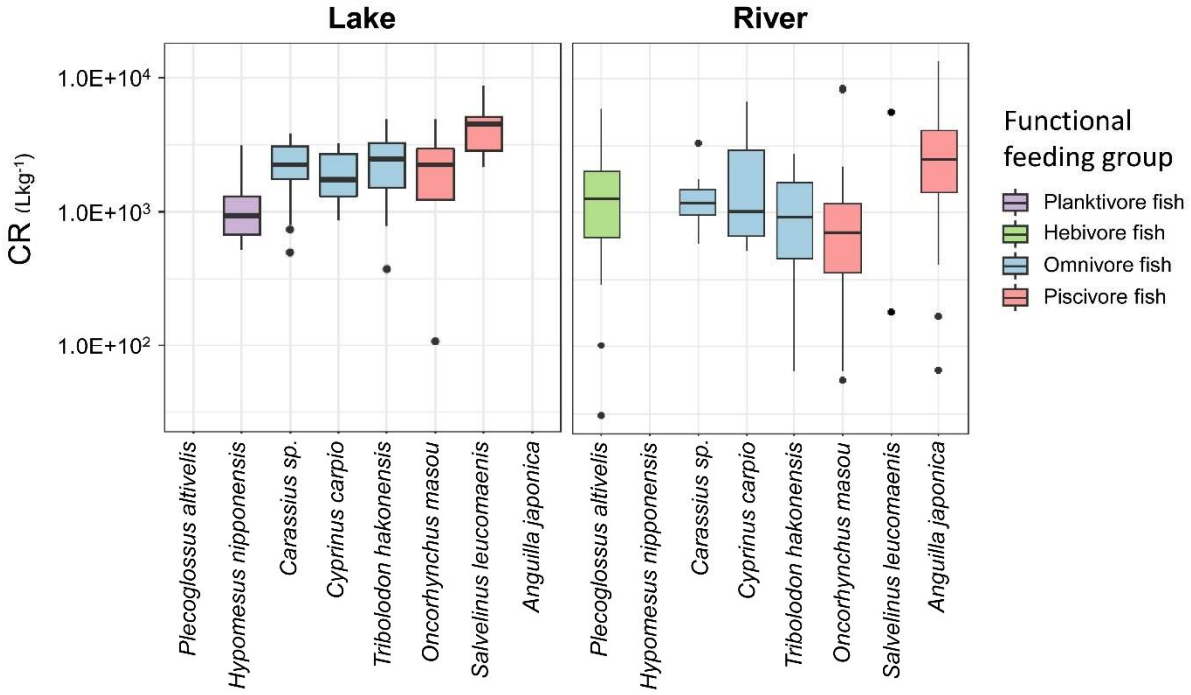

FIG. 6.13. CR values for ^{137}Cs of different species that are important for fisheries (2016–2017). Colours indicate fish functional feeding group. Dark horizontal lines represent median. Boxes represent 25th and 75th percentiles. Bars extend to 5th and 95th percentiles. Dots indicate outliers.

6.4.5. Fish size effect on concentration ratios

To clarify the effect of fish size on CR values for ^{137}Cs for various fish species in lakes, ponds and rivers a linear regression analysis using log-transformed was carried out for CR and fresh weight in fish (Table 6.14) [6.82, 6.90] . Additional data from a survey of fish in forest rivers and irrigation ponds within the designated evacuation zone in Fukushima [6.91] were incorporated into the analysis. The estimated regression parameters suggest that the effect of body size on the CR varied with fish species and ecosystem type. The effect of size was apparent for both lake and pond fish. There was a strong positive correlation between the CR and fish size for every piscivore, especially for Japanese catfish (slope = 0.80). Lake and pond cyprinids also had significant positive correlations between the CR and size with relatively similar slopes and intercepts (slope range: 0.19–0.37; intercept range: 5.1–6.5). For riverine fish, significant positive correlations between the CR and size were observed for *Oncorhynchus masou*, *Salvelinus leucomaenis*, and *Ictalurus punctatus.* No correlation between the CR and size was

observed in any other riverine omnivore or herbivorous fish species except for *Hemibarbus barbus* ($p = 0.02$) and *Tribolodon hakonensis* ($p = 0.002$).

TABLE 6.12. ACTIVITY CONCENTRATION RATIO OF ^{137}CS FOR IMPORTANT FISHERY SPECIES (2016–2017)

Fish species	Water body	Activity concentration ratio *CR* (L/kg FM)							
		N	Median	AM	ASD	GM	GSD	Min.	Max.
Plecoglossus altivelis	River	31	1300	1600	1300	1100	2.9	30	5900
Hypomesus nipponensis	Lake	10	940	1200	760	1000	1.7	520	3100
Carassius sp.	Lake	25	2200	2300	940	2000	1.7	500	3800
Carassius sp.	River	8	1200	1400	840	1200	1.7	580	3300
Cyprinus carpio	Lake	8	1700	2000	910	1800	1.6	870	3200
Cyprinus carpio	River	8	1000	2200	2300	1400	2.7	520	6700
Tribolodon hakonensis	Lake	26	2500	2500	1200	2200	1.8	370	4800
Tribolodon hakonensis	River	46	920	1100	690	820	2.3	64	2700
Oncorhynchus masou	Lake	8	2200	2300	1500	1600	3.3	110	4800
Oncorhynchus masou	River	22	700	1400	2300	650	3.6	56	8400
Salvelinus leucomaenis	Lake	16	4500	4400	1600	4100	1.5	2200	8600
Salvelinus leucomaenis	River	2	2900	2900	3800	1000	11	180	5600
Anguilla japonica	River	21	2500	3000	3000	1800	3.4	65	13000

TABLE 6.13 ACTIVITY CONCENTRATION OF ^{137}CS FOR SPECIES IMPORTANT FOR FISHERIES. MEASUREMENTS MADE IN 2016–2017.

Fish species	Water body	Activity concentration of ^{137}Cs in fish (Bq/kg FM)							
		N	Median	AM	ASD	GM	GSD	Min.	Max.
Plecoglossus altivelis	River	31	44	56	43	39	3	3	170
Hypomesus nipponensis	Lake	10	17	22	13	19	2	9	48
Carassius sp.	Lake	25	25	30	20	24	2	6	82
Carassius sp.	River	8	36	130	160	55	4	11	360
Cyprinus carpio	Lake	8	29	28	13	25	2	10	48
Cyprinus carpio	River	8	160	270	400	86	6	7	1200
Tribolodon hakonensis	Lake	26	29	30	14	26	2	11	67
Tribolodon hakonensis	River	46	19	60	100	23	3	4	350
Oncorhynchus masou	Lake	8	33	32	18	22	4	1	58
Oncorhynchus masou	River	22	11	41	83	12	5	1	320
Salvelinus leucomaenis	Lake	16	42	43	14	42	1	27	86
Salvelinus leucomaenis	River	2	23	23	31	8	11	2	45
Anguilla japonica	River	21	110	300	540	98	5	5	2400

TABLE 6.14. STATISTICAL VALUES FOR THE RELATIONSHIP BETWEEN LOG-TRANSFORMED FISH BODY SIZE AND CR VALUES FOR ^{137}CS

Fish species	Tissue	Slope	Intercept	*p*-value	R^2	N
River						
Oncorhynchus masou (Forest river)	Muscle	0.34	7.6	<0.001	0.12	157
Oncorhynchus masou (Middle and downstream)	Whole	0.27	5.3	0.03	0.07	62
Salvelinus leucomaenis (Forest River)	Muscle	0.61	6.7	<0.001	0.33	135
Micropterus dolomieu	Whole	0.06	6	0.72	0.005	27
Silurus asotus	Whole	0.19	6.2	0.09	0.13	23
Ictalurus punctatus	Whole	0.74	1.8	0.005	0.53	13
Anguilla japonica	Whole	0.10	6.8	0.52	0.02	29
Hemibarbus barbus	Whole	0.23	5.3	0.04	0.15	29
Carassius sp.	Whole	0.07	7.3	0.46	0.03	23
Cyprinus carpio	Whole	0.08	6.2	0.58	0.02	22
Tribolodon hakonensis	Whole	−0.17	7.2	0.002	0.07	123
Misgurnus anguillicaudatus	Whole	−0.31	7.3	0.12	0.05	52
Rhinogobius sp.	Whole	−0.05	6.9	0.66	0.003	61
Plecoglossus altivelis	Whole	−0.05	7.6	0.61	0.004	59
Lake						
Oncorhynchus masou	Whole	0.45	5.2	<0.001	0.32	33
Salvelinus leucomaenis	Whole	0.41	5.7	<0.001	0.34	46
Micropterus dolomieu	Whole	0.46	5.5	<0.001	0.4	65
Micropterus salmoides	Whole	0.45	5.4	0.001	0.76	9
Silurus asotus	Whole	0.82	2.7	0.007	0.38	17
Hemibarbus barbus	Whole	0.19	6.4	0.03	0.11	46
Carassius sp.	Whole	0.27	6.1	<0.001	0.37	73
Cyprinus carpio	Whole	0.14	6.4	0.11	0.15	18
Tribolodon hakonensis	Whole	0.28	6.5	<0.001	0.37	69
Hypomesus nipponensis	Whole	−0.14	7.7	0.31	0.05	22
Irrigation pond						
Micropterus salmoides	Muscle	0.32	6.6	0.002	0.4	21
Common carp	Muscle	0.27	5.1	<0.001	0.59	36
Japanese crucian carp	Muscle	0.28	5.9	0.009	0.48	13
Silver crucian carp	Muscle	0.33	5.2	<0.001	0.32	101

6.4.6. Concentration ratios for other aquatic organisms

The time trends for ^{137}Cs *CR* values of other freshwater aquatic organisms (vegetative litter, aquatic plants, periphytons, planktons, snails, crustaceans, aquatic insects, amphibian adults and larvae) are shown in Fig.6.14 and Table IV.3.

Table IV.4 shows data on time trends of ^{137}Cs activity concentrations for freshwater aquatic organisms from 2011 to 2017. Aquatic plants include submerged and emergent species. Aquatic insects include larvae of order Odonata, Megaloptera, Plecoptera, Ephemeroptera and Trichoptera. Crustaceans include freshwater crab, shrimp, and crayfish. The *CR* values for snails were only calculated from data for the freshwater snail *Semisulcospira libertina*. The dominant amphibian adult species are newts and Rana *spp*.; amphibian larvae include only tadpoles. The ^{137}Cs activity concentrations generally tended to decline each year, except for periphytons. However, a significant time trend of *CR* values could not be identified for any of the categories, except for litter which significantly decreased in both lakes and rivers.

6.4.7. Detailed analysis for radiocaesium transfer to lake fish

6.4.7.1.Description of fish data and sampling sites

Large amounts of data have been compiled for Wakasagi in lakes [6.92] located in areas with relatively high radionuclide depositions of Fukushima, Tochigi and Gunma Prefectures. These data are listed in Table 6.15. Wakasagi is a plankton-feeding fish (common length of adult fish: 15 cm, majority of this species live about 1 year, some can survive for 2–3 years). Changes in ^{134}Cs and ^{137}Cs activity concentrations in water are well reflected in variations of radiocaesium activity concentrations in Wakasagi [6.81]. The data on radiocaesium activity concentrations in freshwater fish were extracted from an open data source on radioactivity in fish [6.92]. The characteristics of the lakes are described in reports by Fukushima and Arai [6.93] and Suzuki et al. [6.81]. The locations of these lakes are shown in Fig. 6.15.

TABLE 6.15. CHARACTERISTICS OF LAKES USED FOR FISH STUDIES

Prefecture	Lake	Altitude (m)	Lake area (km^2)	Mean water depth (m)	Mean water retention time (year)
Fukushima	Akimoto	736	3.9	9.9	0.26
	Hibara	822	10.4	12.0	0.83
	Onogawa	797	1.4	7.9	0.058
Tochigi	Chuzenji	1269	11.5	94.6	6.5
Gunma	Akagi-Onuma	1345	0.83	9.1	2.3
	Haruna	1084	1.24	8.1	—

— no data

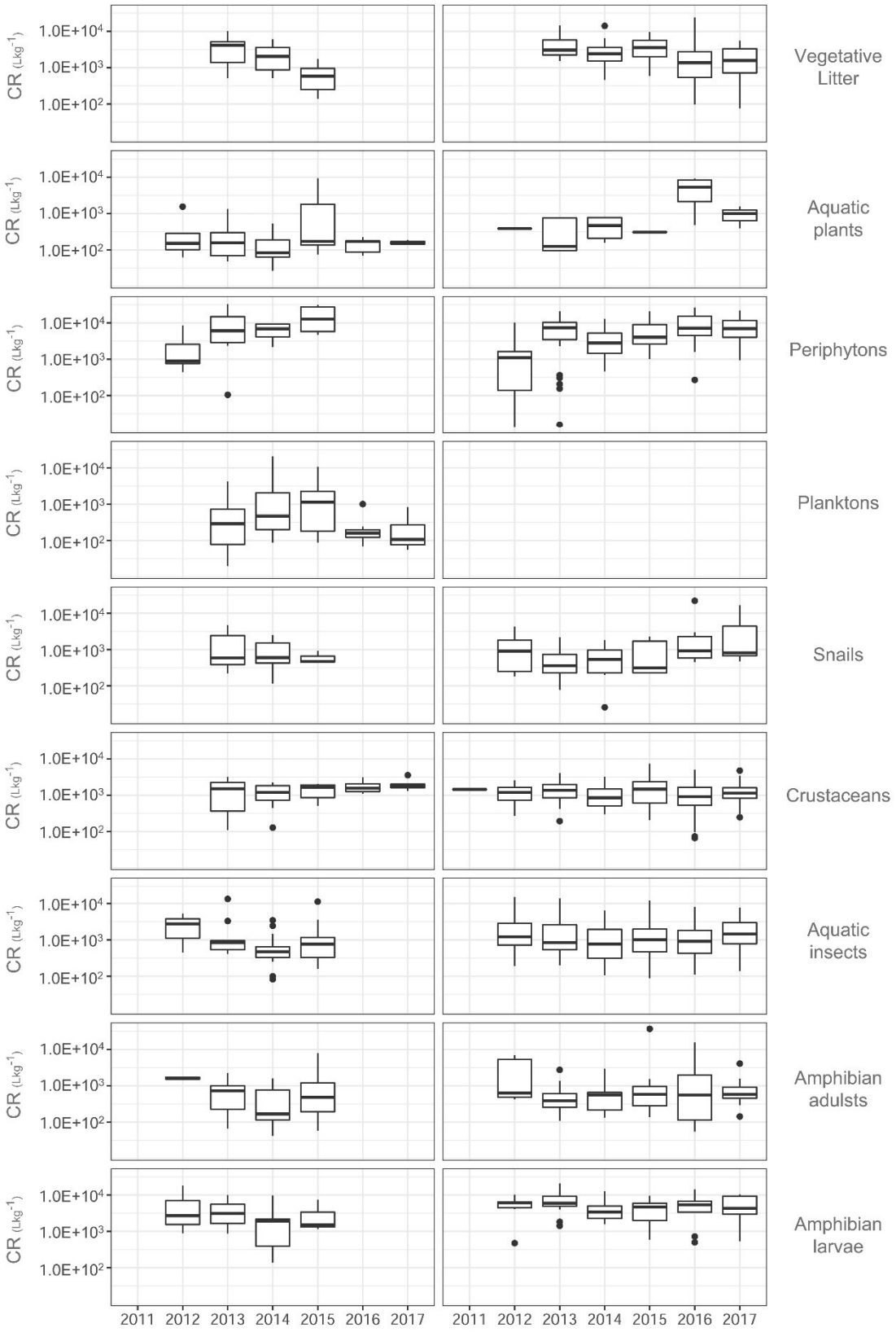

FIG. 6.14. CR values for ^{137}Cs for freshwater organisms from 2011 to 2017. Dark horizontal lines represent median. Boxes represent 25th and 75th percentiles. Whiskers represent 5th and 95th percentiles. Dots indicate outliers.

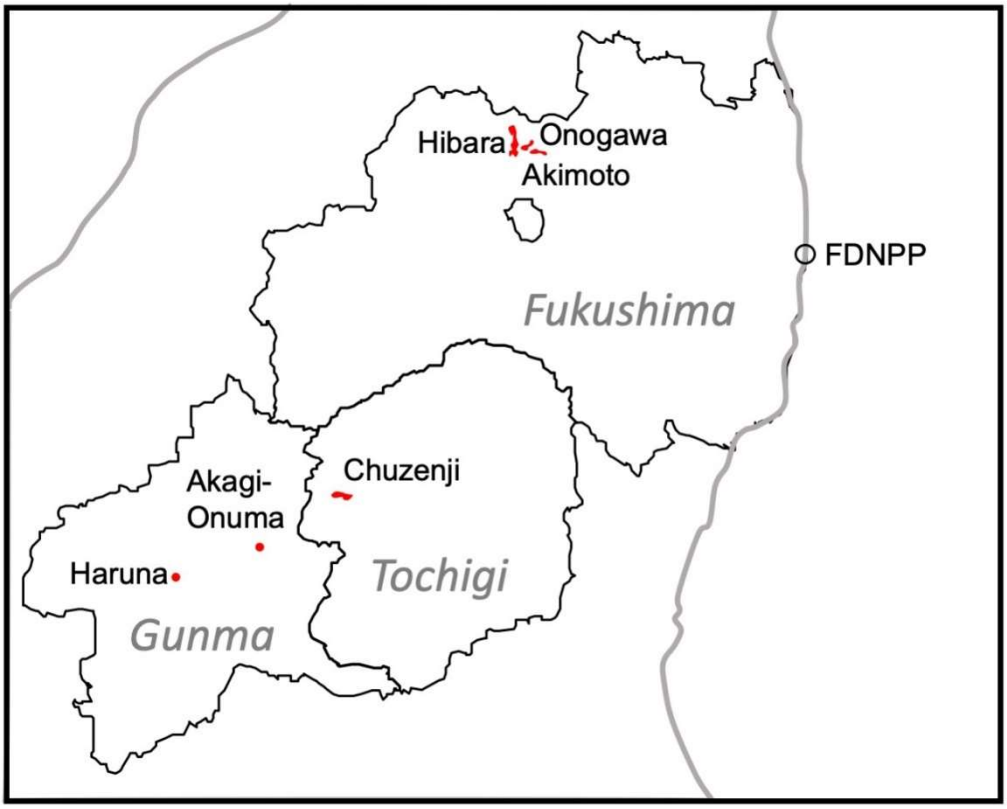

FIG. 6.15. Locations of lakes (indicated by red spots) used for fish studies.

The following *CR* values were reported for aquatic organisms in these lakes [6.86]:

- Wakasagi: 890 ± 200 L/kg;
- Pale chub: 1800 ± 250 L/kg;
- Japanese dace: 2000 ± 580 L/kg;
- Phytoplankton: 720 ± 110 L/kg;
- Zooplankton: 40 ± 14 L/kg.

The *CR* values for fish and zooplankton were within the range of previously reported values [6.72, 6.94]. The phytoplankton *CR* values were five-fold higher than that previous reported by Yankovich et al. [6.94].

A range of factors cause variations in ^{137}Cs activity concentrations in lake fish. Observations made in 2012–2015 indicated a positive correlation between the body mass of Wakasagi and the *CR,* but not in 2016 [6.95]. Other factors influencing the *CR* for fish were feeding habits, retention time of lake water, and variations in ^{137}Cs activity concentrations in lake water [6.81].

6.4.8. Comparison of ^{137}Cs concentration ratios before and after the FDNPP accident

To compare the transfer of ^{137}Cs from water to freshwater fish or other organisms before and after the FDNPP accident, the ^{137}Cs *CR* values from 2015 to 2017 are listed in Table IV.1 and Table IV.3. The data were statistically analysed according to the classification in Table 6.11, because the CR values were relatively stable after 2015. All fish species monitored after the

FDNPP accident are classified as benthopelagic or benthic except for *Hyposesus nipponensis* (Japanese smelt). Because both fish types include piscivorous and non-piscivorous species, the comparison focused on whether fish were piscivorous or not without attributing them to the benthic group. Table 6.16 shows that the geometric mean values for algae and invertebrates in Fukushima prefecture are clearly higher than those obtained before the FDNPP accident. For algae, the measured radiocaesium activity concentrations of sampled periphytons may often include fine clay particles with high radiocaesium activity concentrations due to the difficulty in completely removing such particles from periphytons during sample preparation. For invertebrates, the influence of the low minimum *CR* value (0.005) makes the comparison difficult. Otherwise, there are no significant differences for pre- and post-FDNPP accident data for all trophic levels.

TABLE 6.16: COMPARISON OF PRE- AND POST-FUKUSHIMA (2015–2017) ACCIDENT *CR* VALUES FOR ^{137}CS FOR FRESHWATER ORGANISMS

Aquatic organisms	Pre-accident CR (L/kg FM)					Aquatic organisms	Post-accident CR (L/kg FM)				
	N	GM	GSD	Min.	Max.		N	GM	GSD	Min.	Max.
Algae											
Various type of algae	5	960	2.4	430	3300	Periphytons	72	5900	2.5	270	32000
Macrophytes	3	390	4.0	170	2000	Aquatic plants	27	430	4.8	68	9300
Invertebrates [a]											
Freshwater invertebrates	20	23	75	0.005	6100	Crustaceans	146	1000	2.4	66	7400
						Aquatic insects	175	980	2.9	87	12000
Molluscs (soft tissue)	1	320				Molluscs	21	1100	3.6	226	22000
Amphibian [a]											
Tadpole	3	3000	1.3	2500	4000	Tadpole	34	3300	2.8	500	22000
Frog	2	210	64	160	250	Frog	47	700	3.9	54	37000
Fish [a]											
Benthic	11	2000	1.9	480	4400	Benthic fish	104	520	2.6	49	3900
Non-piscivorous (Forage)	43	980	2.6	75	5200	Bentho-pelagic fish	420	1000	2.6	39	7000
						Pelagic fish	10	19	1.7	9	48
Piscivorous	91	5300	2.2	240	24000	Bentho-pelagic fish	136	1800	3.4	54	11000
						Benthic fish	60	2000	3.1	65	19000

[a] The CR values of invertebrates, tadpole, frog, and fish were whole-body samples in both TECDOC-1616 and the Fukushima data.
[b] The arithmetical mean and the standard deviation are given due to small sample size (N=2).

The time trends of ^{137}Cs *CR* values in freshwater organisms indicate that radiocaesium in freshwater fish had nearly reached equilibrium within 4–5 years after the FDNPP accident. The values are similar to those measured after the Chernobyl NPP accident.

Due to the persistent and continuing high transfer of ^{137}Cs to some important species for fisheries, some *CR* values have continued to exceed 1000. To predict the time-dependence of activity concentrations and *CR* in biota and develop effective measures for reducing radiocaesium activity concentration in fish, it is necessary to understand food web processes impacting on radiocaesium transfers to freshwater fish in more detail.

There was a clear difference between lakes and rivers; the classification of the ^{137}Cs *CR* values based on functional feeding group is considered a meaningful approach that will facilitate understanding of radiocaesium transfers through the aquatic food-web. Therefore, conducting a long-term comprehensive monitoring programme including all relevant transfer routes in freshwater ecosystems is essential to correctly understand the current situation and the future trend of the radiocaesium transfers in aquatic environments.

6.4.9. Summary and limitations

- After the FDNPP accident, the Ministry of the Environment of Japan (MOE) set up an extensive programme to monitor radiocaesium activity concentrations in fish, aquatic biota and water. The data set of MOE does not include additional information on variables such as potassium concentrations and dissolved organic matter of the monitored waters. The resulting MOE data set has been analysed together with data provided from additional field studies on the behaviour of radiocaesium in freshwater lake systems;
- The uptake of radiocaesium by fish and aquatic biota has been quantified using the concentration ratio *CR*. In both rivers and lakes, there is a clear decline in radiocaesium activity concentrations in fish, aquatic biota and water since the FDNPP accident in 2011. With a few exceptions, there is no decline in the *CR* values with time after 2015;
- Clear differences were reported in *CR* values of radiocaesium for aquatic organisms between lakes and rivers;
- Only in lakes, an increase in *CR* values in fish has been reported with trophic level from planktivorous (lowest) to piscivorous fish (highest);
- The effect of fish size on *CR* was demonstrated in river and lake piscivores. Additionally, most omnivores show a significant correlation of ^{137}Cs activity concentration with body size in lakes and ponds;
- *CR* values reported are in general agreement with global data and observations made in Japan before the FDNPP accident.

The analysis is based on data gained during monitoring programmes carried out by the Ministry of the Environment (MOE). The intention of these programmes is primarily the control of radiocaesium activity concentrations in aquatic foods rather than on the performance of scientific analysis. The MOE data set includes the pH-value but the study by Ishii et al. [6.90] showed that there is no correlation between the *CR* and pH. Additional data on water characteristics such as the concentrations of cations, anions, and dissolved organic matter were not obtained during the monitoring programme. Considering the competition between potassium and caesium, it is likely that further consideration of the relationship between the

potassium content of water and the *CR* for ^{137}Cs, would allow a more differentiated analysis of the data set.

Further data are also needed to understand the contribution of differences in the food web to the reported differences in *CR* values for organisms in lakes and rivers.

6.5. EFFECTIVE HALF-LIVES OF RADIOCAESIUM IN LAKE BIOTA

Freshwater fish are traditional foods and important components of the diet in Japan. Therefore, it is important to study the long-term impact and dynamics of radiocaesium in lakes, as well as rivers, coastal areas and oceans. Information outlined here on the dynamics of radiocaesium in lakes with watersheds contaminated by radiocaesium is essential for the population and authorities to appropriately evaluate the impact of the deposited radiocaesium.

Due to low ^{137}Cs activity concentrations in freshwaters, originating from global weapons' fallout, before the FDNPP accident, no detailed study had been carried out in lake environments in Japan. After the FDNPP accident, quantification and prediction of changes with time in components of freshwater systems provided useful information for fishermen, citizens and local governments. The reported data can be used by authorities to make decisions on the suitability of lifting restrictions on fishing and other uses of aquatic systems.

The time-dependence of the ^{137}Cs activity concentration is quantified by the T_{eff} as defined in chapter 2 using open data source information on radiocaesium in fish [6.92]. Before the FDNPP accident, the ^{137}Cs activity concentration in Wakasagi was approximately 1.0–1.4 Bq/kg (FM) at Lake Akagi-Onuma in August 2007 and 2010 and January 2011 [6.81]. There was a sharp increase in radiocaesium activity concentrations in this fish species following the FDNPP accident. The first measurements of radiocaesium in fish were carried out in Hibara lake, Fukushima Prefecture in early May 2011. The subsequent decrease with time after the accident on 11 March 2011 is shown for three lakes in Fig. 6.16. The ^{137}Cs activity concentrations and the rates of decrease differ slightly between lakes.

Equilibrium was almost reached between ^{137}Cs in freshwater fish such as Wakasagi and Japanese dace, and lake water approximately 2000 days (5.5 years) after the FDNPP accident. To describe the time trend of ^{137}Cs in fish, the data were approximated by a single exponential model (SEM) and also a double exponential–model (DEM). The two-component approach simulates the combination of a fast and a slow component [6.96, 6.97]. Table 6.17 shows the effective half-lives for both the single (T_{eff}) and the double exponential model ($T_{eff(fast)}$ and $T_{eff(slow)}$). In all six cases, a second components exists; however, the data are too sparse for a final evaluation, so the data were described by a single exponential model.

For pale chub and Wakasagi, in accordance with Suzuki et al., [6.81, 6.95], double exponential model approaches could be more appropriate. For pale chub, the analysis indicates $T_{eff(fast)}$ and $T_{eff(slow)}$ of 0.5 and 6.4 years, respectively. For Wakasagi and phytoplankton, the application of double exponential models suggests a long slow component with a half-life that is much longer than the observation period of five years. Due to the short observations period compared with the slow component of radiocaesium retention for both biota, these results are associated with large uncertainties and the numerical values are not meaningful for extended time periods. However, it indicates that $T_{eff(slow)}$ of Wakasagi may be long and that the long-term decline may be mainly controlled by the physical half-life, 30.2 y of ^{137}Cs. Since the slow component for Wakasagi and phytoplankton cannot be determined in a reliable manner, the numerical

values are not given in the table. In some European lakes, double exponential models developed for some species have been reported to have T_{eff} of 10 years and more [6.98, 6.99].

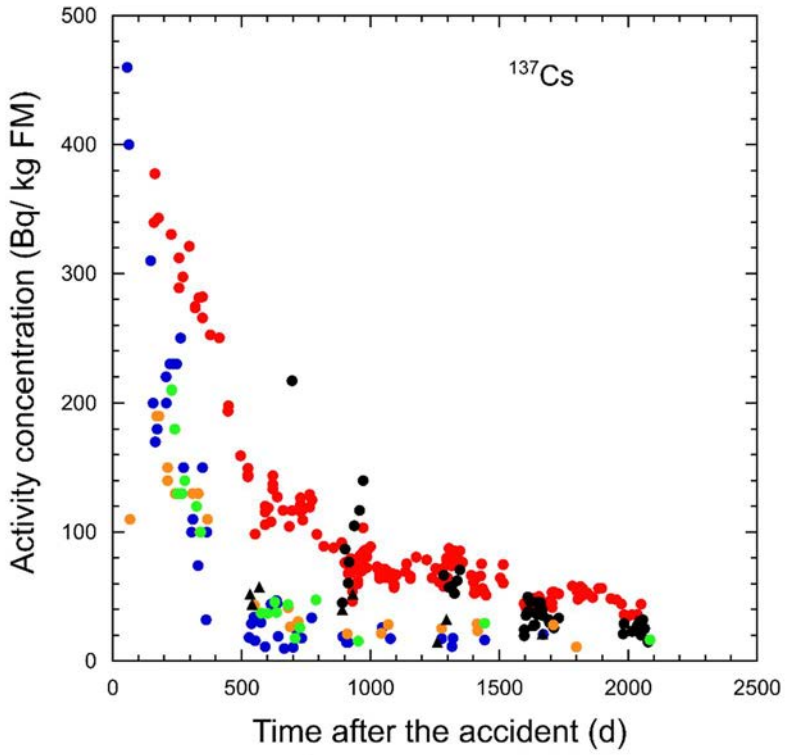

FIG. 6.16. Activity concentration of ^{137}Cs in Wakasagi fish in Gunma prefecture in L. Onuma (red circles) and L. Haruna (orange cicrles), in Fukushima Prefecture in L. Hibara (blue circles), L. Akimoto (orange circles) and L. Onogawa (green circles), in Tichigi Prefecture in L. Chuzenji (black triangles).

The biological half-lives of ^{137}Cs in aquatic organisms generally vary from 10–100 days [6.100]. Since the T_{eff} of ^{137}Cs in aquatic organisms are considerably longer than T_{biol}, the values determined for the T_{eff} mainly reflect the hydrological characteristics and the dynamic behaviour of ^{137}Cs in lakes. Important factors are the in- and outflow of water and ^{137}Cs, the concentration of suspended sediments, the deposition of ^{137}Cs sediments and the resuspension of ^{137}Cs from the bottom sediment, and water characteristics such as pH, and the concentrations of ammonium, potassium and calcium ions [6.81].

The data indicate the existence of a slow component to describe the time-dependence of ^{137}Cs which is much longer than the observation period of 5 years. Due to the short observation period, this component cannot be reliably estimated.

6.5.1. Summary and limitations

- The deposition of ^{137}Cs during the FDNPP accident caused a sharp increase of ^{137}Cs concentrations in water and aquatic organisms. In Japan, before the FDNPP accident, low ^{137}Cs activity concentrations originating from global weapons' fallout were observed in the freshwater environments;

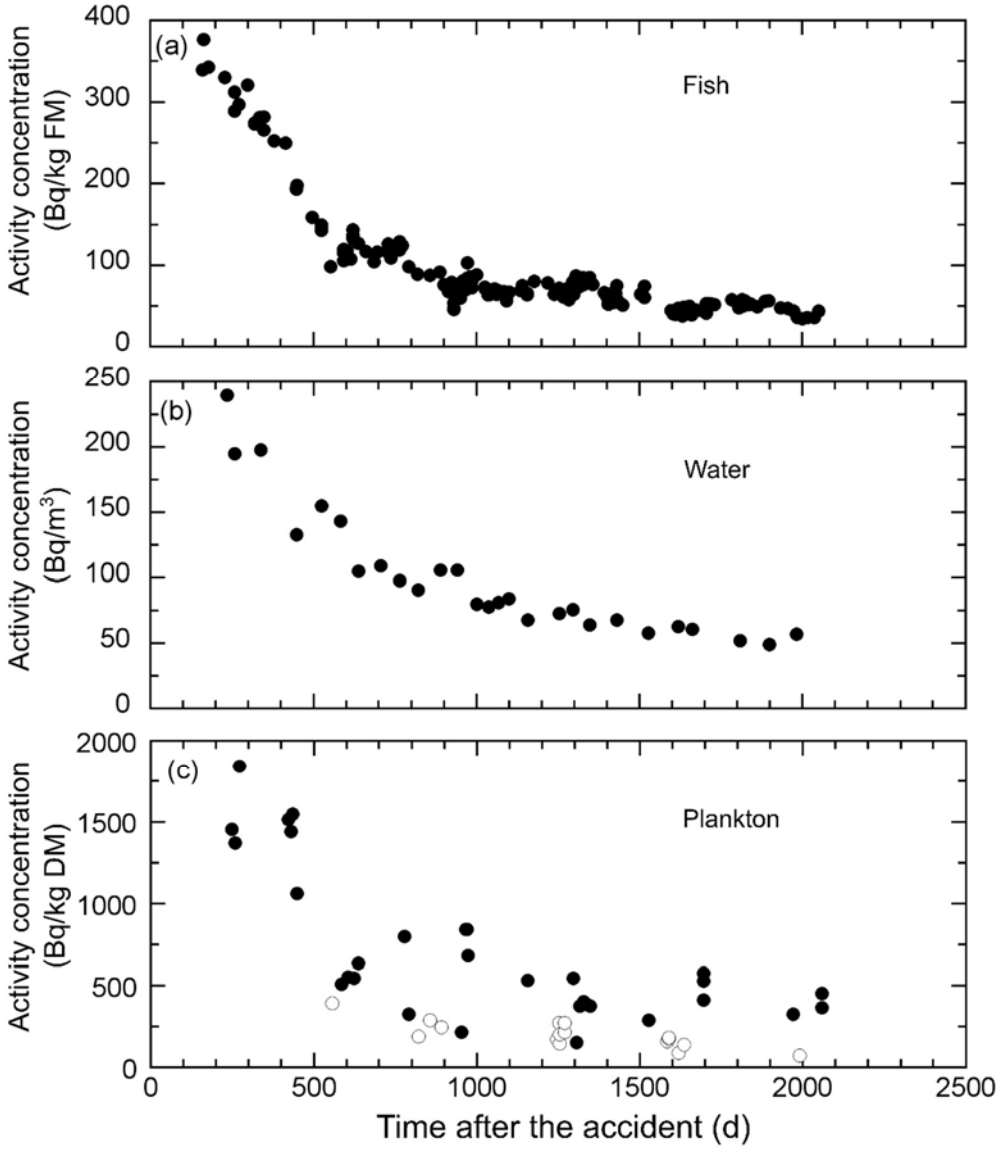

FIG.6.17. Activity concentrations of ^{137}Cs in Wakasagi (a), lake water (b) and plankton (c) in L. Akagi-Onuma as a function of time after the FDNPP accident. The closed and open circles in (c) indicate phytoplankton and zooplankton), respectively.

- Concentration ratios and effective half-lives of radiocaesium for three fish species, phyto- and zooplankton have been estimated from monitoring measurements carried out in 15 lakes located in areas affected by the deposition of radionuclides released during the accident in FDNPP;

- The *CR* values for three commonly eaten lake fish species, Wakasagi, Pale Chub and Japanese Dace, varied between 1000 and 2000 L/kg, with a coefficient of variation of about 15–30%. For phyto- and zooplankton, mean *CR* values were lower at 700 and 40 L/kg respectively;

TABLE 6.17. EFFECTIVE ECOLOGICAL HALF-LIFE OF ^{137}CS IN FRESHWATER FISHES IN LAKE AKAGI-ONUMA.

Species	Components of the exponential decline	T_{eff} or $T_{eff(fast)}$ (year)	$T_{eff(slow)}$ (year)
Wakasagi	Single	1.15	— [a]
	Double (fast and slow)	0.64	Much longer than the observation period [b]
Pale chub	Single	1.72	—
	Double (fast and slow)	0.49	6.4
Japanese dace	Single	2.46	—
Phytoplankton	Single	1.55	—
	Double (fast and slow)	0.74	Much longer than the observation period [b]
Zooplankton	Single	2.30	—

[a] no data
[b] derived from measurements with large variations

- The effective half-lives of ^{137}Cs in aquatic organisms, derived from monitoring measurements, reflect the importance of the hydrological characteristics of the lakes and the dynamic behaviour of ^{137}Cs in those lakes. The decline of ^{137}Cs concentrations from 2011 in most aquatic organisms can be described by a single exponential model (SEM) with effective half-lives in the range of 1.1 to 2.5 years, depending on the species considered;

- In some cases, the data indicated the existence of fast and slow components for describing the decline so a double exponential model (DEM) was applied. In this case, the fast component was equivalent to an effective half-life of 0.5 to 0.8 y. The slow component for Pale Chub is equivalent to a half-life of 6.4 years, whereas for Wakasagi and phytoplankton, the slow component does not indicate any dependence of the ^{137}Cs activity concentration on time. Longer observation periods would be needed to quantify longer time dependencies with more accuracy.

REFERENCES

[6.1] MATSUNAGA, T. et al., Characteristics of Chernobyl-derived radionuclides in particulate form in surface waters in the exclusion zone around the Chernobyl Nuclear Power Plant, J. Contam. Hydrol. **35** 1 (1998) 101.

[6.2] FUKUYAMA, T., TAKENAKA, C., ONDA, Y., 137Cs loss via soil erosion from a mountainous headwater catchment in central Japan, Sci. Total Environ. **350** 1–3 (2005) 238.

[6.3] WAKIYAMA, Y., ONDA, Y., MIZUGAKI, S., ASAI, H., HIRAMATSU, S., Soil erosion rates on forested mountain hillslopes estimated using 137Cs and 210Pbex, Geoderma **159** 1 (2010) 39.

[6.4] TERAMAGE, M.T. et al., The relationship of soil organic carbon to 210Pbex and 137Cs during surface soil erosion in a hillslope forested environment, Geoderma **192** (2013) 59.

[6.5] GOMI, T., SIDLE, R.C., MIYATA, S., KOSUGI, K., ONDA, Y., Dynamic runoff connectivity of overland flow on steep forested hillslopes: Scale effects and runoff transfer, Water Resour. Res. **44** 8 (2008).

[6.6] FUKUYAMA, T., ONDA, Y., TAKENAKA, C., WALLING, D.E., Investigating erosion rates within a Japanese cypress plantation using Cs-137 and Pb-210ex measurements, J. Geophys. Res. Earth Surf. **113** F2 (2008).

[6.7] FUKUYAMA, T. et al., Quantifying the impact of forest management practice on the runoff of the surface-derived suspended sediment using fallout radionuclides, Hydrol. Process. Int. J. **24** 5 (2010) 596.

[6.8] YOSHIMURA, K., ONDA, Y., KATO, H., Evaluation of radiocaesium wash-off by soil erosion from various land uses using USLE plots, J. Environ. Radioact. **139** (2015) 362.

[6.9] NISHIKIORI, T., ITO, S., TSUJI, H., YASUTAKA, T., HAYASHI, S., Influence of Forest Floor Covering on Radiocesium Wash-off Associated with Forest Soil Erosion, J. Jpn. For. Soc. **97** 1 (2015) 63.

[6.10] NIIZATO, T. et al., Input and output budgets of radiocesium concerning the forest floor in the mountain forest of Fukushima released from the TEPCO's Fukushima Dai-ichi nuclear power plant accident, Spec. Issue Radioact. Contam. For. Ecosyst. Chernobyl Fukushima **161** (2016) 11.

[6.11] TAKAHASHI, J., TAMURA, K., SUDA, T., MATSUMURA, R., ONDA, Y., Vertical distribution and temporal changes of 137Cs in soil profiles under various land uses after the Fukushima Dai-ichi Nuclear Power Plant accident, J. Environ. Radioact. **139** (2015) 351.

[6.12] TAKAHASHI, J., ONDA, Y., HIHARA, D., TAMURA, K., Six-year monitoring of the vertical distribution of radiocesium in three forest soils after the Fukushima Dai-ichi Nuclear Power Plant accident, J. Environ. Radioact. **192** (2018) 172.

[6.13] WAKIYAMA, Y., ONDA, Y., YOSHIMURA, K., IGARASHI, Y., KATO, H., Land use types control solid wash-off rate and entrainment coefficient of Fukushima-derived 137Cs, and their time dependence, Spec. Issue Five Years Fukushima **210** (2019) 105990.

[6.14] WISCHMEIER, W.H., SMITH, D.D., Predicting Rainfall Erosion Losses: A Guide to Conservation Planning, Department of Agriculture, Science and Education Administration (1978).

[6.15] IWAGAMI, S. et al., Temporal changes in dissolved 137Cs concentrations in groundwater and stream water in Fukushima after the Fukushima Dai-ichi Nuclear Power Plant accident, J. Environ. Radioact. **166** (2017) 458.

[6.16] YASUTAKA, T., KAWABE, Y., KUROSAWA, A., KOMAI, T., Monitoring Dissolved Radioactive Cesium in Abukuma River in Fukushima Prefecture, Japan (2013) 230.

[6.17] IWAGAMI, S. et al., Six-year monitoring study of 137Cs discharge from headwater catchments after the Fukushima Dai-ichi Nuclear Power Plant accident, J. Environ. Radioact. **210** (2019) 106001.

[6.18] SAKAI, M. et al., Radiocesium leaching from contaminated litter in forest streams, J. Environ. Radioact. **144** (2015) 15.

[6.19] IWAGAMI, S., ONDA, Y., TSUJIMURA, M., ABE, Y., Contribution of radioactive 137Cs discharge by suspended sediment, coarse organic matter, and dissolved fraction from a headwater catchment in Fukushima after the Fukushima Dai-ichi Nuclear Power Plant accident, J. Environ. Radioact. **166** (2017) 466.

[6.20] KATO, H. et al., Six-year monitoring study of radiocesium transfer in forest environments following the Fukushima nuclear power plant accident, J. Environ. Radioact. **210** (2019) 105817.

[6.21] YAMASHITA, M., EGUCHI, S., TATEISHI, T., TSUIKI, M., Species Difference and Yearly Change of Radioactive Cesium Concentration in Grasses, Jpn. J. Grassl. Sci. **62** 3 (2016) 134.

[6.22] TSUJI, H. et al., Factors controlling dissolved 137Cs concentrations in east Japanese Rivers, Sci. Total Environ. **697** (2019) 134093.

[6.23] YAMASHITA, R. et al., Temporal variation and source analysis of radiocesium in an urban river after the 2011 nuclear accident in Fukushima, Japan, J. Water Environ. Technol. **13** 2 (2015) 179.

[6.24] MATSUDA, K. et al., Comparison of radioactive cesium contamination of lake water, bottom sediment, plankton, and freshwater fish among lakes of Fukushima Prefecture, Japan after the Fukushima fallout, Fish. Sci. **81** 4 (2015) 737.

[6.25] MURAKAMI, M. et al., Occurrence and partition ratios of radiocesium in an urban river during dry and wet weather after the 2011 nuclear accident in Fukushima, Water Res. **92** (2016) 87.

[6.26] YOSHIMURA, K., SAITO, K., FUJIWARA, K., Distribution of 137Cs on components in urban area four years after the Fukushima Dai-ichi Nuclear Power Plant accident, J. Environ. Radioact. **178–179** (2017) 48.

[6.27] TANIGUCHI, K. et al., Transport and Redistribution of Radiocesium in Fukushima Fallout through Rivers, Environ. Sci. Technol. **53** 21 (2019) 12339.

[6.28] SANSONE, U., BELLI, M., VOITSEKOVITCH, O.V., KANIVETS, V.V., 137Cs and 90Sr in water and suspended particulate matter of the Dnieper River-Reservoirs System (Ukraine), Sci. Total Environ. **186** 3 (1996) 257.

[6.29] SUZUKI, Y. et al., Effect of the concentration of radiocesium dissolved in irrigation water on the concentration of radiocesium in brown rice, Soil Sci. Plant Nutr. **61** 2 (2015) 191.

[6.30] ZHELEZNYAK, M.J. et al., Mathematical modeling of radionuclide dispersion in the Pripyat-Dnieper aquatic system after the Chernobyl accident, Radiobiol. Radioecol. Vicin. Chernobyl **112** 1 (1992) 89.

[6.31] ONISHI, Y., VOITSEKHOVICH, O.V., ZHELEZNYAK, M.J., Chernobyl - What Have We Learned? The Successes and Failures to Mitigate Water Contamination Over 20 Years, Environmental Pollution, Springer Netherlands X, 291 pp.

[6.32] WAUTERS, J., CREMERS, A., Effect of Particle Concentration and Fixation on Radiocesium Sorption, Environ. Sci. Technol. **30** 10 (1996) 2892.

[6.33] KURIKAMI, H., KITAMURA, A., YOKUDA, S.T., ONISHI, Y., Sediment and 137Cs behaviors in the Ogaki Dam Reservoir during a heavy rainfall event, J. Environ. Radioact. **137** (2014) 10.

[6.34] KURIKAMI, H., FUNAKI, H., MALINS, A., KITAMURA, A., ONISHI, Y., Numerical study of sediment and 137Cs discharge out of reservoirs during various scale rainfall events, J. Environ. Radioact. **164** (2016) 73.

[6.35] MORI, K. et al., Integrated watershed modeling for simulation of spatiotemporal redistribution of post-fallout radionuclides: application in radiocesium fate and transport processes derived from the Fukushima accidents, Environ. Model. Softw. **72** (2015) 126.

[6.36] SAKUMA, K. et al., Characteristics of radio-cesium transport and discharge between different basins near to the Fukushima Dai-ichi Nuclear Power Plant after heavy rainfall events, J. Environ. Radioact. **169–170** (2017) 137.

[6.37] SAKUMA, K. et al., Applicability of Kd for modelling dissolved 137Cs concentrations in Fukushima river water: Case study of the upstream Ota River, J. Environ. Radioact. **184–185** (2018) 53.

[6.38] OCHIAI, S. et al., Effects of radiocesium inventory on 137Cs concentrations in river waters of Fukushima, Japan, under base-flow conditions, J. Environ. Radioact. **144** (2015) 86.

[6.39] YOSHIMURA, K., ONDA, Y., SAKAGUCHI, A., YAMAMOTO, M., MATSUURA, Y., An extensive study of the concentrations of particulate/dissolved radiocaesium derived from the Fukushima Dai-ichi Nuclear Power Plant accident in various river systems and their relationship with catchment inventory, J. Environ. Radioact. **139** (2015) 370.

[6.40] KONOPLEV, A. et al., Radiocesium Solid-Liquid Distribution and Migration in Contaminated Areas after the Accident at Fukushima Dai-Ichi Nuclear Power Plant, New Challenges with New Analytical Technologies, Aristotle University of Thessaloniki, Thessaloniki, Greece (2015) 51–58.

[6.41] TSUKADA, H., NIHIRA, S., WATANABE, T., TAKEDA, S., The 137Cs activity concentration of suspended and dissolved fractions in irrigation waters collected from the 80 km zone around TEPCO's Fukushima Daiichi Nuclear Power Station, J. Environ. Radioact. **178–179** (2017) 354.

[6.42] TSUJI, H. et al., Vertical/spatial movement and accumulation of 137Cs in a shallow lake in the initial phase after the Fukushima Daiichi nuclear power plant accident, Appl. Radiat. Isot. **147** (2019) 59.

[6.43] TSUJI, H. et al., Behavior of dissolved radiocesium in river water in a forested watershed in Fukushima Prefecture, J. Geophys. Res. Biogeosciences **121** 10 (2016) 2588.

[6.44] NAGAO, S. et al., Export of 134 Cs and 137 Cs in the Fukushima river systems at heavy rains by Typhoon Roke in September 2011, Biogeosciences **10** 10 (2013) 6215.

[6.45] UEDA, S. et al., Fluvial discharges of radiocaesium from watersheds contaminated by the Fukushima Dai-ichi Nuclear Power Plant accident, Japan, J. Environ. Radioact. **118** (2013) 96.

[6.46] YAMASHIKI, Y. et al., Release of Radionuclides from Natural River, Abukuma as Suspended Particulate Matter into Pacific Ocean, Disaster Prev. Res. Inst. Annu. **56** A (2013) 25.

[6.47] TANAKA, K., IWATANI, H., SAKAGUCHI, A., TAKAHASHI, Y., ONDA, Y., Relationship between particle size and radiocesium in fluvial suspended sediment

related to the Fukushima Daiichi Nuclear Power Plant accident, J. Radioanal. Nucl. Chem. **301** 2 (2014) 607.

[6.48] TEISHIMA, H., ERIGUCHI, T., YANAGITA, K., HORIGUCHI, F., Distribution of radiocesium in Tokyo Bay after the Fukushima Daiichi Nuclear Power Station accident., J. Adv. Mar. Sci. Technol. Soc. **19** 2 (2014) 1.

[6.49] TSUJI, H., YASUTAKA, T., KAWABE, Y., ONISHI, T., KOMAI, T., Distribution of dissolved and particulate radiocesium concentrations along rivers and the relations between radiocesium concentration and deposition after the nuclear power plant accident in Fukushima, Water Res. **60** (2014) 15.

[6.50] SAKAGUCHI, A. et al., Size distribution studies of 137Cs in river water in the Abukuma Riverine system following the Fukushima Dai-ichi Nuclear Power Plant accident, J. Environ. Radioact. **139** (2015) 379.

[6.51] KINOUCHI, T., YOSHIMURA, K., OMATA, T., Modeling radiocesium transport from a river catchment based on a physically-based distributed hydrological and sediment erosion model, J. Environ. Radioact. **139** (2015) 407.

[6.52] EYROLLE-BOYER, F. et al., Behaviour of radiocaesium in coastal rivers of the Fukushima Prefecture (Japan) during conditions of low flow and low turbidity–insight on the possible role of small particles and detrital organic compounds, J. Environ. Radioact. **151** (2016) 328.

[6.53] KAKEHI, S. et al., Radioactive cesium dynamics derived from hydrographic observations in the Abukuma River Estuary, Japan, J. Environ. Radioact. **153** (2016) 1.

[6.54] NAGAO, S., OCHIAI, S., INOUE, M., KANAMORI, M., SUZUKI, K., 134Cs and 137Cs radioactivity in river waters from the upper tone river, Bunseki Kagaku Jpn. Anal. **66** 4 (2017) 243.

[6.55] WEI, L., KINOUCHI, T., YOSHIMURA, K., VELLEUX, M.L., Modeling watershed-scale 137Cs transport in a forested catchment affected by the Fukushima Dai-ichi Nuclear Power Plant accident, J. Environ. Radioact. **171** (2017) 21.

[6.56] KONOPLEV, A.V. et al., Radiocesium in ponds in the near zone of Fukushima Dai-ichi NPP, Water Resour. **45** 4 (2018) 589.

[6.57] OSAWA, K. et al., Quantification of dissolved and particulate radiocesium fluxes in two rivers draining the main radioactive pollution plume in Fukushima, Japan (2013–2016), Anthropocene **22** (2018) 40.

[6.58] NAKANISHI, T., SAKUMA, K., Trend of 137Cs concentration in river water in the medium term and future following the Fukushima nuclear accident, Chemosphere **215** (2019) 272.

[6.59] PUTYRSKAYA, V., KLEMT, E., RÖLLIN, S., Migration of 137Cs in tributaries, lake water and sediment of Lago Maggiore (Italy, Switzerland) – analysis and comparison with Lago di Lugano and other lakes, J. Environ. Radioact. **100** 1 (2009) 35.

[6.60] HIROSE, K., AOYAMA, M., SUGIMURA, Y., Plutonium and cesium isotopes in river waters in Japan, J. Radioanal. Nucl. Chem. **141** 1 (1990) 191.

[6.61] MARTIN, J.M., THOMAS, A.J., Origins, concentrations and distributions of artificial radionuclides discharged by the Rhône River to the Mediterranean Sea, J. Environ. Radioact. **11** 2 (1990) 105.

[6.62] CERLING, T.E., MORRISON, S.J., SOBOCINSKI, R.W., LARSEN, I.L., Sediment-water interaction in a small stream: Adsorption of 137Cs by bed load sediments, Water Resour. Res. **26** 6 (1990) 1165.

[6.63] MATSUNAGA, T., AMANO, H., YANASE, N., Discharge of dissolved and particulate137Cs in the Kuji River, Japan, Appl. Geochem. **6** 2 (1991) 159.

[6.64] JOSHI, S.R., MCCREA, R.C., Sources and behavior of anthropogenic radionuclides in the Ottawa river waters, Water. Air. Soil Pollut. **62** 1–2 (1992) 167.

[6.65] MARINGER, F., JACHS, P., RANK, D., TSCHURLOVITS, M., On the behaviour of Sr-90 and Cs-137 in water, suspended matter and sediment of the river Danube, (1994).

[6.66] DRNDARSKI, N.D., LAVI, N., Radioactivity in sediments from the Grliska impoundment, Water Res. **30** 6 (1996) 1539.

[6.67] BELLI, M. et al., The role of a spring river as a source of^ 1^ 3^ 7Cs in a lagoon environment: the case of the Stella river (Marano lagoon, Northern Adriatic Sea), Stud. Environ. Sci. **68** (1997) 97.

[6.68] COMANS, R.N.J., HILTON, J., CREMERS, A., GEELHOED-BONOUVRIE, P.A., SMITH, J.T., Interpreting and Predicting in Situ Distribution Coefficients of Radiocaesium in Aquatic Systems, Freshwater and Estuarine Radioecology: Proceedings of an International Seminar, Lisbon, Portugal, 21-25 March 1994, Vol. 68, Elsevier (1997) 129–140.

[6.69] DE LUCA, M.E.M., MARCOS GODOY, J., Mobilization studies of 137Cs in sediments from Rochedo Reservoir, Goiania, Go., Brazil, Stud. Environ. Sci. **68** (1997) 119.

[6.70] TSCHURLOVITS, M., MARINGER, F.J., "In situ assessment of Kd factors in the Austrian part of the Danube river", Studies in Environmental Science, Vol. 68 (DESMET, G. et al., Eds), Elsevier (1997) 255–260.

[6.71] KONOPLEV, A. et al., Comparative study of 137Cs partitioning between solid and liquid phases in Lakes Constance, Lugano and Vorsee, J. Environ. Radioact. **58** 1 (2002) 1.

[6.72] INTERNATIONAL ATOMIC ENERGY AGENCY, Handbook of Parameter Values for the Prediction of Radionuclide Transfer in Terrestrial and Freshwater Environments, Technical Reports Series 472, INTERNATIONAL ATOMIC ENERGY AGENCY, Vienna (2010).

[6.73] BOYER, P., WELLS, C., HOWARD, B., Extended Kd distributions for freshwater environment, J. Environ. Radioact. **192** (2018) 128.

[6.74] TOMCZAK, W., BOYER, P., KRIMISSA, M., RADAKOVITCH, O., Kd distributions in freshwater systems as a function of material type, mass-volume ratio, dissolved organic carbon and pH, Appl. Geochem. **105** (2019) 68.

[6.75] EGUCHI, S., Behavior of radioactive cesium in agricultural environment, Soil Phys. Cond. Plant Growth Jpn. (2017).

[6.76] PHILLIPS, J.M., RUSSELL, M.A., WALLING, D.E., Time-integrated sampling of fluvial suspended sediment: a simple methodology for small catchments, Hydrol. Process. **14** 14 (2000) 2589.

[6.77] HOWARD, B.J. et al., The IAEA handbook on radionuclide transfer to wildlife, Spec. Issue 2011 ICRER Meet. **121** (2013) 55.

[6.78] HOWARD, B.J., LARSSON, C.-M., The ERICA Integrated Approach and its contribution to protection of the environment from ionising radiation., J. Environ. Radioact. **99** 9 (2008) 1361.

[6.79] IGUCHI, K. et al., Cesium-137 discharge into the freshwater fishery ground of grazing fish, ayu Plecoglossus altivelis after the March 2011 Fukushima nuclear accident, Fish. Sci. **79** 6 (2013) 983.

[6.80] MATSUDA, K. et al., Comparison of radioactive cesium contamination of lake water, bottom sediment, plankton, and freshwater fish among lakes of Fukushima Prefecture, Japan after the Fukushima fallout, Fish. Sci. **81** 4 (2015) 737.

[6.81] SUZUKI, K. et al., Radiocesium dynamics in the aquatic ecosystem of Lake Onuma on Mt. Akagi following the Fukushima Dai-ichi Nuclear Power Plant accident, Sci. Total Environ. **622–623** (2018) 1153.

[6.82] ISHII, Y., MATSUZAKI, S.S., HAYASHI, S., Different factors determine 137Cs concentration factors of freshwater fish and aquatic organisms in lake and river ecosystems, J. Environ. Radioact. **213** (2020) 106102.

[6.83] BERESFORD, N.A. et al., A new approach to predicting environmental transfer of radionuclides to wildlife: a demonstration for freshwater fish and caesium, Sci. Total Environ. **463** (2013) 284.

[6.84] INTERNATIONAL ATOMIC ENERGY AGENCY, Quantification of Radionuclide Transfer in Terrestrial and Freshwater Environments for Radiological Assessments, TECDOC Series 1616, INTERNATIONAL ATOMIC ENERGY AGENCY, Vienna (2009).

[6.85] MINISTRY OF ENVIRONMENT (MOE), Radioactive Material Monitoring in the Water Environment and around Fukushima Prefecture. Public Water Areas, MINISTRY OF ENVIRONMENT (MOE), Japan (2019).

[6.86] SUZUKI, K. et al., Radiocesium dynamics in the aquatic ecosystem of Lake Onuma on Mt . Akagi following the Fukushima Dai-ichi Nuclear Power Plant accident, Sci. Total Environ. **622–623** (2018) 1153.

[6.87] IGUCHI, K. et al., Cesium-137 discharge into the freshwater fishery ground of grazing fish, ayu Plecoglossus altivelis after the March 2011 Fukushima nuclear accident, Fish. Sci. **79** 6 (2013) 983.

[6.88] TSUBOI, J., ABE, S., FUJIMOTO, K., KAERIYAMA, H., "Spatiotemporal monitoring of 134 Cs and 137 Cs in Ayu, Plecoglossus altivelis, a microalgae-grazing fish , and in their freshwater habitats in Fukushima", Impacts of the Fukushima Nuclear Accident on Fish and Fishing Grounds (NAKATA, K., SUGISAKI, H., Eds), Springer (2015) 211–219.

[6.89] TAGAMI, K., UCHIDA, S., WOOD, M.D., BERESFORD, N.A., Radiocaesium transfer and radiation exposure of frogs in Fukushima Prefecture, Sci. Rep. **8** 1 (2018) 10662.

[6.90] ISHII, Y., MATSUZAKI, S.S., HAYASHI, S., Data on 137Cs concentration factor of freshwater fish and aquatic organisms in lake and river ecosystems, Data Brief **28** (2020) 105043.

[6.91] WADA, T. et al., Strong contrast of cesium radioactivity between marine and freshwater fish in Fukushima, J. Environ. Radioact. **204** (2019) 132.

[6.92] FISHERIES AGENCY, Results of the Monitoring on Radioactivity Level in Fisheries Products, Ministry of Agriculture, Forestry and Fisheries of Japan.

[6.93] FUKUSHIMA, T., ARAI, H., Radiocesium contamination of lake sediments and fish following the Fukushima nuclear accident and their partition coefficient, Inland Waters **4** 2 (2014) 204.

[6.94] YANKOVICH, T. et al., Establishing a database of radionuclide transfer parameters for freshwater wildlife, J. Environ. Radioact. **126** (2013) 299.

[6.95] SUZUKI, K., WATANABE, S., ONOZEKI, Y., ARAI, H., Body-size effect and dynamics of radiocesium for wakasagi Hypomesus nipponensis, Bunseki Kagaku Jpn. Anal. **66** 3 (2017) 195.

[6.96] JONSSON, B., FORSETH, T., UGEDAL, O., Chernobyl radioactivity persists in fish, Nature **400** 6743 (1999) 417.

[6.97] SMITH, J.T. et al., Chernobyl's legacy in food and water, Nature **405** 6783 (2000) 141.

[6.98] PRÖHL, G. et al., Ecological half-lives of 90Sr and 137Cs in terrestrial and aquatic ecosystems, J. Environ. Radioact. **91** 1 (2006) 41.

[6.99] SMITH, J.T., VOITSEKHOVITCH, O.V., HÅKANSON, L., HILTON, J., A critical review of measures to reduce radioactive doses from drinking water and consumption of freshwater foodstuffs, Remediat. Strateg. **56** 1 (2001) 11.

[6.100] BERESFORD, N.A. et al., Radionuclide biological half-life values for terrestrial and aquatic wildlife, J. Environ. Radioact. **150** (2015) 270.

7. MARINE SYSTEMS

HYOE TAKATA
Institute of Environmental Radioactivity (IER), Fukushima University, JAPAN

MASASHI KUSAKABE
Marine Ecology Research Institute, JAPAN

MATHEW P. JOHANSEN
Australian Nuclear Science and Technology Organisation, AUSTRALIA

HYOJOON JEON
Korea Atomic Energy Research Institute, REPUBLIC OF KOREA

PAUL MCGINNITY
IAEA Environment Laboratories, MONACO

7.1. INTRODUCTION

A large amount of data on radionuclide activity concentrations in seawater, sediments and marine organisms have been systematically collected since 1984 in the seawaters near nuclear power plants and nuclear-reprocessing facilities around Japan. The program has been carried out by the Marine Ecology Research Institute (MERI) under contract initially with Ministry of Education, Culture, Sports, Science and Technology (the former Science and Technology Agency) and since 2013 the Nuclear Regulation Authority. A comprehensive and informative understanding of the marine response to large-scale releases of radionuclides requires an analysis and interpretation of both pre- and post-accident data. The data series include information collected as part of the response to the contamination of marine areas after the FDNPP accident of March 2011.

The FDNPP accident resulted in the world's largest accidental release of radioactivity from a coastal nuclear power plant. As the accident unfolded, it was important to be able reliably to predict the impacts on marine resources. Several early studies highlighted the need for accurate parameters that describe the behaviour of radiocaesium in the seawaters off the FDNPP [7.1–7.6]. From 2011 to 2019, the ^{137}Cs activity concentrations in seawater have cycled through sharp, pulsed increases, followed by gradual decreases. As of 2019, they have already approached the pre-accident values of 2010 in many areas.

In this chapter, radioecological data are provided that can support the assessment of potential internal doses via the human food chain arising as the consequence of a large-scale pulsed inputs into marine systems. The objectives of this chapter are:

- To analyse the data on temporal changes of concentration ratio (CR) in fish;
- To quantity timescales required for contaminated marine biota to return to pre-accident levels;
- To analyse the temporal changes of ^{137}Cs activity concentrations in the seawater and bottom sediments;
- To develop a simple model for the spatiotemporal changes in sediment-water distribution coefficient (K_d) values.

The data help to understand the behaviour and bioavailability of radiocaesium distributed in the coastal areas during the pre-accident and post-accident periods.

7.2. CONCENTRATION RATIOS FOR EDIBLE MARINE SPECIES

The 1984–2010 data reported here provide useful insights on how radionuclides behave in typical ambient conditions. The post-2011 data provide insights into the changes that can occur in marine systems following substantial radiological disruptions such as the FDNPP accident.

7.2.1. Definitions of concentration ratios (*CR*) for edible marine species

Uptake of radionuclides by marine species in steady-state conditions has been widely reported using CR, defined for marine species as the activity concentration within the organism divided by that of its host seawater [7.7–7.9]. CR can be calculated for the whole body of the organism or for specified parts such as edible tissues:

$$CR = \frac{\text{Activity concentration in tissues of biota} \left(\frac{Bq}{kg}\ FM\right)}{\text{Activity concentration in water} \left(\frac{Bq}{L}\right)} \quad (7.1)$$

CR values can serve as reference values for estimating transfer from seawater to marine species and as parameters in models that have been developed for safety assessments of radioactive impacts on the environment [7.10–7.13]. The use of CR values normalizes transfer data which can then be compared across regions and timescales.

In this section, CR values are given for ^{137}Cs in muscle, which is the most commonly consumed marine animal tissue in Japan. Nevertheless, the Japanese diet notably includes a diverse range of marine species, some of which, such as Japanese sand lance (*Ammodytes personatus)* and Japanese anchovy (*Engraulis japonicus*), are consumed whole. The seawater-to-muscle CR values for Cs provided here may slightly overpredict *CR* values for the whole body. However, the difference will not exceed 10% [7.14] as muscle accumulates most of the body burden of caesium [7.15]. Whole-body CR for radiocaesium are compiled in the IAEA TRS 479 report [7.16] where both, arithmetic and geometric means, for which a difference in values indicates an asymmetric distribution, are given for marine fish (AM = 84 L/kg, GM = 48 L/kg), crustaceans (AM = 35 L/kg, GM = 21 L/kg), molluscs (AM = 50 L/kg, GM = 35 L/kg), macroalgae (AM = 96 L/kg, GM = 24 L/kg), and zooplankton (AM = 130 L/kg, GM = 67 L/kg).

There are well-known limitations associated with the CR concept as CR values are intended for application in equilibrium or quasi-equilibrium conditions [7.7, 7.9] which is not the case for the first few years after the FDNPP accident. CR data generally show significant inter-species variation [7.17, 7.18] due to variations in age, size, locations, and feeding basis. This was also reported for several species of marine fish in Japan [7.19]. Intra-species variation in CR values have also been reported amongst age classes and geographic locations [7.19, 7.20].

7.2.2. Datasets

This section builds upon a comprehensive review of ^{137}Cs data [7.21] for marine species and seawater which were sampled annually by MERI from 1984 to 2010 from a series of coastal monitoring stations near nuclear sites around Japan. The dataset has been supplemented with additional pre-FDNPP accident data reported elsewhere, which includes data for algae,

molluscs, crustaceans, and zooplankton, some of which are not typically eaten by humans, but are included here as they are important contributors to the understanding of food-chain contamination [7.22–7.26]. More than 10 000 additional data collected by the [7.27] for Aomori, Iwate, Miyagi, Fukushima, Ibaraki, and Chiba Prefectures from 2011 to 2015 were also included.

The ^{137}Cs activity concentrations in marine species (edible flesh) from 1984 to 2016 (including data after the FDNPP accident) [7.21] are shown in Fig. 7.1 for three areas that have been classified according to prevailing seawater currents [7.28]. The time-series trend indicates that ^{137}Cs activity concentrations in marine species were highest in Area I (Fig. 7.1), close to the FDNPP. In Area I, ^{137}Cs activity concentrations decreased exponentially with time with effective half-lives (T_a) that ranged from 220 to 390 days [7.29]. There were several pulsed responses in ^{137}Cs activity concentrations in fish which lagged behind those of seawater. The time delay prolonged concerns over the safety of fishery products and emphasized the need for management controls over seafood.

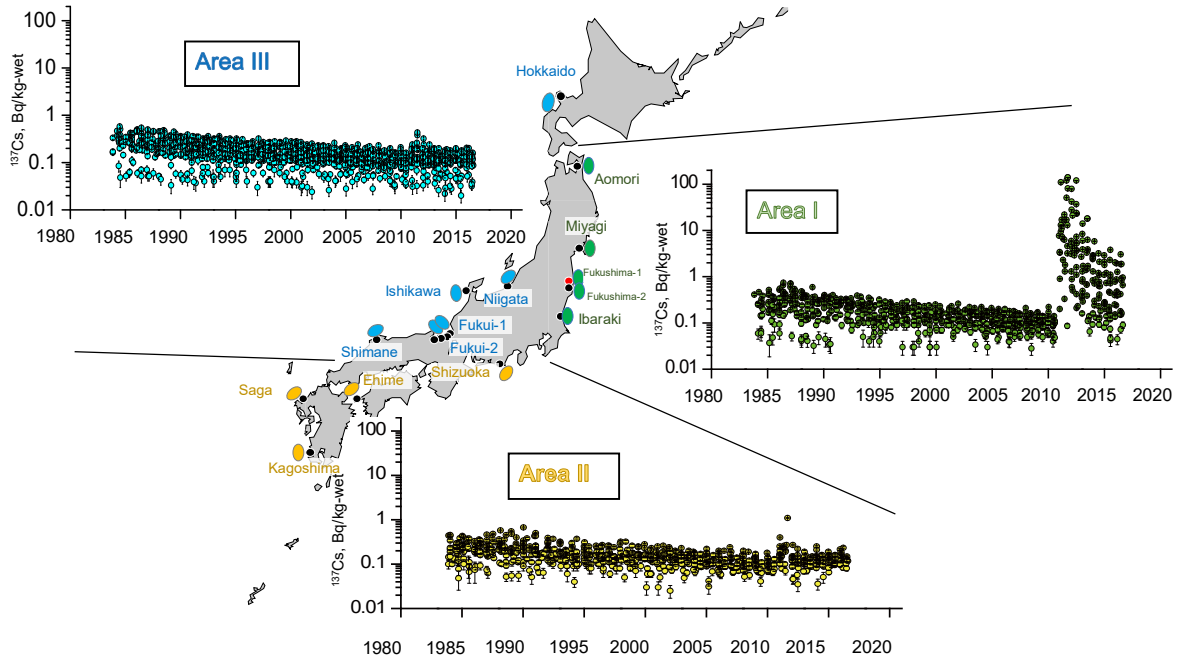

FIG 7.1. Changes with time in the ^{137}Cs activity concentration in marine species (edible flesh) before and after the FDNPP accident based on fifteen sampling sites in three areas adjacent to nuclear power plants in coastal areas around Japan.

7.2.3. CR_{GF} values derived from global fallout (1984–2010)

Global fallout was the primary source for the period 1984–2010, so the *CR* values before the accident are designated as *CR* Global Fallout (CR_{GF}). The muscle-to-seawater CR_{GF} values from 1983 to 2010 of ^{137}Cs in 95 marine species (see Fig 7.2) [7.21] have remained almost constant over time with geometric means varying within a narrow range of 45–72 for Area I, 43–63 for Area II, and 50–64 for Area III. Based on the statistical *t*-test, there were no substantial

differences in CR_{GF} values between the three areas, and there was little change in the CR_{GF} values for each species, with differences between species and within species remaining approximately the same over time between areas. The data indicated that an equilibrium was established in ^{137}Cs activity concentrations between seawater and marine species during the two decades preceding the FDNPP accident. These consistent data established a baseline for typical ambient conditions in the seas around Japan. Therefore, these values have been used as a reference for determining whether values have returned to their pre-accident CR_{GF} levels after the FDNPP accident.

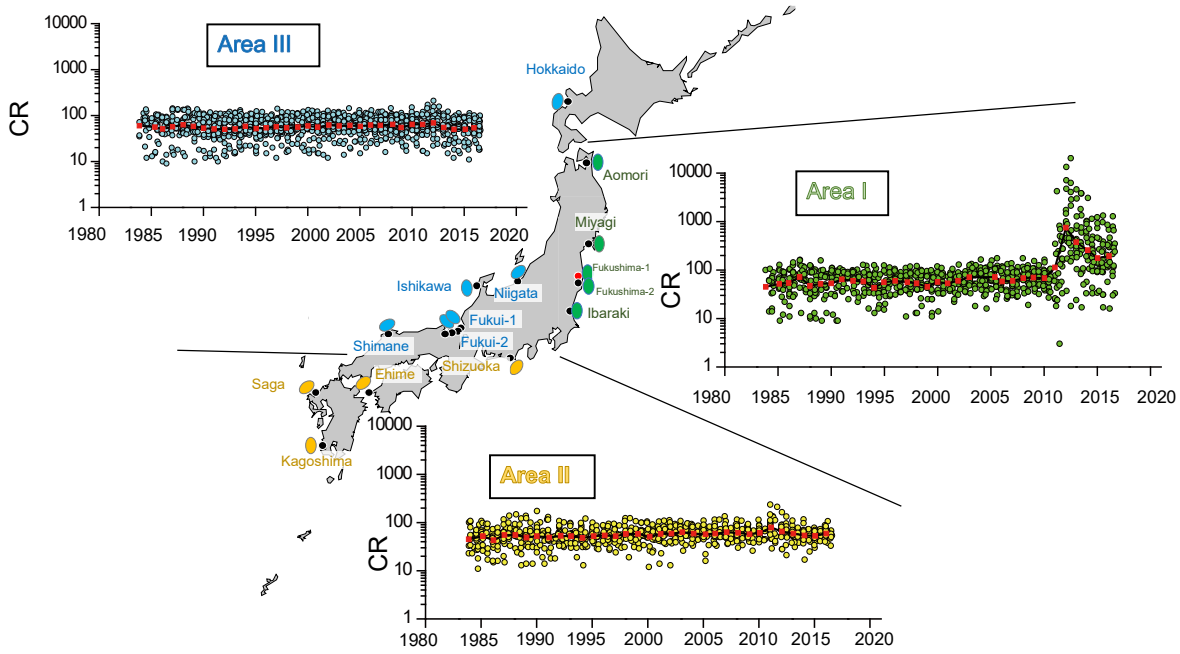

FIG 7.2. CR values of ^{137}Cs for marine species based on three areas classified according to prevailing seawater currents. Red squares represent annual geometric means of CR values in each area. Values prior to 2010 relate to global fallout (CR_{GF}) and those after 2010 are CR_a values (see text).

To evaluate the factors influencing CR_{GF} variation, the values for fish species that had been sampled more than ten times over the 28-year measurement period were analysed. The data indicated that the CR_{GF} intra-species variation (coefficient of variation, CV, of about 30%) is smaller than the inter-species variation (CV of 45%) (see Fig 7.3). The CV for some fish species were relatively high (>30%) including pollack, greenling, stone flounder, and marbled sole whereas brown sole, blue drum and white croaker had relatively low CV (<21%).

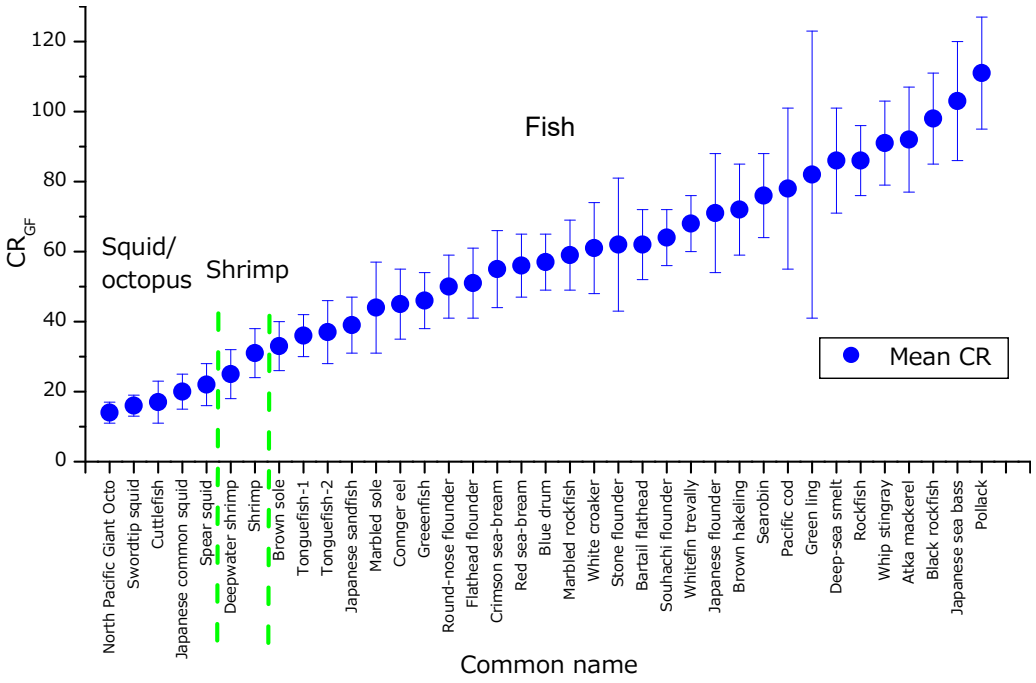

FIG 7.3. Mean CR_{GF} values of ^{137}Cs for frequently sampled marine species over 1984–2010 before the FDNPP accident. Whiskers are plus or minus one standard deviation. Data are from the areas in Fig. 7.2.

Some of the variation in CR_{GF} values can be attributed to variations in diet, age and whether it is a pelagic or demersal fish species. Red sea bream has relatively smaller variation in CR_{GF} values and also little variation in dietary preferences between juveniles and adults according to gut content analysis [7.19]. In contrast, Stone flounders have larger variations in CR_{GF} and substantial changes in their diet as they consume greater proportions of fish with increasing age (higher trophic diet and higher CR_{GF}). The effect of age is further supported by a significant relationship between CR_{GF} and fish size (e.g. for Stone flounder ($r = 0.8$)). Fish size, defined as the body length from the mouth to the end of caudal fin, and CR_{GF} for 16 species were correlated (correlation coefficient of >0.4) [7.21] according to an equation based on the relationship between CR_{GF} and fish size L (cm) for individual fish:

$$CR_{GF\text{-size}} = a\,L + b\,, \tag{7.2}$$

where a and b represent the slope and the intercept of the regression of CR_{GF} versus body size, respectively. The $CR_{GF\text{-size}}$ has been obtained from a restricted range of sampled fish that were a suitable size for the market. Therefore, the relationship may not hold for smaller or larger fish than those considered suitable for consumption.

Differences in habitat may also influence CR_{GF} variation. The seawater temperature and depth were identified as potential factors controlling CR_{GF} for atka mackerel [7.19]. These environmental conditions could differentiate CR_{GF} among species but were not critical factors when assessing CR_{GF} variations between collection sites in the 1984–2010 data which suggests that CR_{GF} variation is more affected by fish size than by seawater depth and temperature.

The difference between whole body and muscle tissue is small (conversion factor is ≈1.1) in [7.16]. Therefore, the ranges of CR_{GF} values between 1984–2010 (L/kg) in Japanese seawater

can be directly compared with the international summary values in [7.10, 7.16]. The CR_{GF} values are similar for a range of different species as follows:

- 10–58 L/kg for shrimp in Japan compared with AM of 53 L/kg (SD = 120, n = 287) for crustaceans in [7.16];
- 9–30 L/kg for squid and octopus compared with 9 L/kg for cephalopods [7.10] and an AM of 50 L/kg for all molluscs (SD = 50, n = 336) in [7.16];
- 15–175 L/kg for fish in Japan compared with AM of 84 L/kg (SD = 120, n = 1812) for fish in [7.16]. The CR_{GF} geometric mean for the seas around Japan (56 L/kg) is similar to the geometric mean (48 L/kg, GSD = 2.9) in the IAEA TRS Report 479 [7.16]. The IAEA summary values representing world-wide data are based on 1812 data entries for fish [7.16], whereas the pre-2011 data base includes more than 2200 entries from the seas around Japan (see Table 7.1) [7.21–7.26].

7.2.4. CR_a values after the FDNPP accident

Since the *CR* concept assumes approximate steady-state conditions, by definition, any *CR* values calculated in the initial months following the FDNPP accident, will be compromised by the rapid changes in ^{137}Cs activity concentration initially in the seawater, then in biota and sediments. This dynamic process that result in disequilibrium of the ratio of ^{137}Cs in biota to seawater raises the question: "How long does the disequilibrium between marine organisms and their host seawater last?".

The analysis in this section utilizes a large quantity of post-2011 data that have been gathered from the seas around Japan. However, because the dynamic post-accident *CR* data are inherently different from the steady-state pre-accident data, a separate notation has been used here, termed here *apparent CR* (CR_a). These CR_a values should not (without clear qualification) be included in general *CR* references as they are not representative of general ambient (quasi-steady state) conditions. They are, however, useful as temporary indicators of disequilibrium and are used here to better define the extent, magnitude and timing of the increase in radiocaesium accumulation in marine species, and to consider when *CR* data have returned to a quasi-steady state.

For Area I (Aomori, Iwate, Miyagi, Fukushima, Ibaraki, and Chiba Prefectures, see Fig. 7.2), CR_a values were calculated from more than 10,000 data published from 2011 to 2015 and are summarized in Table 7.2. The highest CR_a values were observed in Area I which also had the most prolonged response to the input of radiocaesium. The geometric mean of CR_a data in Area I reached a peak in 2012–2013, and by 2015 CR_a values had gradually approached, but typically not reached, the CR_{GF} values estimated for the period before the accident (Fig. 7.2). The delayed peak and slow subsequent reduction were due to the differing reduction rates between concentrations in seawater and marine species (Fig. 7.2). Immediately after the accident, radiocaesium activity concentrations in seawater peaked rapidly, then quickly declined (T_a from several days to several tens of days) due to mixing with open-ocean seawaters with lower radiocaesium activity concentrations [7.30]. In contrast, the T_a of ^{137}Cs in marine species often exceeded several hundred days (e.g., see in [7.31], discussed further in sub-section 7.1.6), resulting in prolonged elevation of ^{137}Cs in marine species relative to the surrounding seawaters.

TABLE 7.1 ARITHMETIC MEAN CR_{GF} VALUES FOR ALGAE, CEPHALOPOD, CRUSTACEAN (SHRIMP), ZOOPLANKTON AND FISH PRIOR TO THE FDNPP ACCIDENT UP TO 2010

Marine group	Common name	Species	CR_{GF}	$CR_{GF\text{-}size}$ [c]		Reference for:	
				a	*b*	Tissue	Host-water
Algae [a]	Hijiki	*Hizikia fusirmis*	48			[7.23]	[7.21]
	Arame	*Eisenia bicyclis*	*38*			[7.23]	[7.21]
	Umitoranoo	*Sargassum thunbergii*	*62*			[7.23]	[7.21]
	Umitoranoo	*Sargassum thunbergii*	64			[7.24]	
	Tsunomata	*Chondrus ocellatus*	*61*			[7.23]	[7.21]
	Harigane	*Ahnfeltia paradoxa*	*56*			[7.23]	[7.21]
	Fukurofunori	*Gloiopeltis furcata*	*51*			[7.23]	[7.21]
	Makonbu	*Laminaria japonica*	*41*			[7.23]	[7.21]
		Ulva pertusa	16			[7.24]	
		Laurencia nipponica	18			[7.24]	
		Neodilsea yendoana	45			[7.24]	
Cephalopod	Cuttlefish	*Sepia (Platysepia) esculenta*	17			[7.21]	
	Japanese common squid	*Todarodes pacificus Steenstrup*	20			[7.21]	
	Northpacific giant octpus	*Octopus (Enteroctopus) dofleini (Wüker)*	14			[7.21]	
Crustacean (shrimp)	Deepwater prawn	*Pandalus eous*		2.7	−15	[7.21]	
	Shrimp		32			[7.21]	
Zooplankton			13			[7.25]	
			11			[7.26]	
Mollusc [b]	Chosen hamaguri	*Maretrix lamarckii*	*35*			[7.23]	[7.21]
		Maretrix lamarckii	28			[7.22]	
		Anadara broughtonii	7			[7.22]	
		Fulvia mutica	13			[7.22]	
		Crassostrea gigas	16			[7.22]	
		Patinopecten yessoensis	18			[7.22]	
		Haliotis discus	24			[7.22]	
		Charonia sauliae	30			[7.22]	
	Kotamagai	*Gomphina melanaegis*	*35*			[7.23]	[7.21]
	Saragai	*Peronidia venulosa*	*65*			[7.23]	[7.21]
	Hotategai	*Patinopecten yessoensis*	*18*			[7.23]	[7.21]
	Ubagai	*Spisula sachalinensis*	*11*			[7.23]	[7.21]

TABLE 7.1 ARITHMETIC MEAN CR_{GF} VALUES FOR ALGAE, CEPHALOPOD, CRUSTACEAN (SHRIMP), ZOOPLANKTON AND FISH PRIOR TO THE FDNPP ACCIDENT UP TO 2010 (cont.)

Marine group	Common name	Species	CR_{GF}	$CR_{GF\text{-}size}$ [c]		Reference for:	
				a	*b*	Tissue	Host-water
Fish	Greenling	*Hexagrammos otakii*		6.7	−144		[7.21]
	Stone flounder	*Kareius bicoloratus*		2.0	−14		[7.21]
	White croaker	*Pennahia argentata*		2.6	4		[7.21]
	Bartail flathead	*Platycephalus sp.2*		0.9	2		[7.21]
	Black rockfish	*Sebastes schlegelii*		1.3	51		[7.21]
	Blue drum	*Nibea mitsukurii*		2.1	2		[7.21]
	Brown hakeling	*Physiculus maximowiczi*		1.5	18		[7.21]
	Conger eel	Conger myriaster		0.5	14		[7.21]
	Japanese flounder	Paralichthys olivaceus		0.7	40		[7.21]
	Marbled rockfish	Sebastiscus marmoratus		1.3	30		[7.21]
	Marbled sole	Pseudopleuronectes yokohamae Günther		0.8	19		[7.21]
	Pacific cod	Gadus macrocephalus		1.2	8		[7.21]
	Round nose flounder	Eopsetta grigorjewi		1.2	14		[7.21]
	Whitefin trevally	Kaiwarinus equula		1.9	31		[7.21]
	Atka mackerel	Pleurogrammus azonus	92				[7.21]
	Brown sole	Pleuronectes herzensteini	33				[7.21]
	Crimson seabream	Evynnis tumifrons	55				[7.21]
	Deep sea smelt	*Glossanodon semifasciatus*	86				[7.21]
	Flathead flounder	Hippoglossoides dubius	51				[7.21]
	Greenfish	Girella punctata	46				[7.21]
	Japanese sandfish	Arctoscopus japonicus	39				[7.21]
	Japanese seaperch	Lateolabrax japonicus	103				[7.21]
	Pollack	Gadus chalcogrammus	111				[7.21]
	Red sea bream	Pagrus major	56				[7.21]
	Rockfish	Sebastes inermis	86				[7.21]
	Searobin	Lepidotrigla microptena	76				[7.21]
	Souhachi flounder	Cleisthenes pinetorum	65				[7.21]
	Tonguefish	Paraplagusia japonica	37				[7.21]
	Whip stingray	Dasyatis akajei	91				[7.21]

[a] entire organism
[b] soft tissue only
[c] see Eq (7.2) for *a* and *b*

In areas II and III, slight CR_a increases for marine species occurred in the first year (2011). However, by the end of 2012, the CR_a values had generally returned to, and have since remained consistent with the CR_{GF} values from before the FDNPP accident (Fig. 7.4). Data after this time can be used in steady-state models to quantify the transfer of ^{137}Cs to marine fish in these areas.

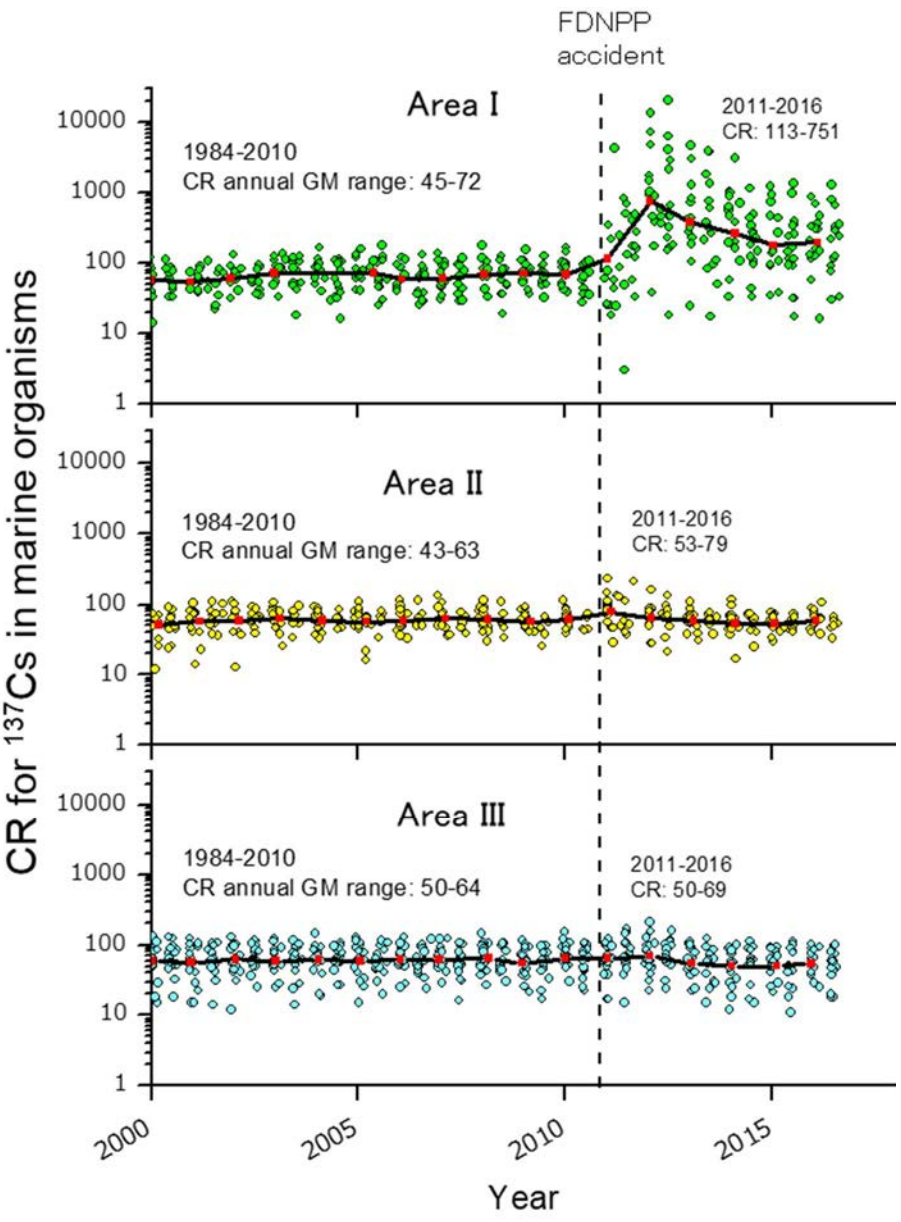

FIG 7.4. CR values of ^{137}Cs for marine species based on three areas classified according to prevailing seawater currents from 2010. Red squares represent annual means of CR values in each area. Values prior to 2010 relate to global fallout (CR_{GF}) and those after 2010 are CR_a values (see text).

TABLE 7.2 APPARENT ACTIVITY CONCENTRATION RATIOS CR_a OF ^{137}CS FOR MARINE FISH IN AREA I AFTER THE FDNPP ACCIDENT

Year	Value[a]	CR_a (L/kg) in prefecture:					
		Aomori	Iwate	Miyagi	Fukushima[b]	Ibaraki	Chiba
2011	N	27	87	95	980	160	84
	min	77	89	8	1	3	14
	max	10500	9800	2900	54200	4400	1800
	GM	920	850	190	512	310	180
	GSD	3.7	2.5	2.9	7.1	2.6	3.2
2012	N	130	270	1000	2800	770	310
	min	33	160	51	8	18	73
	max	22000	15000	57000	76000	17000	24000
	GM	1400	2300	860	1700	640	510
	GSD	3.7	3.3	3.8	3.4	2.9	2.8
2013	N	130	320	700	970	610	220
	min	93	220	130	130	17	120
	max	25000	20000	32000	44000	220000	31000
	GM	1900	1900	1500	2300	1200	670
	GSD	2.7	2.8	3.0	3.0	3.0	2.7
2014	N	110	87	190	6	650	110
	min	50	250	120	260	33	130
	max	5500	7000	25000	1100	23000	9500
	GM	760	950	790	530	890	450
	GSD	2.2	2.4	2.6	1.6	2.5	2.6
2015	N	44	39	140	8	330	59
	min	31	250	92	91	17	120
	max	1300	8800	10000	1300	19000	2600
	GM	290	520	760	510	740	290
	GSD	1.8	2.0	2.7	2.5	2.3	1.9

[a] N is the number of values

[b] Data of the Fisheries Agency for Fukushima Prefecture [7.27] were included until March 2013 because thereafter the percentage of detected samples above the detection limit relative to total collected samples was less than 50%

7.2.5. Effective half-lives (T_a) of CR_a for returning to pre-accident CR values after the FDNPP accident

The CR_a values in the initial dynamic conditions after the FDNPP accident varied widely due to varying activity concentrations in seawater, varying intake rates by biota and the differing, time-dependent retention of radiocaesium in various types of organism. The biological half-life of radiocaesium contributes to the decreasing trend of the CR_a values for different species, including fish, in the seawater offshore of the Fukushima and neighbouring prefectures [7.31, 7.32]. To characterise dynamic changes in CR_a values, Takata et al. [7.21] estimated the time dependence of CR_a for different species using a single-exponential function as:

$$CR_a(t) = \left(CR_a(t_0) - CR_a(\infty)\right) \exp\left(-\frac{\ln 2}{T_a} t\right) + CR_a(\infty), \quad (7.3)$$

where T_a is the half-life (d) characterising the rate at which the post-accident CR_a approaches equilibrium; t_0 is the time when CR_a reached a maximum value within the period of 2012–2013 (day) because CR_a values were highly perturbed during the first year of the accident. Assuming that conditions eventually return to those existing before the accident:

$$\frac{CR_a(t)}{CR_{GF}} = \left(\frac{CR_a(t_0)}{CR_{GF}} - 1\right) \exp\left(-\frac{\ln 2}{T_a} t\right) + 1. \quad (7.4)$$

For many species, the accumulation of ^{137}Cs depends on fish size (see Table 7.1); therefore, the CR_{GF_size} values were used where data existed instead of CR_{GF}.

Of the 29 species for which reference CR_{GF} or $CR_{\mathrm{GF\text{-}size}}$ were obtained, sufficient data were available to estimate T_a values for 16 fish species (Table V.1). For some species, T_a values could be estimated for individual Prefecture sampling areas. Half-lives for CR_a values were obtained from several prefectures for Japanese sea bass, pacific cod, Japanese flounder, stone flounder, greenling, blue drum, and brown sole. Most fish targeted for monitoring schemes were demersal fish species. Pelagic fish are not included in Table V.1 because most of the data were below detection limits and available data were limited because fewer pelagic fish were monitored [7.27]. For fish caught in the seawaters of Fukushima Prefecture, the percentage exceeding 100 Bq/kg FM was distinctly lower for pelagic fish compared with demersal fish [7.29]. The proportion of samples where the radiocaesium activity concentrations were above the detection limit (<10 Bq/kg FM) rapidly decreased for pelagic fish. The rapid reduction is probably because pelagic fish mainly inhabit the surface seawaters which had lower radiocaesium activity concentrations compared with those to which demersal fish were exposed, because they live and feed on or near the bottom. Dietary preference might increase the difference and contribute to the short T_a of pelagic fish which eat small fishes with low radiocaesium.

The T_a data indicate variations among the sampling areas, even within the same species. The slowest re-equilibration rates (and therefore longest T_a) for CR_a were for fish from Ibaraki Prefecture. For example, Japanese flounder (*Paralichthys olivaceus*) had a T_a for CR_a that was more than three times as long in Ibaraki (990 d) as in Iwate (310 d). T_a values from Fukushima Prefecture were also long relative to most other areas (Table V.1).

One contributing factor to the above variation may be that there was a relatively slow reduction of ^{137}Cs activity concentrations in seawater in the areas associated with the longer half-lives. From Aomori to Ibaraki Prefectures, the southward coastal current dominates throughout the year. Initially, in 2011, substantial amounts of seawater with relatively high ^{137}Cs activity concentrations released from the FDNPP were transported southward via coastal currents. Ongoing leakage from the FDNPP also occurred, which has prolonged the elevated radionuclide activity concentrations in some seawaters off both Fukushima and Ibaraki Prefectures. The initially high ^{137}Cs activity concentrations in seawater, as well as the additional ongoing ^{137}Cs releases into these areas would have provided an enhanced accumulation of ^{137}Cs in marine species, their food chains, and area sediments. Such accumulation, as well as more substantial incorporation of ^{137}Cs into marine biota, would result in slower removal rates of ^{137}Cs from seawater, sediments and marine species (larger T_a values) for the Ibaraki and Fukushima Prefectures.

A second type of variation was the differences between the T_a for CR_a among different marine species sampled from the same area. For example, T_a ranged from 310 d (for Blue drum) to 1120 d (for Greenling) in Ibaraki seawaters.

This type of variation is not surprising given that the pre-accident CR_{GF} values also varied between species (Fig. 7.3). A slight ^{137}Cs peak was observed in the seawaters off Fukushima and Miyagi Prefectures after the 1986 Chernobyl accident, and the subsequent ^{137}Cs activity concentration decreased to the background values within 180 d. However, for fish in the same areas, it took much longer than the seawater (approximately, 600 d for Japanese seabass and 860 d for Pacific cod) to return to background values [7.33].

As it is reasonable to assume that the Chernobyl-derived ^{137}Cs was deposited relatively uniformly over the surface seawater of the Fukushima area (consistent with long-range dispersion in a highly diffused plume far from the release point), the differences between species are probably due to species-specific factors including physiological differences in ^{137}Cs retention (e.g. efflux rates) [7.31, 7.32]. The depuration of ^{137}Cs from Rockfish (*Sebastes* spp.) was reported to be relatively slow at 270 d [7.34], which agrees with the relatively high CR_{GF} of this species (Fig. 7.3) and its relatively long T_a for CR_a. When analysed across all species, there was a positive, but only weak ($r = 0.4$) correlation coefficient between the T_a for CR_a. and their respective CR_{GF} values. This correlation suggests that although species-specific efflux rates (or other physiological factors) are important, they do not dominate among the many factors influencing the ^{137}Cs disequilibrium in fish. Had this been valid, then a species with slower Cs efflux rates would have yielded both higher steady-state retention before the accident, and longer recession rates after the accident, but this was not the case for many fish. For example, the T_a of CR_a for marbled sole and brown sole were relatively long, whereas their CR_{GF} values before the accident were relatively low (a mean of less than $\leq$60). In contrast, Pacific cod had a relatively high mean CR_{GF} value of 78, but a relatively short T_a for CR_a. These data, along with gut content analysis on fish from the same sampling stations [7.19] indicate that the longer T_a for CR_a occurs in fish with diets associated with sediments, e.g., predominantly of macro benthos (brown sole) and crustacea-decapoda (red seabream).

Ingested food is generally a more important source of radiocaesium to marine fish than direct intake via seawater [7.19, 7.35]. However, relative inputs of ^{137}Cs can vary by species depending on specific features of their food webs and lifestyle [7.17, 7.19, 7.36, 7.37]. The factors that appear to be important in sustaining elevated ^{137}Cs activity concentrations in marine fish species include:

- Pelagic vs. benthic food sources;
- Length of food chain;
- Feeding preferences;
- The extent to which species are sedentary or migrate into and out of contaminated regions (continuous vs intermittent intake of radiocaesium);
- Longevity and associated generational replacement of less-contaminated specimens.

The disequilibrium between ^{137}Cs in marine organisms of Eastern Japan and that of their host seawater persisted for more than five years in the marine areas closest to the FDNPP, while returning to pre-accident values was faster in more distant areas.

7.3. SEDIMENT DISTRIBUTION COEFFICIENT

7.3.1. Outline of monitoring programme

Most of the data presented in the following sections were derived from the monitoring program carried out by the MERI. Seawater and bottom sediment are collected every year in sampling sites located in the seawaters near each of Japan's coastal nuclear power plants (see Fig. 7.5a for the sampling areas). After the FDNPP accident, an additional ocean monitoring scheme was established with the baseline sampling scheme consisting of 32 sampling sites and sample collection scheduled four times a year (Fig. 7.5b).

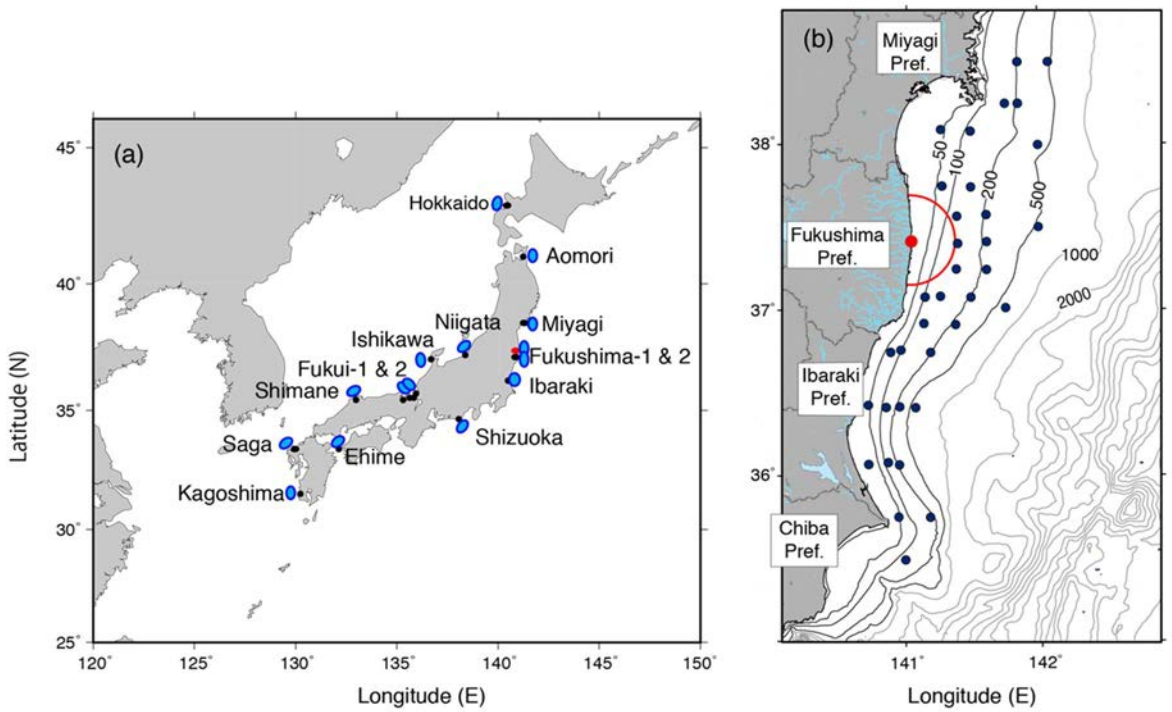

FIG 7.5. (a) Monitoring area and sampling sites. Blue areas are monitoring areas with 4 sampling sites, which are visited once a year. Black dots indicate the locations of nuclear power plants (adapted from Takata et al. [7.28], (b) Sampling sites off Fukushima Prefecture and nearby prefectures. The sampling sites (black dots) are visited 4 times a year. The red circle is at 30 km radius from the Fukushima Daiichi Nuclear Power Plant (FDNPP).

7.3.2. Data sources

The data obtained during the long-term monitoring project have been routinely reported to the relevant governmental authorities every year. The data were also stored in a database and are made freely available online[7]). Some of the monitoring data have been published in the scientific literature (e.g. [7.4–7.6, 7.21, 7.28, 7.30, 7.38–7.42]). After the FDNPP accident, the data derived from the seawaters off Fukushima and nearby prefectures have been uploaded onto the internet as they were reported[8]. The data and figures used in the following sections are mostly adapted from [7.42] unless otherwise stated.

[7] http://search.kankyo-hoshano.go.jp/servlet/search.top
[8] http://radioactivity.nsr.go.jp/en/list/205/list-1.html

7.3.3. Temporal changes of ^{137}Cs in seawater and sediment, and K_d before the FDNPP accident

7.3.3.1. Seawater

The ^{137}Cs activity concentrations in surface and bottom seawaters (up to 10 m above the bottom sediment) in the coastal seawaters around Japan before the FDNPP accident have been compiled in [7.28]. Prior to the Chernobyl accident in 1986, ^{137}Cs activity concentrations in the surface seawaters ranged from 3.3 to 5.6 mBq/L with an arithmetic mean of 4.1 mBq/L. In 1986, ^{137}Cs activity concentrations in the surface seawaters increased to at most 10 mBq/L after the Chernobyl NPP accident. In the following year, 1987, the ^{137}Cs activity concentrations returned to that of previous years at 3.3−4.8 mBq/L. Since then the ^{137}Cs activity concentrations have decreased exponentially; in 2010 they were in a range of 1.1–1.9 mBq/L with an arithmetic mean of 1.5±0.2 mBq/L. The ^{137}Cs activity concentrations in the bottom seawaters are plotted in the upper panel of Fig. 7.6a. Their temporal trend was similar to that of the surface seawater, except for the impact of the Chernobyl accident, which did not appear in the bottom seawaters. The arithmetic mean of ^{137}Cs activity concentrations in the bottom seawater was 4.3 ± 0.4 mBq/L in 1984 and decreased to 1.4 ± 0.3 mBq/L in 2010.

The calculated T_a of ^{137}Cs in bottom seawater ranged from 12.8 to 25.0 y with an arithmetic mean of 17.3 y before the accident (Table V.2). Relatively short T_a were estimated for the area of Miyagi, Fukushima, and Ibaraki areas ranging from 12.8 to 17.4 y (AM = 15.4 y). A relatively long T_a of more than 20 y for bottom seawaters was derived for seawater off Hokkaido and Niigata, in the northern part of the Japan Sea, and is probably due to the prevailing slow exchange of seawater that occurs with the surrounding areas.

T_a values for ^{137}Cs activity concentrations in surface seawater of 16.5 ± 0.9 y (AM ± SD) have also been estimated in the open ocean from the 1950s to 1990s for the western North Pacific in the middle latitudes [7.43]. The temporal trend of ^{137}Cs activity concentrations in coastal seawater is assumed to be controlled by physical processes in the open ocean including: (1) the decline of the surface ^{137}Cs activity concentration from physical decay and vertical mixing of seawater [7.44], and (2) the absence of a physical barrier to prevent active seawater exchange between the coastal area and open ocean leading to the T_a in coastal areas to be similar to those of the open ocean.

7.3.3.2. Sediment

Sediment samples (0–3 cm sediment depths) were analysed for particle-size distribution and radionuclide activity concentrations. Particle-size analysis carried out on samples collected in 2016–2018 Table V.3), indicated a large spatial variation in grain-size distribution as characterized by (silt+clay) contents. Accordingly, the ^{137}Cs activity concentrations in bottom sediment have a much greater spatial variation than seawater. For example, samples from the Niigata area had the highest silt+clay contents (81%), and their ^{137}Cs activity concentrations were also relatively high (Fig. 7.5b). Conversely, samples from the Saga area had the lowest silt+clay contents and had a relatively low ^{137}Cs activity concentration. The temporal changes in ^{137}Cs activity concentrations in the bottom sediment had a similar declining trend to that in seawater (Figs. 7.6a and 7.6b). The geometric mean ^{137}Cs activity concentration in bottom sediment declined from 2.9 Bq/kg DM in 1984 to 1.8 Bq/kg DM in 2010. The T_a varied widely from 10 to 55 years with a mean of 24 years over all the monitored areas, and, more specifically from 12 to 29 y with a mean of 19 y in the Miyagi, Fukushima, and Ibaraki areas (Table V.2). The variability in T_a may be due to the heterogeneous distribution of sediment grain size [7.41].

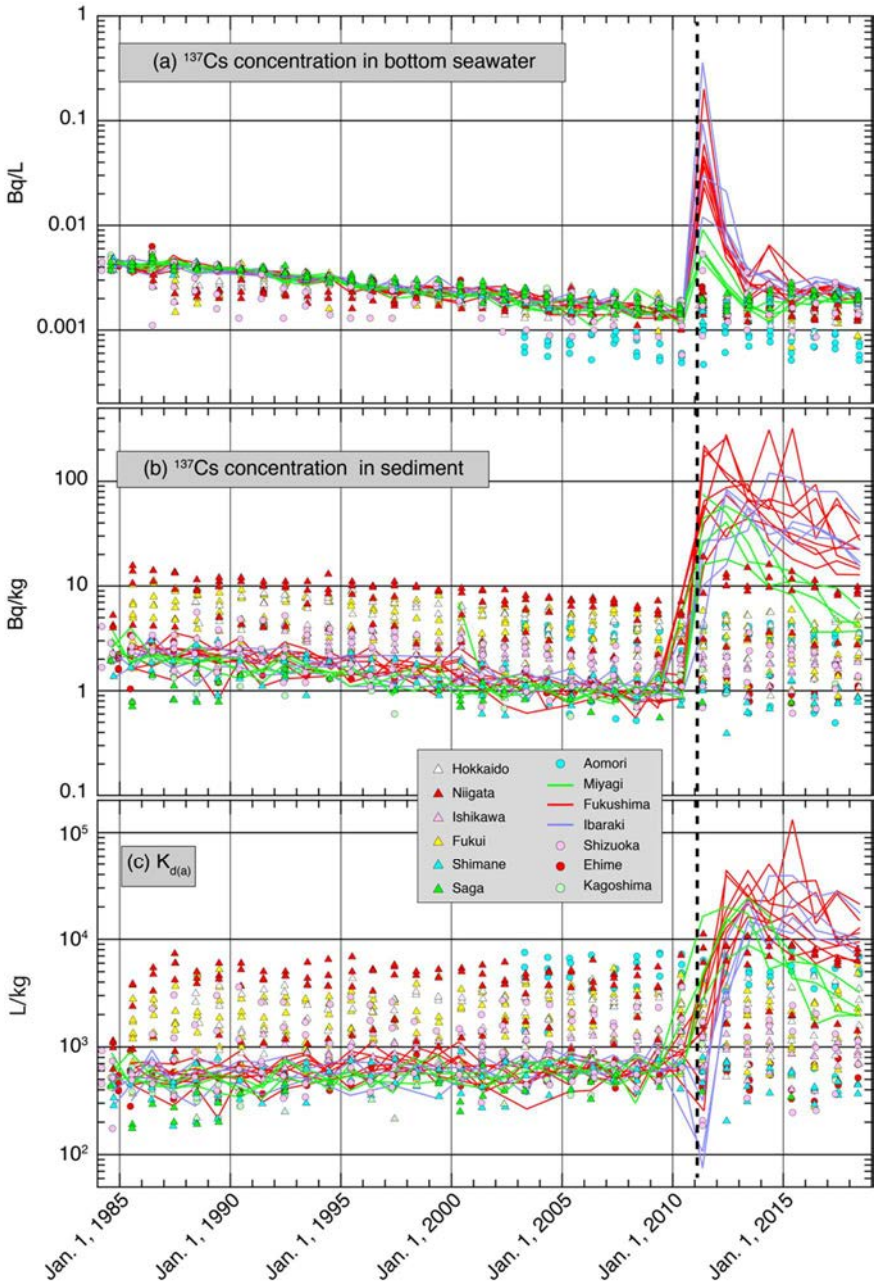

FIG 7.6. Temporal changes of ^{137}Cs activity concentrations in (a) bottom seawater, (b) surface sediment and (c) $K_{d(a)}$ in the sampling areas near all nuclear power plants in Japan. The data derived from areas close to the FDNPP (Miyagi, Fukushima, and Ibaraki) are shown as lines. The black dotted lines indicate the time of the FDNPP accident.

The K_d is defined by a ratio of concentration per mass to concentration per mass or per unit volume [7.10], see Chapter 2 for details. In principle, the K_d is only applicable to a seawater-sediment system that is in equilibrium. However, such equilibrium rarely, if ever, occurs in nature. For example, as shown in Fig. 7.6, the ^{137}Cs activity concentrations in seawater and sediments decreased with time in the 1985–2010 period before the FDNPP accident and exhibited orders of magnitude variability after the accident. An ideal static equilibrium cannot be expected in coastal areas where the ^{137}Cs activity concentrations in both seawater and sediment decrease with time and coastal seawater exchanges freely with open seawater. The main process leading to reduced ^{137}Cs activity concentrations in coastal seawater and sediment

is not solely due to desorption-adsorption processes, but it also involves vertical mixing of seawater in the open ocean. However, over the period of 25 years, the ^{137}Cs activity concentration in seawater only decreased by a factor of 2 to 3 (including radioactive decay), which indicates a very slow decrease. The general trend for the decline of the ^{137}Cs activity concentration in sediments is even less pronounced and there is slight temporal change in the pre-2011 K_d values only on the long-term basis (see below for discussion for the change) Considering the variability of environmental transport processes, this situation is considered to represent a quasi-equilibrium condition[9].

The K_d values derived before the FDNPP accident are summarized in Table V.4 and Figs. 7.6c and 7.7. They ranged widely from 175 L/kg at Shizuoka to 7540 L/kg at Aomori with a geometric mean and median value for all prefectures of 920 L/kg and 720 L/kg, respectively. A major reason for a variation of more than a factor of 40 in K_d is the variation in the physical characteristics of bottom sediment (Table V.2). A quantitative relationship between adsorbed ^{137}Cs on soil and its surface area has been demonstrated [7.46] so the K_d should be related to grain size (Fig. 7.8). The pre-accident data were fitted to a power function and a best-fit curve with $r^2 = 0.78$ was obtained as follows:

$$K_d = 11200\, S^{1.66} \tag{7.5}$$

where S is the specific surface area (m^2/g) of the bottom sediment. This relationship suggests that the spatial variation of K_d in the coastal seawater around Japan reflects the grain-size distribution in the sediments. The notably highest K_d values from Aomori may be ascribed to one of the lowest measured ^{137}Cs activity concentrations in bottom seawater due to the intrusion of deep seawater from the open ocean (Fig. 7.6a), and the relatively large specific surface area of sediments compared with most of the other monitoring sites (Table V.3).

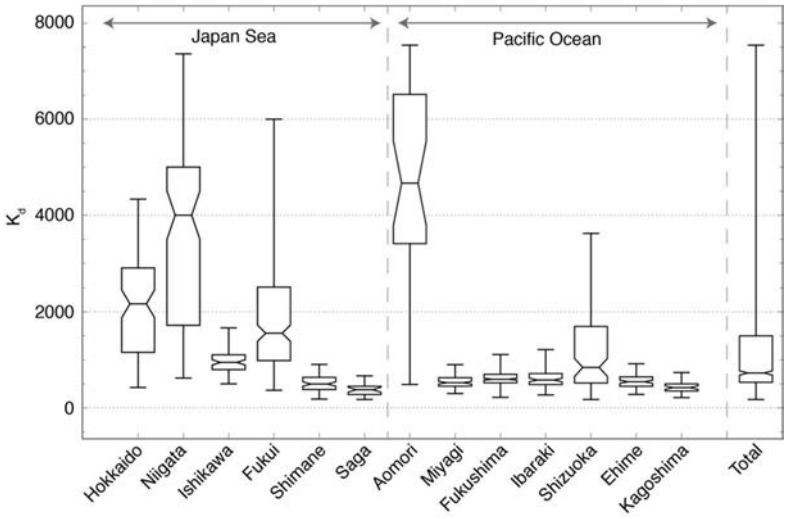

FIG 7.7. Summary of the K_d (L/kg) distribution in the coastal seawater around Japan. The box-whisker-plot shows minima, lower quartiles, medians, upper quartiles and maxima. All data prior to the FDNPP accident (1984–2010).

[9]The assumption of a (quasi-) equilibrium to identify distribution coefficients does not precisely follow the assumptions inherent in the theoretical K_d definition that equilibrium exists and/or that exchanges are wholly reversible and instantaneous [7.45].

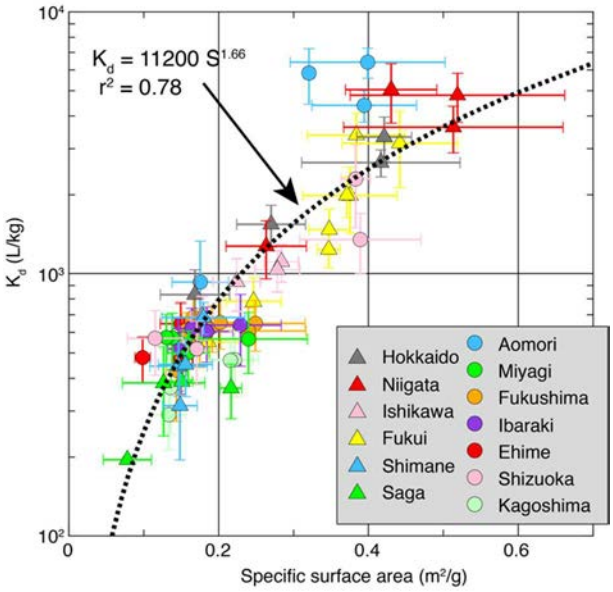

FIG 7.8. Relationship between K_d and specific surface area of the sediments. A dotted line indicates a regression line fitted to the data (see text for detail). All data prior to the FDNPP accident (1984–2010).

7.3.4. Variation of K_d before the FDNPP accident

Many factors may influence K_d in marine systems such as oceanographic setting, flux of the nuclide to the environment, its temporal change, and sediment mineralogy. The IAEA has previously provided a K_d value for Cs at ocean margins of 4000 L/kg [7.10] which is toward the upper end of ranges of coastal K_d values measured at most data sites in Japan (Fig. 7.7). The IAEA value was based the entire marginal ocean using the average concentrations of stable Cs in seawater and sediment, whereas the Japanese data are based on measured ^{137}Cs in both phases. The IAEA document also reported K_d values based on field observations of ^{137}Cs ranging from 300 to 20000 L/kg. MacKenzie *et al* [7.47] reported higher K_d values of 10^4–10^5 L/kg in the Irish Sea based on sediment and ambient interstitial seawater. There are significant differences in the environmental features of the UK data compared with those from Japan. The Irish Sea is a semi-closed sea into which the Sellafield nuclear fuel reprocessing plant has discharged a range of different radionuclides including ^{137}Cs since the 1950s. In contrast, most monitoring areas around Japan are in coastal areas directly facing onto open ocean where global fallout ^{137}Cs was the dominant source, and no discharge of ^{137}Cs from the nuclear power plants had been reported before the FDNPP accident.

The data used for the calculation of K_d in Japan have been obtained continuously over almost three decades at 60 fixed monitoring sites and are specific to ^{137}Cs. Therefore, despite the differences between the IAEA and UK data, the calculated K_d values in Table V.4 and Fig. 7.7 should be robust values applicable to similar ocean margins with respect to the site-specific environmental characteristics and input mode of radionuclides.

As shown above, the T_a of ^{137}Cs in the bottom seawaters and sediments in Japan before the FDNPP accident ranged from 12.8 to 25.0 years and from 10.3 to 55.1 years, respectively (Table V.2). The T_a in sediments were longer than that for seawater (Fig. 7.9), implying that the system has not been in equilibrium and exchange of ^{137}Cs has not been reversible and rapid enough to respond to the change of ^{137}Cs in the bottom seawater on a long-term basis. Generally, the T_a in

the bottom sediment seemed to increase with specific surface area of the sediment (plotted data not shown here), but the relationship was yet to be quantified. A lack of equilibrium will lead to temporal change in K_d values. The geometric mean of K_d in all the monitored coastal seawaters around Japan increased from 640 L/kg in 1984 to 1400 L/kg in 2010. K_d in the seawaters off Miyagi, Fukushima, and Ibaraki Prefectures varied from 520 L/kg to 680 L/kg over the same period (Fig. 7.10). Some of the variability evident in Fig. 7.7 can be attributed to the temporal change of K_d.

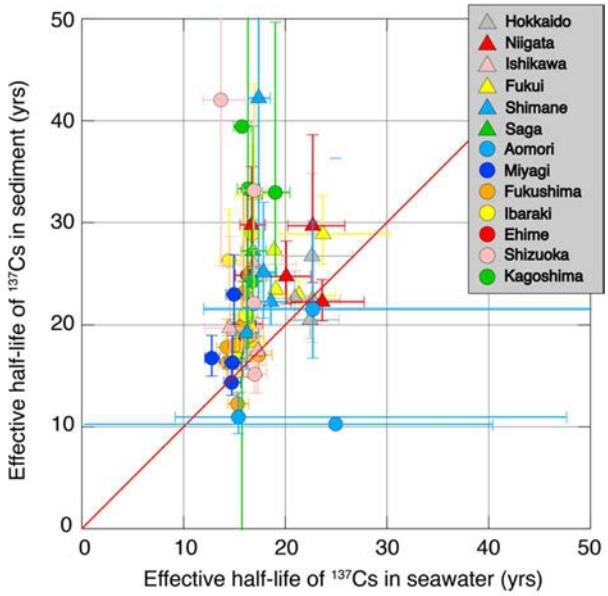

FIG 7.9. Relationship between effective half-lives, T_{eff}, of ^{137}Cs in bottom seawater and surface sediment. All data prior to the FDNPP accident. A red line indicates the 1:1 relationship

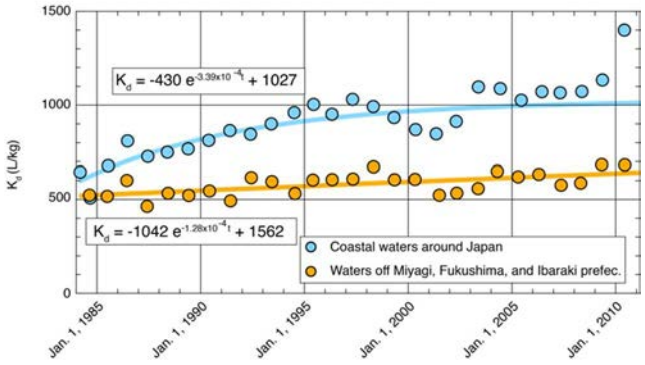

FIG 7.10. Temporal change of the geometric mean of K_d values (L/kg) in the coastal seawater around Japan and the seawaters off Miyagi, Fukushima, and Ibaraki Prefectures (1984–2010).The lines indicate best-fit curves for the geometric means at all of the monitoring data sites (blue) and those in the three prefectures only (orange). See the text for detail of curve fitting.

Compiled data on ^{137}Cs activity concentrations in seawater and sediment from 1964 to 2010 in the seawaters around Japan has been used to calculate K_d values¸ Table 7.3 shows the geometric

means for each decade after 1970 [7.48]. Except for 1964–1969, when global fallout peaked, the geometric mean values have increased from 260 to 580 L/kg. The small increase in K_d with time could be due to ^{137}Cs becoming less mobile with increased duration of retention in the sediment.

TABLE 7.3 TEMPORAL CHANGES OF GEOMETRIC MEANS AND MEDIANS OF K_D (L/KG) IN COASTAL SEAWATER AROUND JAPAN BASED ON THE DATA [7.48].

Monitoring period	N[a]	K_d (L/kg)	
		Median	GM
1964–1969	80	730	680
1970–1979	445	260	330
1980–1989	352	330	350
1990–1999	313	490	490
2000–2010	316	580	580
1964–2010	1506	450	430

[a] N is the number of data

The temporal change of K_d values in coastal areas was quantified using a simple two-box model (see Fig. 7.11) [7.42]. In the box for the coastal seawater, the inventory (Bq) of ^{137}Cs decreases with time. The decline is mainly due to mixing of surface seawater with intermediate and deep seawater and, to a much lesser extent, due to scavenging by particulate matter.

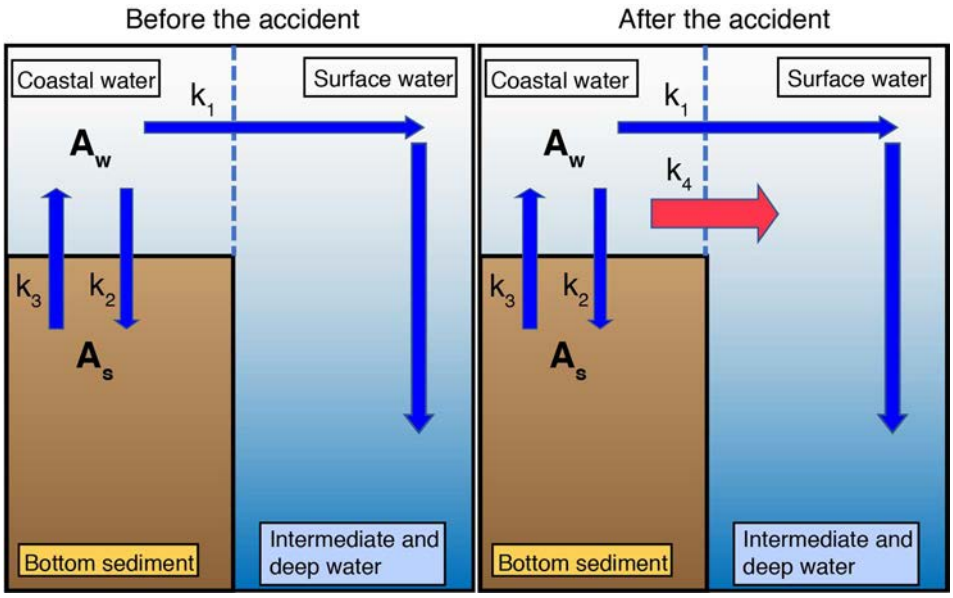

FIG 7.11. Schematic diagram of ^{137}Cs migration in the ocean. The blue arrows indicate the migration of ^{137}Cs before the accident and the red arrow shows the additional pathway for the nuclides after the FDNPP accident. The Fukushima-derived ^{137}Cs may also follow the pre-accident pathway as well to much lesser extent: it is not included in the diagram for simplicity.

The temporal change in ^{137}Cs activity A_w(Bq) in the coastal seawater is expressed as follows:

$$A_w = A_{w_0} e^{-k_1 t} \quad (7.6)$$

where A_{w_0} is the inventory of ^{137}Cs (Bq) as of 1 March 1984 and k_1 is a decline rate of the inventory due to the physical decay of ^{137}Cs and seawater mixing with deep, less contaminated seawater in the open ocean. The contribution of ^{137}Cs fluxes from the seawater to the sediment by scavenging and adsorption, and from sediment to seawater, were assumed to be negligible compared with the mass balance of ^{137}Cs in seawater. This assumption is justified because seawater exchange can be expected to be the dominant mechanism to control the ^{137}Cs activity concentration in seawater as the residence time of seawater in the continental shelf of East Japan have been estimated to be 27–32 d [7.49] and 59 d [7.30], which is much shorter than the T_{eff} of ^{137}Cs activity concentration in seawater (Table V.2). The inventory of ^{137}Cs (Bq) in the sediment is then described as follows:

$$\frac{dA_s}{dt} = k_2 A_w - k_3 A_s \quad (7.7)$$

where A_s is the total activity of ^{137}Cs in the sediment (Bq), k_2 and k_3 are the removal rates of ^{137}Cs from the overlying seawater to the bottom sediment and from the bottom sediment, respectively (year^{-1}). The removal rate k_3 includes physical decay, dissolution/desorption from the sediment, and resuspension and lateral transportation of the sediment. Including the mass of sediment *M* (kg) and seawater volume *V* (L), in order to convert total activity A_w (Bq) and A_s (Bq) to concentrations C_w (Bq/L) and C_s (Bq/kg DM), Eqs (7.6) and (7.7) can be solved for the temporal changes of C_w and C_s, which eventually gives the temporal change of $K_d = C_s/C_w$. Geometric means of ^{137}Cs activity concentrations in bottom seawater and sediments obtained from monitoring data were used to determine the parameters in Eqs (7.6) and (7.7) by curve fitting. Best-fit curves of temporal changes of K_d in the seawaters around Japan and off Miyagi, Fukushima and Ibaraki Prefectures respectively were calculated as follows:

$$K_d = -430\, e^{-3.39\times10^{-4}\, t} + 1027 \quad (7.8)$$

$$K_d = -1042\, e^{-1.28\times10^{-5}\, t} + 1562 \quad (7.9)$$

where t is expressed in days.

Temporal changes of K_d are plotted in Fig. 7.10. The data analysis showed that the K_d values were still in a transient state before the accident but were converging to the $K_{\text{d}\infty}$ values which are 1027 and 1562 in the coastal seawaters around Japan and the seawaters off Miyagi, Fukushima, and Ibaraki Prefectures, respectively. The difference in temporal changes of K_d shown in Fig. 7.10 may be affected by variation in physical characteristics of the sediments (Table V.3).

7.3.5. Temporal changes of ^{137}Cs in seawater and sediment, and $K_{d(a)}$ after the FDNPP accident

7.3.5.1. Seawater

Following the FDNPP accident, ^{137}Cs activity concentrations in surface seawater increased by several orders of magnitude. Temporal trends in ^{137}Cs activity concentrations in bottom seawater in the seawaters off all the nuclear power plants in Japan and off Fukushima and nearby prefectures are shown in Figs. 7.6a and 7.12a, respectively. More than one month after the FDNPP accident, a ^{137}Cs activity concentration of 186 Bq/L was measured in surface

seawater at a site about 30 km to the east of the FDNPP on 15 April, 2011 [7.4], compared with previous values of 1.6 ± 0.3 mBq/L (averaged over 2006–2010 in the seawaters off Fukushima). Subsequently, the ^{137}Cs activity concentrations decreased rapidly until September 2011 [7.4, 7.28, 7.30, 7.50], and after that declined more slowly. As of January 2019, the ^{137}Cs activity concentrations have been close to the pre-accident values. Although the bottom seawater layers from some deep sites shown in blue in Fig.7.12a were much less affected by the accident, the ^{137}Cs activity concentrations followed the same declining trend with time as those of surface seawater.

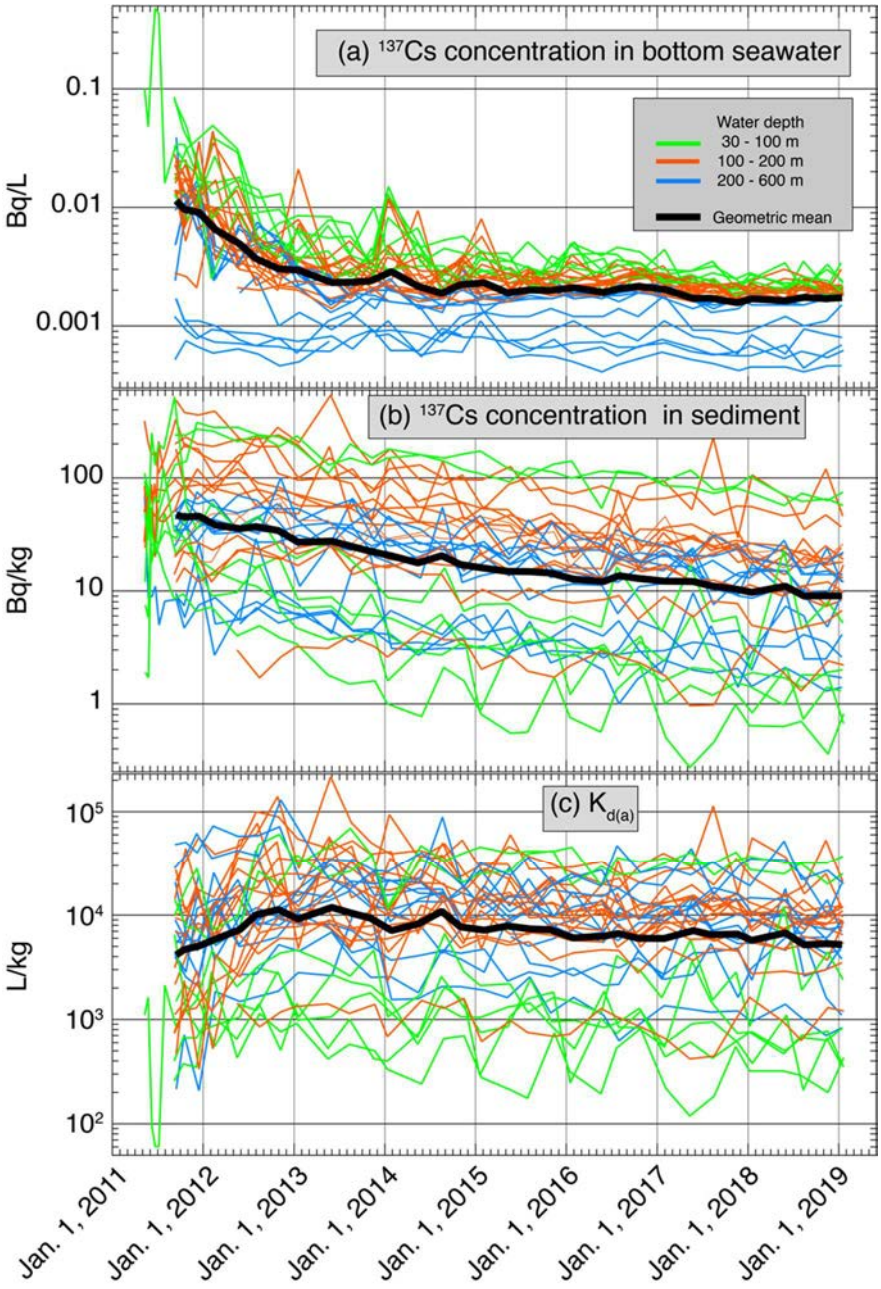

FIG 7.12. Temporal changes in ^{137}Cs activity concentrations in bottom seawater (a) and sediment (b), and of $K_{d(a)}$ (c) in the seawaters off Fukushima and nearby prefectures after the accident.

7.3.5.2. Sediment

Less than one year after the accident, the ^{137}Cs activity concentrations in the sediments increased by up to two orders of magnitude and varied spatially from 1.7 to 580 Bq/kg DM. Close proximity of a sampling station to the FDNPP did not necessarily result in a high ^{137}Cs concentration: the highest values were recorded in the seawaters off Ibaraki and Miyagi prefectures in addition to sites about 30–50 km away from the FDNPP, likely reflecting the initial passage of the contaminated seawater [7.6]. Thereafter, the ^{137}Cs activity concentration in seawater generally decreased with time. A notable feature of the temporal trend is that the ^{137}Cs activity concentration at each monitoring site has not necessarily decreased continuously. Ikenoue *et al* [7.51] reported that the irregular concentration peaks were attributed to the presence of ^{137}Cs-enriched particles that existed in bottom sediments.

The total ^{137}Cs inventory in the upper 3 cm layer of bottom sediments in the entire monitoring area (Fig. 7.5b) decreased from 46×10^{12} Bq in September 2011 to 11×10^{12} Bq in February 2016 with a T_{eff} of 2.3 years [7.41]. The declining rate at each site varied depending on the grain size of the sediments. Data on the temporal change of ^{137}Cs activity concentrations in the bottom sediments are given in Figs. 7.6b and 7.12b. The declining rates of the ^{137}Cs activity concentrations in the sediments are much smaller than those for bottom seawater. The time dependency of K_{d} is discussed below.

7.3.5.3. Post-accident $K_{d(a)}$

As shown above the mass balance of ^{137}Cs in the areas close to the accident site was completely disturbed after 11 March 2011 so that K_d is inappropriate, by definition, for the situation. An apparent distribution coefficient $K_{\text{d(a)}}$, that is used in this section is simply a ratio of ^{137}Cs concentration in sediment to that in seawater. The calculated $K_{\text{d(a)}}$ values varied depending on various factors which influenced the temporal changes of ^{137}Cs activity concentrations in bottom seawater and sediments (Fig. 7.6c). To compare temporal trends and geographical variation of $K_{\text{d(a)}}$ among the monitoring sites, the calculated post-accident $K_{\text{d(a)}}$ values were divided by the pre-accident 5-year-average value of the distribution coefficient K_{d} to provide normalized $K_{\text{d(a)}}$. The normalized $K_{\text{d(a)}}$ was set at a value of 1 for 11 March 2011 (Fig. 7.13).

The impact of the FDNPP accident was only evident in the $K_{d(a)}$ values of Miyagi, Fukushima, and Ibaraki prefectures. Data from the Niigata area (Fig. 7.13) gave higher normalized $K_{d(a)}$ values; however, the increase was less pronounced than for the three sites over the monitoring period and ascribed to the inflow of Fukushima-derived ^{137}Cs via riverine transportation in the Agano River [7.52]. The patterns of temporal changes of normalized $K_{d(a)}$ values were different in the areas off Miyagi, Fukushima and Ibaraki prefectures. Whereas the $K_{d(a)}$ values off the Miyagi area rose by at most 30-fold in two months after the FDNPP accident, they reduced by a factor of ten in the Ibaraki Prefecture. Those in the Fukushima area were intermediate between the other two areas. All of the normalized $K_{d(a)}$ off Ibaraki and a few off Fukushima decreased after the accident and then increased. However, those from other sites off Miyagi and Fukushima did not show any decrease.

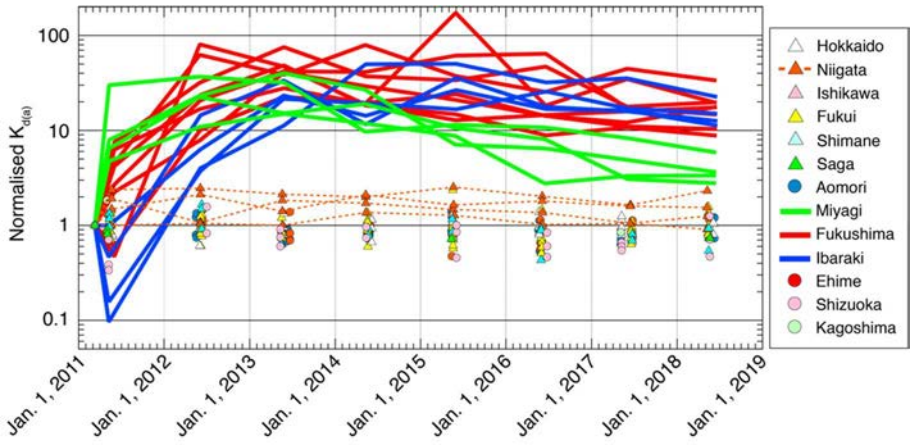

FIG 7.13. Temporal change of normalized $K_{d(a)}$ (L/kg) after the accident in the seawaters off nuclear power plants in Japan. Thick line plots were used for the data from the areas where the impact of the accident was the highest (see Fig. 7.2). Dotted line plots show the data derived from the Niigata area.

Recent studies report on the existence of radiocaesium-micro-particles (CsMP) in the release. Such particles have been detected e.g. in air filters, soil, and surface seawater [7.53]. Due to the high local ^{137}Cs activity concentration, Igarashi *et al* [7.53] identified the influence of the presence of CsMPs on K_d values from measurements carried out in the Kuchibuto River. K_d values were estimated for six samples, with and without taking into account the influence of CsMPs. The values including the CsMPs were a factor of 1.2 to 3 higher. However, it is thought that the abundance of CsMPs in seawater and bottom sediments is lower and the possible impact of the presence of CsMPs is low.

Upon arrival of the contaminated seawater, the $K_{d(a)}$ would be expected to decrease because most of the bottom sediment sample was not yet contaminated [7.45]. The temporal changes of ^{137}Cs activity concentrations in seawater and bottom sediment, and $K_{d(a)}$ are presented in Fig. 7.14. The contaminated seawater mass initially moved to the north after the FDNPP accident, and then part of the seawater mass moved to the south [7.4]. Considering the transport of the contaminated seawater mass, a decrease in the $K_{d(a)}$ should have occurred before the first samples were taken off Miyagi and off part of Fukushima. Thus, following the accident the samples were collected at or after t_2 in Fig.7.14 when $K_{d(a)}$ values were already higher than the pre-accident values. Since the contaminated seawater arrived later at the southern part of the monitoring area, a significant decrease of $K_{d(a)}$ was reported off Ibaraki, i.e., the samples were taken at around t_1. Subsequently, the $K_{d(a)}$ in all three areas became almost constant or slightly declined. Even among the three areas most affected by the FDNPP accident, the $K_{d(a)}$ values ranged by about ten-fold up to 2018.

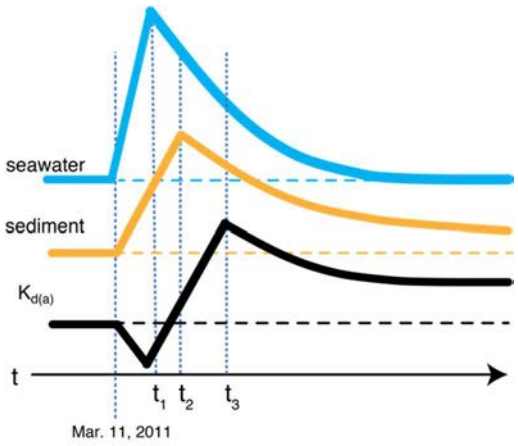

FIG 7.14. Schematic diagram of temporal changes of ^{137}Cs concentrations in seawater and sediment, and $K_{d(a)}$ after the accident in the seawaters off Fukushima and nearby prefectures. Times t_1, t_2 and t_3 denote when each curve reaches its maximum after the accident. The dotted horizontal lines indicate the pre-accident levels.

Another $K_{d(a)}$ dataset [7.42] based on additional comprehensive surveys in the area close to the accident site (Fig. 7.5b) is shown in Fig. 7.12c. The data ranged from 10^2 to ~10^5 L/kg and the geometric mean started increasing from approximately 5000 L/kg in September 2011 and reached a maximum of about 10^4 L/kg in 2013. After that, it gradually decreased.

The temporal changes of ^{137}Cs activity concentrations in seawater and bottom sediments, and of $K_{d(a)}$ after the accident were analysed using the methods described in sub-section 7.2.4. The FDNPP accident released large amounts of ^{137}Cs to the coastal area by direct discharge and through air-borne deposition. The ^{137}Cs that has been released directly from the FDNPP to the coastal area did not follow the same pathway as that of fallout ^{137}Cs, but migrated to the open ocean, initially by dispersion due to the orders of magnitude increase in the amount discharged over a much shorter period (Fig 7.11). If subsequent decreases by dispersion in the amount of ^{137}Cs activity in seawater are assumed to be exponential, then the temporal change of ^{137}Cs (Bq) in the seawater can be expressed as follows:

$$A_w = A_{w1}\, e^{-k_1 t} + A_{w2}\, e^{-k_4 t} \tag{7.10}$$

where A_{w1} and A_{w2} are amounts of ^{137}Cs on March 11, 2011 in the monitored area (Fig. 7.5b) from deposition of radionuclides to the ocean and from liquid radioactive effluents, respectively, and k_4 is a decrease rate of the accident component. Removal of ^{137}Cs from the seawater to sediment was assumed to be negligible in Eq. (7.10), assuming that the dominant mechanism to control the ^{137}Cs in coastal seawater is vertical seawater mixing in the open ocean. The temporal change of ^{137}Cs (Bq) in sediment was formulated as follows:

$$\frac{dA_s}{dt} = k_2 \frac{V}{M}(A_{w1}\, e^{-k_1 t} + A_{w2} e^{-k_4 t}) - k_3 A_s \tag{7.11}$$

As shown above, A_w and A_s in the equations were converted to C_w and C_s, respectively. Then Eq. (7.10) and solution of Eq. (7.11) were fitted to the geometric means of the data obtained in the seawaters off Miyagi, Fukushima, and Ibaraki (Fig. 7.15). The best-fit curves calculated for $K_{d(a)}$ is as follows:

$$K_{d(a)} = 6240 + \frac{-174 + 112000e^{0.00149\,t}}{8.59 + e^{0.00465\,t}} \tag{7.12}$$

Grey marks in Fig.7.15 were calculated from small datasets so that they were not included in the curve fitting. The ^{137}Cs activity concentrations in seawater due to the FDNPP accident decreased faster than those in sediments. The concentrations in seawater are almost at the same level as the pre-accident level in January 2019, whereas those in the sediments are still one order of magnitude higher. Consequently, $K_{d(a)}$ reached a maximum (10,400) in around January 2013 and decreased gradually. The curve fitting predicted that even though the ^{137}Cs activity concentrations in both phases decreased with time, the $K_{d(a)}$ will not return to the pre-accident level (~600) but will converge to a $K_{d\infty}$ of about 6,200.

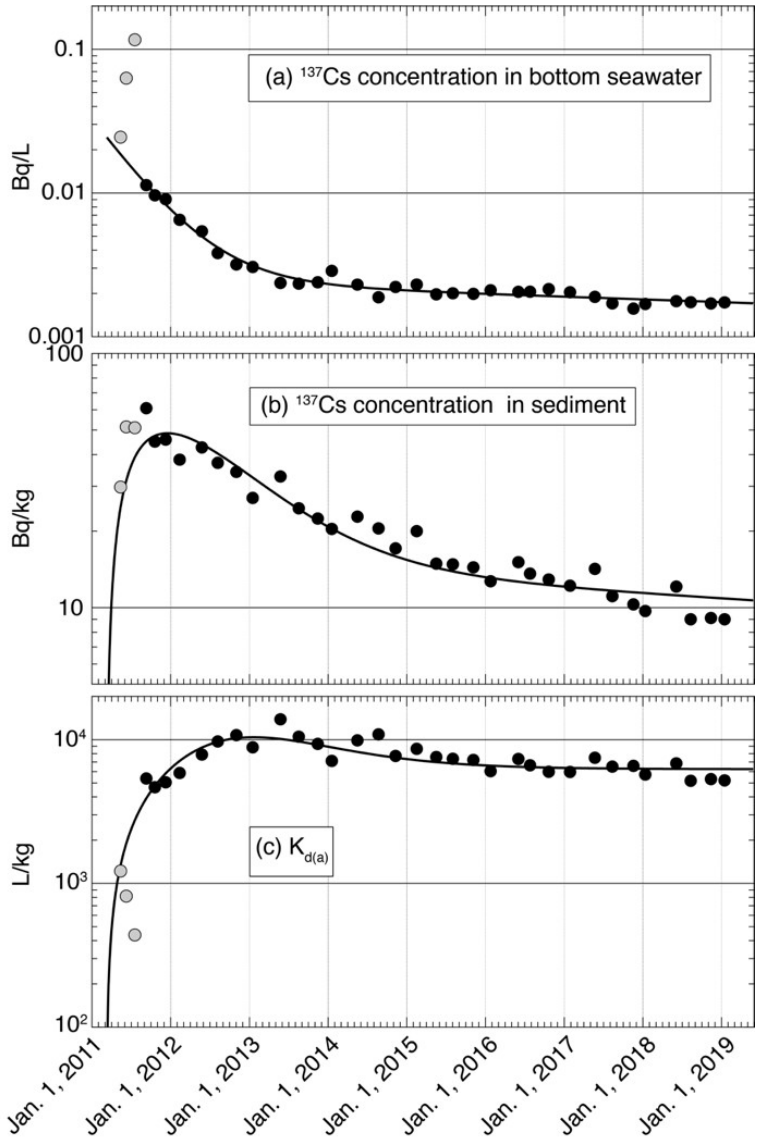

FIG 7.15. Temporal changes in geometric means of ^{137}Cs activity concentrations in bottom seawater (a) and sediment (b), and of $K_{d(a)}$ (c) in the seawaters off Fukushima and nearby prefectures after the FDNPP accident. The lines indicate the best-fit curves based on the model calculation. Data shown in grey were derived from a small dataset and were not included in the regression analysis.

As previously reported (e.g., [7.30, 7.54]), $K_{d(a)}$ values depend on both the chemical and physical characteristics of bottom sediment, which are highly variable especially in coastal areas, resulting in a wide spatial variation. Temporal changes in $K_{d(a)}$ values were also clearly presented in that report. Major factors controlling the temporal changes could be related to the intensity of the input of ^{137}Cs into the marine environment, the post-depositional behaviour of Cs in sediment and the dynamic behaviour of overlying seawater. The time needed to reach the $K_{d\infty}$ is likely to be several decades, during which time the long-lived, anthropogenic radionuclides will be in a transient state in the ocean environment approaching to the dynamic equilibrium state where $K_{d(a)} \approx K_{d\infty}$. Sedimentary environments differ considerably with variable contributions of the factors mentioned above, leading to additional complexity when trying to predict the fate of radionuclides using K_d values, especially in coastal areas.

The model presented here is obviously a simplification of the system considered with its highly variable parameters. In addition, diagenetic processes such as fast and slow reversible adsorption-desorption in sediment and vertical migration of ^{137}Cs in the pore space were not taken into consideration (e.g., [7.55, 7.56]). Re-suspension of bottom sediment and subsequent lateral transportation, which may also play an important role in the mass balance of ^{137}Cs in the bottom sediment, are not included in the model as an input from the highly polluted area to less polluted area [7.41]. Despite these deficiencies, two general conclusions can be drawn from the simple box model based on geometric means in a wide area, summarized as:

- Before the FDNPP accident, the seawater-sediment system with respect to radiocaesium had been in a transient close-to-equilibrium-state with temporally changing K_d gradually approaching to $K_{d\infty}$;
- Once significant amounts of ^{137}Cs and ^{134}Cs were added to the system, the system shifted to a newly established transient state for $K_{d(a)}$ values approaching to a higher $K_{d\infty}$ value which will continue for decades. Such ongoing retention of ^{137}Cs over decadal time scales is consistent with data observed at the Bikini and Eniwetok Atolls where the sediment/seawater activity concentration ratios remain elevated more than 60 years after the US nuclear weapons tests [7.57].

7.4. SUMMARY

Interpretation and analysis of the behaviour of radiocaesium released into the marine system after the FDNPP accident was greatly facilitated by the availability of long-term data from systematic monitoring that has been carried out in the coastal seawaters near the nuclear power plants in Japan. Immediately after the accident, monitoring of seawater, sediments and aquatic organisms in the areas affected by the accident was intensified. Pre-accident data included *CR* values for marine biota and K_d values in marine sediment which provided baseline against which changes were monitored.

7.4.1. Pre-FDNPP accident (1984–2010)

- Pre-accident concentration ratios (*CR)* for aquatic organisms were at an equilibrium whereas the distribution coefficients K_d were still very slowly increasing during the period between 1984–2010;

- Concentration ratios derived from monitoring of ^{137}Cs originating from global fallout CR_{GF} were calculated for 37 species, which were mainly fish but also included crustaceans and

cephalopods. Variation in *CR* values could be explained by several factors, including body size and trophic level;

- Pre-accident geometric mean and median K_d values in the coastal seawaters around Japan were 920 and 720 L/kg, respectively. They are significantly smaller than the mean value of 4000 L/kg from compiled data found in the IAEA report [7.10];

- K_d values varied spatially because, in some regions, there was increased absorption onto bottom sediment consisting of materials with relatively high specific surface area;

- A box model including fallout ^{137}Cs in seawater and bottom sediment indicated that pre-accident geometric mean of K_d values around Japan increased from 600 in 1984 to 1000 in 2010.

7.4.2. After the FDNPP accident

- The *CR* values in affected areas were perturbed due to the imbalance between ^{137}Cs in marine organisms and their host seawater; (termed here "apparent concentration ratios", CR_a). The CR_a values increased sharply after the accident in affected areas. Near the FDNPP they peaked during the years 2012–2013, and subsequently they have gradually returned to the pre-accident background levels (at which time they are suitable for application in steady-state analyses);

- Post-accident half-lives (termed T_a) for CR_a have been derived for quantifying the time until the pre-accident CR values were, or will be, closely approached. The disequilibrium persisted for coastal areas of Eastern Japan even 5 years after the accident;

- Values for T_a vary in the range of 200–1200 days. The T_a data indicate variation among the sampled marine areas, even within the same species. Due to the heterogeneous distribution of the ^{137}Cs plume in seawater, the estimated time span may vary according to the initial pulse amount, ongoing sources, and differences in physiology and diet among marine species;

- By 2019 the activity concentrations of ^{137}Cs in bottom seawaters, once elevated by orders of magnitude, approximately returned to pre-accident values. In comparison, the ^{137}Cs activity concentrations in the bottom sediments decreased at a much slower rate. Consequently, the marine K_d values in impacted areas sharply increased to a maximum and thereafter have not substantially decreased, but have remained relatively constant, which indicates the achievement of (quasi-) equilibrium conditions;

- A box model including ^{137}Cs derived from the accident showed that because the concentration of newly added ^{137}Cs to the bottom sediments has decreased more slowly than that in seawater, the $K_{d(a)}$ values are expected to remain significantly higher than the pre-accident levels.

7.5. LESSONS LEARNED FROM THE ACCIDENT

7.5.1. Importance of systematic monitoring on a long-term basis:

In the case of an accidental release of large amounts of radionuclides to the marine environment, knowledge on background activity concentrations and their temporal trends is essential to evaluate the impact of the accidental release. Gathering and analysis of such data provides a sound basis for prediction of future contaminant distributions in the environment as well as providing a valuable reference basis when releases do occur.

7.5.2. CR_{GF} and CR_a values as indicators of ^{137}Cs transfer to species in host vs post-accident conditions:

CR_{GF} values calculated from long-term monitoring prior to the FDNPP accident provided well-supported parameter values for transfer of ^{137}Cs to marine species in typical (quasi-steady-state conditions) of the NW Pacific Ocean. These parameters are valuable in regional assessments and provide a significant amount of new data that contribute to international databases. In areas affected by the accident, the CR_a values indicate a sharp increase of ^{137}Cs in the tissues of species relative to seawater, the CR_a values exceeded the concentration ratios determined under equilibrium conditions before the accident. The collated data allowed estimation of the time taken for the CR_a in each species to return to the pre-accident CR_{GF} baseline levels. Due to the heterogeneous distribution of the ^{137}Cs plume in seawater, the estimated time span may vary according to the initial radionuclide input, ongoing radionuclide releases, and differences in physiology and diet among marine species. The laboratory analysis detection limits have varied by monitoring area. In some areas, the relatively higher minimum detection limits used in biota monitoring resulted in many non-detections (below MDA, minimum detectable activity) that, although adequate for food safety analysis, has hampered the evaluation of the behaviour of the released ^{137}Cs in the marine environment.

7.5.3. Temporal changes of K_d values:

The temporal trend in the marine K_d values observed after the accident has generally not been well documented. The K_d values determined after the accident are not expected to be the same as those pre-accident because of disturbance in the mass balance of ^{137}Cs in seawater and bottom sediment, and longer effective half-lives of ^{137}Cs in sediments than in seawater, so that validity of the K_d concept, which is based on steady-state assumptions, needs to be carefully examined as it applies to marine systems.

7.5.4. *CR* vs $K_{d(a)}$ values:

CR and $K_{d(a)}$ are based on the similar concept, that is, a ratio of Cs activity concentration in biota or sediment to that in ambient seawater. Yet their temporal changes after the accident differed significantly. The CR_a values increased to the maximum in 1–2 years after the accident and then decreased exponentially with T_a values of 200–1100 days, approaching to the pre-accident level as of 2011; CR_a and T_a depend on biokinetics in marine biota. The $K_{d(a)}$ values also increased till January 2013, then decreased gradually converging to the $K_{d\infty}$ value, which was greater than the pre-accident value by almost two orders of magnitudes. K_d is controlled by the post-depositional behaviour of ^{137}Cs, the main processes may include fast and slow reversible adsorption-desorption in sediment and vertical migration in the pore space.

7.6. LIMITATIONS

- The differences in T_a for CR_a of various species suggests the need for additional analysis on the relative influence of specific types of food webs, food chain lengths (e.g. trophic-level effects), generational replacement, and spatial movement of fish receptors relative to the ongoing contaminant source. Since the CR_a value was highly perturbed during the first year after the accident, equation (7.4) can only be applied to the CR_a after the initial peak occurred in 2011;

- The temporal trend of K_d should be associated with oceanographic features, the temporal pattern of activity of ^{137}Cs released from the accident site, and mineralogical characteristics of sediment to appropriately address the site- and event-specific K_d values and their temporal changes. Development of mathematical models taking into account these factors would be of great help to predict the fate of radionuclides released to the marine environment and eventually to assess radiological impacts to marine organisms and humans.

7.7. REFERENCES

[7.1] BUESSELER, K., AOYAMA, M., FUKASAWA, M., Impacts of the Fukushima Nuclear Power Plants on Marine Radioactivity, Environ. Sci. Technol. **45** 23 (2011) 9931.

[7.2] GARNIER-LAPLACE, J., BEAUGELIN-SEILLER, K., HINTON, T.G., Fukushima Wildlife Dose Reconstruction Signals Ecological Consequences, Environ. Sci. Technol. **45** 12 (2011) 5077.

[7.3] HONDA, M.C. et al., Dispersion of artificial caesium-134 and -137 in the western North Pacific one month after the Fukushima accident, Geochem. J. **46** 1 (2012) e1.

[7.4] OIKAWA, S., TAKATA, H., WATABE, T., MISONOO, J., KUSAKABE, M., Distribution of the Fukushima-derived radionuclides in seawater in the Pacific off the coast of Miyagi, Fukushima, and Ibaraki Prefectures, Japan, Biogeosciences **10** 7 (2013) 5031.

[7.5] WATABE, T. et al., Spatiotemporal distribution of 137Cs in the sea surrounding Japanese Islands in the decades before the disaster at the Fukushima Daiichi Nuclear Power Plant in 2011, Sci. Total Environ. **463–464** (2013) 913.

[7.6] KUSAKABE, M., OIKAWA, S., TAKATA, H., MISONOO, J., Spatiotemporal distributions of Fukushima-derived radionuclides in nearby marine surface sediments, Biogeosciences **10** 7 (2013) 5019.

[7.7] BERESFORD, N.A., The transfer of radionuclides to wildlife, Radiat. Environ. Biophys. **49** 4 (2010) 505.

[7.8] TAKATA, H., AONO, T., TAGAMI, K., UCHIDA, S., Concentration ratios of stable elements for selected biota in Japanese estuarine areas, Radiat. Environ. Biophys. **49** 4 (2010) 591.

[7.9] HOWARD, B.J. et al., The IAEA handbook on radionuclide transfer to wildlife, Spec. Issue 2011 ICRER Meet. **121** (2013) 55.

[7.10] INTERNATIONAL ATOMIC ENERGY AGENCY, Sediment Distribution Coefficients and Concentration Factors for Biota in the Marine Environment, Technical Reports Series 422, IAEA, Vienna (2004).

[7.11] BERESFORD, N.A. et al., Derivation of transfer parameters for use within the ERICA Tool and the default concentration ratios for terrestrial biota, J. Environ. Radioact. **99** 9 (2008) 1393.

[7.12] BROWN, J.E. et al., A new version of the ERICA tool to facilitate impact assessments of radioactivity on wild plants and animals, J. Environ. Radioact. **153** (2016) 141.

[7.13] COPPLESTONE, D., BERESFORD, N.A., BROWN, J.E., YANKOVICH, T., An international database of radionuclide concentration ratios for wildlife: development and uses, J. Environ. Radioact. **126** (2013) 288.

[7.14] YANKOVICH, T.L. et al., Whole-body to tissue concentration ratios for use in biota dose assessments for animals, Radiat. Environ. Biophys. **49** 4 (2010) 549.

[7.15] JOHANSEN, M.P. et al., Radiological Dose Rates to Marine Fish from the Fukushima Daiichi Accident: The First Three Years Across the North Pacific, Environ. Sci. Technol. **49** 3 (2015) 1277.

[7.16] INTERNATIONAL ATOMIC ENERGY AGENCY, Handbook of Parameter Values for the Prediction of Radionuclide Transfer to Wildlife, Technical Reports Series 479, IAEA, Vienna (2014).

[7.17] ROWAN, D.J., CHANT, L.A., RASMUSSEN, J.B., The fate of radiocesium in freshwater communities—Why is biomagnification variable both within and between species?, J. Environ. Radioact. **40** 1 (1998) 15.

[7.18] UGEDAL, O., FORSETH, T., JONSSON, B., NJASTAD, O., Sources of Variation in Radiocaesium Levels Between Individual Fish from a Chernobyl Contaminated Norwegian Lake, J. Appl. Ecol. **32** 2 (1995) 352.

[7.19] FUJIO KASAMATSU, YUSUKE ISHIKAWA, Natural variation of radionuclide 137Cs concentration in marine organisms with special reference to the effect of food habits and trophic level, Mar. Ecol. Prog. Ser. **160** (1997) 109.

[7.20] ELLIOTT, J.M. et al., Sources of Variation in Post-Chernobyl Radiocaesium in Fish from Two Cumbrian Lakes (North-West England), J. Appl. Ecol. **29** 1 (1992) 108.

[7.21] TAKATA, H. et al., A 30-year record reveals re-equilibration rates of 137Cs in marine biota after the Fukushima Dai-ichi nuclear power plant accident: Concentration ratios in pre- and post-event conditions, Sci. Total Environ. **675** (2019) 694.

[7.22] SUZUKI, Y., NAKAHARA, M., NAKAMURA, R., Accumulation of Cesium-137 by Useful Mollusca, NIPPON SUISAN GAKKAISHI **44** 4 (1978) 325.

[7.23] NAGAYA, Y., SUZUKI, Y., NAKAMURA, K., 239, 240Pu and 137Cs Concentrations in Some Marine Organisms, Mostly from the Ibaraki and Aomori Coasts, Japan, 1987-1989, NIPPON SUISAN GAKKAISHI **56** 10 (1990) 1599.

[7.24] TATEDA, Y., KOYANAGI, T., Concentration Factors for Cs-137 in Marine Algae from Japanese Coastal Waters, J. Radiat. Res. (Tokyo) **35** 4 (1994) 213.

[7.25] TATEDA, Y., Concentration Factor of 137Cs for Zooplankton Collected from the Misaki Coastal Water, Fish. Sci. **64** 1 (1998) 176.

[7.26] KAERIYAMA, H., WATABE, T., KUSAKABE, M., 137Cs concentration in zooplankton and its relation to taxonomic composition in the western North Pacific Ocean, J. Environ. Radioact. **99** 12 (2008) 1838.

[7.27] FISHERIES AGENCY, Results of the Monitoring on Radioactivity Level in Fisheries Products, Ministry of Agriculture, Forestry and Fisheries of Japan.

[7.28] TAKATA, H., KUSAKABE, M., INATOMI, N., IKENOUE, T., Appearances of Fukushima Daiichi Nuclear Power Plant-Derived 137Cs in Coastal Waters around Japan: Results from Marine Monitoring off Nuclear Power Plants and Facilities, 1983–2016, Environ. Sci. Technol. **52** 5 (2018) 2629.

[7.29] WADA, T. et al., Effects of the nuclear disaster on marine products in Fukushima: An update after five years, J. Environ. Radioact. **164** (2016) 312.

[7.30] TAKATA, H., AONO, T., TAGAMI, K., UCHIDA, S., A new approach to evaluate factors controlling elemental sediment–seawater distribution coefficients (Kd) in coastal regions, Japan, Sci. Total Environ. **543** (2016) 315.

[7.31] IWATA, K., TAGAMI, K., UCHIDA, S., Ecological Half-Lives of Radiocesium in 16 Species in Marine Biota after the TEPCO's Fukushima Daiichi Nuclear Power Plant Accident, Environ. Sci. Technol. **47** 14 (2013) 7696.

[7.32] TAGAMI, K., UCHIDA, S., Consideration on the Long Ecological Half-Life Component of 137Cs in Demersal Fish Based on Field Observation Results Obtained after the Fukushima Accident, Environ. Sci. Technol. **50** 4 (2016) 1804.

[7.33] YOSHIDA, K., SUZUKI, N., TOMOSADA, A., Time of appearance of the 137Cs peak concentrations and retention time in marine fish under the load to the sea---Based on data before and after the Chernobyl accident and inter-annual variability prediction formula, Rep. Study Environ. Radioact. (2004) 85.

[7.34] MATSUMOTO, A. et al., Biological half-life of radioactive cesium in Japanese rockfish Sebastes cheni contaminated by the Fukushima Daiichi nuclear power plant accident, J. Environ. Radioact. **150** (2015) 68.

[7.35] KASAMASTU, F., Notes on Possible change in the food of Atka Mackerel, Pleurogrammus azonus, taken off Niigata as suggested by recent change of radiocesium concentrations, Bull Jap Soc Fish Ocean. **60** (1996) 227.

[7.36] NARIMATSU, Y. et al., "Why Do the Radionuclide Concentrations of Pacific Cod Depend on the Body Size?", Impacts of the Fukushima Nuclear Accident on Fish and Fishing Grounds (NAKATA, K., SUGISAKI, H., Eds), Springer Japan, Tokyo (2015) 123–137.

[7.37] SHIGENOBU, Y. et al., Radiocesium contamination of greenlings (Hexagrammos otakii) off the coast of Fukushima, Sci. Rep. **4** 1 (2014) 6851.

[7.38] KASAMATSU, F., UEDA, Y., TOMIZAWA, T., NONAKA, N., NAGAYA, Y., Preliminary report on radionuclide concentrations in the bottom waters at the entrance of Wakasa Bay with special reference to the Japan Sea Proper Water, J. Oceanogr. **50** 5 (1994) 589.

[7.39] KASAMATSU, F., INATOMI, N., Effective environmental half-lives of 90Sr and 137Cs in the coastal seawater of Japan, J. Geophys. Res. Oceans **103** C1 (1998) 1209.

[7.40] TAKATA, H. et al., Long-term distribution of radioactive cesium in the coastal seawater and sediments of Japan, Rep Mar Ecol Res Inst 22 (2017) 17.

[7.41] KUSAKABE, M., INATOMI, N., TAKATA, H., IKENOUE, T., Decline in radiocesium in seafloor sediments off Fukushima and nearby prefectures, J. Oceanogr. **73** 5 (2017) 529.

[7.42] KUSAKABE, M., TAKATA, H., Temporal trends of 137Cs concentration in seawaters and bottom sediments in coastal waters around Japan: implications for the Kd concept in the dynamic marine environment, J. Radioanal. Nucl. Chem. **323** 1 (2020) 567.

[7.43] POVINEC, P.P. et al., 90Sr, 137Cs and 239,240Pu concentration surface water time series in the Pacific and Indian Oceans – WOMARS results, J. Environ. Radioact. **81** 1 (2005) 63.

[7.44] HIROSE, K., AOYAMA, M., Analysis of 137Cs and 239,240Pu concentrations in surface waters of the Pacific Ocean, Deep Sea Res. Part II Top. Stud. Oceanogr. **50** 17 (2003) 2675.

[7.45] BOYER, P., WELLS, C., HOWARD, B., Extended Kd distributions for freshwater environment, J. Environ. Radioact. **192** (2018) 128.

[7.46] HE, Q., WALLING, D.E., Interpreting particle size effects in the adsorption of 137Cs and unsupported 210Pb by mineral soils and sediments, J. Environ. Radioact. **30** 2 (1996) 117.

[7.47] MACKENZIE, A.B., COOK, G.T., MCDONALD, P., JONES, S.R., The influence of mixing timescales and re-dissolution processes on the distribution of radionuclides in Northeast Irish Sea sediments, J. Environ. Radioact. **39** 1 (1998) 35.

[7.48] UCHIDA, S., TAGAMI, K., Comparison of coastal area sediment-seawater distribution coefficients (Kd) of stable and radioactive Sr and Cs, Transform. Fate Nat. Anthropog. Radionucl. Environ. **85** (2017) 148.

[7.49] CHARETTE, M.A. et al., Radium-based estimates of cesium isotope transport and total direct ocean discharges from the Fukushima Nuclear Power Plant accident, Biogeosciences **10** 3 (2013) 2159.

[7.50] KUMAMOTO, Y. et al., Radiocesium in North Pacific coastal and offshore areas of Japan within several months after the Fukushima accident, J. Environ. Radioact. **198** (2019) 79.

[7.51] IKENOUE, T., ISHII, N., KUSAKABE, M., TAKATA, H., Contribution of 137Cs-enriched particles to radiocesium concentrations in seafloor sediment: Reconnaissance experiment, PLOS ONE **13** 9 (2018) e0204289.

[7.52] INOUE, M. et al., Spatial variation in low-level 134Cs in the coastal sediments off central Honshu in the Sea of Japan: implications for delivery, migration, and redistribution patterns, J. Oceanogr. **73** 5 (2017) 571.

[7.53] IGARASHI, Y. et al., A review of Cs-bearing microparticles in the environment emitted by the Fukushima Dai-ichi Nuclear Power Plant accident, J. Environ. Radioact. **205–206** (2019) 101.

[7.54] TAKATA, H., TAGAMI, K., AONO, T., UCHIDA, S., Distribution coefficients (Kd) of strontium and significance of oxides and organic matter in controlling its partitioning in coastal regions of Japan, Sci. Total Environ. **490** (2014) 979.

[7.55] MADERICH, V., JUNG, K.T., BROVCHENKO, I., KIM, K.O., Migration of radioactivity in multi-fraction sediments, Environ. Fluid Mech. **17** 6 (2017) 1207.

[7.56] PERIÁÑEZ, R., BROVCHENKO, I., JUNG, K.T., KIM, K.O., MADERICH, V., The marine kd and water/sediment interaction problem, J. Environ. Radioact. **192** (2018) 635.

[7.57] BUESSELER, K.O., CHARETTE, M.A., PIKE, S.M., HENDERSON, P.B., KIPP, L.E., Lingering radioactivity at the Bikini and Enewetak Atolls, Sci. Total Environ. **621** (2018) 1185.

8. FOOD AND CULINARY PROCESSING

KEIKO TAGAMI, SHIGEO UCHIDA
National Institute of Radiological Sciences, National Institutes for Quantum and Radiological Science and Technology, JAPAN

SERGEY FESENKO
Russian Institute of Radiology and AgroEcology, RUSSIAN FEDERATION

GERHARD PRÖHL
Consultant, GERMANY

8.1. INTRODUCTION

Different food processing methods that vary with agricultural and climatic conditions, economic constraints and national or regional traditions are used worldwide. The activity concentrations of radionuclides in food that is consumed are modified by both domestic and industrial food processing such as boiling, removal of certain parts of the raw food (e.g. bran, peel, shell and bone), drying and mixing with other, uncontaminated food components [8.1].

The transfers of radionuclides to foodstuffs described in preceding chapters have been relatively well studied and robust values for quantifying radionuclide transfers to plants and animals are available in international compilations of data (e.g. IAEA-TECDOC-1616) [8.1]. However, the impact of food processing on the amounts of consumed radionuclides can be significant, Therefore, neglecting variations in radionuclide activity concentrations in foodstuffs during food processing can lead to either overestimation (in most cases) or underestimation of the ingestion doses to humans [8.2].

During the management of environmental contamination following nuclear accidents, food processing is considered to be an important option to reduce activity concentrations in foods and to reduce exposures to people [8.3]. During storage and processing of foodstuffs the activity concentrations of short-lived radionuclides (such as ^{131}I) will considerably decrease. Processing of milk with high ^{131}I activity concentrations during the acute phase of the Chernobyl accident and production of long-lasting foodstuffs (such as butter, cheese and dried milk) ensured significant decreases of ^{131}I activity concentrations in these foodstuffs due to radioactive decay before their delayed consumption.

The wastes or by-products generated in food processing may contain radionuclides and the impacts of their disposal or use for other purposes may need to be addressed. Some by-products generated during food processing may be subsequently used as animal feed, or as components used in other processes in the food industry. For example, the bran of rice can be used for preparation of a salt solution “Nukadoko” which is used for making Japanese pickles. Therefore, the use of contaminated bran may result in contamination of pickled products, even though the main ingredients are not contaminated.

Most of the information on changes of radionuclide activity concentrations in foodstuffs during processing and culinary preparation is available for caesium and iodine. The dominance of information on radioisotopes of these elements is due to the experience gained on radionuclide transfers in human food chains during nuclear weapons’ testing and after nuclear accidents. These data have been summarised in several international reviews, such as IAEA-TECDOC 1616 and TRS 472 [8.1, 8.2], and by the Radioactive Waste Management Centre in Japan

(hereafter termed RWMC) and other national reviews [8.4–8.6]. Extensive experience gained after the Chernobyl accident has shown that many commonly used methods of domestic and industrial processing of food products result in significant reductions of radionuclide activity concentrations in many foodstuffs and hence of internal radiation doses to people [8.2, 8.6, 8.7]. After the FDNPP accident, food processing options were considered to reduce radioiodine and radiocaesium concentrations in foodstuffs. However, the wide ranges in previously reported reductions of radioiodine and radiocaesium that occurred after food processing and the special methods of culinary processing of many Japanese foodstuffs such as Tofu and Surimi, limited the usefulness of available food processing data for estimating potential reductions in internal doses and facilitating the carrying out of more realistic dose assessments. In response, the previously reported data on the effects of food processing and culinary preparation reported by RWMC [8.4] were updated using data obtained after the FDNPP accident [8.5].

The consumption of edible wild plants such as new shoots of fern, bamboo, and some herbaceous plants and trees is common in Japan. There are no relevant data on processing of such foodstuffs in TRS-472 and other international reviews. The measurement and collation of such information after the FDNPP accident allowed an extension of the existing database on food processing and may be of particular relevance for countries with similar food consumption habits to those in Japan.

This chapter provides an overview of the data obtained after the FDNPP accident on the modification of radionuclide activity concentrations in foodstuffs during industrial and domestic food processing.

8.2. DEFINITIONS AND CONCEPTS

Three major parameters are normally used to quantify the effects of food processing, namely food processing factor, food processing retention factor and processing efficiency (see Chapter 2).

The food processing factor, F_r, and the food processing retention factor, P_f, are applied to quantify the total loss of radionuclides during processing; they are also used for calculations of individual and collective doses arising from the consumption of contaminated foodstuffs [8.1] (see Chapter 2). These parameters can be also applied for the assessment of the impacts arising from the use of by-products generated during food processing. Since the mass of the processed food can differ from the weight of the raw product, one more parameter is required to provide a relationship between food processing factor and food processing retention factor. The processing efficiency P_e is the ratio of the fresh mass of the processed food (kg FM) to mass of the original raw material (kg FM).

For some foodstuffs (vegetables and fruits), F_r values based on ‘surface contamination’, such as washing, are also presented. It is assumed that the foodstuffs are largely “externally” contaminated because of spraying, resuspension or direct deposition, when the time lag between the contamination event and food processing is short enough to prevent radionuclide transfer from the surface of plants into the inner tissues.

For root crops, surface contamination is largely due to the attachment of contaminated soil particles to the surface of vegetables.

8.3. PROCESSING OF CEREALS

Data on processing of rice, wheat and buckwheat derived after the FDNPP accident are given in Table 8.1. Processing of cereals can include various steps such as milling and production of different end products, including noodles. The efficiency of radionuclide removal from cereals through processing may be up to 90% of the initial radionuclide activity in raw material, depending on the procedure applied (see Table 8.1). In areas affected by the FDNPP accident, the harvest of cereals occurred around six months after the accident and cereals were not directly affected by the deposition. The removal of radionuclide activity from cereals due to washing was low, with a reduction in the radiocaesium activity concentration of only 5% or less of the initial activity present. Other options of food processing, such as the production of flour from grain were more effective. The subsequent use of these methods used for preparation of meals provides products with low radiocaesium activity concentrations (see Table 8.1).

TABLE 8.1. FOOD PROCESSING FACTORS FOR CEREALS [A]

Initial product	Type of rice processing	N	P_f	P_e	F_r	Reference
			Rice			
Brown rice	Milling to white rice	7	0.46 ± 0.03	0.90–0.92	0.42 ± 0.03	[8.8–8.10]
Brown rice	Milling to white rice		— [b]	—	0.2–0.4	[8.1]
Brown rice	Washing	6	0.96 ± 0.03	1.00	0.96 ± 0.03	[8.8, 8.10]
Medium milled rice (excl. white rice)	Washing	7	0.59 ± 0.07	0.96 ± 0.00	0.68 ± 0.08	[8.5, 8.9, 8.11]
White rice	Washing	6	0.58	0.96	0.65 ± 0.05	[8.5, 8.9, 8.11]
Brown rice	Boiling rice after milling to white rice and washing	3	0.13 ± 0.01	2.33	0.30 ± 0.03	[8.5, 8.9]
Medium milled rice (excl. white rice)	Boiling rice after washing	3	0.26 ± 0.00	2.46 ± 0.03	0.64 ± 0.02	[8.9]
White rice	Boiling rice after washing	3	0.27 ± 0.02	2.36 ± 0.11	0.64 ± 0.01	[8.5, 8.9]
White rice	Boiling rice noodle	3	0.33 ± 0.07	1.51 ± 0.02	0.50 ± 0.11	[8.10]
Brown rice	Rice bread	2	0.41	1.97	0.21	[8.5]
			Wheat			
Wheat	Milled outer layer	13	2.17 ± 0.18	0.37 ± 0.03	0.80 ± 0.09	[8.5, 8.12]
Wheat	Milling to white flour	14	0.33	0.56	0.19	[8.5, 8.12]
Wheat	Milling to white flour		—	0.6–0.8	0.2–0.6	[8.1]
Udon noodle (fresh)	Boiling	10	0.07 ± 0.03	2.48 ± 0.44	0.17 ± 0.05	[8.13]
Udon noodle (dried)	Boiling	6	0.08 ± 0.04	2.98 ± 0.42	0.22 ± 0.07	[8.14]
Chinese noodle (fresh)	Boiling	3	0.26	1.8	0.46	[8.5]
Macaroni, spaghetti, pasta	Boiling		—	—	0.1–0.4	[8.1]

TABLE 8.1. FOOD PROCESSING FACTORS FOR CEREALS [A] (cont.)

Initial product	Type of rice processing	N	P_f	P_e	F_r	Reference
			Buckwheat			
Threshed and winnowed	Polished grains	2	0.45	1	0.45	[8.15]
Threshed and winnowed	Polishing and ultrasonic washing	2	0.33	1	0.33	[8.15]
Threshed and winnowed	Milling	2	0.70	0.57	0.40	[8.16]
Buckwheat flour	Boiled noodle	6	0.42 ± 0.07	1.51 ± 0.10	0.64 ± 0.09	[8.16]

[a] the data are shown are either a single value or a mean ± standard deviation or a range
[b] no data

Bran is removed during milling of brown rice (up to the stage of hulled rice). Complete removal of the bran produces white rice that is typically used for cooking. During the transformation of brown rice to white rice, the total weight is reduced by about 90% (i.e. the processing efficiency of this option is about 90%). The distribution of radiocaesium in brown rice is inhomogeneous as the bran is enriched with many microelements and contains higher radiocaesium activity concentrations compared with that of the entire grain [8.17].

Almost 50% of the total Cs is located in the rice bran. When the milling grade of white rice increases (or decreases for P_e), a larger fraction of the bran is removed and the remaining fraction of radiocaesium in rice decreases.

Depending on the use of rice, different milling grades are used during the processing of brown rice. Figure 8.1 shows a strong linear relationship between the food processing factor (P_f) and the milling grade of brown rice. In this figure, the milling grade is quantified by the processing efficiency of brown rice P_e, which decreases from 1 to 0.9–1.0, i.e. the removed fraction of the rice grain increases from 0 to up to 10%. For white rice with the processing efficiency P_e between 0.90 and 0.92 (n = 6) (8–10% of the grain is removed), the arithmetic mean for P_f is 0.46 with a standard deviation of 0.03. The arithmetic mean value for the food processing retention factor F_r is 0.42 ± 0.03 (i.e. 42% of the radiocaesium in the brown rice remained in the white rice).

After milling, rice grains are typically washed several times before cooking. During this process, more radiocaesium is removed from white rice than during the washing of brown rice (Table 8.1). During boiling, the mass of white rice increases 2.3–2.4 times, but no further decrease of caesium content takes place (F_r about 1.0). However, due to the increase of mass with water, radiocaesium activity concentrations in boiled rice decrease.

The removed rice bran can be used to make “Nukadoko” solution by adding salt, water, and other ingredients. Typically, 1 kg of rice bran is mixed with about 1 L of salt water (100–200 g/L); dilution factors for several types of “Nukadoko” samples vary between 0.37–0.55 compared with the initial total Cs in rice bran. The solution that is normally used for making Japanese pickles is called “Nukazuke” (Table 8.2). Tanji et al. [8.12] determined *CR* values between pickled vegetables (using three uncontaminated vegetables) and “Nukadoko” solution and reported *CR* values of 0.2–0.3 after 16 hours pickling. Uncontaminated cucumber contained more radiocaesium (by 2 to 3-fold) when the pickling time of contaminated “Nukadoko” increased [8.12].

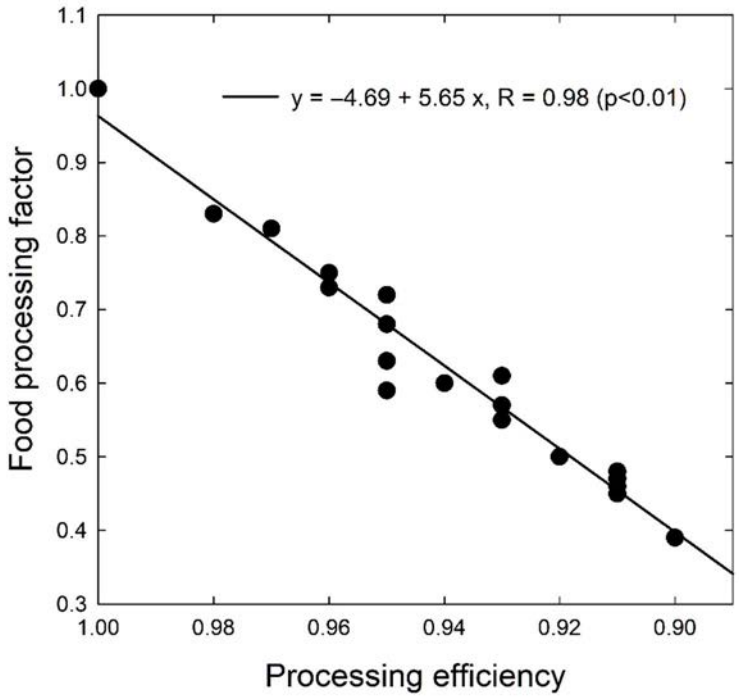

FIG. 8.1. Relationship between the food processing factor P_f of brown rice for radiocaesium and the processing efficiency P_e, which is linked to extent of bran removal; e.g., $P_e = 0.9$ corresponds to removal of 10% of the rice grain.

TABLE 8.2. PROCESSING FACTOR FOR PICKLED VEGETABLES FOR NUKADOKO MADE FROM RICE BRAN [8.12]

Pickled vegetables (time of pickling)	N	Processing factor P_f
Cucumber	4	0.33 ± 0.10
Cucumber (27 hours)	1	0.71
Cucumber (8 days)	1	0.93
Turnip (16 hours)	1	0.21
Carrot (16 hours)	1	0.31
Japanese radish	1	0.20

Radiocaesium was measured during the processing chain of wheat-wheat flour-noodles (Table 8.1). Udon noodles are treated in two ways namely: boiled freshly made Udon noodles or, as commonly done for pasta, freshly made Udon noodles are first dried (to make it non-perishable) and boiled later. In both cases, the F_r values are around 0.2.

8.4. PROCESSING OF SOYBEAN

Soybeans are used for the preparation of many foodstuffs that are widely used in normal Japanese cuisine. For example, Natto is made from fermented boiled soybean and Tofu is made from soy milk (Fig. 8.2). Food processing factors are shown in Table 8.3.

Soaking removed 5–20% of the total radiocaesium (Bq) in soybeans [8.5, 8.18]. The activity concentrations of caesium in the final products (soy milk and curd) are less than half that of the soybean. After squeezing and other processing, radiocaesium activity concentrations in some end food products (Tofu, Miso) are only 15–22% of that in the soybean.

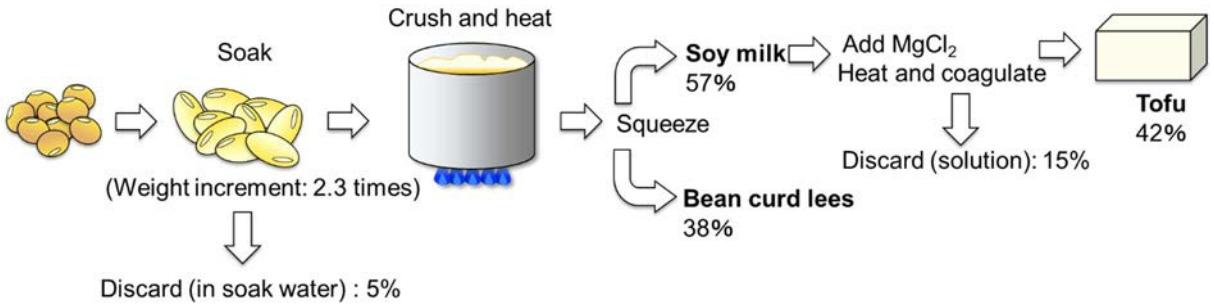

FIG. 8.2. Fluxes of radiocaesium during the processing of soybean.

TABLE 8.3. FOOD PROCESSING FACTORS OF SOYBEAN FOR CS

Product	Type of processing	N	P_f	P_e	F_r	Reference
Soybean	Soaking	4	0.45	2.1	0.95	[8.5]
	Soaking	3	— [a]	—	0.80	[8.18]
Bean curd lees	Squeezing	4	0.20	2.0	0.39	[8.5]
Soymilk	Squeezing	4	0.13	4.4	0.57	[8.5]
Boiled soybean	Boiling	4	0.21	2.4	0.50	[8.5]
	Boiling	3	—	—	0.48–0.53	[8.18]
Steamed soybean	Steaming	4	0.43	2.2	0.94	[8.5]
Tofu	Soaking, boiling, squeezing, doping (see text)	4	0.15	2.8	0.42	[8.5]
Natto	Soaking, boiling, fermenting (see text)	4	0.43	2.1	0.91	[8.5]
Miso	Soaking, boiling, doping, fermenting (see text)	1	0.22	3.7	0.81	[8.5]

[a] no data

8.5. VEGETABLES AND FRUITS

There are several contamination pathways for vegetables and fruits. Leafy vegetables can be contaminated by direct deposition and through uptake of radionuclides by translocation from leaf surfaces and from soil via the roots. The surface of plants can also have resuspended, contaminated adhered soil particles. The significance of these different pathways depends on the contamination scenario, and the plant biomass and structure. Immediately after the deposition of radionuclides, a relatively high fraction may initially be present on plant surfaces, compared with later times after deposition. The partitioning of radionuclides between external deposits and incorporation into plant tissues depends on the time after deposition and the amount of plant biomass present both at the time of deposition and at harvest, such as cabbage,

tomato and radish. For vegetables with an open foliar structure such as spinach, although leaf has a thin structure, there are surface and internal tissue parts thus the same effect can be observed. This effect can be substantial for vegetables and is less pronounced for fruits. Accordingly, the efficiency of some food processing options (F_r and P_f values) differs with time after deposition occurs.

Differences in the efficiency of removal of radionuclides between contamination of plant surface by direct deposition and subsequent phases (internal contamination) were observed after both the Chernobyl and the FDNPP accidents. Therefore, data for vegetables are reported separately for the initial period when deposition occurred and for subsequent periods (Tables 8.4 and 8.5). For oil seed (*Perilla frutescens*), the data are provided in Table 8.6.

The IAEA documents TECDOC 1616 [8.1] and TRS 472 [8.2] provide a wide range of F_r values, from 0.1 to 0.9. The retention of radioiodine and radiocaesium depends on the characteristics of the surface contamination of the crops; therefore, F_r varies with the extent and type of surface contamination. No differences were reported between F_r values for radioiodine and radiocaesium in TRS 472, whereas after the FDNPP accident more radiocaesium was removed compared with radioiodine (although, these values are within the reported ranges of TRS 472 [8.2]).

TABLE 8.4. FOOD PROCESSING RETENTION FACTOR FOR VEGETABLES WITH SURFACE CONTAMINATION OBSERVED SHORTLY AFTER THE FDNPP ACCIDENT

Plant type	Type of processing	FDNPP data						TRS 472 [8.2]	
		N	AM	GM	Minimum	Maximum	Reference	Min	Max
					Radioiodine				
Spinach	Washing	13	0.67	0.67	0.56	0.88	[8.5, 8.19]	0.1	0.9
Spinach	Boiling	1	0.40	n.a.[a]	n.a.	n.a.	[8.5]	0.1	0.5
					Radiotellurium				
Spinach	Washing	10	0.50	0.49	0.38	0.80	[8.5, 8.19]	—[b]	—
Spinach	Boiling	1	0.47	n.a.	n.a.	n.a.	[8.5]	—	—
					Radiocaesium				
Spinach	Washing	13	0.44	0.43	0.29	0.68	[8.5, 8.19]	0.1	0.9
Spinach	Boiling	1	0.27	n.a.	n.a.	n.a.	[8.5]	0.1	0.5

[a] not applicable
[b] no data

After the emergency phase of the FDNPP accident, data for vegetables and fruit processing were only available for radiocaesium when uptake of radionuclides via the roots became the dominating contamination route. Processing factors for washing and boiling for this period (P_f and F_r) were near 1.0, underlining the lower effectiveness of washing of crops that have been harvested at longer times after the deposition occurred.

TABLE 8.5. FOOD PROCESSING RETENTION FACTOR OF VEGETABLES INTERNALLY CONTAMINATED WITH RADIOCAESIUM (VIA ROOT CONTAMINATION)

Type of processing	N	P_f [8.5]	F_r [8.5]			P_e [8.2]		F_r [8.2]	
			GM	Min.	Max.	Min.	Max.	Min.	Max.
Leafy vegetables, washing	15	—[a]	0.84	0.27	1.0	1.0	1.0	0.6	1.0
Leafy vegetables, boiling	21	0.52	0.44	0.04	0.93	0.8	1.0	0.4	0.9
Root crops, peeling	1	0.18	0.16	n.a.[b]	n.a.	0.7	0.9	0.5	0.9
Root vegetables, boiling	1	0.87	0.82	n.a.	n.a.	—	—	—	—
Leafy vegetables and root crops, salting using salt water or soy sauce	5	0.57	0.30	0.13	0.65	—	—	—	—

[a] no data
[b] not available

TABLE 8.6. FOOD PROCESSING FACTORS OF PERILLA OIL SEED (*PERILLA FRUTESCENS*) FOR CS [8.5]

Product	Type of processing	N	P_f	P_e	F_r
Perilla seed	Roasting	3	0.98	0.97	0.92
Perilla seed oil	Pressing	3	0.08	0.34	0.03

Data on fruits processing are given in Table 8.7. These data show the low effectiveness of food processing for radiocaesium removal F_r and a reduction of the radionuclide activity concentrations P_f for nearly all processing options. In contrast, drying or preparation of syrup increased radiocaesium activity concentrations compared with the fresh products. The only effective option was the production of alcoholic drinks from fruits, which provided a two-fold removal of radiocaesium and a three-fold reduction of radiocaesium activity concentrations in the end product.

The data in Table 8.7 also indicate that washing and peeling were only effective soon after the FDNPP accident occurred when the surface contamination was much higher than the contamination of the inner plant tissues.

8.6. BEVERAGES

8.6.1. Tea brewing

Green tea leaves are made from young leaves of tea trees. To produce Japanese green tea, leaves are first steamed for about 15–20 seconds, then the leaves are dried after rolling. Tea leaves are not washed to avoid losing flavour. Varying water temperatures and brewing times used for Japanese green tea had little effect on the amount of radiocaesium extracted (Table 8.8). About 50–70% radiocaesium was extracted from tea leaves for all conditions.

Barley tea is an extract made from roasted barley. During preparation, when roasted barley grains are boiled in water for 5–10 min and then left for different soaking times, the tea colour darkens and the F_r increases, especially after 2 hours soaking time, as shown in Table 8.8. The IAEA TECDOC 1616 provided a range of F_r values of 0.4–0.6 for tea brewing times of only 2–8 minutes [8.1]. Similar values were also reported for herbal tea.

TABLE 8.7. MEAN FOOD PROCESSING FACTORS OF CS IN FRUITS

Type of fruits	Type of processing	N	P_f	P_e	F_r	Reference
	Surface contamination					
Apple	Washing	3	0.93	1.0	0.95	[8.5]
Apple	Washing and peeling	5	0.92	0.78	0.71	[8.5]
Blue berry	Washing	4	1.0	1.0	1.0	[8.5]
Grape	Washing and peeling	2	0.84	0.92	0.77	[8.5]
Japanese apricot	Washing	5	0.65	1.0	0.65	[8.5]
Japanese apricot	Washing and peeling	3	0.50	0.57	0.35	[8.5]
Japanese apricot	Pickled with salt (10–20% weight of total fruits)	6	0.99	0.82	0.81	[8.5]
Loquat	Washing and peeling	2	0.85	0.49	0.41	[8.5]
Peach	Washing	2	0.85	1.0	0.85	[8.5]
Peach	Washing and peeling	5	0.76	0.82	0.62	[8.5]
Peach	Juice production	2	0.95	0.66	0.63	[8.5, 8.20]
Persimmon	Washing and peeling	3	0.76	0.81	0.61	[8.5]
	Internal contamination					
Apple	Washing	3	1.0	1.0	1.0	[8.5]
Apple	Juice production	4	0.89	0.73	0.66	[8.5, 8.20]
Apple	Syrup (10–50% sugar solution without heating)	3	— [a]	2.0	0.14	[8.5, 8.20]
Apple	Pickled in syrup (10–50% sugar solution without heating)	3	0.77	0.99	0.76	[8.5, 8.20]
Apple	Syrup (10–30% sugar with heating)	14	—	—	0.64	[8.5, 8.20]
Apple	Compote (10–30% sugar solution with heating)	14	0.44	1.0	0.44	[8.5, 8.20]
Apple	Drying	2	9.0	0.11	1.0	[8.5]
Blue berry	Jam (sugar, 40–50% of fruits weight)	2	0.87	1.0	0.87	[8.5, 8.20, 8.21]
Fig	Washing	3	1.0	1.0	1.0	[8.5]
Fig	Boiling in syrup	3	1.35	0.65	0.88	[8.5]
Fig	Soaking in syrup	3	0.52	0.94	0.48	[8.5]
Grape	Washing	1	1.0	1.0	1.0	[8.5]
Grape	Washing and peeling	3	0.63	0.70	0.44	[8.5]
Grape	Juice production	3	0.98	0.75	0.74	[8.5]
Grape	Drying	3	3.6	0.29	1.0	[8.5]
Japanese apricot (*Prunus mume*)	Washing	3	0.87	1.0	0.87	[8.5]
Japanese apricot (*Prunus mume*)	Washing and peeling	4	1.1	0.75	0.85	[8.5, 8.22]
Japanese apricot (*Prunus mume*)	Production of Umeshu liquor [b]	12	0.25	3.1	0.78	[8.5, 8.20, 8.23]
Japanese apricot (*Prunus mume*)	Fruits soaked in Umeshu liquor	12	0.46	0.58	0.26	[8.5, 8.20, 8.23]
Japanese apricot (*Prunus mume*)	Pickled with salt of 10–20% weight of total fruits	6	0.75	0.75	0.60	[8.5, 8.20]

TABLE 8.7. MEAN FOOD PROCESSING FACTORS OF CS IN FRUITS (cont.)

Type of fruits	Type of processing	N	P_f	P_e	F_r	Reference
Japanese apricot (*Prunus mume*)	Pickled and dried	6	0.92	0.62	0.56	[8.5, 8.20]
Japanese apricot (*Prunus mume*)	Juice production	3	1.0	0.77	0.77	[8.5]
Japanese apricot (*Prunus mume*)	Jam (sugar, 70% of fruits weight)	6	0.75	1.36	1.0	[8.5]
Oldham blueberry (*Vaccinium oldhamii*)	Jam (sugar, 60% of fruits weight)	1	0.74	1.2	0.9	[8.20]
Peach	Washing and peeling	6	0.93	0.84	0.78	[8.5]
Peach	Compote (35% sugar solution with heating)	3	0.54	0.86	0.46	[8.5, 8.20]
Peach	Soaking in 10–30% sugar solution and drying	2	2.7	0.21	0.58	[8.5, 8.20]
Persimmon	Washing and peeling	6	0.91	0.82	0.76	[8.5, 8.24, 8.25]
Persimmon	Drying after peeling	3	4.6	0.22	1.0	[8.5]
	Drying (Ampogaki)	1	4.2	0.24	1.0	[8.5]
Yuzu (*Citrus* × *junos*)	Washing	3	0.95	1.0	0.95	[8.5]
Yuzu (*Citrus* × *junos*)	Skin only	3	1.1	0.45	0.50	[8.5]
Yuzu (*Citrus* × *junos*)	Flesh only	3	0.61	0.42	0.26	[8.5]
Yuzu (*Citrus* × *junos*)	Marmalade production	3	0.18	2.0	0.36	[8.5]
Yuzu (*Citrus* × *junos*)	Liquor production (the weight proportions are 0.24:1.0:2.4 for sugar, fruit and shochu [c])	3	0.19	2.4	0.46	[8.5]

[a] no data
[b] traditional Japanese liqueur made from Japanese apricot (*Prunus mume*)
[c] Japanese liquor made by distillation

TABLE 8.8. FOOD PROCESSING FACTORS FOR RADIOCAESIUM IN GREEN TEA AND BARLEY TEA

Tea processing	N	P_f	P_e	F_r	Reference
Green tea [a]					
60°C, 1 min (2011 [b])	2	— [c]	43	0.56 ± 0.03	[8.5]
90°C, 1 min (2011 [b])	2	—	43	0.60 ± 0.09	[8.5]
90°C, 1 min (2012 [b])	28	0.015 ± 0.004	30	0.46 ± 0.12	[8.26]
90°C, 2 min (2011 [b])	2	—	20	0.73 ± 0.13	[8.27]
100°C, 10 min (—)	3	—	50	0.64 ± 0.05	[8.28]
Barley tea [d]					
Boiling 5 min and soaked for 5 min	3	—	29	0.15	[8.5]
Boiling 5 min and soaked for 60 min	3	—	29	0.31	[8.5]
Boiling 5 min and soaked for 120 min	3	—	29	0.39	[8.5]

[a] processing factors relative to activity concentrations in dry leaves
[b] tea harvest year
[c] no data
[d] processing factors relative to activity concentration in grain

8.6.2. Alcoholic drinks

Brown rice grain is initially polished in the production of "sake" (Japanese rice wine). During this process, the surface layers are removed, and the remaining mass constitutes 45–70% of the whole grain. The alcohol content of "sake" is generally 14–16% by volume. The remaining rice polish, which has been removed, is used for making products such as rice crackers. During "sake" production, the change in both stable Cs and radiocaesium activity concentrations are similar [8.8, 8.29] (see Table 8.9). When rice is milled to 70% of its initial weight, 0.83–0.85 of the total Cs is removed from the rice grain. The "sake" and "sake cake" products have F_r values of 0.06 and 0.04, respectively. About one third of caesium in the 70% milled rice is removed during washing and soaking.

TABLE 8.9. PRODUCTION OF ALCOHOLOIC DRINKS AND FOOD FROM BROWN RICE. [8.8, 8.29, 8.30]

Processing steps	Stable Cs				^{137}Cs			
	N	P_f	P_e	F_r	N	P_f	P_e	F_r
Milling to 70% by weight	6	0.21	0.7	0.15	1	0.25	0.7	0.17
Sake (rice wine)	3	0.04	1.35	0.056	1	0.04	1.38	0.059
Sake cake	3	0.15	0.23	0.036	1	0.22	0.18	0.038
Shochu (distillate)	1	≈0	0.9	≈0	—[a]	—	—	—

[a] no data

Another Japanese liquor, "Shochu", which contains 25% alcohol by volume, is made from rice, wheat or sweet potato. The production of "Shochu" includes a distillation process, therefore, the radiocaesium content in "Shochu" is negligible and F_r and P_f values are close to zero [8.30].

In IAEA TRS 472 [8.2], values for the food processing retention factor F_r in a range of 0.3–0.7, and for the processing efficiency in a range of 0.6–0.8 are given for grape wine. These values are much higher than those for "sake" (see Table 8.7). For wine, the whole grapes are crushed and the solid parts (peels, stem, etc.) are removed before or during the fermentation. Caesium is water-soluble, therefore a large fraction of the radiocaesium in grapes is present in wine.

8.7. FOOD PROCESSING OF ANIMAL PRODUCTS AND FISH

8.7.1. Meat

Data on food processing of animal products derived after the FDNPP accident are scarce. The lack of data is probably associated with the low contributions of animal products to internal doses to the public, due to low transfers to housed animals and to restrictions on production and distribution of animal products produced in the areas affected by the FDNPP accident. No studies on processing of dairy products, pork or chicken, either for ^{131}I or for ^{137}Cs were generated, although some limited data for ^{137}Cs were reported for beef processing (Table 8.10).

Meat processing can be an effective method for reducing the ^{137}Cs content if an appropriate option is selected (see Table 8.10). Boiling and soaking in salt or acid solution are the most effective types of meat processing leading to a three-fold reduction of radiocaesium activity

concentrations in meat.

TABLE 8.10. EFFECTIVENESS OF ^{137}CS REMOVAL BY MEAT PROCESSING

Type of meat	Type of processing	Fukushima data					TECDOC 1616 [8.1]				
							F_r			P_f	
		N	P_f	P_e	F_r	Ref.	Value [a]	Min	Max	Min	Max
Beef (Rump)	Roasting	3	1.06	0.85	0.91	[8.5]					
Beef (Thick flank)	Roasting	3	1.06	0.86	0.91	[8.5]	0.7	0.5	0.8	0.4	0.7
Beef (Rump)	Boiling	3	0.64	0.64	0.41	[8.5]					
Beef (Thick flank)	Boiling	3	0.52	0.66	0.34	[8.5]	0.4	0.2	0.7	0.5	0.7
Beef (Thick flank)	Stewing	3	0.38	0.43	0.16	[8.5]	— [b]	—	—	—	—
Beef (Rump)	Frying	3	1.16	0.73	0.84	[8.5]	—	—	—	—	—
Beef	Marinating	—	0.33	0.32	0.11	[8.21]	0.5	0.1	0.7	0.9	1.0
Wild boar meat	Boiling	2	0.79	0.72	0.57	[8.31]	—	—	—	—	—

[a] recommended value
[b] no data

Data have been reported on the effect of boiling on the radiocaesium content in wild boar meat [8.31]. Radiocaesium was shown less removable by boiling from wild boar meat than from beef probably due to the tougher texture of wild boar meat compared with beef. Juices produced through cooking meat are often consumed together with meat, therefore, overall, there would be no reduction in radiocaesium consumption.

Figure 8.3 compares *CR* values of radiocaesium in neck, chuck, rib loin, sirloin short plate and rump to silverside with the fat content in each tissue, calculated from the data reported by Nabeshi et al. [8.32]. Radiocaesium activity concentrations in beef are negatively correlated with fat content of beef. For comparison, potassium concentration ratios in different parts of two types of cattle (Wagu and dairy fattened steer) are also plotted using data reported by MEXT Japan in 2019 [8.33]. Potassium follows a similar trend to that for radiocaesium.

8.7.2. Fish

Data for marine fish for “Kamaboko” (processed fishcake), i.e., nibe, Pacific cod, white croaker (used to produce a cured product called “surimi”) and Wakasagi fish that inhabit lakes and estuaries, are reported in Table 8.11.

TABLE 8.11. EFFECTIVENESS OF PROCESSING OF FRESHWATER SPECIES ON ^{137}CS

Type of meat	Type of processing	N	P_f	P_e	F_r	Reference
Kamaboko (fish cake)	Boiling	20	0.24	1	0.24	[8.5, 8.34]
Wakasagi fish	Tempura	3	1.15	0.82	0.94	[8.5, 8.35]
Wakasagi fish	Tempura-marinating	3	0.49	1.47	0.72	[8.5, 8.35]
Wakasagi fish	Roasting	3	1.6	0.6	1.0	[8.5, 8.35]

The data in Table 8.11 show that roasting fish, and to a less extent, cooking tempura, can substantially increase radiocaesium activity concentrations in the final products due to the loss of water during the cooking process. Marinating and boiling of tempura reduce radiocaesium activity concentration in the end product. These data are consistent with those reported in IAEA TECDOC 1616 [8.1] and TRS 472 [8.2]. Although consumption of marine fish and other marine biota is important in Japan, no information on the effect of the different methods of cooking sea food is available in the literature.

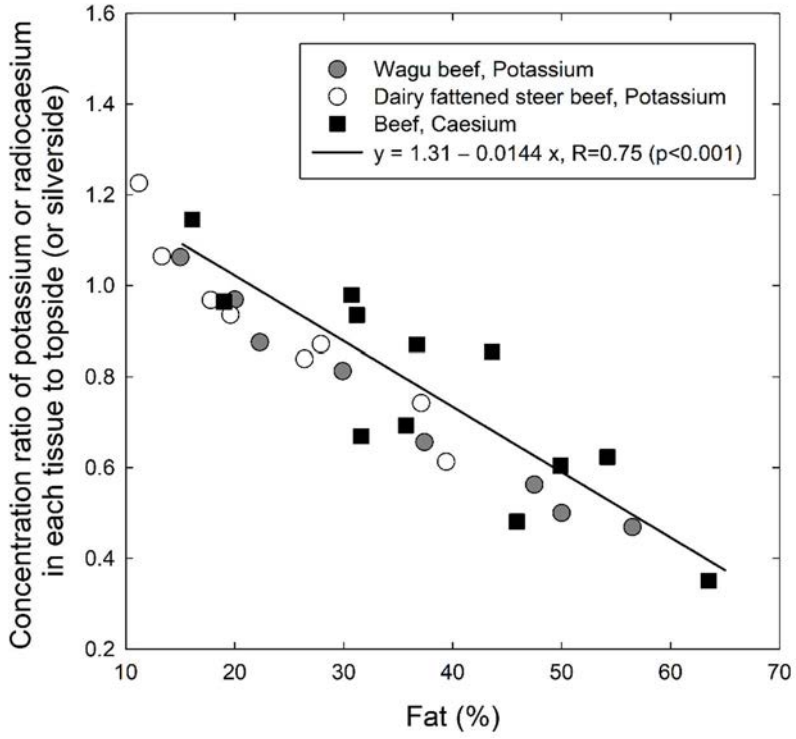

FIG. 8.3. Activity concentrations of radiocaesium and potassium in different beef tissues relative to those in topside (or silverside for radiocaesium) against fat content in tissues (data from [8.32, 8.33]).

8.7.3. Insects

The most popular edible insect in Japan is grasshopper (*Oxya yezoensis* or *Oxya japonica*) or "inago" in Japanese. These insects are pests that eat rice plants and are routinely collected from paddy fields to avoid damage. In Japan, since ancient times and until, approximately, 150 years ago, consumption of this traditional Japanese food served as supply of protein to the diet. After collection, the insects are left for an adequate time periods to allow defecation and then boiled. After all food processing of these insects, the F_r value was reported to be 0.29 [8.36], similar to that after boiling fish.

8.8. WILD EDIBLE PLANTS AND MUSHROOMS

8.8.1. Wild edible plants (Sansai)

Forest is a natural environment that is widely used by the public as a source of many wild foods such as mushrooms, berries, meat of game and medicinal or edible plants. The experience gained after the Chernobyl accident shows that contaminated forest may become a major source of internal exposure for some population groups [8.3]. The significance of the forest in term of internal exposure of the population depends on many factors, including consumption habits [8.3].

In Japan, wild edible plants are called “Sansai” which means vegetables that grew in the wild. For some population groups in Japan, wild edible plants constitute an important component of the diet; this is also the case for many other Pacific countries. Additionally, especially in spring, many Japanese people enjoy eating wild edible plants, such as young shoots of ferns, bamboo and Japanese angelica tree (“tara-no-me”), flower shoots of butterbur, young leaves of mugwort and Japanese parsley. Data on food processing of wild plants are scarce, although their importance was recognized shortly after the FDNPP accident.

As with leafy vegetables, wild edible plants can be affected by direct deposition of radionuclides, which are subsequently transferred to forest soil and then to the internal tissues of plants. The effectiveness of radionuclide removal from surfaces and internal tissues differs; therefore, data on food processing retention factors are reported separately in Tables 8.12 and 8.13.

More radiocaesium is retained after washing and boiling thick pieces of wild plants, such as bamboo or fern shoots, than in the case of leafy vegetables. Making tempura from edible plants does not remove caesium from the product.

8.8.2. Mushrooms

Culinary processing is one of the most effective and technically feasible options for the reduction of radiocaesium in mushrooms (see Table 8.14). Fresh mushrooms are normally washed, boiled or soaked. These options can reduce the radiocaesium activity concentration in cooked mushrooms by more than one order of magnitude [8.3]. Unfortunately, data on mushroom processing after the FDNPP accident are scarce and cover only a limited number of options. Currently available data are similar to those derived after the Chernobyl accident.

The IAEA publications [8.1, 8.2] provide more information on food processing options for reduction of radiocaesium activity concentration in mushrooms. TRS 472 provides a range of values of 0.5–0.95 for the food processing retention factor of fresh mushrooms for ^{137}Cs and a range of F_r values of 0.03–0.3 for boiling [8.2]. These values are similar to those observed in Japan. Also, lower F_r values were given in TRS 472 for the food processing retention factor for soaking dried mushroom in water. Nevertheless, the observed differences should not be overestimated since few observations were made after the FDNPP accident in Japan. Furthermore, different mushroom species may have been analysed and varying processing methods may have been applied to the mushrooms collected in the forests contaminated by the two accidents.

TABLE 8.12. FOOD PROCESSING RETENTION FACTOR F_r OF RADIOVAESIUM IN WILD PLANTS WITH SURFACE CONTAMINATION [8.5, 8.37]

Plant type	Type of processing	N	F_r			
			AM	GM	Min	Max
Radiotellurium						
Wild edible plants, leafy, 5 species [a]	Washing	5	0.69	0.66	0.43	1.0
Wild edible plants, 4 species [b]	Boiling	4	0.36	0.30	0.16	0.76
Radioiodine						
Wild edible plants, leafy, 5 species [a]	Washing	5	0.76	0.75	0.54	0.91
Wild edible plants, petiole, fertile stem, and bulb [c]	Washing	3	0.69	0.65	0.38	0.91
Wild edible plants, 4 species [b]	Boiling	4	0.46	0.42	0.19	0.60
Wild edible plants, petiole, fertile stem, and bulb [c]	Boiling	3	0.37	0.34	0.23	0.59
Radiocaesium						
Wild edible plants, leafy, 5 species [a]	Washing	5	0.74	0.71	0.49	1.0
Wild edible plants, petiole, fertile stem, and bulb [c]	Washing	3	0.80	0.77	0.51	1.0
Wild edible plants, 4 species [b]	Boiling	4	0.36	0.32	0.15	0.58
Wild edible plants, petiole, fertile stem, and bulb [c]	Boiling	3	0.64	0.52	0.38	1.0

[a] leaves of mugwort, dandelion, dock, butterbur, and wild garlic
[b] leaves of mugwort, dandelion, dock, and wild garlic
[c] petiole of butterbur, fertile stem of field horsetail, and bulb of wild garlic

TABLE 8.13. FOOD PROCESSING RETENTION FACTOR F_r OF RADIOCAESIUM IN WILD EDIBLE PLANTS (CONTAMINATED BY ROOT UPTAKE)

Food	Type of processing	N	P_f	F_r			Reference
				GM	Min	Max	
Wild edible plants, leafy [a]	Washing	15	— [b]	0.84	0.27	1.0	[8.5, 8.38]
Wild edible plants, leafy [a]	Boiling [c]	21	0.52	0.44	0.04	0.93	[8.5, 8.38]
Young shoot of ferns	Washing and Boiling [c]	11	0.34	0.34	0.09	0.98	[8.5, 8.38]
Bamboo shoot and root vegetables	Boiling	5	0.73	0.73	0.67	0.82	[8.37, 8.38]
Young shoots of trees (*tara-no-me* and *koshiabura*)	Tempura	2	0.55	1.0	0.98	1.0	[8.21]

[a] butterbur leaves, petioles, mugwort leaves, and dock leaves
[b] no data
[c] *CR* values and weight ratios were available not for all samples, thus affecting estimated P_f

TABLE 8.14. FOOD PROCESSING RETENTION FACTORS OF RADIOCAESIUM IN MUSHROOMS

Type of processing (specimen)	Fukushima data							TRS 472 [8.2]	
	N	P_f	P_e	F_r			Reference	P_e	F_r
				GM	Min	Max			
Washing (*Boletopsis leucomela, Lentinula edodes*)	3	— [a]	1.0	0.92	0.90	0.96	[8.25]	1.0–1.3	0.5–0.95
Boiling [b] (*Pholiota microspora, Armillaria mellea, Hypholoma sublateritium, Sarcodon aspratus*)	6	0.65	0.95	0.36	0.18	0.63	[8.5, 8.39]	0.7–0.9	0.03–0.3
Soaking dried mushroom in water, then discarding the water (*Lentinula edodes*)	3	0.08	6.23 [c]	0.47	—	—	[8.40]	8.3 [c,d]	0.1–0.2

[a] no data
[b] concentration ratios and weight ratios were not obtained for all samples and thus N was smaller in P_f and F_r
[c] P_e is defined relatively mass of dried mushrooms (DM)
[d] deduced from the data in TRS 472 [8.2]

8.9. SUMMARY AND LIMITATIONS

Many methods for processing and culinary preparation of food are applied worldwide. Investigations carried out after the FDNPP accident on food processing are in general agreement with previously reported values. Some detailed information especially for the food processing methods specific to Japan have been obtained after the FDNPP accident and collated in this chapter. These data were not available at the time when IAEA TRS 472 [8.2] or TECDOC 1616 [8.1] were compiled.

Some foods collected from forests, such as bamboo shoots and wild edible plants — known in Japan as “Sansai” — are rarely consumed in non-Asian countries, except for mushrooms and ferns. For “Sansai”, the most frequent culinary preparation methods are “tempura” (which constitutes battered and deep-fried food materials) and boiling for short time after washing. For these cooking processes only a limited reduction in radiocaesium content can be expected during cooking.

Compiled data are available for a small number of food processing methods used in Japan. The low radiocaesium activity concentrations in many foods made it difficult to study the effects of food processing. However, for some products, potassium can be used as an analogue for estimating the modification of radiocaesium contents in food during processing [8.38] and may be helpful in enhancing relevant data for different raw materials and food processing options in the future. More food processing data would be needed to enhance current guidance on: (a) how food processing can be used to reduce radiocaesium intakes in post-accident situations; and (b) providing more realistic estimates of internal dose.

REFERENCES

[8.1] INTERNATIONAL ATOMIC ENERGY AGENCY, Quantification of Radionuclide Transfer in Terrestrial and Freshwater Environments for Radiological Assessments, TECDOC Series 1616, IAEA, Vienna (2009).

[8.2] INTERNATIONAL ATOMIC ENERGY AGENCY, Handbook of Parameter Values for the Prediction of Radionuclide Transfer in Terrestrial and Freshwater Environments, Technical Reports Series 472, IAEA, Vienna (2010).

[8.3] FESENKO, S. et al., Important factors governing exposure of the population and countermeasure application in rural settlements of the Russian Federation in the long term after the Chernobyl accident, J. Environ. Radioact. **56** 1 (2001) 77.

[8.4] RADIOACTIVE WASTE MANAGEMENT CENTER (RWMC), Removal of Radionuclides during Food Processing and Culinary Preparation, 4, Environmental Parameter Series, (1994) p. 54.

[8.5] RADIOACTIVE WASTE MANAGEMENT FUNDING AND RESEARCH CENTER (RWMC), Removal of Radionuclides during Food Processing and Culinary Preparation. Focusing on radiocaesium removal rate data collected in Japan after the Fukushima accident, 4, Supplemental edition of Environmental Parameter Series, (2013) p. 201.

[8.6] NOORDIJK, H., QUINAULT, J.M., The Influence of Food Processing and Culinary Preparation on the Radionuclide Content of Foodstuffs: A Review of Available Data, 1011–4289, INTERNATIONAL ATOMIC ENERGY AGENCY (1992) pp. 35–59.

[8.7] ADRIANO, D.C., DOSWELL, A.C., CIRAVOLO, T.G., III, J.E.P., MCLEOD, K.W., Radionuclide content of selected root vegetables as influenced by culinary preparation, J. Environ. Radioact. **49** 3 (2000) 307.

[8.8] OKUDA, M. et al., The transfer of radioactive cesium and potassium from rice to sake, J. Biosci. Bioeng. **116** 3 (2013) 340.

[8.9] HACHINOHE, M. et al., Distribution of Radioactive Cesium (134Cs plus 137Cs) in Rice Fractions during Polishing and Cooking, J. Food Prot. **78** 3 (2015) 561.

[8.10] HACHINOHE, M., SASAKI, T., SHINDOH, K., OKUNISHI, T., HAMAMATSU, S., Distribution of Radioactive Cesium (137Cs) during Cooking of Rice Noodles with Different Firmness, Nippon Shokuhin Kagaku Kogaku Kaishi **64** 4 (2017) 191.

[8.11] TAGAMI, K., UCHIDA, S., Radiocaesium Food Processing Retention Factors for Rice with Decreasing Yield Rates due to Polishing and Washing, and the Radiocaesium Distribution in Rice Bran, RADIOISOTOPES **61** 5 (2012) 223.

[8.12] TANJI, K., SEKIZAWA, H., YAMASHITA, S., ENDO, A., Dynamics of radiocesium during the processing of grain and rice bran, 113, Special Issue on Radioactive Material Countermeasures, Fukushima Agricultural Technology Centre (2014).

[8.13] HACHINOHE, M. et al., Effect of Noodle Size and Boiling Time on Dynamics of Radioactive Cesium During Cooking of Japanese Udon Noodles, Nippon Shokuhin Kagaku Kogaku Kaishi **61** 1 (2014) 34.

[8.14] HACHINOHE, M. et al., Dynamics of Radioactive Cesium during Noodle Preparation and Cooking of Dried Japanese Udon Noodles, Nippon Shokuhin Kagaku Kogaku Kaishi **62** 1 (2015) 56.

[8.15] KUBO, K. et al., Decreasing radioactive cesium in lodged buckwheat grain after harvest, Plant Prod. Sci. **19** 1 (2016) 91.

[8.16] HACHINOHE, M., NIHEI, N., KAWAMOTO, S., HAMAMATSU, S., Distribution of Radioactive Cesium during Milling and Cooking of Contaminated Buckwheat, J. Food Prot. **81** 6 (2018) 881.

[8.17] TAGAMI, K., UCHIDA, S., Distributions of Inorganic Elements in Brown Rice Determined by ICP-OES and ICP-MS, and Analysis of Their Concentration Changes by Washing, BUNSEKI KAGAKU **65** 9 (2016) 511.

[8.18] KOBAYASHI, M., SAITO, F., Variation in amount of radioactive cesium before and after cooking of soybean, Journal of Japan Disaster Food Society **1** 1 (2014) 59.

[8.19] JAPAN SOCIETY FOR RADIATION SAFETY MANAGEMENT, Interim Report on Removal of Radioactive Materials Attached to Vegetables Contaminated by the Fukushima Daiichi Nuclear Accident, (2011).

[8.20] SEKIZAWA, H., YAMASHITA, S., TANJI, K., Dynamics of radiocesium at fruit processing, Special Issue on Radioactive Material Countermeasures, Fukushima Agricultural Technology Centre (2014) pp. 118–121.

[8.21] NABESHI, H. et al., Effects of Cooking Process on the Changes of Concentration and Total Amount of Radioactive Caesium in Beef, Wild Plants and Fruits, RADIOISOTOPES **65** 2 (2016) 45.

[8.22] TAKATA, D., ET AL., Radioactivity distribution of the fruit trees ascribable to radioactive fallout: A study on stone fruits cultivated in low level radioactivity region, RADIOISOTOPES **61** 6 (2012) 321.

[8.23] OKUDA, M., AKAO, T., SUMIHIRO, M., MIZUNO, M., GOTO-YAMAMOTO, N., Transfer of caesium and potassium from Japanese apricot (Prunus mume Sieb.et Zucc.) to Japanese apricot liqueur (Ume liqueur), J. Inst. Brew. **122** 3 (2016) 473.

[8.24] TAGAMI, K., UCHIDA, S., Effective half-lives of 137Cs from persimmon tree tissue parts in Japan after Fukushima Dai-ichi Nuclear Power Plant accident, J. Environ. Radioact. **141** (2015) 8.

[8.25] KUWAMORI, T. et al., Radioactive cesium-137 contents and their reduction under process of cooking in food products cultivated in Kawauchi, Fukushima Prefecture, Jin-Ai Univ. Res. Bull. **6** (2014) 15.

[8.26] SHIRAKI, Y., TAKEDA, H., OKAMOTO, T., FUNAHASHI, H., KITA, N., Radiocaesium concentration of the first crop of processed tea and its extracts, and the second crop of processed tea manufactured in Kanagawa Prefecture in 2012, RADIOISOTOPES **62** 2 (2013) 83.

[8.27] SHIMIZU, K., Extraction characteristics of radiocaesium in tea leaves contaminated due to the TEPCO's Fukushima Daiichi Nuclear Power Plant accident, J. Jpn. Soc. Radiat. Saf. Manag. **11** 2 (2012) 186.

[8.28] COOK, M.C., STUKEL, M.J., ZHANG, W., MERCIER, J.-F., COOKE, M.W., The determination of Fukushima-derived cesium-134 and cesium-137 in Japanese green tea samples and their distribution subsequent to simulated beverage preparation, J. Environ. Radioact. **153** (2016) 23.

[8.29] OKUDA, M. et al., The transfer of stable ^{133}Cs from rice to Japanese sake, J. Biosci. Bioeng. **114** 6 (2012) 600.

[8.30] OKUDA, M. et al., The behavior of stable ^{133}Cs and other inorganic elements during shochu making, J. Brew. Soc. Jpn. **109** 11 (2014) 808.

[8.31] FUMA, S. et al., Radiocaesium contamination of wild boars in Fukushima and surrounding regions after the Fukushima nuclear accident, J. Environ. Radioact. **164** (2016) 60.

[8.32] NABESHI, H., KIKUCHI, H., TSUTSUMI, T., HACHISUKA, A., MATSUDA, R., Concentration of radioactive cesium in different cuts of beef, J. Food Hyg. Soc. Jpn. **54** 6 (2013) 415.

[8.33] MINISTRY OF EDUCATION, CULTURE, SPORTS, SCIENCE AND TECHNOLOGY, JAPAN, Standard Tables of Food Composition in Japan 2015 (Seventh Revised Edition), (2015).

[8.34] WATABE, S. et al., Removal of Radioactive Caesium Accumulated in Fish Muscle by Washing in the Process of Surimi-Based Productions, RADIOISOTOPES **62** 1 (2013) 31.

[8.35] NABESHI, H., TSUTSUMI, T., HACHISUKA, A., MATSUDA, R., Reduction of radioactive cesium content in pond smelt by cooking, J. Food Hyg. Soc. Jpn. **54** 4 (2013) 303.

[8.36] MITSUHASHI, R. et al., Radioactive caesium contamination in Inago and sustainability of Inago cuisine in Fukushima, J. Food Hyg. Soc. Jpn. **54** 6 (2013) 410.

[8.37] TAGAMI, K., UCHIDA, S., Food processing retention factors for wild plants and rice, Proceedings of the 13th Workshop on Environmental Radioactivity, KEK proceedings, High Energy Accelerator Research Organization, Tsukuba (2012) 154–159.

[8.38] TAGAMI, K., UCHIDA, S., Comparison of food processing retention factors of 137Cs and 40K in vegetables, J. Radioanal. Nucl. Chem. **295** (2013).

[8.39] NISHIUMRA, R., Study on radiocaesium absorption by mushrooms and the nuclide elution from mushrooms, Annual Report of Kinki University Research Reactor AN00063722-20170324–0101, News from the Laboratory 2016, (2017) p. 112.

[8.40] NABESHI, H., TSUTSUMI, T., HACHISUKA, A., MATSUDA, R., Variation in Amount of Radioactive Cesium before and after Cooking of Dry Shiitake and Beef, Food Hyg. Saf. Sci. **54** 1 (2013) 65.

9. CONCLUSIONS

9.1. INTRODUCTION

The accident in the Fukushima-Daiichi Nuclear Power Plant (FDNPP) occurred on 11 March 2011 leading to the release of radionuclides that were dispersed to terrestrial and aquatic environments. The releases of radionuclides that were potentially important contributors to both external and internal doses was much lower than that after the Chernobyl accident. A large fraction of the radionuclides released to the atmosphere was deposited in the ocean thereby reducing the proportion of the release that contaminated freshwater and terrestrial catchments around the FDNPP. The affected area is largely comprised of paddy fields, farmlands, deciduous forests and evergreen coniferous forests, but also inhabited areas were affected. About 80% of Fukushima Prefecture territory is mountainous, and 70% is forested. The Fukushima Prefecture is famous for organic farming, producing high quality rice, fruits, soybeans, and buckwheat. The prefecture also produces vegetables (sweet potato, spinach, cucumber, tomato etc.) and wheat.

Immediately after the accident, intensive monitoring and research programmes were initiated to determine gamma-dose rates and their time-dependence, and to determine radionuclide activity concentrations in environmental media such as soils, plants, foodstuffs, surface seawaters, sediments and aquatic species. The fate of radionuclides deposited on, or released directly to, the Pacific Ocean was addressed by measuring activity concentrations in seawater, suspended and bottom sediments and seafood in the coastal areas and oceans around Japan.

Monitoring programmes were initially designed to provide data relevant to ensuring compliance with radiological criteria relating to activity concentrations in food, and dose rates and annual doses for exposure of workers and members of the public.

Research activities had an initially low priority in the aftermath of the Great Eastern earthquake and tsunami. Nevertheless, studies of radionuclide behaviour in the affected environmental systems gradually commenced where possible. The aim of these activities was to support predictions of radionuclide transfers in the affected environments. They also provided data to explore whether the observations made after the FDNPP accident were consistent with previous global experience regarding the behaviour of radiocaesium in the environment.

The consequences of large-scale releases of radionuclides to the environment depend on many factors, including the duration of the release, activity and composition of radionuclides in the release, meteorological conditions during the release, the season of the year (determining the stage of the development of plants), properties of the environment and the agricultural practices, population density and life style of people in the affected areas, and the implementation of countermeasures and remedial actions. The special features associated with the FDNPP accident are as follows:

- The releases occurred before or, for a few crops, at an early phase of the growing period. Therefore, only residual vegetation left in fields after the last growing season (rice straw), a few types of early growing leafy or perennial crops and evergreen fruit were affected by direct deposition of radioiodine and radiocaesium onto plant canopies;

- Many crops (including rice) and feedstuffs used for animal products were not affected by direct contamination of leaves, so the long-term uptake of radiocaesium from soil was the dominant contamination route for most crops and animal feedstuffs;

- As fruit trees were contaminated during the dormant period, the uptake of radiocaesium through the bark and subsequent distribution in the tree was studied in detail for the first time;

- Farm animals, including dairy cows were housed and being fed with stored feed;

- The vicinity of the FDNPP is a mountainous region with many lakes, ponds, rivers and creeks. Many hills are steep and receive generally high rates of precipitation, enhanced by typhoons which cause high surface run-off and associated flooding, which can enhance radiocaesium transport from the mountains via rivers to the sea;

- Whereas the impact of the Chernobyl accident was largely on terrestrial ecosystems in Europe, the FDNPP accident also affected the marine environment around Japan;

- After the Chernobyl accident, enhanced radiocaesium activity concentrations persisted in foods produced or collected in some agricultural, and semi-natural or extensively used environments all over Europe. The agricultural areas were predominantly podzolic soils in Belarus, Russia and Ukraine whereas the semi-natural or extensively used environments included upland regions in Western Europe countries such as the UK, Ireland, Austria and Scandinavia. Soils in these areas are characterized by low pH, insufficient potassium supply, low clay and high organic matter contents associated with persistently high uptake rates of radiocaesium by plants. Such unimproved lands are often used for milk and meat production, and in some cases for production of robust crops such as rye and potatoes. This phenomenon was of relatively low importance in Japan after the FDNPP accident.

The data compiled within this report were from studies by leading Japanese institutes in their respective fields.

9.2.LESSONS LEARNED FROM POST-ACCIDENT STUDIES

Immediately after deposition of radionuclides to agricultural land, forests and water bodies, there is the most intensive flux of radionuclides between environmental compartments. During this initial period, activity concentrations may change significantly within a short period of time. The transfer processes occurring in this early period may influence the long-term fate of the radionuclides in the environment. Some monitoring campaigns and the experimental studies carried out in Japan used already existing monitoring and research installations for the measurement of radionuclides:

- For the investigation of the behaviour of radiocaesium in forests, installations were used that were already established when the deposition occurred. This allowed unique measurements that elucidated the interception of radionuclides and the loss of radionuclides from forest trees in the very early stage, which could significantly improve the data base on interception and retention;

- Measurements to derive the loss of radiocaesium from farmland due to surface run-off were carried out on existing experimental plots which had been originally set up to measure the loss of soil with water erosion;

- Monitoring of radionuclide levels in seawater, sediments and fishery products has been performed in the coastal areas and oceans around Japan since the 1960s, providing a unique time series of activity concentrations in components of the marine system. K_d-

values for bottom sediments and concentration ratios (from seawater to aquatic organisms) could therefore be derived for conditions that represent equilibrium or quasi-equilibrium conditions. The existence of such data facilitated the analysis and evaluation of the measurements made after March 2011 and allowed prospective assessments of activity concentrations in fish and other sea food, which is extremely important for managing fishing restrictions.

The immediate availability of such installations for monitoring purposes or experimental studies provided an invaluable advantage. Immediately after a release, assessment of the accident consequences solely depends on radioecological models. Since, in the early phase, the radionuclide deposition is inherently uncertain, the results are associated with considerable uncertainties. In this situation, the link of radioecological models with monitoring data represents a powerful tool to enhance the reliability of prospective dose assessments. It also provides valuable input for prioritizing the use of limited monitoring resources.

9.3.SPECIFIC FINDINGS

The report focuses on the description and parametrisation of time-dependent processes that affect the migration of radionuclides in the environment including the transfer through food chains. Here, an emphasis is given to quantifying the following processes.

- Interception of deposited radionuclides by plants;
- Loss of radionuclides from plant surfaces due to weathering and abrasion;
- Systemic transport of radionuclides in plants (translocation);
- Behaviour of radiocaesium in various types of soil;
- Uptake of radionuclides from soil by rice and other agricultural crops and vegetables;
- Transfer of radionuclides from feedstuffs to milk and meat;
- Uptake and distribution of radiocaesium in forest trees;
- Uptake of radiocaesium by wild plants, including mushrooms and berries;
- Transfer of radiocaesium to wild animals;
- Behaviour of radiocaesium in freshwater systems, coastal areas and in the ocean;
- Transport of radiocaesium from catchments through rivers, streams and lakes to the ocean;
- Uptake of radiocaesium by aquatic organisms;
- Modification of radionuclide activity concentrations in food products during food processing and culinary preparation.

The essential findings on these topics are summarized below.

Interception of deposited radionuclides by plants

- Observations and analysis after both the FDNPP accident and the Chernobyl accident give similar values for the initial retention of ^{131}I and ^{137}Cs by plant canopies following atmospheric deposition. The field-based data observed in 2011 are also in general agreement with values from controlled experiments reported in TRS 472 (IAEA 2010);

- Radiocaesium was effectively transported within crops and trees following deposition onto the foliage. Therefore, plant organs and tissues such as grain, fruit and new shoots could become contaminated, even if they were not directly impacted by the initial deposition of radionuclides;

- The results are consistent with global experience.

Transfer of radiocaesium to rice

- Soils in Japan are generally well-fertilised with a sufficiently high potassium status. Consequently, the concentration ratio[10] *CR* values of radiocaesium for rice from soil were generally low compared with other crops. Differences in radiocaesium transfer to rice from varying soil types were of minor importance;

- Rice was not planted when the deposition occurred. The uptake of radiocaesium from paddy field soil was enhanced in the first two to three years after the deposition but returned by the fourth year to CR values that were similar to those observed before the FDNPP accident for global fallout from atmospheric nuclear weapons tests. The comprehensive monitoring of radiocaesium activity concentrations of all brown rice produced in Fukushima prefecture has not exceeded the standard limit since 2015;

- Water from irrigation ponds was not a major source of radiocaesium to rice even though the ponds were often fed by run-off water from contaminated forested catchments.

Uptake of radiocaesium from soil by other agricultural crops

- The *CR* values for leafy vegetables and fodder grass growing in affected areas in 2011 are consistently within an order of magnitude of pre-2011 worldwide experience;

- The variation in measured *CR* values within a soil type for some crops was high, characterised by a factor of 5–50, depending on the crop, so supplementary data on soil properties, such as potassium status, organic matter content, pH and clay content are required to make more robust conclusions.

Loss of radiocaesium from rice paddies with irrigation water

- In 2011, during normal cultivation including flooding, puddling, irrigation and drainage, not more than 1% of the ^{137}Cs inventory was lost to the receiving surface water bodies from experimental rice paddies;

- In the following years, when radiocaesium was mixed with deeper soil layers, it was even less available for surface run-off, with ^{137}Cs loss rates dropping rapidly to well below 0.05%/year.

Fruit trees

- Fruit trees were contaminated by direct deposition of radionuclides on leaves and bark or by uptake of radionuclides from soil. The accident happened before the emergence of leaves, which highlighted the importance of the translocation of radiocaesium from

[10] Ratio of activity concentrations in plant or animal products and soil or water under equilibrium conditions.

bark to fruit. This phenomenon was most pronounced in the first harvest after deposition, but it was also demonstrated to continue to contribute to activity concentrations in fruit over the next few years;

- The application of a *CR*, relating activity concentrations in fruit to those in soil, would not be appropriate to quantify the transfer of radiocaesium to harvested fruit in 2011 since the concentration ratio does not include the uptake of radiocaesium via foliage and bark;

- The relative importance of the uptake via foliage, bark and soil was shown to depend on the stage of development of fruit trees and shrubs at deposition, growth characteristics, plant structure and fruit type. Careful consideration of the contamination routes is necessary to allow reliable predictions of radionuclide activities in fruit subsequent to radionuclide deposition.

Uptake of radiocaesium by green tea

- Transfer parameters for green tea plants are reported here for the first time in an international compilation. Root uptake of radiocaesium is similar to that reported for herbaceous plants;

- Tea is a perennial crop. Radiocaesium activity concentrations in tea leaves observed in 2012 in the newly emerged tea leaves was due to redistribution of radiocaesium that was deposited in 2011 and stored overwinter in old leaves, stems and roots of the tea tree. The GM of effective half-lives of ^{137}Cs from short-term measurements was 50 d and over longer timescales was 420 d on average.

Influence of potassium on uptake of radiocaesium from soil

- For a wide range of crops, the uptake of radiocaesium from soil is influenced by exchangeable potassium concentrations in soil. Additional use of potassium fertilizer was recommended for soils with less than 50 mg/kg DM exchangeable potassium for the first rice crop grown after the FDNPP accident and where the radiocaesium activity concentrations in crops might exceed 100 Bq/kg FM. For buckwheat and soybeans, values of 30 mg/kg and 25 mg/kg were applied respectively. In the longer term, a level of 25 mg/kg of exchangeable potassium was used to identify agricultural fields which needed additional potassium fertilizer to reduce radiocaesium activity concentrations in rice.

Transfer of radiocaesium to animal products

- The contribution of animal products to the internal doses of the members of public in areas affected by the FDNPP accident was much lower than for the Chernobyl accident. The prevailing animal management practices (e.g. housing dairy animals) in Japan and the low importance of farm animal products in the Japanese diet led to a much lower radioiodine and radiocaesium intake via animal products. Correspondingly, milk ingestion was a much less significant exposure pathway after the FDNPP accident as compared with conditions after the Chernobyl accident;

- The transfer parameter data obtained for animal food products are similar to those available before the FDNPP accident.

Forest ecosystems

- Because the FDNPP accident occurred in March 2011, interception of radionuclides by coniferous trees was higher than by deciduous trees which did not have emergent leaves at the time of deposition;

- The reduction in radiocaesium activity in tree canopies after the accident can be described by a two-component exponential model;

- Most aggregated transfer factors T_{ag}[11] determined for wood of cedar, cypress, pine and oak trees were in the range of 10^{-4} to 10^{-3} m²/kg. The T_{ag} values for needles, bark, and branches were higher than those for wood. T_{ag}-values for oak (wood and leaves) are similar to those observed after the Chernobyl accident. T_{ag} values for wood of coniferous trees affected by the Fukushima accident are lower than those reported for the Chernobyl accident. Preliminary results indicate that potassium fertilization in forests may be effective as a remediation option;

- The reductions of radiocaesium activity concentrations of cedar, cypress and pine needles were similar, with effective half-lives in the range of 1–3 years whereas that of pine branches varied from 1 to 4 years. So far, the declines for ^{137}Cs observed after the FDNPP accident have been generally more rapid than those observed after the Chernobyl accident. However, the period of observations after the FDNPP accident has not been long enough to draw final conclusions at the present time;

- T_{ag} values for Sika deer and wild boar in Japan, are similar to those reported for other terrestrial game mammals in IAEA TRS 472;

- Effective half-lives of radiocaesium in forest products such as mushrooms, game and berries after the Chernobyl accident were much longer than those for agricultural products. It is not yet clear whether this is the case for areas affected by the Fukushima accident.

Radiocaesium transport in catchments

Radionuclides deposited in the terrestrial and freshwater environment are re-distributed due to run-off and erosion processes. After the FDNPP accident these processes were studied in field experiments and by analysis of data from environmental monitoring programmes. Emphasis was given to erosion from farmland, pasture and forests, the transport of radiocaesium from rice paddies to rivers, the transport in catchments and the time-dependence of ^{137}Cs activity concentrations in suspended sediments of rivers in Fukushima Prefecture. The main findings are as follows.

Loss of radiocaesium from farmland due to erosion

- The loss of radiocaesium due to water erosion depended on the land use. It increased in the order: grassland and forest < vegetated farmland < bare farmland;

[11] Aggregated transfer factor T_{ag} relates activity concentration in wood or tree parts and radionuclide deposition density (inventory)

- On steep farmland plots — being unvegetated during the whole year due to continuous weeding — water erosion caused radiocaesium losses of about 10% per year, whereas for vegetated farmland plots erosion losses were much lower. On grassland, erosion rates were generally well below 0.01%/year;

- Except for bare farmland, the removal of radiocaesium from affected areas was, in general, a process of minor importance.

Forested catchments

- In forests with steep slopes, erosion losses ranged from 0.001–0.2% per year;

- The results indicate that the fraction of dissolved ^{137}Cs in run-off water has been small. Most ^{137}Cs in run-off water from forested catchments has been bound to suspended sediments;

- In the period 2012–2017, ^{137}Cs bound to organic matter in run-off water declined according to an effective half-life of 0.75–1.8 years;

- The fraction of ^{137}Cs bound to suspended sediments in run-off water has varied widely; activity concentrations of ^{137}Cs bound to organic matter have declined with effective half-times in the range of 1.7–13 years.

Radiocaesium in urban catchments

- In a catchment with more than 50% residential areas, run-off, as quantified by the entrainment coefficient, was initially a factor of 3 higher than in forested areas due to the retarding effect of the vegetation cover;

- During the first four years after the accident, the loss of ^{137}Cs due to run-off in an urban catchment declined according to an effective half-life of 1.5–2 years. Final conclusions about the long-term behaviour cannot be made at the current time.

Radiocaesium in suspended sediments of river water

- The time-dependence of activity concentrations in suspended sediments could be described by described by a two-component exponential function characterized by "fast" and "slow" effective half-lives. At different monitoring sites of the Abukuma River—the major river in the Fukushima prefecture—the fast component of the effective half-life ranged from 0.2–1.6 year, whereas the long-term components were in a range of 1.4–2.7 years;

- Since in the tributaries, monitoring of ^{137}Cs bound to suspended sediments only started in 2012, no short-term component could be identified; the decline was approximated by a single exponential with an AM effective half-life of about 3 years, with a range of 1.0–16.0 years. The results are in general agreement with findings after the Chernobyl accident, but the observation periods after the accidents in FDNPP and Chernobyl are different.

K_d-values in freshwater bodies

- The K_d values for the mainstream of the Abukuma River and the rivers in the coastal region were similar (GM ≈ 2.5×10^5 L/kg), whereas the mean of the values for the tributaries of the Abukuma River was higher by a factor of two;

- The relationships of K_d-values with pH, electrical conductivity (EC), dissolved organic carbon (DOC), inorganic cations and anions have been quantified. The best correlation was found with EC, followed by NH4+ and the concentration of suspended sediments;

- For radiocaesium reported before 2011, the Japanese $K_{d(a)\text{-}SS}$ values for suspended matter had a geometric mean of 5×10^4 L/kg which was not significantly different from combined global data. The GM values of $K_{d(a)\text{-}SS}$[12] (n = 513) for three sampling situations reported in Japan after the FDNPP accident in Fukushima Prefecture were 5–10 times higher than the small number of $K_{d(a)\text{-}SS}$ values (n = 20) measured before the FDNPP accident. The $K_{d(a)\text{-}SS}$ values of a recently developed dataset for radiocaesium provided a GM of 1.4×10^5, L/kg (GSD = 2.67) which is similar and consistent with those reported in Japanese both before and after the FDNPP accident.

Freshwater fish

- A clear decline of radiocaesium activity concentrations in fish, aquatic biota and water has been observed since the FDNPP accident in 2011;

- The GM of *CR* values in 2015–2017 ranged from 650–1800 L/kg for river fish and 1000–4000 L/kg for lake fish. In lakes, radiocaesium activity concentrations in fish increased with the trophic level;

- The GM of *CR* values for Wakasagi, Pale Chub and Japanese dace varied between 1000 and 2000 L/kg, the standard deviation being about 15–30%. GMs of *CR* values of about 700 and 40 L/kg respectively have been derived for phyto- and zooplankton species;

- The reduction of ^{137}Cs in aquatic organism can be approximated by an exponential model with effective half-lives that range from 1.1 to 2.5 years, depending on the species;

- The GM of *CR* values for freshwater fish are in general agreement with global experience and observations made in Japan before the FDNPP accident.

Marine systems

- Monitoring in seawaters around Japan has been performed since the 1960s. Pre-accident *CR* values for equilibrium conditions for a wide spectrum of aquatic organisms are in a range of approximately 10 to 100 L/kg;

- The apparent activity concentration ratio[13] (CR_a) values for various edible aquatic organisms increased sharply after the FDNPP accident in affected areas. Near the FDNPP they were highest in 2012–2013, and then there was a gradual return to pre-accident values. However, the disequilibrium persisted in coastal areas east of Japan

[12] $K_{d(a)\text{-}SS}$: apparent distribution coefficient for suspended sediments
[13] Activity concentration ratio water-aquatic organism under non-equilibrium conditions

even 5 years after the accident. The transition from the 2012/2013 CR_a values to pre-accidental values can be approximated by exponential functions with effective half-lives of 0.5–3.3 years;

- The variations of CR_a values for aquatic organisms was caused by the heterogeneous distribution of ^{137}Cs in seawater, on-going ^{137}Cs input to the sea and differences in physiology, body size, trophic level, habitat and diet among marine species;

- K_{d} values in marine bottom sediments have been monitored since the 1960s with systematic measurements since 1984. Small changes in K_{d} occurred throughout the period from 1984–2010 (by less than a factor of 2) so an equilibrium had not been fully established before the FDNPP accident. Pre-accident geometric mean and median K_{d} values in the coastal seawaters around Japan were 920 and 720 L/kg, respectively;

- By 2019, the activity concentrations of ^{137}Cs in seawaters returned to approximately pre-accident values. However, ^{137}Cs activity concentrations in bottom sediments decreased at a much slower rate. Consequently, the apparent $K_{\mathrm{d(a)\text{-}SS}}$ values for bottom sediments in impacted areas sharply increased to a maximum, and subsequently changed slowly thereafter. Apparent $K_{\mathrm{d(a)}}$ values determined in 2018/2019 were in the range of 5000–7000 L/kg.

Food preparation

Various food processing and culinary preparation methods existing and applied world-wide can reduce radionuclide activity concentrations in food, thus providing a protective effect regarding public exposure. Results of research carried out after the FDNPP accident on food processing are in general agreement with previously reported data as well as significantly extending the available database for food processing methods relevant for Japan and some other Pacific countries.

9.4.KEY RADIOECOLOGICAL LESSONS

Lesson 1. The environmental consequences of the Fukushima Dai-ichi accident were lower than those occurring after the Chernobyl accident partially due to the nature of the releases. After the FDNPP accident, (i) a large fraction of radionuclides was deposited in the ocean and did not affect terrestrial and freshwater foodchains and (ii) the ratio of ^{134}Cs to ^{137}Cs in the release was approximately twice as high as that after the Chernobyl accident, thus the decrease of radiocaesium inventory and corresponding dose rates was faster.

Lesson 2. The immediate initiation of monitoring campaigns and the implementation of food restrictions in the areas in Japan affected after the FDNPP accident mitigated the short and long-term consequences of the deposited radionuclides in Japan. The prevailing highly fertile agricultural soils prevented high uptakes of radiocaesium from soil to crops. Furthermore, the prevailing farming practices, food production and redistribution systems all contributed to minimising potential early impacts of the FDNPP accident.

Lesson 3. The CR values for rice grown under flooded conditions in Japan could be successfully predicted from the K_d and the concentration of exchangeable potassium in the soil solution; other soil constituents did not have a major impact on CR. Remediation strategies for agricultural crops in Japan were successfully and solely focused on the exchangeable potassium status of the soil rather than the intensive multi-factored approach applied for crops after the

Chernobyl accident in the former Soviet Union. The experience in Japan emphasizes the importance of understanding the impact of various soil components on radionuclide transfer to crops and suggests that—for soils with an insufficient supply of potassium—potassium is the key nutrient for remediation measures to reduce the uptake of radiocaesium from soil.

Lesson 4. Some processes such as radiocaesium transfer from bark to fruit and transfer from old to new leaves on tea shrubs were, for the first time, identified as being potentially important after the FDNPP accident, particularly when deposition occurs outside of the growing season. Radiocaesium transfer from outer bark to other tree compartments may affect radiocaesium activity concentrations in tree leaves (needles), branches and wood.

Lesson 5. The Fukushima data on radiocaesium transfer to game do not differ significantly from those for similar game species derived from research after the Chernobyl accident. This makes it possible to use wild animal T_{ag} values observed in different countries for site-specific assessments.

Lesson 6. Radiocaesium activities in rivers and the water column of lakes declined quickly due to dilution and sedimentation of radiocaesium attached to suspended sediments. One consequence was that irrigation water used in paddy fields was not a major continuing source of radiocaesium to rice.

The activity concentrations of ^{137}Cs had returned to approximately pre-accident values in sea water by 2019. CR values for marine and freshwater fish agreed well with data from before the Fukushima accident.

Lesson 7. In aquatic systems, due to rapid and substantial dilution, the radiocaesium activity concentrations in water were low, but radiocaesium CR values for marine and freshwater fish remain elevated partially due to food-web transfers.

Lesson 8. Samples that were collected from previously instrumented forests and other systems for different purposes were effectively utilized and adapted to provide otherwise difficult to obtain information on rates of interception and loss in the first few days and weeks after the FDNPP accident.

APPENDIX I.

SUPPLEMENTARY DATA FOR CHAPTER 2

I.1. SOIL PROPERTIES

TABLE I.1. COMPARISON OF JAPANESE SOIL GROUPS NAMES WITH THE FAO/UNESCO CLASSIFICATION

	Soil Group	FAO/UNESCO 1994 [2.6]	pH (H_2O)	Total C (%)
01	Man-made soils	Urbic Anthrosols	— [a]	—
02	Peat soils	Fibric Histosols	5.6	5.9
03	Muck soils	Terric Histosols	5.9	3.7
04	Podzols	Podzols	—	—
05	Sand-dune Regosols	Regosols/Arensols	5.8	7.6
06	Volcanogenous Regosols	Glyeic, Vitric Andosols	5.9–6.0	3.5–5.1
07	Gleyed Andosols	Andic Gleysols	5.8–5.9	4.7–8.3
08	Wet Andosols	Andic Gleysols	5.9–6.0	4.1–8.3
09	Forest Andosols	Haplic Andosols	—	—
10	Non-allophanic Andosols	Mollic, Umbric Andosols	5.8–6.0	3.5–8.3
11	Andosols	Andosols	5.8–6.0	3.5–8.3
12	Lowland Paddy soils	Eutric Fluvisols/ Eutric Gleysols	5.8–6.2	1.5–2.6
13	Gley Lowland soils	Eutric Fluvisols	5.3–6.0	2.1–3.7
14	Grey Lowland soils	Eutric Fluvisols	5.8–6.0	2.1–4.0
15	Regosolic Lowland soils	Eutric Fluvisols	6.2	1.7
16	Brown Lowland soils	Eutric Cambisols / Eutric Fluvisols	5.8–6.7	1.5–2.7
17	Gley Upland soils	Gleysols	5.5–5.8	2.2–3.7
18	Grey Upland soils	Gleysols	5.8–5.9	2.1–2.5
19	Lithosols	Eutric Leptosols	5.7–5.9	2.5–4.6
20	Terrestrial Regosols	Eutric Regosols	5.8–8.1	1.0–2.5
21	Dark Red soils	Luvisols / Cambisols	6.8–7.6	1.6
22	Red soils	Cambisols / Acrisols	4.8–5.7	1.7–2.8
23	Yellow soils	Cambisols / Acrisols	5.2–6.0	2.2–3.3
24	Brown Forest soils	Cambisols	5.9–6.1	2.4–3.3

[a] no data

I.2. WET TO DRY MASS CONVERSION FACTORS

TABLE I.2. DRY MATTER CONTENT IN AGRICULTURAL CROPS [2.12]

Group	English name	Scientific name	N	Dry matter content (%)	TRS 472 (%)
Cereals	Whole grain, all	*Triticum aestivum L., Oryza sativa subsp. japonica, Zea mays L., Fagopyrum esculentum*	7	87	—[a]
	Wheat, whole grain	*Triticum aestivum L.*	3	88	88
	Wheat, flour	*Triticum aestivum L.*	7	86	—
	Rice, whole grain	*Oryza sativa subsp. japonica*	2	85	—
	Rice, white rice	*Oryza sativa subsp. japonica*	4	86	—
	Rice, bran	*Oryza sativa subsp. japonica*	1	90	—
	Corn, whole grain	*Zea mays L.*	2	86	85
	Buckwheat, whole grain	*Fagopyrum esculentum*	4	87	
Tubers	All	*Ipomoea batatas L., Colocasia esculenta, Solanum tuberosum L., Dioscorea japonica, Helianthus tuberosus, Smallanthus sonchifolius, Sagittaria trifolia L.*	17	27	—
	Sweet potatoes	*Ipomoea batatas L.*	3	35	—
	Taro	*Colocasia esculenta*	5	24	—
	Potatoes	*Solanum tuberosum L.*	1	20	21
	Yam	*Dioscorea japonica*	5	28	—
Nuts	All	*Ginkgo biloba L., Castanea crenata, Castanopsis sp.*	3	49	—
Leguminous vegetables	Mature seeds, all	*Vigna angularis, Phaseolus vulgaris L., Pisum sativum L., Vigna unguiculata, Viciafaba L., Glycine max, Vigna umbellata, Cicer arietinum L., Phaseolus coccineus L., Phaseolus lunatus, Vigna radiata, Lens culinaris, Arachis hypogaea*	19	88	—
	Soybeans, mature seeds	*Glycine max*	5	88	87
	Immature seeds, all	*Phaseolus vulgaris L., Pisum sativum L., Viciafaba L., Arachis hypogaea*	4	32	—
	Immature pods, all	*Phaseolus vulgaris L., Pisum sativum L., Psophocarpu stetragonolobus, Vigna unguiculata ver. Sesquipedalis, Lablab purpureus*	6	9.8	—
	Leaves and stems, all	*Pisum sativum L.*	1	9.1	—
	Sprouts, all	*Medicago sativa L., Glycine max, Vigna mungo, Vigna radiata*	5	5.9	—

See footnote(s) on page 297

TABLE I.2. DRY MATTER CONTENT IN AGRICULTURAL CROPS [2.12] (cont.)

Group	English name	Scientific name	N	Dry matter content (%)	TRS 472 (%)
Leafy vegetables	All (56 species)		74	7.8	—
	Leaves, all (41 species)		59	7.9	
	Cabbage	*Brassica oleracea L. var. capitata*	3	7.8	12
	Lettuce	*Lactuca sativa L.*	7	5.3	8.0
	Spinach	*Spinacia oleracea L.*	3	7.6	8.0
	Welsh onion	*Allium fistulosum L.*	3	9.5	11
	Leaves and stems, all (11 species)		11	7.8	—
	New shoots, all	*Asparagus L., Aralia cordata*	2	6.5	—
	Petiole, all	*Apium graveolens var. dulce, Rheum rhabarbatum L.*	2	6.6	—
Non-leafy vegetables	All (29 species)		43	11	—
	Bulb, all	*Allium cepa L., Allium sativum L., Lilium L., Allium chinense, Cynara scolymus L.*	7	22	—
	Onions	*Allium cepa L.*	3	10	11
	Garlic	*Allium sativum L.*	1	36	
	Flower bud, all	*Cynara scolymus L., Brassica oleracea var. botrytis, Brassica rapa L. var. nippo-oleifera, Allium tuberosum, Brassica oleracea var. italica, Zingiber mioga*	6	10	—
	Cauliflower	*Brassica oleracea var. botrytis*	1	9.2	11
	Broccoli	*Brassica oleracea var. italica*	1	11	—
	Fruit vegetables, all (14 species)		22	8.7	—
	Zucchini	*Cucurbita pepo L.*	1	5.1	5.0
	Tomatoes	*Solanum lycopersicum L.*	2	7.5	6.0
	Eggplant	*Solanum melongena*	2	6.9	—
	Chayote	*Sechiumedule*	2	6.0	—
	Sweet peppers	*Capsicum annuum L.*	4	8.2	—
	Okura	*Abelmoschus esculentus*	1	10	—
	Pumpkin	*Cucurbita moschata, C. maxima, C. pepo*	3	15	7.5
	Cucumber	*Cucumis sativus L.*	1	4.6	5.0
	Sprouts, all	*Raphanus sativus var. longipinnatus, Brassica oleracea var. italica, Persicaria sp.*	3	8.4	—

TABLE I.2. DRY MATTER CONTENT IN AGRICULTURAL CROPS [2.12] (cont.)

Group	English name	Scientific name	N	Dry matter content (%)	TRS 472 (%)
	Stems, all	*Brassica oleracea var. gongylodes, Allium sativum L., Zizania latifolia L.*	3	8.9	—
Root crops	All (11 species)		19	11	—
	Burdock	*Arctiumlappa L.*	1	18	—
	Carrot	*Daucus carota*	6	11	14
	Ginger	*Zingiber officinale*	2	6.2	—
	Japanese radish	*Raphanus sativus var. longipinnatus*	2	5.4	9.0
	Logus root	*Nelumbo nucifera*	1	19	—
	Turnip	*Brassica rapa L. var. rapa*	3	6.2	12
	Wasabi	*Eutrema japonicum*	1	26	—
Mushrooms	Fresh mushrooms, all (16 species)		17	9.1	—
	Shiitake	*Lentinula edodes*	2	11	—
	Nameko	*Pholiota microspora*	1	7.6	—
	Matsutake	*Tricholoma matsutake*	1	12	—
	Dry mushrooms, All	*Auricularia polytricha, Auricularia auricula-judae, Tremella fuciformis, Lentinula edodes, Grifola frondosa*	5	88	—
	Shiitake, dry	*Lentinula edodes*	1	90	—
Fruits	All (63 species)		78	14	—
	Berries, all	*Ribesuva crispa, Vaccinium sp., Morella rubra, Rubus sp.*	4	13	—
	Blueberries	*Vaccinium sp.*	1	14	—
	Raspberries	*Rubus sp.*	1	12	16
	Citreae, all (23 species)		25	13	—
	Satsuma mandarins	*Citrus unshiu*	4	13	—
	Yuzu	*Citrus junos*	1	16	—
	Deciduous trees, all (13 species)		19	15	—
	Apples	*Malus pumila*	2	16	—
	Peaches	*Amygdalus persica L.*	1	11	—
	Plums	*Prunus salicina*	2	13	—
	Sweet cherries	*Prunus avium*	2	18	—
	Kiwifruit	*Actinidia deliciosa*	2	16	—
	Persimmons	*Diospyros kaki*	2	17	—
	Figs	*Ficuscarica L.*	1	15	—
	Japanese apricot	*Prunus mume*	1	9.6	—

TABLE I.2. DRY MATTER CONTENT IN AGRICULTURAL CROPS [2.12] (cont.)

Group	English name	Scientific name	N	Dry matter content (%)	TRS 472 (%)
	Others, all (7 species)		8	16	—
	Loquats	*Eriobotrya japonica*	1	11	—
	Tropical fruits, all (12 species)		14	17	—
	Herbaceous fruits, all	*Fragaria × ananassa Duchesne ex Rozier, Citrullus lanatus, Cucumis melo var. makuwa, Cucumis melo L.*	8	11	—
	Strawberry	*Fragaria × ananassa Duchesne ex Rozier*	1	10	—
	Watermelon	*Citrullus lanatus*	2	10	7.0
	Oriental melon	*Cucumis melo var. makuwa*	2	9.2	—
	Muskmelon	*Cucumis melo L.*	3	12	—

[a] no data

TABLE I.3. DRY MATTER CONTENT IN EDIBLE PLANTS EDIBLE WILD PLANTS [2.12–2.26]

Group	English name	Scientific name	N	Dry matter content (%)
Ferns	All, shoots (4 species)			10
	Ostrich fern	*Matteuccia struthiopteris*	9	11
	Western bracken fern	*Pteridium aquilinum*	11	9.4
	Cinnamon fern	*Osmundastrum cinnamomeum*	4	10
	Asian royal fern	*Osmunda japonica*	15	9.4
Bamboo	All, shoots (2 species)			8.8
	Bamboo shoots	*Phyllostachys heterocycla, P. bambusoides, P. nigra var. henonis etc.*	70	11
	Bamboo shoots	*Sasa kurilensis*	1	7.0
Perennial herbaceous plants	All (17 species)			11
	Long-stamen chive, bulb	*Allium macrostemon*	3	17
	Japanese butterbur, flower bud	*Petasites japonicus*	5	13
	Japanese knotweed, shoots	*Fallopia japonica*	6	6.4
	Nettle family plant, shoots	*Elatostema umbellatum*	1	10
	Momijigasa, shoots	*Parasenecio delphiniifolius*	4	8.7
	Japanese mugwort, shoots	*Artemisia indica var. maximowiczii*	8	15
	Asian fawn lily, shoots	*Erythronium japonicum*	5	11
	Common Sorrel, shoots	*Rumex japonicus*	4	12
	Nokongiku, shoots	*Aster microcephalus var. ovatus*	4	17
	Japanese honeywort, leaves and stems	*Cryptotaenia canadensis subsp. Japonica*	3	10
	Japanese spikenard, shoots	*Aralia cordata*	7	9.3
	Field horsetail, fertile stem	*Equisetum arvense*	6	11
	Butterbur, petiole	*Petasites japonicus*	129	7.2
	Leopard plant, petiole	*Farfugium japonicum*	5	12
	Hosta, shoots	*Hosta sieboldiana*	1	7.4
	Japanese parsley, shoots	*Oenanthe javanica*	3	8.8
	Miyamairakusa, shoots	*Laportea cuspidata*	2	8.3
Deciduous tree	All (9 species)			15
	Koshiabura, shoots	*Eleutherococcus sciadophylloides*	19	13
	Chocolate vine, fruits	*Akebia quinata*	1	16
	Iwagarami, shoots	*Schizophragma hydrangeoides*	8	14
	Climbing Hydrangea, shoots	*Hydrangea petiolaris*	13	13
	Three-leaf akebia, shoots	*Akebia trifoliata*	6	16
	Japanese angelica-tree, shoots	*Aralia elata*	13	12
	Japanese red elder, shoots	*Sambucus sieboldiana var. pinnatisecta*	5	15
	Hanaikada, shoots	*Helwingia japonica*	4	15
	Japanese pepper, shoots	*Zanthoxylum piperitum*	1	17

APPENDIX II.

SUPPLEMENTARY DATA FOR CHAPTER 4

TABLE II.1. EFFECTIVE T_{eff} AND ECOLOGICAL T_{eco} HALF-LIVES OF ^{137}CS, ^{134}CS+^{137}CS AND ^{131}I IN FRESH VEGETABLES AFTER THE FDNPP ACCIDENT

Crop name	Prefecture	Nuclide	Start of sampling in 2011	Sample size	Correlation coefficient	*p*-value	Effective half-life (d)	Ecological half-life (d)
Leafy vegetables								
Spinach	Fukushima	^{137}Cs	28 March	4	−0.99	0.008	7.7	7.7
Shinobufuyuna	Fukushima	^{137}Cs	21 March	5	−0.97	0.005	7.8	7.8
Spinach	Fukushima	^{137}Cs	21 March	4	−0.98	0.019	8.9	8.9
Spinach	Fukushima	^{137}Cs	21 March	4	−0.98	0.024	6.5	6.5
Kukitachina	Fukushima	^{137}Cs	21 March	5	−0.99	0.001	3.2	3.2
Spinach	Ibaraki	$^{134/137}$Cs	30 March	4	−0.97	0.026	10.4	10.0
Kakina	Tochigi	$^{134/137}$Cs	24 March	6	−0.88	0.021	10.5	10.0
Giant butterbur	Chiba	^{137}Cs	28 March	8	−0.96	0.000	7.7	7.7
Spinach	Fukushima	^{131}I	28 March	4	−0.99	0.006	2.8	4.3
Spinach	Fukushima	^{131}I	28 March	4	−1.00	0.003	3.7	6.9
Spinach	Fukushima	^{131}I	21 March	4	−0.97	0.030	5.0	13
Shinobufuyuna	Fukushima	^{131}I	21 March	5	−0.99	0.001	3.9	7.7
Komatsuna	Fukushima	^{131}I	21 March	3	−1.00	0.017	4.3	9.2
Spinach	Fukushima	^{131}I	28 March	4	−1.00	0.003	2.2	3.0
Spinach	Fukushima	^{131}I	21 March	4	−0.97	0.028	5.4	16
Spinach	Fukushima	^{131}I	21 March	4	−1.00	0.002	5.2	15
Spinach	Fukushima	^{131}I	21 March	4	−0.98	0.022	6.0	23
Spinach	Fukushima	^{131}I	21 March	4	−1.00	0.003	4.5	10
Kukitachina	Fukushima	^{131}I	21 March	5	−1.00	0.000	3.2	5.4
Spinach	Fukushima	^{131}I	21 March	5	−0.90	0.039	5.0	13
Spinach	Fukushima	^{131}I	28 March	4	−1.00	0.002	3.3	5.6
Spinach	Chiba	^{131}I	24 March	6	−0.96	0.002	5.6	19
Spinach	Chiba	^{131}I	30 March	6	−0.93	0.008	3.2	5.2
Spinach	Ibaraki	^{131}I	30 March	4	−0.99	0.009	3.7	6.9
Spinach	Saitama	^{131}I	24 March	4	−1.00	0.002	4.3	9.4
Spinach	Saitama	^{131}I	24 March	5	−0.99	0.001	4.4	9.8
Spinach	Tochigi	^{131}I	24 March	4	−0.99	0.015	4.1	8.3
Kakina	Tochigi	^{131}I	24 March	4	−0.98	0.018	2.5	3.6
Spinach	Gunma	^{131}I	24 March	5	−0.98	0.003	5.2	15
Kakina	Gunma	^{131}I	24 March	5	−0.97	0.006	3.6	6.5
Giant butterbur	Chiba	^{131}I	28 March	8	−0.99	<0.0001	3.7	7.0
Flowering head								
Broccoli	Fukushima	^{131}I	21 March	5	−1.00	<0.0001	3.7	6.7
Broccoli	Fukushima	^{131}I	21 March	3	−1.00	0.016	6.2	27
Broccoli	Fukushima	^{131}I	21 March	3	−1.00	0.006	3.8	7.3
Aburana	Fukushima	^{131}I	21 March	4	−0.99	0.010	4.0	8.1
Purple-stem mustard	Fukushima	^{131}I	21 March	4	−0.99	0.010	3.5	6.2
Nabana	Fukushima	^{131}I	24 March	4	−0.98	0.021	4.1	8.3

TABLE II.2. MASS INTERCEPTION FRACTION f_B (m²/kg DM) FOR RADIOCAESIUM (^{137}CS OR ^{134}CS+^{137}CS) AND ^{131}I ESTIMATED FOR LEAFY VEGETABLES AFTER THE FDNPP ACCIDENT

Crop name	Prefecture	Nuclide	f_B (m²/kg DM)
Spinach	Fukushima	^{137}Cs	0.35
Shinobufuyuna	Fukushima	^{137}Cs	0.10
Spinach	Fukushima	^{137}Cs	0.14
Spinach	Fukushima	^{137}Cs	0.07
Kukitachina	Fukushima	^{137}Cs	0.43
Spinach	Ibaraki	$^{134/137}$Cs	0.02
Kakina	Tochigi	$^{134/137}$Cs	0.01
Giant butterbur	Chiba	^{137}Cs	0.21
Spinach	Fukushima	^{131}I	0.04
Spinach	Fukushima	^{131}I	0.05
Spinach	Fukushima	^{131}I	0.10
Shinobufuyuna	Fukushima	^{131}I	0.02
Komatsuna	Fukushima	^{131}I	0.06
Spinach	Fukushima	^{131}I	0.15
Spinach	Fukushima	^{131}I	0.04
Spinach	Fukushima	^{131}I	0.03
Kukitachina	Fukushima	^{131}I	0.15
Spinach	Ibaraki	^{131}I	0.08
Spinach	Saitama	^{131}I	0.03
Spinach	Saitama	^{131}I	0.08
Spinach	Tochigi	^{131}I	0.20
Kakina	Tochigi	^{131}I	0.10
Spinach	Gunma	^{131}I	0.11
Kakina	Gunma	^{131}I	0.08
Giant butterbur	Chiba	^{131}I	0.30

APPENDIX III.

SUPPLEMENTARY DATA FOR CHAPTER 5

III.1. SOIL TO TREE TRANSFER

TABLE III.1. AGGREGATED TRANSFER FACTORS T_{AG} (m^2/kg DM) OF ^{137}CS FOR EACH TREE COMPARTMENT IN 2011–2015 [5.7, 5.9, 5.43–5.46, 5.59, 5.61, 5.65, 5.145]

Species	Year	T_{ag} (m^2/kg DM)			T_{ag} (m^2/kg DM)		
		Mean [a]	Range	N [b]	Mean [a]	Range	N [b]
		Wood			Bark		
Cedar	2011	4.0×10^{-4}	3.0×10^{-4}–5.5×10^{-4}	4	2.1×10^{-2}	1.1×10^{-2}–4.2×10^{-2}	4
	2012	2.1×10^{-4}	7.2×10^{-5}–4.2×10^{-4}	4	1.2×10^{-2}	8.2×10^{-3}–1.9×10^{-2}	4
	2013	6.9×10^{-4}	2.3×10^{-4}–2.8×10^{-3}	6	1.1×10^{-2}	4.0×10^{-3}–2.5×10^{-2}	6
	2014	2.5×10^{-4}	1.8×10^{-4}–4.3×10^{-4}	4	9.5×10^{-3}	3.7×10^{-3}–2.3×10^{-2}	4
	2015	3.9×10^{-4}	1.7×10^{-4}–1.5×10^{-3}	5	1.5×10^{-2}	2.6×10^{-3}–2.7×10^{-2}	19
Cypress	2011	— [c]	—	0	—	—	0
	2012	7.8×10^{-4}	4.2×10^{-4}–1.1×10^{-3}	2	6.5×10^{-2}	6.2×10^{-2}–6.7×10^{-2}	2
	2013	5.7×10^{-4}	4.6×10^{-4}–6.7×10^{-4}	2	3.1×10^{-2}	2.2×10^{-2}–4.1×10^{-2}	2
	2014	6.4×10^{-4}	6.3×10^{-4}–6.5×10^{-4}	2	1.8×10^{-2}	1.0×10^{-2}–2.5×10^{-2}	2
	2015	8.4×10^{-4}	6.0×10^{-4}–1.6×10^{-3}	3	2.0×10^{-2}	8.3×10^{-3}–3.6×10^{-2}	8
Pine	2011	1.2×10^{-4}	n.a. [d]	1	2.4×10^{-2}	n.a.	1
	2012	5.3×10^{-5}	n.a.	1	8.2×10^{-3}	n.a	1
	2013	3.7×10^{-5}	n.a.	1	7.1×10^{-3}	n.a.	1
	2014	4.5×10^{-5}	n.a	1	7.1×10^{-3}	n.a.	1
	2015	4.9×10^{-4}	3.3×10^{-5}–9.5×10^{-4}	2	1.4×10^{-2}	5.0×10^{-3}–3.7×10^{-2}	4
Oak	2011	1.2×10^{-4}	n.a.	1	3.1×10^{-2}	—	1
	2012	4.1×10^{-4}	1.5×10^{-4}–6.7×10^{-4}	2	2.4×10^{-2}	1.3×10^{-2}–3.5×10^{-2}	2
	2013	8.7×10^{-4}	1.8×10^{-4}–1.6×10^{-3}	2	3.5×10^{-2}	1.2×10^{-2}–5.8×10^{-2}	2
	2014	1.0×10^{-3}	3.0×10^{-4}–1.8×10^{-3}	2	2.0×10^{-2}	6.1×10^{-3}–3.4×10^{-2}	2
	2015	1.1×10^{-3}	3.3×10^{-4}–3.1×10^{-3}	3	2.5×10^{-2}	8.9×10^{-3}–4.0×10^{-2}	2
		Needles/leaves			Branches		
Cedar	2011	2.1×10^{-1}	1.4×10^{-1}–4.8×10^{-1}	4	1.0×10^{-1}	4.4×10^{-2}–1.9×10^{-1}	4
	2012	5.0×10^{-2}	3.7×10^{-2}–6.0×10^{-2}	4	3.6×10^{-2}	1.9×10^{-2}–8.3×10^{-2}	4
	2013	3.9×10^{-2}	1.7×10^{-2}–1.2×10^{-1}	25	2.4×10^{-2}	1.1×10^{-2}–6.8×10^{-2}	6
	2014	1.8×10^{-2}	2.7×10^{-3}–8.6×10^{-2}	47	2.4×10^{-2}	6.1×10^{-3}–8.1×10^{-2}	42
	2015	6.9×10^{-3}	1.8×10^{-4}–3.7×10^{-2}	57	7.8×10^{-3}	2.0×10^{-4}–2.5×10^{-2}	21

TABLE III.1. AGGREGATED TRANSFER FACTORS T_{AG} (m^2/kg DM) OF ^{137}CS FOR EACH TREE COMPARTMENT IN 2011–2015 [5.7, 5.9, 5.43–5.46, 5.59, 5.61, 5.65, 5.145] (cont.)

Species	Year	T_{ag} (m^2/kg DM)			T_{ag} (m^2/kg DM)		
		Mean [a]	Range	N [b]	Mean [a]	Range	N [b]
Cypress	2011	—	—	0	—	—	0
	2012	1.4×10^{-1}	1.2×10^{-1}–1.7×10^{-1}	2	4.0×10^{-2}	4.0×10^{-2}–4.1×10^{-2}	2
	2013	6.7×10^{-2}	2.7×10^{-2}–2.1×10^{-1}	5	1.6×10^{-2}	9.3×10^{-3}–2.2×10^{-2}	2
	2014	3.5×10^{-2}	6.7×10^{-3}–8.5×10^{-2}	15	2.7×10^{-2}	4.7×10^{-3}–9.1×10^{-2}	13
	2015	1.4×10^{-2}	2.9×10^{-3}–1.3×10^{-1}	20	9.7×10^{-3}	3.9×10^{-3}–1.6×10^{-2}	9
Pine	2011	2.9×10^{-1}	n.a.	1	6.1×10^{-2}	n.a.	1
	2012	1.9×10^{-2}	n.a.	1	1.4×10^{-2}	n.a.	1
	2013	5.5×10^{-3}	1.6×10^{-3}–2.6×10^{-2}	4	8.7×10^{-3}	n.a	1
	2014	5.7×10^{-3}	8.1×10^{-4}–4.8×10^{-2}	28	1.6×10^{-2}	3.1×10^{-3}–9.9×10^{-2}	27
	2015	3.6×10^{-3}	5.2×10^{-4}–1.7×10^{-2}	27	6.1×10^{-3}	1.3×10^{-3}–1.7×10^{-2}	5
Oak	2011	7.0×10^{-3}	n.a.	1	3.0×10^{-2}	n.a.	1
	2012	4.7×10^{-3}	1.8×10^{-3}–7.6×10^{-3}	2	2.6×10^{-2}	1.4×10^{-2}–3.9×10^{-2}	2
	2013	9.1×10^{-3}	3.6×10^{-3}–1.5×10^{-2}	2	2.1×10^{-2}	9.4×10^{-3}–3.2×10^{-2}	2
	2014	6.2×10^{-3}	2.9×10^{-3}–1.9×10^{-2}	4	1.4×10^{-2}	6.4×10^{-3}–1.9×10^{-2}	4
	2015	1.1×10^{-2}	2.5×10^{-3}–4.3×10^{-2}	3	9.2×10^{-3}	2.9×10^{-3}–2.6×10^{-2}	3

[a] single value (N = 1), arithmetic mean (N = 2), geometric mean (N > 2)
[b] sample size
[c] no data
[d] not applicable

TABLE III.2. NORMALIZED ACTIVITY CONCENTRATIONS, *NC* (m^2/kg DM) OF ^{137}CS FOR NEEDLES AND LEAVES

Tree species	Year	N [a]	*NC* (m^2/kg DM)				
			Median	GM [b]	GSD [c]	Min	Max
Cedar	2011	22	5.8×10^{-2}	5.2×10^{-2}	2.3	1.4×10^{-2}	2.7×10^{-1}
	2012	338	1.2×10^{-2}	1.2×10^{-2}	3.4	5.9×10^{-4}	1.9×10^{-1}
	2013	90	1.2×10^{-2}	1.4×10^{-2}	2.5	1.4×10^{-3}	8.9×10^{-2}
	2014	141	5.4×10^{-3}	6.6×10^{-3}	2.7	8.0×10^{-4}	8.7×10^{-2}
	2015	94	3.6×10^{-3}	3.6×10^{-3}	2.7	9.0×10^{-5}	2.0×10^{-2}
	2016	83	3.2×10^{-3}	3.1×10^{-3}	2.4	3.4×10^{-4}	2.4×10^{-2}
Cypress	2011	15	5.2×10^{-2}	5.2×10^{-2}	1.7	1.4×10^{-2}	1.4×10^{-1}
	2012	7	4.8×10^{-2}	4.7×10^{-2}	1.8	2.3×10^{-2}	1.2×10^{-1}
	2013	19	2.1×10^{-2}	2.1×10^{-2}	2.8	4.6×10^{-3}	1.4×10^{-1}
	2014	51	1.0×10^{-2}	1.1×10^{-2}	2.4	2.4×10^{-3}	9.0×10^{-2}
	2015	43	6.5×10^{-3}	6.8×10^{-3}	2.3	8.2×10^{-4}	3.3×10^{-2}
	2016	26	3.9×10^{-3}	3.7×10^{-3}	3.0	4.0×10^{-4}	2.7×10^{-2}
Pine	2011	7	5.6×10^{-2}	3.9×10^{-2}	3.3	1.0×10^{-2}	2.4×10^{-1}
	2012	11	1.1×10^{-2}	1.1×10^{-2}	2.0	2.7×10^{-3}	2.6×10^{-2}
	2013	31	2.7×10^{-3}	2.5×10^{-3}	2.7	2.7×10^{-4}	3.1×10^{-2}
	2014	75	2.4×10^{-3}	2.4×10^{-3}	2.2	2.9×10^{-4}	2.0×10^{-2}
	2015	35	2.0×10^{-3}	2.2×10^{-3}	2.6	2.4×10^{-4}	1.2×10^{-2}
	2016	21	1.3×10^{-3}	1.3×10^{-3}	3.0	1.9×10^{-4}	6.4×10^{-3}
Oak	2011	6	1.6×10^{-2}	1.5×10^{-2}	2.0	5.4×10^{-3}	3.5×10^{-2}
	2012	21	4.8×10^{-3}	5.2×10^{-3}	2.5	1.3×10^{-3}	3.6×10^{-2}
	2013	27	3.0×10^{-3}	3.9×10^{-3}	4.2	5.2×10^{-4}	7.6×10^{-2}
	2014	19	2.7×10^{-3}	2.3×10^{-3}	3.3	2.0×10^{-4}	1.9×10^{-2}
	2015	24	5.2×10^{-3}	4.2×10^{-3}	3.8	1.7×10^{-4}	4.5×10^{-2}
	2016	10	5.7×10^{-3}	3.7×10^{-3}	4.0	2.0×10^{-4}	1.6×10^{-2}

[a] sample size
[b] unitless
[c] geometric standard deviation

TABLE III.3. NORMALIZED ACTIVITY CONCENTRATIONS, NC (m^2/kg DM) OF ^{137}CS FOR BRANCHES

Tree species	Year	N [a]	*NC* (m^2/kg DM)				
			Median	GM	GSD	Min	Max
Cedar	2011	4	7.4×10^{-2}	7.4×10^{-2}	1.7	4.1×10^{-2}	1.4×10^{-1}
	2012	4	3.8×10^{-2}	3.8×10^{-2}	1.8	1.9×10^{-2}	8.0×10^{-2}
	2013	8	1.9×10^{-2}	1.8×10^{-2}	2.2	6.7×10^{-3}	8.9×10^{-2}
	2014	43	1.1×10^{-2}	1.2×10^{-2}	1.7	3.5×10^{-3}	3.8×10^{-2}
	2015	12	6.5×10^{-3}	2.5×10^{-3}	9.9	6.0×10^{-6}	1.5×10^{-2}
	2016	48	7.8×10^{-3}	7.6×10^{-3}	2.0	8.2×10^{-4}	3.6×10^{-2}
Cypress	2011	0	— [b]	—	—	—	—
	2012	2	2.6×10^{-2}	2.6×10^{-2}	1.2	2.2×10^{-2}	3.0×10^{-2}
	2013	3	8.7×10^{-3}	1.0×10^{-2}	1.5	7.9×10^{-3}	1.7×10^{-2}
	2014	13	9.1×10^{-3}	9.5×10^{-3}	1.7	3.7×10^{-3}	2.5×10^{-2}
	2015	8	4.4×10^{-3}	3.8×10^{-3}	2.0	7.9×10^{-4}	8.3×10^{-3}
	2016	18	6.6×10^{-3}	5.9×10^{-3}	1.7	1.8×10^{-3}	1.2×10^{-2}
Pine	2011	1	5.0×10^{-2}	5.0×10^{-2}	n.a. [c]	5.0×10^{-2}	5.0×10^{-2}
	2012	1	1.6×10^{-2}	1.6×10^{-2}	n.a.	1.6×10^{-2}	1.6×10^{-2}
	2013	3	9.5×10^{-4}	1.9×10^{-3}	4.4	7.2×10^{-4}	1.1×10^{-2}
	2014	40	5.5×10^{-3}	5.4×10^{-3}	2.7	9.9×10^{-5}	2.6×10^{-2}
	2015	8	2.2×10^{-3}	1.1×10^{-3}	8.6	6.0×10^{-6}	5.0×10^{-3}
	2016	32	3.0×10^{-3}	3.0×10^{-3}	3.1	9.9×10^{-5}	5.4×10^{-2}
Oak	2011	1	2.3×10^{-2}	2.3×10^{-2}	n.a.	2.3×10^{-2}	2.3×10^{-2}
	2012	2	2.4×10^{-2}	2.3×10^{-2}	1.6	1.6×10^{-2}	3.2×10^{-2}
	2013	21	1.7×10^{-3}	2.1×10^{-3}	4.0	2.3×10^{-4}	2.1×10^{-2}
	2014	20	2.7×10^{-3}	2.0×10^{-3}	4.9	9.4×10^{-5}	1.6×10^{-2}
	2015	46	1.4×10^{-3}	1.0×10^{-3}	4.7	7.0×10^{-5}	2.2×10^{-2}
	2016	21	5.8×10^{-4}	5.8×10^{-4}	3.8	8.5×10^{-5}	5.9×10^{-3}

[a] sample size
[b] no data
[c] not applicable

TABLE III.4. NORMALIZED ACTIVITY CONCENTRATIONS, NC (m^2/kg DM) OF ^{137}CS FOR BARK

Tree species	Year	N [a]	*NC* (m^2/kg DM)				
			Median	GM	GSD	Min	Max
Cedar	2011	3	1.4×10^{-2}	1.4×10^{-2}	1.8	7.8×10^{-3}	2.4×10^{-2}
	2012	22	1.6×10^{-2}	2.4×10^{-2}	3.5	5.3×10^{-3}	5.9×10^{-1}
	2013	29	9.3×10^{-3}	1.3×10^{-2}	3.2	2.8×10^{-3}	2.7×10^{-1}
	2014	73	1.6×10^{-2}	2.1×10^{-2}	3.3	2.2×10^{-3}	3.4×10^{-1}
	2015	56	9.0×10^{-3}	8.8×10^{-3}	2.6	1.3×10^{-3}	2.0×10^{-1}
	2016	12	7.4×10^{-3}	8.0×10^{-3}	1.4	5.1×10^{-3}	1.5×10^{-2}
Cypress	2011	0	— [b]	—	—	—	—
	2012	2	4.1×10^{-2}	4.1×10^{-2}	n.a. [c]	3.7×10^{-2}	4.6×10^{-2}
	2013	5	2.1×10^{-2}	2.2×10^{-2}	1.2	1.9×10^{-2}	3.1×10^{-2}
	2014	32	1.5×10^{-2}	1.8×10^{-2}	2.4	3.3×10^{-3}	1.1×10^{-1}
	2015	27	6.8×10^{-3}	8.0×10^{-3}	2.3	1.9×10^{-3}	4.1×10^{-2}
	2016	10	1.5×10^{-2}	1.3×10^{-2}	1.8	6.0×10^{-3}	2.5×10^{-2}
Pine	2011	1	2.0×10^{-2}	2.0×10^{-2}	n.a.	n.a.	n.a.
	2012	1	9.5×10^{-3}	9.5×10^{-3}	n.a.	n.a.	n.a.
	2013	14	8.9×10^{-3}	1.1×10^{-2}	4.8	1.8×10^{-4}	1.5×10^{-1}
	2014	66	1.3×10^{-2}	1.4×10^{-2}	3.1	5.7×10^{-5}	1.7×10^{-1}
	2015	34	7.9×10^{-3}	9.1×10^{-3}	2.7	1.6×10^{-3}	1.0×10^{-1}
	2016	6	7.8×10^{-3}	7.7×10^{-3}	1.7	3.6×10^{-3}	1.7×10^{-2}
Oak	2011	1	2.4×10^{-2}	2.4×10^{-2}	n.a.	n.a.	n.a.
	2012	18	3.1×10^{-2}	3.0×10^{-2}	1.7	8.8×10^{-3}	6.0×10^{-2}
	2013	18	1.8×10^{-2}	1.6×10^{-2}	2.0	5.4×10^{-3}	7.3×10^{-2}
	2014	17	1.0×10^{-2}	1.0×10^{-2}	1.7	3.8×10^{-3}	2.4×10^{-2}
	2015	9	6.7×10^{-3}	7.0×10^{-3}	1.8	3.3×10^{-3}	2.6×10^{-2}
	2016	6	1.3×10^{-2}	1.2×10^{-2}	2.3	3.8×10^{-3}	3.0×10^{-2}

[a] sample size
[b] no data
[c] not applicable

TABLE III.5. NORMALIZED ACTIVITY CONCENTRATIONS, NC (m^2/kg DM) OF ^{137}CS FOR WOOD

Tree species	Year	N [a]	*NC* (m^2/kg DM)				
			Median	GM	GSD	Min	Max
Cedar	2011	3	2.5×10^{-4}	2.4×10^{-4}	1.1	2.2×10^{-4}	2.6×10^{-4}
	2012	3	2.5×10^{-4}	2.8×10^{-4}	1.4	2.2×10^{-4}	4.0×10^{-4}
	2013	8	2.7×10^{-4}	3.6×10^{-4}	2.1	1.4×10^{-4}	1.0×10^{-3}
	2014	62	3.9×10^{-4}	3.8×10^{-4}	1.9	3.7×10^{-5}	1.3×10^{-3}
	2015	28	3.1×10^{-4}	3.6×10^{-4}	2.0	8.5×10^{-5}	1.4×10^{-3}
	2016	15	4.8×10^{-4}	5.3×10^{-4}	2.2	1.5×10^{-4}	2.4×10^{-3}
Cypress	2011	0	— [b]	—	—	—	—
	2012	2	4.7×10^{-4}	4.7×10^{-4}	n.a. [c]	3.1×10^{-4}	6.2×10^{-4}
	2013	3	5.6×10^{-4}	5.0×10^{-4}	1.4	3.5×10^{-4}	6.4×10^{-4}
	2014	24	6.9×10^{-4}	6.7×10^{-4}	2.1	1.0×10^{-4}	2.4×10^{-3}
	2015	15	7.8×10^{-4}	7.1×10^{-4}	1.9	1.6×10^{-4}	3.4×10^{-3}
	2016	8	4.8×10^{-4}	4.7×10^{-4}	1.7	1.8×10^{-4}	9.0×10^{-4}
Pine	2011	1	9.9×10^{-5}	9.9×10^{-5}	n.a.	n.a.	n.a.
	2012	1	6.0×10^{-5}	6.0×10^{-5}	n.a.	n.a.	n.a.
	2013	2	8.9×10^{-5}	8.9×10^{-5}	NA	4.6×10^{-5}	1.3×10^{-4}
	2014	42	3.2×10^{-4}	3.1×10^{-4}	2.3	4.1×10^{-5}	3.1×10^{-3}
	2015	16	2.2×10^{-4}	2.6×10^{-4}	2.4	3.7×10^{-5}	9.3×10^{-4}
	2016	9	1.8×10^{-4}	1.9×10^{-4}	4.2	2.6×10^{-5}	1.9×10^{-3}
Oak	2011	1	9.1×10^{-5}	9.1×10^{-5}	n.a.	n.a.	n.a.
	2012	2	3.6×10^{-4}	3.6×10^{-4}	n.a.	1.7×10^{-4}	5.5×10^{-4}
	2013	2	5.4×10^{-4}	5.4×10^{-4}	n.a.	2.2×10^{-4}	8.6×10^{-4}
	2014	2	7.0×10^{-4}	7.0×10^{-4}	n.a.	3.1×10^{-4}	1.1×10^{-3}
	2015	5	4.7×10^{-4}	7.3×10^{-4}	2.4	3.7×10^{-4}	3.0×10^{-3}
	2016	6	5.9×10^{-4}	5.8×10^{-4}	2.0	2.5×10^{-4}	1.5×10^{-3}

[a] sample size
[b] no data
[c] not applicable

III.2. SOIL TO TREE TRANSFER

TABLE III.6. NORMALIZED CONCENTRATIONS (m^2/kg DM) OF ^{137}CS IN CEDAR POLLEN ADOPTED FROM THE SURVEY BY FORESTRY AGENCY [5.146]

Year	N	AM	GM	GSD (unitless)	Min	Max
2011	10	2.1×10^{-2}	1.7×10^{-2}	2.0	4.2×10^{-3}	4.8×10^{-2}
2012	10	9.2×10^{-3}	7.6×10^{-3}	2.0	2.1×10^{-3}	1.8×10^{-2}
2013	10	5.5×10^{-3}	3.4×10^{-3}	2.5	1.3×10^{-3}	2.5×10^{-2}
2014	10	2.8×10^{-3}	2.4×10^{-3}	1.9	7.4×10^{-4}	5.5×10^{-3}
2015	8	1.8×10^{-3}	1.5×10^{-3}	1.9	4.8×10^{-4}	4.0×10^{-3}
2016	8	1.4×10^{-3}	1.3×10^{-3}	1.6	5.5×10^{-4}	2.1×10^{-3}
2017	8	1.1×10^{-3}	9.3×10^{-4}	1.9	4.1×10^{-4}	2.7×10^{-3}
2018	10	1.3×10^{-3}	9.9×10^{-4}	2.6	1.4×10^{-4}	2.5×10^{-3}

TABLE III.7. EFFECTIVE HALF-LIFE T_{eff} (year) VALUES FOR CEDAR POLLEN ADOPTED FROM THE SURVEY BY THE FORESTRY AGENCY [5.146]

Period	N	AM	GM	GSD (unitless)	Min	Max
2011–2014	10	1.27	1.17	1.49	0.76	2.98
2011–2018	10	2.07	1.86	1.60	0.94	4.65

TABLE III.8. NORMALISED ACTIVITY CONCENTRATIONS NC (m^2/kg DM) OF ^{137}CS IN CEDAR POLLEN REPORTED IN A SPATIAL SURVEY [5.77]

Year	N	AM	GM	GSD	Min	Max
2012	67	0.0043	0.0045	2.2	0.00062	0.03

TABLE III.9. INVENTORY RATIOS OF RADIOCAESIUM OF SOIL SURFACE ORGANIC LAYER AND/OR MINERAL SOIL TO AIRBORNE BASED TOTAL INVENTORY [5.7, 5.9, 5.44, 5.46, 5.47, 5.55, 5.58, 5.59, 5.61, 5.62, 5.64, 5.65, 5.79, 5.80, 5.82–5.90]

Forest type	Year	Soil surface organic layer		Mineral soil		Soil surface organic layer and mineral soil		N [b]
		GM [a]	Range	GM	Range	GM	Range	
Evergreen	2011	0.21	9.0×10^{-3}–1.9	0.39	0.024–1.8	0.65	0.095–2.2	210
	2012	0.38	0.14–0.77	0.57	0.27–1.1	1.0	0.59–1.4	14
	2013	0.37	0.11–1.1	0.58	0.23–1.4	1.0	0.47–1.9	23
	2014	0.25	3.3×10^{-3}–1.4	0.29	2.9×10^{-3}–1.6	0.61	6.2×10^{-3}–1.8	93
	2015	0.18	8.6×10^{-4}–0.79	0.45	3.2×10^{-3}–2.1	0.69	4.1×10^{-3}–2.4	99
	2016	0.25	0.014–1.9	0.46	0.047–3.9	0.83	0.27–4.0	90
Deciduous	2011	0.30	0.075–1.5	0.45	0.20–0.99	0.81	0.34–2.5	27
	2012	0.20	0.056–0.48	0.52	0.2–1.2	0.77	0.43–1.5	7
	2013	0.28	0.17–0.35	0.49	0.24–1.2	0.80	0.41–1.6	4
	2014	0.22	0.056–1.3	0.51	0.14–1.1	0.86	0.49–1.5	10
	2015	0.14	0.046–0.33	0.52	0.088–1.7	0.71	0.23–1.7	11
	2016	0.073	7.7×10^{-4}–0.39	0.47	0.12–1.6	0.59	0.12–1.7	17

[a] geometric mean
[b] the number of study sites

TABLE III.10. NORMALIZED ^{137}CS ACTIVITY CONCENTRATION, NC (m^2/kg DM), IN FOREST SOIL ORGANIC LAYER

Tree species	Year	N [a]	*NC* (m^2/kg DM)				
			Median	GM	GSD [b]	Min	Max
Cedar	2011	120	0.29	0.29	1.7	0.016	0.99
	2012	5	0.14	0.12	2.1	0.036	0.29
	2013	12	0.14	0.15	1.7	0.075	0.44
	2014	63	0.14	0.13	1.9	6.0×10^{-3}	0.44
	2015	59	0.10	0.11	1.6	0.036	0.33
	2016	53	0.084	0.084	1.6	0.028	0.20
Cypress	2011	20	0.25	0.26	1.9	0.047	0.65
	2012	3	0.11	0.13	2.6	0.056	0.38
	2013	4	0.15	0.16	1.6	0.11	0.29
	2014	23	0.11	0.10	1.7	0.031	0.30
	2015	27	0.10	0.095	1.8	0.02	0.38
	2016	24	0.072	0.058	2.6	7.6×10^{-3}	0.26
Pine	2011	69	0.38	0.36	1.6	0.072	0.80
	2012	1	0.21	0.21	n.a. [b]	n.a.	n.a.
	2013	9	0.17	0.11	6.7	8.0×10^{-4}	0.48
	2014	57	0.16	0.13	2.3	1.7×10^{-3}	0.47
	2015	33	0.10	0.088	2.8	6.4×10^{-4}	0.38
	2016	30	0.098	0.072	2.6	5.9×10^{-3}	0.20
Oak	2011	16	0.43	0.18	4.9	7.9×10^{-3}	0.95
	2012	5	6.6×10^{-3}	0.024	9.0	3.2×10^{-3}	0.35
	2013	4	0.14	0.084	3.4	0.015	0.22
	2014	8	0.10	0.072	3.2	4.9×10^{-3}	0.17
	2015	12	0.065	0.064	2.0	0.02	0.20
	2016	6	0.064	0.029	8.8	5.9×10^{-4}	0.23

[a] sample size
[b] unitless
[c] not applicable

TABLE III.11. FRACTION RETAINED IN THE SOIL SURFACE ORGANIC LAYER F-lit (%), POSITION OF MIGRATION CENTRE X_c (cm).

Forest type	Sampling date	*F*-lit (%)	X_c (cm)	N	Depth (cm)	Reference
Cedar	2011/6/18	75	3.5	5	14.3	[5.85]
Cedar	2011/6/18	91	3.9	5	14.9	[5.85]
Cedar	2011/7/19	69	2.7	5	12.9	[5.147]
Cedar	2011/7/20	84	2.6	5	13.8	[5.147]
Cedar	2011/6/30	48	1.7	15	9.5	[5.99]
Cedar	2011/7/2	90	1.1	9	4.3	[5.99]
Cedar	2011/8/9	63	3.6	4	20.0	[5.9]
Cedar	2011/9/7	50	4.8	4	20.0	[5.9]
Cedar	2011/8/31	55	3.2	4	20.0	[5.9]
Cedar	2011/11/28	45	3.7	4	20.0	[5.9]
Cedar	2012/1/10	48	1.8	15	9.5	[5.99]
Cedar	2012/1/17	79	1.3	15	9.5	[5.99]
Cedar	2012/8/1	26	3.2	4	20.0	[5.9]
Cedar	2012/8/23	18	3.4	4	20.0	[5.9]
Cedar	2012/8/28	22	2.3	17	17.5	[5.99]
Cedar	2012/8/28	64	2.2	17	17.5	[5.99]
Cedar	2012/9/3	18	3.8	4	20.0	[5.9]
Cedar	2012/9/20	68	3.4	4	20.0	[5.9]
Cedar	2012/10/17	47	2.9	7	17.5	[5.96]
Cedar	2012/10/17	39	4.2	6	9.0	[5.96]
Cedar	2012/10/17	25	4.9	6	9.0	[5.96]
Cedar	2012/10/17	34	4.1	8	25.0	[5.96]
Cedar	2012/10/17	28	5.4	8	25.0	[5.96]
Cedar	2012/10/17	31	4.7	8	25.0	[5.96]
Cedar	2012/10/17	34	3.7	8	25.0	[5.96]
Cedar	2012/10/17	28	4.8	8	25.0	[5.96]
Cedar	2012/10/17	38	6.0	7	17.5	[5.96]
Cedar	2012/12/13	41	3.2	17	17.5	[5.99]
Cedar	2012/12/13	18	1.7	17	17.5	[5.99]
Cedar	2013/7/14	21	1.7	17	17.5	[5.99]
Cedar	2013/7/18	62	1.5	17	17.5	[5.99]
Cedar	2013/8/1	28	4.0	4	20.0	[5.9]
Cedar	2013/8/26	19	3.4	4	20.0	[5.9]
Cedar	2013/8/27	67	3.8	4	20.0	[5.9]
Cedar	2013/9/4	19	3.9	4	20.0	[5.9]

TABLE III.11. FRACTION RETAINED IN THE SOIL SURFACE ORGANIC LAYER F-lit (%), POSITION OF MIGRATION CENTRE X_c (cont.)

Forest type	Sampling date	*F*-lit (%)	X_c (cm)	N	Depth (cm)	Reference
Cedar	2014/7/21	23	2.7	17	17.5	[5.99]
Cedar	2014/7/21	26	1.5	17	17.5	[5.99]
Cedar	2014/7/29	15	4.0	4	20.0	[5.9]
Cedar	2014/8/25	18	3.3	4	20.0	[5.9]
Cedar	2014/8/27	50	3.8	4	20.0	[5.9]
Cedar	2014/9/1	14	3.8	4	20.0	[5.9]
Cedar	2015/7/25	8	2.1	17	17.5	[5.99]
Cedar	2015/7/26	32	2.1	17	17.5	[5.99]
Cedar	2015/8/4	10	4.3	4	20.0	[5.9]
Cedar	2015/8/25	8	3.4	4	20.0	[5.9]
Cedar	2015/8/26	34	3.2	4	20.0	[5.9]
Cedar	2015/9/2	18	5.4	4	20.0	[5.9]
Cedar	2016/8/7	7	3.1	17	17.5	[5.99]
Cedar	2016/8/7	32	2.4	17	17.5	[5.99]
Cedar	2017/7/2	4	4.8	17	17.5	[5.99]
Cedar	2017/7/2	21	2.3	17	17.5	[5.99]
Cypress	2012/2/16	23	3.7	4	20.0	[5.9]
Cypress	2012/8/24	53	4.7	4	20.0	[5.9]
Cypress	2013/1/28	23	4.2	4	20.0	[5.9]
Cypress	2013/8/27	54	6.3	4	20.0	[5.9]
Cypress	2013/9/25	16	4.3	4	20.0	[5.9]
Cypress	2014/8/26	40	4.6	4	20.0	[5.9]
Cypress	2014/9/30	4	3.5	4	20.0	[5.9]
Cypress	2015/8/25	53	4.1	4	20.0	[5.9]
Cypress	2015/9/28	8	3.8	4	20.0	[5.9]
Deciduous	2011/6/18	61	3.1	5	14.0	[5.85]
Deciduous	2011/6/18	50	2.3	5	14.8	[5.85]
Deciduous	2011/7/20	41	2.6	5	12.1	[5.147]
Deciduous	2011/7/20	64	1.9	5	12.7	[5.147]
Deciduous	2011/8/9	60	3.7	4	20.0	[5.9]
Deciduous	2012/8/2	22	3.6	4	20.0	[5.9]
Deciduous	2012/8/24	46	2.9	4	20.0	[5.9]
Deciduous	2012/10/17	29	3.9	8	25.0	[5.96]
Deciduous	2012/10/17	11	5.1	8	25.0	[5.96]

TABLE III.11. FRACTION RETAINED IN THE SOIL SURFACE ORGANIC LAYER F-lit (%), POSITION OF MIGRATION CENTRE X_c (cont.)

Forest type	Sampling date	*F*-lit (%)	X_c (cm)	N	Depth (cm)	Reference
Deciduous	2012/10/17	25	3.4	8	25.0	[5.96]
Deciduous	2012/10/17	32	2.8	8	25.0	[5.96]
Deciduous	2012/10/17	25	3.0	8	25.0	[5.96]
Deciduous	2012/10/17	27	2.8	8	25.0	[5.96]
Deciduous	2012/10/17	26	4.5	8	25.0	[5.96]
Deciduous	2012/10/17	28	3.9	8	25.0	[5.96]
Deciduous	2012/10/17	27	4.0	7	17.5	[5.96]
Deciduous	2013/8/2	20	3.4	4	20.0	[5.9]
Deciduous	2013/8/27	47	4.5	4	20.0	[5.9]
Deciduous	2014/7/30	18	4.2	4	20.0	[5.9]
Deciduous	2014/8/26	29	3.4	4	20.0	[5.9]
Deciduous	2014/10/15	91	5.7	4	17.5	[5.88]
Deciduous	2015/8/5	11	4.7	4	20.0	[5.9]
Deciduous	2015/8/26	38	4.9	4	20.0	[5.9]
Pine	2011/6/18	56	2.3	5	14.7	[5.85]
Pine	2011/7/19	54	4.6	5	13.7	[5.147]
Pine	2011/8/9	56	5.1	4	20.0	[5.9]
Pine	2012/8/2	27	3.9	4	20.0	[5.9]
Pine	2013/8/1	29	3.3	4	20.0	[5.9]
Pine	2014/7/29	21	3.7	4	20.0	[5.9]
Pine	2015/8/4	10	4.8	4	20.0	[5.9]
Mixed	2011/7/1	91	2.3	15	9.5	[5.99]
Mixed	2012/1/10	65	4.2	15	9.5	[5.99]
Mixed	2012/8/27	50	4.7	17	17.5	[5.99]
Mixed	2012/12/11	40	1.9	17	17.5	[5.99]
Mixed	2013/7/13	68	1.5	17	17.5	[5.99]
Mixed	2014/7/22	17	3.7	17	17.5	[5.99]
Mixed	2015/7/25	27	2.7	17	17.5	[5.99]
Mixed	2016/6/25	7	3.4	17	17.5	[5.99]
Mixed	2017/7/2	6	4.6	17	17.5	[5.99]

III.4. MUSHROOMS

TABLE III.12. *NC* (m^2/kg DM) VALUES OF ^{137}CS FOR MUSHROOMS

Species (Japanese name)	Type [a]	D/F [b]	Year	N [c]	GM	GSD	Min	Max
Armillaria mellea	W	0.11	2011	9	1.0×10^{-2}	3.8	1.2×10^{-3}	7.2×10^{-2}
(Naratake)			2012	12	5.5×10^{-2}	3.4	9.1×10^{-3}	7.7×10^{-1}
			2013	5	3.7×10^{-2}	3.7	5.9×10^{-3}	1.8×10^{-1}
			2014	12	3.5×10^{-2}	2.2	3.8×10^{-3}	9.4×10^{-2}
			2015	11	2.4×10^{-2}	1.5	1.3×10^{-2}	5.2×10^{-2}
			2016	15	2.5×10^{-2}	2.6	4.4×10^{-3}	2.0×10^{-1}
			2017	11	3.1×10^{-2}	2.0	6.6×10^{-3}	8.4×10^{-2}
Entoloma sarcopum	M	0.09	2011	6	1.2×10^{-2}	2.4	2.5×10^{-3}	3.5×10^{-2}
(Urabenihoteishimeji)			2012	8	2.6×10^{-2}	4.5	4.9×10^{-3}	4.3×10^{-1}
			2013	7	2.4×10^{-2}	3.3	7.4×10^{-3}	2.6×10^{-1}
			2014	7	1.9×10^{-2}	3.9	4.3×10^{-3}	2.8×10^{-1}
			2015	7	9.7×10^{-3}	1.8	5.5×10^{-3}	3.5×10^{-2}
			2016	5	1.9×10^{-2}	3.8	6.2×10^{-3}	1.7×10^{-1}
			2017	5	2.3×10^{-2}	3.3	7.1×10^{-3}	1.4×10^{-1}
Hygrophorus russula	M	0.13	2011	6	1.9×10^{-2}	1.7	1.0×10^{-2}	3.2×10^{-2}
(Sakurashimeji)			2012	6	4.2×10^{-2}	2.2	1.4×10^{-2}	1.1×10^{-1}
			2013	2	9.1×10^{-2}	1.1	8.4×10^{-2}	1.0×10^{-1}
			2014	6	3.0×10^{-2}	1.8	1.4×10^{-2}	7.3×10^{-2}
			2015	2	4.1×10^{-3}	1.7	2.9×10^{-3}	5.9×10^{-3}
			2016	2	3.2×10^{-2}	2.4	1.7×10^{-2}	6.0×10^{-2}
			2017	2	3.9×10^{-2}	1.4	3.1×10^{-2}	5.0×10^{-2}
Hypholoma sublateritium	W	0.10	2013	2	5.2×10^{-2}	2.2	3.0×10^{-2}	9.0×10^{-2}
(Kuritake)			2014	6	7.4×10^{-2}	3.0	1.9×10^{-2}	3.4×10^{-1}
			2015	2	2.1×10^{-2}	3.8	8.2×10^{-3}	5.5×10^{-2}
			2016	1	6.7×10^{-2}	n.a. [d]	6.7×10^{-2}	6.7×10^{-2}
			2017	3	4.4×10^{-2}	2.2	1.8×10^{-2}	7.4×10^{-2}
Lactarius hatsudake	M	0.11	2011	10	8.0×10^{-2}	3.8	3.2×10^{-3}	4.1×10^{-1}
(Hatsuktake)			2012	2	3.9×10^{-1}	20.3	4.7×10^{-2}	3.3
Lactarius volemus	M	0.11	2011	24	4.0×10^{-2}	7.1	2.0×10^{-3}	2.2
(Chichitake)			2012	19	3.3×10^{-1}	5.1	1.9×10^{-2}	1.1
			2013	3	5.3×10^{-2}	2.1	2.2×10^{-2}	8.2×10^{-2}
			2014	7	3.3×10^{-2}	5.2	4.5×10^{-3}	6.5×10^{-1}
			2015	3	2.0×10^{-2}	3.0	5.9×10^{-3}	4.8×10^{-2}
			2016	3	3.4×10^{-2}	1.6	2.1×10^{-2}	5.6×10^{-2}
			2017	6	2.4×10^{-2}	2.3	9.5×10^{-3}	6.3×10^{-2}

TABLE III.12. *NC* (m^2/kg DM) VALUES OF ^{137}CS FOR MUSHROOMS (cont.)

Species (Japanese name)	Type [a]	D/F [b]	Year	N [c]	GM	GSD	Min	Max
Lepista nuda	L	0.09	2011	2	2.5×10^{-1}	3.1	1.1×10^{-1}	5.6×10^{-1}
(Murasakishimeji)			2012	1	1.8×10^{-2}	n.a.	1.8×10^{-2}	1.8×10^{-2}
			2013	2	5.9×10^{-2}	1.2	5.1×10^{-2}	6.8×10^{-2}
			2015	2	4.1×10^{-2}	4.8	1.4×10^{-2}	1.2×10^{-1}
			2016	2	1.4×10^{-2}	7.1	3.5×10^{-3}	5.6×10^{-2}
			2017	1	2.1×10^{-1}	n.a.	2.1×10^{-1}	2.1×10^{-1}
Leucopaxillus iganteus	L	0.10	2011	8	5.1×10^{-3}	2.5	1.2×10^{-3}	2.6×10^{-2}
(Ohichotake)			2012	4	1.5×10^{-2}	3.8	4.1×10^{-3}	7.4×10^{-2}
			2013	2	2.9×10^{-2}	1.1	2.7×10^{-2}	3.1×10^{-2}
			2014	2	3.1×10^{-2}	1.5	2.3×10^{-2}	4.2×10^{-2}
			2015	1	5.7×10^{-3}	n.a.	5.7×10^{-3}	5.7×10^{-3}
Panellus serotinus	W	0.10	2011	1	1.7×10^{-1}	n.a.	1.7×10^{-1}	1.7×10^{-1}
(Mukitake)			2012	1	2.4×10^{-2}	n.a.	2.4×10^{-2}	2.4×10^{-2}
			2013	7	5.5×10^{-2}	1.9	2.3×10^{-2}	1.8×10^{-1}
			2014	4	7.1×10^{-2}	2.1	3.5×10^{-2}	1.7×10^{-1}
			2015	4	3.2×10^{-2}	2.5	1.2×10^{-2}	7.2×10^{-2}
			2016	3	5.0×10^{-2}	1.5	3.4×10^{-2}	8.0×10^{-2}
			2017	1	1.0×10^{-2}	n.a.	1.0×10^{-2}	1.0×10^{-2}
Pholiota lubrica	L	0.08	2011	1	2.6×10^{-1}	n.a.	2.6×10^{-1}	2.6×10^{-1}
(Chanametsumutake)			2013	7	2.2×10^{-1}	3.0	2.1×10^{-2}	5.7×10^{-1}
			2014	4	2.3×10^{-1}	4.2	5.2×10^{-2}	8.2×10^{-1}
			2015	2	5.0×10^{-1}	1.3	4.1×10^{-1}	6.1×10^{-1}
			2017	2	2.3×10^{-1}	1.3	1.9×10^{-1}	2.7×10^{-1}
Ramaria botrytis	M	0.12	2011	8	6.8×10^{-3}	3.0	1.9×10^{-3}	3.1×10^{-2}
(Houkitake)			2012	1	5.1×10^{-1}	n.a.	5.1×10^{-1}	5.1×10^{-1}
			2014	2	3.9×10^{-2}	1.3	3.3×10^{-2}	4.7×10^{-2}
			2015	2	2.6×10^{-2}	1.6	1.9×10^{-2}	3.5×10^{-2}
			2016	3	2.6×10^{-2}	1.6	1.6×10^{-2}	4.1×10^{-2}
			2017	4	1.1×10^{-2}	1.5	6.8×10^{-3}	1.5×10^{-2}
Sarcodon aspratus	M	0.13	2011	3	2.0×10^{-2}	2.5	1.1×10^{-2}	5.7×10^{-2}
(Koutake)			2012	4	1.1×10^{-1}	2.8	4.0×10^{-2}	4.4×10^{-1}
			2013	6	5.1×10^{-2}	2.9	1.9×10^{-2}	3.7×10^{-1}
			2014	2	5.8×10^{-2}	10.9	1.1×10^{-2}	3.2×10^{-1}
			2015	2	3.9×10^{-2}	1.2	3.5×10^{-2}	4.4×10^{-2}
			2016	4	6.1×10^{-2}	3.7	1.2×10^{-2}	2.3×10^{-1}
			2017	5	4.4×10^{-2}	1.2	3.3×10^{-2}	5.2×10^{-2}

TABLE III.12. *NC* (m^2/kg DM) VALUES OF ^{137}CS FOR MUSHROOMS (cont.)

Species (Japanese name)	Type [a]	D/F [b]	Year	N [c]	GM	GSD	Min	Max
Suillus bovinus	M	0.09	2011	4	6.6×10^{-2}	1.7	3.7×10^{-2}	1.1×10^{-1}
(Amitake)			2012	9	7.1×10^{-2}	5.5	7.8×10^{-3}	1.2
			2015	1	2.7×10^{-3}	n.a.	2.7×10^{-3}	2.7×10^{-3}
			2017	3	1.1×10^{-2}	1.6	6.6×10^{-3}	1.6×10^{-2}
Tricholoma matsutake	M	0.10	2011	5	6.7×10^{-3}	6.0	8.7×10^{-4}	9.9×10^{-2}
(Matsutake)			2012	3	2.4×10^{-2}	6.7	3.7×10^{-3}	1.6×10^{-1}
			2013	9	9.8×10^{-3}	2.0	3.9×10^{-3}	2.8×10^{-2}
			2014	3	1.9×10^{-2}	4.7	3.5×10^{-3}	6.9×10^{-2}
			2015	2	2.3×10^{-2}	1.4	1.8×10^{-2}	3.0×10^{-2}
			2016	4	1.7×10^{-2}	1.4	1.1×10^{-2}	2.4×10^{-2}
			2017	6	1.7×10^{-2}	3.0	5.1×10^{-3}	6.5×10^{-2}
Tricholoma ortentosum	M	0.10	2011	3	2.7×10^{-1}	2.8	1.4×10^{-1}	9.0×10^{-1}
(Shimofurishimeji)			2012	1	3.1×10^{-2}	n.a.	3.1×10^{-2}	3.1×10^{-2}
			2013	1	1.6×10^{-1}	n.a.	1.6×10^{-1}	1.6×10^{-1}
			2014	1	5.5×10^{-3}	n.a.	5.5×10^{-3}	5.5×10^{-3}
			2015	3	6.8×10^{-2}	3.0	3.0×10^{-2}	2.4×10^{-1}
			2016	2	3.9×10^{-2}	1.5	2.9×10^{-2}	5.3×10^{-2}

[a] Types of mushrooms: L (soil litter decomposing fungi), M (mycorrhizal fungi), W (wood decomposing fungi)

[b] D/F ratio: dry to fresh mass ratios that were compiled from the following Refs. [5.111, 5.112, 5.114–5.116, 5.118, 5.119, 5.148, 5.149]

[c] sample size

[d] not applicable

TABLE III.13. *NC* (m^2/kg DM) [a] VALUES OF ^{137}CS FOR EDIBLE WILD PLANTS FROM GOVERNMENTAL MONITORING DATA [b]

Type	Name (ja: Japanese name)	Species	Edible part (dry/wet ratio)	Year	N	GM	GSD	Min	Max
Deciduous tree	Koshiabura (ja)	*Eleutherococcus sciadophylloides*	Shoot (0.13)	2012	57	5.2×10^{-2}	3.4	2.9×10^{-3}	8.6×10^{-1}
				2013	59	6.9×10^{-2}	2.9	3.6×10^{-3}	1.1×10
				2014	23	7.6×10^{-2}	2.6	1.4×10^{-2}	7.2×10^{-1}
				2015	21	1.1×10^{-1}	2.6	2.3×10^{-2}	6.4×10^{-1}
				2016	19	1.3×10^{-1}	3.1	1.0×10^{-2}	1.0
				2017	14	7.6×10^{-2}	2.6	4.9×10^{-3}	2.1×10^{-1}
				2018	48	8.7×10^{-2}	2.7	6.4×10^{-3}	4.2×10^{-1}
	Walnut	*Juglans sp*.	Seed (—[c])	2012	8	4.6×10^{-4}	3.1	1.3×10^{-4}	2.9×10^{-3}
				2013	12	5.0×10^{-4}	2.3	1.4×10^{-4}	2.7×10^{-3}
				2014	15	3.8×10^{-4}	1.6	1.6×10^{-4}	6.4×10^{-4}
				2015	19	3.3×10^{-4}	2.2	6.6×10^{-5}	1.1×10^{-3}
				2016	14	3.6×10^{-4}	2.9	5.1×10^{-5}	3.2×10^{-3}
				2017	16	3.8×10^{-4}	2.6	5.8×10^{-5}	2.3×10^{-3}
Deciduous shrub	Japanese pepper	*Zanthoxylum piperitum*	Shoot (0.17)	2012	14	1.5×10^{-2}	2.9	2.0×10^{-3}	9.7×10^{-2}
				2013	10	5.4×10^{-3}	2.5	2.2×10^{-3}	2.3×10^{-2}
				2014	4	3.9×10^{-3}	3.5	8.2×10^{-4}	1.7×10^{-2}
				2015	3	4.2×10^{-3}	2.1	1.9×10^{-3}	8.0×10^{-3}
				2016	6	2.8×10^{-3}	1.6	1.1×10^{-3}	3.8×10^{-3}
				2017	2	5.9×10^{-3}	1.2	5.3×10^{-3}	6.6×10^{-3}
				2018	4	3.0×10^{-3}	3.6	6.9×10^{-4}	1.4×10^{-2}
	Taranome (ja)	*Aralia elata*	Shoot (0.12)	2012	77	1.0×10^{-2}	3.5	5.9×10^{-4}	2.7×10^{-1}
				2013	75	9.3×10^{-3}	4.1	2.5×10^{-4}	2.4×10^{-1}
				2014	46	1.2×10^{-2}	4.8	5.5×10^{-4}	3.4×10^{-1}
				2015	57	2.5×10^{-2}	2.9	1.1×10^{-3}	1.4×10^{-1}
				2016	93	1.2×10^{-2}	4.4	2.3×10^{-4}	4.3×10^{-1}
				2017	91	1.3×10^{-2}	3.6	2.5×10^{-4}	1.3×10^{-1}
				2018	123	1.7×10^{-2}	3.5	4.4×10^{-4}	4.1×10^{-1}
Perennial herb	Butterbur leafstalk	*Petasites japonicus*	Leafstalk (0.07)	2012	21	3.6×10^{-3}	5.3	3.6×10^{-4}	1.9×10^{-1}
				2013	42	2.4×10^{-3}	3.4	3.2×10^{-4}	6.8×10^{-2}
				2014	16	1.3×10^{-3}	4.0	1.7×10^{-4}	3.8×10^{-2}
				2015	21	7.9×10^{-4}	2.2	1.7×10^{-4}	4.3×10^{-3}
				2016	18	9.2×10^{-4}	2.9	2.1×10^{-4}	1.1×10^{-2}
				2017	2	4.2×10^{-4}	1.3	3.6×10^{-4}	5.0×10^{-4}
				2018	4	9.5×10^{-4}	1.7	5.2×10^{-4}	1.6×10^{-3}
	Butterbur scape	*Petasites japonicus*	Scape (0.13)	2011	3	2.4×10^{-3}	1.5	1.5×10^{-3}	3.2×10^{-3}
				2012	51	3.2×10^{-3}	2.9	3.7×10^{-4}	6.7×10^{-2}
				2013	24	2.6×10^{-3}	3.1	5.1×10^{-4}	2.5×10^{-2}
				2014	30	1.4×10^{-3}	2.4	2.8×10^{-4}	1.2×10^{-2}
				2015	21	1.2×10^{-3}	2.4	1.9×10^{-4}	4.7×10^{-3}

TABLE III.13. *NC* (m^2/kg DM) [a] VALUES OF ^{137}CS FOR EDIBLE WILD PLANTS FROM GOVERNMENTAL MONITORING DATA [b] (cont.)

Type	Name (ja: Japanese name)	Species	Edible part (dry/wet ratio)	Year	N	GM	GSD	Min	Max
				2016	29	1.3×10^{-3}	2.3	3.7×10^{-4}	9.0×10^{-3}
				2017	11	8.7×10^{-4}	1.9	3.6×10^{-4}	3.2×10^{-3}
				2018	15	1.5×10^{-3}	2.1	5.5×10^{-4}	8.2×10^{-3}
	Japanese mugwort	*Artemisia indica var. maximowiczii*	Shoot (0.15)	2013	1	1.8×10^{-3}	n.a.[d]	1.8×10^{-3}	1.8×10^{-3}
				2014	1	6.4×10^{-4}	n.a.	6.4×10^{-4}	6.4×10^{-4}
				2017	2	4.5×10^{-3}	2.1	2.6×10^{-3}	7.6×10^{-3}
	Japanese parsley	*Oenanthe javanica*	Stem, root (0.09)	2011	7	6.1×10^{-3}	5.0	5.8×10^{-4}	1.0×10^{-1}
				2012	6	1.5×10^{-2}	7.0	1.3×10^{-3}	1.6×10^{-1}
				2014	2	1.5×10^{-3}	1.6	1.1×10^{-3}	2.1×10^{-3}
				2015	21	1.2×10^{-2}	1.4	6.1×10^{-3}	2.8×10^{-2}
				2017	1	5.3×10^{-3}	n.a.	5.3×10^{-3}	5.3×10^{-3}
	Miyamairakusa (ja)	*Laportea cuspidata*	Stem (0.08)	2012	3	2.9×10^{-3}	1.8	1.8×10^{-3}	5.5×10^{-3}
				2013	6	4.5×10^{-3}	2.2	1.7×10^{-3}	1.7×10^{-2}
				2014	3	6.7×10^{-3}	2.3	3.2×10^{-3}	1.7×10^{-2}
				2015	3	6.8×10^{-3}	1.1	6.2×10^{-3}	7.2×10^{-3}
				2016	7	5.9×10^{-3}	3.8	1.0×10^{-3}	4.6×10^{-2}
				2017	5	3.8×10^{-3}	2.0	1.5×10^{-3}	9.8×10^{-3}
				2018	1	6.5×10^{-3}	n.a.	6.5×10^{-3}	6.5×10^{-3}
	Momijigasa (ja)	*Parasenecio delphiniifolius*	Shoot (0.09)	2012	11	7.0×10^{-3}	3.4	1.0×10^{-3}	3.5×10^{-2}
				2013	9	4.3×10^{-3}	2.4	1.1×10^{-3}	1.7×10^{-2}
				2014	9	2.5×10^{-3}	2.2	8.3×10^{-4}	1.2×10^{-2}
				2015	5	2.0×10^{-3}	2.4	8.3×10^{-4}	7.8×10^{-3}
				2016	12	4.6×10^{-3}	3.0	7.8×10^{-4}	1.8×10^{-2}
				2017	9	2.8×10^{-3}	4.7	6.9×10^{-4}	4.3×10^{-2}
				2018	8	3.3×10^{-3}	2.2	1.1×10^{-3}	7.7×10^{-3}
	Oobagiboushi (ja)	*Hosta sieboldiana*	Shoot (0.07)	2012	1	3.4×10^{-3}	n.a.	3.4×10^{-3}	3.4×10^{-3}
				2013	4	1.2×10^{-3}	2.3	4.0×10^{-4}	2.9×10^{-3}
				2014	5	2.5×10^{-3}	3.9	3.6×10^{-4}	1.6×10^{-2}
				2015	5	4.9×10^{-3}	3.0	1.4×10^{-3}	2.1×10^{-2}
				2016	2	1.4×10^{-2}	1.7	9.5×10^{-3}	2.0×10^{-2}
				2017	2	1.4×10^{-3}	1.9	8.9×10^{-4}	2.2×10^{-3}
				2018	3	6.4×10^{-4}	4.0	2.4×10^{-4}	3.1×10^{-3}
	Udo (ja)	*Aralia cordata*	Shoot, stem (0.09)	2012	12	2.1×10^{-3}	4.8	2.1×10^{-4}	2.6×10^{-2}
				2013	22	2.6×10^{-3}	3.3	1.6×10^{-4}	1.5×10^{-2}
				2014	21	2.0×10^{-3}	4.3	1.3×10^{-4}	3.4×10^{-2}
				2015	13	1.1×10^{-3}	3.6	2.1×10^{-4}	1.0×10^{-2}
				2016	4	1.5×10^{-3}	1.7	9.2×10^{-4}	2.9×10^{-3}
				2017	4	1.7×10^{-3}	2.0	8.1×10^{-4}	3.7×10^{-3}
				2018	1	2.6×10^{-3}	n.a.	2.6×10^{-3}	2.6×10^{-3}

TABLE III.13. *NC* (m^2/kg DM) [a] VALUES OF ^{137}CS FOR EDIBLE WILD PLANTS FROM GOVERNMENTAL MONITORING DATA [b] (cont.)

Type	Name (ja: Japanese name)	Species	Edible part (dry/wet ratio)	Year	N	GM	GSD	Min	Max
	Uwabamisou (ja)	*Elatostema umbellatum*	Stem (0.10)	2012	30	6.9×10^{-3}	3.9	7.2×10^{-4}	8.0×10^{-2}
				2013	32	7.6×10^{-3}	3.4	1.1×10^{-3}	9.6×10^{-2}
				2014	22	3.4×10^{-3}	2.2	6.8×10^{-4}	1.4×10^{-2}
				2015	13	5.1×10^{-3}	2.8	5.3×10^{-4}	2.6×10^{-2}
				2016	25	1.0×10^{-2}	3.6	8.5×10^{-4}	1.2×10^{-1}
				2017	22	5.0×10^{-3}	2.8	7.9×10^{-4}	2.2×10^{-2}
				2018	17	3.5×10^{-3}	3.9	5.3×10^{-4}	4.8×10^{-2}
Bamboo	Bamboo shoot	*Phyllostachys bambusoides, P. heterocycle, P. nigra var. henonis* etc.	Shoot (0.11)	2011	69	2.4×10^{-2}	1.7	7.1×10^{-3}	9.3×10^{-2}
				2012	206	2.2×10^{-2}	3.0	1.8×10^{-3}	1.9×10^{-1}
				2013	426	9.4×10^{-3}	2.5	8.0×10^{-4}	6.5×10^{-2}
				2014	629	5.7×10^{-3}	2.3	4.6×10^{-4}	5.7×10^{-2}
				2015	330	4.7×10^{-3}	2.7	4.3×10^{-4}	6.8×10^{-2}
				2016	690	5.0×10^{-3}	3.1	4.4×10^{-4}	3.8×10^{-1}
				2017	497	4.3×10^{-3}	3.2	2.9×10^{-4}	3.1×10^{-1}
				2018	455	4.8×10^{-3}	3.3	2.6×10^{-4}	4.0×10^{-1}
	Nemagaritake (ja)	*Sasa kurilensis*	Shoot (0.07)	2011	7	6.4×10^{-3}	1.7	3.1×10^{-3}	1.2×10^{-2}
				2012	11	8.6×10^{-3}	4.6	9.4×10^{-4}	1.8×10^{-1}
				2013	8	6.3×10^{-3}	2.3	2.2×10^{-3}	3.0×10^{-2}
				2014	11	8.3×10^{-3}	3.0	2.1×10^{-3}	7.1×10^{-2}
				2015	7	4.4×10^{-3}	3.2	1.4×10^{-3}	4.1×10^{-2}
				2016	10	9.3×10^{-3}	2.8	2.9×10^{-3}	8.7×10^{-2}
				2017	6	6.8×10^{-3}	2.1	2.9×10^{-3}	1.9×10^{-2}
				2018	51	1.7×10^{-2}	3.2	1.5×10^{-3}	1.3×10^{-1}
Perennial fern	Ostrich fern	*Matteuccia struthiopteris*	Shoot (0.11)	2012	60	1.0×10^{-2}	3.5	8.8×10^{-4}	3.9×10^{-1}
				2013	61	9.9×10^{-3}	4.7	2.5×10^{-4}	3.6×10^{-1}
				2014	68	1.5×10^{-2}	3.9	4.5×10^{-4}	3.4×10^{-1}
				2015	42	9.5×10^{-3}	7.0	3.5×10^{-4}	2.1×10^{-1}
				2016	80	1.2×10^{-2}	3.4	1.5×10^{-4}	2.1×10^{-1}
				2017	92	9.5×10^{-3}	2.6	3.2×10^{-4}	9.9×10^{-2}
				2018	28	8.3×10^{-3}	3.3	4.4×10^{-4}	4.3×10^{-2}
	Western bracken fern	*Pteridium aquilinum*	Shoot (0.09)	2012	54	5.4×10^{-3}	5.1	1.4×10^{-4}	3.3×10^{-1}
				2013	57	4.5×10^{-3}	6.0	3.0×10^{-4}	5.1×10^{-1}
				2014	52	3.0×10^{-3}	4.6	1.8×10^{-4}	9.1×10^{-2}
				2015	52	1.5×10^{-2}	8.5	3.7×10^{-4}	1.2
				2016	46	4.1×10^{-3}	5.3	3.1×10^{-4}	6.4×10^{-1}
				2017	25	2.2×10^{-3}	2.9	3.3×10^{-4}	1.6×10^{-2}
				2018	73	2.0×10^{-2}	5.9	2.4×10^{-4}	8.3×10^{-1}

TABLE III.13. *NC* (m^2/kg DM) [a] VALUES OF ^{137}CS FOR EDIBLE WILD PLANTS FROM GOVERNMENTAL MONITORING DATA [b] (cont.)

Type	Name (ja: Japanese name)	Species	Edible part (dry/wet ratio)	Year	N	GM	GSD	Min	Max
	Zenmai (ja)	*Osmunda japonica*	Shoot (0.09)	2012	20	3.2×10^{-2}	4.3	3.2×10^{-3}	3.8×10^{-1}
				2013	23	8.9×10^{-3}	4.0	7.6×10^{-4}	1.5×10^{-1}
				2014	15	8.0×10^{-3}	5.9	4.5×10^{-4}	1.2×10^{-1}
				2015	27	4.2×10^{-2}	4.5	2.1×10^{-3}	8.6×10^{-1}
				2016	22	1.8×10^{-2}	4.6	5.1×10^{-4}	3.5×10^{-1}
				2017	18	8.5×10^{-3}	3.2	1.1×10^{-3}	3.8×10^{-2}
				2018	24	2.0×10^{-2}	3.4	1.1×10^{-3}	2.1×10^{-1}
Vine	Chocolate vine	*Akebia quinata* (*A. trifoliata*)	Fruit (0.16)	2011	13	3.0×10^{-3}	2.2	6.4×10^{-4}	1.1×10^{-2}
				2012	8	1.7×10^{-3}	2.9	4.0×10^{-4}	6.2×10^{-3}
				2013	5	1.8×10^{-3}	3.1	4.9×10^{-4}	1.0×10^{-2}
				2014	3	1.1×10^{-3}	2.9	3.2×10^{-4}	2.0×10^{-3}
				2015	5	3.0×10^{-4}	3.1	9.6×10^{-5}	1.4×10^{-3}

[a] *NC* was converted to dry weight basis (m^2 kg^{-1} DM) from fresh weight basis (m^2/kg FM) using wet/dry ratios [5.124, 5.125, 5.158–5.160, 5.150–5.157].

[b] Data indicating cultivated samples were excluded from analysis. However, data taken in 2011 did not have any information indicating cultivation.

[c] not applicable, T_{ag_T} results were shown as fresh weight basis due to missing dry/wet ratio for walnut

[d] not applicable

APPENDIX IV.

SUPPLEMENTARY DATA FOR CHAPTER 6

TABLE IV.1. FISH ^{137}CS *CR* (L/kg) FOR FUNCTIONAL FEEDING GROUPS AT EACH SAMPLING TIME FROM 2011 TO 2017

Fish feeding group	Water body	Year	N	Concentration ratio CR (L/kg FM)						
				Median	AM	ASD	GM	GSD	Min.	Max.
Herbivore fish	River	2011	26	1300	1300	760	1100	2.3	83	3600
	River	2012	11	1500	1900	1300	1500	2.1	460	4300
	River	2013	11	620	630	320	530	2.0	100	1200
	River	2014	11	440	630	860	340	3.2	50	3100
	River	2015	6	1400	1200	680	910	2.4	220	1800
	River	2016	17	1100	1300	960	850	3.3	30	3100
	River	2017	14	1600	1900	1500	1400	2.2	290	5900
Omnivore fish	Lake	2011	4	2200	2200	260	2200	1.1	1800	2400
	Lake	2012	57	2100	3000	2400	2200	2.4	84	10000
	Lake	2013	59	1800	2300	1800	1600	2.6	84	7400
	Lake	2014	61	1800	2000	1200	1700	2.0	320	5000
	Lake	2015	55	2000	1900	1000	1600	2.0	160	4400
	Lake	2016	61	1800	2000	1000	1700	1.8	370	4800
	Lake	2017	35	1900	2200	1100	1900	1.8	410	4400
	River	2011	11	1900	3400	3400	2400	2.4	510	12000
	River	2012	84	1400	2200	2800	1300	3.2	60	18000
	River	2013	96	860	1300	1200	840	2.7	56	5700
	River	2014	113	670	910	910	580	2.8	42	4800
	River	2015	125	1000	1300	1200	790	3.0	67	7000
	River	2016	123	580	890	950	560	2.8	39	6700
	River	2017	125	860	1000	780	770	2.2	100	4100
Piscivore fish	Lake	2011	4	6300	6000	1000	5900	1.2	4500	6900
	Lake	2012	61	9200	17000	18000	9700	3.1	940	65000
	Lake	2013	49	3800	6000	8700	3900	2.3	430	55000
	Lake	2014	34	3400	4600	3800	3300	2.3	460	19000
	Lake	2015	37	3600	4300	2600	3400	2.2	280	11000
	Lake	2016	32	4300	5100	3700	4100	1.9	1100	19000
	Lake	2017	31	2900	3900	3100	2900	2.5	110	15000
	River	2011	4	1200	3000	4400	1200	5.2	220	9500
	River	2012	23	2500	4300	5300	1900	5.0	17	22000
	River	2013	31	850	1900	4500	820	3.1	69	24000
	River	2014	33	330	560	490	390	2.4	110	1800
	River	2015	23	430	1100	1300	600	3.3	54	4600
	River	2016	26	1300	1900	2600	1100	3.1	56	13000
	River	2017	47	1400	2300	2300	1300	3.5	65	8600
Planktivore fish	Lake	2011	3	1500	2300	1300	2000	1.7	1400	3800
	Lake	2012	12	1300	1600	1100	1400	1.6	730	5000
	Lake	2013	18	980	1100	540	1000	1.6	320	2700
	Lake	2014	17	1000	1000	210	990	1.3	530	1300
	Lake	2015	14	910	890	160	880	1.2	600	1300
	Lake	2016	6	790	850	290	810	1.4	520	1300
	Lake	2017	4	1400	1600	1000	1400	1.9	630	3100

TABLE IV.2. FISH ^{137}CS ACTIVITY CONCENTRATIONS (Bq/kg) FOR FUNCTIONAL FEEDING GROUPS AT EACH SAMPLING TIME FROM 2011 TO 2017

Fish feeding group	Water body	Year	Activity concentration for fish (Bq/kg FM)							
			N	Median	AM	ASD	GM	GS	Min	Max
Herbivore fish	River	2011	26	32	75	93	32	4.6	0.5	340
	River	2012	11	170	360	430	220	2.8	51	1500
	River	2013	11	42	66	72	41	2.9	4.5	230
	River	2014	11	38	150	280	47	4.5	10	960
	River	2015	6	84	98	51	88	1.7	49	170
	River	2016	17	50	53	39	37	2.8	2.5	140
	River	2017	14	34	59	49	41	2.5	10	170
Omnivore fish	Lake	2011	4	99	160	130	130	2	91	360
	Lake	2012	57	110	180	180	110	3	3.2	750
	Lake	2013	59	48	74	95	45	2.7	1.8	480
	Lake	2014	61	33	48	52	32	2.4	4.4	260
	Lake	2015	55	28	37	36	26	2.4	4.5	190
	Lake	2016	61	25	27	18	22	2	3.9	98
	Lake	2017	35	27	27	17	22	2	4.4	82
	River	2011	11	200	340	420	200	2.9	35	1500
	River	2012	84	120	310	720	120	3.6	20	6200
	River	2013	96	55	260	470	82	4.4	8.6	2800
	River	2014	110	28	150	290	47	4.4	5.5	1600
	River	2015	130	25	110	220	34	4.1	5.2	1400
	River	2016	120	13	68	160	19	3.9	3.2	1200
	River	2017	130	13	48	93	17	3.6	0.8	480
Piscivore fish	Lake	2011	4	270	250	44	250	1.2	190	290
	Lake	2012	61	490	1100	1140	470	4.4	6.1	3600
	Lake	2013	49	81	220	360	110	2.8	24	1800
	Lake	2014	34	65	140	240	71	2.8	6.4	1000
	Lake	2015	37	61	110	130	69	2.6	5.9	510
	Lake	2016	32	49	91	110	58	2.4	11	560
	Lake	2017	31	39	58	74	36	2.9	0.9	410
	River	2011	4	260	250	200	180	2.9	50	440
	River	2012	23	210	580	1400	190	5.1	1.1	6700
	River	2013	31	61	160	260	64	4.2	7	1300
	River	2014	33	28	44	47	29	2.5	4.6	210
	River	2015	23	22	70	130	28	3.6	3.8	550
	River	2016	26	37	170	470	44	4.1	4.6	2400
	River	2017	47	25	99	190	28	5.2	1.1	1000
Planktivore fish	Lake	2011	3	290	250	82	240	1.4	160	310
	Lake	2012	12	140	120	78	98	2.1	36	280
	Lake	2013	18	72	66	32	57	1.8	17	130
	Lake	2014	17	66	61	21	55	1.7	16	85
	Lake	2015	14	44	42	24	35	2	9.5	95
	Lake	2016	6	15	22	16	18	2	8.8	48
	Lake	2017	4	23	22	7	21	1.4	14	30

TABLE IV.3. ACTIVITY CONCENTRATION RATIO OF ^{137}CS FOR FRESHWATER AQUATIC ORGANISMS SAMPLED IN 2011–2017

Aquatic organism	Water body	Year	Concentration ratio CR (L/kg FM)							
			N	Median	AM	SD	GM	GSD	Min.	Max.
Vegetative litter	Lake	2013	11	4200	3700	2800	2700	2.5	510	10000
	Lake	2014	12	2100	2600	1900	1900	2.3	520	6100
	Lake	2015	6	580	720	610	510	2.7	140	1700
	River	2013	16	3100	4700	3700	3800	2.0	1500	14000
	River	2014	24	2400	3200	2900	2400	2.2	460	14200
	River	2015	12	3700	4200	3000	3000	2.5	590	9600
	River	2016	27	1400	3100	5000	1400	3.8	97	24000
	River	2017	20	1600	2100	1700	1400	2.9	76	5500
Aquatic plants	Lake	2012	8	150	340	500	190	2.7	62	1500
	Lake	2013	10	160	310	400	170	3.0	48	1300
	Lake	2014	10	83	170	170	110	2.6	26	530
	Lake	2015	10	170	1600	2900	420	5.6	74	9300
	Lake	2016	5	170	150	66	130	1.7	68	230
	Lake	2017	4	160	160	22	160	1.1	140	190
	River	2012	1	390	390	—	390	—	390	390
	River	2013	5	130	370	360	230	3.0	92	780
	River	2014	5	470	480	300	390	2.1	160	800
	River	2015	1	310	310	—	310	—	310	310
	River	2016	4	5800	5300	4100	3300	3.9	480	9300
	River	2017	3	1000	990	580	850	2.0	390	1600
Periphytons	Lake	2012	9	900	2500	2900	1500	2.9	440	8600
	Lake	2013	7	6100	11000	12000	4500	6.7	110	33000
	Lake	2014	4	7200	6600	3600	5600	2.0	2200	9800
	Lake	2015	4	16000	17000	14000	13000	2.7	4700	32000
	River	2012	11	1100	2000	3100	570	7.2	13	10000
	River	2013	29	7300	7600	5500	4000	5.5	16	21000
	River	2014	24	2800	4000	3300	2800	2.4	460	13000
	River	2015	24	4100	6500	5600	4500	2.5	1000	21000
	River	2016	21	7200	9400	7000	6400	2.9	270	27000
	River	2017	23	7000	8200	5400	6500	2.1	950	22000
Planktons	Lake	2013	12	290	720	1200	270	4.6	19	4200
	Lake	2014	11	470	3100	6200	720	5.7	88	21000
	Lake	2015	9	1100	2500	3500	840	5.6	86	11000
	Lake	2016	8	160	260	310	180	2.2	68	1000
	Lake	2017	5	110	260	320	160	3.0	56	820

TABLE IV.3. ACTIVITY CONCENTRATION RATIO OF ^{137}CS FOR FRESHWATER AQUATIC ORGANISMS SAMPLED IN 2011–2017 (cont.)

Aquatic organisms	Water body	Year	Concentration ratio CR (L/kg FM)							
			N	Median	AM	ASD	GM	GSD	Min.	Max.
Snails	Lake	2013	5	590	1700	1900	900	3.6	220	4800
Snails	Lake	2014	7	600	1100	950	690	2.9	120	2600
Snails	Lake	2015	3	470	620	270	580	1.5	450	930
Snails	River	2012	9	910	1500	1600	850	3.3	190	4300
Snails	River	2013	9	360	620	670	390	2.8	79	2200
Snails	River	2014	16	540	660	540	440	2.9	26	1800
Snails	River	2015	5	310	950	970	580	3.1	230	2300
Snails	River	2016	7	920	4200	8000	1500	3.9	450	22000
Snails	River	2017	6	830	4500	6700	1700	4.4	480	17000
Crustaceans	Lake	2013	11	1500	1400	1100	870	3.3	110	3200
Crustaceans	Lake	2014	10	1200	1200	740	960	2.4	130	2200
Crustaceans	Lake	2015	9	1600	1400	600	1300	1.7	510	2000
Crustaceans	Lake	2016	4	1600	1800	910	1700	1.6	1100	3100
Crustaceans	Lake	2017	5	1800	2100	870	1900	1.5	1300	3600
Crustaceans	River	2011	1	1400	1400	NA	1400	NA	1400	1400
Crustaceans	River	2012	18	1200	1200	670	1000	2.0	270	2600
Crustaceans	River	2013	42	1400	1600	960	1300	2.0	190	4100
Crustaceans	River	2014	46	850	1100	710	860	1.9	300	3200
Crustaceans	River	2015	44	1500	1600	1300	1200	2.3	200	7400
Crustaceans	River	2016	42	910	1200	1000	750	3.0	66	5000
Crustaceans	River	2017	42	1100	1300	850	1100	1.9	250	4800
Aquatic insects	Lake	2012	3	2800	2800	2400	1900	3.6	450	5300
Aquatic insects	Lake	2013	10	840	2200	4000	1100	2.9	420	13000
Aquatic insects	Lake	2014	16	480	790	920	490	2.7	83	3500
Aquatic insects	Lake	2015	16	780	1600	2700	750	3.2	160	11000
Aquatic insects	River	2012	34	1200	2500	3000	1500	2.8	190	15000
Aquatic insects	River	2013	64	840	1900	2400	1100	2.8	200	14000
Aquatic insects	River	2014	78	770	1300	1400	780	2.9	110	6500
Aquatic insects	River	2015	67	1000	1600	2000	920	2.9	87	12000
Aquatic insects	River	2016	49	920	1500	1700	850	3	110	8200
Aquatic insects	River	2017	43	1500	2100	1900	1400	2.6	140	7700

TABLE IV.3. ACTIVITY CONCENTRATION RATIO OF ^{137}CS FOR FRESHWATER AQUATIC ORGANISMS SAMPLED IN 2011–2017 (cont.)

Aquatic organisms	Water body	Year	Concentration ratio CR (L/kg FM)							
			N	Median	AM	ASD	GM	GSD	Min.	Max.
Amphibian adults	Lake	2012	2	1600	1600	260	1600	1.2	1400	1800
Amphibian adults	Lake	2013	10	740	810	690	490	3.4	65	2200
Amphibian adults	Lake	2014	12	170	480	550	260	3.3	41	1600
Amphibian adults	Lake	2015	13	480	1200	2100	500	3.9	58	7800
Amphibian adults	River	2012	9	630	2500	2700	1300	3.4	430	6900
Amphibian adults	River	2013	14	380	630	690	430	2.3	110	2700
Amphibian adults	River	2014	19	560	620	650	440	2.3	130	3000
Amphibian adults	River	2015	9	580	4600	12000	740	5.1	140	37000
Amphibian adults	River	2016	12	560	2100	4300	570	5.5	54	15000
Amphibian adults	River	2017	18	580	890	890	660	2.1	140	4100
Amphibian larvae	Lake	2012	3	2700	7300	9600	3500	4.6	900	18000
Amphibian larvae	Lake	2013	3	3100	4700	4800	3000	3.4	870	10000
Amphibian larvae	Lake	2014	6	1900	2700	3600	1200	4.9	140	9900
Amphibian larvae	Lake	2015	3	1500	3400	3600	2400	2.8	1200	7500
Amphibian larvae	River	2012	8	6100	5600	2800	4400	2.6	480	10000
Amphibian larvae	River	2013	14	6000	7500	5200	6000	2.1	1400	21000
Amphibian larvae	River	2014	10	3500	4500	3400	3600	1.9	1600	13000
Amphibian larvae	River	2015	8	4700	4700	3200	3500	2.5	590	9500
Amphibian larvae	River	2016	9	5400	5400	4100	3700	3	500	14000
Amphibian larvae	River	2017	8	4600	5600	3800	4100	2.7	530	10000

TABLE IV.4. ACTIVITY CONCENTRATION OF ^{137}CS FOR FRESHWATER AQUATIC ORGANISMS FROM 2011 TO 2017

Aquatic organisms	Water body	Year	^{137}Cs activity concentration (Bq/kg FM)							
			N	Median	AM	SD	GM	GSD	Min.	Max.
Vegetative litter	Lake	2013	11	110	160	150	95	3.3	13	400
Vegetative litter	Lake	2014	12	60	140	190	64	3.5	15	600
Vegetative litter	Lake	2015	6	19	21	19	11	4.3	2	48
Vegetative litter	River	2013	16	210	430	690	220	3.2	23	2900
Vegetative litter	River	2014	24	180	280	270	180	2.7	24	890
Vegetative litter	River	2015	12	73	160	180	77	3.7	18	500
Vegetative litter	River	2016	27	33	150	350	43	4.4	1	1700
Vegetative litter	River	2017	20	38	54	54	28	4.3	1	190
Aquatic plants	Lake	2012	8	7	8.4	8.1	6.1	2.3	2	27
Aquatic plants	Lake	2013	10	6	9.3	11	5.5	3.0	1	38
Aquatic plants	Lake	2014	10	2	3.4	3	2.2	2.8	0	9
Aquatic plants	Lake	2015	10	2	26	50	5.5	6.4	1	160
Aquatic plants	Lake	2016	5	2	1.4	0.6	1.3	1.7	1	2
Aquatic plants	Lake	2017	4	1	1.3	0.2	1.3	1.2	1	2
Aquatic plants	River	2012	1	62	62	NA	62	NA	62	62
Aquatic plants	River	2013	5	49	73	79	47	2.9	10	210
Aquatic plants	River	2014	5	19	61	100	26	3.6	10	240
Aquatic plants	River	2015	1	7	6.7	NA	6.7	NA	7	7
Aquatic plants	River	2016	4	350	400	390	220	4.1	39	870
Aquatic plants	River	2017	3	15	30	32	21	2.9	9	67
Periphytons	Lake	2012	9	80	220	350	97	3.6	26	1100
Periphytons	Lake	2013	7	430	790	820	260	10.1	3	2300
Periphytons	Lake	2014	4	450	570	370	500	1.8	280	1100
Periphytons	Lake	2015	4	850	940	660	760	2.2	370	1700
Periphytons	River	2012	11	110	150	160	54	7.4	1	440
Periphytons	River	2013	29	310	1200	1800	390	5.4	6	6000
Periphytons	River	2014	24	180	340	380	220	2.4	59	1400
Periphytons	River	2015	24	190	410	850	180	3.1	22	4200
Periphytons	River	2016	21	160	460	680	230	2.9	60	2500
Periphytons	River	2017	23	110	240	310	140	2.9	32	1100
Planktons	Lake	2013	12	17	25	33	11	4.7	1.0	120
Planktons	Lake	2014	11	21	66	110	24	4.4	4.0	380
Planktons	Lake	2015	9	14	42	56	20	4.0	2.0	170
Planktons	Lake	2016	8	4	7.8	11	4.1	3.2	1.0	35
Planktons	Lake	2017	5	4	8.1	11	4.7	2.9	2.0	27

TABLE IV.4. ACTIVITY CONCENTRATION OF ^{137}CS FOR FRESHWATER AQUATIC ORGANISMS FROM 2011 TO 2017 (cont.)

Aquatic organisms	Water body	Year	^{137}Cs activity concentration (Bq/kg FM)							
			N	Median	AM	SD	GM	GSD	Min.	Max.
Snails	Lake	2013	5	41	43	42	27	3.3	6.0	110
Snails	Lake	2014	7	22	30	28	19	3.0	3.0	82
Snails	Lake	2015	3	7	10	5.1	9.4	1.6	7.0	16
Snails	River	2012	9	100	120	110	75	2.9	15	290
Snails	River	2013	9	19	33	26	26	2.1	11	81
Snails	River	2014	16	72	90	87	55	3.1	10	310
Snails	River	2015	5	20	34	29	24	2.6	7.0	77
Snails	River	2016	7	23	120	130	49	4.6	11	310
Snails	River	2017	6	49	88	95	44	4.1	9.0	230
Crustaceans	Lake	2013	11	38	55	66	28	3.7	4.0	210
Crustaceans	Lake	2014	10	35	49	41	32	2.9	4.0	120
Crustaceans	Lake	2015	9	31	37	27	29	2.2	9.0	96
Crustaceans	Lake	2016	4	25	25	8.5	24	1.4	16	33
Crustaceans	Lake	2017	5	19	21	5.2	21	1.3	17	30
Crustaceans	River	2011	1	100	100	n.a.	100	n.a.	100	100
Crustaceans	River	2012	18	91	160	200	99	2.7	18	830
Crustaceans	River	2013	42	120	260	310	120	3.7	18	1100
Crustaceans	River	2014	46	110	210	260	87	3.9	11	860
Crustaceans	River	2015	44	61	130	160	61	3.4	8.0	610
Crustaceans	River	2016	42	28	90	140	38	3.5	5.0	650
Crustaceans	River	2017	42	27	65	110	29	3.3	5	480
Aquatic insects	Lake	2012	3	370	370	320	250	3.6	59	690
Aquatic insects	Lake	2013	10	63	160	290	77	3.2	11	970
Aquatic insects	Lake	2014	16	40	64	110	28	3.8	2.0	450
Aquatic insects	Lake	2015	16	24	52	64	28	3.3	2.0	180
Aquatic insects	River	2012	34	92	220	280	100	3.8	9.0	1100
Aquatic insects	River	2013	64	81	180	240	77	3.8	5.0	1000
Aquatic insects	River	2014	78	56	150	230	61	4.1	5.0	1100
Aquatic insects	River	2015	67	32	78	100	36	3.7	2.0	400
Aquatic insects	River	2016	49	27	70	120	32	3.5	2.0	790
Aquatic insects	River	2017	43	28	83	130	33	4.1	2.0	640

TABLE IV.4. ACTIVITY CONCENTRATION OF ^{137}CS FOR FRESHWATER AQUATIC ORGANISMS FROM 2011 TO 2017 (cont.)

Aquatic organisms	Water body	Year	^{137}Cs activity concentration (Bq/kg FM)							
			N	Median	AM	SD	GM	GSD	Min.	Max.
Amphibian adults	Lake	2012	2	49	49	7.8	48	1.2	43	54
Amphibian adults	Lake	2013	10	16	18	14	12	2.9	2.0	41
Amphibian adults	Lake	2014	12	6	10	9.4	5.6	3.1	1.0	27
Amphibian adults	Lake	2015	13	8	61	180	7.6	5.9	1.0	670
Amphibian adults	River	2012	9	63	120	86	89	2.2	33	250
Amphibian adults	River	2013	14	22	25	14	22	1.8	8.0	47
Amphibian adults	River	2014	19	17	38	48	23	2.5	8.0	190
Amphibian adults	River	2015	9	17	70	110	28	3.9	9.0	290
Amphibian adults	River	2016	12	16	52	100	19	3.9	4.0	370
Amphibian adults	River	2017	18	13	24	24	15	2.8	3.0	95
Amphibian larvae	Lake	2012	3	81	140	160	88	3.5	26	320
Amphibian larvae	Lake	2013	3	81	110	110	72	3.4	20	230
Amphibian larvae	Lake	2014	6	31	46	62	21	4.5	2.0	170
Amphibian larvae	Lake	2015	3	26	54	58	36	2.9	15	120
Amphibian larvae	River	2012	8	450	450	290	370	2.1	92	990
Amphibian larvae	River	2013	14	300	550	700	370	2.2	190	2800
Amphibian larvae	River	2014	10	200	430	470	270	2.7	75	1400
Amphibian larvae	River	2015	8	140	240	270	150	3.1	19	850
Amphibian larvae	River	2016	9	150	400	540	190	3.6	40	1700
Amphibian larvae	River	2017	8	96	120	73	100	1.7	51	280

APPENDIX V.

SUPPLEMENTARY DATA FOR CHAPTER 7

TABLE V.1. EFFECTIVE HALF-LIFE (SEE EQ. 7.3) AND CR_a VALUES IN DIFFERENT PREFECTURES FOR FIVE YEARS AFTER THE FDNPP ACCIDENT

Common name	Half-life (day)	Area	Sample size N and CR_a (L/kg) values and statistics[a] in year:																							
			2011					2012					2013					2014					2015				
			N	AM	SD	GM	GSD	N	AM	SD	GM	GSD	N	AM	SD	GM	GSD	N	AM	SD	GM	GSD	N	AM	SD	GM	GSD
Greenling	651	Aomori	2	423	109	—[b]	—	3	—	—	247	1.5	1	271	n.a.[c]	—	—	1	106	n.a.	—	—	1	105	n.a.	—	—
	—	Iwate	—	—	—	—	—	1	706	n.a.	—	—	—	—	—	—	—	—	—	—	—	—	—	—	—	—	—
	—	Miyagi	2	227	25	—	—	56	—	—	526	2.6	9	—	—	861	3.2	2	355	30	—	—	2	125	18	—	—
	—	Fukushima	69	—	—	1212	5.3	231	—	—	2558	3.5	66	—	—	2547	2.9	—	—	—	—	—	—	—	—	—	—
	1117	Ibaraki	1	4400	n.a.	—	—	13	—	—	978	1.9	14	—	—	999	1.8	12	—	—	694	1.3	6	—	—	596	1.3
Stone flounder	—	Miyagi	—	—	—	—	—	23	—	—	1667	2.1	22	—	—	2627	2.0	2	3033	424	—	—	—	—	—	—	—
	—	Fukushima	30	—	—	1627	9.5	103	—	—	2164	4.0	30	—	—	1740	3.6	—	—	—	—	—	—	—	—	—	—
	862	Ibaraki	4	—	—	562	1.3	33	—	—	781	1.9	34	—	—	739	1.9	18	—	—	458	1.8	8	—	—	869	3.7
	490	Chiba	—	—	—	—	—	7	—	—	362	1.6	7	—	—	237	1.4	3	—	—	259	1.3	—	—	—	—	—
White croaker	—	Miyagi	—	—	—	—	—	2	928	201	—	—	1	1208	n.a.	—	—	—	—	—	—	—	—	—	—	—	—
	—	Fukushima	7	—	—	749	4.4	45	—	—	1154	2.7	5	—	—	2680	1.8	—	—	—	—	—	—	—	—	—	—
	—	Ibaraki	—	—	—	—	—	—	—	—	—	—	—	—	—	—	—	—	—	—	—	—	—	—	—	—	—
	—	Chiba	1	812	n.a.	—	—	—	—	—	—	—	1	217	n.a.	—	—	—	—	—	—	—	—	—	—	—	—
Bartail flathead	—	Miyagi	—	—	—	—	—	2	2512	979	—	—	2	1481	47	—	—	—	—	—	—	—	—	—	—	—	—
	—	Fukushima	4	—	—	93	5.0	32	—	—	1014	3.7	28	—	—	1156	2.3	—	—	—	—	—	—	—	—	—	—
	1066	Ibaraki	—	—	—	—	—	2	1660	350	—	—	1	2066	n.a.	—	—	2	1001	109	—	—	1	932	n.a.	—	—
Black rockfish	624	Aomori	1	77	n.a.	—	—	3	—	—	308	2.8	3	—	—	145.9	1.9	1	195	—	—	—	2	120	42	—	—
	—	Iwate	—	—	—	—	—	4	—	—	1606	3.6	—	—	—	—	—	—	—	—	—	—	—	—	—	—	—
	—	Fukushima	5	—	—	142	4.5	27	—	—	1249	4.2	14	—	—	2347	4.4	—	—	—	—	—	—	—	—	—	—
Blue drum	195	Miyagi	—	—	—	—	—	3	—	—	4481	1.6	8	—	—	1068	2.1	—	—	—	—	—	—	—	—	—	—
	—	Fukushima	8	—	—	167	4.3	65	—	—	958	2.7	2	1035	954	—	—	—	—	—	—	—	—	—	—	—	—
	309	Ibaraki	1	1638	n.a.	—	—	5	—	—	—	1.6	1	746	n.a.	—	—	3	—	—	442	2.1	1	277	n.a.	—	—

TABLE V.1. EFFECTIVE HALF-LIFE (SEE EQ. 7.3) AND CR_a VALUES IN DIFFERENT PREFECTURES FOR FIVE YEARS AFTER THE FDNPP ACCIDENT (cont.)

Common name	Half-life (day)	Area	Sample size N and CR_a (L/kg) values and statistics[a] in year:																							
			2011					2012					2013					2014					2015				
			N	AM	SD	GM	GSD	N	AM	SD	GM	GSD	N	AM	SD	GM	GSD	N	AM	SD	GM	GSD	N	AM	SD	GM	GSD
Brown hakeling	—	Iwate	—	—	—	—	—	1	387	n.a.	—	—	—	—	—	—	—	—	—	—	—	—	—	—	—	—	—
	—	Miyagi	3	—	—	224	1.5	14	—	—	282	1.7	1	249	n.a.	—	—	1	381	n.a.	—	—	—	—	—	—	—
	—	Fukushima	31	—	—	1072	4.3	92	—	—	1872	3.1	19	—	—	2252	2.5	—	—	—	—	—	—	—	—	—	—
	—	Ibaraki	—	—	—	—	—	3	—	—	560	2.7	—	—	—	—	—	—	—	—	—	—	—	—	—	—	—
Conger eel	—	Iwate	—	—	—	—	—	3	—	—	240	1.2	—	—	—	—	—	—	—	—	—	—	—	—	—	—	—
	624	Miyagi	2	265	255	—	—	22	—	—	444	2.3	11	—	—	382	1.4	4	—	—	208	1.7	3	—	—	161	1.9
	—	Fukushima	29	—	—	348	4.6	76	—	—	1698	3.0	9	—	—	2426	1.3	—	—	—	—	—	—	—	—	—	—
	—	Ibaraki	7	—	—	485	1.6	13	—	—	573	1.9	2	961	214	—	—	2	142	36	—	—	10	—	—	403	1.5
	—	Chiba	—	—	—	—	—	4	—	—	190	1.8	1	195	n.a.	—	—	3	—	—	195	1.3	—	—	—	—	—
Japanese flounder	471	Aomori	10	—	—	372	1.4	18	—	—	1193	3.2	13	—	—	2076	2.3	13	—	—	572	2.0	2	146	47	—	—
	314	Iwate	2	340	136	—	—	1	2667	n.a.	—	—	1	2636	n.a.	—	—	2	620	140	—	—	1	273	n.a.	—	—
	521	Miyagi	5	—	—	567	2.4	131	—	—	1670	2.8	197	—	—	1842	2.4	48	—	—	649	2.5	23	—	—	494	2.1
	—	Fukushima	111	—	—	415	8.6	303	—	—	1814	3.6	83	—	—	1810	3.3	1	557	n.a.	—	—	2	1033	421	—	—
	987	Ibaraki	15	—	—	584	2.3	143	—	—	841	2.0	109	—	—	686	2.1	76	—	—	372	1.9	64	—	—	481	1.7
	537	Chiba	—	—	—	—	—	43	—	—	799	2.2	11	—	—	465	1.7	11	—	—	363	2.2	3	—	—	200	1.6
Marbled sole	—	Iwate	—	—	—	—	—	7	—	—	385	1.1	—	—	—	—	—	—	—	—	—	—	—	—	—	—	—
	—	Miyagi	1	84	n.a.	—	—	51	—	—	617	2.5	18	—	—	1253	2.2	2	832	629	—	—	3	—	—	496	1.8
	—	Fukushima	58	—	—	1273	6.3	170	—	—	2292	4.0	52	—	—	2276	2.9	—	—	—	—	—	—	—	—	—	—
	—	Ibaraki	15	—	—	318	2.9	55	—	—	674	2.3	18	—	—	853	1.8	26	—	—	719	1.9	10	—	—	866	1.7
	479	Chiba	1	347	n.a.	—	—	8	—	—	463	1.5	5	—	—	281	1.2	—	—	—	—	—	—	—	—	—	—
Pacific cod	314	Aomori	7	—	—	5166	2.2	76	—	—	2504	3.0	99	—	—	2330	2.3	83	—	—	864	2.0	36	—	—	345	1.4
	264	Iwate	8	—	—	2506	2.7	177	—	—	4326	2.0	294	—	—	2190	2.6	59	—	—	1310	2.4	18	—	—	669	1.6
	380	Miyagi	5	—	—	409	4.7	105	—	—	1993	2.7	59	—	—	2994	2.3	29	—	—	947	2.9	13	—	—	450	2.0
	—	Fukushima	21	—	—	736	7.2	113	—	—	2968	3.1	66	—	—	2287	2.6	3	—	—	419	1.6	2	278	264	—	—
	409	Ibaraki	—	—	—	—	—	50	—	—	2396	2.3	151	—	—	2503	2.1	162	—	—	1088	2.2	12	—	—	700	2.1

TABLE V.1. EFFECTIVE HALF-LIFE (SEE EQ. 7.3) AND CR_a VALUES IN DIFFERENT PREFECTURES FOR FIVE YEARS AFTER THE FDNPP ACCIDENT (cont.)

Common name	Half-life (day)	Area	Sample size N and CR_a (L/kg) values and statistics [a] in year:																							
			2011					2012					2013					2014					2015				
			N	AM	SD	GM	GSD	N	AM	SD	GM	GSD	N	AM	SD	GM	GSD	N	AM	SD	GM	GSD	N	AM	SD	GM	GSD
Round-nose Flounder *Eopsetta grigorjewi*	—	Aomori	—	—	—	—	—	1	322	n.a.	—	—	—	—	—	—	—	—	—	—	—	—	—	—	—	—	—
	—	Iwate	—	—	—	—	—	1	417	n.a.	—	—	—	—	—	—	—	—	—	—	—	—	—	—	—	—	—
	—	Miyagi	—	—	—	—	—	2	620	489	—	—	—	—	—	—	—	—	—	—	—	—	—	—	—	—	—
	—	Fukushima	15	—	—	664	2.6	55	—	—	2609	3.4	16	—	—	2563	2.3	—	—	—	—	—	—	—	—	—	—
	—	Ibaraki	7	—	—	566	1.2	23	—	—	582	2.0	5	—	—	677	2.0	3	—	—	375	1.6	1	164	n.a.	—	—
	438	Chiba	—	—	—	—	—	3	—	—	840	2.2	3	—	—	279	1.2	4	—	—	304	1.4	—	—	—	—	—
Brown sole *Pleuronectes herzensteini*	—	Miyagi	3	—	—	242	1.5	34	—	—	869	2.2	12	—	—	1150	1.4	3	—	—	596	1.5	3	—	—	376	1.7
	1240	Fukushima	46	—	—	878	3.9	137	—	—	2045	2.9	45	—	—	1632	2.4	2	813	460	—	—	3	—	—	770	1.8
	688	Ibaraki	8	—	—	456	1.3	11	—	—	723	1.6	—	—	—	—	—	1	350	n.a.	—	—	1	208	n.a.	—	—
Crimson seabream *Evynnis tumifrons*	—	Miyagi	—	—	—	—	—	6	—	—	1431	1.2	—	—	—	—	—	—	—	—	—	—	1	342	n.a.	—	—
	—	Fukushima	16	—	—	257	5.1	18	—	—	590	3.9	1	1501	n.a.	—	—	—	—	—	—	—	—	—	—	—	—
	735	Chiba	—	—	—	—	—	5	—	—	763	2.2	5	—	—	352	1.6	1	439	n.a.	—	—	3	—	—	306	1.7
Deep-sea smelt *Glossanodon semifasciatus*	—	Ibaraki	—	—	—	—	—	5	—	—	159	1.8	—	—	—	—	—	—	—	—	—	—	—	—	—	—	—
Flathead flounder *Hippoglossoides dubius*	—	Iwate	—	—	—	—	—	1	706	—	—	—	—	—	—	—	—	—	—	—	—	—	—	—	—	—	—
	—	Miyagi	3	—	—	93	1.5	24	—	—	294	1.6	1	611	n.a.	—	—	—	—	—	—	—	3	—	—	362	1.8
	—	Fukushima	2	1334	1663	—	—	18	—	—	1358	2.4	10	—	—	3956	2.1	—	—	—	—	—	—	—	—	—	—
	—	Ibaraki	3	—	—	422	1.1	17	—	—	698	1.8	1	1722	n.a.	—	—	—	—	—	—	—	—	—	—	—	—
Japanese sea bass *Lateolabrax japonicus*	—	Iwate	—	—	—	—	—	2	2231	2691	—	—	—	—	—	—	—	—	—	—	—	—	—	—	—	—	—
	665	Miyagi	1	1671	n.a.	—	—	115	—	—	4906	1.9	145	—	—	3874	1.8	53	—	—	1501	1.7	64	—	—	1822	1.7
	—	Fukushima	19	—	—	839	9.9	86	—	—	2400	3.6	23	—	—	3708	2.7	—	—	—	—	—	—	—	—	—	—
	825	Ibaraki	1	3277	n.a.	—	—	37	—	—	1744	2.0	124	—	—	3055	1.9	246	—	—	1577	1.7	143	—	—	1211	1.8
	679	Chiba	2	—	—	373	1.04	57	—	—	1197	2.6	81	—	—	1000	2.6	43	—	—	760	3.0	22	—	—	346	2.1

TABLE V.1. EFFECTIVE HALF-LIFE (SEE EQ. 7.3) AND CR_a VALUES IN DIFFERENT PREFECTURES FOR FIVE YEARS AFTER THE FDNPP ACCIDENT (cont.)

Common name	Half-life (day)	Area	Sample size N and CR_a (L/kg) values and statistics[a] in year:																							
			2011					2012					2013					2014					2015				
			N	AM	SD	GM	GSD	N	AM	SD	GM	GSD	N	AM	SD	GM	GSD	N	AM	SD	GM	GSD	N	AM	SD	GM	GSD
Pollack Gadus chalcogrammus Pallas	867	Aomori	7	—	—	1044	2.2	7	—	—	838	1.9	5	—	—	410	1.3	6	—	—	650	1.5	1	297	n.a.	—	—
	—	Iwate	—	—	—	—	—	20	—	—	458	1.9	1	1015	n.a.	—	—	—	—	—	—	—	—	—	—	—	—
	—	Miyagi	3	—	—	238	1.6	31	—	—	476	2.6	2	328	41	—	—	5	—	—	289	1.6	1	269	n.a.	—	—
	—	Fukushima	2	784	45	—	—	11	—	—	1514	2.6	4	—	—	4318	1.4	—	—	—	—	—	—	—	—	—	—
	—	Ibaraki	1	562	n.a.	—	—	4	—	—	485	1.6	—	—	—	—	—	—	—	—	—	—	—	—	—	—	—
Red seabream	—	Miyagi	—	—	—	—	—	1	2711	n.a.	—	—	—	—	—	—	—	—	—	—	—	—	5	—	—	330	1.2
Pagrus major	756	Ibaraki	4	—	—	588	1.2	13	—	—	902	1.9	4	—	—	376	1.4	2	253	100	—	—	4	—	—	392	1.9
Rockfish Sebastes inermis Cuvier	—	Fukushima	21	—	—	477	3.2	101	—	—	2709	3.0	29	—	—	3103	2.5	—	—	—	—	—	—	—	—	—	—
Searobin Lepidotrigla microptena	—	Miyagi	—	—	—	—	—	3	—	—	2032	1.9	—	—	—	—	—	1	558	n.a.	—	—	—	—	—	—	—
	—	Fukushima	32	—	—	1033	3.5	78	—	—	1395	2.5	9	—	—	1594	2.0	—	—	—	—	—	—	—	—	—	—
	539	Ibaraki	5	—	—	475	1.2	21	—	—	955	1.8	6	—	—	473	1.8	4	—	—	256	1.4	1	461	n.a.	—	—
	—	Iwate	—	—	—	—	—	1	385	n.a.	—	—	—	—	—	—	—	—	—	—	—	—	—	—	—	—	—
Souhachi-flounder	—	Miyagi	6	—	—	743	1.7	—	—	—	—	—	—	—	—	—	—	1	192	n.a.	—	—	—	—	—	—	—
Cleisthenes pinetorum	—	Ibaraki	—	—	—	—	—	—	—	—	—	—	—	—	—	—	—	—	—	—	—	—	4	—	—	238	1.4
Tonguefish Paraplagusia japonica	—	Fukushima	1	1136	—	—	—	16	—	—	725	2.3	—	—	—	—	—	—	—	—	—	—	—	—	—	—	—
	—	Ibaraki	1	467	—	—	—	1	324	n.a.	—	—	—	—	—	—	—	—	—	—	—	—	—	—	—	—	—
	—	Chiba	1	170	—	—	—	3	—	—	588	1.9	—	—	—	—	—	1	183	—	—	—	—	—	—	—	—
Whip stingray Dasyatis akajei	—	Ibaraki	—	—	—	—	—	3	—	—	821	1.8	2	6156	4924	—	—	3	—	—	1310	1.6	4	—	—	3181	1.7
	—	Chiba	—	—	—	—	—	—	—	—	—	—	—	—	—	—	—	2	922	438	—	—	—	—	—	—	—

[a] mean (AM), standard deviation (SD), geometric mean (GM), geometric standard deviation (GSD)
[b] no data
[c] not applicable

TABLE V.2. MEAN EFFECTIVE HALF-LIVES (T_{eff}) OF ^{137}CS (1984–2010) IN MARINE AREAS OF JAPAN BEFORE THE FDNPP ACCIDENT [7.42]

Prefecture	Effective half-life T_{eff} (a)			
	Bottom seawater		Sediment	
	Mean	Range	Mean	Range
Aomori	19.0	13.2–25.0	14.3	10.3–21.5
Miyagi	14.6	12.8–16.2	18.1	16.3–22.9
Fukushima	15.6	14.3–17.4	18.1	12.3–23.5
Ibaraki	15.8	14.5–16.7	23.4	17.0–28.8
Shizuoka	15.8	13.7–17.0	28.0	15.2–41.4
Ehime	16.2	15.9–16.5	21.0	19.0–24.8
Kagoshima	16.9	15.4–18.6	34.6	24.1–55.1
Hokkaido	22.2	21.0–22.7	23.1	20.7–26.7
Niigata	20.8	16.7–23.6	34.4	29.0–49.2
Ishikawa	16.1	14.3–17.3	19.7	16.1–25.9
Fukui	18.5	16.1–23.5	23.7	18.3–32.9
Shimane	17.5	16.2–18.6	27.2	19.2–42.2
Saga	16.2	15.5–16.8	27.3	27.3–27.3
Miyagi, Fukushima, Ibaraki	15.4	12.8–17.4	19.4	12.3–28.8
All areas	17.3	12.8–25.0	23.6	10.3–55.1

TABLE V.3. SUMMARY OF PARTICLE SIZE ANALYSIS (STUDIED IN 2016–2018 [7.42])

Prefecture	Silt and clay content (%)		Specific surface area (m^2/g DM)	
	Mean	Range	Mean	Range
Aomori	55	7–82	0.32	0.12–0.53
Miyagi	28	16–49	0.17	0.10–0.32
Fukushima	35	13–64	0.19	0.12–0.34
Ibaraki	39	17–80	0.18	0.13–0.27
Shizuoka	48	2–87	0.26	0.07–0.50
Ehime	13	3–22	0.14	0.08–0.20
Kagoshima	17	2–34	0.18	0.11–0.26
Hokkaido	69	12–97	0.32	0.10–0.56
Niigata	81	21–100	0.43	0.22–0.70
Ishikawa	51	20–71	0.24	0.16–0.31
Fukui	78	16–100	0.34	0.14–0.50
Shimane	21	5–41	0.16	0.09–0.23
Saga	11	1–22	0.14	0.03–0.24
Miyagi, Fukushima, Ibaraki	34	13–80	0.18	0.10–0.34

TABLE V.4. SUMMARY OF $K_{d(a)}$ (L/kg) VALUES IN COASTAL AREAS AROUND JAPAN BEFORE THE FDNPP ACCIDENT (1984–2010) [7.42]

Area	Prefecture	N	$K_{d(a)}$ (L/kg)			
			Maximum	Minimum	GM (GSD)	Median
Japan Sea	Hokkaido	89	4330	425	1810 (1.8)	2167
	Niigata	105	7360	620	3110 (1.9)	4000
	Ishikawa	77	1670	500	921 (1.3)	947
	Fukui	200	6000	367	1510 (1.9)	1556
	Shimane	78	905	183	488 (1.4)	497
	Saga	27	667	175	341 (1.4)	379
Pacific Ocean	Aomori	31	7540	488	3540 (2.3)	4667
	Miyagi	96	900	300	536 (1.3)	525
	Fukushima	186	1110	219	597 (1.2)	596
	Ibaraki	92	1210	270	573 (1.3)	581
	Shizuoka	98	3620	175	937 (2.0)	842
	Ehime	80	919	281	544 (1.3)	544
	Kagoshima	42	737	214	414 (1.4)	422
Total		1201	7540	175	923 (2.2)	719

ABBREVIATIONS

AM	arithmetic mean
ANOVA	analysis of variance
ANSTO	Australian Nuclear Science and Technology Organisation
BIOMASS	IAEA Programme on Biosphere Modelling and Assessment
CEA	Commissariat á l'Energie Atomique
CEC	cation exchange capacity
DM	dry mass
EMRAS	Environmental Models for Radiation Safety
FAO	Food and Agriculture Organization
FARC	Fukushima Agricultural Technology Centre, Japan
FDNPP	Fukushima Daiichi Nuclear Power Plant
FM	fresh mass
GM	geometric mean
GSD	geometric standard deviation
IAEA	International Atomic Energy Agency
ICRP	International Commission on Radiological Protection
ICRU	International Commission on Radiation Units and Measurements
ICSA	Intensive Contamination Survey Area (in Japan)
IER	Institute of Environmental Radioactivity, Japan
IRSN	Institute for Radiological Protection and Nuclear Safety, France
JCAC	Japan Chemical Analysis Centre, Japan
KAERI	Korea Atomic Energy Research Institute, Korea
MAFF	Ministry of Agriculture, Forestry and Fisheries, Japan
MEXT	Ministry of Education, Culture, Sports, Science and Technology, Japan
MODARIA	Models and Data for Radiological Impact Assessment
NPP	nuclear power plant
NRA	Nuclear Regulation Authority
RIP	radiocaesium interception potential
SD	standard deviation
SDA	Special Decontamination Area (in Japan)
TRS	Technical Report Series
UKCEH	UK Centre for Ecology & Hydrology, United Kingdom
UNESCO	United Nations Educational, Scientific and Cultural Organization
UNSCEAR	United Nations Scientific Committee on the Effects of Atomic Radiation

CONTRIBUTORS TO DRAFTING AND REVIEW

Beresford, N.A.	UK Centre for Ecology and Hydrology, United Kingdom
Bildstein, O.	Commissariat á l'Energie Atomique, France
Boyer, P.	Institut de Radioprotection et de Sûreté Nucléaire, France
Brown, J.	International Atomic Energy Agency
Carini, F.	Università Cattolica del Sacro Cuore, Italy
Choi, Y-H.	Korea Atomic Energy Research Institute, Republic of Korea
Eguchi, S.	National Agriculture and Food Research Organization, Japan
Fesenko, S.	Russian Institute Radiology and Agroecology, Russian Federation
Fujimura, S.	National Agriculture and Food Research Organization, Japan
Garcia-Sanchez, L.	Institut de Radioprotection et de Sûreté Nucléaire, France
Hashimoto, S.	Forestry and Forest Products Research Institute, Japan
Hayashi, S.	National Institute for Environmental Studies, Japan
Howard, B.J.	School of Bioscience, University of Nottingham and Fellow of UK Centre for Ecology and Hydrology, United Kingdom
Howard, D.C.	UK Centre for Ecology and Hydrology, United Kingdom
Imamura, N.	Forestry and Forest Products Research Institute, Japan
Ishii, N.	National Institutes for Quantum and Radiological Science and Technology, Japan
Ishii, Y.	National Institute for Environmental Studies, Japan
Iurian, A.-R.	International Atomic Energy Agency
Jeong, H.	Korea Atomic Energy Research Institute, Republic of Korea
Johansen, M.P.	Australian Nuclear Science and Technology Organisation, Australia
Kaneko, S.	Forestry and Forest Products Research Institute, Japan
Kato, H.	University of Tsukuba, Japan
Komatsu, M.	Forestry and Forest Products Research Institute, Japan
Konoplev, A.	Fukushima University, Japan
Kusakabe, M.	Marine Ecology Research Institute, Japan

Matsunami, H.	National Agriculture and Food Research Organization, Japan
McGinnity, P.	International Atomic Energy Agency
Mori, A.	International Atomic Energy Agency
Nagao, S.	Kanazawa University, Japan
Nishina, K.	National Institute for Environmental Studies, Japan
Ohashi, S.	Forestry and Forest Products Research Institute, Japan
Onda, Y.	University of Tsukuba, Japan
Pröhl, G.	Consultant, Germany
Saito, T.	Fukushima Agricultural Technology Centre, Japan
Sato, M.	Fukushima University, Japan
Shaw, G.	University of Nottingham, United Kingdom
Shinano, T.	Hokkaido University, Japan
Suzuki, K.	Gunma Prefectural Fisheries Experiment Station, Japan
Tagami, K.	National Institutes for Quantum and Radiological Science and Technology, Japan
Takata, D.	Fukushima University, Japan
Takata, H.	Fukushima University, Japan
Taniguchi, K.	Fukushima Prefectural Centre for Environmental Creation, Japan
Thiry, Y.	Agence Nationale pour la Gestion des Déchets Radioactifs, France
Thorne, M.	Mike Thorne Ltd, United Kingdom
Tsuji, H.	National Institute for Environmental Studies, Japan
Tsukada, H.	Fukushima University, Japan
Uchida, S.	National Institutes for Quantum and Radiological Science and Technology, Japan
Uematsu, S.	University of Tsukuba, Japan
Ulanowski, A.	International Atomic Energy Agency
Vidal, M.	University of Barcelona, Spain
Watanabe, S.	Gunma Prefectural Fisheries Experiment Station, Japan

Wood, M.D.	University of Salford, United Kingdom
Yamaguchi, N.	National Agriculture and Food Research Organization, Japan
Yasuda, H.	Hiroshima University, Japan
Yoschenko, V.	Fukushima University, Japan

LIST OF WORKING GROUP 4, SUBGROUP 2 PARTICIPANTS

Aono, T.	National Institute of Radiological Sciences, Japan
Asano, K.	Fukushima University, Japan
Barnett, C.L.	UK Centre for Ecology and Hydrology, United Kingdom
Beresford, N.A.	UK Centre for Ecology and Hydrology, United Kingdom
Bildstein, O.	Commissariat á l'Energie Atomique, France
Boyer, P.	Institut de Radioprotection et de Sûreté Nucléaire, France
Brown, J.	International Atomic Energy Agency
Choi, Y-H.	Korea Atomic Energy Research Institute, Republic of Korea
Eguchi, S.	National Agriculture and Food Research Organization, Japan
Fesenko, S.	Russian Institute Radiology and Agroecology, Russian Federation
Garcia-Sanchez, L.	Institut de Radioprotection et de Sûreté Nucléaire, France
Hashimoto, S.	Forestry and Forest Products Research Institute, Japan
Hayashi, S.	National Institute for Environmental Studies, Japan
Howard, B.J.	School of Bioscience, University of Nottingham and Fellow of UK Centre for Ecology and Hydrology, United Kingdom
Howard, D.C.	UK Centre for Ecology and Hydrology, United Kingdom
Imamura, N.	Forestry and Forest Products Research Institute, Japan
Iosjpe, M.	Norwegian Radiation and Nuclear Safety Authority, Norway
Ishida, K.	Nuclear Waste Management Organization, Japan
Ishii, N.	National Institutes for Quantum and Radiological Science and Technology, Japan
Ishiniwa, H.	Fukushima University, Japan
Iurian, A-R.	International Atomic Energy Agency
Jeong, H.	Korea Atomic Energy Research Institute, Republic of Korea
Johansen, M.P.	Australian Nuclear Science and Technology Organisation, Australia
Kaneko, S.	Forestry and Forest Products Research Institute, Japan
Kato, H.	University of Tsukuba, Japan

Kelleher, K.	Environmental Protection Agency, Republic of Ireland
Kim, S.	Korea Atomic Energy Research Institute, Republic of Korea
Kobayashi, R.	University of Tokyo, Japan
Komatsu, M.	Forestry and Forest Products Research Institute, Japan
Konoplev, A.	Fukushima University, Japan
Kubota, T.	National Agriculture and Food Research Organization, Japan
Kusakabe, M.	Marine Ecology Research Institute, Japan
Kuusisto, J.	Posiva Oy, Finland
Lahdenperä, A-M.	AINS Group, Finland
Matsunami, H.	National Agriculture and Food Research Organization, Japan
McGinnity, P.	International Atomic Energy Agency
Men, W.	State Oceanic Administration, People's Republic of China
Miura, S.	Forestry and Forest Products Research Institute, Japan
Mizushima, I.	Fukushima University, Japan
Monfort, M.	Commissariat á l'Energie Atomique, France
Mori, A.	International Atomic Energy Agency
Nagata, H.	Fukushima University, Japan
Nakanishi, T.	Japan Atomic Energy Agency, Japan
Nishina, K.	National Institute for Environmental Studies, Japan
Ohashi, S.	Forestry and Forest Products Research Institute, Japan
Ohta, M.	Japan Atomic Energy Agency, Japan
Onda, Y.	University of Tsukuba, Japan
Osvath, I.	International Atomic Energy Agency
Phaneuf, M.	Canadian Nuclear Safety Commission, Canada
Pröhl, G.	Consultant, Germany
Rigol, A.	University of Barcelona, Spain
Saito, T.	Fukushima Agricultural Technology Centre, Japan
Shaw, G.	University of Nottingham, United Kingdom
Shinano, T.	Hokkaido University, Japan

Tagami, K.	National Institutes for Quantum and Radiological Science and Technology, Japan
Takata, H.	Fukushima University, Japan
Takeda, A.	Institute for Environmental Sciences, Japan
Tanaka, T.	Electricité de France, France
Thiry, Y.	Agence Nationale pour la Gestion des Déchets Radioactifs, France
Tsuji, H.	National Institute for Environmental Studies, Japan
Tsukada, H.	Fukushima University, Japan
Tsumune, D.	Central Research Institute of Electric Power Industry, Japan
Tsuruta, T.	Japan Atomic Energy Agency, Japan
Uchida, S.	National Institutes for Quantum and Radiological Science and Technology, Japan
Ulanowski, A.	International Atomic Energy Agency
Vidal, M.	University of Barcelona, Spain
Yamaguchi, N.	National Agriculture and Food Research Organization, Japan
Yunxuan, L.	National Security Commission, People's Republic of China

MODARIA II Technical Meetings, IAEA Headquarters, Vienna

31 October – 4 November 2016, 30 October – 3 November 2017, 22–25 October 2018, 21–24 October 2019

Interim Working Group Meetings, MODARIA II Working Group 4, Subgroup 2

Tsukuba, Japan: 10–12 July 2017
Fukushima, Japan: 6–8 June 2018
Vienna, Austria: 27–31 May 2019

Consultants Meetings

Vienna, Austria: 10–14 December 2018, 26–30 August 2019

IAEA
International Atomic Energy Agency

No. 26

ORDERING LOCALLY

IAEA priced publications may be purchased from the sources listed below or from major local booksellers.

Orders for unpriced publications should be made directly to the IAEA. The contact details are given at the end of this list.

NORTH AMERICA

Bernan / Rowman & Littlefield

15250 NBN Way, Blue Ridge Summit, PA 17214, USA
Telephone: +1 800 462 6420 • Fax: +1 800 338 4550

Email: orders@rowman.com • Web site: www.rowman.com/bernan

REST OF WORLD

Please contact your preferred local supplier, or our lead distributor:

Eurospan Group

Gray's Inn House
127 Clerkenwell Road
London EC1R 5DB
United Kingdom

Trade orders and enquiries:

Telephone: +44 (0)176 760 4972 • Fax: +44 (0)176 760 1640
Email: eurospan@turpin-distribution.com

Individual orders:

www.eurospanbookstore.com/iaea

For further information:

Telephone: +44 (0)207 240 0856 • Fax: +44 (0)207 379 0609
Email: info@eurospangroup.com • Web site: www.eurospangroup.com

Orders for both priced and unpriced publications may be addressed directly to:

Marketing and Sales Unit
International Atomic Energy Agency
Vienna International Centre, PO Box 100, 1400 Vienna, Austria
Telephone: +43 1 2600 22529 or 22530 • Fax: +43 1 26007 22529
Email: sales.publications@iaea.org • Web site: www.iaea.org/publications

International Atomic Energy Agency
Vienna